

Acta

Morphologica

Academiae
Scientiarum
Hungaricae

ADIUVANTIBUS

I. TÖRŐ, J. BALÓ, E. BEREGLI, P. ENDES,
B. HALÁSZ, H. JELLINEK, I. KROMPECHER,
K. LAPIS, GY. RAPPAY, GY. ROMHÁNYI, P. RÖHLICH,
J. SUGÁR, J. SZENTÁGOTHAÍ, I. TARISKA

REDIGIT

E. SOMOGYI

TOMUS XXV * FASCICULUS I



Akadémiai Kiadó Budapest

1977

ACTA MORPH. HUNG.

ACTA MORPHOLOGICA

A MAGYAR TUDOMÁNYOS AKADÉMIA ORVOSTUDOMÁNYI KÖZLEMÉNYEI

SZERKESZTŐSÉG ÉS KIADÓHIVATAL: 1054 BUDAPEST, ALKOTMÁNY U. 21.

Az Acta Morphologica angol nyelven közöl értekezéseket a kísérletes orvostudomány tárgyköréből.

Az Acta Morphologica változó terjedelmű füzetekben jelenik meg. Több füzet alkot egy kötetet.

A közlésre szánt kéziratok a következő címre küldendőek;

Acta Morphologica, 1091 Budapest, Üllői u. 93.

Ugyanerre a címre küldendő minden szerkesztőségi és kiadóhivatali levelezés.

Megrendelhető a belföld számára az Akadémiai Kiadónál (1368 Budapest Pf. 24. Bankszámla 215-11488), a külföld számára pedig a „Kultúra” Külkereskedelmi Vállalatnál (1389 Budapest 62, P.O.B. 149 Bankszámla; 218-10990) vagy annak külföldi képviselőitől és bizományosainál.

Die Acta Morphologica veröffentlichen Abhandlungen aus dem Bereiche der experimental-medizinischen Wissenschaften in englischer Sprache.

Die Acta Morphologica erscheinen in Heften wechselnden Umfanges. Mehrere Hefte bilden einen Band.

Die zur Veröffentlichung bestimmten Manuskripte sind an folgende Adresse zu senden:

Acta Morphologica, H-1091 Budapest, Üllői u. 93.

An die gleiche Anschrift ist auch jede für die Schriftleitung und den Verlag bestimmte Korrespondenz zu richten. Abonnementspreis pro Band: \$ 36.00.

Bestellbar bei Außenhandelsunternehmen »Kultúra« (1389 Budapest 62, P.O.B. 149. Bankkonto Nr. 218-10990) oder bei seinen Auslandsvertretungen und Kommissionären.

Acta Morphologica

Academiae Scientiarum Hungaricae

Adiuvantibus

I. Törő, J. Baló, E. Beregi, P. Endes, B. Halász, H. Jellinek,
I. Krompecher, K. Lapis, Gy. Rappay, Gy. Romhányi,
P. Röhlich, J. Sugár, J. Szentágothai, I. Tariska

Redigit

E. Somogyi

Tomus XXV



Akadémiai Kiadó, Budapest

1977



ACTA MORPHOLOGICA

TOMUS XXV

INDEX

<i>Mitro, A.—Kiss, A.</i> : The Ependyma of the Ventriculus Mesencephali in the Rat	1
<i>Kovács, P.—Csaba, Gy.</i> : Evidence of the Heterogeneity of Mast Cell Population Based on their Biogenic Amine Content	9
<i>Kovács, P.—Csaba, Gy.</i> : Biogenic Amine and Amine Precursor Uptake by Mast Cells . . .	19
<i>Csonka, Éva—Bernolák, B.—Koch, A. S.—Jellinek, H.</i> : Scanning Electron Microscopic Examination of <i>in Vitro</i> Cultured Cells by Different Methods	25
<i>Kasinathan, S.—Basu, S. L.—Vijayam Sriramulu</i> : Cell Types of the Pars Distalis: Seasonal Changes in Secretory Activity and Effect of Steroids on Spermatogenesis in <i>Rana Hexadactyla</i>	35
<i>Khalil, S. H.—Lázár, Gy.</i> : Nucleus Isthmi of the Frog: Structure and Tecto-Isthmic Projection	51
<i>Ormos, J.—Engelhardt, J.—Mágori, Anikó</i> : Postmortem Diagnostics of Renal Diseases from Semithin Sections	61
Recensiones	71
<i>Bély, M.—Kempelen, I.</i> : Early Diagnosis of Cancer by Gastric Biopsy	73
<i>Beiléri, I.—Bély, M.</i> : Dangers of Positive Pressure Respiration Breathing with Special Reference to the So-called "Surfactant Factor"	91
<i>Fodor, I.</i> : Histogenesis of Beryllium-Induced Bone Tumours	99
<i>Keller, Mária—Tanka, D.</i> : Effect of Ultrasonic Treatment on the Organs of Experimental Animals III. Enzyme-Histochemical Examination of the Prolonged Effect . . .	107
<i>Neumark, T.</i> : Cell-to-Cell Contacts Between Lymphoreticular Cells in Rheumatoid Synovial Membrane	121
<i>Tanka, D.—Keller Mária</i> : Electron Transporting Enzymes of Rheumatoid Connective Tissue	137
<i>Csonka Éva—Bernolák, B.—Koch, A. S.—Jellinek, H.</i> : Influence of Membrane Active Substances on Cell Surface Morphology of Cultured Aortic Endothelial Cells . .	147
<i>Sidhu, K. S.—Guraya, S. S.</i> : Comparative Dimensional Characteristics of Spermatozoa in Muridae	161
<i>Chaldakov, G. N.—Nikolov, S.—Vancov, V.</i> : Fine Morphological Aspects of the Secretory Process in Arterial Smooth Muscle Cells. II. Role of Microtubules	167
<i>Záborszky, L.—Brownstein, M. J.—Palkovits, M.</i> : Ascending Projections to the Hypothalamus and Limbic Nuclei from the Dorsolateral Pontine Tegmentum: A Biochemical and Electron Microscopic Study	181
<i>Pálvölgyi, R.—Péntek, Z.</i> : Xeroradiographic Demonstration of Soft Tissues of the Extremities	189
<i>Kausz Mária—Réthelyi, M.</i> : Descending Course of Primary Afferent Collaterals in the Cat's Spinal Cord (Short Communication)	197
Recensiones	203
<i>Fehér, J.</i> : Myofibre Abnormalities of Orbicular Muscle in Malposition of the Eyelid . .	205
<i>Törő, I.</i> : Influence of the Intestinal Epithelium to the Plasma cell Differentiation injected Into the Thymus	219
<i>Tompa, Anna—Lapis, K.—Schaff, Zsuzsa—Mészáros, K.—Mandl, J.—Garzó, T.—Antoni, F.</i> : Cytoplasmic Aggregates in D-Galactosamine Induced Liver Injury	239
<i>Ambach, G.—Palkovits, M.</i> : Blood Supply of the Rat Hypothalamus. V. The Medial Hypothalamus (Nucleus Ventromedialis, Nucleus Dorsomedialis, Nucleus Perifornicalis)	259

<i>Somogyi, E.—Sótonyi, P.—Nemes, A.—Juhász-Nagy, S.:</i> Intermittent Hypoxic Loading: A Model System to Study the Early Stages of Myocardial Lesions. (Short communication)	279
<i>Paál, Mária—Bajtai, G.—Ambrus, Mária—Horváth, Györgyi—Kovács, Márta—Barna, K.:</i> Detection of Hepatitis B Surface Antigen in Isolated Hepatocytes	285
<i>Decastello, Alice—Remenár, Éva—Tóth, Jeanette—Pozderka, Borbála—Bartók, I.:</i> Post- Mortem Detection of Early Myocardial Infarction by Determination of the Tissue K ⁺ /N ⁺ Ratio	289
Recensiones	297

INDEX AUTORUM

A

- Ambach, G.—Palkovits, M.: 259
Ambrus, Mária vide Paál, Mária—Bajtai, G.—Horváth Györgyi—Kovács, Márta—Barna, K.: 285
Antoni, F. vide Tompa, Anna—Lapis, K.—Schaff, Zsuzsa—Mészáros, K.—Mandl, J.—Garzó, T.: 239

B

- Bajtai, G. vide Paál, Mária—Ambrus, Mária—Horváth, Györgyi—Kovács, Márta—Barna, K.: 285
Barna, K. vide Paál Mária—Bajtai G.—Ambrus, Mária—Horváth, Györgyi—Kovács, Márta: 285
Bartók, I. vide Decastello, Alice—Remenár, Éva—Tóth, Jeanette—Pozderka, Borbála: 289
Basu, S. L. vide Kasinathan, S.—Sriramulu, V.: 35
Bély, M.—Kempelen, I.: 73
Bély, M. vide Betléri I.: 91
Betléri, I.—Bély M.: 91
Bernolák, B. vide Csonka, Éva—Koch, A. S. Jellinek, H.: 25
Bernolák, B. vide Csonka, Éva—Koch, S. A.—Jellinek, H.: 147
Brownstein, M. J. vide Záborszky, L.—Palkovits, M.: 181

C

- Chaldakov, G. N.—Nikolov, S.—Vancov, V.: 167

Cs

- Csaba, Gy. vide Kovács, P.: 9
Csaba, Gy. vide Kovács P.: 19
Csonka, Éva—Bernolák, B.—Koch, A. S.—Jellinek, H.: 25
Csonka, Éva—Bernolák, B.—Koch, A. S.—Jellinek, H.: 147

D

- Decastello, Alice—Remenár, Éva—Tóth, Jeanette—Pozderka, Borbála—Bartók, I.: 289

E

Engelhardt, J. vide Ormos, J.—Mágori, Anikó: 61

F

Fehér, J.: 205

Fodor, I.: 99

G

Garzó, T. vide Tompa, Anna—Lapis, K.—Schaff, Zsuzsa—Mészáros, K.—Mandl, J.—Antoni, F.: 239

Guraya, S. S. vide Sidhu, K. S.: 161

H

Horváth, Györgyi vide Paál, Mária—Bajtai, G.—Ambrus, Mária—Kovács, Márta—Barna, K.: 285

J

Jellinek, H. vide Csonka, Éva—Bernolák, B.—Koch, A. S.: 25

Jellinek, H. vide Csonka, Éva—Bernolák, B.—Koch, A. S.: 147

Juhász-Nagy, S. vide Somogyi, E.—Sótonyi, P.—Nemes, A.: 279

K

Kasinathan, S.—Basu, S. L.—Sriramulu, V.: 35

Kausz, Mária—Réthelyi, M.: 197

Keller, Mária—Tanka, D.: 107

Keller, Mária vide Tanka, D.: 137

Kempelen, I. vide Bély, M.: 73

Khalil, S. H.—Lázár, Gy.: 51

Kiss, A. vide Mitro, A.: 1

Koch, A. S. vide Csonka, Éva—Bernolák, B.—Jellinek, H.: 25

Koch, A. S. vide Csonka, Éva—Bernolák, B.—Jellinek, H.: 147

Kovács, P.—Csaba, Gy.: 9

Kovács, P.—Csaba, Gy.: 19

Kovács, Márta vide Paál Mária—Bajtai, G.—Ambrus, Mária—Horváth, Györgyi—Barna, K.: 285

L

Lapis, K. vide Tompa, Anna—Schaff, Zsuzsa—Mészáros, K.—Mandl, J.—Garzó, T.—Antoni, F.: 239

Lázár, Gy. vide Khalil, S. H.: 51

M

Mandl, J. vide Tompa, Anna—Lapis, K.—Schaff, Zsuzsa—Mészáros, K.—Garzó, T.—Antoni, F.: 239

Mágori, Anikó vide Ormos, J.—Engelhardt, J.: 61

Mészáros, K. vide Tompa, Anna—Lapis, K.—Schaff, Zsuzsa—Mandl, J.—Garzó, T.—Antoni, F.: 239

Mitro, A.—Kiss, A.: 1

N

Nemes, A. vide Somogyi, E.—Sótonyi, P.—Juhász-Nagy, S.: 279
 Neumark, T.: 121
 Nikolov, S. vide Chaldakov, G. N.—Vancov, V.: 167

O

Ormos, J.—Engelhardt, J.—Mágori, Anikó: 61

P

Paál, Mária—Bajtai, G.—Ambrus, Mária—Horváth, Györgyi—Kovács, Márta—Barna, K.: 285
 Palkovits, M. vide Záborszky, L.—Brownstein, M. J.: 181
 Palkovits, M. vide Ambach, G.: 259
 Pálvölgyi, R.—Péntek, Z.: 189
 Péntek, Z. vide Pálvölgyi, R.: 189
 Pozderka, Borbála vide Decastello, Alice—Remenár, Éva—Tóth, Jeanette—Bartók, I.: 289

R

Remenár, Éva vide Decastello, Alice—Tóth, Jeanette—Pozderka, Borbála—Bartók, I.: 289
 Réthelyi, M. vide Kausz, Mária: 197

S

Schaff, Zsuzsa vide Tompa, Anna—Lapis, K.—Mészáros, K.—Mandl, J.—Garzó, T.—Antoni, F.: 239
 Sidhu, K. S.—Guraya, S. S.: 161
 Sriramulu, V. vide Kasinathan, S.—Basu, S. L.: 35
 Somogyi, E.—Sótonyi, P.—Nemes, A.—Juhász-Nagy, S.: 279
 Sótonyi, P. vide Somogyi, E.—Nemes, A.—Juhász-Nagy, S.: 279

T

Tanka, D. vide Keller, Mária: 107
 Tanka, D.—Keller, Mária: 137
 Tompa, Anna—Lapis, K.—Schaff, Zsuzsa—Mészáros, K.—Mandl, J.—Garzó, T.—Antoni, F.: 239
 Tóth, Jeanette vide Decastello, Alice—Remenár, Éva—Pozderka, Borbála—Bartók, I.: 289
 Törő, I.: 219

V

Vancov, V. vide Chaldakov, G. N.—Nikolov, S.: 167

Z

Záborszky, L.—Brownstein, M. J.—Palkovits, M.: 181



Institute of Experimental Endocrinology,
Slovak Academy of Sciences, Bratislava, Czechoslovakia

THE EPENDYMA OF THE VENTRICULUS MESENCEPHALI IN THE RAT

A. MITRO and A. KISS

(Received February 26, 1976)

The ventriculus mesencephali in the rat proceeds in the colliculi posterior region from the mesencephalic aqueduct in the dorsal direction. The ependymal lining is formed by flat, cuboid and cylindrical cells. The cylindrical cells, which occur in all parts of the ventriculus mesencephali, are the most numerous. The cuboid cells are localized mainly in the anterior part, the flat ones in the posterior part of the ventriculus mesencephali. Some cuboid and cylindrical cells have short basal processes. Among the ependymal cells, there are cells with long basal processes. The ependyma is at sites interrupted by flocks of ependymal cells. On the cell surface, there are cilia, microvilli and protoplasmic extrusions. The cell nuclei are spherical to oval. Supraependymally, there are homogeneous globules and intraventricular fibres.

The histological variability of ependymal cells may point to the active participation of these cells in functional processes, even within such a small part of the ventricle system as the ventriculus mesencephali.

Introduction

The internal surface of brain ventricles and the central canal is covered with epithelium, as described first by PURKYNĚ [16] and confirmed by KOELIKER [10]. An extensive study of the structure of this epithelium, the ependyma was made by STUDNICKA [21] and its possible functions were described by AGDUHR [1]. Further authors [7, 8, 11, 15 etc.] have pointed to the structural peculiarities of the ependyma in various animals species.

Morphological investigations of rats ependyma [5, 19, 22] have shown great structural variations, and attributed diverse functions to their tissue, such as secretory, transport absorptive and receptor functions, among others [9, 11, 23].

The present paper deals with the ependymal lining in the region of the ventriculus mesencephali in the rat. The ventriculus mesencephali represents part of the cerebral ventricle system. It is localized ventrally to the cerebellum and proceeds in the form of a recessus from the aqueductus mesencephali in dorsal direction [25]. It was called posterior collicular recessus [25] or ventriculus mesencephali by WESTERGAARD [24] who followed its ontogenesis. BÖHME and FRANZ [4] who made casts of the ventricles, called it "recessus colliculi caudalis". The main object of the present paper was to solve the question whether the ependymal cells of the ventriculus mesencephali were identical or exhibited regional differences.

Material and methods

Eight adult male rats weighing 200—250 g were used. For light microscopy, the brains were fixed in 8% formalin and embedded into paraffin, with their bases oriented parallel to the horizontal plane. The brains were cut in frontal and sagittal planes, the sections were stained with haematoxylin.

For electron microscopy, the brains were cut in the mediosagittal plain. Onto the cut surface 2.5% glutaraldehyde was dropped immediately (50—60 sec after decapitation) and small pieces of brain tissue from selected regions were obtained. These specimens were further fixed in 2.5% glutaraldehyde in a rotating device and postfixed with 1% osmic acid for two hours, then embedded in Durcupan. Semithin sections were stained with toluidine blue. Ultra-thin sections were contrasted with uranyl acetate in veronal buffer and with Reynolds's solution.

The shape and position of the ventriculus mesencephali within the whole ventricle system is shown in Fig. 1.

For further examination, three regions of the ventriculus mesencephali were chosen, the initial part of the ventriculus mesencephali (IVM), its apex (AVM) and its posterior part (FVM) (Fig. 2/A).

The examined regions were subdivided into the following parts, with respect to their shape in the frontal section of brain (Figs 2/B, C):

1. The region of IVM — a) upper part (U), b) middle part (M), c) lower part (L).
2. The region of AVM — a) upper part (U), b) lower part (L).
3. The region of FVM — a) upper part (U), b) lower part (L).

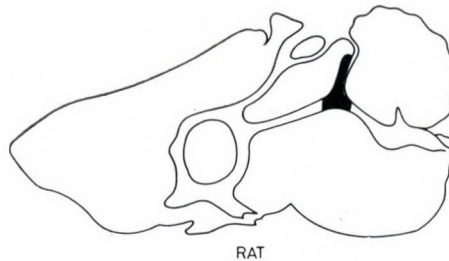


Fig. 1. Medio sagittal section through the brain of the rat. Black — ventriculus mesencephali

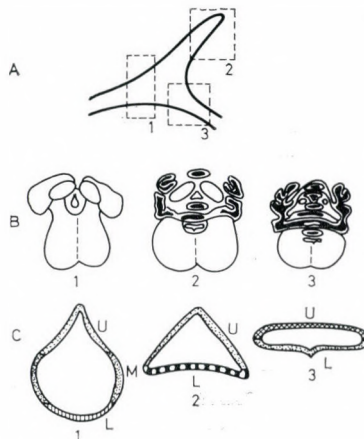


Fig. 2. Regions of the ventriculus mesencephali in the mediosagittal plane (A) and on frontal sections (B) and division of these regions in individual parts (C). U — upper part, M — middle part, L — lower part. Ependyma: dotted-cylindrical; vertically dashed-cuboid; crosswise dashed-flat to cuboid; thick lines-cuboid to cylindrical

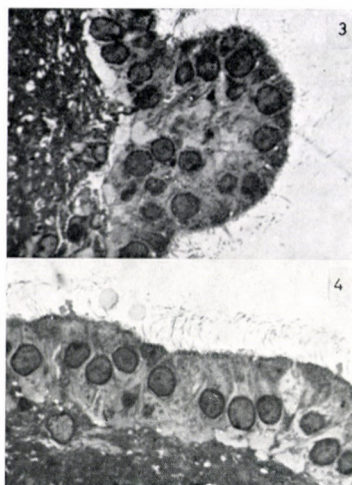


Fig. 3. Single layer of cylindrical ependyma, interrupted by a flock of ependymal cells $\times 1400$
 Fig. 4. Single layer on cylindrical ependyma. Among the cilia, supraependymal particles are present $\times 1400$

Results

Light microscopy

The IVM had the form of a short channel. In the frontal section it was round in shape with one apex-like formation in its upper part.

The upper part was covered with an undulating single layer of ependyma, composed of cylindrical cells with large oval nuclei. The medium part was lined by cylindrical ependyma, which was interrupted on several places by flocks of ependymal cells. In the basal parts some ependymal projected as short processes extending under the neighbouring ependymal cells (Fig. 2/C). Between the ependymal cells, there were some cells having long basal processes (tanocytes). The surface of ependymal cells in this region was covered with cilia. The apex of the IVM had the form of a cone. In the frontal section it was triangular in shape with irregularly undulating walls.

The upper part of this region was covered in some places with a single layer, in other places with stratified ependyma formed by high cylindrical cells with large round or oval nuclei. The lower part of this region consisted of a single layer of cylindrical and cuboid ependyma (Fig. 2/C). In smaller numbers, there occurred ependymal cells with short basal processes. Tanocytes were observed sporadically. The surface of ependymal cells was covered with cilia.

The posterior part of the IVM had the form of a short flat channel. In the frontal section it had a fissure-like appearance.

Its upper part was covered with a single ependymal layer composed of cubic and flat cells covered with cilia. The lower part was lined with a single ependymal layer composed of cylindrical cells between which there occurred some cells with short basal processes (Fig. 2/C). In some areas under this layer, there was a further layer composed of cylindrical and cubic cells. These cells did not reach the lumen. Between these two layers of ependymal cells, there were many capillaries.

Localization of the different types of ependymal cell is demonstrated in Fig. 2/C.

Electron microscopy

In the initial region of the IVM, the luminal surface of ependymal cells is bordered by small cell extrusions close to each other and of various shapes. Small microvilli are also present. The cilia are long and disproportionally distributed over the apical surface of ependymal cells. Their basal parts form small groups lying closely under the cell surface. The ependymal cells near the membrane cells form complex interdigitations and their ventricular surfaces are joined by numerous zonulae adherentes above or below which may be zonulae occludentes. The nuclei are excentric, their chromatin is unequally dispersed and forms small aggregations along the nuclear membrane. The mitochondria are oval to longitudinal. The Golgi apparatus is small. Ribosomes form small aggregations. Between the basal parts of the cells, bundles of non-myelinated and some sporadic myelinated nerve fibres are present. In the subependymal layer, glial cells are seen (Fig. 6); their dark nuclei are surrounded by narrow rings of cytoplasm.

In the apical region of the IVM, the surface of ependymal cells is supplied with microvilli (Fig. 5) and ramified cell extrusions. Adjacent ependymal cells form small interdigitations. The nuclei of ependymal cells are large and with their long axis is often oriented parallel to the cell surface. The mitochondria are oval or bent. The Golgi apparatus and short membrane fragments of endoplasmatic reticulum appear in the apical part of the cells. Dense bodies can also be observed. The size and structure of the bodies bear a striking similarity to the lipofusins as described by BLAKEMORE and JOLY [3] and others. In the supraependymal region nerve fibres and oval homogeneous structures occur but no synapses. The intraventricular nerve fibres contain electron-lucent vesicles up to nm in diameter.

In the posterior region of the IVM the surface of ependymal cells is supplied with extrusions and microvilli. Pinocytic vesicles are not seen. In some places, there are large bulbous projections having broad or narrow basal parts (Fig. 7). Cilia are present in small amounts. The nuclei are large. The chromatin is unequally dispersed over the nucleus. The mitochondria are mostly

longitudinal, often grouped in the apical part of the cell. The Golgi apparatus is large, its cisterns are well-developed and surround small vesicles. There are no granulated vesicles. The ribosomes are free or associated with the lamellae of the endoplasmatic reticulum. In the supraependymal region, there are nerve fibres and round homogeneous structures.

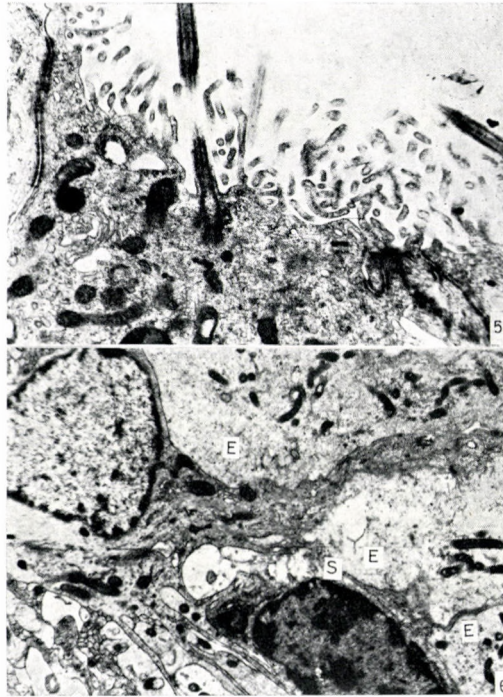


Fig. 5. Apical surface of an ependymal cell densely covered with microvilli $\times 16,000$

Fig. 6. A subependymal cell (S) in close contact with the basal parts of ependymal cells (E) $\times 11,500$

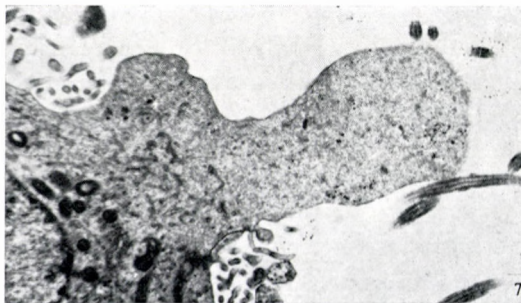


Fig. 7. Cytoplasmic extrusions of the apical part of an ependymal cell $\times 19,500$

Discussion

According to our results, the ependymal cells lying in the different regions of the IVM, show three types.

The first type is cylindrical with archwise shaped basal parts. These cells are the dominant components of the ependyma in all regions of the IVM. MILLHOUSE [14] considered these cells "typical ependymal cells of mammals". They occur in all regions of the cerebral ventricles. Some of them have short processes which penetrate under the neighbouring ependymal cells or are immersed in the adjacent neuropil.

The second type of cells is cuboid, it occurs in all regions of the IVM. The majority has archwise shaped basal parts and the minority short basal processes. The latter cells are comparable with the so-called irregular cuboid ependymal cells described in the lateral ventricle of rats by WESTERGAARD [24].

The third type of cell is flat; these occur in the posterior region of the IVM. Their basal parts are shaped archwise.

In all regions of the IVM, there were a few cells with long processes running into the adjacent neuropil. This type conforms with the so-called tanyocyte ependymal cells described in the shark *Scyliorhinus caniculus* by HORSTMANN [8]. In the rat, tanyocytes occur mostly in the third ventricle and vary in shape, localization and histoenzymatic activity [2, 6, 12, 17]. In the IVM the tanyocytes are distributed unequally between the other ependymal cells.

The luminal surface of ependymal cells, incessantly exposed to the CSF, plays a role in the exchange of biologically active compounds between CSF and ependyma. It represents the so-called first barrier in the transfer of compounds. Formations bordering the surface of ependymal cells — cilia and microvilli — are also important in this respect. In the IVM cilia varying in length occur in small groups unequally distributed over the whole surface of ependymal cells. In the ventricle system of the rat, cilia-free areas occur only in the lower part of the third ventricle [19] or in the area postrema [20]. Among the cilia there are microvilli in varying numbers. At sites the cell extrusions emerge from the surface on broad cytoplasmic pedicles. In other areas the protoplasmic globules are mostly connected with the apical surface by means of narrow stalks of cytoplasm. Although in some places these formations have no contact with the cell, it is probable that the protoplasmic globules are bulging from the ependymal cell surface and influence the composition of the CSF. MILHORAT et al. [13] suggest that cerebrospinal fluid is formed not only in the choroid plexus but also in the ependymal lining of the ventricles.

In the IVM, we found two types of supraependymal structures. In the apical and posterior parts there are non-myelinated nervous fibres, occurring

individually or in small groups. There are also homogeneous round formations; these correspond to the free supraependymal homogeneous spherical structures described in the rabbit by SCHWANITZ [18]. They occur in the apical and posterior regions of the IVM. Their origin cannot be determined unequivocally. It is supposed that in this part of the ventricular system accidental deposits of free supraependymal structures may occur due to the circulation of CSF and the production of whirls.

In the IVM there is no type of ependymal cell which would be characteristic of the region. The ependymal lining exhibits local differences in ependymal stratification, in the occurrence of folds and cell accumulations. There are likewise differences in the distribution of cilia, microvilli, cell extrusions, nervous fibres and supraependymal structures.

The morphological features of the ependymal cells of the IVM are supposed to indicate their absorbing function (microvilli), their ability to transport substances (tanycytes) and their role in the exchange of materials between CSF and nervous system (intraventricular nervous fibres). Those cells do not seem to represent a passive barrier but rather a physiologically active component of the ventricle system.

REFERENCES

1. AGDUHR, E.: (1932) Choroid Plexus and Ependyma. In: *Cytology and Cellular Pathology of the Nervous System*. Ed. W. Penfield, Hober, New York, vol. 2, pp. 537—573.
2. AKMAYEV, I. G., FIDELINA, O. V.: (1974) Morphological aspects of the hypothalamic-hypophyseal system. *Cell Tissue Res.* **152**, 403—410.
3. BLAKEMORE, W. F., JOLLY, R. D.: (1972) The subependymal plate and associated ependyma in the dog. *Neurocytol.* **1**, 69—84.
4. BÖHME, G., FRANZ, B.: (1967) Die Binnenräume des Gehirns von Ratte und Maus. *Acta anat. (Basel)* **68**, 199—206.
5. BRIGHTMAN, M. W.: (1965) The distribution within the brain of ferritin injected into cerebrospinal fluid compartments. I. Ependymal distribution. *J. Cell Biol.* **26**, 99—123.
6. COLMANT, H. J.: (1967) Über die Wandstruktur des dritten Ventrikels der Albinoratte. *Histochemie* **11**, 40—61.
7. FLEISCHHAUER, K.: (1960) Fluoreszenzmikroskopische Untersuchungen an der Faserghia. I. Beobachtungen an den Wandungen der Hirnventrikel der Katze (Seitenventrikel, III. Ventrikel). *Z. Zellforsch.* **51**, 467—496.
8. HORSTMANN, E.: (1954) Die Faserghia des Selachiergehirn. *Z. Zellforsch.* **39**, 588—617.
9. KNOWLES, F.: (1974) Cerebrospinal fluid and endocrine regulation. In: *Ependyma and Neurohormonal regulation*. Ed. A. Mitro. Veda, Bratislava, pp. 11—28.
10. KOELLIKER, R. A.: (1864) *Handbuch der Gewebelehre*. 2. Auflage. Engelmann, Leipzig.
11. LEONHARDT, H.: (1969) Ependym. In: *Symposium über Zirkumventrikuläre Organe und Liquor*. Reinhardtbrunn 1968. Ed. G. Sterba, G. Fischer, Jena, pp. 177—190.
12. LUPPA, H., FEUSTEL, G.: (1971) Location and characterization of hydrolytic enzymes of the IIIrd ventricle lining in the region of the recessus infundibularis of the rat. A study on the function of the ependyma. *Brain Res.* **29**, 253—270.
13. MILHORAT, T. H., HAMMOCK, M. K., FENSTERMACHER, J. D., RALL, D. P., LEVIN, V. A.: (1971) Cerebrospinal fluid production by the choroid plexus and brain. *Science*, **173**, 330—332.
14. MILLHOUSE, O. E.: (1972) Light and electron microscopic studies of the ventricular wall. *Z. Zellforsch.* **127**, 149—174.
15. PERSONEN, N.: (1940) Über die intraependymalen Nervelemente. *Anat. Anz.* **90**, 193—223 (87).
16. PURKYNĚ, J.: (1836) Über Flimmerbewegungen im Gehirn. *Arch. Anat.* 289—290.
17. SCHIEBLER, T. H., MITRO, A.: (1969) Über die Entwicklung des Ependyms. In: *Symposium über Zirkumventrikuläre Organe und Liquor*. Reinhardtbrunn 1968. Ed. G. Sterba, G. Fischer, Jena, pp. 177—190.
18. SCHWANITZ, W.: (1969) Die topographische Verteilung supraependymaler Strukturen in den Ventrikeln und im Zentralkanal des Kaninchengehirns. *Z. Zellforsch.* **100**, 536—551.
19. SCHACHENMAYR, W.: (1967) Über die Entwicklung von Ependym

und Plexus chorioideus der Ratte. *Z. Zellforsch.* **77**, 25—53. — 20. SPACEK, J., PARIZEK, J.: (1968) The structure of the area postrema of the rat. *Acta morph. Acad. Sci. hung.* **17** (1), pp. 17—34. — 21. STUDNÍČKA, F. K.: (1900) Untersuchungen über den Bau des Enzymes der nervösen Zentralorgane. *Anat. Hefte* **15**, 303—430. — 22. TEICHMANN, I., VIGH, B. and AROS, B.: (1966) Histochemical studies on Gomori-positive substances. II. The Gomori-positive material of a special ependymal formation (recessus organ) in the ventral part of the rat's third cerebral ventricle. *Acta biol. Acad. Sci. hung.* **17**, 13—29 (65). — 23. VIGH, B.: (1971) Das Paraventrikularorgan und das Zirkumventrikuläre System des Gehirns. *Akadémiai Kiadó, Budapest*. — 24. WESTERGAARD, E.: (1970) The lateral cerebral ventricles and the ventricular walls. *Andelsbogtrykkeriet, Odense*. — 25. WISLOCKI, G. B., LEDUC, E. H.: (1954) The cytology of the subcommissural organ, Reissner's fiber, periventricular glial cells and posterior collicular recess of the rat's brain. *J. comp. Neurol.* **2**, 283—309.

DAS EPENDYM DES VENTRICULUS MESENCEPHALI

A. MITRO und A. KISS

Der Ventriculus mesencephali bei Ratten zieht sich im Gebiete des Colliculus dorsalis des Aqueductus mesencephalon. Das Ependym bilden Plattenepithel, kubische Epithel und zylindrisches Epithel. In größter Zahl kommen in allen Teilen des Ventriculus mesencephali die zylindrischen Epithelzellen vor. Die kubischen Epithelzellen kommen hauptsächlich im vorderen Teil des Ventriculus mesencephali, die Plattenepithelzellen — im hinteren Teil dieses Gebildes vor. Einige kubische und zylindrische Epithelzellen besitzen kurze basale Fortsätze, einige Ependymzellen besitzen lange Fortsätze. Das Ependym wird an einigen Stellen durch ependymale Zellgruppen abgelöst (?). An den Zelloberflächen kommen Flimmerhärchen, Mikrovilli und Protoplasmaausbuchtungen vor. Die Zellkerne sind rund bis oval. Supraependymal kommen homogene Kügelchen und intraventrikuläre Fasern vor.

Die histologische Veränderlichkeit der Ependymzellen weist darauf hin, daß diese Zellen aktiv an funktionellen Prozessen teilnehmen, wenn auch auf solch kleinen Gebieten, wie Ventrikulärsystem des ventrikulären Teils des Ventriculus mesencephali.

ЭПЕНДИМА ЖЕЛУДОЧЕК МЕЗОЦЕФАЛА У КРЫС

А. МИТРО, и А. КИШ

Желудочек мезоцефала у крыс распространяется у задней части бугорка от водопровода мезоцефала в дорсальном направлении. Эпендима выстилает плоским кубическим и цилиндрическим эпителиальными клетками. В обеих частях желудочка мезоцефала в большинстве цилиндрические эпителиальные клетки наблюдаются. Кубические эпителиальные клетки располагаются главным образом в передней, и плоские эпителиальные клетки задней части мезоцефала. У нескольких кубических и цилиндрических клеток короткие базальные отростки. Одни эпендимальные клетки имеют длинные отростки. Кой-где эпендима заменяется группами эпендимальных клеток (?). На поверхностях клеток реснички микровилли и отростки протоплазма видны. Ядра клеток круглые и овальные. В супраэпендимальной части гомогенные шарики и интравентрикулярные волокна наблюдаются.

Гистологическая разнообразность эпендимальных клеток намекает на активность клеток принимающиеся в функциональных процессах, хотя в той части как вентрикулярная система желудочка мезоцефала.

Alexander MITRO } Institute of Experimental Endocrinology,
Alexander KISS } SAV, Vlárská ul. 3., 80936 Bratislava, Czechoslovakia

Institute of Biology, Semmelweis University Medical School, Budapest

EVIDENCE OF THE HETEROGENEITY OF MAST CELL POPULATION BASED ON THEIR BIOGENIC AMINE CONTENT

P. KOVÁCS and G. CSABA

(Received March 25, 1976)

The heterogeneity of the mast cells localized in various organs has been demonstrated by histochemical determination in their indole amine and histamine content. The strongest amine reaction was found in the mast cells in the mesenterium and peritoneal fluid where their maturation occurs. The reaction of the subcutaneous connective tissue is weaker; in the thyroid gland the reaction is weak as well as diffuse. In the thymus the mast cells localized along the vessels give a strong histamine reaction. The experiments support previously published data concerning the heterogeneity of mast cell populations.

The first observations concerning the mast cells reach back to the second half of the last century [21]. The component serving for their demonstration by inducing metachromasia in the granules, the presence of heparin was detected by JORPES et al. [23]. The other discovery of high importance concerning the composition of mast cell granules was made by RILEY and WEST [27] who demonstrated a close relation between the histamine content and the number of mast cells in the tissues as well as the binding of histamine to heparin in the granules. Then BENDITT et al. [1] demonstrated the presence in murine and rat mast cells of another biogenic amine; serotonin.

COMBS, et al. [3] by means of alcian blue–safranin staining could differentiate mast cells in various stages of maturation in the rat embryo. These mast cells in various degrees of maturation demonstrate marked differences in the quality of the acid polysaccharides as well as in the quantity of biogenic amines and in their maturational and the acid polysaccharide–biogenic amine — basic protein ratio [7, 11].

In earlier studies we have examined the heterogeneity of the mast cell population, based on their polysaccharide content [19]. In the present work we studied amine content of the mast cells in the organs and attempted to establish the functional relation between polysaccharide and amine content. The reason for this was that in our previous work [19] only the quantitative and qualitative differences in mucopolysaccharide content were evaluated as the cause of the heterogeneity of mast cells, whereas heterogeneity of the amines

has been neglected. In addition, the biogenic amine content of the mast cells has an important physiologic function, as it participates in a number of processes of induction and regulation, in anaphylactic reactions, *etc.* Several authors have pointed out [4, 9] that the mast cell population increased by treatment with carcinogenic agents, contains a particularly large amount of serotonin.

Materials and methods

The examinations were carried out in male Wistar CB rats of 100 g body weight. Mast cells were studied in membrane preparations of mesenterium, and subcutaneous connective tissue, thick drop of peritoneal fluid, fixed paraffin or fresh cryostat sections of thymus, lymph node, thyroid gland, lung, and heart muscle.

Histochemical reactions

a) For histamine: OPT (orthophthalaldehyde) reaction [24, 26]; Reinecke salt amine precipitation [28] followed by diazotized sulphanilic acid staining in fresh, unfixed cryostat sections;

b) for serotonin: paraformaldehyde vaporization (Falc's method; [26]; the specificity was controlled by borohydride test; post-coupled benzilene reaction [22] in formaldehyde-fixed paraffin sections;

c) polysaccharide : amine ratio: alcian blue-safranin reaction formaldehyde-fixed paraffin sections;

d) in addition, the following reactions were performed: Schmorl's ferri-ferricyanide reaction [5], diazotized safranin, *p*-dimethylaminobenzaldehyde and the Fast Garnet GBC reactions [25], and the xanthydrol reaction [29]. In our examinations these had not proved specific for amines, therefore their results will not be discussed.

Results

Histamine

The strongest reaction was obtained with Reinecke salt in the mesenteric mast cells (Fig. 1) and a considerably weaker one in connective tissue (Fig. 2). In the thymus the mast cells along the vessels, which could be identified also by their shape and localization (Fig. 3), gave an intense fluorescence, but in these cells thiazine dyes caused frequently no metachromatic staining. In the peritoneal mast cells the Reinecke reaction was marked (Fig. 4); the mast cells in the lymph nodes produced a fluorescence of about the same intensity (Fig. 5). In these two organs the strong reaction observed in some small lymphoid cells was conspicuous. In the thyroid gland and the heart muscle the reaction was rather weak, whereas in the lung the mast cells could not be differentiated: in a great number of cells the fluorescence was weak and diffuse. The results were supported by the diazotized sulphanilic acid reaction performed subsequent to dark-field examination, as well as by OPT fluorescence, which supplied results similar to the Reinecke salt method.

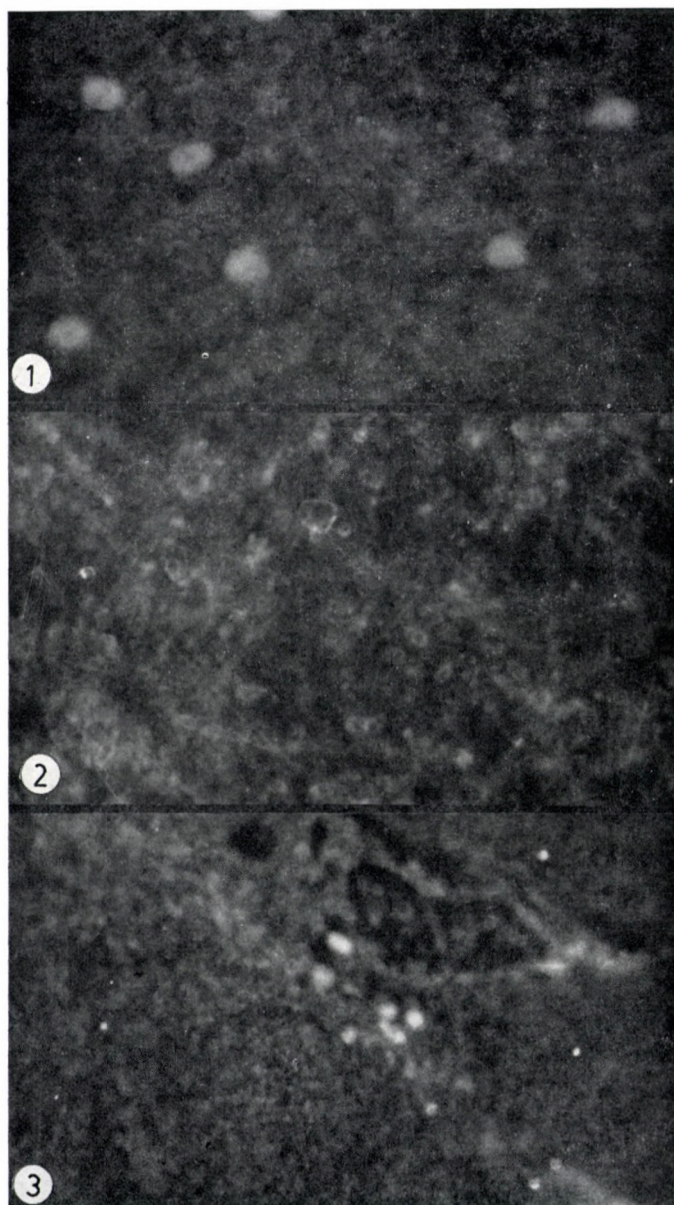


Fig. 1. Mesenteric mast cells treated with Reinecke salt. Dark-field picture $\times 320$

Fig. 2. Mast cell group localized in subcutaneous connective tissue, treated with Reinecke salt. Dark-field picture, $\times 160$

Fig. 3. In the thymus the mast cells localized around the vessels give a strong reaction with Reinecke salt. Dark-field picture, $\times 160$

Indoles

With paraformaldehyde vaporization by the Falek method, the strongest fluorescence was obtained in the mesenteric mast cells (Fig. 6). The fluorescence was weaker in both the peritoneal (Fig. 7) and the subcutaneous connective tissue (Fig. 8) mast cells. The fluorescence of thyroid gland (Fig. 9) and lymph node mast cells were rather weak. In lymph node macrophages (Fig. 10) an intense yellow autofluorescence, similar as that of the Gömöri-positive cells of the thymus, was observed. Results for the heart and lungs were not evaluable.

These results were supported by those obtained with the post-coupled benzyldene reaction. It was conspicuous that the Gömöri-positive cells of the thymus and the lymph node macrophages gave an identical reaction. A similar picture was obtained in the small lymphoid mast cells of the peritoneal fluid (Fig. 11) and the lymph nodes (Fig. 12).

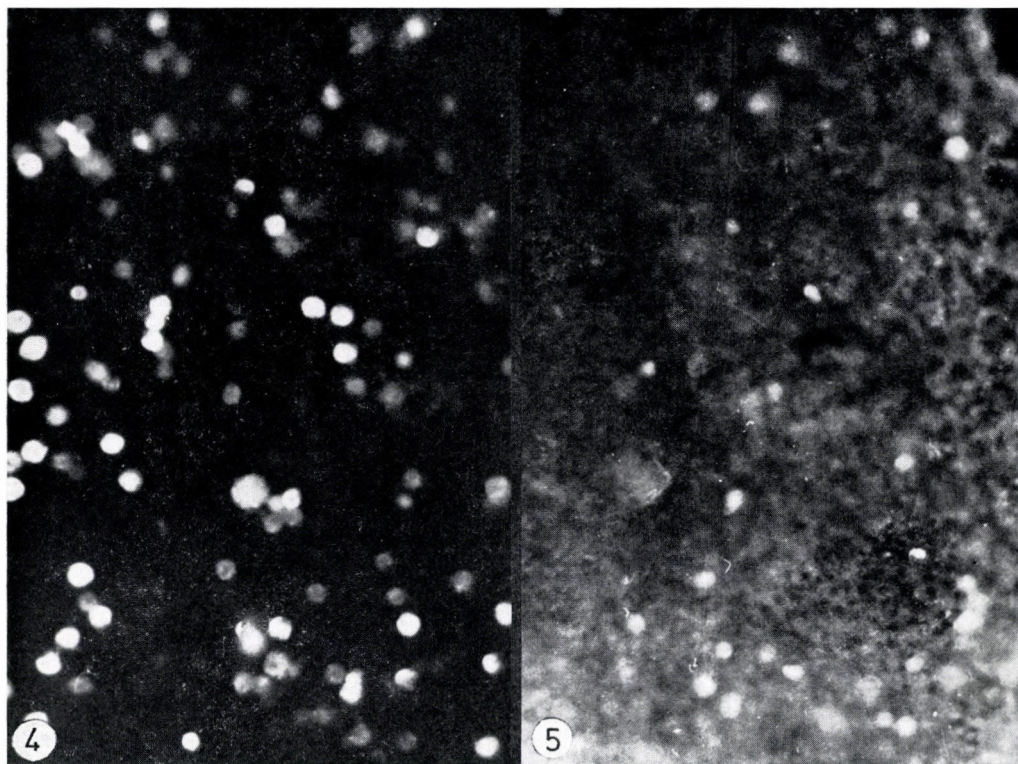


Fig. 4. The peritoneal mast cells and the small lymphoid cells give a strong reaction with Reinecke salt. Dark-field picture, $\times 160$

Fig. 5. The mast cells and some of the small lymphoid cells of the lymph nodes give a strong reaction with Reinecke salt. Dark-field picture, $\times 160$

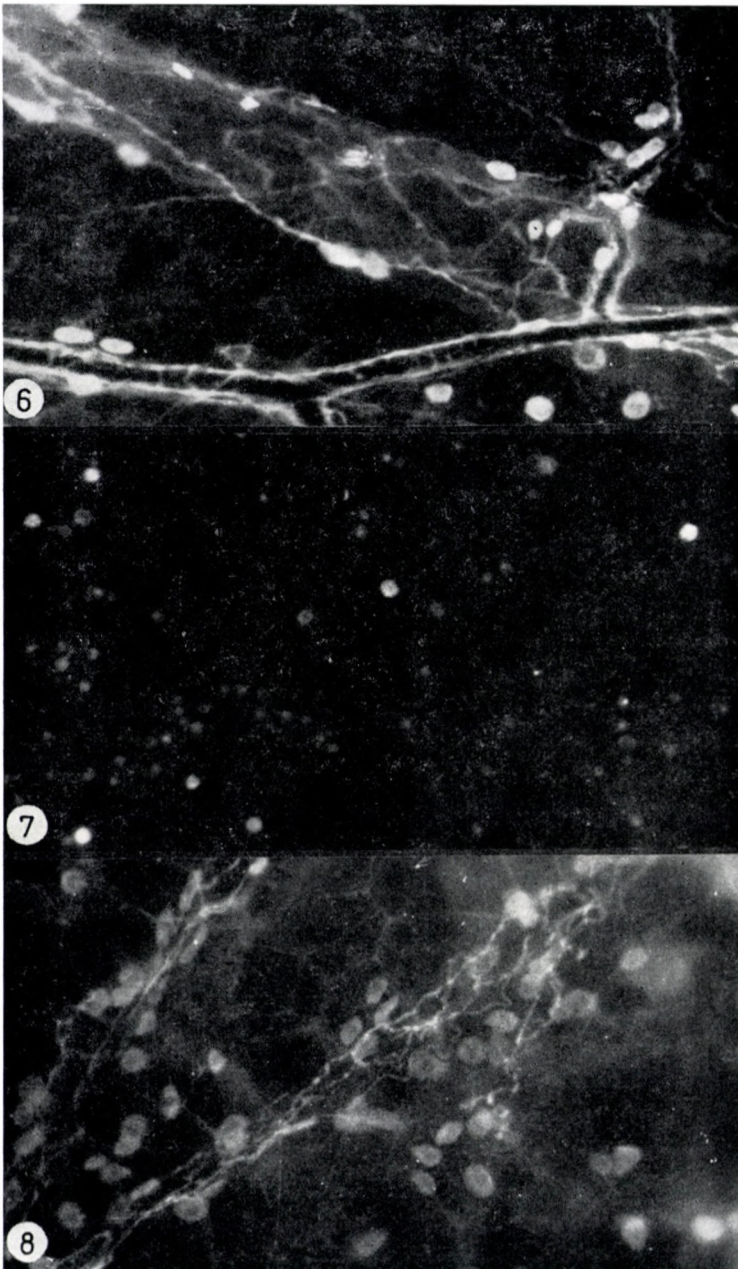


Fig. 6. Mesenteric mast cells give a strong reaction on paraformaldehyde vaporization according to the Falck method, $\times 160$

Fig. 7. Peritoneal mast cells give a moderately strong reaction with the Falck method, $\times 160$

Fig. 8. Subcutaneous connective tissue mast cells appear clearly with the Falck method, $\times 160$

Alcian blue-safranin staining

The results were identical with those described previously.

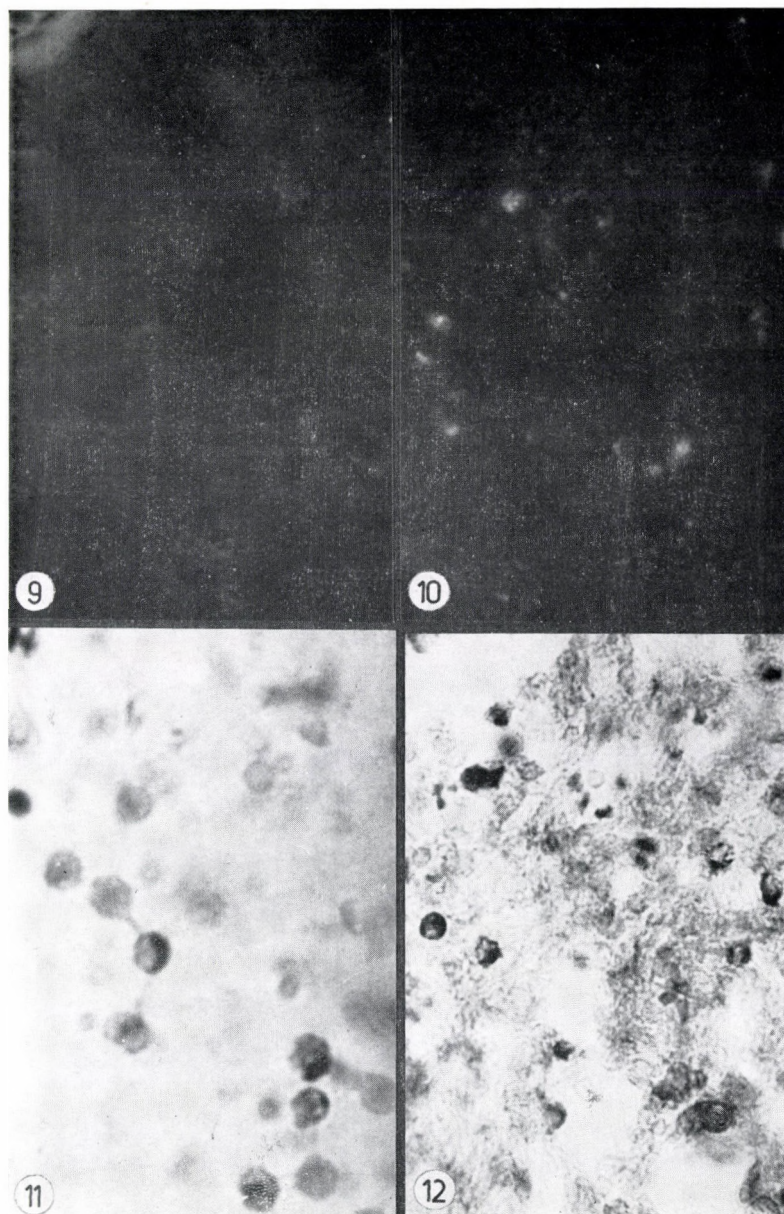


Fig. 9. Thyroid gland mast cells giving a weak Falck reaction, $\times 160$

Fig. 10. Yellowish autofluorescence of cells in lymph nodes, $\times 160$

Fig. 11. Lymphoid mast cells in the peritoneal fluid give a strong benzylidene reaction, $\times 360$

Fig. 12. The mast cells of lymphoid character in the lymph nodes give a strong benzylidene reaction, $\times 160$

Discussion

The results demonstrated that the mast cell population heterogeneous in mucopolysaccharide content [19], histochemical behaviour [11], and labelled precursor uptake [17] was dissimilar also in biogenic amine content.

In rat mast cells the heparin : histamine : serotonin ratio is 3 : 1 : 0.1 [12]. It was obvious already from previous experiments [8, 11] that the same ratio would not be valid for every mast cell, the maturation of such cells being mirrored by the ratio of the granule components. Mature mast cells are not uniform in the various organs; some show a vivid metabolism, some a slow one [2, 10], some are able to take up complete granule components [15, 16], whereas others cannot even take up precursors [17]. Thus it may be supposed that the mast cells are adapting themselves to the organ where they are localized.

In the present experiments the strongest reactions for both amines were seen in the mesenterial, subcutaneous connective tissue and peritoneal fluid mast cells. Among these the mesenterial and the peritoneal fluid mast cells were outstanding by their least sulphated mucopolysaccharide content. At the same time the mast cells of the subcutaneous connective tissue are strongly sulphated. On this basis an inversed ratio of the amine content and the degree of sulphation could not be stated. Taking, however, into consideration the intense metabolism the mast cells of the mesenterium and the peritoneal cavity, whereas the subcutaneous connective tissue mast cells are so-called end-product cells [11], the hypothesis seems permissible that the amine reaction is stronger — more amine is perhaps present? — in the active mast cells where the mucopolysaccharide is less sulphated. It is also possible that the stronger sulphated mucopolysaccharide binds the amines more strongly and so their demonstration is more difficult.

Among the peritoneal mast cells the small lymphoid ones yielded particularly strong indole and histamine reactions. This would support our observation [8] of an amine excess in the alcian blue positive small mast cells, which would induce increased heparin synthesis [6]. By such means in the safranin positive mast cells with mixed granulation the amine : heparin ratio will be balanced [11]. The peritoneal and the mesenterial mast cells form a homogeneous population. Maturation of the lymphoid cells which had migrated from the thymus into the peritoneal cavity, where the maturation process started, would continue in the mesentery [13]. This might be the cause of reactions of similar type.

The reaction of the thymus mast cells was a special problem. These cells failed to give any reaction characteristic of serotonin, while the mast cells localized along the vessels were conspicuous by their strong histamine reaction. Their majority gave Reinecke positive, but failed to stain with thiazine dyes.

In contrast, other connective tissue mast cells stained with thiazine, but did not react with Reinecke salt. Similarly, the Reinecke positive mast cells in the thymus did not stain with alcian blue-safranin either. The phenomenon cannot be explained on the basis of the present experiments. The Gömöri positive cells of the thymus [14, 18, 20] gave a characteristic indole reaction, but these could be differentiated from the mast cells.

The thyroid gland mast cells are characterized by serotonin uptake and delivery [15, 16]. Despite this fact, or just for this reason, only a weak, diffuse reaction was obtained for both amines. Their demonstration might have been presented by binding the most acid polysaccharide [19] or else, in view of their migration, only a small quantity of amines may have been present in the cells.

The amine reaction was weak in the few pulmonary mast cells. In our previous experiments [19] sulphatation of the mucopolysaccharides was of a similarly low degree, referring to the possibility that the rat lung is not a mast cell organ.

Summing up, the biogenic amine and mucopolysaccharide content of the mast cells is different in the various organs; on an increase of the degree of sulphatation the amine content, or perhaps its demonstrability, might be decreased. In the active, maturing mast cells the amine content is higher, but the thyroid mast cells form an exception. The findings support our previous observations concerning the heterogeneity of the mast cell population. Thus heterogeneity manifests itself in the ratio of the granule components, as well as in the activity of cells and the intensity of their metabolism.

REFERENCES

1. BENDITT, E. P., WONG, R. L., ARASE, M., ROEPER, E.: (1955) 5-hydroxytryptamine in mast cells. *Proc. Soc. exp. Biol. (N. Y.)* **90**, 303—304. — 2. BURTON, A. L.: (1963) Studies on living normal mast cells. *Ann. N. Y. Acad. Sci.* **103**, 245—262. — 3. COMBS, J. W., LAGUNOFF, D., BENDITT, E. P.: (1965) Differentiation and proliferation of embryonic mast cells of the rat. *J. Cell Biol.* **25**, 577—592. — 4. COUPLAND, R. E., RILEY, J. F.: (1960) Mast cells and 5-hydroxytryptamine in precancerous mouse skin. *Nature (Lond.)* **187**, 1128—1129. — 5. COUPLAND, R. E., HEATH, I. E.: (1961) Chromaffin cells, mast cells and melatonin. *J. Endocr.* **22**, 59—69. — 6. CSABA, G.: (1969) Mechanism of the formation of mast cell granules. III. Self regulating system of granule formation. *Acta biol. Acad. Sci. hung.* **20**, 211—218. — 7. CSABA, G.: (1969) Mechanism of the formation of mast cell granules. II. Cell free model. *Acta biol. Acad. Sci. hung.* **20**, 205—210. — 8. CSABA, G., SURJÁN, L. JR., FISCHER, J., KISS, J., TÖRÖK, I. JR.: (1969) On the mechanism of mast cell function. Effect of glucocorticoids on the mast cells of normal and thymectomized rats. *Acta biol. Acad. Sci. hung.* **20**, 57—74. — 9. CSABA, G., FORGÁCS, A.: (1970) Behaviour of mast cells in the skin of mice treated with benzpyren. *Acta morph. Acad. Sci. hung.* **18**, 17—22. — 10. CSABA, G., TÖRÖK, O.: (1970) Physiology of mast cells. I. Behaviour of mast cells in tissue culture. *Acta biol. Acad. Sci. hung.* **21**, 63—74. — 11. CSABA, G.: (1971) Mechanism of the formation of mast cell granules. VII. Participation of amines and basic proteins in the formation of the mast cell granule. Analysis of the heterogeneity of mast cells. *Acta biol. Acad. Sci. hung.* **22**, 155—168. — 12. CSABA, G.: (1972) Regulation of Mast Cell Formation. *Akadémiai Kiadó, Budapest.* — 13. CSABA, G., TÖRÖK, O.: (1972) Physiology of mast cells. IV. Role of blood transport in the transformation of mast cells. *Acta biol. Acad. Sci. hung.* **23**, 369—376. — 14. CSABA, G.: (1973)

An attempt to demonstrate endocrine cells in the rat thymus. *Endocr. exp.* **7**, 99-105. — 15. CSABA, G., BARÁTH, P.: (1973) Tritiated 5-hydroxytryptamine uptake of the mast cells in the rat thyroid gland. *Neuroendocrinology* **12**, 67-70. — 16. CSABA, G., BARÁTH, P.: (1974) Effect of pinealectomy on the ^3H -5-HT uptake of mast cells in the thyroid gland of the rat. *Acta anat. (Basel)* **89**, 442-451. — 17. CSABA, G., BARÁTH, P.: (1974) Heterogeneity of mast cell population as emerging from studies with labelled amines and amine precursors. *Acta biol. Acad. Sci. hung.* **25**, 323-325. — 18. CSABA, G., TÖRÖK, O.: (1974) Examination of the Gomori positive cells of the thymus in tissue culture. *Endocr. exp.* **8**, 3-12. — 19. CSABA, G., KOVÁCS, P.: (1976) Demonstration of the heterogeneity of the mast cell population on the basis of the mucopolysaccharide content. *Acta morph. Acad. Sci. hung.* **23**, 227-233. — 20. CSABA, G., KOVÁCS, P., TÖRÖK, O.: (1977) Gomori positive cells in the rat thymus. In preparation. — 21. EHRLICH, P.: (1877) Beiträge zur Kenntnis der Anilinfärbungen und ihrer Verwendung in der mikroskopischen Technik. *Arch. mikr. anat. Forsch.* **13**, 263-301. — 22. GLENNER, G. G. LILLIE, R. D.: (1957) The histochemical demonstration of indole derivatives by the post-coupled dimethylaminobenzylidene reaction. *J. Histochem. Cytochem.* **1**, 276-279. — 23. JORPES, J. E., HOLMGREN, H., WILANDER, O.: (1937) Über das Vorkommen von Heparin in den Gefäßwänden und in den Augen. *Z. mikr. anat. Forsch.* **42**, 279-300. — 24. JUHLIN, L., SHELLEY, W. B.: (1966) Detection of histamine by a new fluorescent o-phthalaldehyde stain. *J. Histochem. Cytochem.* **14**, 525-532. — 25. LILLIE, R. D., PIZZOLATO, P., WACCA, L. L., CATALANO, R. A., DONALDSON, P. T.: (1973) Histochemical azocoupling reactions. *J. Histochem. Cytochem.* **21**, 455-463. — 26. PEARSE, A. G. E.: (1968) *Histochemistry*. Little, Brown and Co., Boston. — 27. RILEY, J. F., WEST, G. B.: (1953) The presence of histamine in tissue mast cells. *J. Physiol. (London)* **120**, 528-537. — 28. SCHAUER, A., WERLE, A.: (1959) Zur histochemischen Darstellung des Histamins der Mastzellen. *Z. ges. exper. Med.* **131**, 100-104. — 29. SOLCIA, E., SAMPIETRO, R.: (1967) Indole nature of enterochromaffin substance. *Nature (Lond.)* **214**, 196-197.

NACHWEIS DER HETEROGENITÄT DER MASTZELLENPOPULATION AUF GRUND DES BIOGENAMID-GEHALTES

P. KOVÁCS und GY. CSABA

Mit Hilfe der biochemischen Verfahren zur Ermittlung der Indolamine und des Histamins läßt sich die Heterogenität des Amingehaltes der in verschiedenen Organen lokalisierten Mastzellen nachweisen. Die stärkste Aminreaktion erfolgt in den Mastzellen des Mesenterium und der peritonealen Flüssigkeit, wo auch die Reifung der Mastzellen vor sich geht. Die Reaktion des Bindegewebes ist geringer, die der Schilddrüse ist ebenfalls schwach und diffus. Im Thymus geben die neben den Gefäßen gelegenen Mastzellen eine starke Histaminreaktion. Die experimentalen Ergebnisse bekräftigen die schon früher beschriebene Heterogenität der Mastzellenpopulation.

ДОКАЗАТЕЛЬСТВО РАЗНОРОДНОСТИ ПОПУЛЯЦИИ ТУЧНЫХ КЛЕТОК НА ОСНОВЕ СОДЕРЖАНИЯ БИОГЕННЫХ АМИНОВ

П. КОВАЧ и Д. ЧАБА

При помощи гистохимических методов исследования, служащих для выявления индоламинов и гистамина, можно выявить разнородность содержания аминов в тучных клетках, расположенных в различных органах. Наиболее сильную реакцию на амины показывают тучные клетки брыжейки и брюшинной жидкости, где происходит созревание тучных клеток. Реакция подложной соединительной ткани менее сильна, а реакция щитовидной железы слаба и диффузна. В зубной железе сильную реакцию на гистамин дают тучные клетки, располагающиеся вдоль кровеносных сосудов. Результаты исследований подкрепляют уже раньше описанную разнородность популяции тучных клеток.

Péter Kovács } Semmelweis Orvostudományi Egyetem, Biológiai Intézet,
György Csaba } H-1450 Budapest, Tűzoltó u. 58., Hungary

Institute of Biology, Semmelweis University Medical School, Budapest

BIOGENIC AMINE AND AMINE PRECURSOR UPTAKE BY MAST CELLS

P. KOVÁCS and GY. CSABA

(Received May 3, 1976)

The mast cell population is heterogeneous concerning its amine precursor and amine uptake. The immature cells incorporate amine precursors, but in more advanced stages of their maturation they take up only 5-HTP. The mature cells do not take up precursors only 5-HT. The thyroid gland and heart muscle mast cells take up the highest amount of 5-HT; this may be related with some specific function of the mast cells in these two organs. Neither of the mast cells would take up histamine, the compound is synthesised by the cells.

Introduction

RILEY and WEST [13] were the first to show that the mast cell granules contained histamine in addition to heparin. BENDITT et al. [2] demonstrated the presence of another biogenic amine, serotonin, in mouse and rat mast cells.

The question arose whether the biogenic amines would be formed in the mast cells, or are taken up and stored in these. WERLE and SCHAUER [16], soon after the discovery of RILEY and WEST [13] separated from extracts mast cell-rich tissues (pleura, peritoneum) a fraction of high histidine decarboxylase activity. Later WEISSBACH et al. [15] showed that histidine can be decarboxylized in two enzymatic ways. One of the enzymes is an aspecific amino acid-decarboxylase, its chief substrate being DOPA, but it decarboxylates also 5-HTP, tyrosine, phenylalanine, and to a lesser extent histidine. The other enzyme is a specific histidine-decarboxylase.

LAGUNOFF et al. [11] as well as HAGEN and LEE [8] demonstrated in mast cell-rich skin extracts of rats and mice a 5-HTP decarboxylase, then LAGUNOFF and BENDITT [12] found this enzyme in isolated mast cells. WEISSBACH et al. [15] tested in mastocytoma extracts an aspecific enzyme decarboxylating aromatic amino acids.

These data point to the possibility that mast cells can produce biogenic amines by themselves. It is not clear, however, whether they could take up amine precursors and amines. In certain mast cells aminopeptidases can namely be demonstrated, as well as enzymes which can split larger protein molecules [14] and thus supply amine precursors. According to other reports [1, 4] the

mast cells of certain organs are capable of amine precursor and even of complete biogenic amine uptake [3, 5].

In previous experiments considerable differences in acid polysaccharide [7] and biogenic content were observed in mast cells originating from different organs of the rat [10]. In the present work it was therefore studied whether there was any difference in amine precursor and biogenic amine uptake between mast cells originating from different rat organs, and how these differences could be correlated with the degree of maturation, physiological functions and histochemical characteristics of the mast cells.

Materials and methods

The experiments were carried out in 80 g male Wistar CB rats, using two animals for each material. For MAO inhibition, each animal received 250 mg/kg body weight of nialamide (Nuredal EGYT), intraperitoneally, dissolved in n/5 HCL. After 30 minutes 125 μ Ci 3 H-histidine (spec. act.: 1 Ci/mM, Amersham), 125 μ Ci 3 H-histamine (spec. act.: 56 Ci/mM, Amersham), 125 μ Ci 3 H-5-HTP (5-hydroxytryptophan, spec. act.: 8.2 Ci/mM Amersham) or 125 μ Ci 3 H-5-HT (serotonin, spec. act.: 10.7 Ci/mM, Amersham) were injected intravenously. After 1 hour the animals were killed by an overdose of ether. The mesenterium, subcutaneous connective tissue, lymph node, heart and lung were removed fixed in 3% glutaraldehyde, and embedded in Durcupan ACM. Semithin sections were covered with Ilford K 5; after exposition for 28 days they were developed with ORWO R 09 developer. Staining was performed with Nuclear Fast red.

Results

3 H5HTP was taken up most intensively by the mesenterial mast cells (Fig. 1); uptake by the lymph node (Fig. 2) and heart mast cells was less intense, and nil by the connective tissue or pulmonary mast cells.

3 H-5-HT was incorporated at the highest intensity by the heart muscle mast cells (Fig. 3); incorporation by the mesenterium (Fig. 4) and lymph node (Fig. 5) mast cells was less intense. In about one-third of the subcutaneous connective tissue cells (Fig. 6) 1 or 2 grains can be found per cell. This seemed specific, since there were no grains present among the cells. Some pulmonary epithelial cells showed intense 5-HT uptake.

3 H-histidine and 3 H-histamine were not incorporated by the mast cells of the examined organs.

Discussion

In mast cell formation the thymocytes occupy a fundamental position, but the cells do not reach the mast cell form in the thymus [6]. They are transported into the peritoneal cavity, where each stage of maturation from the lymphocyte to the safranin-positive mast cells can be found. Still the maturation

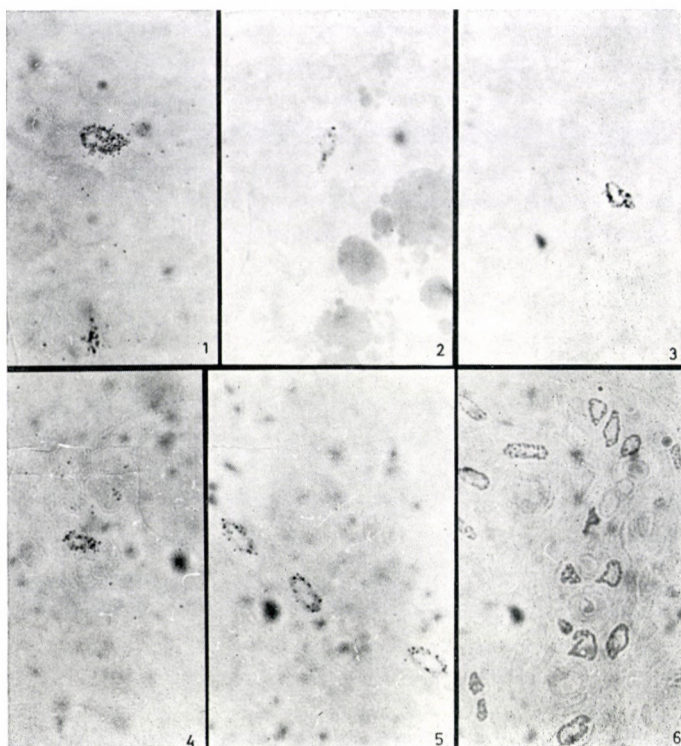


Fig. 1. Mesenterium, 5-HTP

Fig. 2. Lymph node, 5-HTP

Fig. 3. Heart muscle, 5-HT

Fig. 4. Mesenterium, 5-HT

Fig. 5. Lymph node, 5-HT

Fig. 6. Subcutaneous connective tissue, 5-HT. Numerous mast cells in a group; no grains above them

Labelled amine and amine precursor uptake of mast cells localized in various organs. Magnification: $\times 1000$; Stain: Nuclear Fast red

tion is not yet complete, but the cells migrate presumably through the mesenterium and possibly reach through the blood stream the organ where they exert their function [6]. Therefore, even if the homogeneity of the whole mast cell population concerning its origin and basic components is accepted, the histochemical and functional characteristics of the single mast cell groups are different. This manifests itself well in the sulphatation of their mucopolysaccharide content [7] as well as in their biogenic amine content [10]. Some of our previous experiments even indicated differences in their amine and amine precursor uptake [1—5]. When the mast cells are classified according to their degree of maturation, it appears that the most immature forms can be found in the peritoneal cavity [6]. These cells can incorporate 5-HTP and histidine [4], thus they take up each precursor characteristic of the rat mast cell, but they do not take up complete amines. Thus, amine synthesis occurs in these cells.

In the mesenterium cells are still taking up 5-HTP (this could be demonstrated only by the use of high specific activities in the present experiments), but no histidine, indicating that histamine synthesis has already been complete or no new synthesis had started while 5-HT synthesis was still in progress. The mature cells localized in the organs are taking up scarcely any precursors, or none at all, indicating that their synthesis has ceased. On the other hand, the majority of cells are able to take up serotonin. This ability is characteristic of the thyroid gland mast cells in the first place [3, 5] and may be related to the thyroid regulation of these cells. Serotonin uptake occurs by the heart muscle mast cells, too, perhaps owing to their specific function [9].

Thus, the mast cell in the course of its maturation changes into such an end-product cell, which has lost its synthetising activity but maintained its amine-mediating, or transport function. In this respect there are quantitative differences in the various mast cells; the least active are the subcutaneous connective tissue mast cells. This cell type is outstanding also by its failure to take up precursors, not even 5-HTP. It should be emphasized that the mediating function of the mast cells, namely their amine uptake and transport, is restricted to serotonin. The cells can synthetise and release histamine, but cannot take it up in its complete form. The explanation of the differences in uptake between the two amines requires further investigations.

REFERENCES

1. BARÁTH, P., CSABA, G.: (1974) Biogenic amine and amine precursor uptake by thyroid mast cells. *Acta morph. Acad. Sci. hung.* **22**, 327—330. — 2. BENDITT, E. P., WONG, R. L. ARASE, M., ROEPER, E.: (1955) 5-Hydroxytryptamine in mast cells. *Proc. Soc. exp. Biol. (N. Y.)* **90**, 303—304. — 3. CSABA, G., BARÁTH, P.: (1973) Tritiated 5-hydroxytryptamine uptake of the mast cells in the rat thyroid gland. *Neuroendocrinology* **12**, 67—70. — 4. CSABA, G., BARÁTH, P.: (1974) Heterogeneity of mast cell population as emerging from studies with labelled amines and amine precursors. *Acta biol. Acad. Sci. hung.* **25**, 323—325. — 5. CSABA, G., BARÁTH, P.: (1974) Effect of pinealectomy on the ^3H -5-HT uptake of mast cells in the thyroid gland of the rat. *Acta anat. (Basel)* **89**, 442—451. — 6. CSABA, G., TÖRÖK, O.: (1974) Physiology of mast cells IV. Role of blood transport in the formation of mast cells. *Acta biol. Acad. Sci. hung.* **23**, 369—376. — 7. CSABA, G., KOVÁCS, P.: (1976) Proof of the heterogeneity of mast cell population based on mucopolysaccharide content. (A hízósejtpopuláció heterogenitásának bizonyítása a mukopoliszacharida tartalom alapján.) *Acta morph. Acad. Sci. hung.* In press. — 8. HAGEN, P., LEE, F. L.: (1958) Amino acid decarboxylases of mouse mast cells. *J. Physiol. (Lond.)* **143**, 7—8. — 9. HEINE, H., FÖRSTER, F. J.: (1974) Zur Morphologie der Beziehungen zwischen Mast- und Muskelzellen bei Säugetieren. *Acta anat. (Basel)* **89**, 387—400. — 10. KOVÁCS, P., CSABA, G.: (1976) Proof of the heterogeneity of mast cell population based on the biogenic amine content. (Hung.: A hízósejtpopuláció heterogenitásának bizonyítása a biogénamin tartalom alapján.) *Acta morph. Acad. Sci. hung.* In press. — 11. LAGUNOFF, D., LAM, K. B., ROEPER, E., BENDITT, E. P.: (1957) 5-Hydroxytryptamine formation from 5-hydroxytryptophan by mast cells. *Fed. Proc.* **16**, 363. — 12. LAGUNOFF, D., BENDITT, E. P.: (1959) 5-Hydroxytryptophan decarboxylase activity in rat mast cells. *Amer. J. Physiol.* **196**, 993—997. — 13. RILEY, J., WEST, G. B.: (1953) The presence of histamine in tissue mast cells. *J. Physiol. (Lond.)* **120**, 528—537. — 14. SCHAUER, A.: (1964) *Die Mastzellen*. Gustav Fischer Verlag, Stuttgart. — 15. WEISSBACH, H. W., LOVENBERG, W., UDENFRIEND, S.: (1961) Characteristics of mammalian histidine decarboxylating enzymes. *Biochem. biophys. Acta (Amst.)* **50**, 177—179. — 16. WERLE, E., SCHAUER, A.: (1956) Histamin in Nerven. *Z. ges. exp. Med.* **127**, 16—21.

DIE AUFNAHME BIOGENER AMINE ODER AMIN-PRÄKURSOREN
DURCH DIE MASTZELLEN

P. KOVÁCS und G. CSABA

In bezug auf die Aminvorläufer- und Aminaufnahme ist die Mastzellenpopulation uneinheitlich. Von den unreifen Zellen werden die Amin-Präkursoren aufgenommen, bei fortschreitender Reifung nehmen sie jedoch nur noch 5-HTP auf. Die reifen Zellen nehmen keine Präkursoren mehr auf, doch sind sie — in unterschiedlichem Grade — zur Aufnahme von 5HT fähig. Die Mastzellen der Schilddrüse und des Herzmuskels nehmen das meiste 5HT auf, was mit ihrer speziellen Funktion in diesen beiden Organen zusammenhängen dürfte. Keine der Mastzellen nimmt fertiges Histamin auf, sie können dieses nur synthetisieren.

ПРИЕМ БИОГЕННЫХ АМИНОВ И ПРЕКУРСОРОВ АМИНОВ ТУЧНЫМИ
КЛЕТКАМИ

П. КОВАЧ и Д. ЧАБА

С точки зрения приема прекурсоров аминов и аминов популяция тучных клеток неоднородна. Незрелые клетки поглощают прекурсоры, однако, по мере продвижения созревания они поглощают только 5HTP. Зрелые клетки не поглощают прекурсоров, однако они — в различной степени — способны к приему 5HT. Тучные клетки щитовидной железы и сердечной мышцы поглощают наибольшее количество 5HT, что повидимому связано с их специальной функцией в этих двух органах. Ни одна из тучных клеток не усваивает готовый гистамин, они способны только к синтезу гистамина.

Dr. Péter Kovács	}	Semmelweis Orvostudományi Egyetem, Biológiai Intézet, H-1450 Budapest, Tűzoltó u. 58., Hungary
Dr. György Csaba		

Second Department of Pathology, Semmelweis Medical University, Budapest

SCANNING ELECTRON MICROSCOPIC EXAMINATION OF *IN VITRO* CULTURED CELLS BY DIFFERENT METHODS

Éva CSONKA, B. BERNOLÁK, A. S. KOCH and H. JELLINEK

(Received October 26, 1976)

1. The morphology of cultured aortic endothelial cells was studied by scanning electron microscopy. The cells were prepared for examination by three different procedures: two involved fixation, the third only drying in vacuum.
2. To check the efficiency of the methods of preparation, three non-endothelial cell lines were processed similarly and examined for SEM morphology.
3. The images of the cell surfaces were found to differ depending on the method of preparation and the value of the methodical approach clearly varied with the type of the cell. It is concluded that for studying cell morphology by SEM the method of preparation should carefully be selected.

Study, *in vivo* of the individual cellular components of the vessel wall would require complicated methodical approaches. In order to surmount this difficulty, cell lines representing homogenous populations have increasingly been preferred for investigations into normal and pathological conditions.

Studies on cultured cells have been promoted by the marked improvement of the culturing techniques during the last decade. The development and maintenance of pure aortic endothelium and pure aortic smooth muscle cells was reported for the first time from this laboratory in 1973 [2]. Similar cultures have been obtained by other authors [4, 5] chiefly from veins, and attempts at isolating them from the aorta have been reported only recently [6].

The electron microscopic morphology of the isolated cells has been accepted as the most reliable means of identification. The aortic endothelial and smooth muscle cell lines isolated in this laboratory were therefore identified by transmission electron microscopic criteria [3].

Further examinations by scanning electron microscopy are the subject of this report. Since the usual fixing procedures did not always yield preparations of satisfactory quality, especially in respect of reproducibility, the processing of the specimens was modified and other cell lines, partly our own isolates, partly international standard cell strains, were similarly examined for comparison.

Materials and methods

Cell cultures

Passages 7–10 of the endothelial cell line E-203, isolated in this laboratory from miniature pig (Minnesota) aorta.

Passages 2–5 of the smooth muscle cell line S-215, isolated in this laboratory from miniature pig (Minnesota) aorta.

Passages 104–110 of the aortic smooth muscle cell line S-76, which became heteroploidic during cultivation. This cell line, too, was isolated in this laboratory from miniature pig (Minnesota) aorta.

HeLa, international standard cell strain.

For scanning electron microscopy, coverslip cultures were prepared in Leighton tubes from all examined cell lines, using 10% calf serum containing synthetic Parker-199 medium throughout.

Processing for scanning electron microscopy

1. Coverslip cultures were fixed for 2 hours in 6% glutaraldehyde containing Holt solution, were washed in phosphate buffered saline after fixation, and dehydrated in step-graded ethanol and acetone.

2. The monolayer grown on the coverslip was washed in phosphate buffered saline, rinsed in distilled water 3 times for 1 second each, mounted immediately on copper plate and dried in vacuo. Vapour pressure was reduced gradually to 10^{-3} mm Hg in 10 minutes, and to $5 \cdot 10^{-5}$ mm Hg in another 10 minutes.

3. The cells were fixed for 2 hours at room temperature in cacodylate buffer containing 1.2% glutaraldehyde and 0.1% ruthenium red. After fixation the cells were dehydrated in step-graded acetone.

Pieces of the coverslip carrying the differently processed cells were mounted on copper plates with collodion, coated by a 50 Å thick layer of carbon and a 200 Å thick layer of gold, and shadowed by copper at an angle of 20°.

Electron microscopy

The preparations were examined in a scanning adapter connected with a JEM 100 B electron microscope, at 40 KV voltage and 60 μ beam amperage.

Results

Evaluation of the results was made by comparison of the electron micrographs taken at 1000, 3000 and 10,000 fold magnifications of each of 4 different cell lines processed in 3 different ways.

(Fig. 1/a–c) The electron micrographs of a fixed preparation do not reflect quite correctly the characteristic morphological features of the endothelial cells.

(Fig. 1a/c) The fixed cells are shrunken, whereas the non-fixed preparations clearly show the mosaic-like fitting of the cells, as well as the typical endothelial border (Fig. 1/b).

The appearance of the cell surfaces depends on the method of processing. The nucleus and nucleolus are conspicuously visualized by the usual fixation procedure (Fig. 1/a), while fixation with ruthenium red results in a practically homogeneous appearance of the cell surface (Fig. 1/c).

(Fig. 2/a–c) Differences in fixation cause less variation in the appearance of smooth muscle cells than in the endothelial cells. The nucleolus is more

conspicuous in the fixed preparations than in unfixed ones and the arrangement of the myofilaments is least visible in specimens fixed with ruthenium red (2/c).

(Fig. 3/a—c) Cell line S-76 isolated and maintained in this laboratory, had originally been a regular smooth muscle cell culture, to judge by its characteristics, but in the 21st passage it became polymorphous and heteroploidic in a single step. Like the endothelial cells also showed different surface morphology, depending on the type of processing. The fixed cells are carrying microvilli on their surfaces (Fig. 3/a). The villous structures can easily be differentiated in conventionally fixed preparations, whereas on fixation with ruthenium red they appear thicker and more densely arranged (Fig. 3/c). In non-fixed preparations the helter-skelter surface structures are flat, but the nucleus and nucleolus are more easily visible than in the fixed preparations (Fig. 3/b).

(Fig. 4/a—c) The electron micrographs of HeLa cells remind of those of S-76 cells, except that the villous outgrowths on the surface are considerably denser (Fig. 4/a). In preparations treated with ruthenium red, the villous structures appear as irregularly ordered depositions (Fig. 4/c). The characteristic large nuclei of the HeLa cells are visible only in unfixed preparations (Fig. 4/b).

Discussion

The problems met with in the scanning electron microscopic study of cultured endothelial cells have induced us to prefer for such studies non-fixed cells in a practically natural state. This approach also involves certain artefacts, which may mislead the investigator [1]. Cell lines other than aortic endothelium had therefore been included in the study with the express purpose of showing that the simplified processing proposed by us does not blur the specific morphological characteristics of the different cell types.

The electron microscopic image of the surface of fixed HeLa cells corresponds to that found by other authors using a different fixing procedure [7]. The fixed preparations of HeLa cells were in fact fairly uncharacteristic.

Processing without fixation proved to be the method of choice with the endothelial cell because it prevented its shrinking. The possibility was also explored whether rapid rinsing in distilled water damaged the cells. It was concluded that if the osmotic changes concomitant upon chemical alterations in the environment of the cell are of short duration and during this critical period the shape and surface morphology of the cell can be brought into a form that will not become altered, the culture so processed is suited for scanning EM-studies. If after the rapid rinsing the moist preparation is immediately exposed to vacuum, rapid evaporation causes reduction of the temperature to such a low degree that the water retained in the cell with frozen and subli-

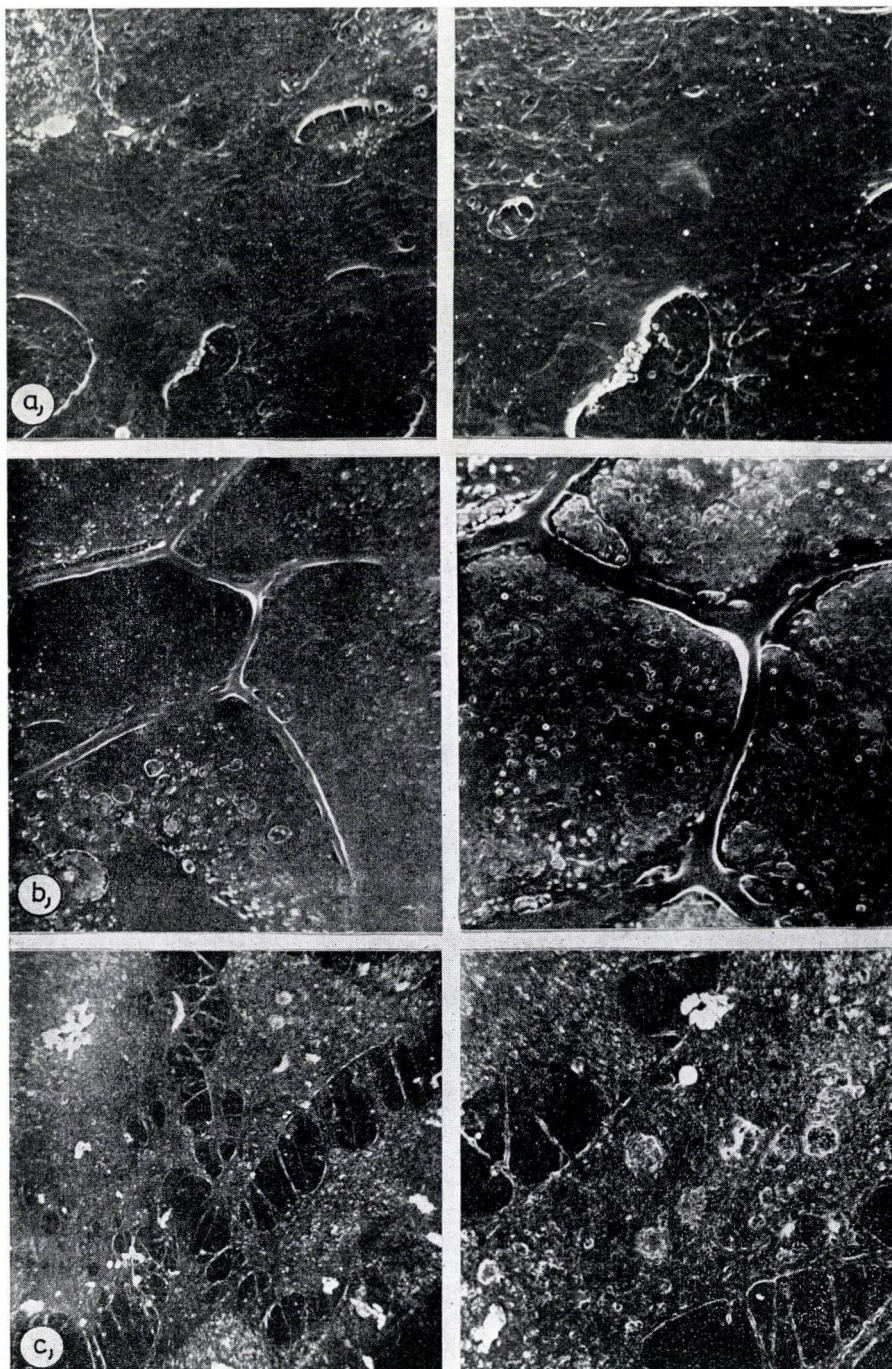


Fig. 1. Scanning electron micrographs of E-203 cultured aortic endothelial cells prepared by various techniques. a) preparation treated with Holt's fixing solution. $\times 1000$, $\times 3000$; b) preparation dried in vacuo. $\times 1000$, $\times 3000$; c) preparation treated with ruthenium red and glutaraldehyde. $\times 1000$, $\times 3000$

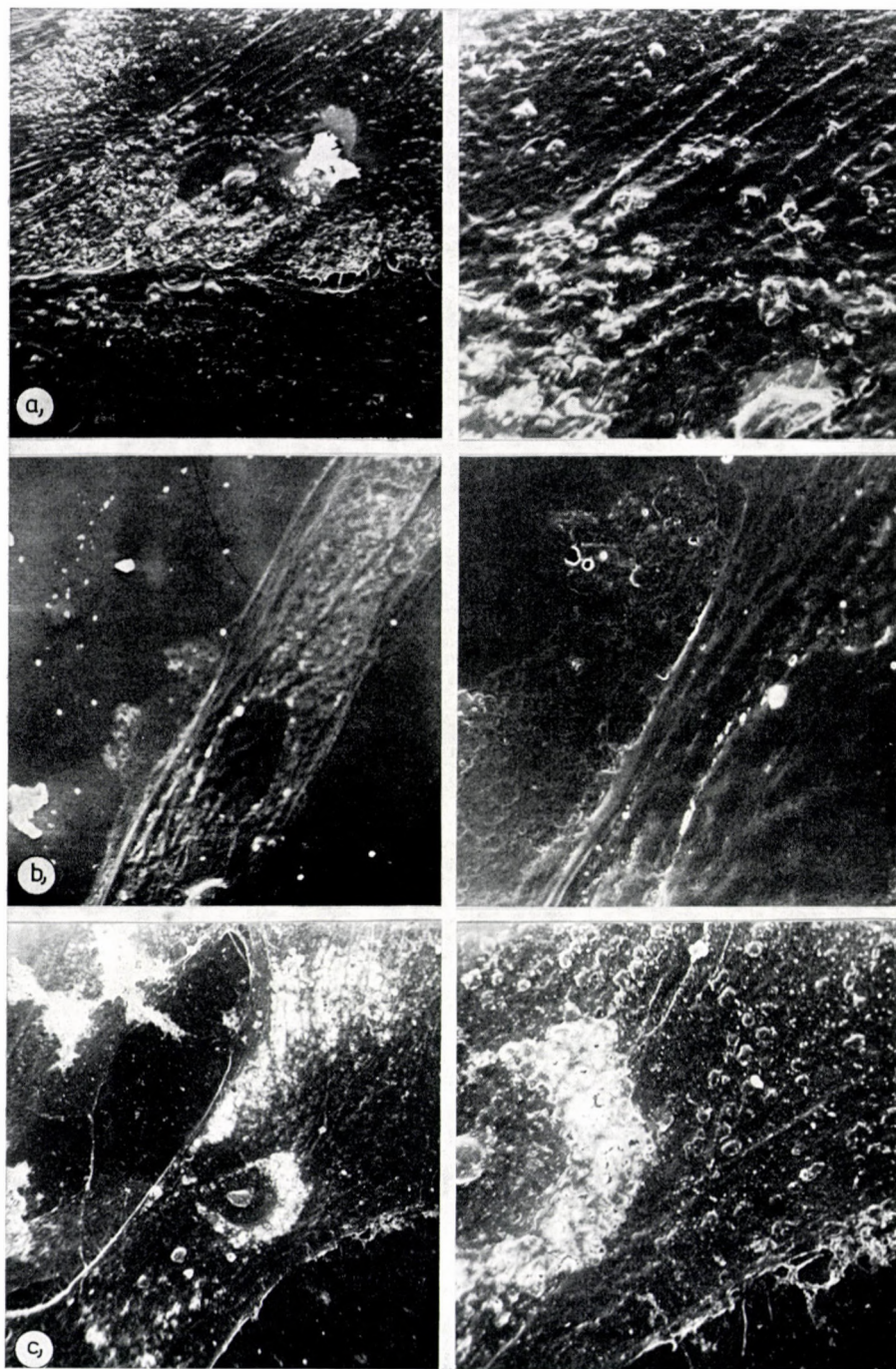


Fig. 2. Scanning electron micrographs of S-215 cultured aortic smooth muscle cells prepared by various techniques. a) preparation treated with Holt's fixing solution. $\times 1000$, $\times 3000$; b) preparation dried in vacuo $\times 1000$, $\times 3000$; c) preparation fixed with ruthenium red and glutaraldehyde $\times 1000$, $\times 3000$

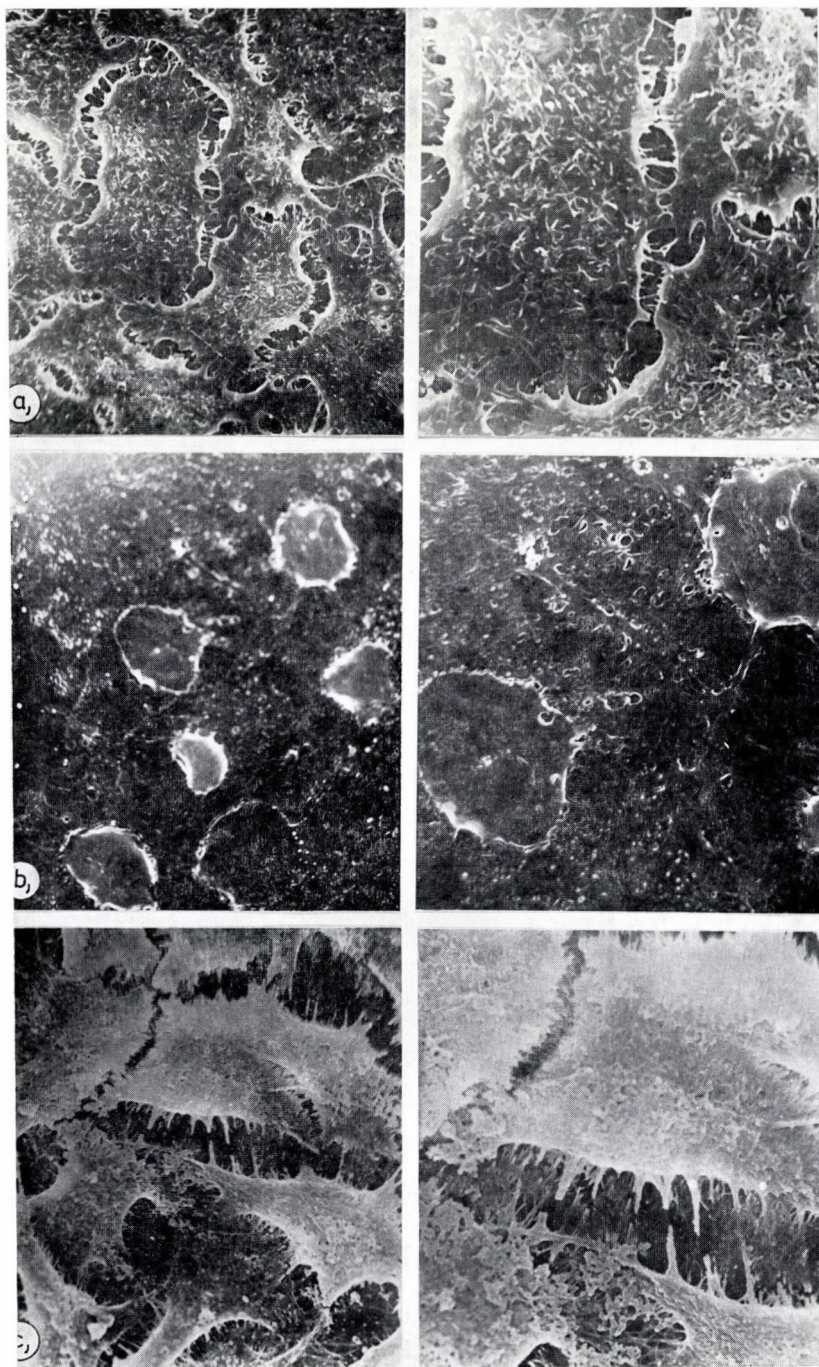


Fig. 3. Electron micrographs of the S-76 cultured aortic smooth muscle cell mutant differently prepared by various techniques. a) preparation treated with Holt's fixing solution. $\times 1000$, $\times 3000$; b) preparation dried in vacuo $\times 1000$, $\times 3000$; c) preparation fixed with ruthenium red and glutaraldehyde $\times 1000$, $\times 3000$

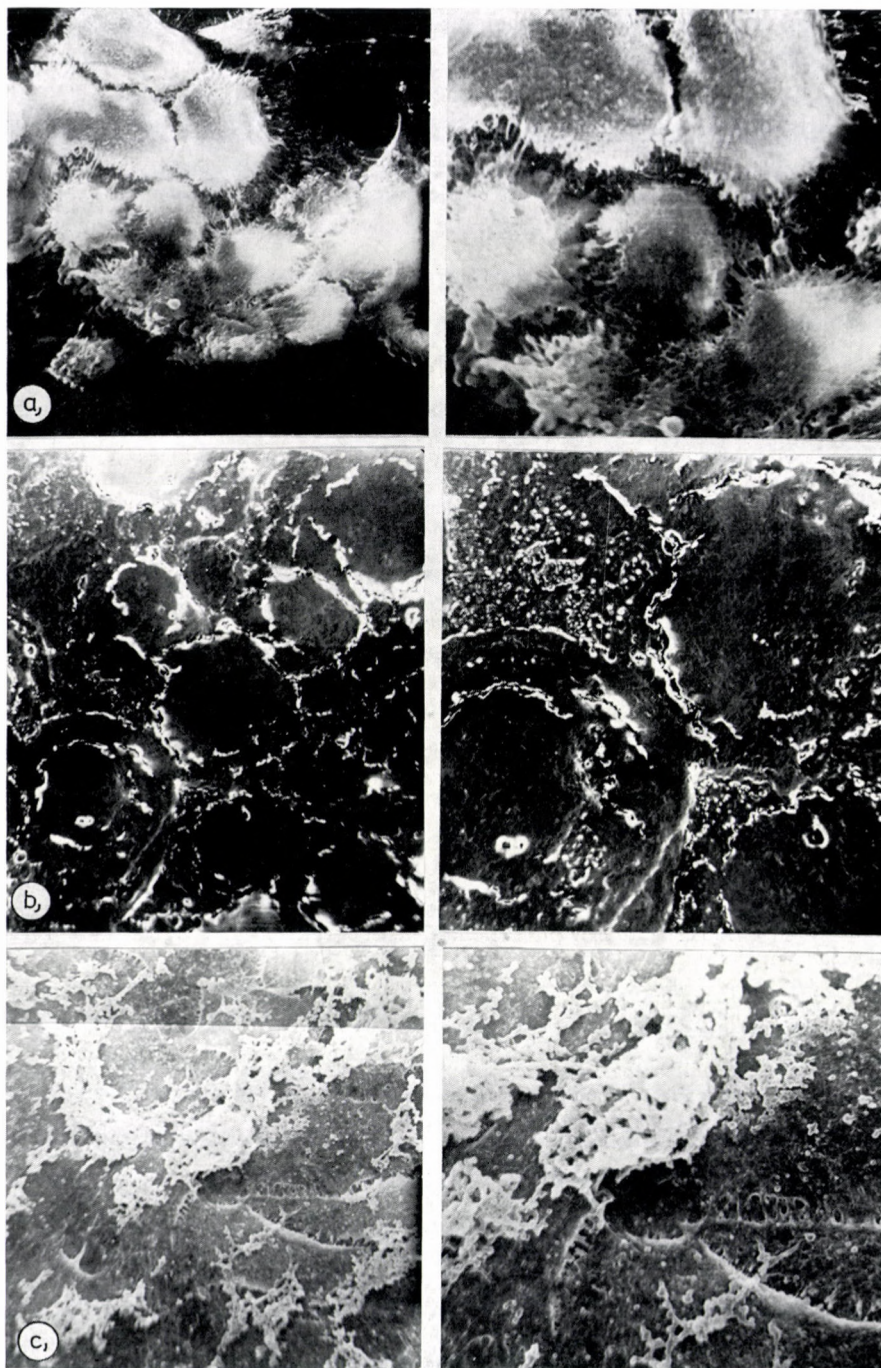


Fig. 4. Electron micrographs of the HeLa international standard cell strain prepared by various methods. a) preparation treated with Holt's fixing solution $\times 1000$, $\times 3000$; b) preparation dried in vacuo $\times 1000$, $\times 3000$; c) preparation fixed with ruthenium red and glutaraldehyde $\times 1000$, $\times 3000$

mation from the frozen state will not affect the morphological details. Great caution should be exercised with the rate of pressure reduction, as already referred to in the foregoing. If pressure is reduced too rapidly the cells may burst instead of being frozen as a result of heat loss through evaporation.

In summary, scanning electron microscopy offers valuable information about the ultrastructural details of the cell surface if the methodical approach is carefully chosen according to the detail or type of cell under examination.

REFERENCES

1. BOYDE, A., VESELY, P.: Comparison of fixation and drying procedures for preparation of some cultured cell lines for examination in the SEM. In: Scanning Electron Microscopy. (Part 2.) Proceedings of the Workshop on Biological Specimen Preparation for Scanning Electronmicroscopy (Johari, O. and Corvin, I. eds) IITRI, Chicago p. 317 (1972). — 2. CSONKA, É., KÁDÁR, A., KERÉNYI, T., JELLINEK, H.: (1973) Morphology of cultured endothelial and smooth muscle cells of different origin. Acta morph. Acad. Sci. hung. Suppl. **14**, 18. — 3. CSONKA, É., KERÉNYI, T., KOCH, A. S., JELLINEK, H.: (1975) In vitro cultivation and identification of aortic endothelium from miniature pig. Arterial Wall, **3**, 31—37. — 4. JAFFE, H. A., NACHMAN, R. L., BECKER, C. G., MINICK, C. R.: (1973) Culture of human endothelial cells derived from umbilical veins. Identification by morphological and immunological criteria. J. clin. Invest. **52**, 2745—2756. — 5. LEWIS, L. J., HOAK, J. C., MACA, R. D., FRY, G. L.: (1973) Replication of human endothelial cells in culture. Science, **181**, 453—454. — 6. SLATER, D. E., SLOAN, J. M.: (1975) The porcine endothelial cell in tissue culture. Atherosclerosis, **21**, 259—272. — 7. TSURUHARA, T., AMANO, H., SUZUKI, M., MATSUO, T.: (1972) Examination of the focus of Variola virus-infected HeLa cells by scanning electron microscopy. J. Electr. Micr. **21**, 149—150.

SCANNING ELEKTRONENMIKROSKOPISCHE UNTERSUCHUNG IN VITRO GEZÜCHTETER ZELLEN MIT VERSCHIEDENEN METHODEN

ÉVA CSONKA, B. BERNOLÁK, A. S. KOCH und H. JELLINEK

1. Verfasser untersuchten mittels scanning elektronenmikroskopischer Methode die Morphologie in vitro gezüchteter Endothelialzellen. Sie benutzen drei verschiedene Vorbereitungsmethoden, in zwei Fällen fixierten sie die Zellen, während nach der dritten Methode die Präparate ohne Fixierung in Vakuum getrocknet wurden.

2. Zur Kontrolle der verschiedenen Methoden untersuchten Verfasser auch die Morphologie von Zellkulturen dreier verschiedener Typen mittels der von ihnen angewandten Methode.

3. Verfasser stellten fest, daß scanning elektronenmikroskopische Aufnahme von auf verschiedene Art vorbereiteten Zellkulturen ein ziemlich abweichendes Oberflächenbild zeigten. Deshalb muß bei der Durchführung solcher morphologischer Untersuchungen — je nach dem Ziel des Versuches — immer die entsprechende Methode gewählt werden.

ОТРАЖАТЕЛЬНОЕ (СКАНИРОВАННОЕ) ЭЛЕКТРОННОМИКРОСКОПИЧЕСКОЕ ИССЛЕДОВАНИЕ КЛЕТОК, КУЛЬТИВИРОВАННЫХ IN VITRO И ПОДГОТОВЛЕННЫХ РАЗЛИЧНЫМИ МЕТОДАМИ

ЕВА ЧОНКА, Б. БЕРНОЛАК, А. Ш. КОХ и Х. ЙЕЛЛИНЕК

1. Морфология клеток эндотелия аорты, культивированных in vitro, была изучена при помощи отражательного (сканирование) электронномикроскопического метода. Для подготовки материала применялись три различных метода. В двух случаях клетки были фиксированы, а при третьем методе препараты были высушены в вакууме без фиксации.

2. В целях проверки различных методов подготовки, кроме эндотелиальных клеток, сравнивалась морфология культур еще трех клеточных типов при применении тех же методов для подготовки.

3. Было установлено, что при методе отражательной электронной микроскопии различными способами подготовленных клеточных культур получают довольно отклоняющиеся картины поверхности. Поэтому, для таких морфологических исследований — в зависимости от цели эксперимента — всегда приходится выбрать наиболее подходящую методику подготовки препаратов.

Éva CSONKA	{	Semmelweis Orvostudományi Egyetem
B. BERNOLÁK		II. sz. Kórbonctani Intézet,
A. S. КОСН		H-1091 Budapest, Üllői u. 93. Hungary
H. JELLINEK		

Department of Biology Jawaharlal Institute of Postgraduate Medical Education
and Research, Pondicherry and Department of Zoology, Annamalai University,
Annamalai Nagar, India

CELL TYPES OF THE PARS DISTALIS: SEASONAL CHANGES IN SECRETORY ACTIVITY AND EFFECT OF STEROIDS ON SPERMATOGENESIS IN *RANA HEXADACTYLA*

S. KASINATHAN, S. L. BASU and VIJAYAM SRIRAMULU

(Received October 27, 1976)

Cytomorphological features and tinctorial affinities of the adeno-hypophyseal gonadotrophs have been studied in stained preparations of the pituitary of adult male frogs *Rana hexadactyla* Lesson, at monthly intervals during a calendar year. All the five morphologically distinct cell types showed a progressive increase in size from August to February, followed by a decrease from March to July. Extrusion of the synthesized product occurred in the summer and during this period production was low. Injection of steroids *viz.* stilboestrol, testosterone, oestradiol, doca and cortisol, interfered with the elaboration and secretion of gonadotropins, the adeno-hypophyseal feedback mechanism, and the sensitivity of the germinal epithelium. Changes in gonadotropins secretion and their impact on the testis are discussed.]

Cytological studies in several species of amphibia have brought to light the existence in the pars distalis of different cell types with specific tinctorial affinities [5, 10—12, 14, 21, 24, 31, 35]. These studies have also pointed out the involvement of hypophyseal gonadotropins in the regulation of reproductive cycles. The mechanisms regulating these processes are complex. A survey of the literature has shown that the level of hypophyseal gonadotropins varies considerably from season to season, and elaboration and secretion of the hormones by the concerned cell types is largely under the influence of the physical factors of the environment. The responsiveness of the germinal epithelium and the extent to which it is sensitive to hormonal priming are dependent on the internal physiological rhythms to bring about a hormone-mediated response. In a previous study on *Rana hexadactyla* [1, 2] the spermatogenic cycle has been found to be continuous and, by administering pituitary extracts, KASINATHAN et al. [21] found an enhancement of spermatogenic activity and interstitial development in the testis of the recipient frogs. In the present investigation we have studied [1] the seasonal changes in the secretory activity of the pars distalis cell types, and [2] the influence of steroids on the hypophyseal cell types and the impact of the latter on spermatogenic activity in *Rana hexadactyla* Lesson.

Material and methods

Adult male frogs of 65 g average body weight and approximately 80 mm snout to vent length were used. The frogs were kept under uniform conditions and were allowed to feed *ad libitum* on live earthworms provided in a wire mesh box and left in a corner of the aquarium on a stone slab. The frogs were divided into different lots, each lot consisting of five specimens and were treated with hormones as detailed below:

1. *Stilboestrol*: a) 1.25 mg suspended in 1 ml of amphibian Ringer was injected in a single dose in each frog belonging to the first lot, for fifteen days; b) 1.25 mg dissolved in 1.25 ml of amphibian Ringer was administered in five doses of 0.25 ml each in the second group of frogs of the first lot at intervals of 48 hours for 15 days.

2. *Testosterone*: In the second lot of frogs 1 mg of testosterone dissolved in 1 ml of amphibian Ringer was injected every day for 15 days.

3. *Oestradiol*: 5 mg of oestradiol was suspended in 15 ml of amphibian Ringer. Of this, 1 ml was administered to each of the frogs of lot three. The treatment was continued for 15 days.

4. *Deoxycorticosterone acetate* (DOCA): 7.5 mg of DOCA was suspended in 15 ml of amphibian Ringer and each frog of lot four received 1 ml of this hormone and the treatment was continued for 15 days.

5. *Cortisol*: 0.5 mg of cortisol, suspended in 1 ml of amphibian Ringer was given a single daily dose to each frog of lot five, for 15 days.

The hormones used were obtained in the form of microcrystals and suspended separately in amphibian Ringer prior to administration. Control frogs injected with an equal quantity of placebo and amphibian Ringer solution were kept together with the experimental ones. The frogs were killed after a fortnight and the gonads and pituitaries were collected. Pituitaries were fixed in Bouin's sublimate solution, embedded in paraffin, sectioned at $3\ \mu$ and stained with:

1. CLEVELAND and WOLFE's trichrome stain [18];
2. periodic acid Schiff (PAS) Orange G (OG) [17];
3. HALMI's [16] aldehyde fuchsin (AF);
4. GABE's [15] AF with HALMI's [16] counter stain;
5. HERLANT's [18] Alcian blue (AB) pH 3.0 with Pas and OG;
6. Aldehyde thionine (AT) [14].

Results

Five chromophilic granular cell types were clearly discernible on the basis of tinctorial affinities in the pars distalis region of the pituitary gland of *Rana hexadactyla*. These cell types have been grouped under acidophilic types 1 and 2 (A_1 and A_2) and basophilic types, 1, 2 and 3 (B_1 , B_2 , B_3); their tinctorial affinities are summarized in Table I.

Distribution of cell types (Fig. 2)

In general, A_1 and A_2 cells are distributed throughout the gland. A_1 cells are more towards the ventral or rostral region of the pars distalis while A_2 cells are present in its posterior or dorsocaudal region. The ventrocaudal region mostly contains B_1 cells, whereas B_2 cells are distributed throughout the gland, but those occurring in the rostral region are larger than those in the caudal region. In the anterior region these cells are less abundant. B_3 cells are found chiefly in the anteroventral region and these cells line the capillaries entering the pars distalis from the median eminence.

Seasonal cycle of pituitary cell types

Acidophils (A₁). The A₁ cells are in general tall and columnar but exhibit variations in size, shape and appearance. The amount of granules in their cytoplasm depends on the stage of secretory activity. In pituitary samples collected during November and December, the A₁ cells are large their cytoplasm fully loaded with the synthesized product (Fig. 3). In the months January to April the nucleus loses its smooth outline, appears irregular and shows a gradual reduction in size followed by partial degranulation of the accumulated product (Figs 4, 5). The acidophils exhibit a maximum reduction in their size, and the remaining granules; tightly packed in the cytoplasm, undergo degranulation during May to August. Thereafter, in September to October, the cells show signs of renewed activity as evidenced by an increase in volume and a steady accumulation of the synthesized products. The granules are coarse.

Acidophils (A₂). A₂ cells are small narrow elongated cells. The nature of the cytoplasmic granules and their staining affinity are similar to those of A₁ cells. These cells show reduction in size during January to April (Figs. 4 and 5) followed by degranulation from May to August. From September onwards, the cells renewed activity like A₁ cells. With Brooks' stain [4] these cells stain a brownish orange and can clearly be differentiated from A₁ cells which stain red. The dorsocaudal region of the pars distalis contains a few A₂ cells.

Basophils (B₁). Basophilic cells (B₁) are either spherical or slightly elongated. Their cytoplasm contains cyanophilic granules which exhibit a strong affinity for PAS-Alcian blue when stained with HERLANT's [18] technique. Though these cells are distributed throughout the lobe they are found in large numbers in the ventrocaudal region of the pars distalis. Samples of pituitary collected during March and April show B₁ cells with their cytoplasm loaded with cyanophilic granules. No appreciable modification is noticed during April, May and June (Fig. 5). Degranulation of these cells is evident in July, August and September; the volume of the nucleus is less during August. From October to March (Fig. 1) the nucleus shows a steady increase in volume and the cytoplasm does not show much change in respect of its staining affinities or granulation.

Basophils (B₂). Basophilic type B₂ cells are tall columnar and are positive with PAS, HERLANT's [19] CLEVELAND and WOLFE's trichrome dyes [18]. The cytoplasm of these cells contains both cyanophilic and coarse orangeophilic granules. B₂ cells are more numerous than B₁ cells and are found distributed

Table I

Tinctorial affinities of basophils and acidophils in the pars distalis of Rana hexadactyla Lesson

Staining technique employed	Cell types					
	basophils				acidophils	
	B ₁	B ₂	B ₃		A ₁	A ₂
		Coarse inclusions	Fine granules			
1. CLEVELAND and WOLFE's trichrome	blue	orange	blue	pinkish violet	orange	reddish orange
2. Periodic acid — Schiff (PAS) Orange G(OG) HERLANT, 1956	light purple	orange purple	blue	reddish pink	orange	orange
3. BROOK's azofuchsin triple stain	green	red	green	green	orange red	brownish orange
4. HERLANT's AB (pH 3.0) PAS Orange G	blue	blue purple or unstained	blue	brownish pink	orange	orange
5. GABE's AF plus Halmi's counter stain	purple violet	purple	deep orange, purple	greyish	orange	orange or greyish brown
6. AF + PAS + OG	light purple	purple	deep orange, purple	reddish pink	orange	orange
7. MALLORY's (AF, AB)	blue	blue	blue	blue	red	red
8. MONROE Former	green	purple	purple	bright red	red	red
9. GREENER and LILLIE	blue	blue	blue	blue black	dark red	dark red

throughout the pars distalis. The cells found in the rostral region are larger and more densely granulated than those in the caudal region.

In pituitary samples collected from November to January the B₂ cells are confined to the rostral region, and exhibit secretory activity with their cytoplasm full of orangeophilic and cyanophilic granules. These cells show an intense affinity for PAS. An increase in the percentage of these cells is observable in samples of pituitary collected during February and March. The nucleus is big in these cells and the cytoplasmic granules appear AB, AT, PAS and OG positive. Release of orangeophilic granules occurs from April onwards (Fig. 5) and along with the processes of degranulation the cell shows a gradual reduction in size and nuclear volume. This is especially pronounced in samples collected during August. Such cells appear more chromophobic, irregular in shape and the nucleus shows a reduction in volume. During September and October an increase in the size of the cell and nucleus occurs (Fig. 1) followed

Table II

Characteristic features and the seasonal variations in pars distalis cell types in Rana hexadactyla Lesson

		Jan.	Feb.	Mar.	Apr.	May	Jun.	Jul.	Aug.	Sept.	Oct.	Nov.	Dec.
A ₁	CP	19.30	17.90	18.50	19.10	21.10	22.10	21.80	23.10	23.40	21.80	22.30	20.00
	ND	12.30	14.00	10.20	8.80	8.40	8.10	7.90	7.00	8.40	9.60	10.50	11.40
	g	—	—	+	—	+	—	—	+	++	++	+	+
A ₂	CP	18.70	16.50	17.20	18.60	20.00	20.30	21.30	20.90	21.20	19.20	17.90	18.10
	ND	8.10	8.80	7.70	6.30	6.00	5.80	5.40	5.60	6.30	6.70	7.00	7.70
	g	—	—	+	—	+	—	—	+	++	++	+	+
B ₁	CP	20.50	21.40	21.10	21.90	20.10	19.60	19.30	18.70	18.10	20.00	19.60	20.00
	ND	8.80	9.60	9.10	7.00	6.30	6.00	5.60	4.80	6.70	7.00	7.70	8.10
	g	—	—	+	+	+	—	—	—	—	+	+	+
B ₂	CP	31.70	31.00	33.20	33.40	28.50	31.00	28.40	25.30	27.00	30.10	31.70	31.90
	ND	11.40	12.30	10.50	8.80	7.90	7.40	7.00	6.70	7.90	8.80	9.60	10.50
	g	++	++	++	+++	+	+	—	—	++	+	++	++
B ₃	CP	4.80	9.00	8.90	8.20	4.20	4.10	4.10	5.60	6.90	7.20	7.50	7.90
	ND	9.80	10.50	11.20	7.70	7.00	6.70	6.30	5.30	7.00	8.10	9.80	9.10
	g	++	++	—	—	—	—	—	—	++	++	++	++
Chromophobe		5.40	2.20	2.60	—	6.20	3.20	5.10	5.40	3.70	2.10	1.10	1.50

CP: cell population

ND: nuclear diameter in μ

g: granulation

by a gradual accumulation of granules in the cytoplasm. First, orangeophilic granules appear, but their accumulation is slow and restricted to a particular zone within the cell.

Basophil (B₃). B₃ cells are encountered in the medioventral region of the pars distalis bordering the blood vessel that penetrates this region from the median eminence. The cells are elongated and columnar and the cytoplasmic granules are positive to PAS, erythrosin and Orange G. Pituitary samples collected from November to February reveal a heavy accumulation of PAS positive granulae in the cytoplasm. The nuclei in these cells is well developed and oval in shape (Fig. 1). Vacuolization of the cytoplasm and shrinkage of the nucleus is evident in March pituitary samples. Degranulation takes place during April (Fig. 5) and these cells show a reduction in size which is pronounced in July.

The characteristic seasonal changes of the nuclear size of the pars distalis cell types are given in Table II.

Effect of steroids on pituitary cell types

The cytomorphology of the hypophyseal gonadotrops, their number and secretory activity in steroid treated frogs, are given in Table III. In the placebo controls injected with amphibian Ringer hypophyseal cytology, does not differ from that of the normal male specimens (Fig. 6).

Table III

Comparative effect of steroid hormones on spermatogenesis and hypophyseal gonadotrops of Rana hexadactyla Lesson

Treatment	Hypophyseal gonadotrops				Spermatogenesis	
	Cell dimension	Cell population	Activity of pituitary	Nature of granulation	Activity of germinal epithelium	Spermatogenic stages
Stilboestrol	Hyper-trophy Hyper-plasia	In: Nil DC: B ₂ , B ₃ & A ₃	Moderately active	Granulated	Inactive	DC All stages
Testosterone	Shrink-age	In: Nil DC: B ₂	Less active	Granulated	Inactive	DC II
Oestradiol	Regression	In: Nil DC: All cells	Less active	Granulated	Inactive	DC All stages
DOCA and cortisol	Atrophy	In: Nil DC: All cells	Low and fibrosis	De-granulated	Inactive	DC II and IV

In: increase
DC: decrease

Effect of a booster dose of stilboestrol

Specimens treated with a single booster dose of stilboestrol show distorted histoarchitecture of the pars distalis. Types 2 and 3 basophils, (B_2 , B_3) and A_2 acidophils are the most affected. In some pituitaries the basophils are so atrophic that a distinction between B_2 and B_3 cells is not possible (Fig. 7). The acidophils shows hypertrophy and each cell has a large spherical nucleus which is pushed to a corner. In the extracellular spaces of the pituitary a heavy accumulation of orangeophilic granules occurs. Colloid material is found in the sinusoidal spaces.

Effect of a split dose of stilboestrol

The cytological features of the basophils and acidophils in the pituitary of frogs treated with split dose of stilboestrol are unchanged. B_2 , B_3 cells appear moderately active but are small. The acidophils exhibit an accumulation of stainable material in their cytoplasm. Large sinusoidal spaces and extensive ramification of the connective tissue appear to be characteristic of the pituitary of frogs receiving split doses of stilboestrol (Fig. 8).

Effect of testosterone

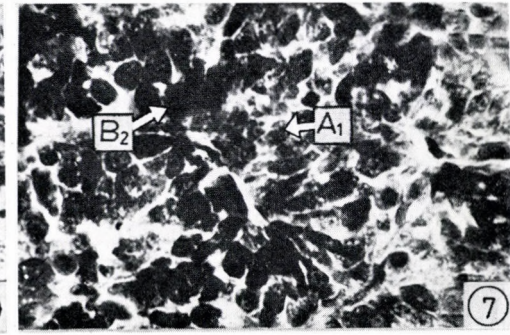
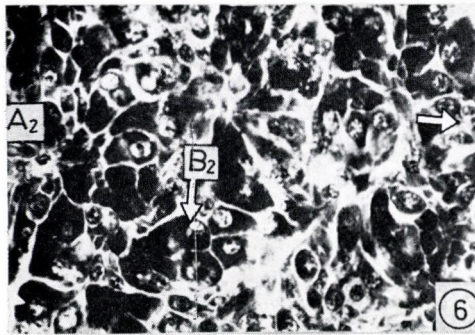
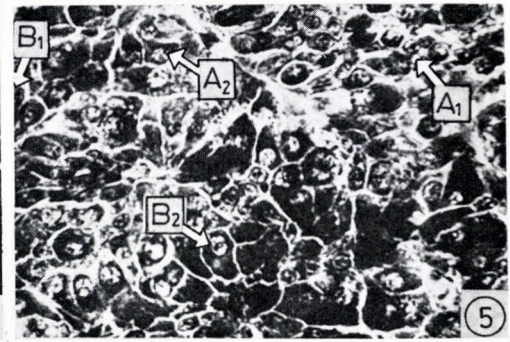
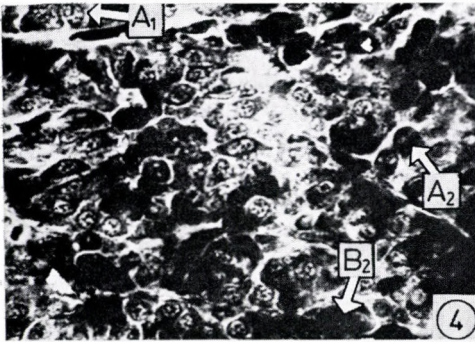
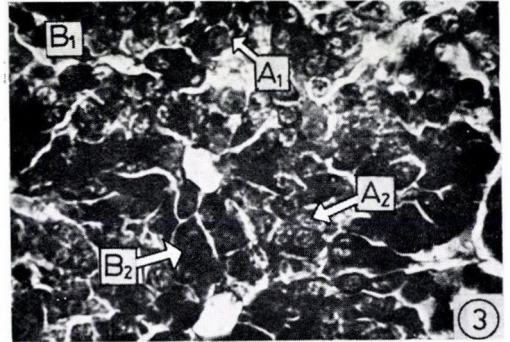
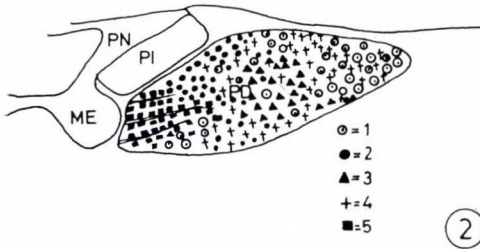
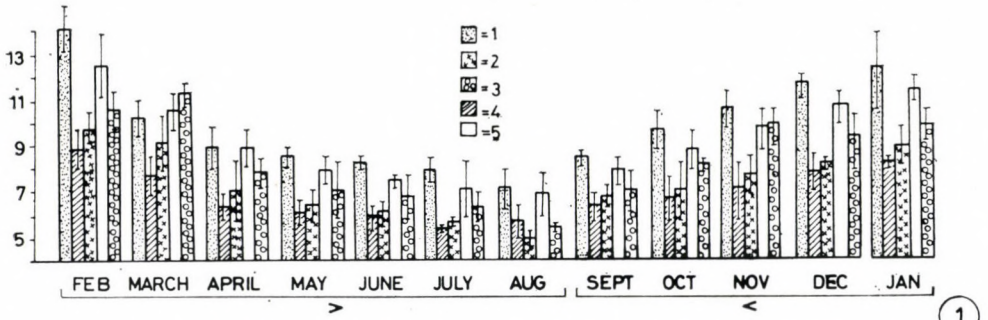
Testosterone selectively affected the B_2 cells while the other cell types retained their cytomorphological features and tinctorial affinities. The B_2 cells are somewhat reduced in size; their nuclei are hyperchromatic, oval in outline and shrunken. The cytoplasm is heavily granulated. The reduction in the size of the cell and the granules in the cytoplasm point to increased secretory activity (Fig. 9).

Effect of oestradiol

Oestradiol treatment resulted in the regression of all acidophils and basophils. The sparse distribution of orangeophilic granules and the occurrence of numerous vacuoles in the cytoplasm of B_2 cells suggests an augmented production of secretory material.

Effect of deoxycorticosterone

In deoxycorticosterone treated frogs the pars distalis showed extensive fibrosis. The acidophils and basophils have lost their characteristic cellular morphology and the secretory granules (Fig. 10).



Effect of cortisol

Extensive ramification of the connective tissue and complete atrophy of the pituitary gland was noticed in frogs treated with cortisol. Basophils and acidophils showed a regression and the cytoplasm contained sparse granulations (Fig. 11).

Spermatogenic cycle in Rana hexadactyla

In *Rana hexadactyla* the spermatogenic cycle is continuous and cells in different stages of spermatogenic activity are encountered in the tubular lumina throughout the year. A quantitative study disclosed a regular rhythmic wave of spermatogenic activity. Primary spermatogonia are less from January to July (2.96—2.97) (Figs 12 and 13), but show a progressive increase thereafter reaching a maximum (7.37) in November (Fig. 14). Secondary spermatogonia (stage-I) show an abrupt rise in August (5.61) whereas in other months this number is low (1.78—3.13); stage-III is higher from September to March (7.30—6.83); stage-IV is low from March to June (2.95—2.98) while stage-V is less, especially during spermiation time. Spermiation takes place in April though sperms are found throughout the year.

Effect of steroids on spermatogenesis

Oestradiol and stilboestrol are detrimental to spermatogenesis, causing extensive damage to the testicular tissues. DOCA and cortisol are similarly inhibitory on the wave of spermatogenesis. If administered for a prolonged period, they bring about testicular atrophy and fibrosis. When the frogs are treated with testosterone, spermatogenetic cells are normally inhibited at the secondary spermatogonial stage (Fig. 15) without further detrimental effect

←

Fig. 1. Seasonal changes in nuclear size. 1. Acidophil Type 1; 2. Basophil Type 1; 3. Basophil Type 3; 4. Acidophil Type 2; 5. Basophil Type 2

in μ . > Significant decrease in size ($P < 0.05$) < Significant increase in size

Fig. 2. Distribution of cells in median sagittal section of pars distalis in *Rana hexadactyla* Lesson. 1. Acidophil Type 1; 2. Acidophil Type 2; 3. Basophil Type 1; 4. Basophil Type 2; 5. Basophil Type 3. PD = pars distalis; PI = pars intermedia; PN = pars nervosa; ME = median eminence

Figs 3—5. T. S. of the pars distalis of the pituitary of the frog stained with Cleveland and Wolfe's trichrome. $\times 1200$

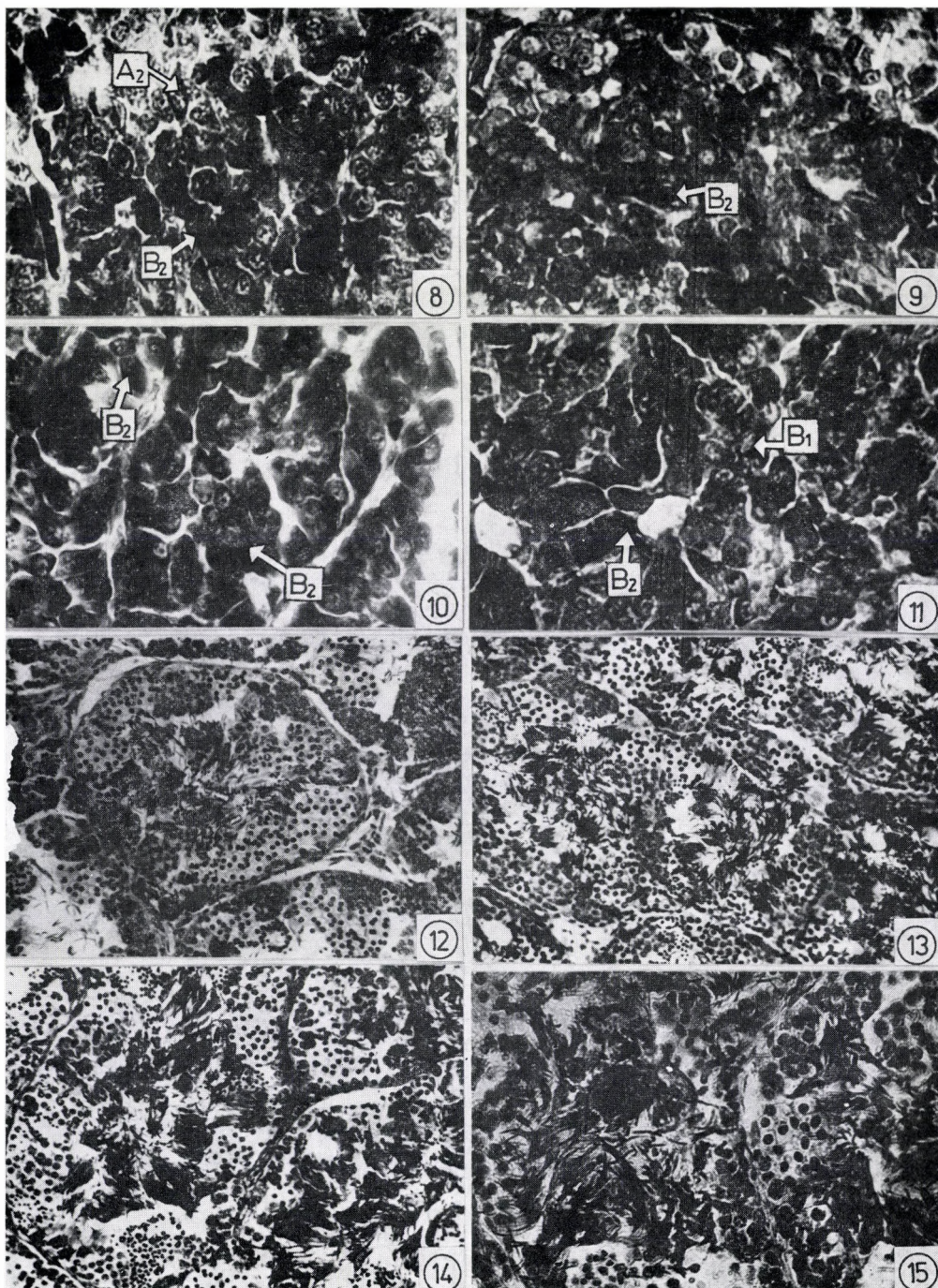
Fig. 3: February, granulated cells

Fig. 4: April, strong degranulation of B_3

Fig. 5: November, reggranulated cells

Fig. 6. T. S. of the pituitary of control frog showing the distribution of different cell types. $\times 1200$

Fig. 7. T. S. of the pituitary of frog treated with booster dose of stilboestrol. Hypertrophy of A_1 cells and the distortion of B_2 cells. Accumulation of orangeophilic and acidophilic granules on extracellular spaces. $\times 1200$



on the spermatocytes and other advanced stages in the seminiferous tubules. Withdrawal of testosterone is followed by recovery, but this was not the case with the other steroids.

Discussion

It has been observed in the present investigation, that the different types of cells of the pars distalis exhibit a similar trend in secretory activity. The cells attain their maximum size, and the amount of granules in the cytoplasm is highest by the end of February. This is followed by a period of degranulation and a gradual release of secretory granules in mid-summer. This phenomenon observed in *Rana hexadactyla* appears to be different from that reported for other species [6, 24, 45—47].

There are characteristic differences in the degranulation of acidophils and basophils. Acidophils (A_1) are relatively inert: it is only during the time of strong extrusion that cells of this type appear partly granulated whereas the period of gradual release is characterized by a shrinkage of the cells. Basophils (B_3) lose most of their granules at the peak of reproductive activity, and in the remaining period they are sparsely granulated. On the other hand, basophils (B_2) after losing the orange granules accumulate new granules in April. VAN OORDT and LOFTS [42] interpreted this as a sign of gonadotropin storage due to a negative feedback testicular hormones. DOER-SCHOTT [7, 8], RIECKEN et al. [28] and WACHTLER and PEARSE [44] have drawn attention to the presence of acid phosphatase in the large orangeophilic granules, which would suggest that lysosomal activity was involved in the extrusion of secretory products. DOER-SCHOTT [7] and VAN OORDT [39] described a second wave of degranulation in the type 2 from June to August. Degranulation cannot solely be ascribed to increased extrusion but may partly be due to a decreased production of secretory granules. This is supported by the decrease in size of the nuclear apparatus, which starts in March and ends in August, when the cells attain their smallest dimensions.

Exogenous steroid caused extensive damage to the basophils, in particular to B_2 and B_3 cells, and to a little extent also to the acidophils in the pars

←
Fig. 8. T. S. of the pituitary of frog treated with split dose of stilboestrol. Clear distinction between B_2 cells and the granular nature of acidophilic cells and large sinusoidal spaces. $\times 1200$

Fig. 9. T. S. of the pituitary of frog treated with testosterone. Cytomorphological change of B_2 cells and their granulation. $\times 1200$

Fig. 10. T. S. of the pituitary of frog treated with DOCA. Atrophic pituitary cells and dense vacuolization and poor granulation in the cytoplasm. $\times 1200$

Fig. 11. T. S. of the pituitary of frog treated with cortisol. Regressive changes of the cells and wide ramification of connective tissue and inhibition of secretory activity. $\times 1200$

Figs 12—14. T. S. of the testis of frog stained with haemalum eosin. $\times 400$

Fig. 12: February, decrease of primary spermatogonia

Fig. 13: July, overall acceleration of spermatogenetic activity

Fig. 14: October, increase and well developed spermatogonia

Fig. 15. T. S. of the testis of frog treated with testosterone for one month. $\times 400$

distalis. Even though the pattern of response of these cell types varies with the type of hormone administered, changes occurred in the cytomorphological features, tinctorial affinities and secretory activity. From the nature of granulation and other cytomorphological conditions, it appears that the B_2 and B_3 cells of testosterone treated frogs are slightly active, whereas in other hormone treated frogs they are atrophied. The B_2 and B_3 cells, though reduced in size, showed cytoplasmic granulation indicating the storage of synthesized materials. Since B_2 and B_3 cells were selectively affected by the hormone treatment, these two types of cells seem to be sensitive to the administered hormone. As derangement of spermatogenic activity and atrophy of the B_2 and B_3 cells run parallel under the influence of administered hormone(s) there is evidence to believe that in untreated *R. hexadactyla*, these two types of basophilis are involved in the regulation of spermatogenic activity. The functional significance of these two types of cells and their role in the regulation of reproductive activity needs further elucidation.

In the pars distalis of the amphibian adenohypophysis, five different cell types have been identified [36, 41] and of these B_2 and B_3 are concerned with the secretion of gonadotropins. Based on studies on *Pleurodeles waltlii*, PASTEELS [25, 26] suggested that B_2 cells are the source of FSH like hormone, while B_3 cells are concerned with the production of LH or ICSH hormones. In *P. waltlii*, homoplastic transplantation of adenohypophysis led to a regression of B_1 and B_2 and atrophy of B_3 cells in the pituitary, and affected the interstitial tissue in the testis and also the secondary sexual characteristics of the recipient frogs. PASTEELS [25, 26] therefore concluded that B_3 cells are the source of ICSH like hormone. VAN OORDT [41] suggested a correlation between B_3 cells and the cycle of interstitial cells in the testis of the common frog. Following heteroplastic transplantation of the pars distalis, VAN OORDT [37] and VAN DONGEN et al. [32] observed atrophy of Leydig cells, testis, thumb pads of *Bufo bufo* and a complete disappearance of B_3 cells from the hypophysis. SAXEN et al. [29] VAN OORDT [38, 40], KERR [22] and STREB [30] stated that in amphibians B_1 cells are thyrotropic cells whereas in *Rana temporaria*, DOER-SCHOTT [9, 13] consider the B_3 cells to be thyrotropic. Such considerations do not, however, exclude the possibility that these cells exert a corticotropic function.

The existence of a parallelism between the activity of B_3 cells and interstitial function, both under normal and experimental conditions, led VAN OORDT and LOFTS [42] to conclude that this basophil is the source of ICSH like hormone. Studying B_3 cells as well as interstitial and interrenal cells during a circennial cycle [34, 43] and under the influence of high temperature [33], it was observed that changes in the activity of the cells run parallel in the three different tissues. In *Rana temporaria* activation of B_3 cells coincided with interrenal stimulation while the interstitial cells regressed [33]. As the

influence of B_3 cells on the interrenal tissue was more profound than on the interstitium of the testis, it led the authors to suggest that B_3 cells are corticotropic rather than gonadotropic. VAN OORDT et al. [43] suggested that the activity of B_3 cells corresponds to yearly changes in the production of testicular hormones, and corticoids, leaving the question open whether B_3 cells produce ICSH-like hormone or ACTH. KASINATHAN and BASU [20] also found that exogenous steroid hormone leads to a decrease in interrenal activity and a regression of interstitium in the testis. In the present study, the pituitary of frogs treated with steroid showed B_3 cell hyperplasia and granulation. Concomitant with these changes, spermatogenesis was affected and the interstitium was reduced. These observations corroborate the suggestion of VAN OORDT and LOFTS [42] that B_3 is chiefly concerned with the production of ICSH-like hormone and corticoids.

The relationship between the pars distalis and the target organ is evidenced by the fact that the secretory activity of pars distalis during April coincides with the maximum activity of the testis. Spermiation and initial multiplication of primary spermatogonia take place during the period of strong extrusion of B_2 cells of the pars distalis. In *Rana temporaria* it has been shown that secretory activity of the pars distalis runs parallel with the functional differentiation of the testis. In the absence of gonadotropins, lipid materials accumulate in the Sertoli cells, resulting in the degeneration of secondary spermatogonia. After the release of gonadotropins, clearing away of lipid material occurs leading to renewal of the spermatogenic activity, i.e. secondary spermatocytes are differentiated into sperms [23]. In the present study too, primary spermatogonia decreased in number from January to July and then increased to a maximum in November. The B_2 cell types exhibit a similar trend in their numerical occurrence. In *Rana hexadactyla* spermatogenic activity is dependent on the gonadotropins of B_2 , as the activity in these two runs parallel. In temperate frogs, spermatogenesis is discontinuous and spermatogenic activity is arrested during the winter, whereas during the summer it is accelerated due to the renewal of gonadotropin secretion. This aspect is clearly illustrated by the granulation and degranulation in the B_2 cells and this fact has been taken into consideration for implicating the hormonal control of spermatogenic activity in temperate frogs. On the other hand, in the present investigation spermatogenic activity was continuous in the tropical frog, *Rana hexadactyla*. Synthesis of gonadotropins by B_2 cells appears to be continuous within no marked variations in extrusion of the elaborated products. Further, spermatogenic activity also shows waxing and waning, spread over to the entire circennial cycle.

Thus, impairment in the function of B_2 cells leads to an inhibition of gametogenic activity. The data presented seem to indicate that gonadotropic activity of the B_2 cells mainly influence gametogenesis. The secretory activity

of the gonadotrops in turn depends on the circulating steroid level within the organism. The renewed activity of the germinal epithelium is less under the influence of steroid hormone treatment than is the spermatogenic activity of the cells proliferating prior to hormone treatment, which continues unhampered. KASINATHAN and BASU [20] reported that exogenous steroids act by two pathways. First, the adenohypophyseal feedback mechanism is interrupted and the second possible pathway is a direct action of the hormone on the germinal epithelium of the testis leading to an inhibition of the further differentiation of spermatogenic stages. BASU [3] showed *in vitro* that spermatogenic cells are affected directly by steroids. The present series of experiments has lent additional support to the finding that steroids not only decrease FSH and LH output from the gonadotrops but also alter their cytomorphological characteristics. The magnitude of these changes varies and is dependent on the type of steroid administered.

REFERENCES

1. BASU, S. L.: (1968) Effects of testosterone and estrogen on spermatogenesis in *Rana hexadactyla* Lesson. J. exp. Zool. **169** (2), 133. — 2. BASU, S. L.: (1969) Effect of hormones on the salient spermatogenesis *in vivo* and *in vitro*. Gen. Comp. Endocr. Suppl. **2**, 203. — 3. BASU, S. L.: (1973) Maintenance of isolated testicular tubules of albino rats in organ culture. Ind. J. exp. Biol. **11** (4), 326. — 4. BROOKS, L. D.: (1967) A stain for differentiating two types of acidophils in the pituitary. Gen. comp. Endocr. **9**, 436. — 5. COPELAND, D. L.: (1943) Cytology of the pituitary gland in developing and adult *Triturus viridescens*. J. Morph. **72**, 379. — 6. DENT, J. N.: (1961) Seasonal and sexual variations in the pituitary gland of *Triturus viridescens*. Anat. Rec. **141**, 85. — 7. DOER-SCHOTT, J.: (1962) Évolution des cellules gonadotrophes Bo au cours du cycle annuel chez la grenouille rousse *Rana temporaria*. Étude au microscope électronique; observations histochemiques et cytophysiologiques. Gen. Comp. Endocrinol. **2**, 541. — 8. DOER-SCHOTT: (1964) Localisation au microscope électronique de l'activité phosphatase acide dans les cellules B de l'hypophyse de la grenouille rousse *Rana temporaria*. C. R. Acad. Sci. (Paris). **258**, 1621. — 9. DOERR-SCHOTT, J.: (1965) Étude aux microscopes optique et électronique des différents types des cellules de la pars distalis et de la pars intermedia de *Triturus marmoratus*. Ann. Endocr. **27**, 101. — 10. DOERR-SCHOTT, J.: (1965a) Étude comparative de la cytologie et de l'ultrastructure de l'hypophyse distale de trois espèces d'amphibiens Anoures: *Rana temporaria* L., *Bufo vulgaris* Laur: *Xenopus laevis*. D. Gen. Comp. Endocr. **5**, 631. — 11. DOERR-SCHOTT, J.: (1965b) L'hypophyse de crapaud: *Bufo vulgaris* Laur. Étude comparative aux microscopes optique et électronique. Compt. R. Acad. Sci. (Paris) **260**, 283. — 12. DOERR-SCHOTT, J.: (1966) Modifications ultra-structurales des cellules thyrotrophes de l'hypophyse distale de la grenouille rousse après thyroïdectomie. C. R. Acad. Sci. (Paris) **262**, 1973. — 13. DOERR-SCHOTT, J.: (1968) Cytologie et physiologie de l'adenohypophyse des amphibiens. Ann. Biol. **7**, 189. — 14. EZRIN, C., MURRAY, S.: (1963) The cells of the human adenohypophysis in pregnancy, thyroid disease and adrenal cortical disorders. Coll. Int. Nat. Rech. Sci. **128**, 183. — 15. GABE, M.: (1953) Sur quelques applications de la coloration par la fuchsine-paraldehyde. Bull. Micr. appl. **3**, 153. — 16. HALMI, N. S.: (1952) Differentiation of two types of basophils in the adenohypophysis of the rat and the mouse. Stain Technol. **27**, 61. — 17. HERLANT, M.: (1956) Correlations hypophyso-génitales chez la femelle de la chauve-souris, *Myotis myotis* (Berkhausen). Arch. Biol. **67**, 89. — 18. HERLANT, M.: (1960) Étude critique de deux techniques nouvelles destinées à mettre en évidence les différentes catégories cellulaires présentes dans la glande pituitaire. Bull. Micr. appl. **10**, 37. — 19. HERLANT, M.: (1964) The cells of the adenohypophysis and their functional significance. Int. Rev. Cytol. **17**, 299. — 20. KASINATHAN, S., BASU, S. L.: (1972) Seasonal variation and exogenous hormonal effect on the interrenal glands of *Rana hexadactyla* Lesson.

- Proc. Ind. Acad. Sci. **75** (4), 191. — 21. KASINATHAN, S., BASU, S. L., SRIRAMULU, V.: (1974) Effect of pituitary extracts on the hypophyseal gonadotrophs and its relation to spermatogenesis in *Rana hexadactyla* Lesson. J. Exp. Zool. **187** (2), 233. — 22. KERR, T.: (1966) The development of the pituitary in *Xenopus laevis* Daudin. Gen. Comp. Endocr. **6**, 303. — 23. LOFTS, B.: (1961) The effects of follicle stimulating hormone and leutinizing hormone on the testis of hypophysectomised frogs (*Rana temporaria*). Gen. Comp. Endocr. **1**, 179. — 24. MILLER, M. R., ROBBINS, M. E.: (1955) Cyclic changes in the pituitary gland of the urodele amphibian *Taricha torosa* (*Triturus torosus*). Anat. Rec. **122**, 105. — 25. PASTEELS, J. L.: (1957) Recherches experimentales sur la rôle de l'hypothalamus dans la differentiation cytologique de l'hypophyse chez *Pleurodeles waltlii*. Arch. Biol. (Liege) **68**, 65. — 26. PASTEELS, J. L.: (1960) Étude experimentale des différentes categories d'elements chromophiles de l'hypophyse adulte de *Pleurodeles waltlii*. Arch. Biol. (Liege) **71**, 409. — 27. RASTOGI, R. K., CHIEFTI, G.: (1970) Cytological changes in the pars distalis of pituitary of the green frog *Rana esculenta* L. during the reproductive cycle. Z. Zellforsch. **111**, 505. — 28. RIECKEN, E. O., NUNN, R. E., WACHTLER, K., PEARSE, A. G. E.: (1965) Electron cytochemical demonstration of acid phosphatase in the globular basophils of the amphibian pituitary. J. roy. micr. Soc. **84**, 509. — 29. SAXEN, L., SAXEN, E., TOIVONEN, S., SALIMAKI, K.: (1957) The anterior pituitary and thyroid function during normal and abnormal development of frog. Ann. Zool. Soc. "Vanamo". **18**, 1. — 30. STREB, M.: (1967) Experimentelle Untersuchungen über die Beziehung zwischen Schilddrüse und Hypophyse während der Larvalentwicklung und Metamorphose von *Xenopus laevis* Daudin. Z. Zellforsch. **82**, 407. — 31. TUCHMANN-DUPLESSIS, H.: (1945) Correlations hypophysoendocrines chez le triton. Determinisme hormonal des caracteres sexuels secondaires. Actual. Scient. Industr. Paris. (Hermann). **987**, 1. — 32. VAN DONGEN, W. J., JORGENSEN, C. B., LARSEN, L. O., ROSENKILDE, P., LOFTS, B., VAN OORDT, P. G. W. J.: (1966) Function and cytology of the normal and autotransplanted pars distalis of the hypophysis in the toad *Bufo bufo* (L). Gen. Comp. Endocr. **6**, 491. — 33. VAN KEMENADE, J. A. M.: (1969) Effects of a rise in ambient temperature on the pars distalis of the pituitary, the interrenal gland and the interstitial tissue of the testis in the common frog *Rana temporaria* during hibernation. Z. Zellforsch. **95**, 620. — 34. VAN KEMENADE, J. A. M., VAN OORDT, P. G. W. J.: (1968) Seasonal changes in the endocrine organs of the male common frog *Rana temporaria*. The interrenal tissue. Z. Zellforsch. **91**, 96. — 35. VAN OORDT, P. G. W. J.: (1961) The gonadotrophin producing and other cell types in the distal lobes of the pituitary of the common frog, *Rana temporaria*. Gen. Comp. Endocrinol. **1**, 364. — 36. VAN OORDT, P. G. W. J.: (1963a) Identification of the gonadotrophin producing cells in the pituitary of common frog, *Rana temporaria*. Acta. Physiol. Pharmacol. Neerlandica. **12**. North-Holland Publishing Co. Amsterdam. — 37. VAN OORDT, P. G. W. J.: (1963b) Cytological aspects of normal and autotransplanted pituitaries of *Bufo bufo*. Gen. Comp. Endocr. **3**, 736 (abstr.). — 38. VAN OORDT, P. G. W. J.: (1963c) Cell types in the pars distalis of the amphibian pituitary. Coll. Int. Cent. nat. Rech. Sci. Cytologie de l'adenohypophyse. **128**, 301. — 39. VAN OORDT, P. G. W. J.: (1965) Nomenclature of the hormone producing cells of the adenohypophysis. In Perspectives in Endocrinology (ed. E. J. W. Barrington and C. B. Jorgensen) 405. New York and London, Academic Press. — 40. VAN OORDT, P. G. W. J.: (1966) Changes in the pituitary of common toad, *Bufo bufo* during metamorphosis and the identification of thyrotrophic cells. Z. Zellforsch. **75**, 47. — 41. VAN OORDT, P. G. W. J.: (1968) The analysis and identification of the hormone producing cells of the adenohypophysis. In "Perspectives of Endocrinology — Hormones in the life of lower vertebrates" (Ed. E. J. W. Barrington and C. B. Jorgensen). — 42. VAN OORDT, P. G. W. J., LOFTS, B.: (1963) The effects of high temperature on gonadotrophin secretion in the male common frog (*Rana temporaria*) during autumn. J. Endocr. **27**, 137. — 43. VAN OORDT, P. G. W. J., VAN DONGEN, W. J., LOFTS, B.: (1968) Seasonal changes in the endocrine organs of the male common frog *Rana temporaria* I. The pars distalis of the adenohypophysis. Z. Zellforsch. **88**, 549. — 44. WACHTLER, K., PEARSE, A. G. E.: (1966) The histochemical demonstration of five lysosomal enzymes in the pars distalis of amphibian pituitary. Z. Zellforsch. **69**, 326. — 45. ZUBER VOGELI, M.: (1953) L'histophysiologie de l'hypophyse de *Bufo vulgaris* L. Archs. Anat. **35**, 77. — 46. ZUBER VOGELI, M.: (1966) Les variations cytologiques de l'hypophyse distale du male de *Nectophrynoides occidentalis* au cours du cycle annuel. Gen. Comp. Endocr. **7**, 492. — 47. ZUBER VOGELI, M., HERLANT, M.: (1964) Étude cytologique des formes cellulaires presentes dans l'ante hypophyse de *Nectophrynoides occidentalis* (Angel). C. R. Acad. Sci. (Paris) **258**, 3367.

SAISONALE SCHWANKUNGEN DER SEKRETORISCHEN AKTIVITÄT
DER ZELLTYPEN DES PARS DISTALIS UND IHRE EINWIRKUNG
AUF DIE TESTIS UND AUF DIE INTERRENALEN DRÜSEN
BEI *RANA HEXADACTYLA* LESSON

S. KASINATHAN, S. L. BASU und VIJAYAM SRIRAMULU

Im distalen Teil der Adenohypophyse des Froschmännchens der *Hexadactyla* Lesson untersuchten Verfasser 5 morphologisch verschiedene Zelltypen an gefärbten Präparaten der Hypophyse, welche im Laufe des Jahres monatlich gesammelt wurden. Alle Zelltypen wiesen von August bis Februar progressives Wachstum auf, nach welchen von März bis Juli eine Verringerung auftrat. Die Ausstoßung des synthetisierten Produktes ging im Sommer vor sich und während der Periode der Ausstoßung war die Synthese gering. Die Besprechung enthält die zyklischen Änderungen der sekretorischen Aktivität der im Pars distalis vorkommenden Zelltypen und ihre Wirkung auf die Testis und die interrenalen Drüsen.

СЕЗОНАЛЬНЫЕ КОЛЕБАНИЯ СЕКРЕТОРНОЙ АКТИВНОСТИ КЛЕТОК ТИПОВ
PARS DISTALIS, ЕГО ВЛИЯНИЕ НА ЯИЧКО И ИНТЕРРЕНАЛЬНЫЕ
ЖЕЛЕЗЫ И *RANA HEXADACTYLA* LESSON

Ш. КАШИНАТАН, С. Л. БАШУ и В. ШИРАМУЛУ

Авторы изучали в 5 морфологически разнообразных типов клеток в дистальной аденогипофиза самца лягушки *Rana Hexadactyla* Lesson в окрашенных препаратах с гипофизов собранных в течение одного года. Все типы клеток с августа по февраль повышаются и понижаются с марта по июль. Удаление синтетического продукта произошло летом и в периоде удаления продукция была малая. Дискуссия содержит циклические изменения секреторной активности типов клеток найденных в дистальной части, и их влияние на яичко и на интраренальные железы.

S. KASINATHAN } Department of Biology, Jawaharlal Institute of Postgraduate
S. L. BASU } Medical Education and Research, Pondicherry-605006, India

Vijayam SRIRAMULU: Department of Zoology, Annamalai University,
Annamalai Nagar, India

Institute of Anatomy, Histology and Embryology, University Medical School, Pécs

NUCLEUS ISTHMI OF THE FROG: STRUCTURE AND TECTO-ISTHMIC PROJECTION

S. H. KHALIL and GY. LÁZÁR

(Received November 23, 1976)

The morphology of neurons in the isthmic nucleus was studied with the Golgi technique. Most of the neurons have thick dendrites covered with lamelliform dendritic processes.

The tecto-isthmic projection was investigated with the Fink—Heimer technique after partial tectal lesions. The anteromedial part of the tectum projects on the dorsal and anterior part, the caudomedial tectal region on the dorsal and posterior part of the nucleus. The posterolateral tectal area projects on the anterolateral part of the nucleus, and the axons originating in the anterolateral tectal quadrant terminate in its ventral and caudal part.

The isthmic nucleus (IN) is one of the most obscure structures in the frog brain, though its topography and cytoarchitecture is well-known from many descriptions [1, 3, 4, 5, 12]. Several fibre pathways associated with the nucleus were also described in intact animals [1, 5, 12], and LARSELL [5] studied its neurons with the Golgi technique. The function of the nucleus is, however, unknown.

In birds, the isthmo-optic nucleus is more or less similar in structure and connections. This nucleus is involved into a topographically organized retinal feed-back loop [9, 10]. The functional significance of the tecto-isthmo-retinal pathway was disclosed in electrophysiological and behavioural studies [11].

In frogs, similarly as in birds, the retinotectal projection is organized topographically. RUBINSON [13] showed that the isthmic nucleus receives a strong tectal projection, and more recently the existence of reciprocal connections between the tectum and isthmic nucleus was confirmed in anatomical studies (Kicliter, personal communication; 14).

In the present investigations we studied whether in the frog the tecto-isthmic projection was topographically organized. The structure of the nucleus was studied with the Golgi technique in order to make a basis for further electronmicroscopic investigations concerning its synaptology.

Material and methods

The normal architecture of the nucleus has been studied with routine neurohistological staining techniques in *Rana esculenta*. In our earlier investigations on the frog visual system, over one hundred brains were prepared with the rapid Golgi technique. This material was used in the present studies to investigate the morphology of cells and fibre terminals.

To analyse topographical relationships in the tecto-isthmic projection, small pieces of the anterolateral, anteromedial, posterolateral and the posteromedial parts of the tectum were removed by suction in 32 animals. The animals were killed 5–7 days after the lesion by intracardial perfusion of 10% formaldehyde. For further fixation, the brains were removed and kept in the same fixative in the refrigerator for 2 weeks then they were embedded in egg yolk. Frozen sections, 25 μm in thickness, were prepared. Denegenerated terminals were impregnated by the Fink–Heimer technique [2].

Results

Structure of the isthmic nucleus (IN)

The IN is interposed between the rhombencephalon and the tegmentum mesencephali, just below the caudal pole of the tectum. It is roughly ovoid in shape with the medial part slightly impressed (Fig. 5). The diameter of the nucleus is 300 μm in the mediolateral, and 500 μm in the dorsoventral direction in a middle-sized frog (body weight 70 g). The IN has a cortex formed by a few rows of cells and the marrow with scattered neurons in the centre. The marrow is surrounded by a neuropil. The cortex is interrupted by a hilus at the ventrolateral part (Fig. 5).

In Golgi preparations two kinds of neurons can be distinguished in the cortex. One of them has an almost spherical, large perikaryon. One or two short, thick dendrites originate from it, which give origin to several side branches in the neuropil and among cells in the medulla. Sometimes the main dendrite is larger and usually follows the curvature of the cortical cell row, and the secondary branches point radially towards the centre of the nucleus (Fig. 1; Fig. 5 C1 neurones). Smaller branches are covered with dendritic appendages. These are similar to the plasma processes characteristic of ependymo-glial cells, but they are less in number. We could not reliably identify the axons of these cells.

The second type of neurons is very similar to the small pear-shaped cells described in the tectum [8]. The piriform perikaryon is small. A main dendrite emerges from the tip of the perikaryon and points towards the centre of the nucleus (Fig. 2; Fig. 5 C2 neurones). The dendrites arborize either in the neuropil or among the neurones in the marrow. Only a few spines and appendages occur on these dendrites. In some cases, the axons of these cells were also impregnated; they left the nucleus ventrally or laterally, but could only be traced for a short distance.

The majority of neurons in the marrow is similar to those in the cortex but the dendrites may be oriented in either direction.

In smaller numbers, two other types of neurons can be distinguished in the marrow. One of them has a large irregular perikaryon. Usually more than two thick, uneven main dendrites originate from it with a few secondary branches (Fig. 3; Fig. 5 M1 neurones). The other type of cell has a middle-sized fusiform perikaryon from the two poles of which originate the dendrites (Fig. 5 M2 neurons). In a few cases the axons of marrow cells were also impregnated. Usually they were lost among cells within the marrow, but a few axons could be followed to the hilus or to the lateral wall of the nucleus.

Tectal fibres reach the IN alongside the whole dorsolateral circumference including the hilus and enter the marrow. Inside the nucleus the fibres break up into small, broom-like end-arbors (Figs 4, 5). The terminals form a dense network among the cells in the marrow and the neuropil but do not reach the perikarya of cortical cells.

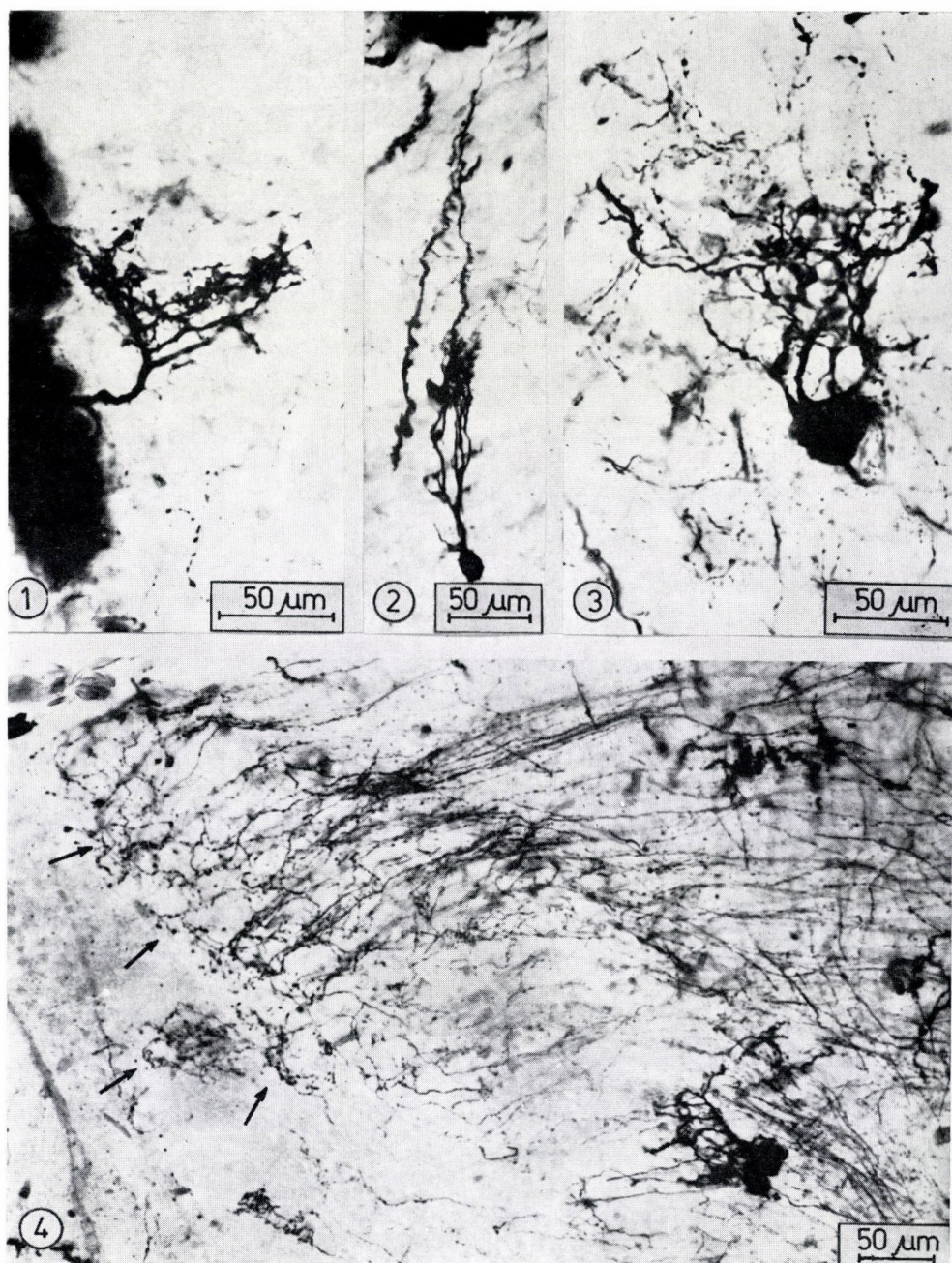
Topographical organization of the tecto-isthmic projection

A small lesion in the tectum resulted in degeneration in circumscribed areas inside the IN. The location of degenerated terminals depended on the location of lesions in the tectum. It means that the tecto-isthmic projection is organized topographically. The border of a single degenerated spot is always sharp, but the projection fields of neighbouring distinct tectal areas overlap. This fact makes it difficult to reconstruct the exact topography of the tectal projection.

After an anteromedial tectal lesion degenerated fragments were distributed dorsally in the anterior half of the IN, and spread medially in more caudal sections, but did not reach the caudal end (Figs 6, 10).

When the lesion had destroyed the caudomedial part of the tectum, degenerated terminals were found also dorsally and dorsomedially but mostly in the caudal half of the IN. In the anterior one fourth there was no degeneration. Fragments of terminals appeared in the dorsal part of the nucleus at a distance of 80–90 μm from the anterior end, and the tectal projection area extended ventralwards in more posterior levels (Figs 7, 10). The projection areas of anteromedial and posteromedial parts of the tectum overlap in the middle zone (along the anteroposterior axis) of the IN.

A lesion in the posterolateral part of the tectum resulted in degeneration in the anterolateral part of the IN. In the anterior one fourth, degenerated terminals fill almost the whole cross section area, and only a narrow strip is empty along the medial side of the nucleus. More caudally, the degeneration was located dorsolaterally, but the caudal one fourth did not show signs of



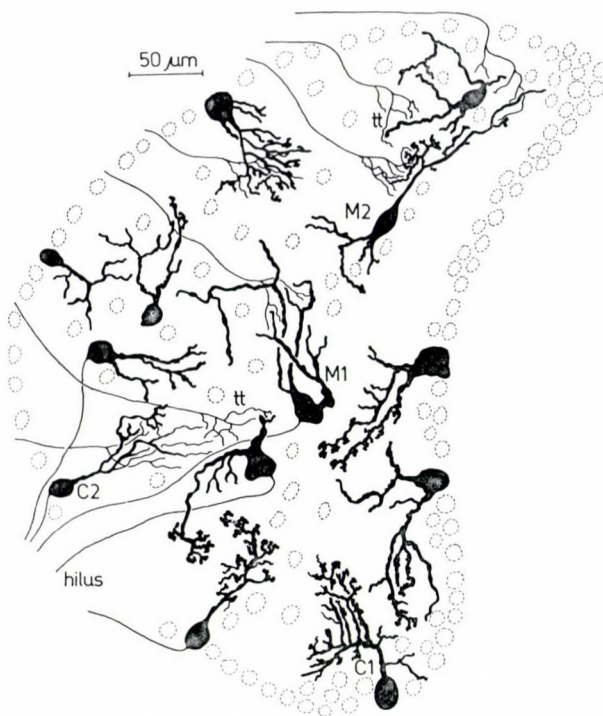


Fig. 5. Neuron types in the isthmus nucleus. Perikaryons and dendrites were drawn with the aid of a camera lucida, axons and tectal terminals are schematized. C1, C2 — cortical cells; M1, M2 — marrow cells; tt — tectal terminals. Coronal plane. Dorsal is upward, medial is to the right

degeneration (Figs 8, 10). The projection of the anteromedial and posterolateral tectal areas overlap to some extent (Fig. 10).

When lesions were made in the anterolateral part of the tectum, degenerated terminals were found in the ventral and caudal part of the IN. The anterior one fourth of the nucleus was free of degeneration. In more caudal sections degenerated terminals appeared in the ventrolateral part located close to the hilus of the nucleus. The area occupied by degenerated fibres extended dorsally and was shifted medialwards in the posterior half of the nucleus. In some cases, the ventrolateral part of the nucleus did not contain degenerated fragments in the most caudal sections. The tectal projection area was located ventromedially in such cases (Fig. 9).

Fig. 1. Cortical cell with curved main dendrite and with dendritic processes. The perikaryon is covered with precipitate

Fig. 2. Cortical cell resembling pear-shaped tectal neurones

Fig. 3. Marrow cell with multipolar perikaryon

Fig. 4. Tectal terminals (arrows) and two cortical cells in the isthmus nucleus. Rapid Golgi technique. The bar is 50 μm in each figure



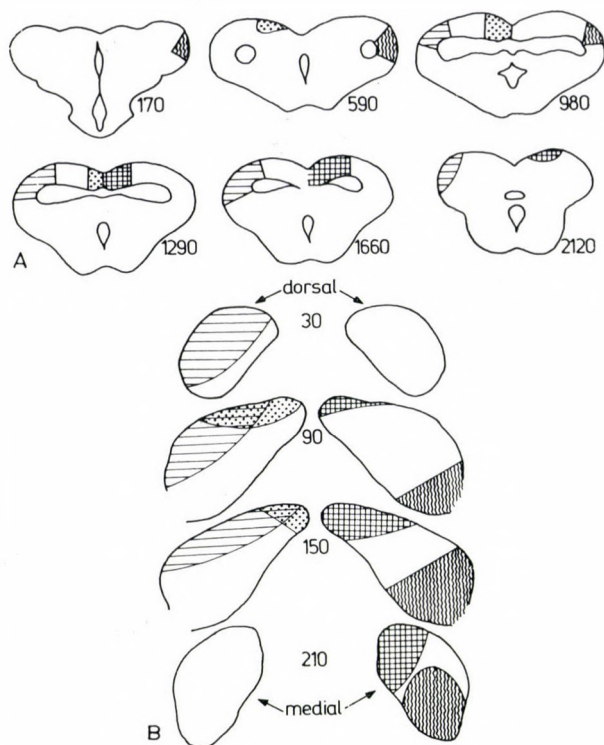


Fig. 10. Schematic representation of the tecto-isthmic projection after partial tectal lesions. The figures show the distance in μm from the anterior pole of the tectum (A), and of the isthmic nucleus (B). Patterns in the drawings of tectal cross sections (A) show the destroyed tectal area. The same patterns were applied to show the projection of the corresponding tectal area on the cross sections of the isthmus (B).

Discussion

The present Golgi studies showed that a number of neurones in the IN are peculiar in form when compared to the rest of nerve cells in other brain areas. Unusually thick dendrites and several irregular lamelliform dendritic processes give a characteristic appearance of these neurones. The significance

Figs 6–9. Distribution of degenerated axon terminals in the isthmus nucleus after lesions made in the anteromedial (6), posteromedial (7), posterolateral (8) and in the anterolateral parts (9) of the tectum. Numbers in the upper right corner indicate in μm the approximate distance of the sections from the anterior pole of the nucleus. Dashed lines indicate the extension of degeneration. Coronal sections. Dorsal is upward. M — medial. Fink—Heimer technique.

The bar is 50 μm in each figure

of the processes is unknown. Further electron microscopic studies are necessary to elucidate the synaptic relations of these structures.

The topography of the tecto-isthmic projection is not as clear as the topography of the retino-tectal projection. The projections of the anterolateral and posterolateral tectal regions are well separated, but fibres originating from anteromedial and posteromedial tectal areas overlap to some extent. The medial edge of the tectum is much shorter than the lateral circumference, and lesions in the anterior and posterior parts of this edge are located very close to each other. In fact, in our cases there was always a small overlap between the destroyed anteromedial and posteromedial tectal regions and this may have caused the overlap of projections.

The tectal anatomy may cause another difficulty in interpretation. In the case of *e.g.* posterolateral lesions, fibres originating from the anteromedial part of the tectum may be interrupted. The overlap of projections of the anteromedial and posterolateral tectal areas may be attributed to this situation. Taking into account the scantiness of degeneration technique in this case, tracing techniques should be used to obtain a more accurate topography of the tecto-isthmic projection.

In another series of experiments [7], the transneuronal transport of radioactive substances was investigated in the frog visual system with the autoradiographic technique. In one case only the anterolateral part of the tectum was labelled after tritiated proline injection into the corresponding eye. Subsequently, transneuronal labelling was restricted to the ventrolateral part of the IN. In another case almost the whole tectum was labelled except its anterolateral part. There was no transneuronal labelling in the ventrolateral part of the IN in this case, but the rest of the nucleus was labelled. This corresponds well to the results obtained with degeneration technique.

In birds a topographically organized feed-back loop was found between the retina and the tectum through the isthmo-optic nucleus [9, 10]. We do not know whether in the frog the IN projects on the retina. SCALIA [14] using the horse-radish peroxidase technique did not find direct isthmoretinal connections. In other investigations [6, 13] degenerated fibres were found in the optic nerve after tectal removal but SCALIA [14] could not confirm their existence. Provided the results obtained with the horse-radish technique are reliable, this may mean that neither the IN nor the tectum is involved in a feed-back loop to the retina in frogs, and so the role of the IN and especially of its topographically organized tectal afferents remains obscure. Electrophysiological studies may solve the problem of whether a direct connection exists or not between the retina and the isthmic nucleus.

REFERENCES

1. ARIENS KAPPERS, C. U., HUBER, C. G., CROSBY, E. C.: (1960) *The Comparative Anatomy of the Nervous System of Vertebrates, Including Man*. Hafner, New York.
2. FINK, P., HEIMER, L.: (1967) Two methods for selective impregnation of degenerating axons and their synaptic endings in the central nervous system. *Brain Res.* **4**, 369–374.
3. GAUPP, E.: *Anatomie des Frosches*. Vieweg, Braunschweig (1899).
4. KREHT, H.: (1940) Die markhaltigen Fasersysteme im Gehirn der Anuren und Urodelen und ihre Myelogenie; zugleich ein kritischer Beitrag zu den Flechsig'schen myelogenetischen Grundgesetzen. II. Kleinhirn, Mittelhirn und Endhirn. *Z. mikr.-anat. Forsch.* **48**, 191–286.
5. LARSELL, O.: (1924) The nucleus Isthmi of the Frog. *J. comp. Neurol.* **36**, 309–322.
6. LÁZÁR, GY.: (1969) Efferent Pathways of the optic tectum in the frog. *Acta biol. Acad. Sci. hung.* **20**, 171–183.
7. LÁZÁR, GY.: (1976) Transneuronal transport in the frog visual system. *Brain Res.* **109**, 623–627.
8. LÁZÁR, GY., SZÉKELY, GY.: (1967) Golgi studies on the optic center of the frog. *J. Hirnforsch.* **9**, 329–344.
9. MCGILL, J. J., POWELL, T. P. S., COWAN, W. M.: (1966a) The retinal representation upon the optic tectum and isthmooptic nucleus in the pigeon. *J. Anat.* **100**, 5–33.
10. — (1966b) The organization of the projection of the centrifugal fibres to the retina in the pigeon. *J. Anat.* **100**, 35–49.
11. MILES, F. A.: (1972) Centrifugal control of the avian retina. I–V. *Brain Res.* **48**, 65–156.
12. RÖTHIG, P.: (1927) Beiträge zum Studium des Zentralnervensystems der Wirbeltiere. 11. Über die Faserzüge im Mittelhirn, Kleinhirn und der Medulla oblongata der Urodelen und Anuren. *Z. mikr.-anat. Forsch.* **10**, 381–472.
13. RUBINSON, K.: (1968) Projections of the tectum opticum of the frog brain. *Behav. Evol.* **1**, 529–561.
14. SCALIA, F.: (1976) The optic pathway of the frog: nuclear organization and connections. In: *Frog Neurobiology*. Ed. by R. Llinás and W. Precht. Springer, Berlin—Heidelberg—New York. pp. 386–406.

DER ZELLKERN DES NUCLEUS ISTHMI BEIM FROSCH: AUFBAU (STRUKTUR) UND TECTO-ISTHMISCHE PROJEKTION

S. H. KHALIL und GY. LÁZÁR

Die Morphologie der Nervenzellen des Nucleus isthmi wurde mit der Golgi-Methode untersucht. Die Mehrzahl der Neuronen besitzt dicke Dendriten, die mit plattenartigen dendritischen Fortsätzen besetzt sind.

Die tecto-isthmische Projektion wurde nach partiellen Tectumläsionen mit der Fink-Heimerschen Methode untersucht. Der anteromediale Teil des Tectums projiziert sich dorsal auf den Vorderteil des Nucleus, während der kaudomediale Teil auf dem hinteren Teil des Nucleus, gleichfalls dorsal zur Darstellung kommt. Das posterolaterale Tectumgebiet wird auf den anterolateralen Teil des Nucleus projiziert und diejenigen Axone, die vom anterolateralen Quadranten des Tectums ausgehen, enden ventral im kaudalen Teil des Nucleus isthmi.

КЛЕТОЧНОЕ ЯДРО NUCLEUS ISTHMI У ЛЯГУШКИ: СТРОЕНИЕ (СТРУКТУРА) И ЕГО ТЕКТО-ИСТМИЧЕСКАЯ ПРОЕКЦИЯ

Ш. Х. КХАЛИЛ и ДЬ. ЛАЗАР

Морфология нервных клеток nucleus isthmi была изучена методом Гольджи. Большинство нейронов обладает толстыми дендритами, которые покрыты пластинчатыми дендритическими отростками.

Текто-истмическая проекция была изучена после частичных повреждений крыши методом Финк-Геймера. На дорсальной стороне anteromedialная часть крыши проецируется на переднюю часть ядра, а kaudomedialная часть — на заднюю часть ядра, так же дорсально. Постеролатеральная область крыши проецируется на anterolateralную часть ядра, причем аксоны, исходящие из anterolateralного квадранта крыши кончаются на вентральной стороне каудальной части nucleus isthmi.

S. H. KHALIL: Zoology Department, Faculty of Science,
Moharram Bey Alexandria, Egypt

Gyula LÁZÁR: Department of Anatomy, University Medical School,
H-7643 Pécs, Hungary

Institute of Pathological Anatomy, University Medical School, Szeged

POSTMORTEM DIAGNOSTICS OF RENAL DISEASES FROM SEMITHIN SECTIONS*

J. ORMOS, J. ENGELHARDT and Anikó MÁGORI

(Received April 17, 1976)

For the light microscopic postmortem study of mostly glomerular renal diseases, in addition to the paraffin technique, 0.5 μ thick (semithin) sections from material fixed in buffered formaldehyde and embedded in methacrylate or Durcupan ACM were used. The method allows for eventual electron microscopic examinations. The semithin sections were stained with methylene blue combined with basic fuchsin, as well as with periodic acid–silver methamine. The method is not a substitution, but the supplementation of the paraffin technique and is suited for the clarification of numerous fine details: in some cases the exact diagnosis was made in this way.

Introduction

Kidney specimens from necropsy material have been studied in semithin sections after methacrylate or Durcupan ACM embedding.

Materials and methods

The kidneys obtained from 47 selected necropsies of subjects with glomerular renal disease without conspicuous autolytic phenomena and from 8 nephrectomies were examined. In four cases each, paraffin-embedded specimens were studied. The time between death and fixing of the material varied from 5 to 27 hours. The $2 \times 2 \times 2$ mm specimens taken from the cortical and from the medullary substance were fixed in formaldehyde buffered with distilled water solution of NaOH and NaH_2PO_4 for several days. After 2 hours post-fixation in 1% OsO_4 and dehydration in an alcohol series the blocks were embedded in methyl-butyl-methacrylate or Durcupan ACM and semithin (0.5 to 1.0 μ) sections were prepared with the LKB Ultratome I. For staining, the combination of methylene blue and basic fuchsin (M–F) and periodic acid–silver methenamine (PASM) were applied. With M–F, removal of the embedding material is not necessary but staining must be performed by vaporization. Before PASM staining the sections are treated with saturated alcoholic KOH solution for 15 minutes. In some cases ultrathin sections were also prepared: these were studied after contrasting with uranyl acetate and lead citrate with SEM 3–1 electron microscope. For the examination of material fixed in 4% non-neutralized formaldehyde and embedded in paraffin, the $2 \times 2 \times 2$ mm pieces after deparaffination were postfixed in 2.5% glutaraldehyde for 2 hours then with OsO_4 for 1 hour. Subsequent embedding, cutting and staining were performed as described above.

Results

The details of the glomerular capillaries and of Bowman's capsule appeared clearly; frequently even the immune complex deposits could be seen (Figs 1, 2 and 3). In one case the so-called dense deposit type of

* Based on a paper at the Balaton Conference on Electron Microscopy, Veszprém, 1975. Supported by Grant 4–07–0301–01–0/O from the Hungarian Ministry of Health.

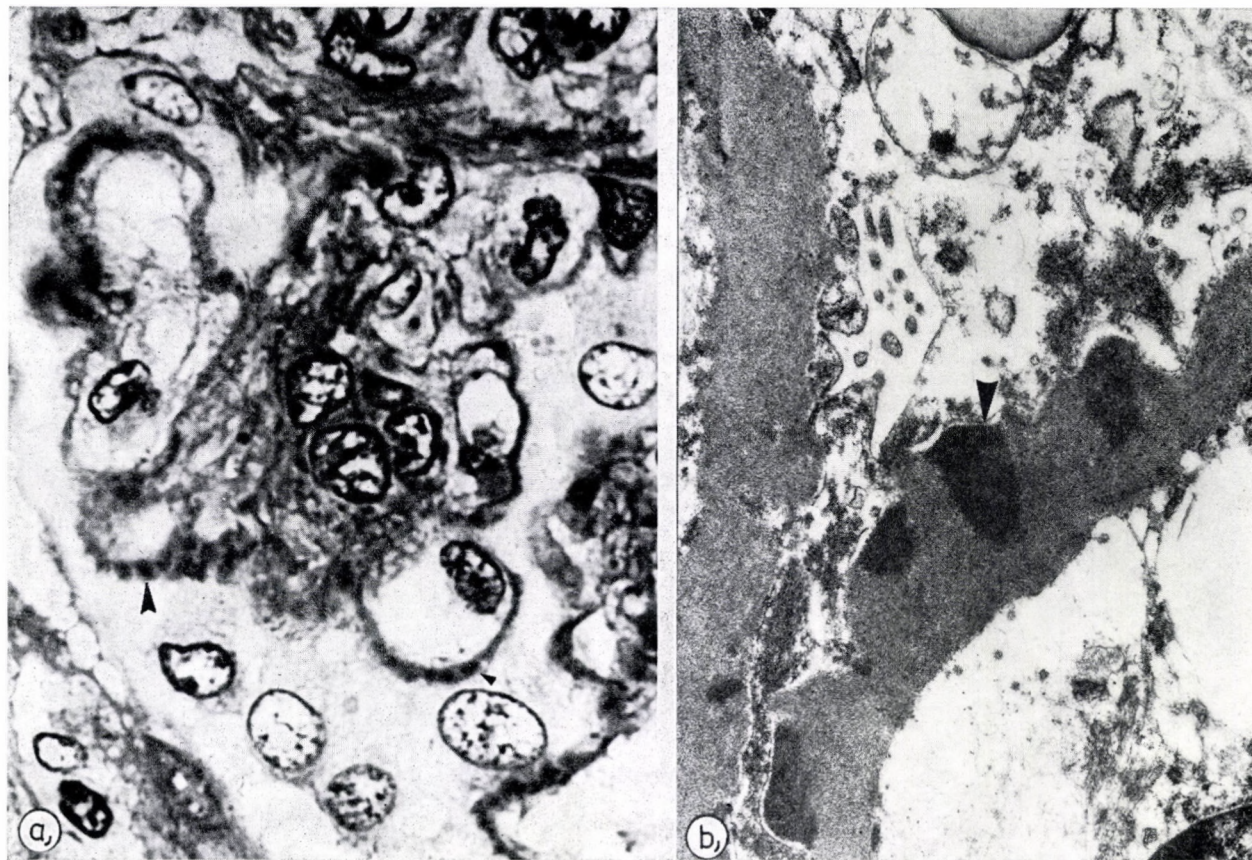


Fig. 1. Diffuse mesangio-proliferative glomerulonephritis. Immune complex deposits on the external surface of the capillary wall (arrow). a) Semithin section, Durcupan ACM embedding, M-F stain, $\times 1400$. b) The subepithelial immune complex deposits can be seen on the electron microscopical picture despite postmortem autolysis. Uranyl acetate and lead citrate, $\times 23,000$

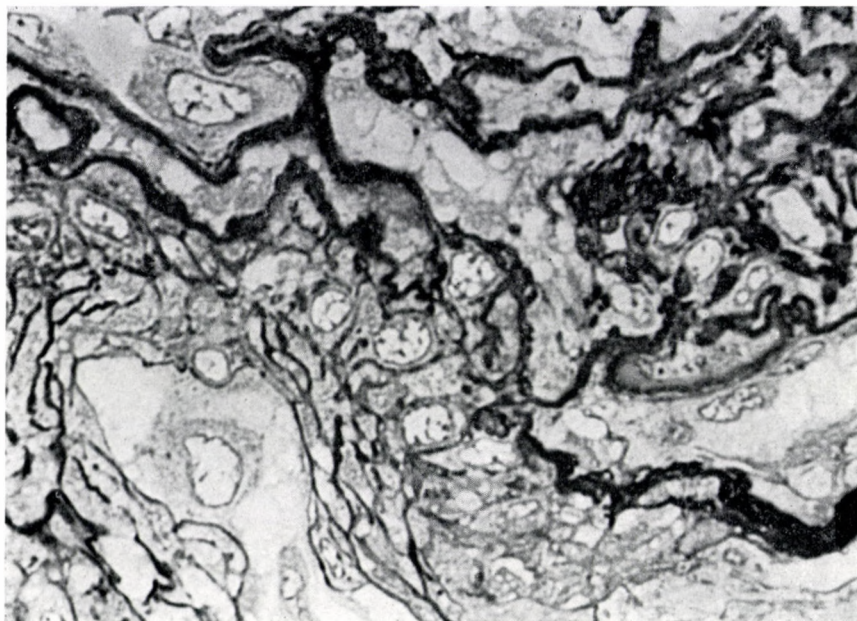


Fig. 2. Lupus nephritis. Glomerulus with afferent arteriole. In the capillary walls immune deposits can be seen ("wire loop lesion"). Semithin section, methacrylate embedding, PASM stain, $\times 1400$

mesangiocapillary glomerulonephritis in an end-stage kidney could be recognized in material embedded previously in paraffin. It was possible to differentiate the podocytes and sometimes their finer details (processes granulation, fusion of foot processes) (Figs 4 and 5). In hyaline glomeruli, PASM staining demonstrated the basement membrane network and the M–F staining the cell residues.

In a case where the clinical data pointed with great certainty to renal disease, but in the paraffin sections and even in the semithin sections, with PASM staining only glomeruli of normal appearance could be seen by M–F staining the disappearance of foot processes and podocyte activity could be suspected. This was verified by electron microscopy of the material fixed 5 hours after death, thus the diagnosis of minimal change could be stated. In another case, necropsy was performed 27 hours after death. In the paraffin sections the glomeruli contained an increased number of cells. In M–F stained semithin sections the presence of characteristic humps could be demonstrated; this was verified by electron microscopy, establishing the diagnosis of immune complex (post-streptococcal) glomerulonephritis (Fig. 1).

Thickness and structure (Fig. 6) of the tubular epithelium, its eventual multilayer composition (Fig. 7), multiplication of the tubular basement mem-

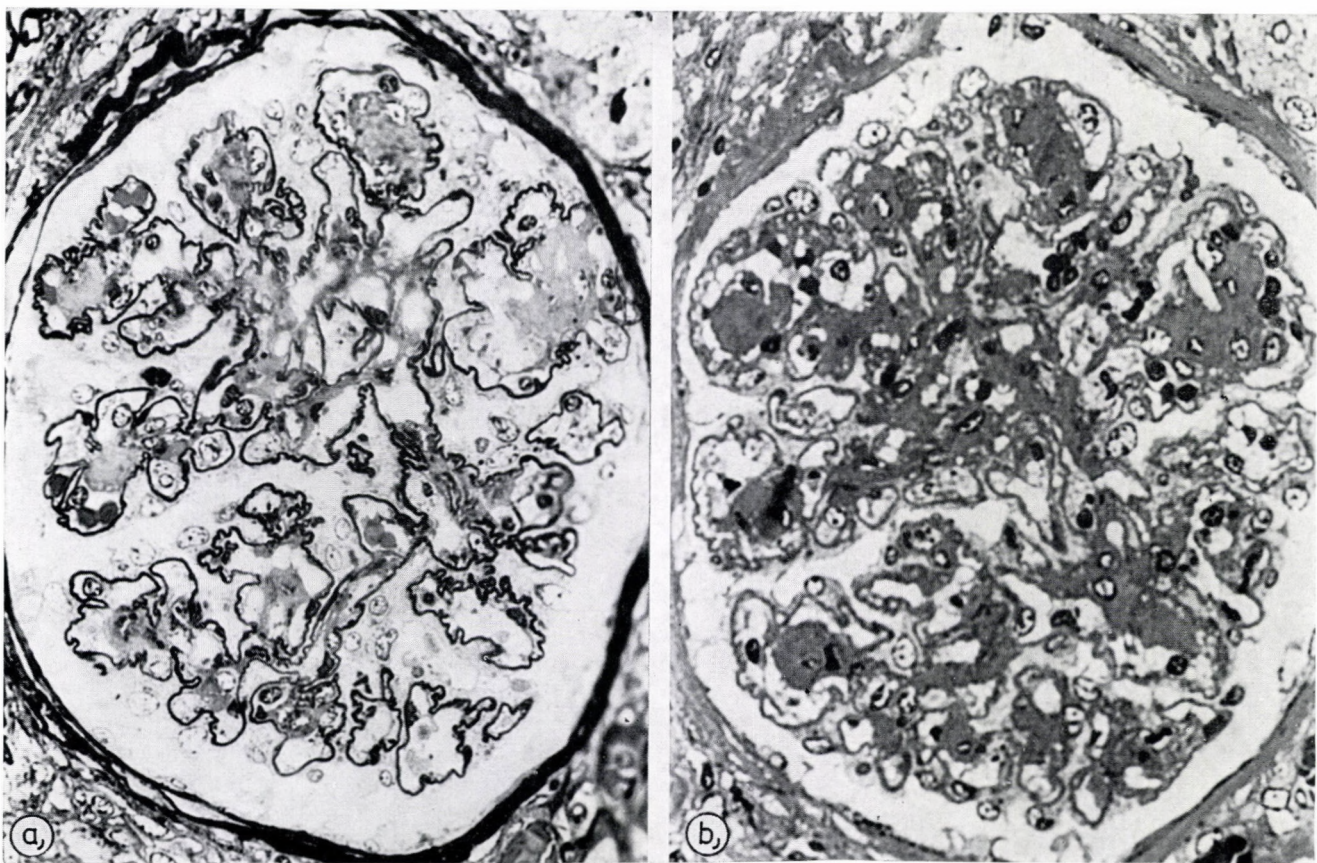


Fig. 3. Diabetic glomerulosclerosis. The two staining methods supplement each other. Semithin section, Durcupan ACM embedding. a) PASM stain, $\times 1400$, b) M-F stain, $\times 1400$

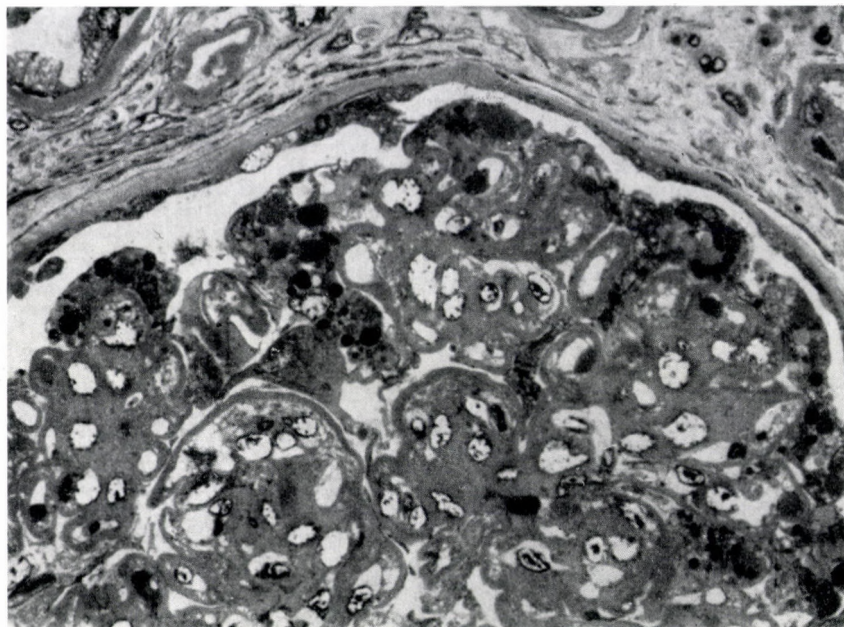


Fig. 4. Diabetic glomerulosclerosis. Conspicuous thickening of glomerular capillary and tubular basement membrane; numerous inclusions formed in podocytes. Semithin section, methacrylate embedding, M-F stain, $\times 560$

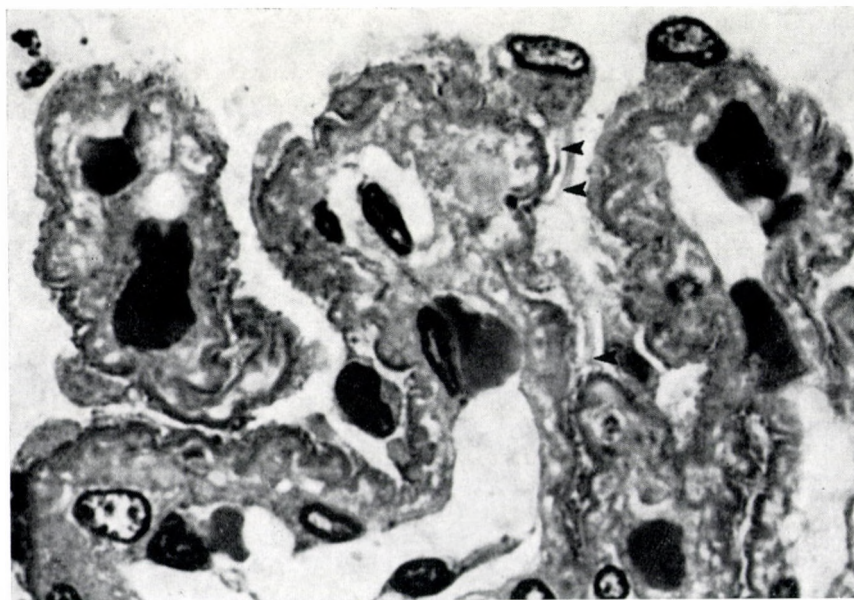


Fig. 5. Lupus nephritis. Despite postmortem damage many details of the capillary wall are preserved, even primary processes of the podocytes (arrow). Semithin section, methacrylate embedding, M-F stain, $\times 1400$

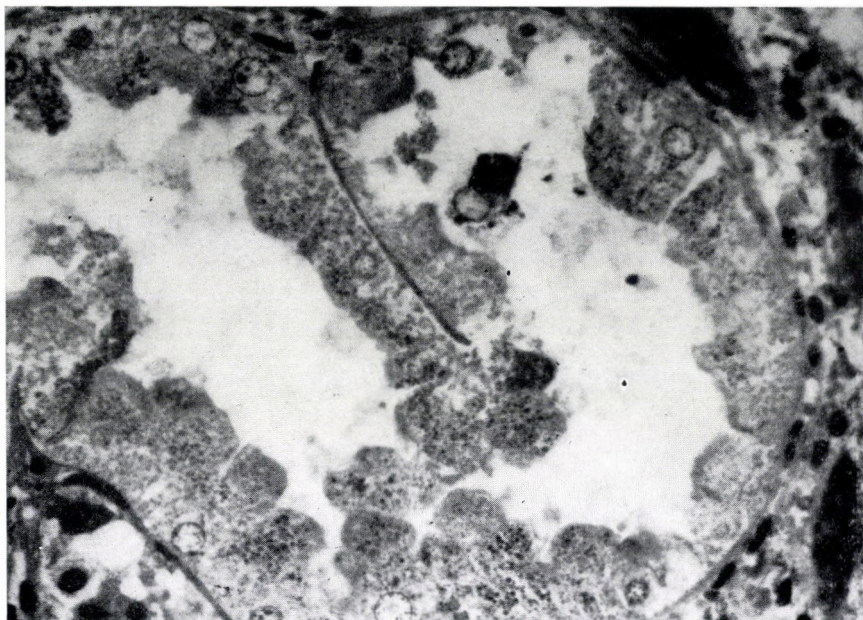


Fig. 6. Lupus nephritis. Hypertrophic proximal convoluted tubule. The rich granulation of the epithelial cells points to ample organelle content. Semithin section, methacrylate embedding, M-F stain, $\times 560$

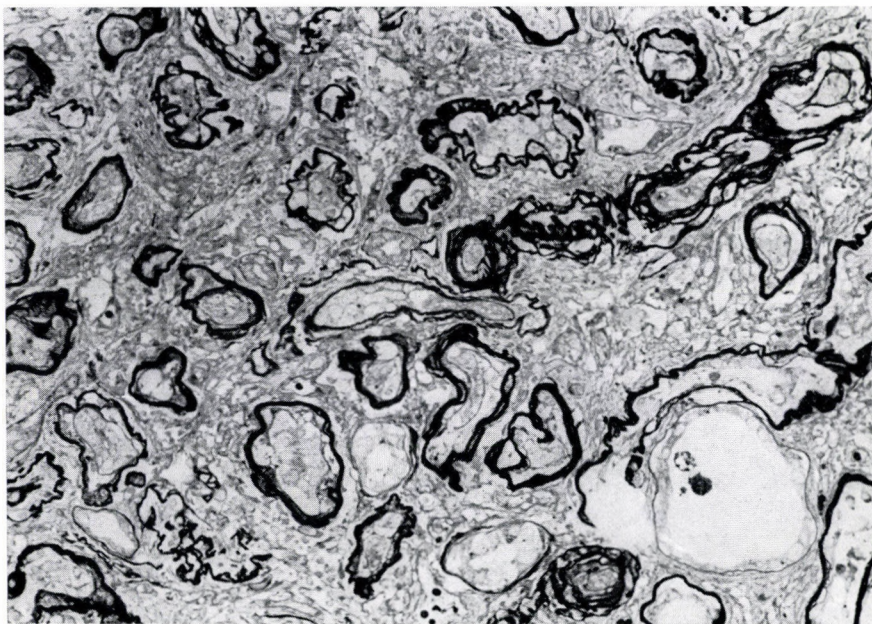


Fig. 7. Diabetic nephropathy. The complicated structure of the basement membrane of the atrophic tubuli is clearly seen. Semithin section, Durcupan ACM embedding, PASM stain, $\times 224$

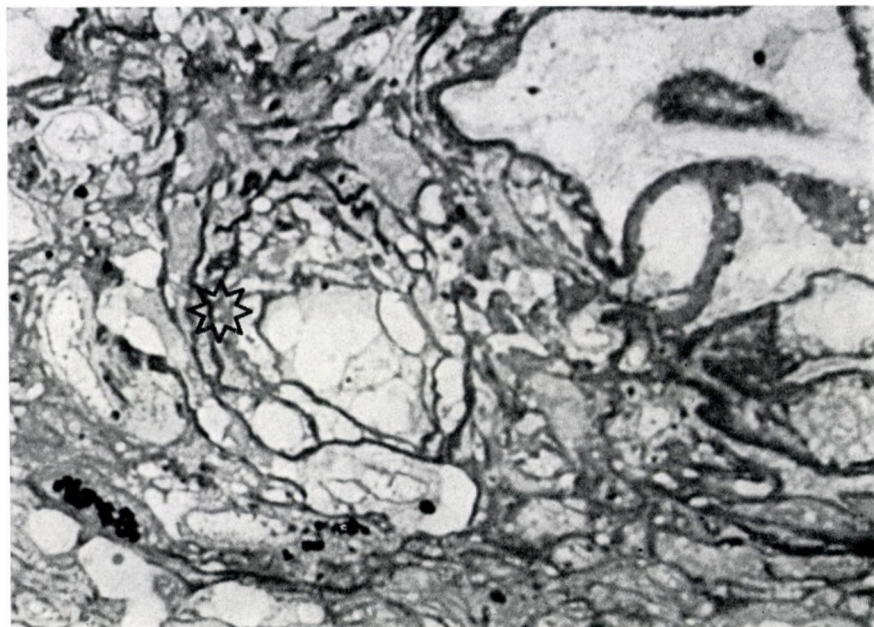


Fig. 8. Lupus nephritis. Basement membrane network (+) and juxtaglomerular granules in the wall of the afferent arteriole. Semithin section, methacrylate embedding, PASM stain, $\times 1400$

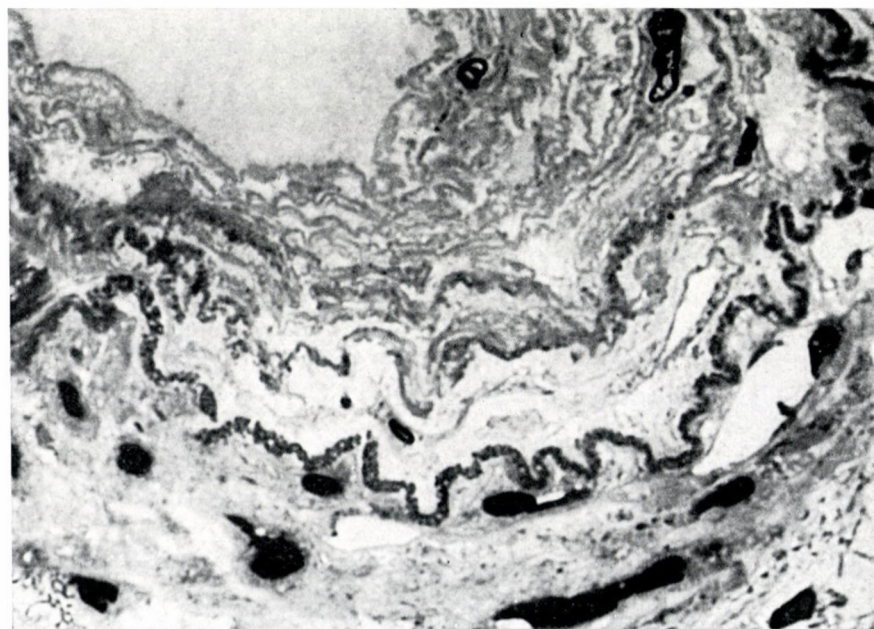


Fig. 9. Chronic pyelonephritis. Part of arterial wall. In some places the inhomogeneity of the elastic fibres is clearly seen. Semithin section, methacrylate embedding, M-F stain, $\times 1400$

brane, and the composition of cylinders were clearly revealed together with the structure of the vascular walls, the width of the lumina and the basement membrane network. Even the inhomogeneity of the elastica could clearly be observed (Figs 8 and 9).

Discussion

Several authors have emphasized the advantages of semithin sections over the paraffin technique [1, 2, 4—6, 11]. The greatest advantage in post-mortem renal diagnostics is the reliable demonstration of fine details, and in some cases the correct diagnosis can be made this way or with electron microscopy performed on the same tissue. In the small specimens, autolysis is prevented sooner by the rapid fixation. Plastics embedding induces less shrinking than paraffin. The 0.5—1.0 μ thick sections demonstrate finer details than the 4—8 μ thick paraffin sections, they can be studied under higher power.

It should be recognized, however, that the semithin technique is more material and time-consuming than the renal paraffin processing, the sections are less extensive, the use of specific stains is restricted and the time between death and fixation must not be more than 18 hours. Beside the time factor other factors (e.g. temperature) might be also of importance. In addition, due to the higher magnification and the richness of details the deceptive post-mortem artifacts may appear more abundant.

Among the fixatives described by CARSON et al. [3] we applied Millonig's phosphate-buffered formaldehyde, mentioned under D./3/, thus fixation allows both light and electron microscopic examinations. The material is not expensive so that it can be used instead of the usual, unbuffered formaldehyde. It is recommended to use 1 mm specimens prepared inside the fixative to allow rapid fixation. Some authors [2, 7, 10, 15] applied OsO_4 or glutaraldehyde fixation for the preparation of semithin sections. We performed postfixation in OsO_4 . Plastics are harder than paraffin and than the tissue components, therefore the block is of more even consistence and ultramicrotomic sections can be prepared. The possibility of the re-examination of specimens embedded into paraffin many years before is also provided, as the tissue piece regained from the block can be re-embedded into methacrylate or Durcupan ACM [5].

The M-F staining method is actually the combination of two stains described by MORGENSTERN [14]. This together with the PASM stain described by JONES [8] supplement each other well. Their joint application offers ample information and takes little time. In renal routine diagnostics these two staining methods are usually sufficient and other procedures [2, 5—7, 9—12, 15] can be dispensed with. The PASM method stains essentially the same structures

as PAS [8, 13], but the contours are better defined and the fine structures and details are more clearly outlined. Material embedded into methacrylate can be stained somewhat more easily than that embedded in Durcupan ACM.

The sections were covered with the embedding plastics. According to LYNN [9, 11] in this way a higher resolution power can be achieved by immersion. We applied plastics in the first place to prevent the fading under Canada-balsam.

The method described will not substitute the paraffin technique but supplements it supplying useful new informations chiefly about glomerular renal diseases.

Acknowledgements

We are indebted to Mrs. Mária ELHARDT, Mrs. Jenő SZAMOSVÁRI, Mrs. Olga HAJNAL and Mrs. Magda SZUPERA for technical assistance.

REFERENCES

1. AGODOA, L. C. Y., STRIKER, G. E., CHI, E.: (1975) Glycol methacrylate embedding of renal biopsy specimens for light microscopy. *Amer. J. clin. Path.* **64**, 655—660. — 2. CARDNO, S., STEINER, J. W.: (1965) Improvement of staining technics for thin sections of epoxy-embedded tissue. *Amer. J. clin. Path.* **43**, 1—8. — 3. CARSON, F. L., MARTIN, J. H., LYNN, J. A.: (1973) Formalin fixation for electron microscopy: a re-evaluation. *Amer. J. clin. Path.* **59**, 365—373. — 4. DITSCHERLEIN, G., DENA, R.: (1972) Zur Aussagekraft von versilberten Semidünnschnitten in der histologischen Diagnostik von Nierenveränderungen. *Zbl. allg. Path.* **116**, 113—120. — 5. DITSCHERLEIN, G., DENA, R.: (1974) Einfache Semidünnschnittmethode, welche die Anwendung verschiedener Routinefärbungen gestattet. *Z. med. Labortechnik* **15**, 302—306. — 6. GERMAIN, J. P.: (1974) Epoxy resin embedding and light microscopy, its advantages and disadvantages. *Science Tools* **21**, 30—32. — 7. JENNINGS, B. M., FARQUHAR, M. G., MOON, H. D.: (1959) Staining methods for osmium methacrylate sections. *Amer. J. Path.* **35**, 991—997. — 8. JONES, D. B.: (1957) Nephrotic glomerulonephritis. *Amer. J. Path.* **33**, 313—330. — 9. LYNN, J. A.: (1965) Rapid toluidene blue staining of Epon-embedded and mounted "adjacent" sections. *Amer. J. clin. Path.* **44**, 57—58. — 10. LYNN, J. A., MARTIN, J. H., RACE, G. J.: (1966) Recent improvements of histologic technics for the combined light and electron microscopic examination of surgical specimens. *Amer. J. clin. Path.* **45**, 704—713. — 11. LYNN, J. A.: (1975) "Adjacent" sections: a bridge in the gap between light and electron microscopy. *Human Path.* **6**, 400—402. — 12. MARTIN, J. H., LYNN, J. A., NICKEY, W. M.: (1966) A rapid polychrome stain for epoxy-embedded tissue. *Amer. J. clin. Path.* **46**, 250—251. — 13. MCMANUS, J. F. A.: (1948) The periodic acid routine applied to the kidney. *Amer. J. Path.* **24**, 643—653. — 14. MÖRGENSTERN, E.: (1969) Vergleichende lichtoptische Untersuchungen im Rahmen elektronenmikroskopischer Arbeiten an ultradünnen Schnitten. II. Färbemethoden. *Mikroskopie* **25**, 250—260. — 15. TRUMP, B. F., SMUCKER, E. A., BENDETT, E. P.: (1961) A method for staining epoxy sections for light microscopy. *J. Ultrastruct. Res.* **5**, 343—348.

DIE ANWENDUNG VON SEMIDÜNNNSCHNITTEN BEI DER POSTMORTALEN MORPHOLOGISCHEN DIAGNOSTIK DER NIERENKRANKHEITEN

J. ORMOS, J. ENGELHARDT und A. MÁGORI

Bei der lichtmikroskopischen Bewertung in postmortalem Material vorkommender verschiedener, hauptsächlich glomerulärer Nierenkrankheiten benutzten Verfasser neben der gewöhnlichen Paraffintechnik auch Semidünnschnitte von $0,5\ \mu$, zu welchen sie gepufferten Formalin und Methakrylat oder Durcupan ACM-Einbettung benutzten. Diese Methode ermöglicht auch eine evtl. elektronenmikroskopische Untersuchung. Die Semidünnschnitte färbten Verfasser mittels mit Methylenblau kombinierten basischen Fuchsin, sowie mit perjodsaurem Silbermethenamin. Diese, die Paraffintechnik nicht ersetzende, sondern ergänzende Methode ist zum Nachweis viel feinerer Details anwendbar, und in einigen Fällen ist somit — mittels Licht- oder elektronenmikroskopischer Untersuchung — nur solcherweise die genaue Diagnosestellung möglich.

ПРИМЕНЕНИЕ ПОЛУ-ТОНКИХ СРЕЗОВ В ПОСМЕРТНОЙ МОРФОЛОГИЧЕСКОЙ ДИАГНОСТИКЕ ЗАБОЛЕВАНИЙ ПОЧКИ

Е. ОРМОШ, Е. ЭНГЕЛЬХАРД и А. МАГОРИ

Авторы про помощи оптического микроскопа, кроме обычной методики парафина употребляли и полу-тонкие срезы (0,5) для оценки заболеваний почки применяя фиксативом забуференный формалин и заливанием метакриллат или Durcupan ACM. Эта методика и электронномикроскопически применяемая. Полу-тонкие срезы были окрашены основным фуксином комбинированном метиленовой синькой и метенамином перйодата серебра. Эта дополнительная и не замещающая технику парафина методика способна к выяснению деталей, в некоторых случаях только таким путем возможно ставить точный диагноз при помощи оптического и электронномикроскопического микроскопа.

Jenő ORMOS	}	Szegedi Orvostudományi Egyetem,
József ENGELHARDT		Kórbonctani Intézet, H-6701 Szeged,
Anikó MÁGORI		Pf. 401, Hungary

RECENSIONES

JELLINEK, H. and TÓTH, F.: *Functional Pathology of the Endometrium and Cervical Biopsy Specimens*. Akadémiai Kiadó, Budapest 1976. 299 pages with 196 figures

The literature of gynaecological pathology has become richer by this important monograph which may justly claim the interest of specialists of the subject.

The major part of the book deals with investigations concerning the endometrium and with the systematization of pertaining data. In these chapters the knowledge acquired during the last seven decades is reviewed and presented in an easily understandable manner. Knowledge of the changes occurring in the endometrium is indispensable for the gynaecological pathologist as well as for all those, who intend to be engaged in gynaecological endocrinology. In our days when reliable information can be obtained on the actual endocrinological state of the organism by up to date methods, e.g. gas chromatography or radioimmune assay, it is still the endometrium, as the target organ of the female sexual hormones which supplies the best information on the disturbance of female sexual function.

The last 15 years brought a rapid development in the pharmacology of steroid hormones. The appearance of synthetic norsteroids resulted in a world-wide use of hormonal contraception; simultaneously the treatment of functional female sterility received new stimulus and achieved promising results by the detection of clomiphene citrate. The effect on the organism of these compounds can best be appreciated by the histological changes observed in the endometrium. Thus the investigations into the normal and pathological changes occurring in the endometrium by various, histological, histochemical and cytochemical methods have an immense literature.

The authors have integrated the accumulated material in a fortunate manner, in such a way that the reader will not be lost in details and will be supplied with an answer to any of the actually emerging problems.

The first chapters of the book deal with the physiological function of the endometrium, the morphological manifestations of the cyclic changes, the hormone-dependent changes of the subcellular particles. All these are convincingly demonstrated by excellent electron micrographs. Then the pathological changes of the endometrium are discussed from the clinical aspect. In these chapters the readers obtain adequate answers to almost every questions from classic knowledge to the analysis of the effect and critical evaluation of upto date contraceptive drugs. The demonstration by excellent pictures of the endometrial changes following the administration of hormonal contraceptives and IUD is perhaps the most valuable chapter of the monography and it supplies up to date informations to be utilized in everyday practice by both the clinician and the gynaecologist-pathologist.

Compared with the rich content and colourful abundance of pictures of the chapters concerning the endometrium, the chapters on the cervix are considerably more modest. The authors seemed to be less stimulated by these chapters; the statements discussed on these pages are less new and even the illustrations are less colourful. These chapters may be considered a kind of addition. Compared with its clinical significance, the discussion of the changes of the cervix is also somewhat restricted.

The monograph ends with an abundant list of references where the interested reader or the investigator of the subject may find an ample choice of pertaining data.

I. ZOLTÁN

ROMEN, W.: *Zur Pathogenese der Glomerulosklerose*

Gustav Fischer Verlag, Stuttgart—New York, 1976. 87 pages with 39 pictures. Price: DM 38.—

This book is the 102nd of the "Veröffentlichungen aus der Pathologie" series.

In the introduction the author discusses the term sclerosis remarking that in pathology sclerosis means hardening associated with fibrosis. A more adequate term is not recommended. It is said that "glomerulosclerosis" indicates some degenerative non-inflammatory alteration of the glomeruli, where an increase in amount the glomerular basement membrane (GBM)

and the mesangial matrix (MM) is the most characteristic sign. The pathogenetic factors may be diabetes, hypertension, poisoning, ageing, among others. The main question of the examinations is whether the various aetiological factors leading to glomerulosclerosis, act by the same or by different mechanisms. As the problem cannot be studied in biopsy or necropsy material, the process was reproduced under various experimental conditions. The problem of GBM and MM formation was also investigated since these seem to be closely connected with the question.

The development of glomerulosclerosis was studied by light microscopy, electron microscopy and autoradiography in 4 groups of rats:

- a) in the course of spontaneous ageing;
- b) following subtotal 5/6 nephrectomy;
- c) after subtotal constriction of the renal vein
- d) in the course of acute and chronic N-nitrosomorpholine poisoning.

The results indicate that the various factors act by different routes. Following 5/6 nephrectomy, increased production of GBM and MM, in hypoxia produced by inhibition of the venous flow, after N nitrosomorpholine poisoning as well as following spontaneous ageing, the decrease of the process of decomposition will produce the alteration, with certain differences. The autoradiographic findings pointed to the podocytic origin of GBM and the production of MM by mesangial cells.

Though the problem is briefly mentioned it is not sufficiently emphasised why in glomerulosclerosis GBM thickening and MM increase are consequently associated, whereas these are different in cellular origin. A more detailed discussion of diabetic glomerulosclerosis would have been welcome.

The majority of the figures are electron micrographs; they are demonstrative and convincing. The book reflects adequately the accuracy of the experiments performed and of the process of evaluation.

H. JELLINEK

DANIEL, P. M. and PRICHARD, M. L.: *Studies of the Hypothalamus and the Pituitary Gland. With Special Reference to the Effects of Transection of the Pituitary Stalk*. Alden Press, Oxford. 1975. 216 pages with 104 illustrations. Price: £ 3.00

This monograph, first published in 1975 as Supplementum 201 to *Acta Endocrinologica* vol. 80, is an excellent summary of the nearly 25 years research of the authors and their collaborators on the effects of interruption of the neurovascular link by which the pituitary gland is connected to the brain. The investigations were made both on human material and on experimental animals of several species *i.e.* monkeys, sheep, goats, rats and ferrets. The authors are internationally known experts in the field and have probably the largest material on the morphological alterations of transection of the pituitary stalk. They describe, among others, that there are two groups of portal vessels, each of which drains a primary capillary bed in a specific segment of the neural component of the pituitary and supplies a particular territory in the pars distalis. Further, they determined the volumes of the territories supplied by the two groups of vessels and also the changes in volume of the parts of the pituitary gland after severing the pituitary stalk.

In the first part a brief summary of the anatomy of the hypothalamus and the pituitary gland is given and the neurohumoral mechanism controlling pituitary functions is briefly discussed. The second part is concerned with the local effects of pituitary stalk section and of hypophysectomy dealing separately with the morphological alterations proximal to the site of the surgical lesion (hypothalamus, pituitary stalk) and with those distal to it (various parts of the pituitary). In the third part remote effects of the mentioned intervention are described such as diabetes insipidus, alterations in growth, in the endocrine target organs and in reproduction and lactation. The documentation of the text is excellent, all illustrations are of high quality. The techniques used are briefly described in an appendix and this is followed by an author and subject index. The book is recommended for pathomorphologists, neuroendocrinologists and clinicians, particularly for postgraduates.

B. HALÁSZ

INDEX

Morphologica Normalis et Experimentalis

<i>Mitro, A.—Kiss, A.</i> : The Ependyma of the Ventriculus Mesencephali in the Rat	1
<i>Kovács, P.—Csaba, Gy.</i> : Evidence of the Heterogeneity of Mast Cell Population Based on their Biogenic Amine Content	9
<i>Kovács, P.—Csaba, Gy.</i> : Biogenic Amine and Amine Precursor Uptake by Mast Cells . . .	19
<i>Csonka, Éva—Bernolák, B.—Koch, A. S.—Jellinek, H.</i> : Scanning Electron Microscopic Examination of <i>in Vitro</i> Cultured Cells by Different Methods	25
<i>Kasinathan, S.—Basu, S. L.—Vijayam Sriramulu</i> : Cell Types of the Pars Distalis: Seasonal Changes in Secretory Activity and Effect of Steroids on Spermatogenesis in <i>Rana Hexadactyla</i>	35
<i>Khalil, S. H.—Lázár, Gy.</i> : Nucleus Isthmi of the Frog: Structure and Tecto-Isthmic Projection	51

Pathologia

<i>Ormos, J.—Engelhardt, J.—Mágori, Anikó</i> : Postmortem Diagnostics of Renal Diseases from Semithin Sections	61
Recensiones	71

Printed in Hungary

A kiadásért felel az Akadémiai Kiadó igazgatója

Műszaki szerkesztő: Zacsik Annamária

A kézirat nyomdába érkezett: 1977. IX. 22. — Terjedelem: 6,65 (A/5) ív, 23 ábra

77.4954 Akadémiai Nyomda, Budapest — Felelős vezető: Bernát György

The Acta Morphologica publish papers on experimental medical subjects in English. The Acta Morphologica appear in parts of varying size, making up volumes. Manuscripts should be addressed to:

Acta Morphologica, H-1091 Budapest, Üllői u. 93.

Correspondence with the editors and publishers should be sent to the same address. The rate of subscription is \$ 36.00 per volume.

Orders may be placed with "Kultúra" Foreign Trade Company (1389 Budapest 62, P.O.B. 149. Account No. 218-10990) or with representatives abroad.

Les Acta Morphologica paraissent en anglais et publient des travaux du domaine des sciences médicales expérimentales.

Les Acta Morphologica sont publiés sous forme de fascicules qui seront réunis en volumes.

On est prié d'envoyer les manuscrits destinés à la rédaction à l'adresse suivante:

Acta Morphologica, H-1091 Budapest, Üllői u. 93.

Toute correspondance doit être envoyée à cette même adresse.

Le prix de l'abonnement est de \$ 36.00 par volume.

On peut s'abonner à l'Entreprise du Commerce Extérieur « Kultúra » (1389 Budapest 62, P.O.B. 149. Compte-courant No. 218-10990) ou à l'étranger chez tous les représentants ou dépositaires.

«Acta Morphologica» публикуют трактаты из области экспериментальных медицинских наук на английском языке.

«Acta Morphologica» выходят отдельными выпусками разного объема. Несколько выпусков составляют один том.

Предназначенные для публикации авторские рукописи следует направлять по адресу:

Acta Morphologica, H-1091 Budapest, Üllői u. 93.

По этому же адресу направлять всякую корреспонденцию для редакции и администрации. Подписная цена — \$ 36.00 за том.

Заказы принимает предприятие по внешней торговле «Kultúra» (1389 Budapest 62, P. O. B. 149. Текущий счет № 218-10990) или его заграничные представительства и уполномоченные.

Reviews of the Hungarian Academy of Sciences are obtainable
at the following addresses:

- AUSTRALIA**
C.B.D. LIBRARY AND SUBSCRIPTION SERVICE,
Box 4886, G.P.O., *Sydney N.S.W. 2001*
COSMOS BOOKSHOP, 145 Ackland Street, *St. Kilda (Melbourne), Victoria 3182*
- AUSTRIA**
GLOBUS, Höchstädtplatz 3, *1200 Wien XX*
- BELGIUM**
OFFICE INTERNATIONAL DE LIBRAIRIE, 30
Avenue Marnix, *1050 Bruxelles*
LIBRAIRIE DU MONDE ENTIER, 162 Rue du
Midi, *1000 Bruxelles*
- BULGARIA**
HEMUS, Bulvar Ruszki 6, *Sofia*
- CANADA**
PANNONIA BOOKS, P.O. Box 1017, Postal Sta-
tion "B", *Toronto, Ontario M5T 2T8*
- CHINA**
CNPICOR, Periodical Department, P.O. Box 50,
Peking
- CZECHOSLOVAKIA**
MAD'ARSKÁ KULTURA, Národní třída 22,
115 66 Praha
PNS DOVOZ TISKU, Vinohradská 46, *Praha 2*
PNS DOVOZ TLAČE, *Bratislava 2*
- DENMARK**
EJNAR MUNKSGAARD, Norregade 6, *1165 Copenhagen*
- FINLAND**
AKATEEMINEN KIRJAKAUPPA, P.O. Box 128,
SF-00101 Helsinki 10
- FRANCE**
EUROPERIODIQUES S. A., 31 Avenue de Ver-
sailles, *78170 La Celle St. Cloud*
LIBRAIRIE LAVOISIER, 11 rue Lavoisier, *75008 Paris*
OFFICE INTERNATIONAL DE DOCUMENTA-
TION ET LIBRAIRIE, 48 rue Gay-Lussac, *75240 Paris Cedex 05*
- GERMAN DEMOCRATIC REPUBLIC**
HAUS DER UNGARISCHEN KULTUR, Karl-
Liebknecht-Straße 9, *DDR-102 Berlin*
DEUTSCHE POST ZEITUNGSVERTRIEBSAMT,
Straße der Pariser Kommune 3-4, *DDR-104 Berlin*
- GERMAN FEDERAL REPUBLIC**
KUNST UND WISSEN ERICH BIEBER, Postfach
46, *7000 Stuttgart 1*
- GREAT BRITAIN**
BLACKWELL'S PERIODICALS DIVISION, Hythe
Bridge Street, *Oxford OX1 2ET*
BUMPUS, HALDANE AND MAXWELL LTD.,
Cowper Works, *Olney, Bucks MK46 4BN*
COLLET'S HOLDINGS LTD., Denington Estate,
Wellingborough, Northants NN8 2QT
WM. DAWSON AND SONS LTD., Cannon House,
Folkestone, Kent CT19 5EE
H. K. LEWIS AND CO., 136 Gower Street, *London WC1E 6BS*
- GREECE**
KOSTARAKIS BROTHERS, International Book-
sellers, 2 Hippokratous Street, *Athens-143*
- HOLLAND**
MEULENHOF-BRUNA B.V., Beulingstraat 2,
Amsterdam
MARTINUS NIJHOFF B.V., Lange Voorhou-
9-11, *Den Haag*
- INDIA**
ALLIED PUBLISHING PRIVATE LTD., 13/14
Asaf Ali Road, *New Delhi 110001*
150 B-6 Mount Road, *Madras 600002*
INTERNATIONAL BOOK HOUSE PVT. LTD.,
Madame Cama Road, *Bombay 400039*
THE STATE TRADING CORPORATION OF
INDIA LTS., Books Import Division, Chandralok,
36 Janpath, *New Delhi 110001*
- ITALY**
EUGENIO CARLUCCI, P.O. Box 252, *70100 Bari*
INTERSCIENTIA, Via Mazzé 28, *10149 Torino*
LIBRERIA COMMISSIONARIA SANSONI, Via
Lamarmora 45, *50121 Firenze*
SANTO VANASIA, Via M. Macchi 58, *20124 Milano*
D. E. A., Via Lima 28, *00198 Roma*
- JAPAN**
KINOKUNIYA BOOK-STORE CO. LTD., 17-7
Shinjuku-ku 3 chome, Shinjuku-ku, *Tokyo 160-91*
MARUZEN COMPANY LTD., Book Department,
P.O. Box 5050 Tokyo International, *Tokyo 100-31*
NAUKA LTD. IMPORT DEPARTMENT, 2-30-19
Minami Ikebukuro, Toshima-ku, *Tokyo 171*
- KOREA**
CHULPANMUL, *Phenjan*
- NORWAY**
TANUM-CAMMERMEYER, Karl Johansgatan
41-43, *1000 Oslo*
- POLAND**
WĘGIERSKI INSTYTUT KULTURY, Marszał-
kowska 80, *Warszawa*
KOP I W ul. Towarowa 28 00-958 *Warszawa*
- ROUMANIA**
D. E. P., *Bucureşti*
ROMLIBRI, Str. Biserica Amzei 7, *Bucureşti*
- SOVIET UNION**
SOJUZPETCHATJ — IMPORT, *Moscow*
and the post offices in each town
MEZHDUNARODNAYA KNIGA, *Moscow G-200*
- SPAIN**
DIAZ DE SANTOS, Lagasca 95, *Madrid 6*
- SWEDEN**
ALMQVIST AND WIKSELL, Gamla Brogatan 26,
101 20 Stockholm
GUMPERTS UNIVERSITETSBOKHANDEL AB,
Box 346, *401 25 Göteborg 1*
- SWITZERLAND**
KARGER LIBRI AG, Petersgraben 31, *4011 Basel*
- USA**
EBSCO SUBSCRIPTION SERVICES, P.O. Box
1943, *Birmingham, Alabama 35201*
F. W. FAXON COMPANY, INC., 15 Southwest
Park, *Westwood, Mass. 02090*
THE MOORE-COTTRELL SUBSCRIPTION
AGENCIES, North Cohocton, *N. Y. 14868*
READ-MORE PUBLICATIONS, INC., 140 Cedar
Street, *New York, N. Y. 10006*
STECHERT-MACMILLAN, INC., 7250 Westfield
Avenue, *Pennsauken N. J. 08110*
- VIETNAM**
XUNHASABA, 32, Hai Ba Trung, *Hanoi*
- YUGOSLAVIA**
JUGOSLAVENSKA KNJIGA, Terazije 27, *Beograd*
FORUM Vojvode Mišića 1, *21000 Novi Sad*

Acta

Morphologica

Academiae
Scientiarum
Hungaricae

ADIUUVANTIBUS

I. TÖRŐ, J. BALÓ, E. BEREĞI, P. ENDES,
B. HALÁSZ, H. JELLINEK, I. KROMPECHER,
K. LAPIS, GY. RAPPAY, GY. ROMHÁNYI, P. RÖHLICH,
J. SUGÁR, J. SZENTÁGOTHAÍ, I. TARISKA

REDIGIT

E. SOMOGYI

TOMUS XXV * FASCICULI 2-3



1977

Akadémiai Kiadó Budapest

ACTA MORPHOLOGICA

A MAGYAR TUDOMÁNYOS AKADÉMIA
ORVOSTUDOMÁNYI KÖZLEMÉNYEI

SZERKESZTŐSÉG ÉS KIADÓHIVATAL: 1054 BUDAPEST, ALKOTMÁNY U. 21.

Az Acta Morphologica angol nyelven közöl értekezéseket a kísérletes orvostudomány tárgyköréből.

Az Acta Morphologica változó terjedelmű füzetekben jelenik meg. Több füzet alkot egy kötetet.

A közlésre szánt kéziratok a következő címre küldendők:

Acta Morphologica, 1091 Budapest, Üllői út 93.

Ugyanerre a címre küldendő minden szerkesztőségi és kiadóhivatali levelezés.

Megrendelhető a belföld számára az Akadémiai Kiadónál (1368 Budapest Pf. 24. Bankszámla: 215-11488), a külföld számára pedig a „Kultura” Külkereskedelmi Vállalatnál (1389 Budapest 62, P.O.B. 149 Bankszámla: 218-10990) vagy annak külföldi képviselőinél.

Die Acta Morphologica veröffentlichen Abhandlungen aus dem Bereich der experimental-medizinischen Wissenschaften in englischer Sprache.

Die Acta Morphologica erscheinen in Heften wechselnden Umfanges. Mehrere Hefte bilden einen Band.

Die zur Veröffentlichung bestimmten Manuskripte sind an folgende Adresse zu senden:

Acta Morphologica, 1091 Budapest, Üllői út 93.

An die gleiche Anschrift ist jede für die Schriftleitung und den Verlag bestimmte Korrespondenz zu richten. Abonnementspreis pro Band: \$ 36.00.

Bestellbar bei »Kultura« Außenhandelsunternehmen (1389 Budapest 62, P.O.B. 149. Bankkonto Nr. 218-10990) oder seinen Auslandsvertretungen.

National Institute of Rheumatology and Physiotherapy, Budapest

EARLY DIAGNOSIS OF CANCER BY GASTRICBIOPSY

M. BÉLY and I. KEMPELEN

(Received October 5, 1976)

On the basis of 350 gastric biopsies the difficulties of early diagnosis of cancer are discussed. The technical and morphological stumbling blocks of evaluation are reviewed. The differences between the gross and microscopic diagnoses, the more important causes of histologic error are dealt with.

Biopsy plays a most important role in the early diagnosis of gastric cancer [4, 5, 8, 10, 13]. The clinician calls a cancer an early one if it is small, localized, produces few or non-typical symptoms and is difficult to diagnose [14, 15]. In pathology, the difficulty of an interpretation of the term "early cancer" lies in the fact that in the case of a structure showing irregular polymorphism of nuclei, forms dividing with polychromasia, etc., the process is not yet a cancer [2, 3, 9, 12]. All the pathologist can say in such cases is that malignant transformation is conceivable or that there is good reason to suspect malignancy. A certainly cancerous form is not early, because it is independent of the size of the primary focus and metastases may occur in that stage already. As far as prognosis is concerned, it is said [11] that it is the depth of infiltration that is decisive, the superficial area plays no role [3]. Although metastases may occur also with the form localized to the mucosa and the submucosa, it is more benign [11], just like a lympho-plasmocytic infiltration, secondary follicle formation, adjacent reactive fibrosis may be indicative of an increased systemic defensive activity [2, 6, 7]. According to the definition by the Japanese Gastroenterological Endoscopic Society, early cancer is localized to the tunica propria and submucosa [1]. Therefore it is fully justified to use the synonymous expression "superficial cancer".

The following brief survey has been prepared on grounds of 350 biopsies performed in 1974/75, with the Olympus JEB-2 duodenoscope and the Olympus GIFK oesophago-gastro-duodenoscope. The diagnosis of cancer on the basis of biopsy was confirmed, or the erroneous diagnosis corrected, by examination of a gastric resection specimen.

The experience and skill of the examiner play a decisive role in the recognition of superficial or early cancer. Most frequently, the early cancer is 5 sg. cm,

In honour of the 70th anniversary of Professor K. FARKAS.

or often less than 2 sg. cm in size, located to the corpus-antrum junction of the lesser curvature. It is often multicentric, and it depends on the experience of the examiner whether the specimen is taken from that area.

On the basis of the gross appearance the following forms can be distinguished:

- I. Protruding, polypous type
- II. Superficial type
 - a.) elevated
 - b.) flat
 - c.) depressed
- III. Excavated type

Radiologically, the polypous and the ulcerative forms are easily detectable, while type II is difficult to recognize. It is exclusively by means of biopsy that forms I and III can be differentiated from benign mucosal polyp or peptic ulcer, and that type II can be recognized [5].

Sometimes it is merely by chance that the area judged to be pathological is pinched, because the instrument may always be dislodged a few mm as a result of peristalsis. Superficial cancer never develops when the gastric mucosa is intact or normal. Practically always more or less marked inflammation, hyperaemia, increased tendency to bleeding may be seen [13, 14, 15]. Thus, a bleeding following biopsy may make a subsequent control examination unfeasible. Since this is not one of the typical sources of error in histological processing and evaluation, we do not wish to deal with it here. It follows from the nature of the intervention that the specimen obtained is usually small and damaged. Irregular or atypical patterns may often be visible in independent fragments, but taken out of its environment it is difficult or even impossible to say whether there is an infiltration. In such cases, it may be necessary to repeat the biopsy [6, 7]. Histologically, the following forms may be distinguished.

- a) adenocarcinoma (Figs 1 and 2)
- b) signet-ring cell, mucus producing cancer (Figs 3 and 4)
- c) anaplastic cancer (Fig. 5)
- d) mixed form cancer (Fig. 6)

Glands lined on the inside with several layers of increased basophilic epithelium, irregular in polarity and shape may be traced back to cell proliferation caused by inflammatory irritation or an occlusion of the glandular lumina (Fig. 7).

Numerous divisions of nuclei, polymorphism, polychromasia of nuclei, nuclei of increased size, or ballooning ones with several nucleoli may occur in

every kind of chronic inflammation and do not necessarily indicate malignancy (Fig. 8).

An increase in the number of goblet cells, a transformation of the gastric mucosa reminiscent of intestinal mucosa by themselves do not indicate precancerosis. Such changes frequently occur in aged patients with chronic gastritis, without the detection of malignant transformation on repeated examinations [2, 10] (Figs 9, 10).

Clumsy cell forms vagueness of the glandular structure even if restricted to just one group of glands may justifiably arouse the suspicion of malignant transformation (Fig. 11).

A disorganized structure, infiltrative growth unequivocally indicate malignancy. Mistakes are, of course, possible even in such cases. On the basis of

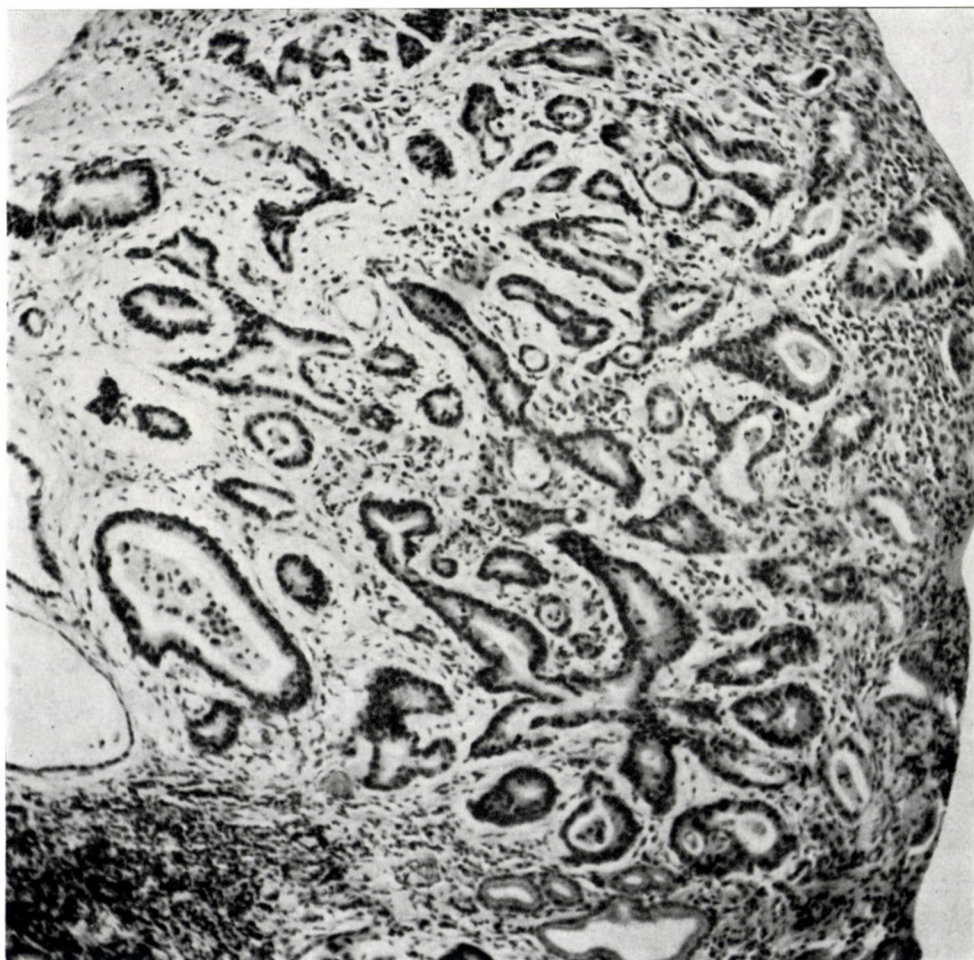


Fig. 1. Adenocarcinoma

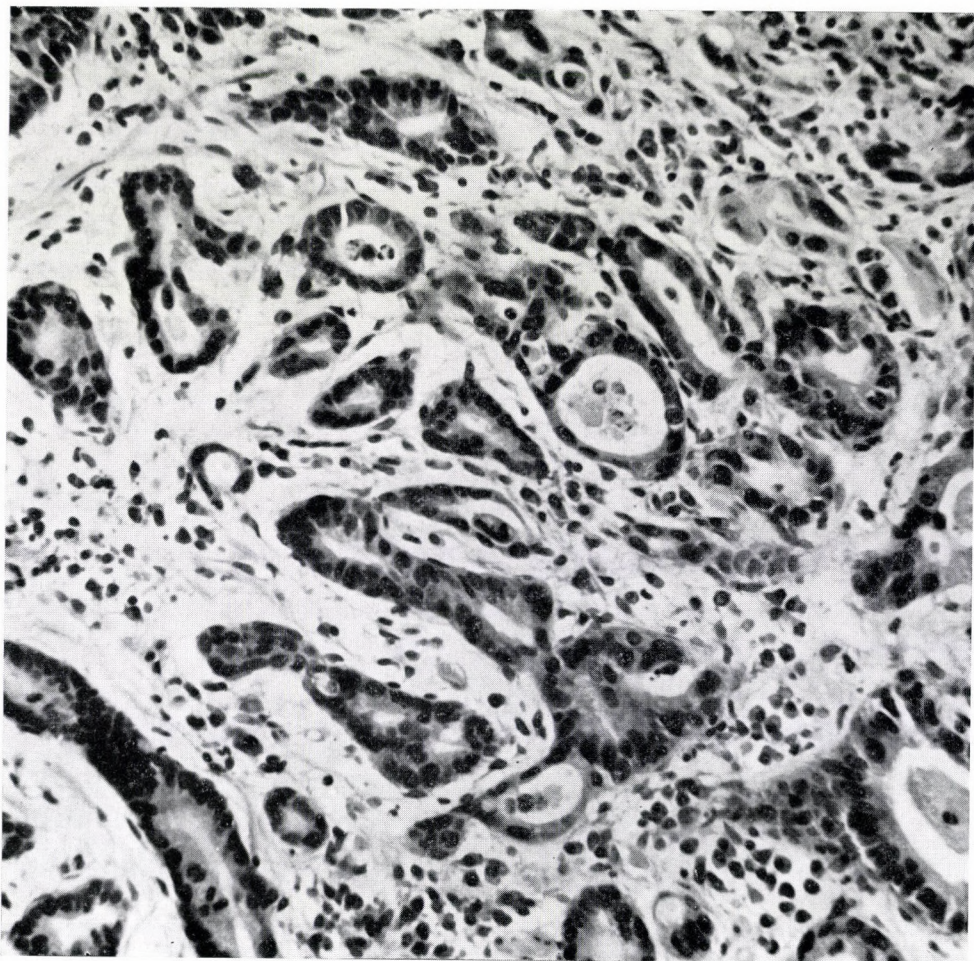


Fig. 2. Adenocarcinoma

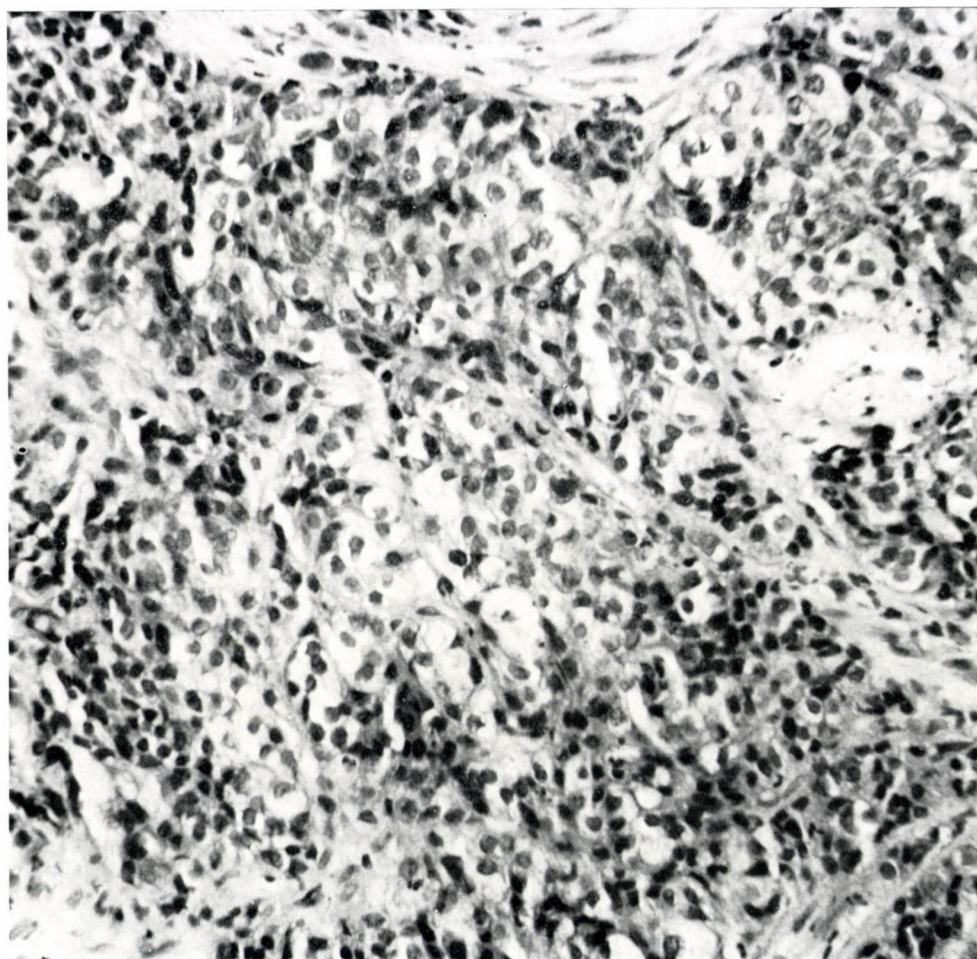


Fig. 3. Cc muciparum

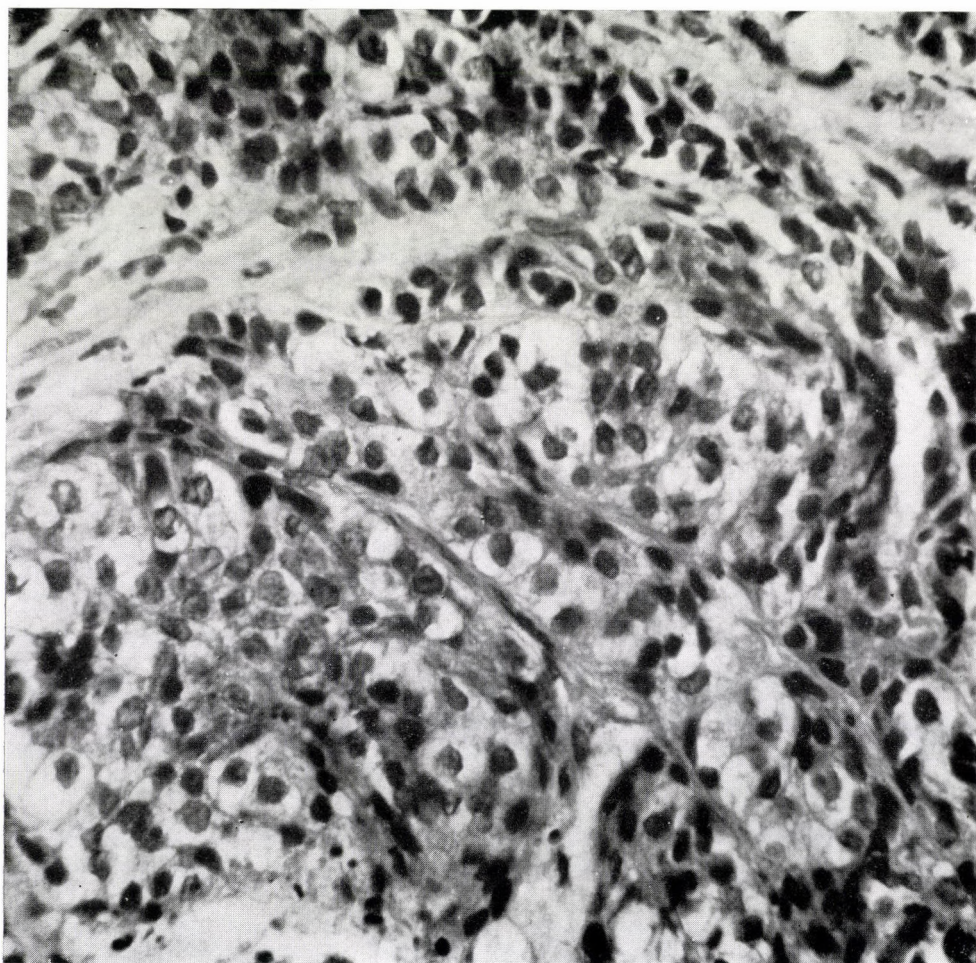


Fig. 4. Cc muciparum

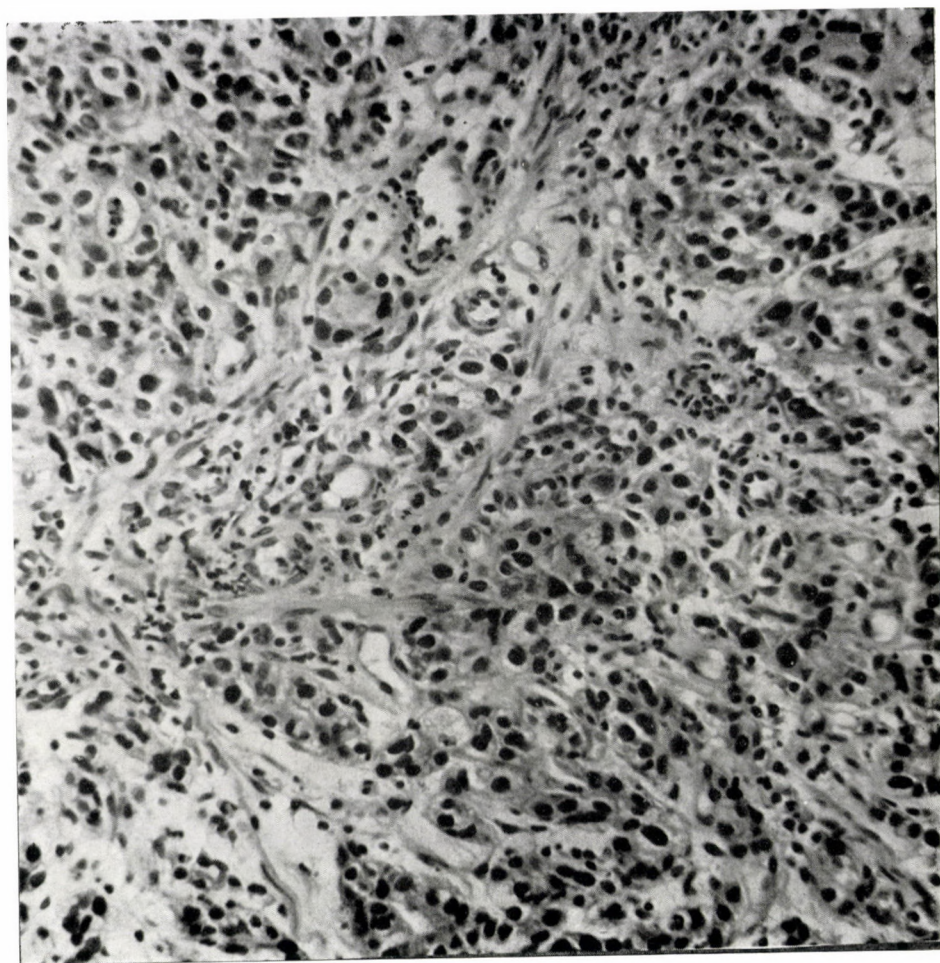


Fig. 5. Cc anaplasticum

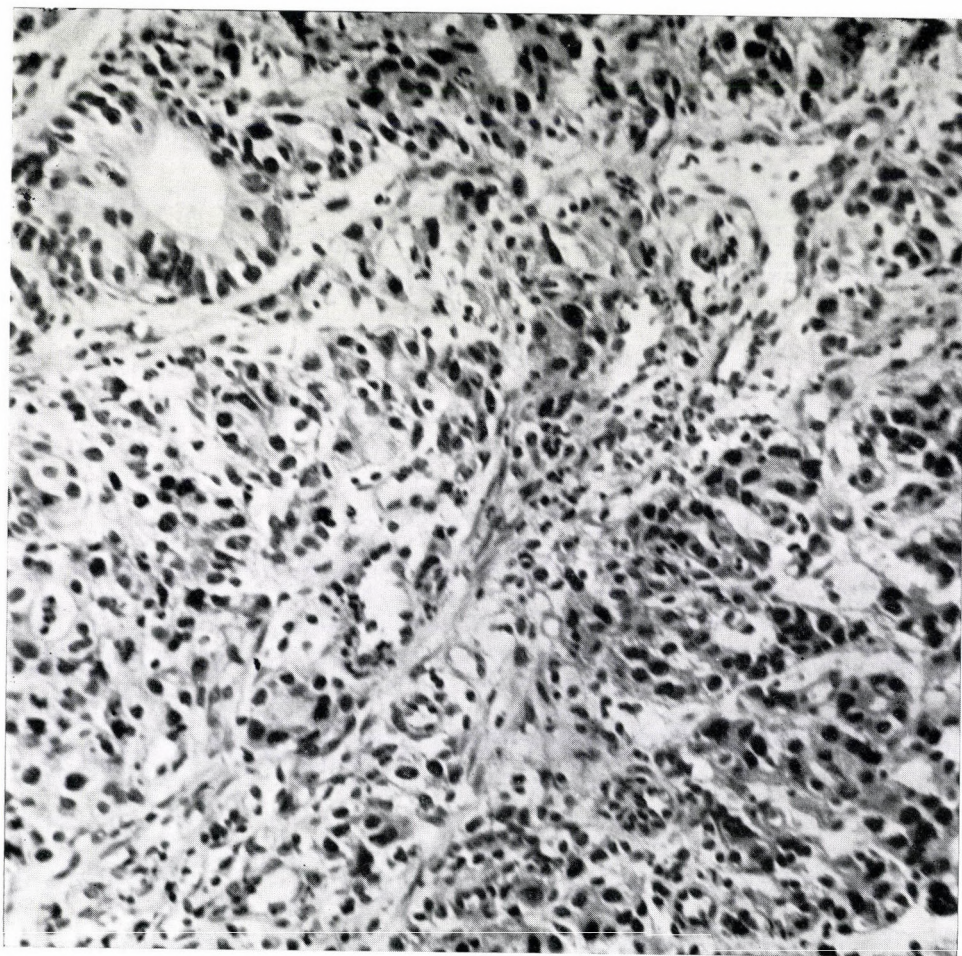


Fig. 6. Mixed form of cancer

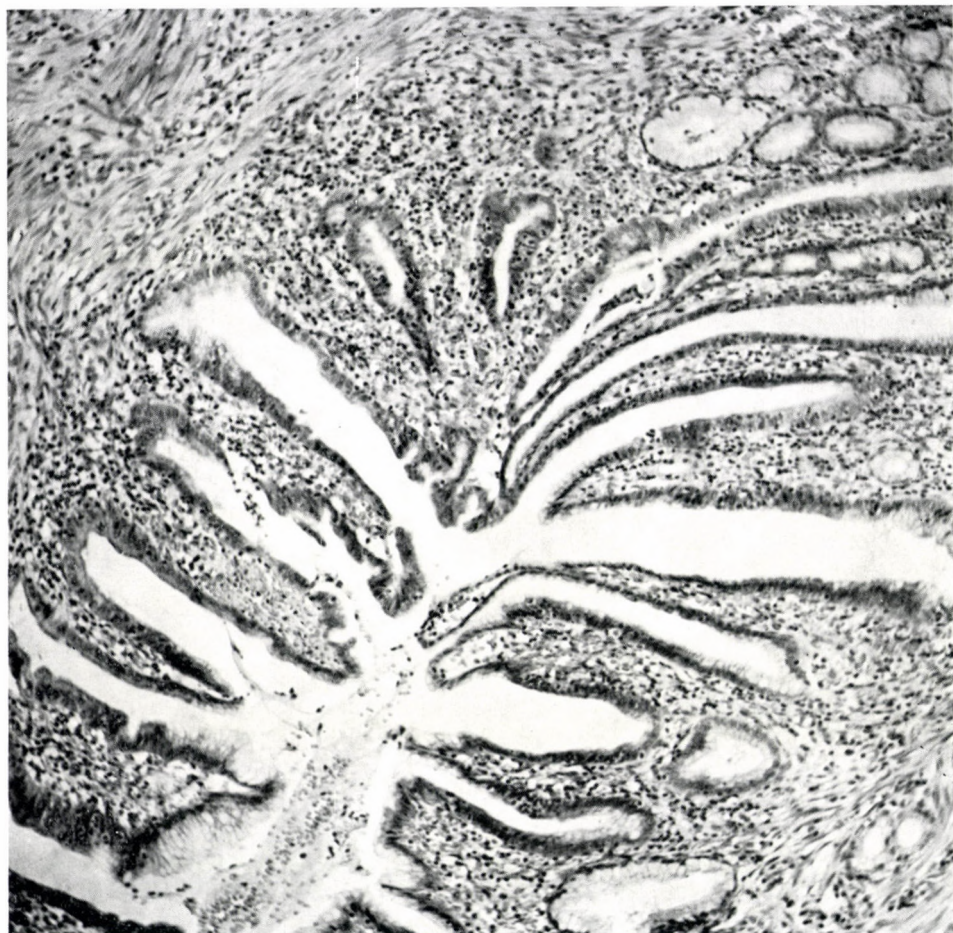


Fig. 7. Changes caused by inflammatory irritation

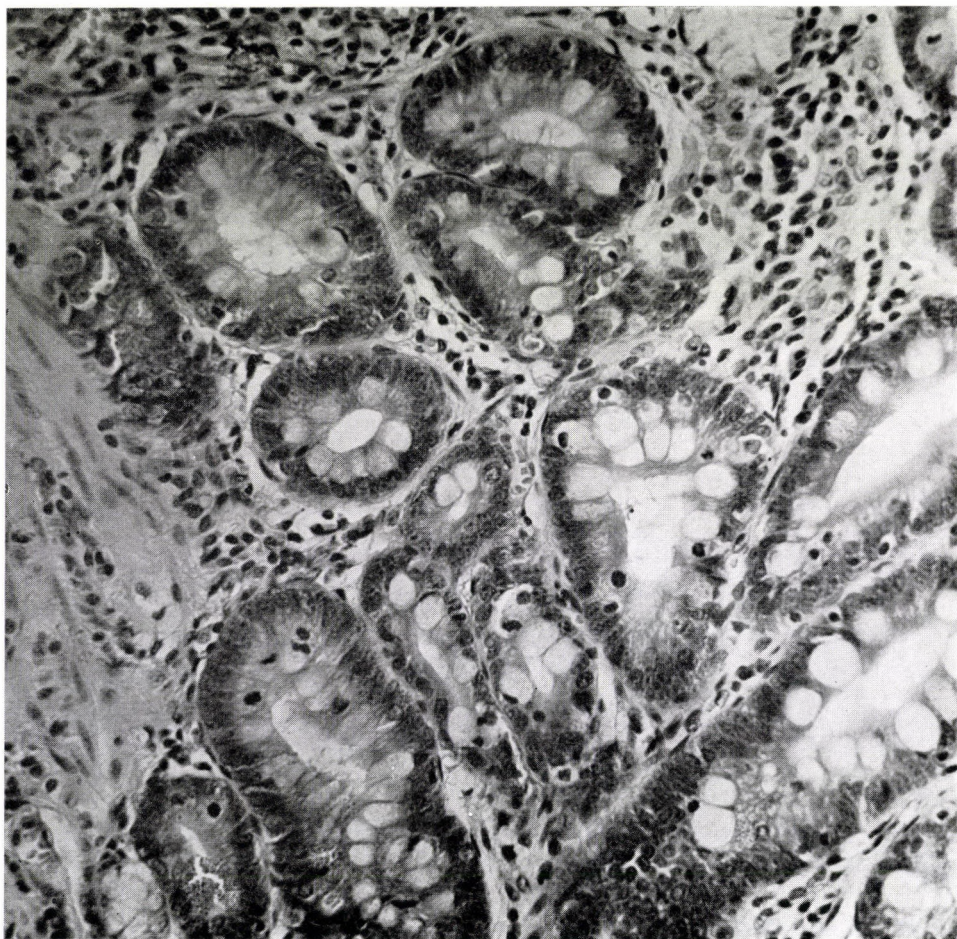


Fig. 8. Changes caused by inflammatory irritation



Fig. 9. Changes caused by inflammatory irritation



Fig. 10. Changes caused by inflammatory irritation

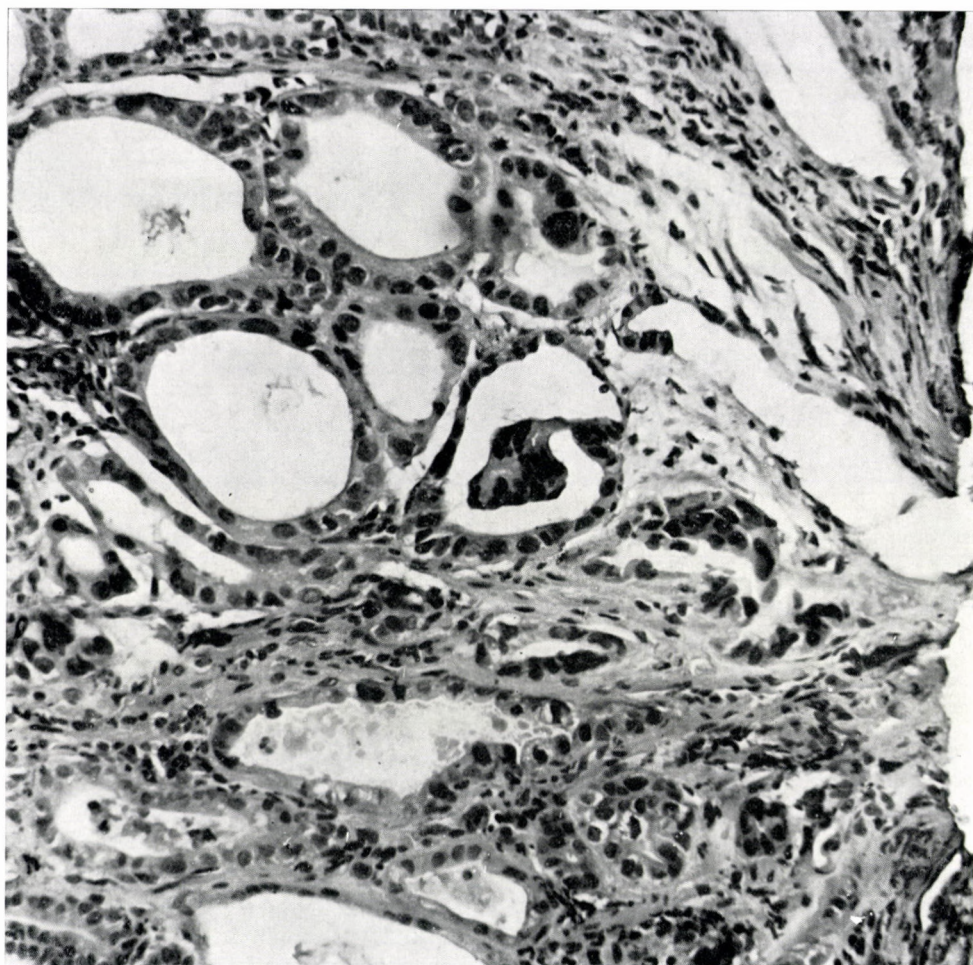


Fig. 11. Clumsy cell form vagueness of the glandular structure

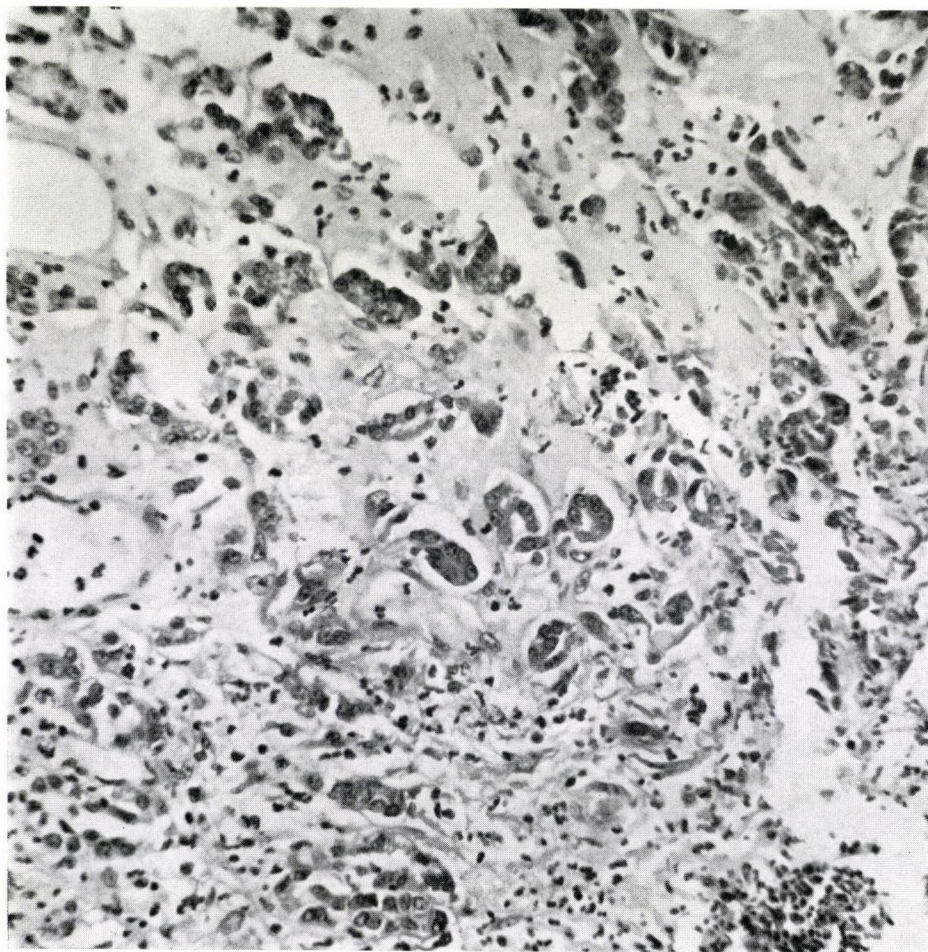


Fig. 12. Pancreatic structure caused by chronic pancreatitis

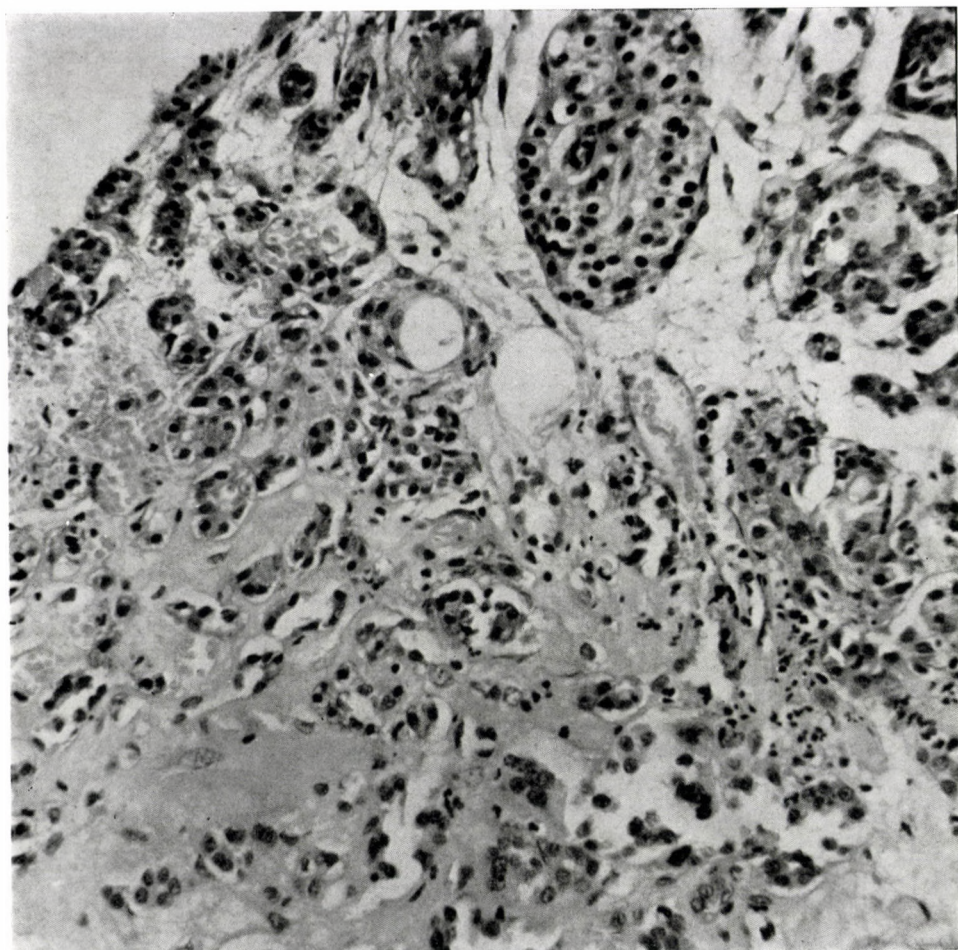


Fig. 13. Pancreatic structure caused by chronic pancreatitis

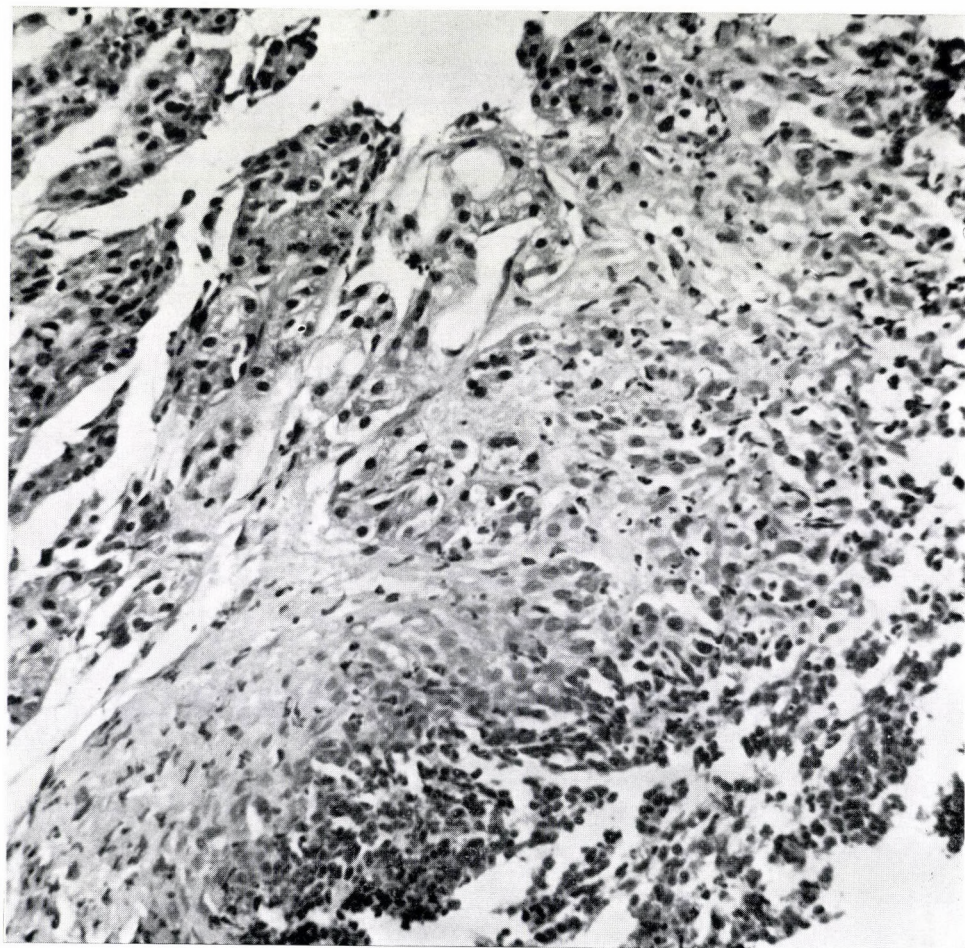


Fig. 14. Pancreatic structure caused by chronic pancreatitis

studying 12 to 14 pictures, we have suggested cancer, which actually proved to be the base of a chronic ulcer penetrating into the pancreas, pancreatic tissue brought into turmoil by chronic pancreatitis. Possibly the site of biopsy could have suggested pancreatic involvement in this case. The correct diagnosis was established by studying the resected stomach.

The gross appearance often arouses the suspicion of malignancy, which cannot be corroborated by biopsy, or merely a tentative diagnosis may be set up. For instance, intact mucosa may be pinched from over a submucosal cancer growing infiltratively.

On the other hand, a change believed to be benign on gross examination may prove to be malignant. The diagnostic score may be improved when the gross and microscopic findings are controlled with examination of the resected specimen, and when the endoscopic studies are made jointly by the physician and the morphologist where this is feasible. The opinion proffered will be more adequate in possession of both the gross and the microscopic evidence than it is when based exclusively on the histologic findings.

REFERENCES

1. ASHIZAWA, S., KIDOKORO, T.: Endoscopic Color Atlas of Gastric Disease. G. Thieme Verlag, Stuttgart p. 5., 1971. — 2. BÉLY, M., KEMPELEN, I.: Die Fallen der Gastrobiopsie, die Schwierigkeiten der Morphologischen Auswertung bei durch Operation Bestätigten Fällen. 3. European Congress of Gastrointestinal Endoscopy. Abstr. p. 143. Hungarian Society of Gastroenterology, Budapest 1976. — 3. CAIN, H., KRAUS, B.: (1973) Frühcarcinom des Magens (Morphologische Beobachtungen und Probleme). Dtsch. med. Wschr. **98**, 1591—1595. — 4. DVORSKY, A.: (1975) 15 years experiences in endoscopy of the cancer of the stomach. Akt. Gastrol. **4**, 211—213. — 5. ELSTER, K., KOLACHEK, F., SHIMAMOTO, K., FREITAG, H.: (1975) Early gastric cancer experience in Germany. Endoscopy **7**, 5—10. — 6. FIGUS, I. A., SIMON, I., BAJTAI, A., BÁNKY, GY.: (1971) A krónikus gastritis II. Röntgen és gastroscopos vizsgálatok. Orv. Hetil. **112**, 668—672. — 7. FIGUS, I. A., SIMON, I., BAJTAI, A., BÁNKY, GY., SZABÓ, I.: (1976) Endoscopos electrocauterus beavatkozások a gyomorban. Orv. Hetil. **117**, 715—718. — 8. FRÜHMORGEN, P., CLASSEN, M., HERMANEK, P., DEMLING, L.: (1972) Diagnostik des Magencarcinoms mit Glasfaserendoscopen. Dtsch. med. Wschr. **97**, 1443—1447. — 9. GRUNMAN, E.: (1975) Histologic types and possible initial stages in early gastric carcinoma. Beitr. path. Anat. **154**, 256—280. — 10. KOBAYASHI, S., YOSHI, Y., KASOGAI, T.: (1976) Biopsy and cytology in the diagnosis of early gastric cancer. Endoscopy, **8**, 53—59. — 11. KONJETZNY, G. E.: (1940) Der oberflächliche Schleimhautkrebs des Magens. Chirurg **12**, 192—196. — 12. KRAUSPE, C., GUSSE, W.: (1961) Über Frühstadien des Magencarcinoms. Verh. dtsch. ges. Path. **45**, 183—190. — 13. REISSI, H., LEDERER, B., SCHWAMBERGER, K., FALSER, N., WALTER, W.: (1976) Early gastric cancer — our results. Akt. Gastrologie **5**, 161—196. — 14. RÖSCH, W., KOCH, H.: (1976) Early gastric cancer: gross aspect and biopsy. Akt. Gastrol. **5**, 239—251. — 15. SAKITA, T., OGURO, Y., YOSHIMORI, M.: (1976) Recent advances in endoscopic diagnosis and treatment of early gastric cancer. Akt. Gastrol. **5**, 213—227.

DIE FRÜHDIAGNOSE DES KREBSSES MIT HILFE DER GASTROBIOPSIE

M. BÉLY und I. KEMPELEN

Die Schwierigkeiten der Frühdiagnose des Krebses werden aufgrund von 350 Gastrobiopsien erörtert und eine Übersicht der technischen und morphologischen Probleme der Auswertung gegeben.

Im weiteren werden die Unterschiede der makro- und mikroskopischen Diagnosen aufgezeigt, ferner die wichtigsten Ursachen der histologischen Fehlinterpretationen besprochen.

РАННИЙ ДИАГНОЗ РАКА С ПОМОЩЬЮ ГАСТРОБИОПСИИ

М. БЕЛЬ и И. КЕМПЕЛЕН

На основе результата 350 гастробиопсий обсуждаются трудности раннего диагноза рака и дается обзор технических и морфологических проблем оценки полученных данных.

В дальнейшем указываются на разницы макро- и микроскопических диагнозов и на важнейшие причины ошибочных гистологических результатов.

Dr. Miklós BÉLY }
Dr. Imre KEMPELEN } Országos Reuma és Fizioterápiás Intézet,
 1525 Budapest, Pf. 54., Hungary

National Institute of Rheumatology and Physiotherapy, Budapest

DANGERS OF POSITIVE PRESSURE RESPIRATION BREATHING WITH SPECIAL REFERENCE TO THE SO-CALLED “SURFACTANT FACTOR”

I. BETLÉRI and M. BÉLY

(Received October 5, 1976)

Atelectasis and emphysema have been induced in rabbits after anaesthesia and IPPB for one hour at 30 cm water pressure. The pulmonary surfactant became coarsely granular and appeared in the form of large drops. A correlation is suggested to exist between this phenomenon and the atelectasis and emphysema which developed during IPPB.

There are numerous data on the role of pulmonary surfactant (PS) in the development of intra- and postoperative pulmonary changes such as emphysema, atelectasis, etc. PS is produced or excreted by the II-type pneumocyte of the alveolar wall [8].

PS is a glyco-lipoprotein containing phospholipid. Of the lipid portion, 60% is dipalmitin-lecithin. It also contains small amounts of other phospholipids, and is ultraviolet-fluorescent. Metabolic and electron microscopic studies have shown that PS is excreted as a lipoprotein. It is easy to demonstrate its carbohydrate component, while demonstration of its lipid factor requires cytochemical procedures. ADAMSON and BOWDEN [1] identified PS by means of the tricomplex flocculation method of DERMER [3]. While MEBAN [7] in electron microscopic studies by the gluteraldehyde method could prove that the granulated pneumocytes were actively involved in the synthesis of PS and were not merely in its excretion. In their electron microscopic studies DELARUE et al. [2] found the size to vary from 100 to 600 Å and showed that it contained high amounts of carbohydrate. SCARPELLI [10] identified also neutral fats in the substance and GIESEKING [5] found in the 6 month fetus the osmiophilic lamellated bodies corresponding to preformed SF in the II pneumocytes, and arising from osmiophilic globular inclusions. The sonic was shown by the light and electron microscopic studies of JÓZSA and RÉFFY [6] performed with ROMHÁNYI's method [9].

The role of the PS is to ensure the constancy of surface tension in the alveoli, to facilitate gas exchange, to protect underlying tissues from exsiccation.

In honour of the 70th anniversary of Professor K. FARKAS.

There are forces which increase, and others which decrease the alveolar surface.

1. *Mechanical forces*

- a) tissue elasticity \uparrow \downarrow *
- b) pleural pressure \uparrow
- c) pulmonary capillary pressure \downarrow

2. *Colloidosmotic forces*

- a) colloidosmotic pressure in the pulmonary capillaries \uparrow
- b) colloidosmotic pressure in the tissue interspaces \downarrow

3. *Surface forces* (Fig. 7)

Note: the arrows pointing upward indicate an increase, those pointing downward indicate a reduction of the alveolar surface.

In rabbits subjected to positive pressure respirator treatment we have studied the morphological sequelae visible in the lungs, with special attention to the PS.

Adult male and female rabbits in the supine position were anaesthetized with droperidol with fentanyl then the trachea was incised and a rubber tube was fixed in place, airproof. This was attached to the UNA II anaesthesia apparatus and the animals were respired for one hour in a semi-closed system with an 1 : 2 mixture of oxygen–nitrogen oxide.

Three animals served as controls. Three animals were anaesthetized as described above, intubated and allowed to breathe spontaneously for one hour.

Three animals after relaxation with 0.05 mg/kg body weight of pancuronium bromide were respired manually at 20 cm water pressure. Six animals like in the previous group were respired manually at 30 cm water pressure.

After one hour breathing, while still under anaesthesia, the animals were killed by opening the chest and taking out the lungs. After gross examination, specimens were taken to make frozen sections, paraffin-embedded sections and for electron microscopic study by the ruthenium red procedure.

* The smaller the radius of the alveolus, the thicker the PS film present in it, and the lower the surface tension, the easier dilates the alveolus. This means that when the alveolus is over-dilated, the surface tension of the PS film lining it increases, preventing further dilatation. Thus, PS keeps up an equilibrium as far as the internal diameter of the alveoli is concerned, and so prevents emphysema and atelectasis. Consequently, a deficiency of PS, due to its insufficient production or increased utilization has a causal role in the development of both emphysema and atelectasis.

Results

The lungs from the intubated and spontaneously respiration animals exhibited neither gross, nor microscopic changes, as compared to the controls.

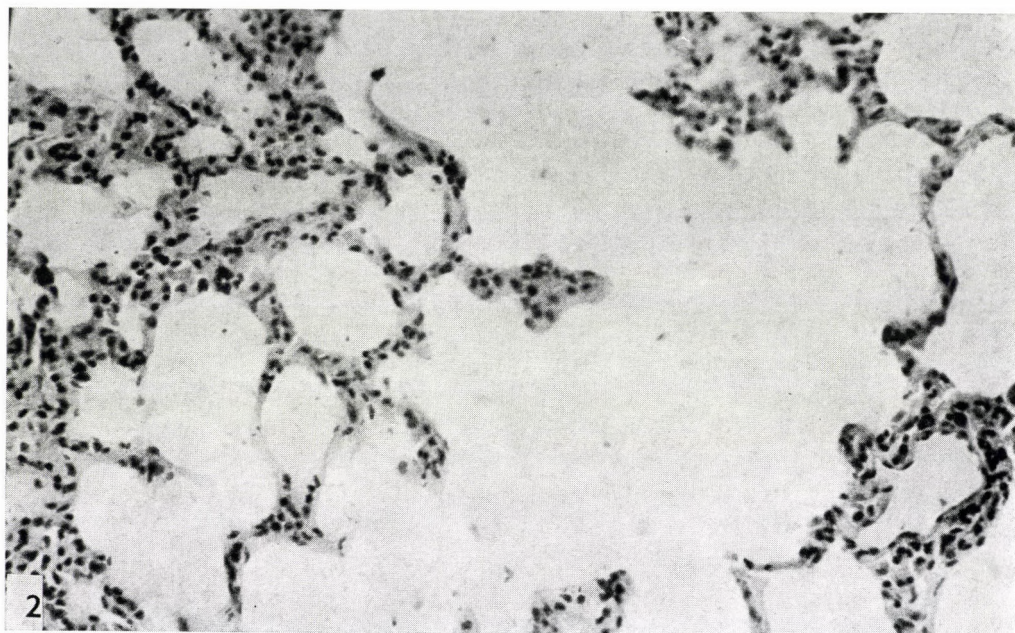
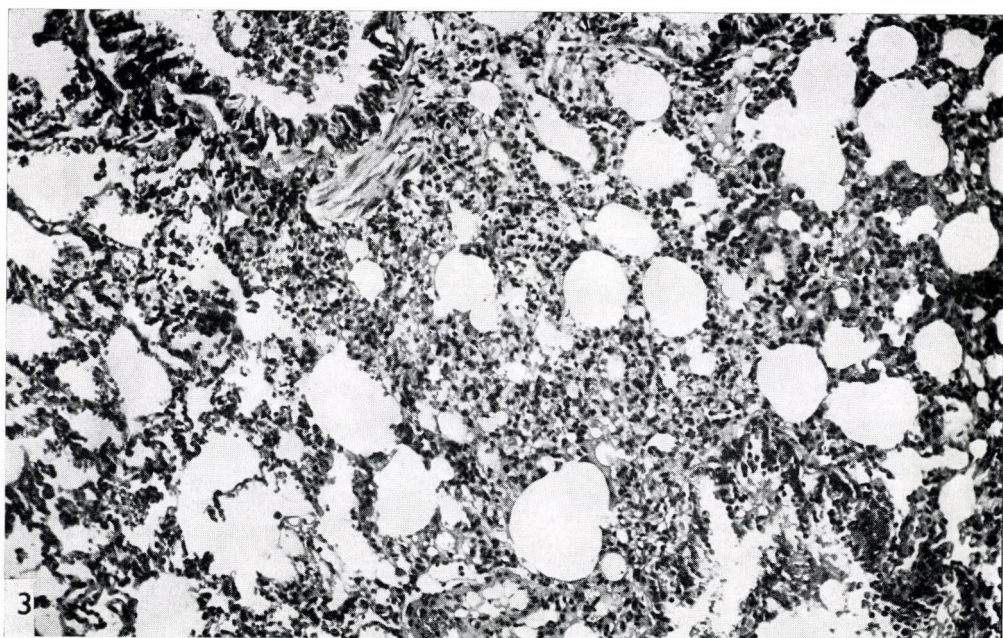
Among the animals subjected to IPPB, significant changes were found mainly in the 30 cm water pressure group. The lungs of these animals appeared to be emphysematous but at the same time in every animal there were scattered confluent areas of atelectasis, particularly in the lower lobes (Fig. 1). In the bronchi at sites marked hyperaemia and increased mucus production were visible.



Fig. 1

The embedded section were stained with haematoxylineosin and by the PAS method. In these sections, atelectasis was clearly visible beside a bullous, confluent emphysema (Figs 2 and 3).

By studying in polarized light frozen sections treated with the metachromatic method [9] we could identify the PS. This under normal conditions appears as a brilliant thin yellowish layer evenly covering the alveolar lumen, in sharp contrast to the dark base. This was what we saw also in sections obtained from the control animals (Fig. 4.). In contrast, in the lungs of animals respiration at 30 cm water pressure, the PS appeared in the form of coarse granules like

*Fig. 2**Fig. 3*

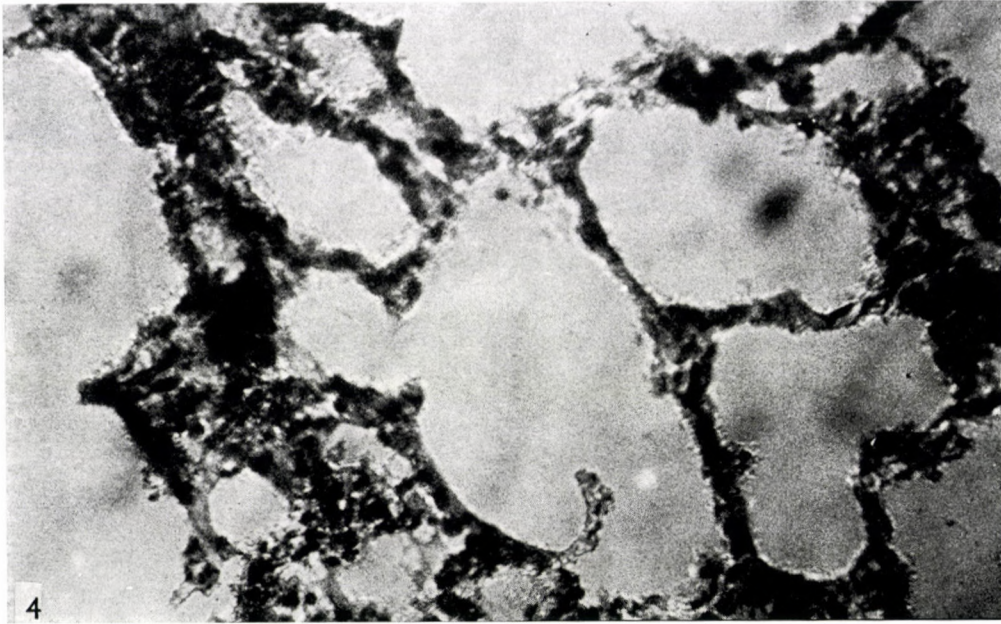


Fig. 4

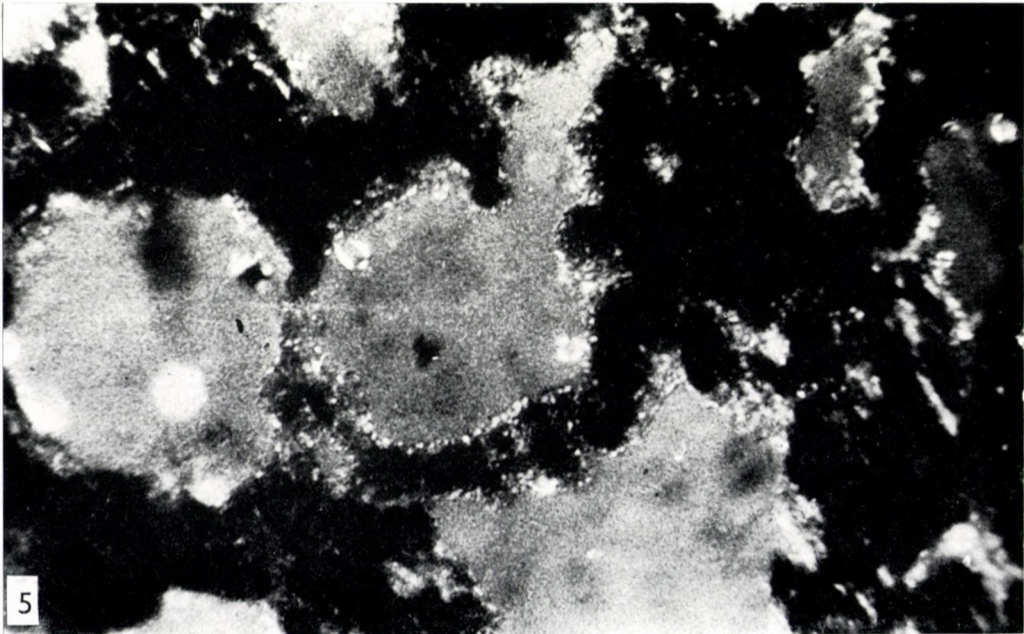


Fig. 5

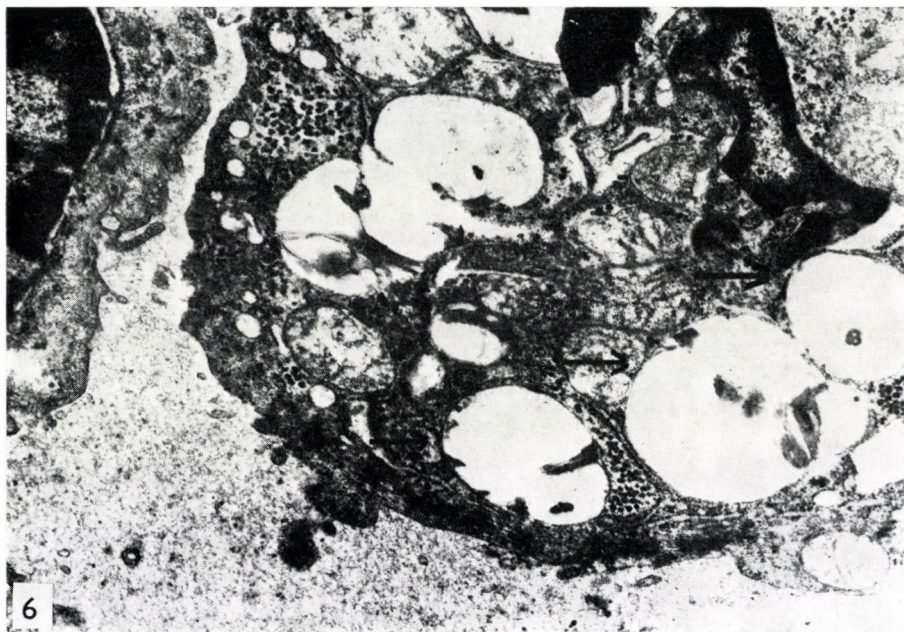


Fig. 6

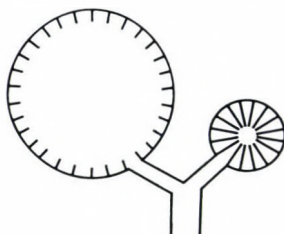


Fig. 7

brilliant dewdrops at sites. Their distribution was uneven, and the appearance of the changes varied from lung area. The granular, drop-like transformation of the material could be observed in the emphysematous and atelectatic areas observed in the emphysematous and atelectatic areas alike (Fig. 5.).

In electron microscopic investigations we have succeeded in identifying the material, like JÓZSA and RÉFFY [6] as well as other investigators did, and could demonstrate the osmiophilic bodies of the granulated pneumocytes (Fig. 6.)

Discussion

Anaesthesia is now almost invariably performed by intubation. Its potential hazards, complications and some eventual untoward, although indirect, effects respiratory balance are well-known. Still the procedure interferes profoundly with the mechanism of respiration. Irrespective of the technique employed, IPPB replaces the work of the elastic skeletal structure of the chest, which exerts its effect through a negative intrathoracic pressure. In IPPB this is done by a pump system combined with valves. Plainly speaking: we pump air into the respiratory pathways from the outside, creating therein pressures higher than the physiologic. This is of no consequence as long as we have to deal with a lung capable of sufficient adaptation. We attain our goal: we introduce an ideal mixture of gases into the respiratory tract, in quantities always meeting the actual demands. But when the adaptability of the respiratory and circulatory systems is impaired, for instance as a result of the common wear and tear diseases (emphysema, arteriosclerosis), these potential advantages may easily turn into iatrogenic hazards. IPPB may expose the emphysematous lung tissue of diminished elasticity to severe mechanical insult: the alveoli will continue to rupture, and even pneumothorax may ensue. It is also known that more or less extensive areas of atelectasis can be found in the lower pulmonary lobes of persons who died hours or days after surgery, just as well as in those subjected to mechanical respiration.

No far-reaching human pathological conclusions can be drawn from our studies. Still, we may seek a correlation between the morphological transformation of the PS and the emphysema and atelectasis which developed simultaneously during respiration at pressures exceeding the physiologically permissible one. We cannot say whether it is the secretory activity of the granulated pneumocytes that suffers or the physicochemical properties of the substance protecting the alveolar wall are changed by it.

There seem to be differences in this kind of sensitivity among the various species of animals. This is suggested by the investigations of FRANK et al. [4] who could not reproduce the changes described by us in dogs under somewhat similar experimental conditions. It remains, to be seen how the human lung behaves in this respect. All these require further investigations, first of all on human material.

REFERENCES

1. ADAMSON, I. Y. R., D. H. BOWDEN: (1970) Oxygen poisoning in mice. Ultrastructural and surfactant studies during exposure and recovery. *Arch. Path.* **90**, 463—472. — 2. DELAURE, J. S., R. KHALIFAT: (1969) Démonstration ultrastructurale de polysaccharides dont certains acides, dans le film de surface de l'alvéole pulmonaire. *Poumon et Cœur* **25**, 213—218. — 3. DERMER, G. B.: (1970) The pulmonary surfactant content within type II alveolar cells. *J. Ultrastruct. Res.* **33**, 306—317. — 4. FRANK, J., W. NOACK, P. P. LUNKENHEIMER, H.

ISING, H. KELLER, H. H. DICKHUTH, W. RAFFLENBEUL, M. JACOBSON: (1975) Light- and electron microscopic investigations of pulmonary tissue after high-frequency positive pressure ventilation. — *Anaesthesist* **24**, 171—176. — 5. GIESEKING, R.: (1971) Elektronmikroskopische Befunde beim Atemnotsyndrom. *Verh. dtsch. ges. Path.*, **55**, 22—39. — 6. JÓZSA, L., A. RÉFFY: (1975) Light- and electron microscopic studies of the pulmonary alveolar surfactant. *Acta Biochem. (Jena)* **53**, 58—69. — 7. MEBAN, C.: (1972) The inclusion bodies in granular pneumocytes of hamster lung. *J. Anat.*, **112**, 195—206. — 8. VON NEERGARD, K.: (1929) Neue Auffassungen über einen Grundbegriff der Alveolarmechanismen. *Z. ges. exp. Med.*, **66**, 373—394. — 9. ROMHÁNYI, GY.: cit. JÓZSA, L., A. RÉFFY. — 10. SCARPELLI, E. M.: *The Surfactant System of the Lung*. Lea & Febiger, Philadelphia 1968.

GEFAHREN BEI DER BEATMUNG MIT POSITIVEN DRUCK UNTER BESONDERER BERÜCKSICHTUNG DES SOG. "SURFACTANT-FACTORS"

I. BETLÉRY und M. BÉLY

In der Lunge narkotisierter Kaninchen wurde durch intratracheale Beatmung bei 30 cm-H₂O-Druck im halbgeschlossenen Kreisrespirator-System im einstündigen Experiment Atelektase und Emphysem herbeigeführt. Bei der mikroskopischen Untersuchung der Gefrierschnitte ließ sich mit dem Romhányischen metachromatischen Verfahren beobachten, daß der die Innenfläche der Alveolen auskleidende sog. surfactant factor zu groben Schollen und großen Tropfen verwandelt wird. Die Autoren vermuten zwischen dieser Erscheinung und der im Verlauf der Überdruckbeatmung entstandenen Atelektase und dem Emphysem einen kausalen Zusammenhang. Für die Klärung der humanpathologischen Bedeutung dieser Frage sind weitere Untersuchungen erforderlich.

ОПАСНОСТИ ВЫДЫХАНИЯ ПРИ ПОЛОЖИТЕЛЬНОМ ДАВЛЕНИИ, С ОСОБЫМ ВНИМАНИЕМ НА ТАК НАЗ. SURFACTANT ФАКТОР.

И. БЕТЛЕРИ и М. БЕЛИ

В легких наркотизированных кроликов авторы вызвали путем внутритрахеального дыхания при давлении в 30 см H₂O в полужамкнутой системе в одночасовом эксперименте ателектаз и эмфизему. При микроскопическом исследовании замороженных срезов метachromaticким методом Ромханы наблюдали, что выстилающий внутреннюю поверхность альвеол так наз. surfactant factor показывает крупноглобчатое, крупнокапельное превращение. Между этим явлением и ателектазом и эмфиземой, возникающими при искусственном дыхании повышенным давлением, авторы полагают причинную связь. Для выяснения патологического значения этого вопроса для человека необходимо провести еще дальнейшие исследования.

Dr. István BETLÉRY } Országos Reuma és Fizioterápiás Intézet,
Dr. Miklós BÉLY } H-1525 Budapest, Pf. 54., Hungary

National Institute of Rheumatology and Physiotherapy, Budapest

HISTOGENESIS OF BERYLLIUM-INDUCED BONE TUMOURS

I. FODOR

(Received October 5, 1976)

In response to beryllium treatment, irregular bone formation starts mainly in the marrow cavity of long bones, preceding neoplastic growth. Irregular medullary bone formation may be connected with the endosteum, but usually it develops in the bone marrow, independently of the endosteum. Osteogenesis in the bone marrow may be preceded by fibrosis but irregular bone may be formed also without any previous histological change in the bone marrow.

The tumour develops directly from the medullary bone. The prolonged irritation causes abnormal osteogenesis, which ultimately turns into neoplastic proliferation. Thus, the beryllium-induced bone sarcoma is, from histogenesis point of view, a hyperplaseogenic tumour.

Irregular bone formation is considered a preblastomatous change, because it is closely connected with the development of the tumour and precedes it in time.

The multiplicity of the tumour is explained by the "neoplastic field" theory of WILLIS.

Intravenous administration of poorly soluble beryllium compounds was found to induce tumour formation in rabbits. The tumour corresponds to human osteogenic sarcoma. To follow the phases of bone tumour genesis, we have undertaken to study the histogenesis of bone tumour developing under the effect of beryllium.

Material and methods

Sixty rabbits of 6 months mean age and 1300 to 1500 g in weight, were treated with a 1% beryllium oxide suspension in 5 ml physiologic NaCl solution, administered into an ear vein once a week for 25 weeks. The bones to be studied were fixed in 8% formalin and decalcinated in 10% neutral EDTA. Paraffin sections were prepared and stained with haematoxylin-eosin, azan, methylene blue picrofuchsin, or impregnated with silver.

Results

Following treatment, beryllium oxide granules accumulated in the bone marrow throughout the skeletal system. The granules were found intracellularly in phagocytes with PAS-positive eccentric nuclei, visible in groups or scattered (Fig. 1). Around the beryllium granules the bone marrow became poor in cells, the haemopoietic elements decreased in number. Focal proliferation of reticulum cells occurred in the diaphysis and metaphysis of the long tubular

* In honour of the 70th anniversary of Professor K. FARKAS.

bones in the first place (Fig. 2). The cells became elongated fibroblast-like and fibrous foci developed. Within these, the fibres had homogenized, the homogenous mass enclosing some single cells gave rise to connective tissue osteoid arises, with trabeculae displaying an irregular mesh structure. Apart from form of osteogenesis, islets composed of spongy bone tissue may arise, even without fibrous transformation of the bone marrow (Fig. 3). The bone trabeculae correspond to "spinned" bone. Osteoclasts occur only occasionally, there is no sign of bone tissue breakdown. The medullary "beryllium bone" thus produced may fill the entire marrow cavity. In the spongy part of the metaphysis the beryllium bone is deposited on the surface of the trabeculae of the primary or secondary spongiosa. Deposition seems to take place in phases, beryllium bone and normal bone are formed alternately and mosaic structure develops in addition to the excessive narrowing of the marrow cavities.

In these changes there are no atypical cells, the bone forming matrix is not sarcomatous and there is no cartilage formation either, although this is common in tumours.

The fully developed tumour can readily be differentiated from the medullary or beryllium bone, because the tumour has a sarcomatous stroma, but there are many transitional forms from the typical beryllium bone to the certainly atypical bone sarcoma (Fig. 4). Where the fibrosis of the marrow

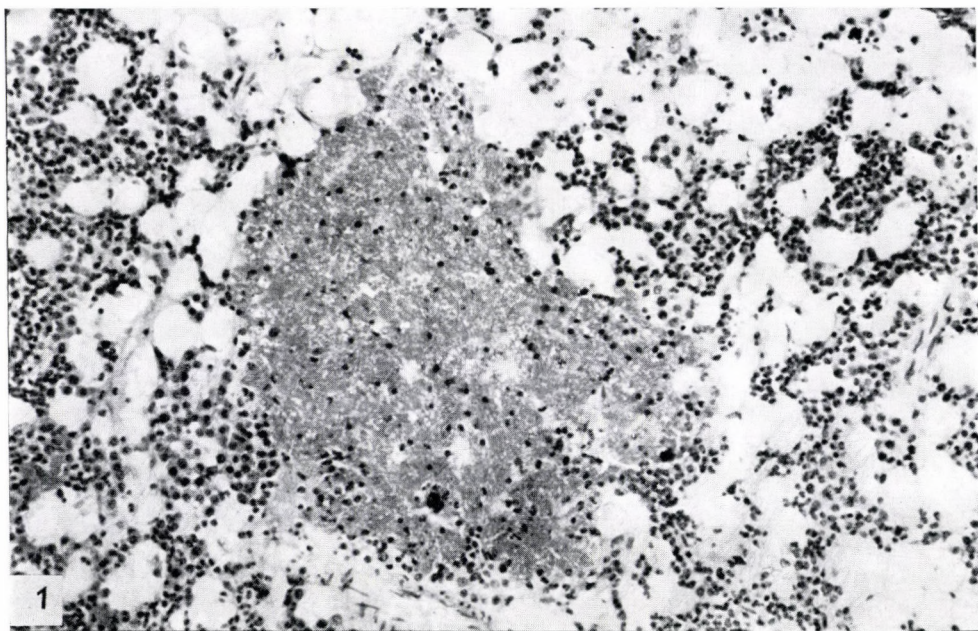


Fig. 1. Phagocytes containing beryllium oxide in the haemopoietic bone marrow. Haematoxylin-eosin, $\times 80$



Fig. 2. Focal reticulum cell proliferation in the metaphysis of the tibia. Haematoxylin-eosin, $\times 80$

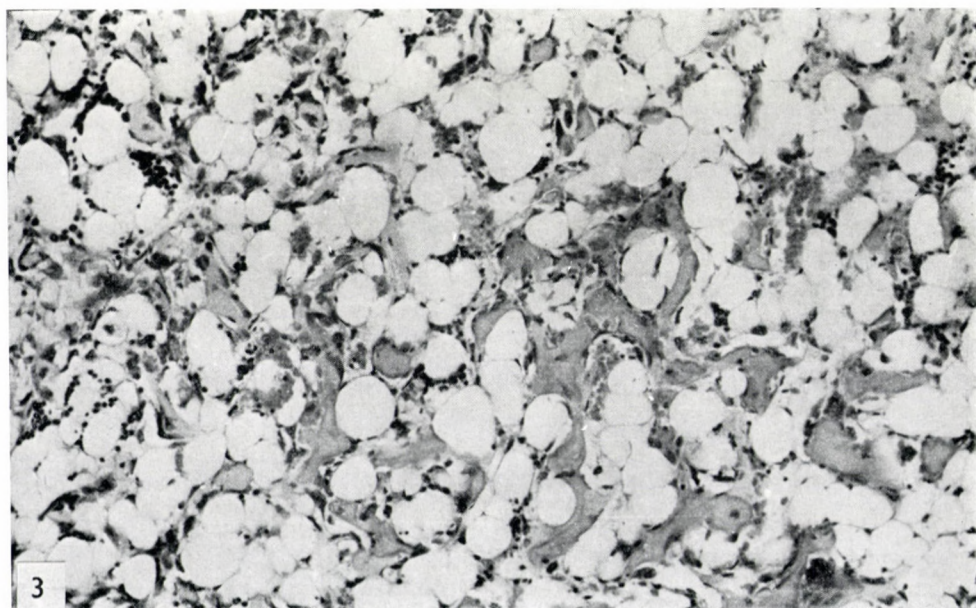


Fig. 3. Osteogenesis in bone marrow without fibrous transformation. Haematoxylin-eosin, $\times 80$

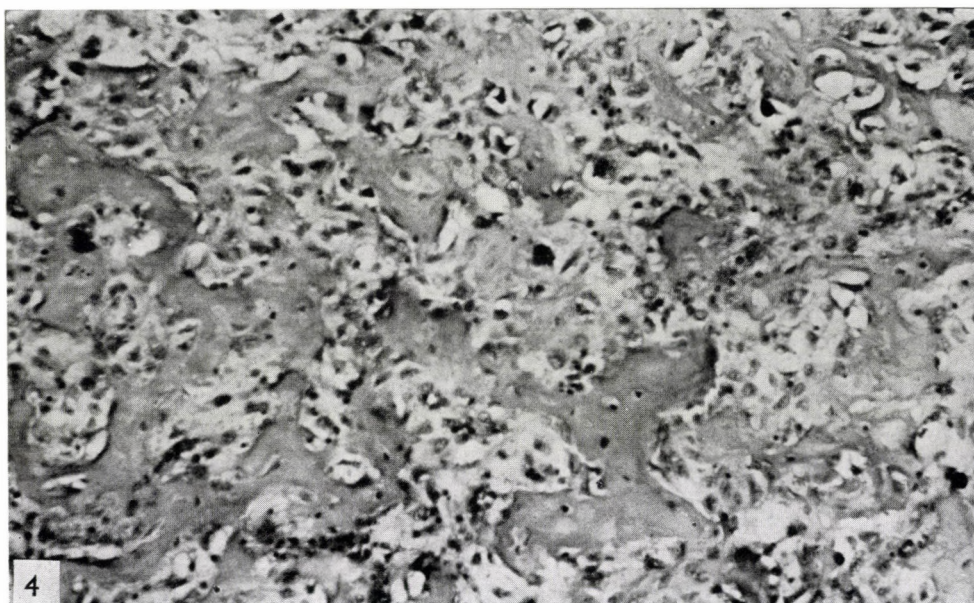


Fig. 4. Neoplastic transformation of medullary bone. Haematoxylin-eosin. $\times 80$

preceded medullary osteogenesis, the stroma becomes more and more cellular and polymorphous and develops into atypical tumour tissue without any sharp borderline. A similar change occurs in the medullary bone tissue which has developed without marrow fibrosis. Of the 60 beryllium-treated animals, 29 survived till the end of the experiment. Of these, 21 had developed sarcoma, while in 8 rabbits beryllium bone tissue could be demonstrated.

Discussion

As far as the changes preceding tumour development are concerned, beryllium accumulation in the bone marrow has been observed also by BARNES et al. [1]. TAPP [11] injected beryllium oxide into the metaphysis of the tibia, and found there a granuloma two months later. The central part of the granuloma was necrosed, this was surrounded by giant cells containing beryllium, and this in turn was surrounded by an inflammatory halo. According to our findings no such granuloma develops when the beryllium is injected intravenously.

CLOUDMAN et al. [2] reported that in response to the intravenous administration of zinc beryllium sillicate the cortex of the long tubular bones of rabbits was unevenly thickened 94 days after the onset of treatment. DUTRA and LARGENT [4] described fibrous foci in the bone marrow, mainly at the end

of tubular bones. JANES et al. [6, 7] observed sclerosis of the tubular bones in animals that developed tumour subsequently. Mineralization and blood supply of this abnormal bone were studied by microradiography by KELLY et al. [8]. They found that the mineral content of the medullary abnormal bone was higher than that of the surrounding normal bone, some lacunae showed calcification and, as demonstrated by filling the blood vessels with indigo gelatin, the blood supply was reduced by the medullary bone formation which filled the marrow cavities.

KELLY et al. [8] consider medullary bone formation to be of endosteal origin. TAPP [11], after implanting beryllium into the marrow cavity, observed endosteal bone formation, but this was absorbed after 8 to 9 months. The phenomenon is a reaction to the inflammation around the granuloma rather than a direct beryllium effect.

According to our findings, medullary bone formation may be connected with the endosteum but it mostly arises in the bone marrow, independently of the endosteum. TAPP [11] emphasized that the development of medullary bone is preceded by no change of any kind. According to BARNES et al. [1] fibrosis of the marrow develops and the medullary bone grows within the fibrotic areas. In our own material we have found examples for both types of bone formation.

The correlation between medullary bone and tumour has been studied by several authors. TAPP [11] found no transition between medullary bone formation and the tumour. According to BARNAS et al. [1] the medullary bone which developed the soil of marrow fibrosis would directly continue to develop into tumour.

In our own material we found several transient forms between medullary bone and neoplastic proliferation, irrespective of the fact whether the medullary bone had developed from marrow fibrosis or without it.

We regard the changes developing in the bones in response to beryllium, particularly the irregular medullary bone formation, as presarcomatous ones, in view of the close connection with the tumour and the fact that the changes precede the development of tumour.

From the point of view of histogenesis, the beryllium-induced bone sarcoma is a hyperplaseogenic growth. The long-lasting stimulation causes irregular bone formation, which ultimately turns into neoplastic proliferation. The increased rate of bone formation may be one of the conditions of the development of bone tumour. It has been known for long that the malignant tumours of bones, particularly the osteogenic sarcomas, arise during the phase of active growth and mainly in the metaphysis of long bones showing the fastest rate of growth [3, 10]. The role of proliferative activity is supported also by the fact that after growth has come to an end, the bone tumours usually arise from bones with increased metabolism. Illustrative of this are Paget's

disease, hyperparathyroidism, chronic osteomyelitis, bone infarction, the callus of fractures and exposure to ionizing radiation [9].

The bone tumours induced by beryllium are often multiple ones. The explanation is obvious. Most of the intravenously administered and poorly soluble beryllium oxide is stored in the reticuloendothelial system of the bone marrow, where it exerts a prolonged action as it slowly dissolves. This way the entire skeletogenic tissue becomes a potentially neoplastic field [12]. Within this, simultaneously or subsequently the connections necessary for neoplastic growth may arise at several sites.

REFERENCES

1. BARNES, J. M., F. A. DENZ, H. A. SISSONS: (1950) Beryllium bone sarcomata in rabbits. *Brit. J. Cancer* **4**, 212—222. — 2. CLODUMAN, A. M., D. VINNIG, S. BARKULIS, J. J. NICKSON: (1949) Bone changes observed following intravenous injections of beryllium. *Amer. J. Path.* **25**, 810—811. — 3. CODMAN, E. A.: Bone sarcoma, P. Hoeber, New York 1925. — 4. DUTRA, F. R., E. J. LARGENT: (1950) Osteosarcoma induced by beryllium oxide. *Amer. J. Path.* **26**, 197—209. — 5. GARDNER, L. U., H. F. HESLINGTON: (1946) Osteosarcomata from intravenous beryllium compounds in rabbits. *Fed. Proc.* **5**, 221—225. — 6. JANES, J. M., G. M. HIGGINS, J. F. HERRICK: (1954) Beryllium induced osteogenic sarcoma in rabbits. *J. Bone Jt Surg.* **36B**, 543—552. — 7. JANES, J. M., G. M. HIGGINS, J. F. HERRICK: (1956) The influence of splenectomy on the induction of osteogenic sarcoma in rabbits. — *J. Bone Jt Surg.* **38A**, 809—816. — 8. KELLY, P. J., J. M. JANES, L. F. A. PETERSON: (1961) The effect of beryllium on bone. — *J. Bone Jt Surg.* **43A**, 829—844. — 9. PUTSCHAR, W. G. J.: In: *Handbuch der Allgemeinen Pathologie* Vol. III/2. pp. 363—439. Springer-Verlag, Berlin—Göttingen—Heidelberg 1960. — 10. SCHINZ, H. R., E. UEHLINGER: (1931) Zur Diagnose, Differentialdiagnose und Therapie der primären Geschwülste und Zysten des Knochensystems. *Ergebn. med. Strahlenforsch.* **5**, 389—397. — 11. TAPP, E.: (1969) Changes in rabbit tibia due to direct implantation of beryllium salts. *Arch. Path.* **88**, 521—529. — 12. WILLIS, R. A.: *Pathology of Tumours*. Butterworth & Co, London 1953.

HISTOGENESE DER MIT BERYLLIUM HERBEIGEFÜHRTEN KNOCHENGESCHWÜLSTE

I. FODOR

In der Markhöhle der langen Röhrenknochen setzt unter Berylliumwirkung — noch vor der Tumorentstehung — eine unregelmäßige Knochenbildung ein. Entsprechend den Untersuchungen des Autors kann zwar irregulärer medullärer Knochen auch im Zusammenhang mit dem Endost entstehen, bildet sich aber im Großteil der Fälle dennoch unabhängig davon, im Knochenmark. Im letzteren kann der Knochenbildung eine Markfibrose vorangehen, doch irregulärer Knochen kann auch ohne jede vorangehende histologische Veränderung des Knochenmarks entstehen.

In bezug auf die gegenseitigen Beziehungen zwischen medullärem Knochen und später entstehendem Tumor wird festgestellt, daß die Geschwulst unmittelbar aus dem medullären Knochen entsteht. Der anhaltende Reiz ruft eine abnormale Knochenbildung hervor, die schließlich in eine sarkomatöse Wucherung übergeht. Das mit Beryllium herbeigeführte Knochensarkom ist somit in bezug auf seine Histogenese eine hyperplastogene Geschwulst.

Die irreguläre Knochenbildung wird vom Autor als präblastomatische Veränderung angesehen, die mit der Geschwulstentstehung in engem Zusammenhang steht und zeitlich ihr vorangeht. Die Komplexität des Tumors wird mit der "neoplastischen-Feld-Theorie" von Willis erklärt.

ГИСТОГЕНЕЗ КОСТНЫХ ОПУХОЛЕЙ, ВЫЗВАННЫХ БЕРИЛЛИЕМ

И. ФОДОР

Под влиянием бериллия в мозговой полости длинных костей — до развития опухоли — начинается образование нерегулярной кости. Согласно исследованиям автора нерегулярная медуллярная кость может образоваться в связи с внутренней надкостницей, однако в большинстве случаев она возникает все же, независимо от последней, в костном мозге. Образованию кости в костном мозге может предшествовать фиброз костного мозга, но нерегулярная кость может создаться и без предшествующего гистологического изменения мозга.

Относительно взаимоотношения нерегулярной медуллярной кости и развивающейся в последствии опухоли было установлено, что опухоль развивается непосредственно из медуллярной кости. Постоянное раздражение вызывает ненормальное костеобразование, которое затем переходит в карциноматозное разрастание. Следовательно, вызванный бериллием костной рак с точки зрения гистогенеза представляет собой гиперпластогенную опухоль.

Автор придерживается того мнения, что ненормальное костеобразование представляет собой предбластоматозное изменение, так как оно тесно связано с образованием опухоли и во времени предшествует последнему. Сложность опухоли автором объясняется теорией «неопластического поля» Виллиса.

Dr. István Fodor } Országos Reuma és Fizioterápiás Intézet,
H-1525 Budapest, Pf. 54., Hungary

National Institute of Rheumatism and Physiotherapy Budapest, Hungary

EFFECT OF ULTRASONIC TREATMENT ON THE ORGANS OF EXPERIMENTAL ANIMALS. III. ENZYME-HISTOCHEMICAL EXAMINATION OF THE PROLONGED EFFECT

Mária KELLER and D. TANKA

(Received October 5, 1976)

The protracted effect of ultrasound treatment on the parenchymatous organs of rats has been studied histochemically at 1 to 10-day intervals. As a result of the altered redox conditions it is the oxidative enzymes in the first place that react to ultrasound treatment and their normalization takes a long time. Exposure decreased the activity of lysosomal enzymes and in the cell membrane the alkaline phosphatase and ATP-ase too. The activity of hydrolases returned to normal parallel with the normalization of the microscopic structure.

In studies of the effect exerted by ultrasound on macromolecules and biological substances, attention have been focussed on the changes produced by mechanical vibrations in the first place [19]. Evidence has been scarce concerning the mechanism of action in the background of the changes. We may read about effects of ultrasound on biological systems — organisms — as well as about the possibilities of therapeutic use also in the publications by Hungarian authors [7], who surveyed the literature in detail and described their own observations.

According to our observations [8, 9] the oxidative enzymes react much more sensitivity than the hydrolytic ones to sonication *in vivo*. In this paper we shall discuss the protracted effect of ultrasound and seek the answer to the question as to the changes in enzymatic activity are reversible and how long it would take for them to return to normal.

Materials and methods

A total of 90 Wistar rats weighing 120 to 150 g were exposed to ventro-dorsal ultrasound treatment* with a dose of 0.3 and 0.5 W/square cm, for 2 minutes. The effect was studied in 4 rats daily and control animal at intervals of 1 to 10 days. After killing, the liver, kidneys and spleen were processed immediately.

Part of the material was fixed in formalin and embedded in paraffin for microscopic examination. Liver specimens were fixed also in ethanol. The oxidative enzymes were

In honour of the 70th anniversary of Professor K. FARKAS.

* TUR—US-5 therapeutic ultrasound equipment, VEB Transformatoren und Röntgenwerke, DRESDEN, DDR. The used frequency was 800 kHz.

demonstrated in unfixed cyrostat sections 4 microns thick, while the hydrolytic enzymes were processed in a similar way, after fixation in neutral formol at +4 °C.

The activities of the following enzymes were determined.

1. Lactate dehydrogenase (EC.1.1.1.27.) -LDH- (12)
2. Malate dehydrogenase (EC.1.1.1.37.) -MDH- (12)
3. Succinic dehydrogenase (EC.1.3.99.1.) -SDH- (15)
4. Iso-citrate dehydrogenase (EC.1.1.1.42.) -i-CDH- (17)
5. NADH diaphorase (EC.1.6.99.1.) — (12)
6. Cytochrome oxidase (EC.1.9.3.1.), (5)
7. Adenosine triphosphatase (Mg-avid-ATP-ase), (16)
8. Phosphorylase (EC.2.4.1.1.), (20, 11, 13)
9. Ascorbic acid dehydrogenase
10. Monoamine oxidase (EC.1.4.3.4.) -MAO- (10)
11. 11-beta-hydroxysteroid dehydrogenase (18)
12. Arylesterase (carboxylesterase) (EC.3.1.1.2.), (2)
13. Acid phosphatase (EC.3.1.3.2.), (1)
14. Alkaline phosphatase (EC.3.1.3.1.), (3)
15. Leucine aminopeptidase (EC.3.4.1.1.) -LAP- (4)

For the demonstration of dehydrogenases, *p*-nitro-blue tetrazolium was used. To control the histochemical reaction, the sections were heated at 90 °C.

Results

1. *LIVER*. After sonication with 0.3 W or 0.5 W, passive hyperaemia and hydropic degeneration were observed. They persisted for 6 to 7 days, and after exposure to 0.5 W until the 10th day

In the liver of the animals exposed to 0.3 W and killed immediately after treatment, increased SDH and ascorbic acid dehydrogenase activity were demonstrated. This increased SDH activity persisted throughout, while ascorbic acid dehydrogenase activity decreased sharply, as early as 24 hours later. Following exposure to 0.5 W, the reverse took place, with the SDH activity decreasing throughout, (Fig. 1) as opposed to the ascorbic acid dehydrogenase activity which increased from the 2nd day on. The decrease of activity presented itself centrolobularly, *i.e.* in those groups of cells which were damaged also morphologically. The changes of cytochrome oxidase, (Fig. 2.) DPNH diaphorase, (Fig. 3) as well as of the LDH and MDH activities were similar to those of the SDH, but differed from that in localization, the decrease of activity being observable at the periphery of the lobules.

When studying LDH and MDH we found, unlike in the other cases, a slightly increased reaction centrolobularly on the 5th to 7th days. Throughout the period of observation the activity of i-CDH and MAO was increased, particularly in the cells around the central veins. The activity of the enzyme catalysing the hydrocortisone-cortisone conversion was increased in the entire liver lobule following exposure to 0.3 W (Fig. 4). Treatment with 0.5 W was followed by an initial decrease in activity, then, on the 2nd day, by an increased activity centrolobularly.

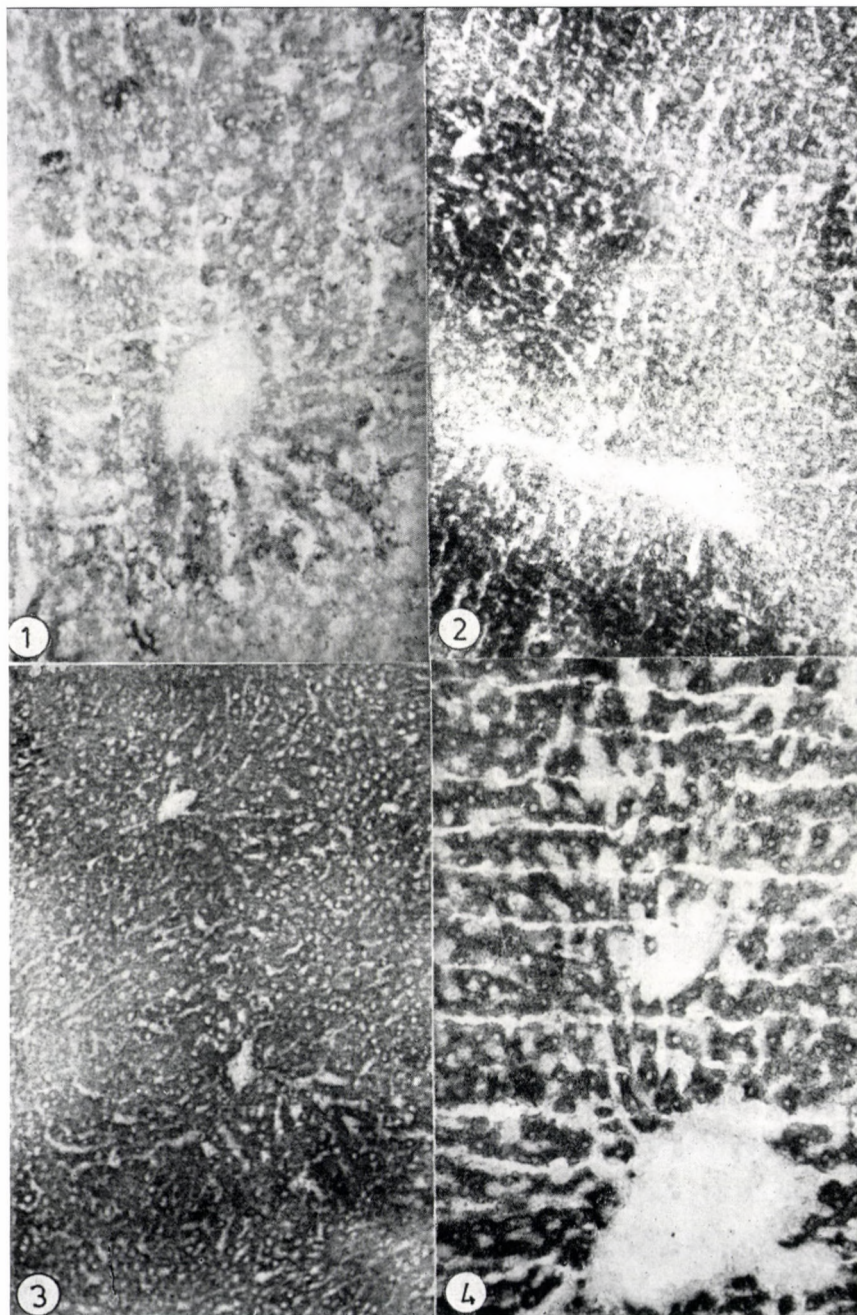


Fig. 1. Decreased succinic dehydrogenase reaction in the centrolobular liver cells after treatment (0.5 W). $\times 30$

Fig. 2. Cytochrome oxidase reaction in the liver on the 2nd day (0.5 W). $\times 30$

Fig. 3. Increased NADH diaphorase reaction in the liver on the 2nd day (0.5 W). $\times 30$

Fig. 4. 11-beta-hydroxysteroid dehydrogenase activity in the liver, after 0.3 W. $\times 30$

In general, the activity of the lysosomal enzymes studied decreased, centrolobularly following exposure to the 0.3 W dose, and peripherally in the first place following treatment with 0.5 W (Fig. 5). In the dilated sinusoids large numbers of enzyme-active Kupffer's cells could be demonstrated. After exposure to 0.5 W, the alkaline phosphatase active cells almost flooded the liver lobule, while there was a decrease in ATP-ase activity. Following 0.5 W treatment, at 3 to 5 days an intensive enzyme reaction could be observed in the dilated sinusoids around the central veins, showing a star-shaped pattern radiating toward the periphery (Fig. 6).

In response to treatment, aminopeptidase activity greatly increased in the entire liver lobule (Fig. 7). This increased reaction persisted throughout the experimental period.

The histochemically demonstrable glycogen content of the liver decreased in both cases. After formalin fixation, only a few cells around the central veins showed PAS positivity. (Fig. 8). Considerably more glycogen could be demonstrated following fixation in alcohol. Regeneration began on the 3rd—4th days.

The activity of phosphorylase, the enzyme breaking down glycogen, likewise decreased, with only a few active cell groups demonstrable in periportal region (Fig. 9). Normalization of the enzyme reaction began as late as 8 to 10 days after treatment (Fig. 10).

2. *KIDNEY*. The hydropic degeneration that developed after treatment persisted even on the 6th or 7th day, the tubules of the cortex were dilated, the brush border decreased in diameter, passive hyperaemia developed at the cortico-medullary junction.

After exposure to 0.5 W, the above changes were accompanied by vacuolar degeneration of the tubules, which subsided in about 10 days.

After treatment with the 0.3 W dose, SDH activity was retained in the dilated contorted tubules of the cortex. In the lumen, slightly active granules, presumably remnants of detached epithelial cells, could be observed (Fig. 11). After exposure to 0.5 W some tubules of the cortex showed increased, while, others showed decreased activity (Fig. 12.). On 0.3 W treatment ascorbic acid dehydrogenase was almost totally inactive in the outer zone of the cortex and the medulla showed diminished activity. Regeneration started after the 5th day. (Fig. 13). On the other hand, following treatment with the 0.5 W dose it was only on the 1st and 2nd days that we found a slightly decreased enzyme reaction in the cortex. The changes of DPNH diaphorase activity were similar, but the decrease was noted mainly at the cortico-medullary junction, in the inner zone of the cortex (Fig. 14). Inactivation of the enzyme was more marked on exposure to the 0.3 W dose. Likewise, LDH and MDH activities decreased following exposure to 0.3 W. The absence of reaction was especially obvious in the outer zone of the cortex. Following 0.5 W treatment the activ-

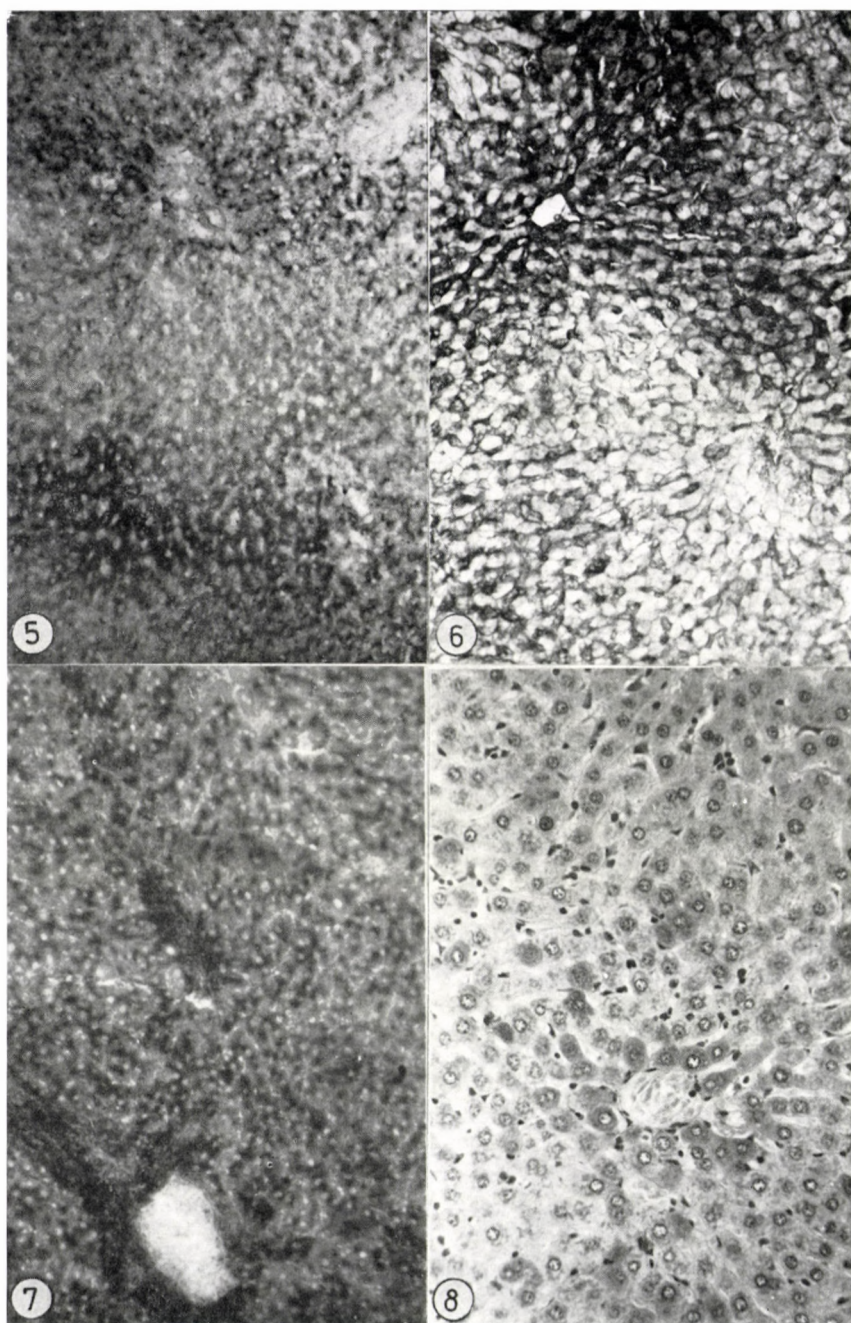


Fig. 5. Decreased arylesterase reaction in the peripheral cells of liver lobule. $\times 30$

Fig. 6. Adenosine triphosphatase activity after 0.5 W on the 5th day. $\times 30$

Fig. 7. Increased leucine aminopeptidase reaction in the liver. $\times 30$

Fig. 8. A few PAS positive cells around the central veins in the liver. $\times 30$

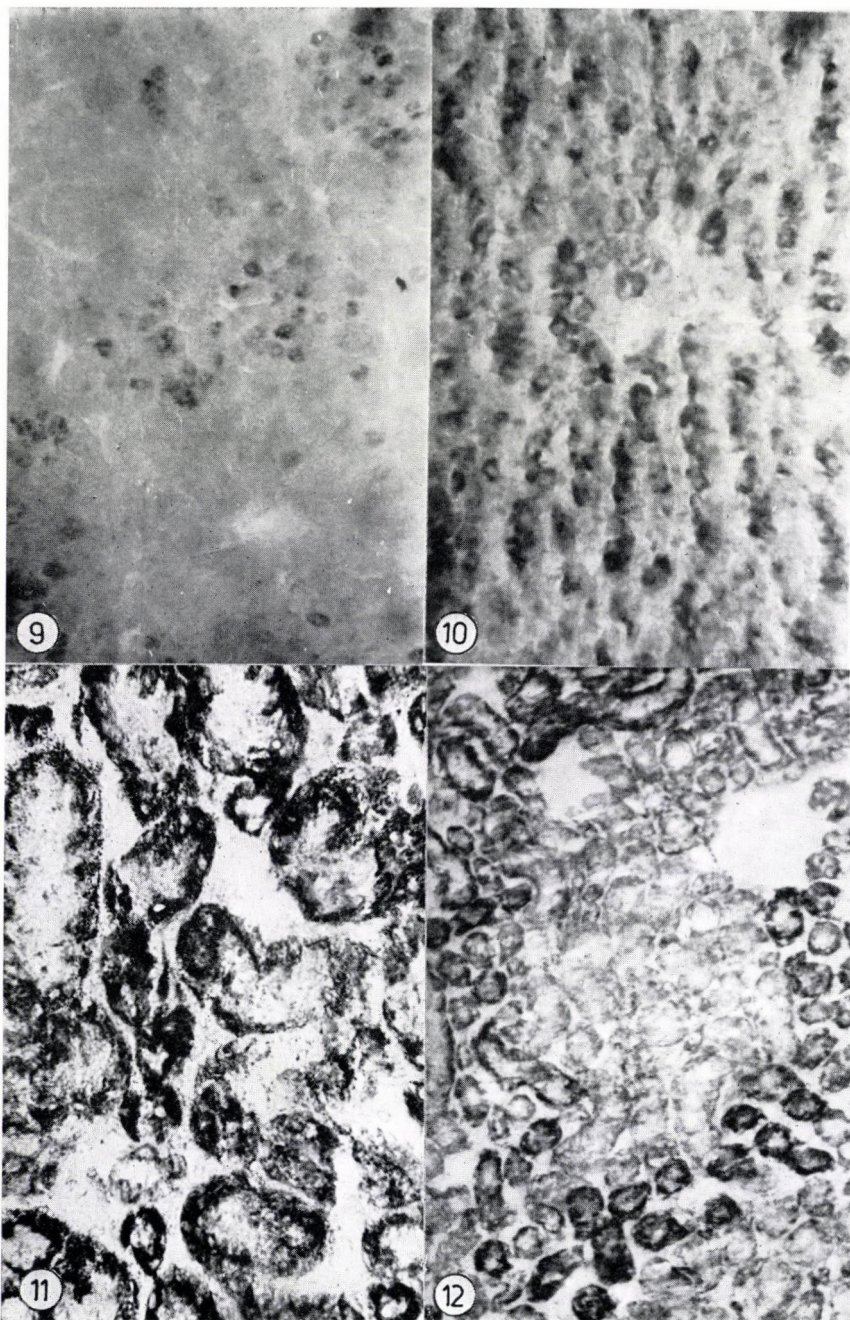


Fig. 9. Low phosphorylase activity in the liver after both doses. $\times 30$

Fig. 10. Reactivated phosphorylase reaction on 10th day. $\times 30$

Fig. 11. Succinic dehydrogenase reaction in the renal cortex, after treatment with 0.3 W. $\times 80$

Fig. 12. Some tubules of the cortex show a decreased succinic dehydrogenase reaction after 0.5 W dose. $\times 30$

ity of MDH, i-CDH (Fig. 15) and 11-beta-hydroxysteroid dehydrogenase increased, while on exposure to 0.3 W the initially increased reaction of the later enzyme decreased at 24 hours (Fig. 16). Particularly in the outer cortical zone the activity of carotochrome oxidase (Fig. 17) and MAO decreased after both doses.

The changes in the activities of the lysosomal enzymes reflect the changes in structural relations. In the cortex the detached, damaged remnants of epithelial cells appeared as esterase active granules (Fig. 18), while in the outer zone of the cortex, in the tubular cytoplasm acid phosphatase active granules were observed. The brush border of the primary convoluted tubules is narrow, its alkaline phosphatase and ATP-ase activities diminished or ceased. With regeneration of the renal tissue, as seen under the microscope, the normalization of hydrolases began.

Aminopeptidase activity increased following exposure to either dose, but after treatment with 0.3 W the increase appeared only on the 4th—5th day.

3. *SPLEEN*. Following treatment, many cells with PAS positive cytoplasm appear in the pulp. During the first days, strong haemosiderin pigmentation indicative of erythrocyte disintegration was visible.

Some of the oxidative enzymes studied gave only minimal reactions in the spleen, therefore the changes cannot be demonstrated histochemically or are hardly noticeable. The activity of the dehydrogenases requiring co-enzyme decreased throughout the period of observation; the decrease was slighter in the case of i-CDH. DPNH diaphorase activity of the pulp also decreased, while that of the germinative centres was retained. The activity of 11-beta-hydroxysteroid dehydrogenase increased.

Carboxylesterase (Fig. 19) and acid phosphatase activity decreased and it was only after the disappearance of the haemosiderin pigment that normalization begun, first in the follicles, then also in the pulp.

On treatment with 0.3 W, the alkaline phosphatase reaction diminished, while following exposure to 0.5 W, large enzyme-active cell groups were visible around the follicles. ATP-ase activity increased on the 3rd or 4th day mainly in the cells of the germinative centre (Fig. 20).

Unlike in the other organs, the activity of aminopeptidase decreased throughout.

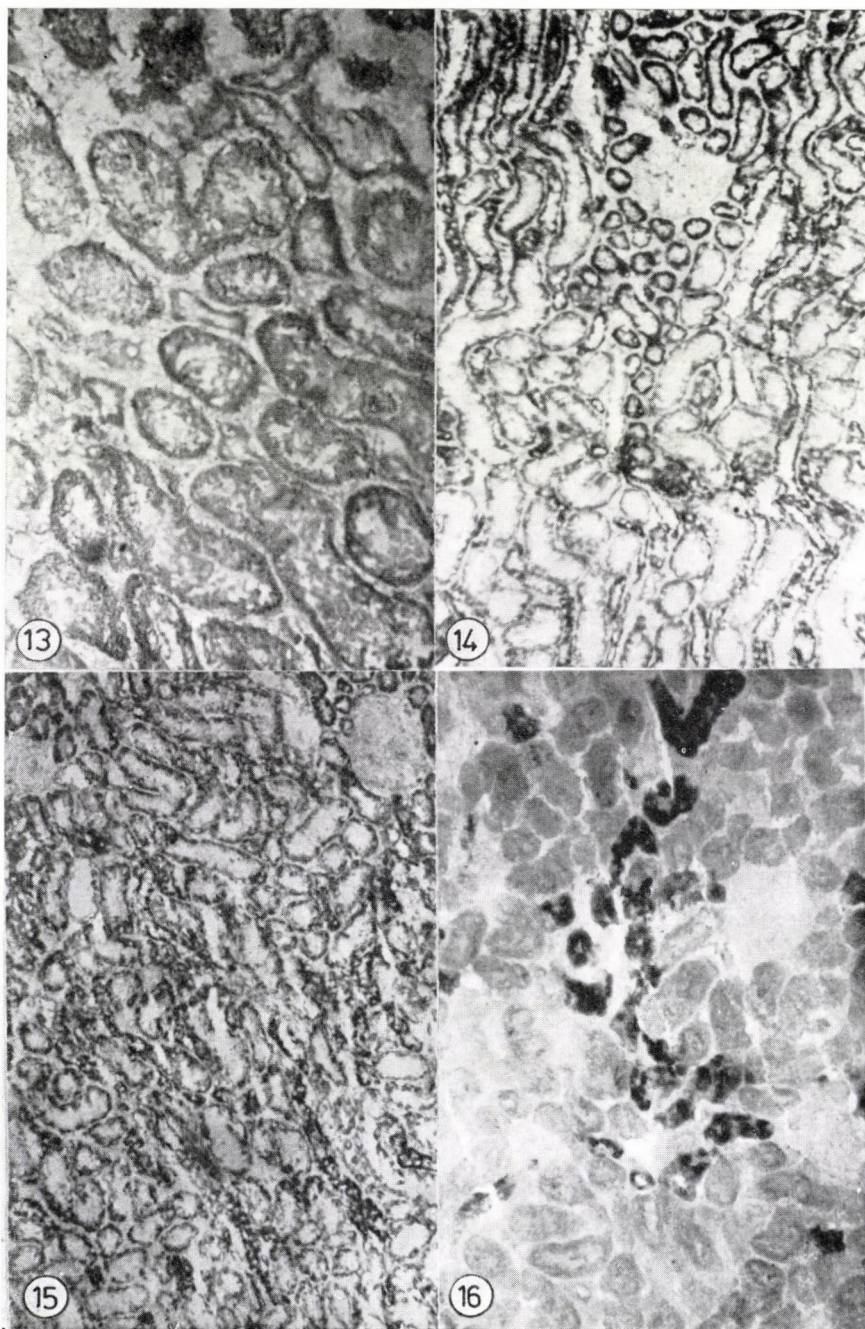


Fig. 13. Nearly normal ascorbic acid dehydrogenase reaction in the renal cortex on the 8th day. $\times 30$

Fig. 14. Decreased NADH diaphorase reaction in the cortico medullary junction of the kidney. (0.5 W). $\times 30$

Fig. 15. Increased isocitrate dehydrogenase reaction in the renal cortex (0.5 W). $\times 30$

Fig. 16. 11-beta hydroxysteroid dehydrogenase reaction after 24 hours in the kidney (0.3 W). $\times 30$

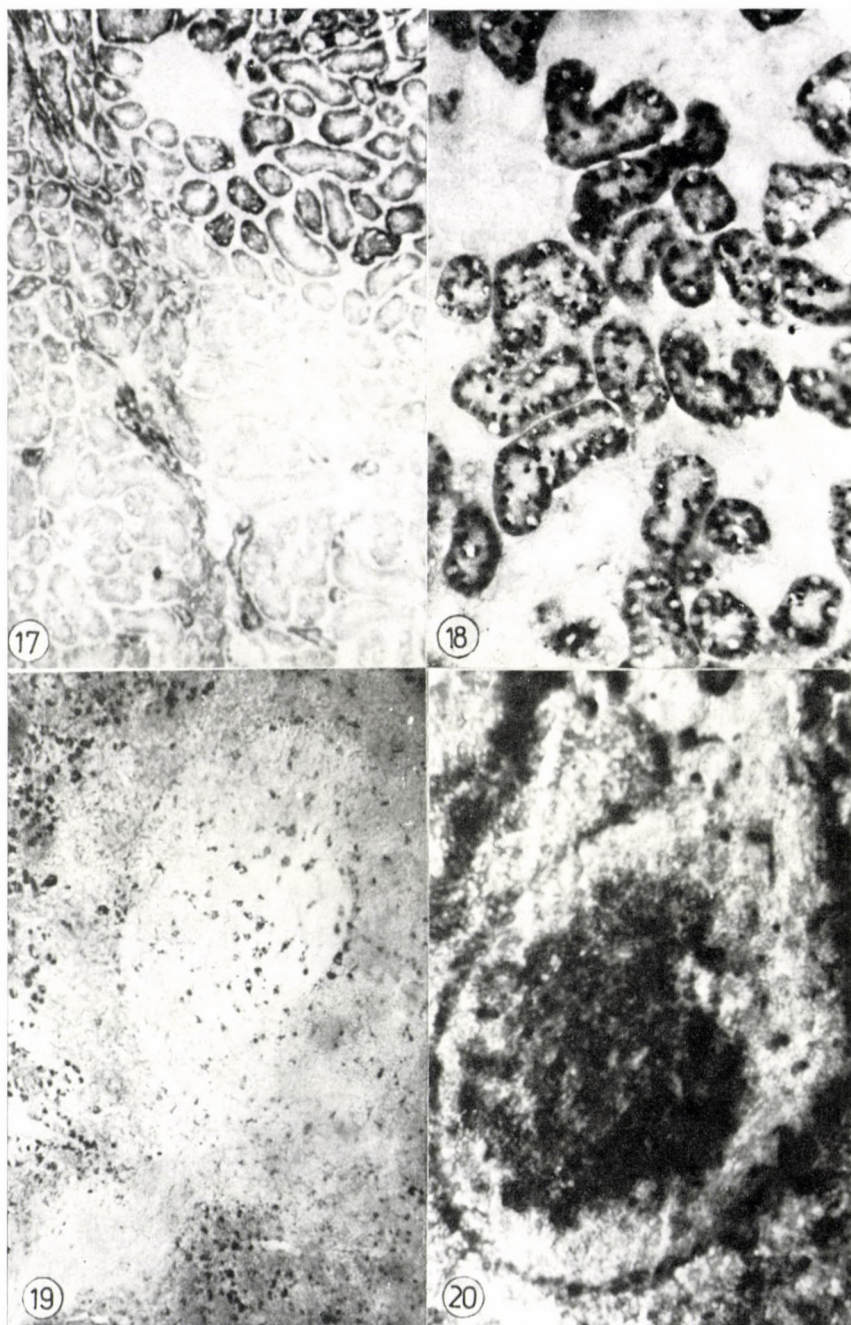


Fig. 17. Decreased cytochrome oxidase reaction in the inner cortical zone and persisting activity in the external zone of the kidney. $\times 30$

Fig. 18. Arylesterase active granules in the cortical tubules on 2nd day (0.3 W). $\times 30$

Fig. 19. Decreased arylesterase reaction in Malpighi body on the 4th day. (0.5 W). $\times 80$

Fig. 20. Increased adenosine triphosphatase activity in spleen on 4th day after 0.5 W dose. $\times 130$

Discussion

The morphological changes induced by ultrasound have extensively been described in the literature, but enzyme chemical studies have been carried out in a few cases only [7, 12], and even these were restricted to single lysosomal enzymes. Investigations involving sonication *in vivo* and extending to oxidative enzymes, or studies concerned with the protracted affect of ultrasonic treatment have not been published in the literature at our disposal.

The structural changes are produced by mechanical vibration. The extent of the damage depends on the intensity and frequency of sonication; these determine whether the changes will be macromolecular or will affect the cell organelles too. The altered structure alone would suffice to change cellular metabolic processes, causing them to deviate from the normal.

The physical effect is, however, accompanied by physicochemical and biochemical reactions. On the wall of the cavitation hollows electrical double layers develop, the electric charges shift on the cellular membranes, the redox potential is altered. It is the above phenomena that are responsible in the first place for the changes observed in the activities of the oxidases.

It should be borne in mind that the microwaves create compression and dilatation, which may interfere with the physiological pulsation of mitochondria, damaging their membrane or altering their permeability. This phenomenon may play a role in the changes of mitochondrial enzyme activities.

The changes resulting in cell membrane potentials and permeability can be followed by studying the activity of alkaline phosphatase and ATP-ase.

TAYLOR and POND [22] using higher doses than those applied by us, found increased acid phosphatase activity in the rat liver, which they attributed to a disintegration of lysosomes. In our own experiments we investigated two lysosomal enzymes and found that their activity decreased. This was assumed to be due to some damage to the protein components of the enzymes or to the development of some inhibitor substance. Ultrasound is used for the treatment of chronic inflammation, among others. If we realize that inflammatory processes are usually characterized by increased lysosomal enzyme activity, the above observations may prove helpful in the choice of the therapeutic dose. In this respect we have a few experimental data [14]. We induced arthritis in rats with the contents of granuloma pouch and treated it with 0.3 W intensity ultrasound. In response to treatment there was clinical improvement, the microscopic appearance of the joint hardly differed from that of the untreated animal and the lysosomal enzyme activities were similar to those of the controls.

The increased enzyme activity found in Kupffer's cells may be considered an indicator of RES activation. The readiness of ultrasound to mobilize the

RES, as well as the sensitive functional reaction of the spleen suggest that the intervention might affect immunological processes.

The increase in local temperature in response to the absorbed energy affects the cell membranes; their permeability and the metabolic rate are increased. The friction due to the accelerated molecular movement is held responsible for the depolymerizing effect of ultrasound, as has already been suggested by SZENT-GYÖRGYI [19].

The enhanced peptic activity is presumably due to an accumulation of the breakdown products of proteins depolymerized by the ultrasound, which are further broken down by this enzyme, among others. It is not by chance that the activation of aminopeptidase takes place mainly in the liver, which plays a detoxifying role in the organism.

The other biopolymer the changes of which were followed was the liver glycogen, which in accordance with published data [17, 23] became depolymerized. This was indicated in the formalin-fixed material by the fact that the PAS reaction demonstrated glycogen in a few cells only, the breakdown products, the oligo and disaccharides being water-soluble. In the alcohol-fixed material considerably more cells showed PAS positivity. The same phenomenon can be observed after X-ray irradiation [6, 21] as confirmed by determining the molecular weight by ultracentrifugation.

Phosphorylase activity decreased after ultrasound treatment. The simultaneous disappearance from the cells of glycogen and of the enzyme breaking down glycogen is merely an apparent contradiction, because glycogen was broken down as a result of depolymerization, and it is just these accumulated breakdown products that inhibit the activity of the enzyme.

Thus, it may be stated the physical stimulation of the organism evokes an immediate response, which triggers off a series of physicochemical and biochemical reaction. The response is not specific, but of general validity. The induced reactions, the changed metabolic processes persist for a long time after *in vivo* treatment. This fact is not negligible from the point of view of therapeutic and diagnostic use.

The experimental results will allow to set precisely the optimum dose causing inhibition of lysosomal enzymes as also the intervals between treatments. The observations made on experimental animals should be taken into consideration also when using ultrasound for modern diagnostic purposes, with special attention devoted to the choice of the proper, innocuous doses.

REFERENCES

1. BARKA T.: (1960) A simple azo-dye method for histochemical demonstration of acid-phosphatase. *Nature*, (Lond.) **187**, 248—249. — 2. BURSTONE, M. S.: (1957) The cytochemical localization of esterase. *J. nat. Cancer Inst.* **18**, 167—170. — 3. BURSTONE, M. S.: (1958) Histochemical comparison of naphthol-AS-phosphates for the demonstration of phos-

phatases. J. nat. Cancer Inst. **29**, 601–615. — 4. BURSTONE, M. S., J. E. FOLK: (1956) Histochemical demonstration of aminopeptidase. J. Histochem. Cytochem. **4**, 217–226. — 5. BURSTONE, M. S.: (1960) Histochemical demonstration of cytochrome oxidase with new amine reagents. J. Histochem. Cytochem. **8**, 63–70. — 6. DÁVID G., D. TANKA, A. CZUPPON: (1964) A máj glikogén tartalmában és a máj-glikogén molekulaszervezetében bekövetkező változások teljesest röntgenbesugárzás és nitrogénmustár mérgezés hatására. Magy. Radiol. **16**, 246–250. — 7. FARKAS, K., J. IRÁNYI: Az ultrahang. Medicina, Budapest 1965. — 8. FARKAS K., M. KELLER, D. TANKA: (1972) Effect of ultrasonic treatment on the organs of experimental animals. I. Enzyme-histochemical alterations in the liver, spleen and kidney of animals killed immediately after ultrasonic treatment. Acta morph. Acad. Sci. hung. **20**, 171–183. — 9. FARKAS, K., M. KELLER, D. TANKA: (1972) Effect of ultrasonic treatment on the organs of experimental animals. II. Quantitative enzyme-chemical alterations in liver, spleen and kidney of animals sacrificed immediately after treatment. Acta morph. Acad. Sci. hung. **21**, 49–55. — 10. GLENNER, G. G., H. J. BURTNER, A. W. BROWN: (1957) The histochemical demonstration of monoamine oxidase activity by tetrazolium salts. J. Histochem. Cytochem. **5**, 591–600. — 11. GODLEWSKI, H. G.: (1960) Application of ethylene-diamino-tetraacetic acid (EDTA) in the histochemical method for demonstration of phosphorylase and branching enzyme. Bull. Acad. Sci. **8**, 441–444. — 12. HESS, R., D. G. SCARPELLI, A. G. E. PEARSE: (1958) The cytochemical localisation of oxidative enzymes. II. Pyridine nucleotide linked dehydrogenases. J. biophys. biochem. Cytol. **4**, 753–769. — 13. KELLER M., D. TANKA: (1965) Preservation of the iodine-glycogen complex of the phosphorylase reaction. — Acta histochem. (Jena) **22**, 73–76. — 14. KELLER M., D. TANKA: (1973) Development of experimental arthritis in ultrasound treated animals. Acta morph. Acad. Sci. hung., Suppl. 14. p. 77. — 15. NACHLAS, N. M., K. C. TSOU, E. DESOUSA, C. S. CHANG, A. M. SELIGMAN: (1957) Cytochemical demonstration of succinic dehydrogenase by the use of new p-nitro-phenyl substituted ditetrazole. J. Histochem. Cytochem. **5**, 420–436. — 16. PADYKULA, H. A., E. HERMAN: (1955) The specificity of the histochemical method for adenosinetriphosphatase. J. Histochem. Cytochem. **3**, 170–195. — 17. PEARSE, A. G. E.: Histochemistry. Theoretical and Applied. J. A. Churchill Ltd., London 1961. — 18. PEARSON, B., F. GROSE: (1959) Histochemical demonstration of 17-beta-hydroxysteroid dehydrogenase by use of tetrazolium salt. Proc. Soc. exp. Biol. (N. Y.) **100**, 636–638. — 19. SZENT-GYÖRGYI A.: (1933) Chemical and biological effects of ultrasonic radiation. Nature (Lond.) **131**, 278. 20. TAKEUCHI, T., H. KURIAKI: (1955) Histochemical demonstration of phosphorylase in animal tissues. J. Histochem. Cytochem. **3**, 153–160. — 21. TANKA D.: (1967) A sugárrezisztens szervek funkcionális morfológiai károsodásáról. Thesis, Budapest — 22. TAYLOR, K. J. W., J. POND: (1970) The effects of ultrasound of varying frequencies on rat liver. J. Path. **100**, 287–293. — 23. VALTONEN, E.: (1967) Influence of ultrasonic radiation in the medical therapeutic range on the fine structure of the liver parenchymal cells. Virchows Arch. path. Anat. **343**, 26–33.

DIE WIRKUNG DER ULTRASCHALLTHERAPIE AUF DIE ORGANE DER VERSUCHSTIERE III. ENZYMHIStOCHEMISCHE UNTERSUCHUNG DER VERZÖGERTEN WIRKUNG

MÁRIA KELLER und D. TANKA

Die Wirkung der Ultraschallbehandlung auf die parenchymatösen Organe weißer Ratten wurde unter experimentellen Bedingungen in 1–10tägigen Intervallen nach der Behandlung analysiert. Bei der histochemischen Untersuchung wurde festgestellt, daß die Ultraschallbehandlung die Veränderung der Redoxprozesse bewirkt, wobei in erster Linie die oxydativen Enzyme reagieren. Die Aktivitätsänderung normalisiert sich erst nach mehreren Tagen. Die Aktivität der lysosomalen Enzyme nimmt in Abhängigkeit von der Dosis ab. In ähnlicher Weise wird auch die sich auf die Membran lokalisierende alkalische Phosphatase und die ATPase inaktiviert. Parallel mit der Normalisierung des morphologischen Bildes kehrt auch die Aktivität der hydrolytischen Enzyme zurück. Zusammenfassend läßt sich sagen, daß die unter Ultraschalleinfluß im biologischen Medium entstehenden Veränderungen äußerst komplex sind und im lebenden Organismus sich eine komplexe Wirkung geltend macht.

ДЕЙСТВИЕ УЛЬТРАЗВУКОВОЙ ТЕРАПИИ НА ОРГАНЫ ПОДОПЫТНЫХ
ЖИВОТНЫХ
III. ЭНЗИМОГИСТОЛОГИЧЕСКОЕ ИССЛЕДОВАНИЕ ЗАПАЗДЫВАЮЩЕГО
ДЕЙСТВИЯ

МАРИЯ КЕЛЛЕР и Д. ТАНКА

Действие ультразвуков было изучено в экспериментальных условиях на паренхиматозных органах белых крыс в 1—10-дневных интервалах после применения ультразвуков. В ходе гистохимических исследований удалось установить, что под влиянием ультразвуковой терапии изменяются окислительно-восстановительные процессы. Железа всего реагируют окислительные ферменты, и изменение активности нормализуется только по истечении нескольких дней. Активность лизосомальных ферментов понижается в зависимости от применяемой дозы. Подобную инактивизацию показывает также щелочная фосфатаза и АТФ-аза, локализованные в перепонке. Одновременно с нормализацией морфологической картины активность гидролитических энзимов возвращается к норме. Подытоживая можно сказать, что изменения, возникающие в биологической среде под влиянием ультразвуков крайне сложные и что в живом организме проявляется комплексное действие.

Dr. Mária KELLER } Országos Reuma és Fizioterápiás Intézet,
Dr. Dezső TANKA } H-1525 Budapest, Pf. 54., Hungary

National Institute of Rheumatism and Physiotherapy, Budapest

CELL-TO-CELL CONTACTS BETWEEN LYMPHORETICULAR CELLS IN RHEUMATOID SYNOVIAL MEMBRANE

T. NEUMARK

(Received October 5, 1976)

Nodular type and diffuse perivascular lymphoid cell infiltrates in rheumatoid synovial membranes from 72 patients were examined under the electron microscope. Attempts were made to describe the ultrastructural relations of the cells examined, and to classify the different types of cell-to-cell contacts between them. Members of a complex series, composed of gradually differentiating forms of cell contacts beginning from simple membrane adherences and interdigitations and gap junctions; minute filamentous intercellular bridges; subsurface confronting cisternae and desmosome-like structures, are described and suggested as function-dependent morphological representatives of sites of cellular interactions.

The general phenomenon of cell-to-cell contact may require a direct interaction between the surface of neighbouring cells resulting in the formation of specialized junctions. These cell interactions could play an essential role in several types of communication phenomena such as the immune response, cell fusion, ionic coupling, metabolic co-operation, intercellular adhesion, etc. [4, 6, 19].

Intercellular contacts between lymphoreticular cells in the rheumatoid synovial membrane have been described earlier [21, 22, 23]. The present study is further electron microscopic analysis of the different types of intercellular contacts between cells in the lymphoid cell infiltrates found in the synovial membrane of joints affected by rheumatoid arthritis.

Material and methods

Synovial membranes were obtained during synovectomy of the knee of 72 patients suffering from rheumatoid arthritis of the definite or classical type by the American Rheumatism Association criteria [29]. Most samples were collected from the parapatellar region of the knee. For electron microscopy small tissue fragments, 1 mm in diameter, were fixed immediately in Karnovsky's fluid [17] and postfixed with buffered 1% osmium tetroxide. After dehydration in graded ethanol series, the specimens were embedded in Durcupan ACM (Fluka) and thick and ultrathin sections were cut with glass knives on a Reichert OM-U2 ultramicrotome. During dehydration the specimens were stained with 1% uranyl acetate in 70% ethanol. Ultrathin sections were mounted on uncoated copper grids, stained with lead citrate and uranyl acetate. 4–5 grids from each block were examined with a TESLA BS-513A electron microscope using an accelerating voltage of 80 kV. Semi-thick sections of approximately 1 μ m, stained with toluidin blue, were used to select areas of the synovial membranes that contained both diffuse and nodular types of lymphoid cell infiltrates.

In honour of the 70th anniversary of Professor K. FARKAS.

Results

Under the light microscope, accumulations of macrophages intermingled with several differentiating forms of the lymphocyte plasma cell transformation line simply called (lymphoid cells) were consistently found around the small blood vessels in the sublining or deeper layers of the rheumatoid synovial membrane. In 26 of the 72 patients, characteristic nodular type lymphoid cell aggregates were found around blood vessels, very similar to the primary follicles in lymph nodes. Germinal centres were also apparent in 2—3 of the 26 samples (Fig. 1).

Both the simple nodular lymphoid cell infiltrates and those which resemble the secondary follicles, demonstrated an unexpected ultrastructural complexity. The central part of the aggregate contained mainly closely packed small and somewhat larger lymphocytes intermingled with dendritic cells and macrophages (Fig. 2). Lymphoblasts, mitotic forms of lymphoid cells and tingible-body macrophages were also observed in this area (Fig. 3). The periphery of the nodular cell aggregates as well as the areas with diffuse accumulation of lymphoid cells were characterized by looser connections of the cells and an increased plasma cell infiltration. Some areas of the central part of the nodular cell aggregates consisted of little else but interdigitating cytoplasmic extensions and cytoplasmic infolds. The interspace between adjacent cells, filled by an electron-opaque material, appeared as an irregular labyrinth resulting from the numerous infoldings and interdigitations of cell processes.

The low power electron micrographs of the nodular lymphoid cell infiltrate revealed simple junctional areas and some kind of apparent membrane specialization of the opposed cell membranes. At higher magnification it was clearly seen that the opposing cell membranes ran parallel to each other, in a straight line or in a wavy course, separated over most of the junctional area by a remarkably constant gap less than 100 Å in diameter. In such cases, the profiles of cytoplasmic processes in close contact were frequently indistinguishable from those of the lymphocytes. In some cases, within these zones of cell contact, local differentiations of the plasma membranes between the somatic zones of opposed cells or between their larger cell processes could also be seen. The total thickness at these regions was reduced to about 200 Å, and although the structure of the contact was not clearly seen, the intercellular gap often consisted of electron dense punctations or septa corresponding in appearance to a classical gap junction (Fig. 4). Generally, the above-mentioned types of cell contact were the consistent feature of this area.

At some distinct areas, either between slender cytoplasmic processes of macrophages and lymphoid cells, or between their perikaryons, fine intercellular filaments about 80 Å in diameter seemed to bridge over the intercellular space as minute filamentous bridges. On the other hand, at some points the

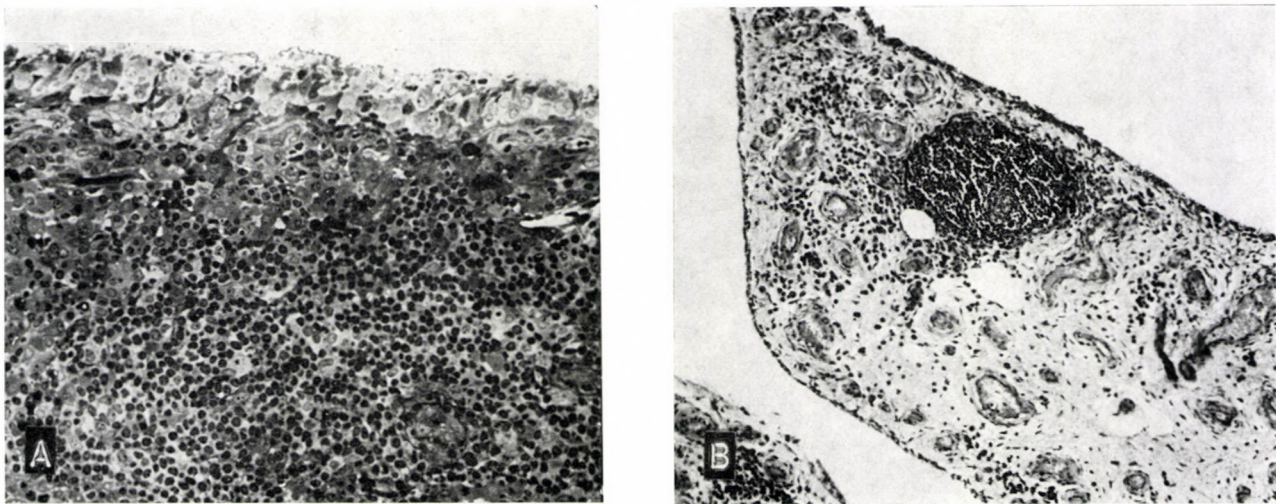


Fig. 1. H. E. sections from rheumatoid synovial membranes. A) diffuse lymphoid cell infiltration in the subsynovial layer. $\times 230$. B) Dense nodular type lymphoid cell aggregate containing germinal centre $\times 100$

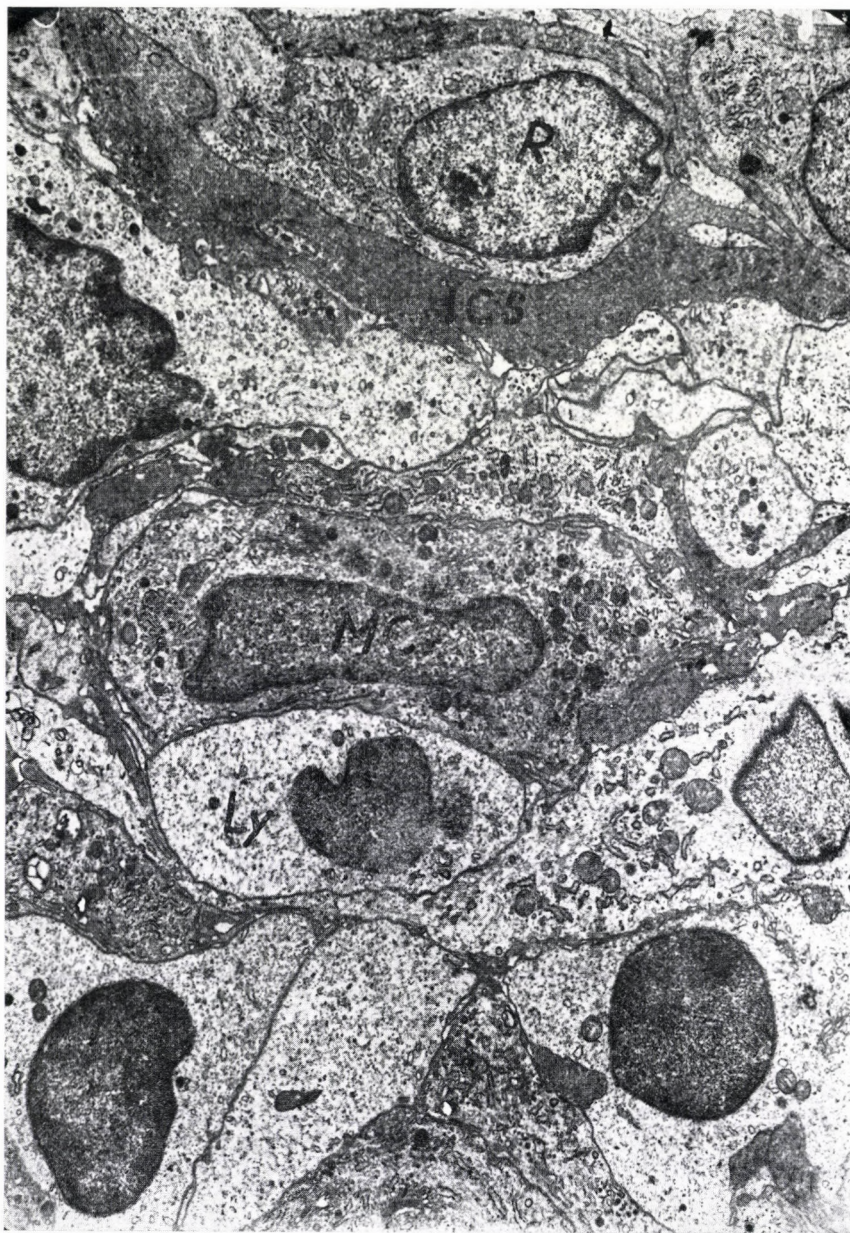


Fig. 2. Mixed cell population in the central part of a nodular type lymphoid cell aggregate taken from a rheumatoid synovial membrane. Note the accumulation of electron-opaque material within the intercellular spaces and the labyrinth of plasma; membrane infoldings and interdigitations. ICS = intercellular space; Ly = lymphocyte; MC = macrophage; R = reticular cell, $\times 5200$

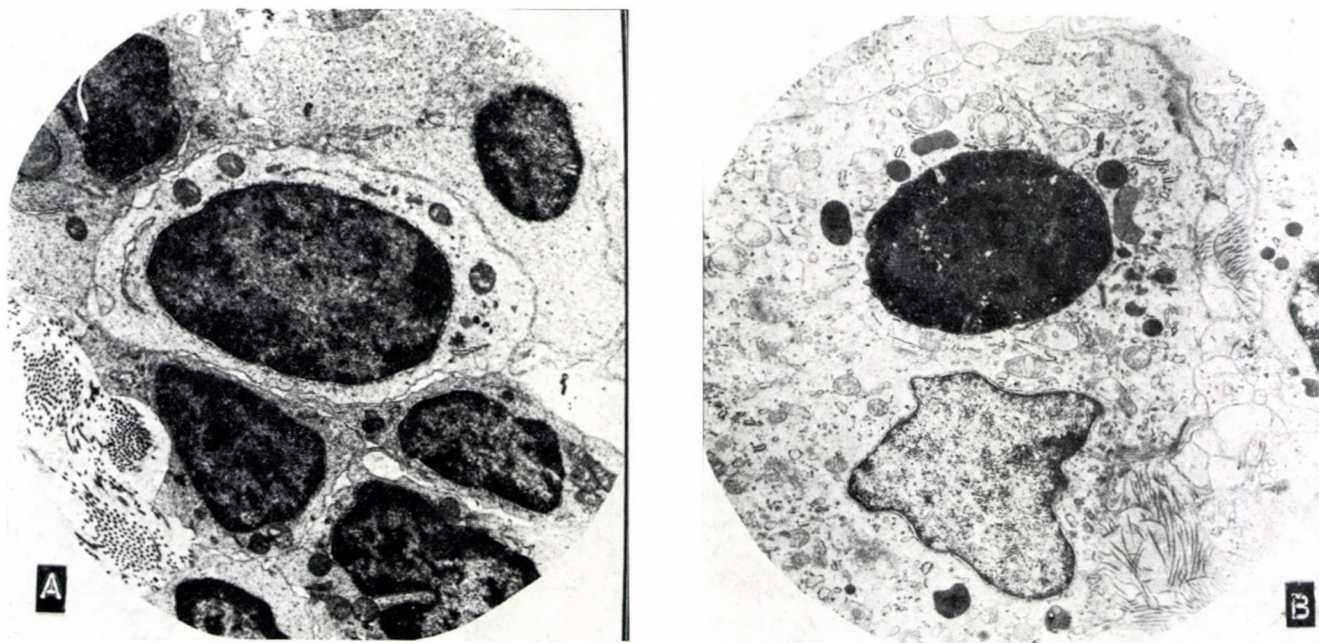


Fig. 3. A) Lymphoblast surrounded by small lymphocytes and B) a tingible-body macrophage in a nodular type lymphoid cell aggregate, A = $\times 4000$, B = $\times 7300$

intercellular gap between opposed cell membranes became as narrow as 50 Å or less. At such focal membrane contacts, circumscribed dense areas appeared in the underlying cytoplasm of both cells. In some cases, lymphocytes were seen attached to a macrophage or fibroblast by pseudopods which penetrated into the target cell. Although the total thickness of cell contact here was also approx. 250 Å in diameter, focal contacts could be seen between cell membranes suggestive of gap or tight junctions (Figs 4 and 5). In addition to these types of cell-to-cell contacts, complete fusion of plasma membranes, resulting in the formation of narrow cytoplasmic bridges between lymphoid cells, was observed in a few cases. This type of cell contact was characterized by the presence of continuous cytoplasmic material in the bridge between adjacent cells and the clear continuity of the plasma membranes joining the two cells (Fig. 5c). Their actual existence as channels was proved by goniometric measurements.

The above-mentioned forms of cell-to-cell contacts can readily be distinguished from desmosome-like structures to be found especially between macrophages and fibroblasts, but almost never between lymphoid cells. Desmosome-like structures were usually observed around the nodular lymphoid cell aggregates and also between lining cells, and could be classified as fascial or zonular adherents. The total thickness of the cell contact in this case was about 250–350 Å, and the intercellular space was filled by a material of moderate electron density, often showing a structured pattern. The opposing cell membranes of the two cells ran parallel in a straight line for several microns, and a condensation of dense filamentous material could be found in the cytoplasm along the adherens junctions. In some cases, small circumscribed contacts especially between cell processes of the above-mentioned cells, could also be observed. Short intracellular filaments and small granules embedded in a dense material, within the cytoplasm attaching to the inner surfaces of each participating plasma membrane also characterized this type of cell contact. Occasionally, fine filaments or tubules were bridging over intercellular space (Fig. 6).

Characteristic structures, so-called subsurface cisternae were observed immediately under the plasma membrane at the junctional zones between lymphoid cells, either in unilaterally or bilaterally, forming a confronting complex of such subsurface cisternae (Fig. 7). In almost all cases of such flattened vesicles, their continuity with the rough ER was clearly demonstrated. In one case, as is shown in Fig. 7b, the cavity of one member of the confronting pair of these subsurface cisternae was detectable directly next to that of an extremely dilated rough-surface cisterna within an almost fully developed plasma cell.

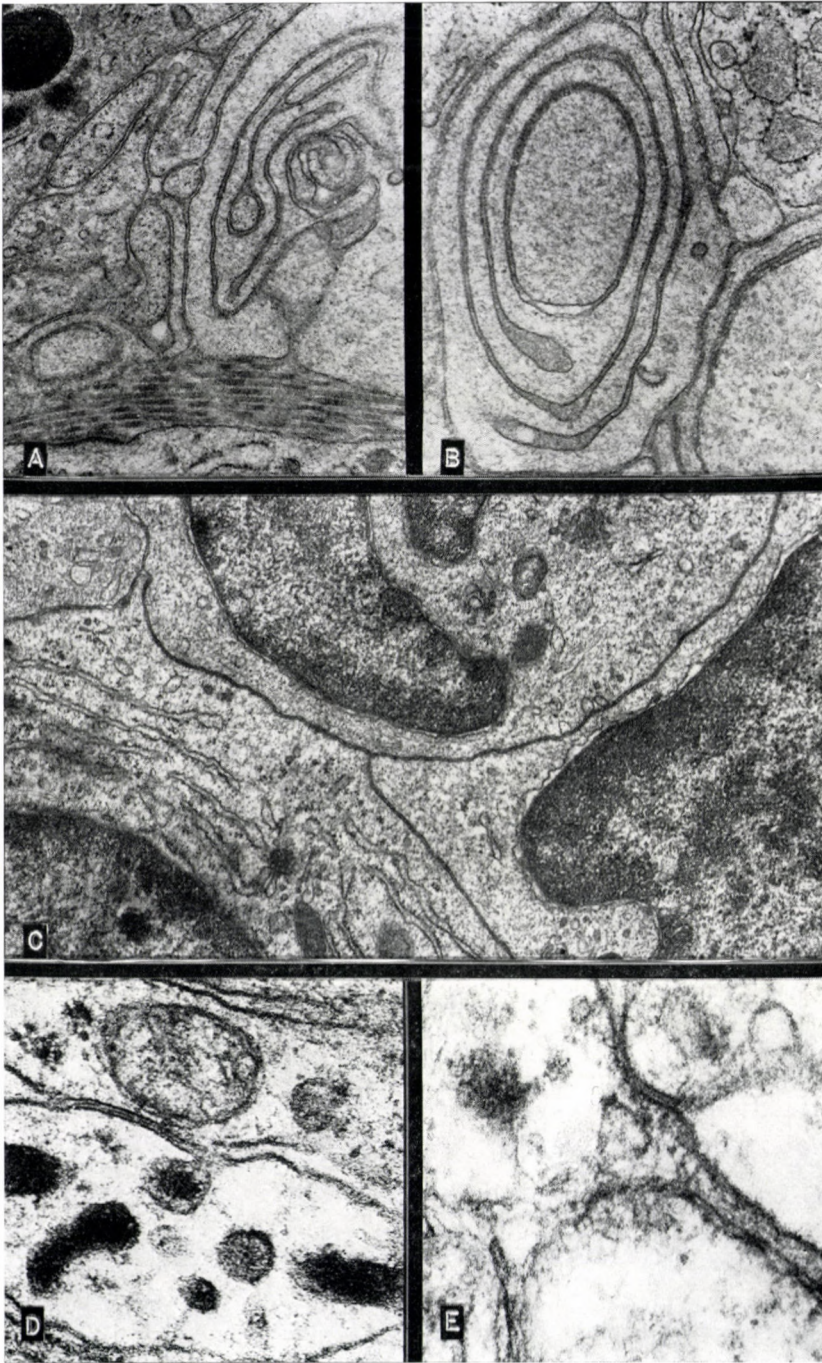


Fig. 4. A) and B) Interdigitating cytoplasmic extensions and cytoplasmic infoldings between lymphoreticular cells. Note in fig. B the electron-opaque material in the intercellular space A = $\times 22,000$, B = $\times 34,200$. C) Close membrane apposition and apparent membrane modification between lymphoid cells. $\times 22,600$. D) Tight junction between interdigitating cell processes of a lymphoid cell and macrophage $\times 89,000$. E) Circumscribed gap junction between two fibroblasts. $\times 107,600$

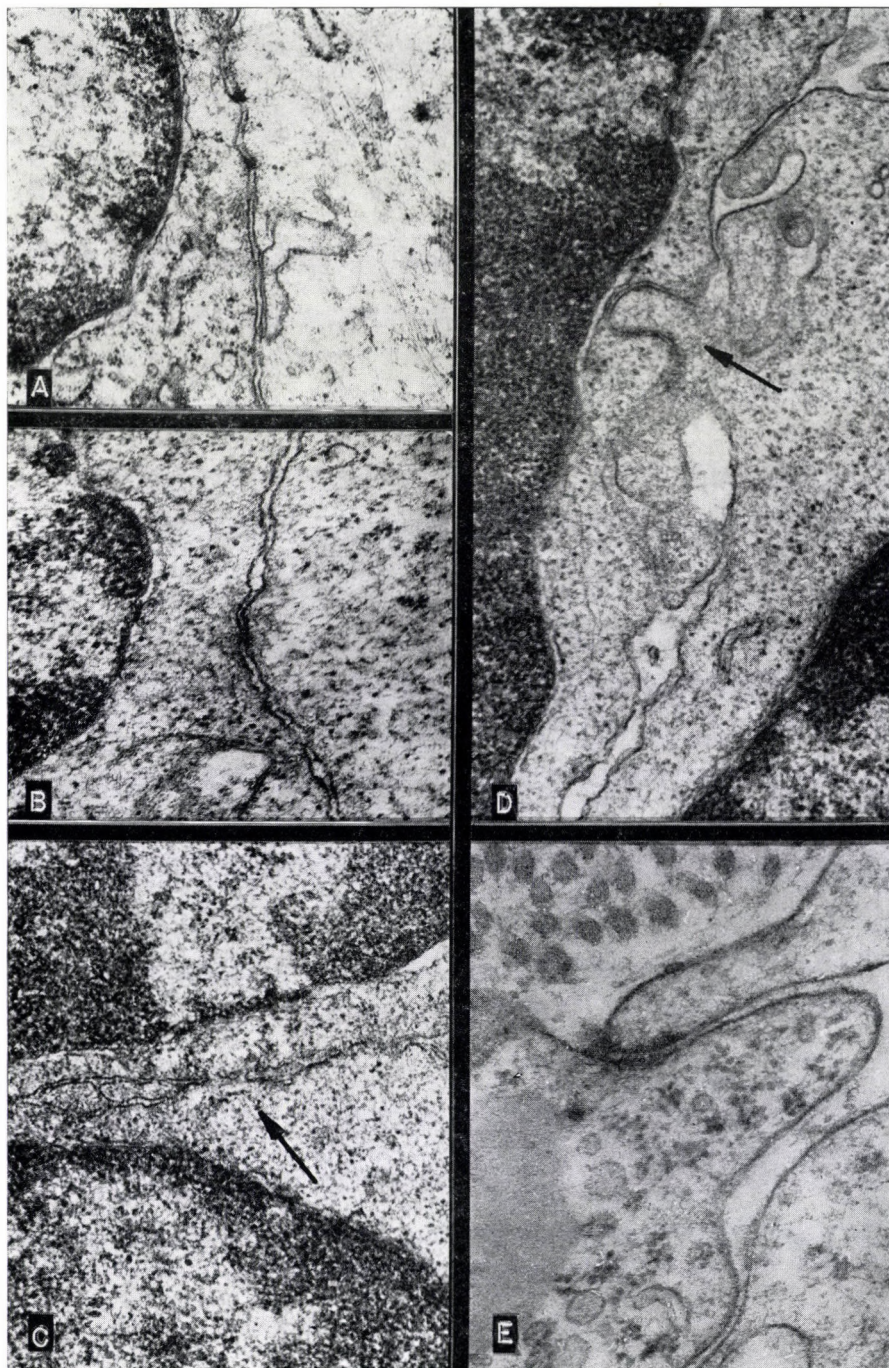


Fig. 5. A) and B) Focal cell junctions between lymphoid cells. Note in Fig. A the existence of a surface cistern along a close membrane opposition. A = $\times 40,000$, B = $\times 53,400$. C) Cytoplasmic bridges (arrow) between two lymphocytes $\times 45,200$. D) Arrow indicates a single pseudopod penetrating in the target cell. Both cells are lymphocytes $\times 42,750$. E) Cell contact zone between fibroblasts. Septate-like filaments cross the intercellular space $\times 72,250$

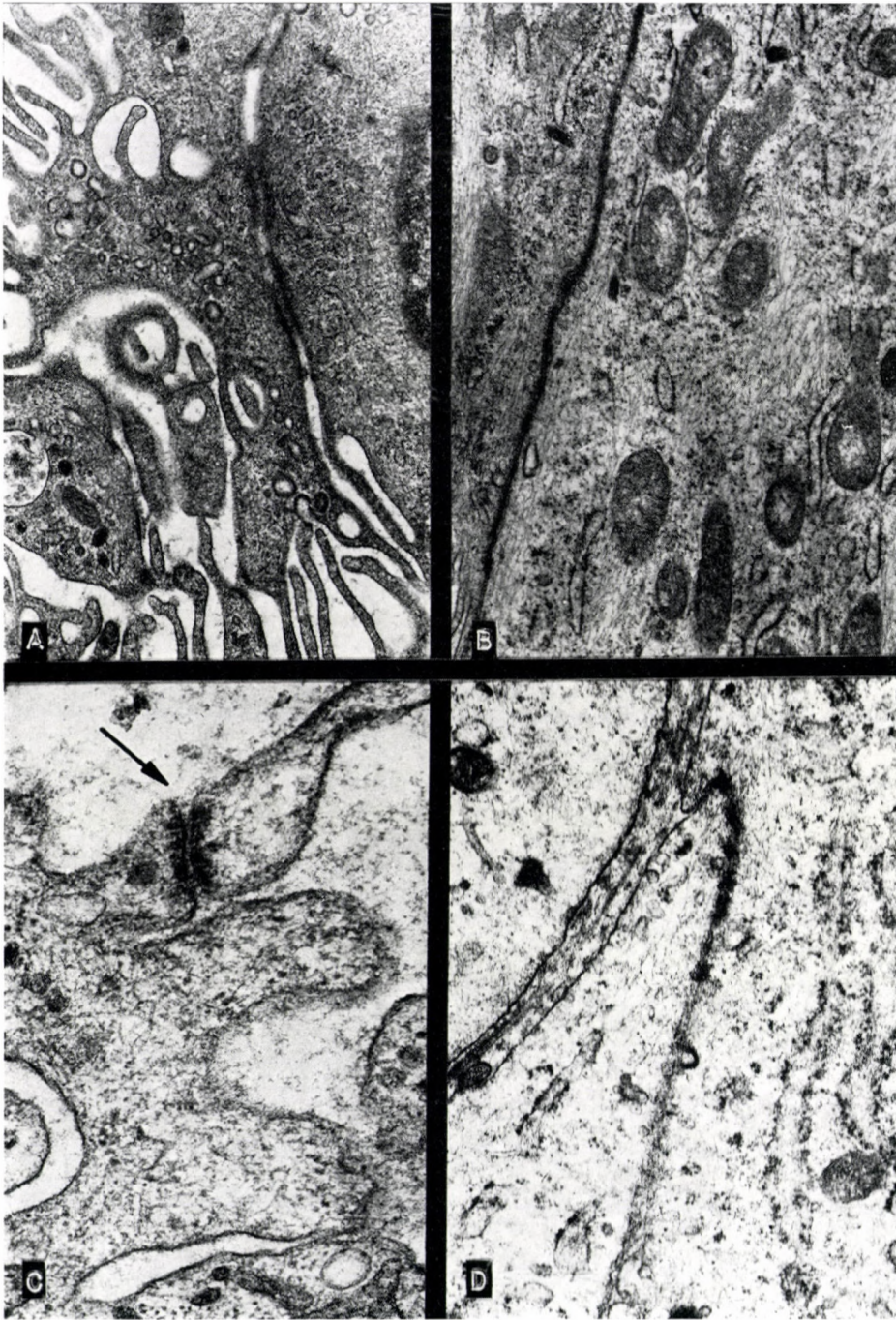


Fig. 6. A) Desmosomes between A type lining cells, $\times 22,600$. B) Adhering fascia between two fibroblasts, $\times 22,600$. C) Desmosome-like contact between processes of macrophages. Arrow indicates a narrow cylindrical cytoplasmic bridge between cell processes, $\times 71,200$. D) Multiple focal desmosome-like contact between fibroblasts, $\times 40,000$

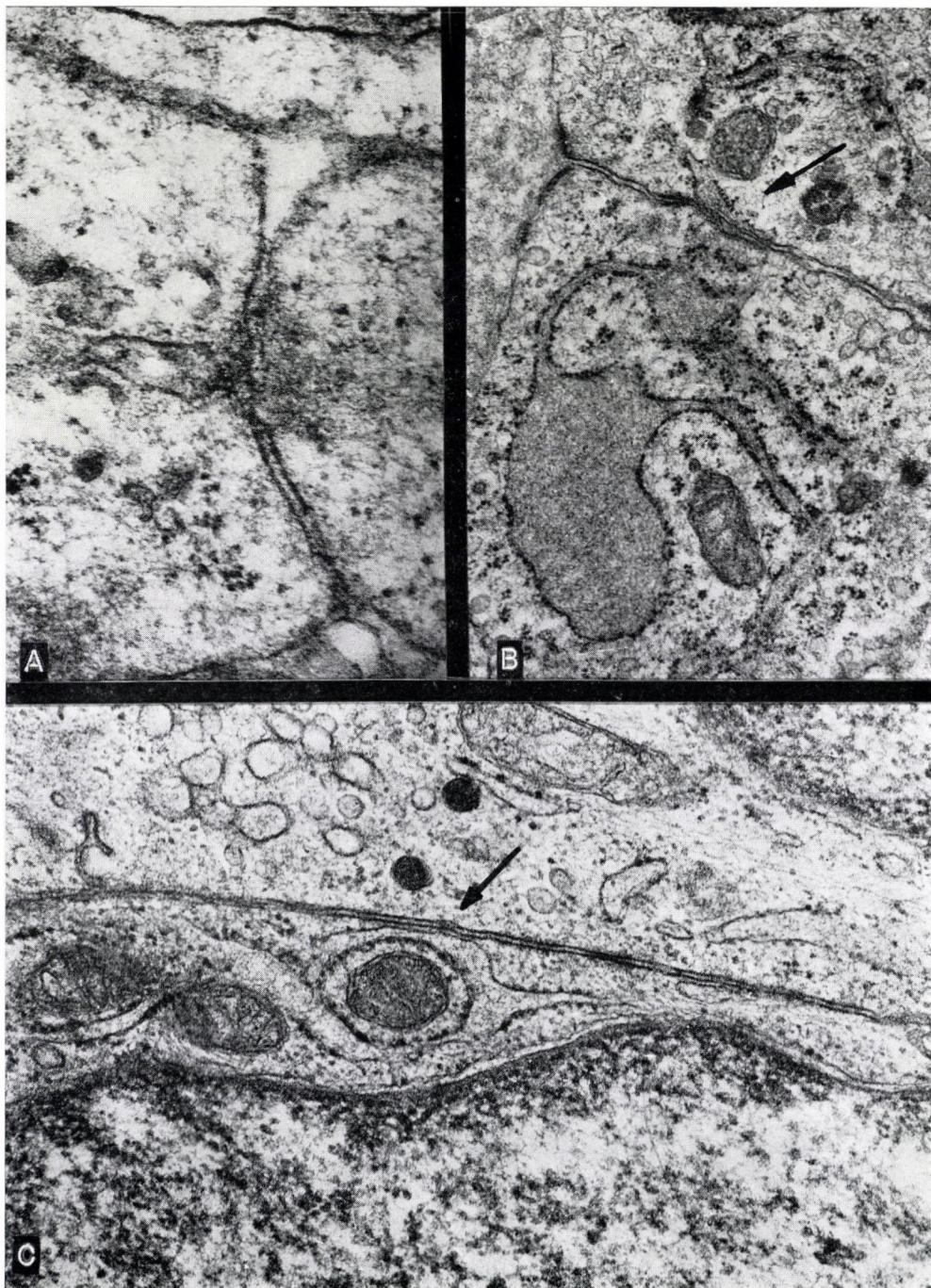


Fig. 7. A) Cell contact zones between lymphocytes. A fibrillar material is attached convergently to it, $\times 71,200$. B) Confronting subsurface cisternae with a contact zone between lymphoid cells (arrow) $\times 33,300$. C) Close membrane opposition between macrophage and fibroblast. Arrow indicates a surface cistern $\times 51,300$

Discussion

The term junction generally refers to a variety of contacts between cells or between cells and a closely opposed extracellular structure. This can be characterized as a specialized region of short-range contact between two cells which is associated with the differentiation of the contributing cell surface membranes and the intervening intercellular material. Junctions between cells can be classified into two large categories. In the first, plasma membranes of neighbouring cells appear to come into direct contact as seen in electron micrographs of standard thin sections. In the second category, plasma membranes of adjacent cells are separated by an interspace of 150–350 Å that contains electron-dense material. The term *occludens* is used for a junction where the adjacent plasma membranes of cells are in contact. The term *adhering* describes a junction where by adjacent cell membranes are not in direct contact but are attached to each other by a proteinaceous material in the interspace [34].

As seen in thin sections, an adhering junction is composed of parallel plasma membranes that are connected at their intercellular side by a thick belt (*zonula*), sheet (*fascia*) or disc (*macula*) of electron-dense material. This intercellular material can show different electron densities and structural arrangements. In the cytoplasm along an adhering junction is a condensation of filamentous material. This type of junction provides regions of strong attachment of cells and serves as anchoring site for cytoplasmic filaments.

The characteristic feature of tight junctions in ultra-thin sections is that the trilaminar plasma membranes of adjacent cells come into intimate contact and their outer leaflets appear to fuse. The total thickness of the junction is usually less than the sum of the thickness of the two plasma membranes. This type of junction forms a local permeability barrier to the passage of molecules and the flow of small ions by occluding the interspace between adjacent cells.

One of the most common forms of cell junction is the gap junction, now widely implicated in intercellular communication, in cell-to-cell transfer of ions and molecules. By standard thin-section electron microscopy the gap junction is not always easy to differentiate from the real tight junction. The first clear indication that the gap junctions and tight junctions are separate entities was provided by REVEL and KARNOVSKY [28]. In ultra-thin sections, both gap junctions and tight junctions can appear as a membrane modification where plasma membranes come into intimate opposition. It was demonstrated that a 20–40 Å electron-lucent zone of space is to be seen between the outer leaflets of membranes forming the gap junctions. This gap increases the overall thickness of the junction to more than twice the thickness of non-junctional plasma membranes and this is one of the most important differences

in appearance between the gap and the tight junction. In addition, there are other important structural differences between the two types of junctions. At present, it seems that gap junctions serve at least two functions: cell adhesion — which is a function shared with occludents and adherents, and direct cell-to-cell communication which may be mediated by gap junctions alone. However, it must be stressed that data on the real function of gap junctions are fragmentary.

An encouraging approach to the characterization of the structure of cell junction is not always easy. Often only an isolated electron microscopic photograph itself does not allow unambiguous interpretation and in many studies insufficient data are available to establish a junctional class. Therefore, in many cases, it would be better to use some non-committed term such as close opposition or contact zones unless adequate data were obtained about the nature of the studied cell contact.

The presence of different types of cell junctions between lining cells has so far been observed only in the animal synovial membrane [10, 30]. In contrast with observation intercellular contacts do not exist in normal condition between lining cells in the human synovial membrane. However, in pathological conditions such as RA, beside interdigitation of filopodia desmosomal contacts can frequently be seen between A type synovial cells [2, 9], but it must be emphasized that these contacts are not specific indicators of the pathological events in RA.

The complex interdigitations and membrane infoldings between lymphoreticular cells found in abundance especially in dense modular cell infiltrates in the rheumatoid synovium, closely resembled in ultrastructural aspect those in a lymphoid tissue following antigenic stimulation [11, 12, 13, 24, 27, 30, 35]. The intercellular contact between macrophage and lymphoid cells suggest a particular interest because macrophages appear to play an essential role in the process of antigen recognition inducing lymphocyte proliferation and in antibody formation [1, 5, 7, 14, 20, 26, 32, 33]. The direct intercellular contacts between these cells may be regarded as a morphological sign of the above-mentioned immune process in the rheumatoid synovial membrane. The occurrence of blast cells with several differentiating forms of the lymphocyte-plasma cell transformation line, the degenerated remnants of cells together with cells similar to the tingible body macrophages may also support this suggestion [8, 18]. Furthermore, the several membrane adherences, especially those between macrophages and lymphoid cells described in multiple myeloma [3] and the specific lymphocyte — target cell interaction, observed between stimulated lymphocytes and fibroblasts [16], can also be considered the site of specific immunological reactions. Close contact between lymphoid cells and macrophages in the rheumatoid synovium has recently been described by ISHIKAWA and ZIFF [15].

Subsurface cisternae associated with cell contact zones located either confronting on one side, are widely suggested as praecursors of special close junctions or desmosomes [35]. Mitochondria, free ribosomes and fine fibrillar substance were often found associated with the contact zones, giving the impression of some functional importance. In contrast, along a real gap or tight junction, cytoplasmic organelles have not been observed.

At present, an unanimous functional interpretation of intercellular junctions appears impossible. The presence of different types of direct cell contact adherence zones and the filamentous intercellular bridges, raises the question whether they are perhaps specific temporary structures, holding together a given population of cells for close cellular interactions. There is a body of evidence that a direct contact or a close cell association is required for immune induction between lymphoid cells themselves and between lymphoid cells and macrophages [26]. It is therefore interesting to speculate on the possibility that the cell contacts observed in our material might prove the site of a direct cellular interaction through which an exchange of mediators might occur perpetuating the autoimmune processes in the rheumatoid synovium. Further extensive studies are, however, required to support this assumption.

REFERENCES

1. ASKONAS, B. A., RHODES, J. M.: (1965) Immunogenecity of antigen containing ribonucleic acid preparations from macrophages. *Nature (Lond.)* **205**, 470–474. — 2. AUBÖCK, L., FLADERER, H., KLEIN, G.: (1974) Neue ultrastrukturelle Befunde an der Synovialis bei progredient chronischer Polyarthrit. *Z. Rheumatol.* **33**, 87–106. — 3. BLOM, J.: (1973) The ultrastructure of contact zones between plasma cells and dendritic macrophages from patients with multiple myeloma. *Acta path. microbiol. scand. Section A*, **81**, 734–736. — 4. FARQUHAR, M. G., PALADE, G. E.: (1965) Cell junctions in amphibian skin. *J. Cell Biol.* **26**, 263–291. — 5. FELDMAN, M.: (1972) Cell interactions in the immune response in vitro. II. The requirement for macrophages in lymphoid cell collaboration. *J. exp. Med.* **135**, 1049–1058. — 6. GILULA, N. B., REEVES, O. R., STEINBACH, A.: (1972) Metabolic coupling, ionic coupling and cell contacts. *Nature, (Lond.)* **235**, 262–265. — 7. GOTTLIEB, A. A., GLISIN, V. R., DOTY, P.: (1967) Studies on macrophage RNA involved in antibody production. *Proc. nat. Acad. Sci. (Wash.)* **57**, 1849–1856. — 8. GRANGER, G. A., WILLIAMS, T. W.: (1968) Lymphocyte cytotoxicity in vitro: Activation and release of a cytotoxic factor. *Nature (Lond.)* **218**, 1253–54. — 9. GRIMLEY, P. M., SOKOLOGG, L.: (1966) Synovial giant cells in rheumatoid arthritis. *Amer. J. Path.* **49**, 931–954. — 10. GROTH, H. P.: (1975) Cellular contacts in the synovial membrane of the cat and the rabbit. An ultrastructural study. *Cell Tiss. Res.* **164**, 525–541. — 11. HANNA, M. G., JR., MAKINODAN, T., FISCHER, W. D.: Lymphatic tissue germinal center localisation of I^{125} -labelled heterologous and isologous macroglobulins. In: *Germinal Centers of Immune Responses* (H. Cortier, N. Odartchenko, R. Schindler and C. C. Congdon, eds.) Springer-Verlag, Heidelberg—Berlin—New York, 1967, p. 68. — 12. HANNA, M. G., JR., SZAKAL, A. K.: (1968) Localization of (I^{125})-labelled antigen in germinal centers of mouse spleen. *Histologic and ultrastructural autoradiographic studies of the secondary immune reaction.* *J. Immunol.* **101**, 949–954. — 13. HANNA, M. G., JR., NETTESHEIM, P., WALBURG, M. E., JR.: A comparative study of immune reaction in germfree and conventional mice. In: *Advances in Experimental Medicine and Biology* (E. A. Mirand and N. Back, eds.) Vol. 3. Plenum Prgss, New York, 1969. — 14. HERSCH, E. M., HARRIS J. E.: (1968) Macrophage-lymphocyte interaction in the antigen-induced blastogenic response of human peripheral blood leukocytes. *J. Immunol.* **100**, 1184–1195. — 15. ISHIKAWA, H., ZIFF, M.: (1976)

Electron microscopic observations in immunoreactive cells in the rheumatoid synovial membrane. *Arthritis and Rheumatism*. **19**, 1–14. — 16. KALINA, M., GIUSBURG, H.: (1975) Ultrastructural aspects of the adherence to target cells of in vitro differentiated lymphocytes. *Proc. Soc. exp. Biol. (N. Y.)* **149**, 796–799. — 17. KARNOVSKY, M. J.: (1965) Formaldehyde-Glutaraldehyde fixative of high osmolality for use in electron microscopy. *J. Cell Biol.* **27**, 137A. — 18. KOBAYASHI, I., ZIFF, M.: (1973) Electron microscopic studies of lymphoid cells in the rheumatoid synovial membrane. *Arth and Rheum.* **16**, 471–486. — 19. LOEWENSTEIN, W. R.: (1973) Membrane junctions in growth and differentiation. *Fed. Proc.* **32**, 60–64. — 20. MILLER, J. J., NOSSAL, G. J. V.: (1964) Antigens in immunity. VI. The phagocytic reticulum of lymph node follicles. *J. exp. Med.* **120**, 1075–1082. — 21. NEUMARK, T., FARKAS, K.: (1973) Ultrastructural aspects of lymphoreticular cells in rheumatoid synovium. *Ann. rheum. Dis.* **32**, 524–530. — 22. NEUMARK, T., FARKAS, K.: (1973) Electron microscopic examination of immunocompetent cells in rheumatoid synovial membrane. *Acta morph. Acad. Sci. hung.* **21**, 105–119. — 23. NEUMARK, T., FARKAS, K.: Virus-like particles and some ultrastructural aspects of immunocompetent cells in rheumatoid synovial membrane. In: *Infection and Immunology in the Rheumatic Diseases*. Ed: D. C. Dumonde. Blackwell Oxford, London, Edinburgh, Melbourne. 1976. p. 225. — 24. NOSSAL, G. J. V., ABBOT, A., MITCHELL, J., LUMMUS, Z.: (1968) Antigen in immunity. XV. Ultrastructural features on antigen capture in primary and secondary lymphoid follicles. *J. exp. Med.* **127**, 277–290. — 25. NOSSAL, G. J. V., ADA, G. L. Antigens, Lymphoid Cells and the Immune-Response. Academic Press, New York. 1971. — 26. NOSSAL, G. J. V.: Cooperative coupling in the immune system. In: *Functional Linkage in Biomolecular Systems*. Ed. F. O. Schmitt, D. M. Schneider and D. M. Crothers, Raven Press, New York, 1975. p. 181. — 27. DEPETRIS, S., KARLSBAD, G., PERNIS, S., TURK, J. L.: (1966) Ultrastructure of cells present in lymph node during the development of contact sensitivity. *Int. Arch. Allergy*. **29**, 112–130. — 28. REVEL, J. P., KARNOVSKY, M. J.: (1967) Hexagonal array of subunits intercellular junctions of the mouse heart and liver. *J. Cell Biol.* **33**, C7–C12. — 29. ROPES, M. V., BENNETT, G. A., COBB, S., JACOX, R., JESSAR, S. A.: (1959) Diagnostic criteria for rheumatoid arthritis, 1958 revision. *Ann. rheum. Dis.* **18**, 49–53. — 30. ROY, S., GHADIALLY, F. N.: (1967) Ultrastructure of normal rat synovial membrane. *Ann. rheum. Dis.* **26**, 26–38. — 31. TURK, J. L.: (1967) Cytology of the induction of hypersensitivity. *Brit. med. Bull.* **23**, 3–8. — 32. UNANUE, E. R., ASKONAS, B. A. (1968) Persistence of immunogenicity of antigen after uptake by macrophages. *J. exp. Med.* **127**, 915–926. — 33. WALDRON, J. A. JR., HORN, R. G., ROSENTHAL, A. S.: (1973) Antigen induced proliferation of guinea pig lymphocytes in vitro: Obligatory role of macrophages in the recognition. *J. Immunol.* **111**, 58–64. — 34. WEINSTEIN, R. S., MCNUTT, N. S.: (1972) Cell junctions. *New Engl. J. Med.* **286**, 521–524. — 35. WEIS, P.: (1968) Confronting subsurface cisternae in chick embryo spinal ganglia. *J. Cell Biol.* **39**, 485–488.

ZELLKONTAKTE ZWISCHEN DEN LYMPHORETIKULÄREN ZELLEN DER RHEUMATOIDEN SYNOVIALMEMBRAN

T. NEUMARK

Die operativ entfernte Synovialmembran von 72 an rheumatoider Arthritis leidenden Kranken wurde elektronenmikroskopisch untersucht.

Die Untersuchungen richteten sich in erster Linie auf die Erforschung der Zellkontakte zwischen den die subsynoviale Schicht infiltrierenden, herdige und diffuse lymphoidzellige Infiltrate bildenden Zellen. Im Untersuchungsgut wurden zahlreiche Typen von Zellkontakten erkannt, wie einfache Zelleninterdigitation und Membranadhäsionen unterschiedlichen Typs, gap and tight junction, Bildung von zytoplasmatischen und fibrillären Brücken. Diese Zellkontakte können als morphologische Manifestationen funktionsabhängiger interzellulärer Wechselwirkungen aufgefaßt werden.

КЛЕТОЧНЫЕ СОЕДИНЕНИЯ МЕЖДУ ЛИМФОРЕТИКУЛЯРНЫМИ КЛЕТКАМИ
РЕВМАТОИДНОЙ СИНОВИАЛЬНОЙ ОБОЛОЧКИ

Т. НЕЙМАРК

Оперетивно удаленные синовиальные оболочки 72 больных ревматоидным артритом были изучены в электронном микроскопе.

Исследования были направлены в первую очередь на выяснение клеточных связей между клетками, пропитывающих субсиновиальный слой и образующих очаговую и диффузную лимфоклеточную инфильтрацию. В исследованном материале наблюдались многочисленные типы клеточных связей: простая интердигитация, мембранное притяжение, различных типов, gap and tight junction, образование цитоплазматических и фибриллярных мостов. Эти клеточные связи можно рассматривать как морфологические проявления зависимых от функции межклеточных взаимодействий.

Dr. Tamás NEUMARK } Országos Reuma és Fizioterápiás Intézet,
H-1525 Budapest, Pf. 54., Hungary

National Institute of Rheumatism and Physiotherapy, Budapest

ELECTRON TRANSPORTING ENZYMES OF RHEUMATOID CONNECTIVE TISSUE

D. TANKA and Mária KELLER

(Received October 5, 1976)

The oxidative enzyme system of the synovial membrane and rheumatoid node from rheumatoid arthritic patients has been studied by histochemical and biochemical methods. As compared to the control synovial membranes, succinic dehydrogenase activity was substantially higher in the rheumatoid arthritic synovial membranes, and was still higher in the rheumatoid nodes, in which only the cells forming the palisade had succinic dehydrogenase activity. As compared to the controls, in response to menadione succinic dehydrogenase was significantly activated. The reducible ubiquinone content of the rheumatoid synovial membrane and the rheumatoid node was by several orders of magnitude higher than in the controls.

Several theories have been put forward to explain the pathogenesis of rheumatoid arthritis. Each consideration has its realistic foundation, but none of them will fully explain the pathological process and the effect of the therapeutic procedures. It can hardly be disputed that immunological events play a significant role in the pathological process or its phases [3]. The release of lysosomal enzymes [15] occupies a prominent place among the aetiological factors. Less attention has been devoted to the metabolism of rheumatoid connective tissue and to the electron transport mechanism.

Material and methods

Fresh surgical specimens from rheumatoid arthritic patients (synovial membrane, rheumatoid nodule) and synovial tissue obtained 4 to 6 hours after death were studied. Fresh cadaver synovial membrane was used as the control. Processing began 10 minutes after operation or autopsy. From part of the tissue specimens 4 micron cryostat sections were prepared without fixation; the other part was used for biochemical studies of the following enzymes.

For the demonstration of dehydrogenases, *p*-nitrotriazolium blue (NBT) was used as the hydrogen acceptor, at an end concentration of 0.01%.

1. Succinic dehydrogenase (E.C.1.3.99.1) substrate: 30 mM sodium succinate, 0.1 M Sørensen buffer, pH 7.4. Incubation for 25 minutes [6].

2. Succinic dehydrogenase + menadione: to the above incubating mixture 0.1% menadione was added. Incubation for 25 minutes [13, 12, 14].

3. Lactate dehydrogenase (E.C.1.1.1.27) substrate: 10 mM sodium lactate, 0.75 mM NAD, 20 mM Mg chloride, 15 mM sodium cyanide, 0.1 M Sørensen buffer, pH 7.4. Incubation for 35 minutes [5].

4. Malate dehydrogenase (E.C.1.1.1.37) substrate: 10 mM sodium malate, 0.75 mM NAD, 20 mM Mg chloride, 15 mM sodium cyanide, 0.1 M Sørensen buffer, pH 7.4. Incubation for 35 minutes [5].

In honour of the 70th anniversary of Professor K. FARKAS.

5. i-citrate dehydrogenase (E.C.1.1.1.42) substrate: 10 mM sodium citrate, 0.75 mM NADP, 15 mM sodium cyanide, 0.1 M Sörensen buffer, pH 7.4. Incubation for 35 minutes [7].
6. DPNH-diaphorase (E.C.1.6.99.1) substrate: 0.1 mM NADH₂, 0.2 M tris-HCl buffer, pH 8.0. Incubation for 10 minutes [5].
7. Cytochrome c oxidase (E.C.1.9.3.1) indicators: 0.2 mM *p*-amino diphenylamine and 0.1% neotetrazolium chloride, 0.1 M Sörensen buffer pH 7.2. Incubation for 35 minutes [1].
8. Demonstration of quinones: indicators: 40 mM hydroquinone and 0.01% tetranitro-tetrazolium blue (TNBT), 0.1 M Sörensen buffer pH 7.6. Incubation for 15 minutes [11].

Quantitative enzyme activity assays:

The tissue specimens, after adding to them distilled water in a ratio of 1:10 net weight, were homogenized with an ULTRATHURAX bladed homogenator, centrifuged at 5000 r. p. m. and the supernatans were processed, adding each time 0.2 ml to the appropriate incubating mixture. Except for two cases, the histochemical incubating mixture was used for the quantitative assays, but instead of nitro-BT iodo-nitrotetrazolium blue (INT) was used, at a concentration of 0.1 mg/ml. The formazane formed was measured at 5000 nm, in 1 ml cuvette, with a Spektromom 202 photometer.

1. Succinic dehydrogenase: substrate 20 mM sodium succinate, 0.01 M Sörensen buffer, which contained in physiological proportion sodium chloride, potassium chloride and calcium chloride. Incubation for 15 minutes [8].
2. Succinic dehydrogenase + menadione: to the above incubating mixture was added 0.1% menadione. Incubation for 15 minutes [2].
3. Lactate dehydrogenase: substrate 10 mM sodium lactate, 0.4 mM NAD, 0.2 mM magnesium chloride, 1.5 mM sodium cyanide, 0.1 M Sörensen buffer, pH 7.4. Incubation for 10 minutes.
4. Malate dehydrogenase: substrate 10 mM sodium malate, 0.4 mM NAD, 2 mM magnesium chloride, 1.5 mM sodium cyanide, 0.1 M Sörensen buffer pH 7.4. Incubation for 10 minutes.
5. i-citrate dehydrogenase (E.C.1.1.1.41) substrate: 10 mM sodium i-citrate, 0.4 mM NAD, 1.5 mM sodium cyanide, 0.1 M Sörensen buffer pH 7.4. Incubation for 10 minutes.
6. DPNH-diaphorase: substrate 0.4 mM NADH₂, 0.2 N. Tris-HCl buffer pH 8.0. Incubation for 5 minutes.
7. Cytochrome c oxidase: indicators: 0.2 mM *p*-amino-diphenylamine, 0.2 mM *p*-metoxy-*p*-phenylene diamine, 0.1 M Sörensen buffer pH 7.2. Incubation for 10 minutes.
8. Quinone determination: indicator: 4 mM hydroquinone, 0.1 M Sörensen buffer pH 7.6. Incubation for 15 minutes.
9. Protein was determined by the biuret reaction.

The enzyme activities were so calculated that serial dilutions were prepared from INT, then it was converted to formazan by means of alkaline ascorbic acid reduction. The diagram of formazan concentration was plotted.

Ubiquinone assay [2, 4]. A predetermined quantity of the specimen was dehydrated by braying with sodium sulphate, then it was extracted according to Soxhlet with ethanol containing alkaline pyrogallol. The extract was purified by shaking out with *n*-heptane, concentrated by vacuum distillation, and the residue was dissolved in chloroform.

The chloroform solution was chromatographed on Silicagel G plate, in 1:1 mixture of benzene-chloroform. The ubiquinone fraction detected in UV light was eluted in ethanol, spectrophotometrized at 2750 and 2900 nm, then, after borohydride reduction, the extinctions were determined again at the wave lengths specified above. The difference at 2750 nm represented the so-called reducible ubiquinone content.

Results

In the synovial membranes studied by histochemical methods the most intensive oxidative activity was usually found in the lining cells. There was also significant activity in the areas of inflammatory (lymphoid) infiltration (Figs 1 and 2). In the control synovial membranes the activity of the cells covering

the surface was more intensive than that of the connective tissue cells under the surface. An exception was succinic dehydrogenase activity. In the control synovial membrane this activity was absent or could hardly be detected. In the specimens from rheumatoid arthritis patients succinic dehydrogenase activity was slightly increased, almost escaping detection under the microscope. On adding menadione to the incubating solution, the activity increased. In this case the covering cells and the elements of round cell infiltration showed somewhat more intensive activity than the connective tissue cells of the ground tissue.

A different pattern of enzyme activity distribution was found in the rheumatoid nodules. The activities of the dehydrogenases tested were more intensive in the cells forming the palisade demarcating the fibrinoid, than in the cells of the granulation tissue, although the latter showed considerable enzyme activities (Figs 3—7). Here too, succinic dehydrogenase was an exception. While its activity was marked in the cells forming the palisade, it was hardly demonstrable in the granulation tissue (Fig 8). In response to menadione the enzyme activity of the palisade cells increased slightly, hardly discernible under the microscope, whereas a significant activation of succinic dehydrogenase resulted in the cells of the granulation tissue (Fig. 9). Histochemical studies of the distribution of tissue ubiquinone (quinone) revealed high activity in the cells forming the palisade and a low activity in the granulation tissue cells (Fig. 10).

The results of quantitative enzyme activity and ubiquinone assays carried out in synovial tissue and in the rheumatoid nodule corresponded well to the values estimated histochemically. As compared to the controls, the activity of the oxidative enzymes tested was higher. The value for succinic dehydrogenase was hardly different from that found in the control synovial tissue. It was, however, conspicuous, how markedly succinic dehydrogenase activity increased in response to menadione (Table I). The total quinone content in the rheumatoid arthritic synovial membranes was almost threefold that in the controls. The reducible ubiquinone content increased by one order of magnitude as compared to the control (Table II).

In the rheumatoid nodes oxidative enzyme activities were high and so was the activity of succinic dehydrogenase. The quantity of succinic dehydrogenase activated with menadione was less than on the rheumatoid synovial membrane. As compared to the control synovial membrane, the reducible ubiquinone content was two orders of magnitude lower, and as compared to the rheumatoid arthritic synovial, one order of magnitude lower.

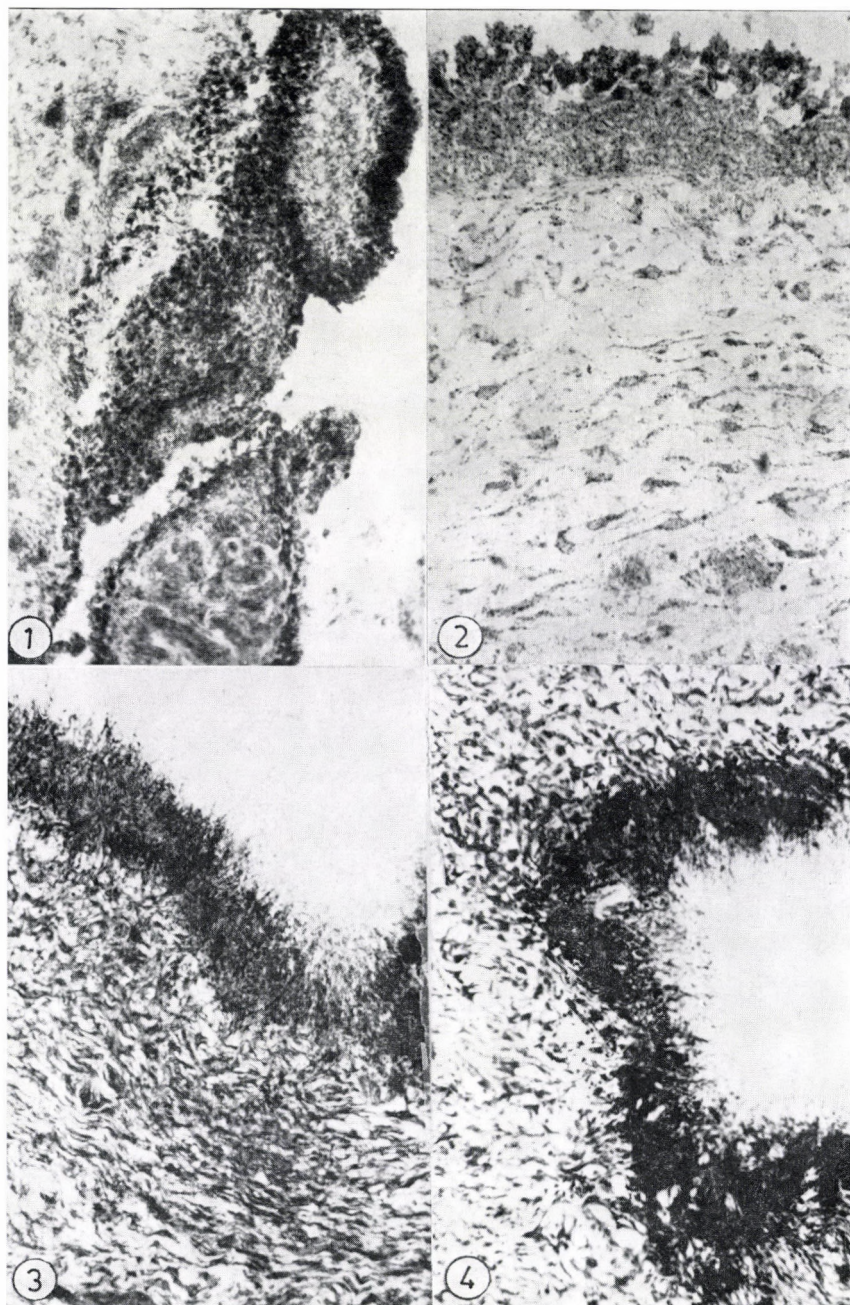


Fig. 1. Intensive lactate dehydrogenase reaction in the lining cells of the synovial and in lymphoid infiltration. $\times 30$

Fig. 2. Malate dehydrogenase activity of synovial membrane in p. c. p. $\times 30$

Fig. 3. Intensive lactate dehydrogenase reaction in the palisade cells and the granulations tissue of the rheumatoid nodule. $\times 30$

Fig. 4. Malate dehydrogenase reaction to the rheumatoid nodule; the localization is similar to that of lactate dehydrogenase. $\times 30$

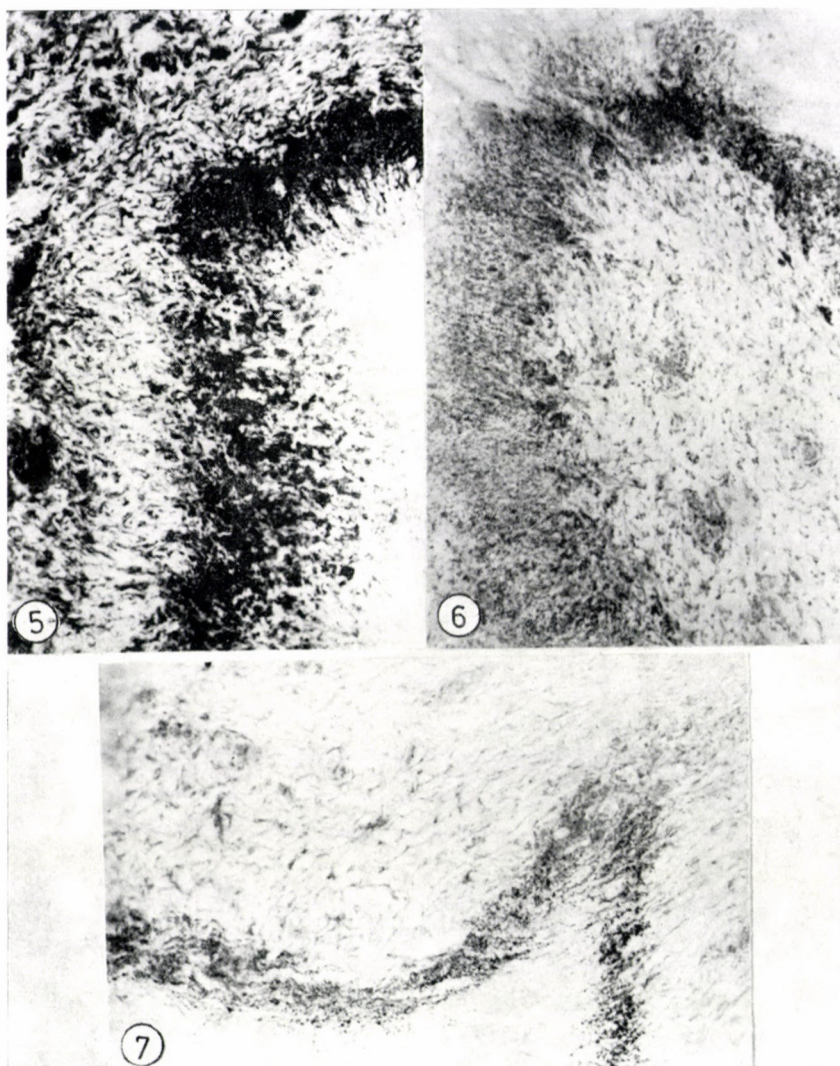


Fig. 5. NADH diaphorase reaction in rheumatoid nodule, similar in localization to that of lactate dehydrogenase. $\times 30$

Fig. 6. Isocitrate dehydrogenase activity of rheumatoid nodule. The localization is similar to the previous one but of less intensity than the others. $\times 30$

Fig. 7. Cytochrome oxidase activity. Medium reaction in the fibrinoid demarcating cells and weaker one in the granulation tissue. $\times 30$

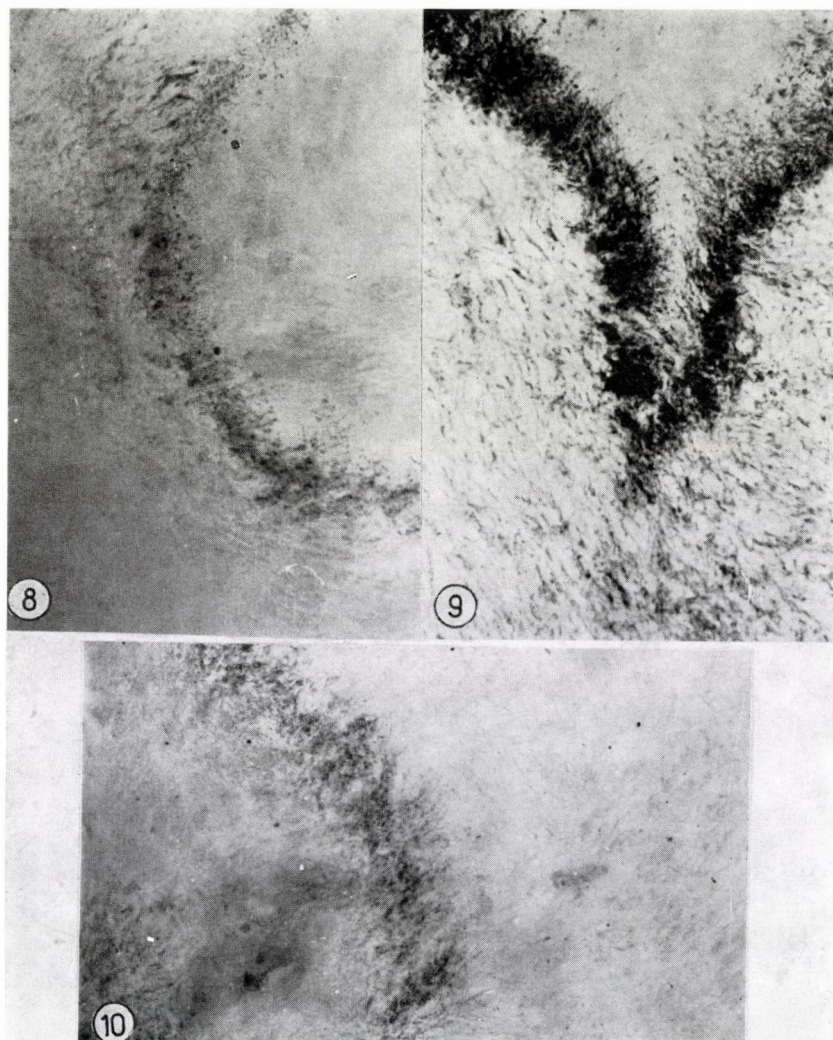


Fig. 8. Succinic dehydrogenase reaction demonstrated only in the palisade cells. $\times 30$

Fig. 9. Under the effect of menadione succinic dehydrogenase activity of the palisade cells increased, and appeared in the granulation tissue too. $\times 30$

Fig. 10. High ubiquinone content in the palisade cells and low in the granulation tissue. $\times 30$

Table I

The used materials	SDH	SOH K _s	LDH	MDH
	mg formazan/100 mg protein			
Syn. autopsy cont.	2.1 —	2.5 —	3.7 —	5.1 —
Syn. autopsy p.c.p.	1.8 p < 0.03	10.3 p < 0.11	6.1 p < 0.03	4.4 p < 0.09
Syn. biopsy p.c.p.	3.9 p < 0.16	5.9 p < 0.05	7.6 p < 0.07	5.1 p < 0.06
Rheumatoid nod.	3.5 —	5.3 —	7.5 p < 0.12	6.2 p < 0.14

The used materials	i-COH	DPNH D.	CYT. Ox.	QUINONE
	mg formazan/100 mg protein			
Syn. autopsy cont.	—	3.5 —	—	4.6 —
Syn. autopsy p.c.p.	4.1 p < 0.08	4.8 p < 0.11	10.8 —	16.4 p < 0.09
Syn. biopsy p.c.p.	7.9 —	7.1 p < 0.12	12.5 —	14.6 p < 0.07
Rheumatoid nod.	—	9.8 —	18.3 —	19.2 p < 0.18

Table II

The used materials	Ox.	Red.	Reducible
	CoQ Cont. in mg/100g wet weight		
Syn. autopsy cont.	0.73 —	1.98 —	0.01 —
Syn. autopsy p.c.p.	0.88 p < 0.05	3.63 p < 0.03	0.22 p < 0.01
Syn. biopsy p.c.p.	0.76 p < 0.01	2.68 p < 0.01	0.28 p < 0.01
Rheumatoid nod.	8.20 p < 0.09	16.06 p < 0.10	2.02 p < 0.07

Discussion

Our investigations have confirmed the hypothesis that the metabolism of the rheumatoid arthritic synovial membrane and of the connective tissue cells of the rheumatoid node was significantly different from that of the synovial membranes from non-rheumatoid arthritic patients. In general, an increased oxidative metabolism is to be reckoned with in inflammatory processes. This was the case also with rheumatoid arthritis, as indicated by the higher activities of the dehydrogenases investigated as compared with those in the controls.

A substantial difference was demonstrated between the succinic dehydrogenase activity of the rheumatoid arthritic granuloma (Meynet's node) and that demonstrable histochemically in other granulative joint diseases (gout, pseudogout) [9, 10]. Special attention has to be paid to the difference in succinic dehydrogenase activity between the cells demarcating the fibrinoid (those forming the palisade) and the chronic granulation tissue surrounding it. The high succinic dehydrogenase activity of the demarcating cells has made us to study the ubiquinone content of this structure, and it was observed that the ubiquinone content of the cells forming the palisade was significantly higher than that of the connective tissue cells of granulation tissue.

The rheumatoid synovial membranes contained much more reducible ubiquinone, which can be utilized in biological oxidation, than the controls, but there was a conspicuous quantity of reducible ubiquinone in the rheumatoid node, too. On the basis of the histochemical evidence it may be assumed that most of the latter is to be found in the cells forming the palisade. This seemed to follow from the histochemical and biochemical tests carried out with menadione.

In general, the activity of succinic dehydrogenase activated by menadione increased in the synovial membrane, but, as suggested by the histochemical evidence, in the rheumatoid node the activation can be demonstrated in the granulation tissue in the first place. This observation may be supplied only by further investigations.

It is suggested that the granulation tissue displays a low succinic dehydrogenase activity because it contains little ubiquinone necessary for activation. Thus, the succinic dehydrogenase enzyme molecule is present in the cells but the optimum amount required for activation is missing. Another possibility is that the granulation tissue contains such a succinic dehydrogenase isoenzyme which requires some other quantity of, ubiquinone for its activation. The latter seems to be supported by the fact that, according to our disk electrophoretic studies, menadione would activate merely one of the succinic dehydrogenase isoenzymes.

REFERENCES

1. BURSTONE, M. S.: Enzyme Histochemistry. Acad. Press, New York 1962. — 2. CRANE, F. L., HATEFI, Y., LESTER, R. L.: (1957) Isolation of quinone from beef heart mitochondria. *Biochem. biophys. Acta* **25**, 220—221. — 3. FARKAS, K.: (1969) Új szempontok az idült rheuma kórfejlődésének magyarázatához. *Rheumat. Balneol. Allergol.* **10**, 65—75. — 4. GODINER, M. H., TRUMPOWER, B. L., CARPENTER, P. C., OLSON, R. E.: (1970) The biosynthesis of ubiquinone in muscle from normal and genetically dystrophic mice. *Arch. Biochem. Biophys.* **140**, 39—46. — 5. HESS, R., SCARPELLI, D. G., PEARSE, A. G. E.: (1958) The cytochemical localisation of oxidative enzymes. II. Pyridine nucleotide linked dehydrogenases. *J. Biophys. Biochem. Cytol.* **4**, 753—760. — 6. NACHLAS, M. M., TSOU, K. C., DeSOUSA, E., CHANG, C. S., SELIGMAN, A. M.: (1957) Cytochemical demonstration of succinic dehydrogenase by the use of a new p-nitro-phenyl substituted ditetrazole. *J. Histochem. Cytochem.* **5**, 420—436. — 7. PEARSE, A. G. E.: *Histochemistry, Theoretical and Applied*. Ed. J. Churchill, Ltd. London 1968. — 8. TANKA, D.: (1967) A sugárrezisztens szervek morfológiai károsodásáról. Thesis, Budapest. — 9. TANKA, D.: (1973) Enzyme histochemical studies of the rheumatoid nodule. *Morph. és Ig. Orvosi Szemle.* **13**, 303—311. — 10. TANKA, D., MITUSZOVA, L., KELLER, M.: Enzyme histochemical changes of the synovial membrane in gouty arthritis. In press. *Ann. Rheum.* — 11. TRANZER, J. P., PEARSE, A. G. E.: (1963) Cytochemical demonstration of ubiquinones in animal tissues. *Nature (Lond.)* **199**, 1063—1066. — 12. WATTENBERG, L. W., LEONG, J. L.: (1960) Effect of co-enzyme Q_{10} and menadione on succinic dehydrogenase activity as measured by tetrazolium salt reduction. *J. Histochem. Cytochem.* **8**, 296—303. — 13. WATTENBERG, L. W.: Histochemical studies of the effects of co-enzyme Q_{10} and Menadione on oxidative enzymes in normal and neoplastic cells. In: *Ciba Foundation Symposium on Quinones in Electron Transport*. J. A. Churchill Ltd., London 1961. p. 367. — 14. WATTENBERG, L. W.: (1961) The effects of quinones on the activity of flavoprotein dehydrogenase systems as measured by tetrazolium salt reduction. *Ann. Histochem.* **6**, 305—310. — 15. WEISSMAN, G.: Lysosomes and the mediation of tissue injury in arthritis. In: *Rheumatoid Arthritis*. Ed.: W. Müller, H. G. Hartworth and K. Fehr. Academic Press, New York 1971. pp. 141—154.

HISTOCHEMISCHE UND BIOCHEMISCHE UNTERSUCHUNG DER ELEKTRONEN-
TRANSPORTIERENDEN ENZYME DES RHEUMATOIDEN BINDEGEWEBES

D. TANKA und MÁRIA KELLER

Das oxydative Enzymsystem der Membrana synovialis bzw. des rheumatoiden Knotens von Kranken mit rheumatoider Arthritis wurde mittels histochemischer und biochemischer Verfahren untersucht. Den Ergebnissen nach ist in der Membrana synovialis der Kranken mit rheumatoider Arthritis die Sukzinodehydrogenaseaktivität wesentlich höher als in den Kontroll-Synovialmembranen, aber noch erheblicher ist sie in den rheumatoiden Knoten, in denen nur die die Palisade bildenden Zellen eine Sukzinodehydrogenaseaktivität aufweisen. Mit Menadion läßt sich im Vergleich zu den Kontrollen sehr bedeutende Sukzinodehydrogenaseaktivisierung aufzeigen. Der Gehalt an reduzierbarem Ubiquinon ist in der rheumatoiden Membrana synovialis und in den rheumatoiden Knoten um mehrere Größenordnungen höher als in den Kontrollen.

ГИСТОХИМИЧЕСКОЕ И БИОХИМИЧЕСКОЕ ИЗУЧЕНИЕ
ЭЛЕКТРОННОТРАНСПОРТНЫХ ЭНЗИМОВ РЕВМАТОИДНОЙ
СОЕДИНИТЕЛЬНОЙ ТКАНИ

Д. ТАНКА и МАРИЯ КЕЛЛЕР

Окислительная энзиматическая система синовиальной оболочки или ревматоидного узла больных ревматоидным артритом была изучена с помощью гистохимических и биохимических методов. Согласно результатам в синовиальной оболочке больных ревма-

тоидным артритом активность сукцинодегидрогеназы намного выше чем в контрольных синовиальных оболочках, и она еще выше в ревматоидных узлах, в которых активность сукцинодегидрогеназы выявляема только в клетках, образующих палисад. При помощи менадиона удалось выявить по сравнению с контролями очень значительную активность сукцинодегидрогеназы. Содержание восстанавливаемого убихинона в ревматоидной синовиальной оболочке и в ревматоидных узлах превышает на многие порядки величин его концентрацию в контролях.

Dr. Dezső TANKA } Országos Reuma és Fizioterápiás Intézet,
Dr. Mária KELLER } H-1525 Budapest, Pf. 54., Hungary

Second Institute of Pathology, Semmelweis University Medical School, Budapest

INFLUENCE OF MEMBRANE ACTIVE SUBSTANCES ON CELL SURFACE MORPHOLOGY OF CULTURED AORTIC ENDOTHELIAL CELLS

Éva CSONKA, B. BERNOLÁK, A. S. KOCH and H. JELLINEK

(Received October 26, 1976)

1. The changes occurring on the surface of cultured aortic endothelial cells under the influence of exogenous cholesterol, lysolecithin, or cholesterol + lysolecithin were pursued by scanning and transmission electron microscopy.

2. Both compounds were found to cause surface changes under different quantitative relations, as shown by scanning electron microscopy of unfixed preparations. The changes were less significant in preparations fixed prior to the scanning — or transmission electron microscopic examination.

3. Other cell lines maintained in this laboratory and similarly treated with cholesterol, were found to be less responsive than the endothelial cells.

4. Cholesterol content was determined by thin layer chromatography in six different cell lines, before and after the addition of cholesterol. Only the endothelial cells showed a notable rise of cholesterol content after treatment. This fact may confirm our finding that cholesterol induced morphological changes were demonstrable only in the endothelial cells.

Among the cellular components of the vascular wall the endothelial cells play in all probability a major role in the development of initial atherosclerotic changes. Various blood-borne materials, which may injure the vessel wall, are contacting the endothelial cells first, and the permeability of the endothelial cell membranes among others allows the passage of such materials across, or their deposition, in the vessel wall. The influence of membrane active substances has chiefly been studied *in vitro* cell cultures, because the *in vivo* approach is extremely difficult. Since the various cell types may have dissimilar functions, cultured homogeneous cell populations are the ideal models for such investigations.

In this laboratory a pure endothelial cell line [2, 3] was obtained from pig aortic endothelium. The cultured cells were identified as true endothelium, by light and electron-microscopic morphology. Among the many factors involved in atherogenesis, cholesterol and lysolecithin were studied for this influence on cultured endothelial cells, in the first stage chiefly by morphological methods. Both compounds are acting on the cell membrane. It is known that a high-cholesterol diet injures the aortic endothelial cells of experimental animals [1]. Cholesterol, being a normal component of the cell membrane, influences its physical and chemical properties, including permeability. Lysolecithin has been shown to be present at elevated levels in the intima and media

of the atherosclerotic aorta [5]. It is also known that lysolecithin injures the cell membrane.

In view of these considerations, the probable injury of the surfaces of *in vitro* cultured aortic endothelial cells by cholesterol and lysolecithin was studied by scanning and transmission electron microscopy. Other cell lines available in this laboratory were similarly examined for comparison. Furthermore, the cholesterol contents of *in vitro* cultured endothelial and other cells were assessed by thin layer chromatography before and after the addition of cholesterol.

Materials and methods

Cell cultures

Passages 7 to 10 of the miniature-pig aortic endothelial cell culture BAEC-203 (Budapest Aortic Endothelial Cell Line), maintained in this laboratory.

Passages 104 to 110 of the modified heteroploid aortic smooth muscle cell line BASC-76 (Budapest Aortic Smooth Cell Line), obtained from miniature-pig aorta and maintained in this laboratory.

Guinea-pig fibroblast cell line T-23, maintained in this laboratory.

Monkey kidney epithelial cell line III/1 (National Institute of Public Health, Budapest).

HeLa international standard cell strain.

BHK suckling hamster kidney cells, international standard strain.

All cell cultures used in the experiment were grown in Parker-199 medium containing 10% calf serum. Cultures grown in 2 litre Roux-flasks were used for thin layer chromatography, and coverslip cultures grown in Leighton tubes for scanning electron microscopy.

Treatment with cholesterol and lysolecithin

A 10^{-2} M stock solution was prepared from cholesterol (NBC, USA, S. C. W. grade) in dimethyl formamide (Form-dimethyl-amide, BDH, England). Further dilutions of the stock solution, ranging from 10^{-4} M to 10^{-2} M, were prepared in Parker-199 medium containing 10% calf serum. The endothelial cells were incubated in the nutrient media containing different concentrations of cholesterol at 37 °C for 24 hours.

The lysolecithin (Calbiochem. Lot. 400205 B grade M. W. 497.7) stock solution, also 10^{-2} M, was prepared in PBS (pH 7.2), to which crystalline bovine albumin was added. Further dilutions were prepared as above, in Parker-199 medium containing 10% calf serum. The cells were incubated in the lysolecithin-containing medium for 24 hours.

Thin layer chromatography

Cells cultured in Roux-flasks were washed in PBS, detached from the glass by treatment with 0.25% trypsin and 0.1% versene, and dissolved in PBS. The cell suspension so obtained was washed by centrifugation in PBS. In each test 3×10^7 cells were used, in 1 ml total volume. The cells were disrupted by three cycles of freezing and thawing, then incubated for 5 minutes in a 50 °C water bath after the addition of 10 ml chloroform-methanol (1 : 1) mixture, and passed through filter paper. The filtrate was evaporated and the residue was resuspended in 1 ml chloroform-methanol (1 : 1) mixture.

The cholesterol content of the nutrient media was determined by shaking out three times with chloroform-methanol (1 : 1) in 10 ml lots, then treated further as above. The calf serum added to the nutrient medium was checked by processing a 1 ml amount of it in the undiluted state as above.

The cholesterol control series was diluted in chloroform-methanol (1 : 1).

Thin layer chromatography was carried out as proposed by PILZ and FRICK [4] and ZÖLLNER and WOLFRAM [9] using PcJ gram Sil. G. Macherey-Nagel plates.

Scanning electron microscopy

1. The coverslip cultures were washed in PBS, rinsed three times for 1 second in distilled water and were immediately mounted on copper plate and dried in vacuum. Pressure was reduced gradually to 10^{-3} mm Hg in 10 minutes, and to 5×10^{-5} mm Hg in another 10 minutes. The coverslip cultures were fixed for 2 hours in 6% glutaraldehyde containing Holt solution, washed in phosphate buffered saline after fixation, and dehydrated in step-graded ethanol and acetone.

Pieces of the coverslip, carrying the differently processed cells were coated with carbon (50 Å thick) and gold (200 Å thick), and shadowed with copper at the angle of 20° . The preparations were examined in a scanning adapter connected with a JEM 100 B electron microscope, at 40 KV voltage and 60 μ beam amperage.

Transmission electron microscopy

For transmission electron microscopy the cells were grown in Falcon plastic flasks. After outgrowth of the cell sheet, the preparation was fixed in 2.5% glutaraldehyde for 1 hour and postfixed in 1% OsO_4 for 30 minutes. Both fixing procedure were followed by washing for 2×10 minutes in phosphate buffer pH 7.3. After rapid dehydration in step-graded ethanol, the specimens were embedded in Araldite. The ultrathin sections were stained with uranyl acetate and lead citrate. The preparations were examined in a JEM 100 B electron microscope.

Results

Figure 1. The endothelial cells incubated in the presence of cholesterol at various concentrations carried on their surfaces many small pits about 1500 Å in diameter, and the cell margins were indefinite. The degree of this superficial change was decreasing as the concentration of cholesterol was reduced.

Figure 2/a—g. Since at low magnification, many pits were seen on the surface of untreated endothelial cells, high magnification scanning electron micrographs were prepared of cholesterol treated and untreated cells for the sake of comparison. The pits on the untreated cells were considerably larger and dissimilar in size as compared to the pits treated cells, which had a more even appearance. At high magnification the cell surface appeared smooth, and the configurations seen under low power as small rosette-like groups were identified as gaps through which the original cell surface became visible. In the control cells, the structures appearing like pits under low power were indentified as small pores in an intricate surface structure.

Figure 3. Since the cholesterol dilutions were prepared in dimethyl-formamide, the 10^{-4}M dilution of cholesterol contained 10^{-3} (v/v) concentration of the diluent. For this reason, the diluent was checked for influence on the cell surface. It did in fact cause changes on the cell surface, thus, the alteration caused by 10^{-4}M cholesterol in 10^{-3} (v/v) dimethyl formamide were attributed to both compounds.

Scanning electron micrographs were made of the cholesterol treated laboratory cell lines, for the sake of comparison. These were in fact considerably less affected by cholesterol than the endothelial cells, and did not show significant morphological changes. Since the different cell cultures

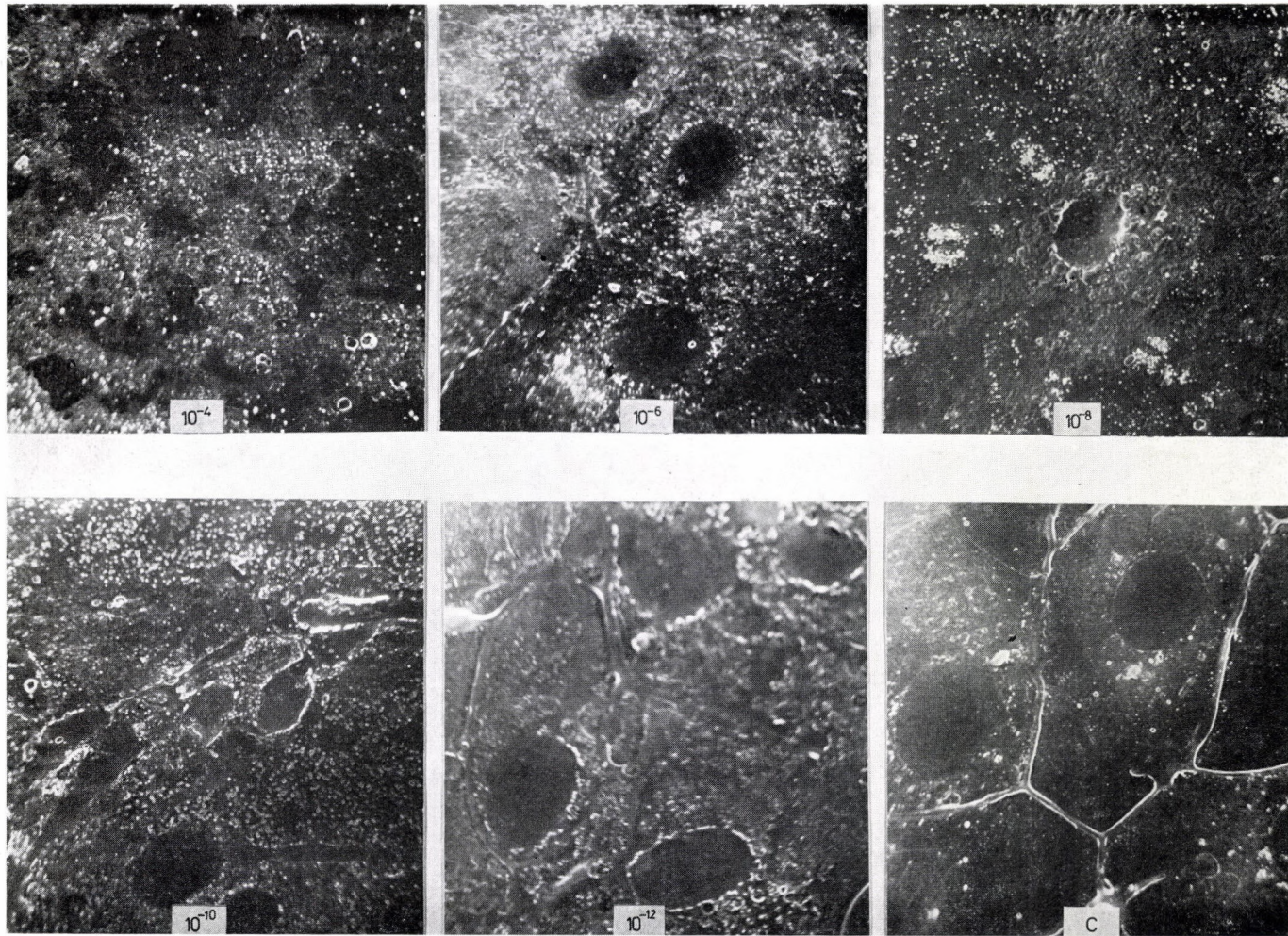


Fig. 1. Scanning electron micrograph of endothelial cells treated with cholesterol at different concentrations. C = control. $\times 2000$

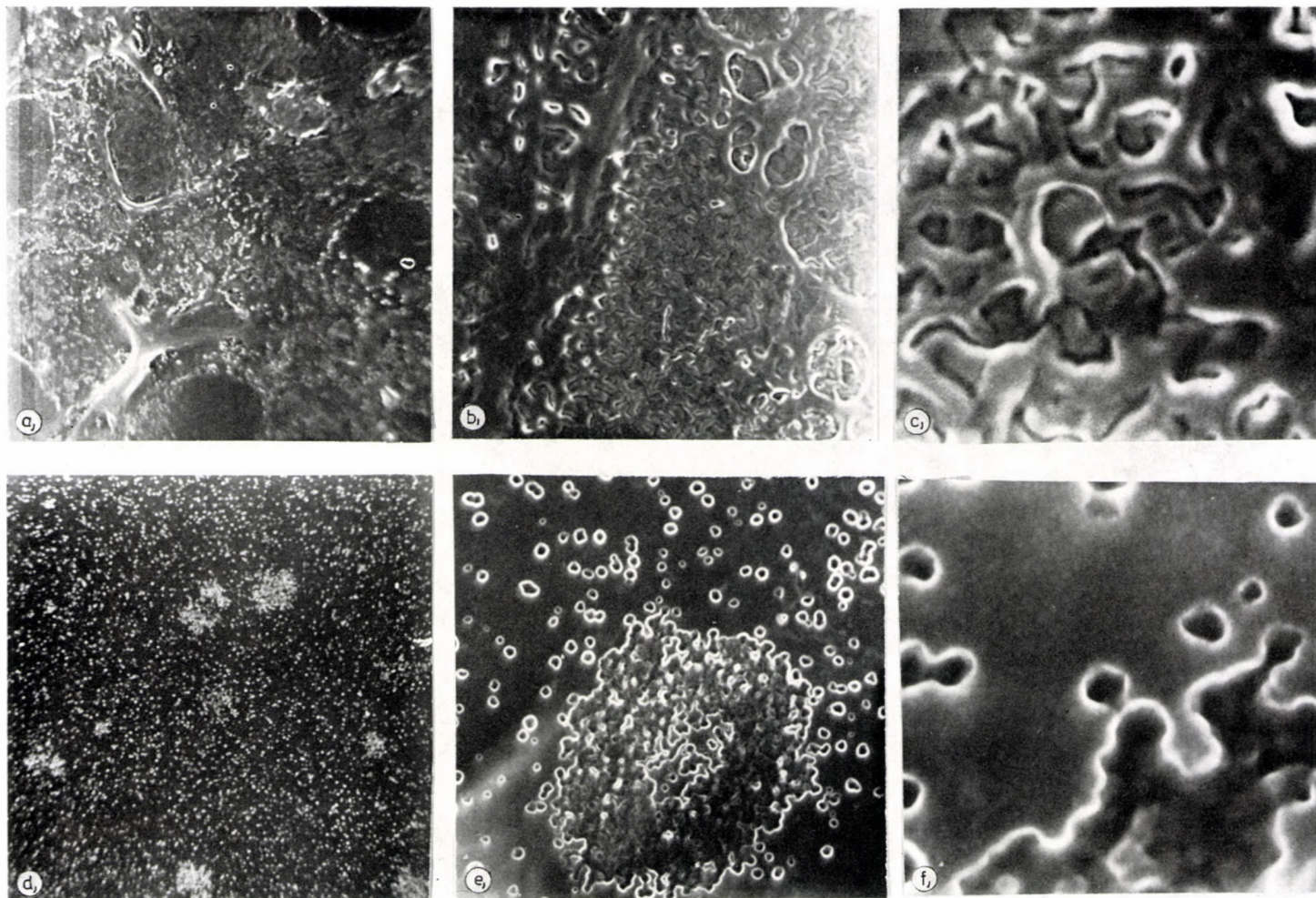


Fig. 2. Scanning electron micrographs of cultured endothelial cells treated and not treated with 10^{-4} M cholesterol. a) Untreated cell, $\times 1500$; b) untreated cell, $\times 10,000$; c) untreated cell, $\times 50,000$; d) cell treated with 10^{-4} M cholesterol, $\times 1500$; e) cell treated with 10^{-4} M cholesterol, $\times 10,000$; f) cell treated with 10^{-4} M cholesterol, $\times 50,000$

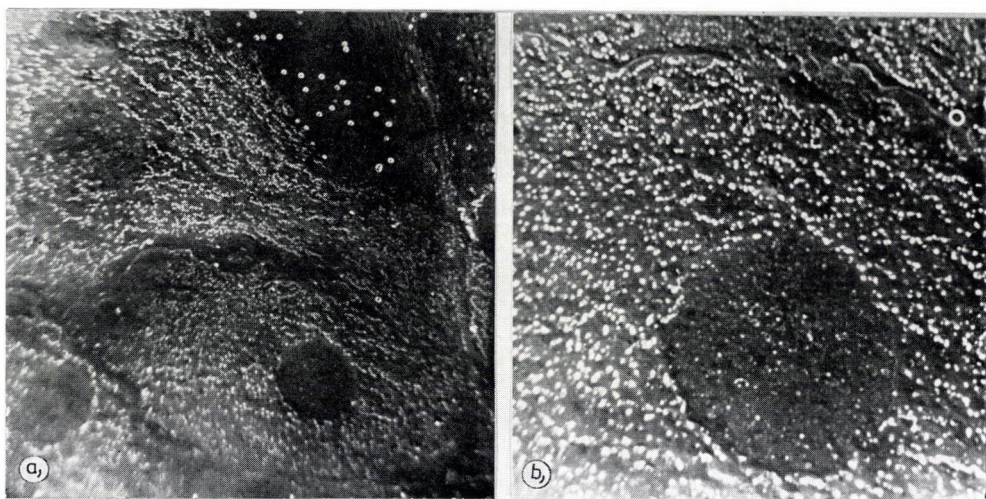


Fig. 3. Scanning electron micrographs of dimethyl formamide-treated endothelial cells.
a) $\times 1500$; b) $\times 3000$

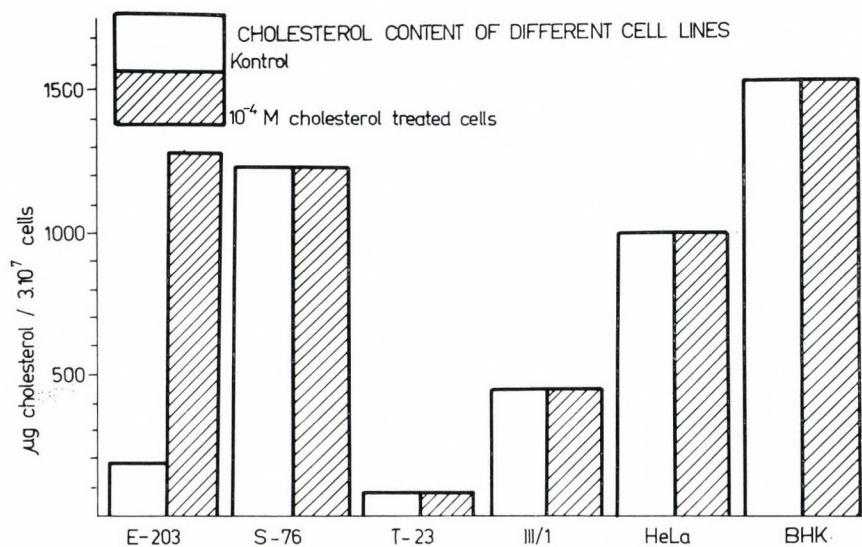
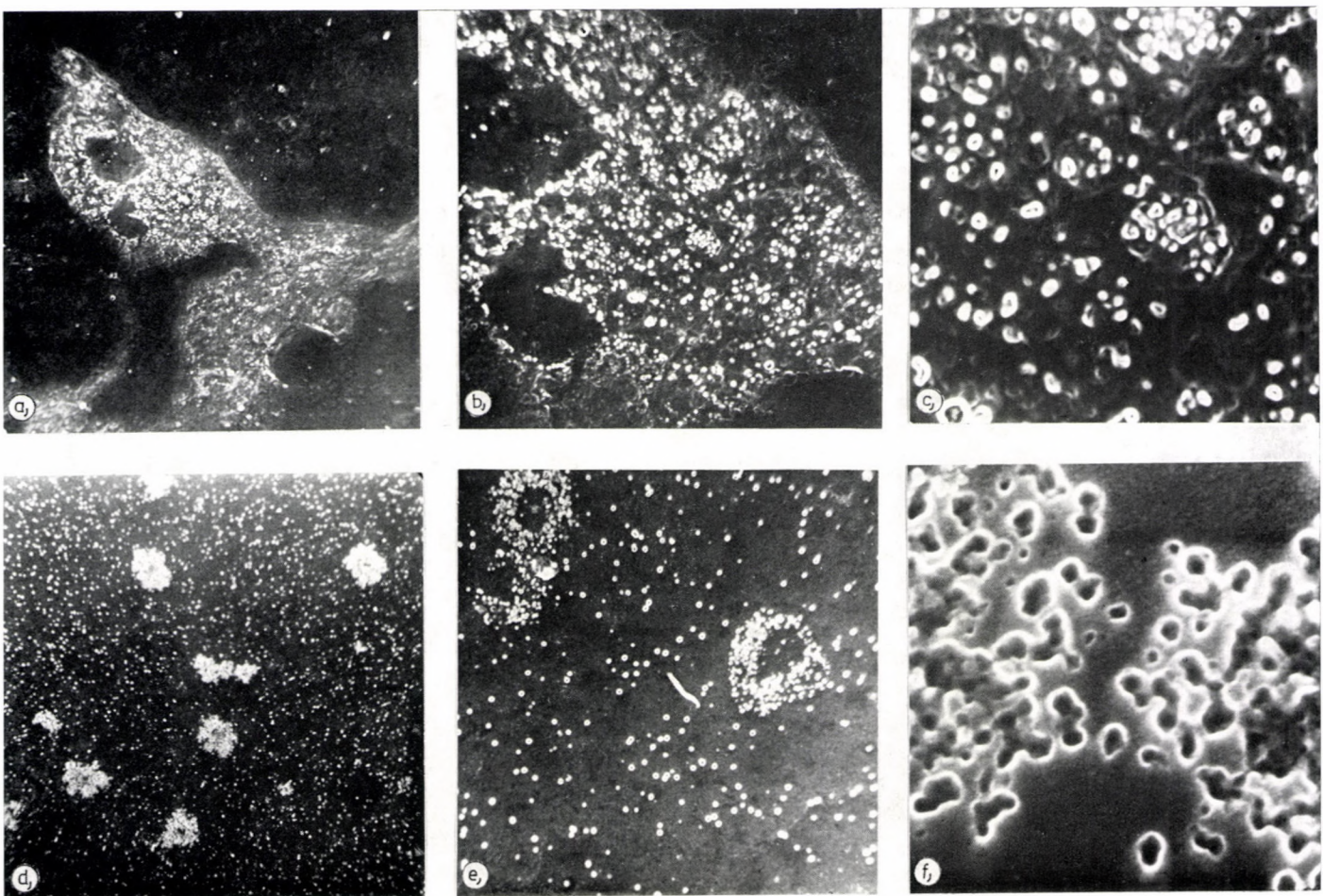


Fig. 4. Cholesterol content in various cell lines

*Fig. 5*

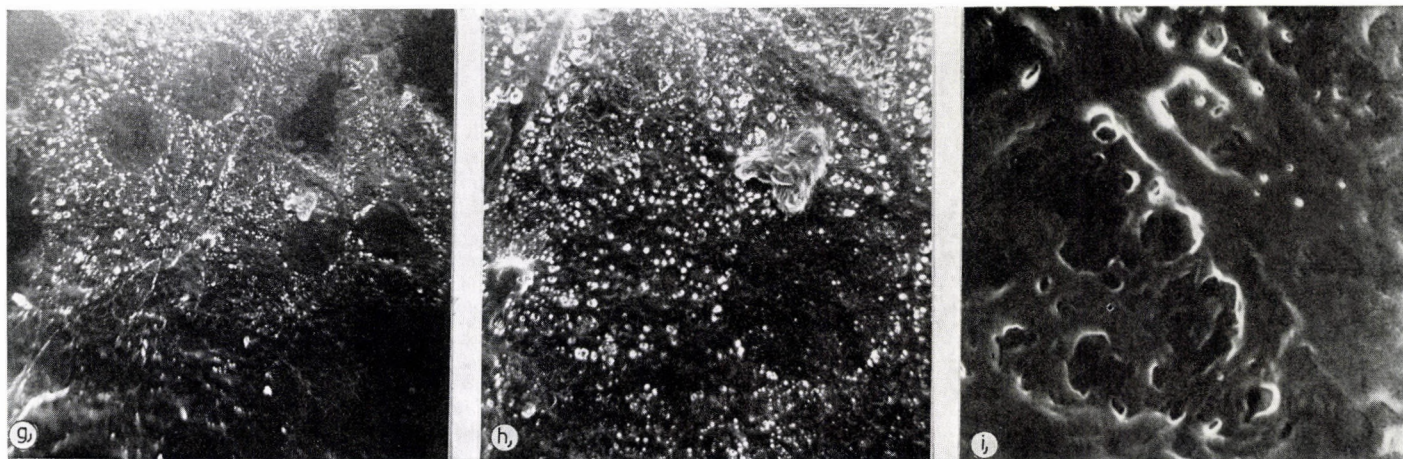


Fig. 5. Effect of cholesterol and lysolecithin on cultured endothelial cells. Effect of treatment with lysolecithin. a—b—c) cells treated with 10^{-4} M lysolecithin $\times 1000$, $\times 3000$, $\times 20,000$; d—e—f) cells treated with 10^{-4} M lysolecithin for 24 hours $\times 1000$, $\times 3000$, $\times 10,000$; g—h—i) effect of treatment with lysolecithin-cholesterol

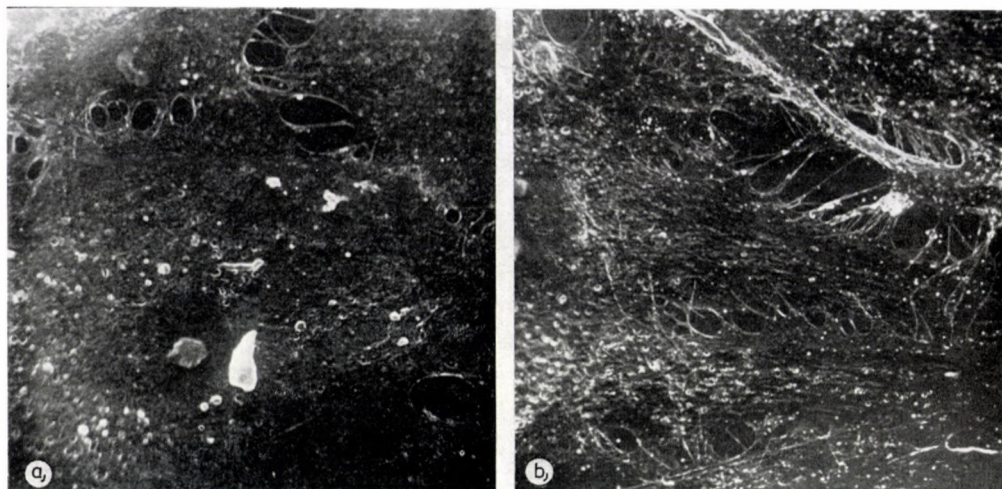


Fig. 6. Scanning electron micrographs of fixed endothelial cells treated and not treated with 10^{-4} M cholesterol. a) untreated cells, $\times 2000$; b) cell treated with 10^{-4} M cholesterol. $\times 2000$

responded in a different manner, they were examined by thin layer chromatography for cholesterol content before and after treatment.

Figure 4. The cholesterol contents of the examined cells differed with the types although the same nutrient medium was used for all. The cholesterol content did not change on 24 hour incubation with 10^{-4} M cholesterol in any type except in the endothelial cell, in which it rose considerably.

Figure 5 a—i. Treatment of the cells with 10^{-4} M lysolecithin caused much less pronounced changes than treatment with cholesterol at an identical concentration (Fig. 5 a—c). If after 24-hour exposure to lysolecithin the cells were additionally treated with cholesterol, the surface changes reached maximum degree (Fig. 5 d—f). If, however, 10^{-4} M lysolecithin and 10^{-4} M cholesterol were added simultaneously to the nutrient medium in which the cells were incubated for 24 hours, only moderate changes developed on the surface (Fig. 5 g—i).

Figure 6/a—b. Cell morphology is obviously affected by the fixation procedures. Transmission electron microscopic examinations cannot be performed on unfixed preparations. Thus, for comparison, cholesterol treated and fixed endothelial cells were studied also by scanning electron microscopy. In fixed preparations the differences between the cholesterol treated and control cells were unimportant. The morphology of the cultured endothelial cells was, however, fairly different according to the method of fixation.

Figure 7/a—c. By transmission electron microscopy the effect of 10^{-4} M cholesterol was demonstrable by the significant increase in the number of lipid inclusions, as compared to the control. At lower concentrations of added

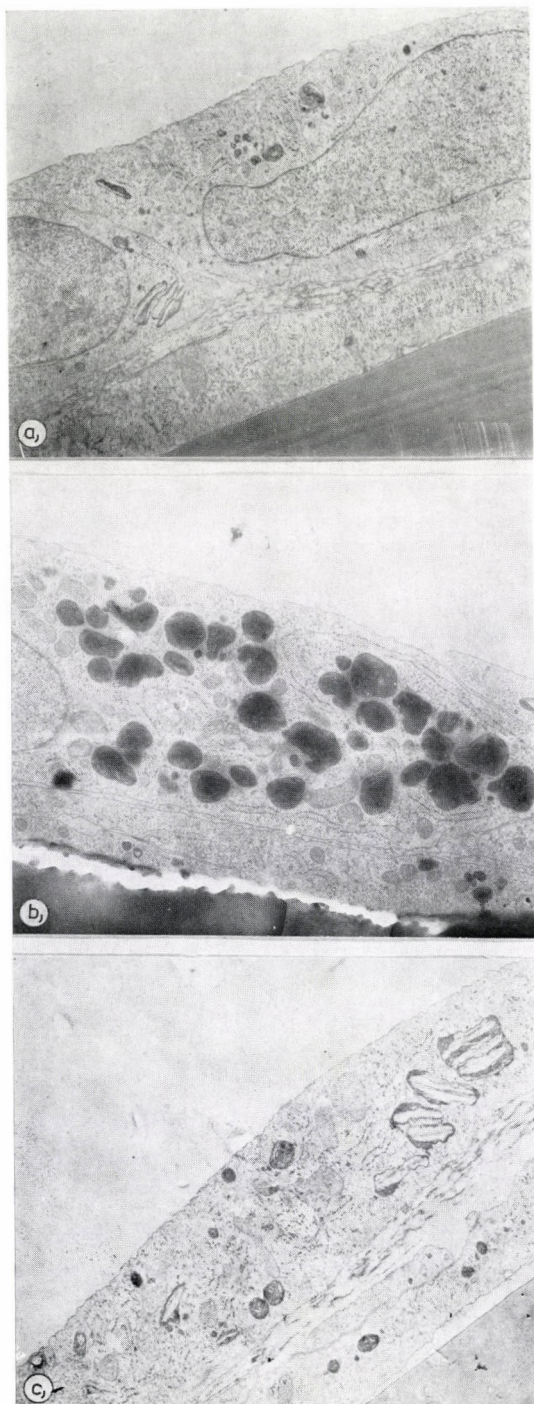


Fig. 7. Transmission electron micrographs of cholesterol and lysolecithin treated cultured endothelial cells. a) untreated control cell, $\times 8000$; b) cell treated with 10^{-4} M cholesterol, $\times 8000$; c) cell treated with 10^{-4} M cholesterol and 10^{-4} M lysolecithin, $\times 8000$

cholesterol the number of lipid inclusions was not significantly higher than usually seen in cultured cells. If, however, 10^{-4}M cholesterol and 10^{-4}M lysolecithin were added simultaneously to the cells for 24 hours, only moderate changes were observed. This was in accordance with the observations made by scanning electron microscopy.

Discussion

The present results clearly show that the different cell types responded in a different manner to exogenous cholesterol. The still diploidic endothelial cell culture was more sensitive to cholesterol than were the two other cell lines. As to the morphological details of the change, our interpretation is still hypothetical. Reference should be made to the observation of ROTHBLAT [7, 8] that on exposure to hyperlipaemic serum many vacuoles are in the cytoplasm of *in vitro* cultured hepatoma cells and the isolated vacuoles contained cholesterol ester. On the other hand, not all cell types accumulated cholesterol in this manner.

Reduction of cell membrane fluidity is another known effect of cholesterol. The change, taking place in the membrane structure of endothelial cells under the influence of cholesterol, is probably such that the subsequent short exposure to distilled water can bring about visible changes on the surface. Rinsing of untreated control cells in distilled water did no result in similar changes. The intensity (degree) of the changes was decreasing parallel with the rising dilutions of cholesterol. This can be regarded as an indirect proof of the specificity of the cholesterol effect.

As revealed both by SEM and TEM, only minimal changes occurred in a second experimental series, in which equimolar quantities of cholesterol and lysolecithin were simultaneously added to the cell suspension. The observation [6] that cholesterol and lysolecithin form a stable complex and eliminate each other's action when mixed at equimolar concentrations, may account for the phenomenon.

The surface of untreated cells studied by scanning electron microscopy of unfixed preparations was considered to represent the least distorted normal morphology. The changes observed after treatment with cholesterol at low concentrations were therefore accepted as signs of a specific effect. Fixation procedures themselves may cause some minor changes in the normal ultrastructure, thus, probably masking the fine effects of low concentrations of cholesterol on the weak molecular interactions within the cell membrane.

We are aware that when evaluating the cell culture experiments, consideration should be given to the fact that scores of factors other than cholesterol are influencing the function of the same cells *in vivo*. The experimental results obtained with *in vivo* cultured cells are related to isolated functions, and conclusions to *in vivo* relations can only be drawn from them with due criticism.

REFERENCES

1. BONDJERS, G., BJÖRKERUD, S.: (1973) Cholesterol accumulation and content in regions with defined endothelial integrity in the normal rabbit aorta. *Atherosclerosis* **17**, 71—83. — 2. CSONKA, É., KÁDÁR, A., KERÉNYI, T., JELLINEK, H.: (1973) Morphology of cultured endothelial and smooth muscle cells of different origin. *Acta morph. Acad. Sci. hung. Suppl.* **14**, 18. — 3. CSONKA, É., KERÉNYI, T., KOCH, A. S., JELLINEK, H.: (1975) In vitro cultivation and identification of aortic endothelium from miniature pig. *Arterial Wall Vol. III.*, pp. 31—37. — 4. PILZ, H., FRICK, E.: (1966) Dünnschichtchromatographische Lipoidmuster von normalen menschlichen Serum und Liquor Cerebrospinalis. *Klin. Wschr.* **44**, 780. — 5. PORTMAN, O. W., ILLINGWORTH, D. H.: (1974) Metabolism of lysolecithin in vivo and in vitro with particular emphasis on the arterial wall. *Biochem. biophys. Acta (Aust.)* **348**, 136—144. — 6. RAND, R. P., PANGBORN, W. A., PURDON, A. D., TINKER, D. O.: (1975) Lysolecithin and cholesterol interact stoichiometrically forming bimolecular lamellar structures in the presence of excess water or lysolecithin or cholesterol. *Canad. J. Bioch.* **53**, 189—195. — 7. ROTHBLAT, G. H., BODY, R., CHERI DEAL.: (1971) Cholesterol biosynthesis in WI-38 and WI-38VAL3A tissue culture cells. *Exp. Cell Res.* **67**, 436—440. — 8. ROTHBLAT, G. H.: (1974) Cholesteryl ester metabolism in tissue culture cells. I. Accumulation in Fu5AH hepatoma cells. *Lipids* **9**, 526—535. — 9. ZÖLLNER, N., WOLFRAM, G.: (1962) Untersuchungen über die Dünnschichtchromatographie von Lipoiden. *Klin. Wschr.* **40**, 1098.

DIE UNTERSUCHUNG DER WIRKUNG MEMBRANAKTIVER STOFFE AUF DER MORPHOLOGIE DER OBERFLÄCHE GEZÜCHTETER ENDOTHELIALZELLEN DER AORTA

É. CSONKA, B. BERNOLÁK, A. S. KOCH und H. JELLINEK

1. Verfasser untersuchten mittels scanning- und transmissions-elektronenmikroskopischer Methode die auf der Oberfläche der in vitro gezüchteten Endothelialzellen der Aorta vor sich gehenden Veränderungen unter Einwirkung Cholesterin, Lysolecithin und auf Wirkung beider Stoffe gemeinsam.
2. Beide untersuchten Verbindungen riefen unter verschiedenen qualitativen Bedingungen Veränderungen an der Zelloberfläche hervor, wenn die Zellen im unfixiertem Zustand mittels scanning-elektronenmikroskopischer Methode untersucht wurden. Die Veränderungen waren weniger bewertbar, wenn die Zellen in fixiertem Zustand mittels scanning-Methode oder mittels Transmissions-Elektronenmikroskopes untersucht wurden.
3. Zecks Vergleiches untersuchten Verfasser auch die Zelloberfläche verschiedener Laboratoriums-Zellkulturen nach Behandlung mit Cholesterin und diese reagierten weniger auf die Cholesterinbehandlung als die Endothelialen Zellen.
4. Mittels Dünnschichtchromatographie verglichen Verfasser den Cholesteringehalt von sechs verschiedenen Zellkulturen vor und nach Hinzugabe von Cholesterin. Nur bei den endothelialen Zellen vergrößerte sich auf Einwirkung exogenen Cholesterins der Cholesteringehalt bedeutend. Das unterstützt jene Beobachtung, laut welcher die durch Cholesterin hervorgerufenen bedeutenden morphologischen Veränderungen nur an einer Kultur von Endothelialzellen beobachtet werden konnten.

ИЗУЧЕНИЕ МЕМБРАННО-АКТИВНЫХ ВЕЩЕСТВ НА МОРФОЛОГИЮ ПОВЕРХНОСТИ КУЛЬТИВИРОВАННЫХ ЭНДОТЕЛИАЛЬНЫХ КЛЕТОК АОРТЫ

ЕВА ЧОНКА, Б. БЕРНОЛАК, А. Ш. КОХ, Х. ЙЕЛЛИНЕК

1. Авторы изучали методом отражательной (сканирование) и трансмиссионной электронной микроскопии изменения, происходящие под действием холестерина, лизолецитина или после совместного введения этих веществ на поверхности эндотелиальных клеток аорты, культивированных in vitro.
2. В случае изучения клеток без фиксации методом отражательной электронной микроскопии оба соединения вызвали изменения поверхности клеток, при различных количественных условиях. Изменения были труднее оценимы, когда клетки изучались методом отражательной или трансмиссионной электронной микроскопии без фиксации.

3. В целях сравнения изучалась также поверхность клеток других лабораторных клеточных культур, после введения холестерина. Оказалось, что они реагировали в меньшей мере на холестерин, чем эндотелиальные клетки.

4. Методом хроматографии на тонком слое авторы сравнивали содержание холестерина в различных клеточных культур до и после добавления холестерина. Под влиянием экзогенного холестерина значительное повышение его содержания наблюдалось только в эндотелиальных клетках. Этим подкрепляется прежнее наблюдение авторов, согласно которому более значительные морфологические изменения, вызванные холестерином, удалось выявить только в культурах эндотелиальных клеток.

Dr. Éva CSONKA	} Semmelweis Orvostudományi Egyetem
Dr. Béla BERNOLÁK	
Dr. A. Sándor KOCH	
Dr. Harry JELLINEK	
	} II. sz. Kórbonctani Intézet
	} H-1450 Budapest, Üllői út 93., Hungary

Department of Zoology, College of Basic Sciences and Humanities, Punjab Agricultural University, Ludhiana, India

COMPARATIVE DIMENSIONAL CHARACTERISTICS OF SPERMATOOZOA IN MURIDAE

K. S. SIDHU and S. S. GURAYA

(Received December 11, 1976)

A comparative study has been made of the dimensional characteristics in six species of Muridae (*Malardia meltda*, *Bandicota bengalensis*, *Albino rat*, *Rattus norvegicus*, *Mus booduga*, *Rattus rattus*). Characteristic differences were found in the dimensions of their spermatozoa. Head dimensions *viz.*, acrosome length, width, area and post-acrosomal area, vary significantly between different species but the differences are significant within individuals of the same species. Flagellum dimensions *viz.*, mid-piece length, breadth, area and main-piece length also vary significantly between different species; within individuals of the same species the differences are not significant except for mid-piece breadth, which varies significantly both between and within the species. The ratio of flagellum to head varies significantly between species but the difference is not significant within individuals of the same species. The significance of the variabilities is discussed.

Introduction

Variations in the phenotype of spermatozoa in different vertebrate and invertebrate species, independent of age and other non-genetic factors have been reported [2, 5, 6, 9, 14]. BEATTY [3] suggested the genetic control of the size and shape of different parts of organelles of mammalian spermatozoa. BRADEN [6] demonstrated the first genetically controlled differences in size and shape of the mouse spermatozoon head. Inherited variations in the dimensions of spermatozoa have been shown to exist between inbred strains, which are not affected by the environment. The present study was undertaken to determine the degree of variability in comparative dimensional characteristics of spermatozoa in some closely related species of Muridae. An additional aim was to determine whether the dimensional characteristics of spermatozoa can be used for taxonomical purposes.

Material and methods

Sexually mature soft furred field rat (*Malardia meltda*), Indian mole rat (*Bandicota bengalensis*), Indian field mouse (*Mus booduga*), albino rat, Norwegian rat (*Rattus norvegicus*) and house rat (*Rattus rattus*) were collected from fields and houses. The testicles were taken out, the epididymes were separated and washed in physiological saline. Caudal segments of epididymes were minced and sperms were suspended in physiological saline.

Smears of semen were prepared on glass slides, fixed in aqueous Bouin's fluid for 2 hours, washed in running water and then mordented in 4% iron aluminium for 1/2 hour, washed

in water and stained with iron haematoxylin overnight. After repeated washing in running water for one hour, the smears were dehydrated in alcohol series and mounted in DPX.

Dimensions of spermatozoa were measured according to the method of BEATTY [3] using a camera lucida. Statistical analysis was made to test the significance of results.

Observations

Mean spermatozoal dimensions in the different species are given in Table I, the results of statistical analysis in Table II.

Of the head characteristics, acrosome length, width and area, and post-acrosomal area differed significantly in the six species investigated. Differences in these characteristics in individuals of the same species were not significant.

Of the flagellum characteristics, mid-piece length (but not mid-piece breadth), mid-piece area and main-piece length varied significantly between different species, but within the individuals of the same species these characteristics did not differ significantly except for mid-piece breadth, which varied significantly.

The ratio of flagellum to head also varied significantly between different species but in the individuals of same species the differences were not significant.

Discussion

FRIEND [11] was the first to demonstrate differences in spermatozoon dimensions in different mammalian species and genetic differences were demonstrated in living spermatozoa of inbred mouse strains [7, 8]. BEATTY and SHARMA [5] found a significant variability in several characteristics of spermatozoa including breadth and area of the head. In the present study, isolated characteristics of the head *viz.* acrosome length, acrosome width, acrosome area, and postacrosomal area, have been shown to vary significantly in the six different species (see Table I). The spermatozoa of *Rattus rattus* had the largest acrosome area while those of *Rattus norvegicus* showed the smallest acrosome area among the six species investigated. The spermatozoa of *Rattus norvegicus* had the longest and thinnest acrosome. Those of *Rattus rattus* had the thickest acrosome. This variability in the dimensions of sperm organelles suggests that the genotype influences the spermatozoal head shape. Acrosome area in *Millardia melitana*, *Bandicota bengalensis* and, to some extent, in the *albino rat* was almost similar. This homogeneity of their acrosome areas implies that factors such as age, weight and environment have little effect in altering the mean acrosomal area; this homogeneity was observed by BEATTY and SHARMA [5] in mice spermatozoa.

Characteristics of the flagellum *viz.* mid-piece length, mid-piece width, mid-piece area and main-piece length varied significantly between different

Table I

*Mean dimensional characteristics of spermatozoa in different species of Muridae***

Species	Head				Flagellum			
	Dimensions (microns)				Dimensions (microns)			
	Acrosomal length	Acrosome width	Acrosome area	Postacrosome area	Mid-piece length	Mid-piece width	Mid-piece area	Main-piece length
<i>Millardia meltda</i>	6.80	2.40	15.60	5.75	25.40	0.90	22.85	91.60
<i>Bandicota bengalensis</i>	5.10	3.00	15.30	6.60	22.20	0.85	18.85	56.20
<i>Albino rat</i>	5.80	2.70	14.54	5.15	23.60	0.80	18.85	70.00
<i>Rattus norvegicus</i>	7.70	1.50	11.60	3.825	55.00	0.60	33.00	70.00
<i>Mus booduga</i>	6.50	3.00	19.50	6.45	22.00	0.75	16.50	78.00
<i>Rattus rattus</i>	6.80	3.20	21.75	6.70	23.00	0.55	12.60	55.00

* Five samples in each case

+ Number of cells counted per five samples

Table II

'F' values to test the significance of differences in spermatozoal dimensions between and within different species of Muridae

Sources of variation	Acrosome length	Acrosome width	Acrosome area	Post-acrosomal area	Mid-piece length	Mid-piece breadth	Mid-piece area	Main-piece length	Ratio of flagellum to head
Between species	24.87*	14.33*	10.16*	6.112*	129.55*	0.969*	19.53*	45.89*	11.113*
Within species	0.202**	0.090**	0.986**	0.123**	0.043**	0.292*	2.55**	0.701**	0.133**

* Significant at 1% and 5% levels

** Insignificant at 1% and 5% levels

species (Table II), while their variability was not significant in individuals belonging to the same species. An exception was mid-piece breadth, which varied significantly within individuals of the same species but the differences were not significant between different species. This suggests that mid-piece breadth may be susceptible to environmental and other non-genetic factors [1].

The inheritance of flagellum length in different strains of mice has been reported [4, 5]. There occur significant strain differences in mid-piece length and breadth. Similar observations have been made in bull and goat spermatozoa [9, 12]. In the present study a significant variation was observed in the mid-piece area of spermatozoa in different species, but no significant difference in mid-piece breadth could be found as reported also by SHARMA [13]. Differences in mid-piece breadth were observed in different individuals of bull spermatozoa by MUKHERJEE and SINGH [12] who attributed these differences to the low magnification at measurements.

The ratio of flagellum to head varied significantly species between but not significantly within the same species.

The present study showed conspicuous variations in the dimensional characteristics of spermatozoa between different species of Muridae, which along with other methods might be used, for zoological classification at the species levels. Since mid-piece breadth varied significantly within the individuals of the same species, this characteristic is susceptible to environmental and other nongenetic factors, hence cannot be used for classification.

The physiological significance of the variations in spermatozoal dimensions in different species is not known. There is some selection of a particular sperm shape during evolution. Since the variability of flagellum dimensions was comparatively more significant than the variability of head dimensions selection of this character seems to have been favoured during the evolution of sperm structure. Morphology of the spermatozoon is believed to be related in some way to the mode of fertilization [10].

Future studies should be carried out to determine the specific role of these variations in relation to sperm transport, maturation, fertilization problems, etc.

REFERENCES

1. BEATTY, R. A.: (1969b) A genetic study of spermatozoan dimensions in mice selected for body weight. *Ind. J. Hered.* **1**, 9—21. — 2. BEATTY, R. A.: (1970) Genetics of mammalian gamete. *Biol. Rev.* **45**, 73—119. — 3. BEATTY, R. A.: (1971) Phenotype of spermatozoa in relation to genetic content. In: Sex ratio at birth. Prospects for control symposium of the American Society of Animal Sciences. (Eds C. A. Kiddy and H. D. Hafs). pp. 10—18. — 4. BEATTY, R. A.: (1972) Genetic aspects of spermatozoa. In: *Proc. Int. Symp. on the Genetics of the Spermatozoon*. (Eds Beatty, R. A. and S. Gluecksohn-Waelsch p. 406. — 5. BEATTY, R. A., SHARMA K. N.: (1960) Genetics of gametes. III Strain differences in spermatozoa from eight inbred strains of mice. *Proc. roy. Soc. Edinb. B* **68**, 25—53. — 6. BRADEN, A. W. H.: (1956) Studies on mammalian ova. Ph. D. Thesis, Univ. Edinburgh p. 60. — 7. BRADEN,

A. W. H. (1957b) Differences between inbred strains of mice in the morphology of the gametes. *Anat. Rec.* **127**, 270. — 8. BRADEN, A. W. H.: (1959) Strain differences in the morphology of the gametes of the mouse. *Aust. J. biol. Sci.* **120**, 65—71. — 9. DASS, D., SIDHU N. S.: (1975) The size of spermatozoa from black bengal and barbari goats (*Capra hircus*) *J. Reprod. Fert.* **44**, 333—334. — 10. FRANZEN, A.: (1970) Phylogenetic aspects of the morphology of spermatozoa and spermiogenesis. In: *Comparative Spermatology* (Ed. B. Baccetti) London 1970. — 11. FRIEND, G. F.: (1956) The sperms of the British Muridae. *Q. J. microsc. Sci.* **78**, 419—443. — 12. MUKHERJEE, D. P., SINGH, S. P.: (1965) Breed differences in characteristics of bull spermatozoa *Ind. J. vet. Sci.* **35**, 213—220. — 13. SHARMA, K. N.: (1960) Genetics of gametes. IV. The phenotype of mouse spermatozoa in four inbred strains and their F-1 crosses. *Proc. roy. Soc. Edinb. B.* **68**, 54—71. 14. WILLIAM, D. A., BEATTY R. A., BURGOYNE P. S.: (1970) Multivariate analysis in the genetics of spermatozoon dimension in mice. *Proc. roy. Soc. B.* **175**, 313—331.

VERGLEICHENDE UNTERSUCHUNGEN DES SPERMATOZOEN-DURCHMESSERS VON MURIDAE-ARTEN

K. S. SIDHU und S. S. GURAYA

Bei der vergleichenden Untersuchung von 6 Muridae-Arten (*Malardia melitana*, *Bandicota bengalensis*, *Albino rat*, *Rattus norvegicus*, *Mus booduga*, *Rattus rattus*) wurden in den Dimensionen der Spermatozoen eigenartige Unterschiede gefunden. Der Durchmesser des Kopfes, die Länge, Breite und Fläche der Acrosome sowie die Fläche der Postacrosome zeigen bei den verschiedenen Arten erhebliche Unterschiede. Innerhalb der gleichen Art sind jedoch die Abweichungen unbedeutend. Der Schwanzdurchmesser, die Länge, Breite und Fläche des Mittelabschnitts der Spermatozoen sowie die Länge des Hauptteils sind bei den einzelnen Arten stark unterschiedlich, während diese Abweichungen innerhalb der Art nur gering sind, mit Ausnahme der Breite des mittleren Teils, die sowohl zwischenartlich als auch innerhalb der Art bedeutende Abweichungen zeigt.

Die Verhältniszahl von Kopf und Schwanz zeigt zwischen den einzelnen Arten erhebliche Unterschiede, innerhalb der Art ist aber die Abweichung minimal. In der Arbeit wird die Bedeutung dieser Variabilität diskutiert.

СРАВНИТЕЛЬНОЕ ИССЛЕДОВАНИЕ ДИАМЕТРА СПЕРМАТОЗОИДОВ У ВИДОВ РОДА MURIDAE

К. С. СИДХУ и С. С. ГУРАЙЯ

При сравнительном исследовании 6 видов рода Muridae (*Malardia melitana*, *Bandicota bengalensis*, *Albino rat*, *Rattus norvegicus*, *Mus booduga*, *Rattus rattus*) авторы наблюдали своеобразные различия в размерах сперматозоидов. Диаметр головки, длина, ширина и площадь акросом, а также площадь постакросом показывают у отдельных видов значительные отклонения. В пределах вида, однако, отклонения незначительны. Диаметр хвоста, длина, ширина и площадь среднего участка сперматозоидов, а также длина главной части показывают значительные различия у отдельных видов, тогда как эти различия в пределах вида только небольшие, за исключением ширины среднего участка в которой выявляемы различия как между отдельными видами, так и в пределах одного и того же вида.

Относительное число головки и хвоста показывает между отдельными видами существенные отклонения, однако в пределах одного и того же вида различия минимальны. В работе обсуждается значение этой изменчивости.

Kuldip S. Sidhu }
Sardul S. Guraya } Punjab Agricultural University Ludhiana, India

Department of Anatomy and Histology, Medical Faculty, Varna, Bulgaria

FINE MORPHOLOGICAL ASPECTS OF THE SECRETORY PROCESS IN ARTERIAL SMOOTH MUSCLE CELLS. II. ROLE OF MICROTUBULES

G. N. CHALDAKOV, S. NIKOLOV and V. VANCOV

(Received June 2, 1977)

Preliminary results are presented regarding the role of the microtubular system in the secretory process in the rabbit aorta and pulmonary trunk smooth muscle cells. The results are based on electron microscopic findings of the effect of colchicine *in vivo*. On colchicine treatment an accumulation of secretory granules versus a vacuolar type of dilatation of the rough endoplasmic reticulum cisternae distinguishes two groups of smooth muscle cells. It is suggested that two secretory pathways operate in these cells, and that the cell microtubular status plays a key role in triggering one or the other pathway.

Introduction

Smooth muscle cells (SMC) of the arterial wall are well known to be capable of synthesizing and excreting the precursors of extracellular matrix components [9, 10, 11, 13, 22, 23, 26, 27]. Still, few fine morphological data are available concerning their secretory pathways [24]. Recently, Golgi-derived secretory granules (SGr) and a well-developed microtubule system have been demonstrated in the developing rabbit arterial SMC [5].

The aim of the present experiment was to evaluate the possible role of microtubules (Mt) in the secretory process in these cells based primarily on colchicine treatment *in vivo*. The preliminary results of this study will be described here.

Material and methods

Four 20-day-old rabbits were used in the present experiment. Two of them were not treated (controls) and the other two were injected intraperitoneally with colchicine (0.125 mg per 100 g/body weight). Four hours later the animals were sacrificed and longitudinal strips were taken from their aortic arch, thoracic aorta and pulmonary trunk. These strips and the corresponding strips from the controls were immediately immersed in cold 3% glutaraldehyde for two hours and postfixed in cold 1% osmium tetroxide, both in 0.1 M phosphate buffer, pH 7.4. Dehydration was carried out in alcohol and acetone, and embedding in Durcupan ACM (Fluka). Ultrathin sections were stained with uranyl acetate and lead citrate. A JEM 7A electron microscope was used.

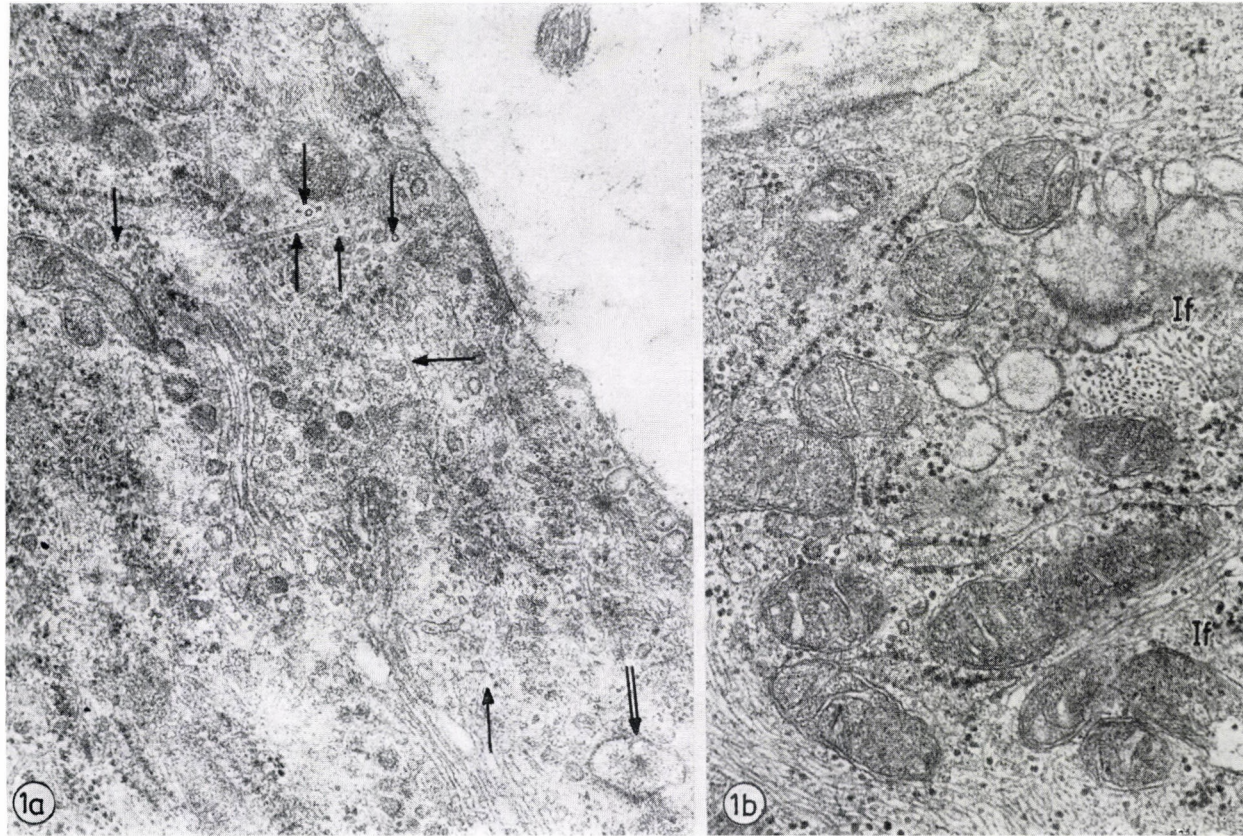


Fig. 1/a. A pulmonary trunk SMC from a control rabbit. Cross- and longitudinally sectioned microtubules (single arrows) are apparent. The Golgi-complex consists of flattened cisternae and small vesicles. A single secretory granule is noted (double arrow). $\times 20,000$

Fig. 1/b. SMC from colchicine-treated rabbit. This cell contains no microtubules. Increase in number of intermediate filaments (If) and accumulation of Golgi-derived vacuoles. $\times 20,000$

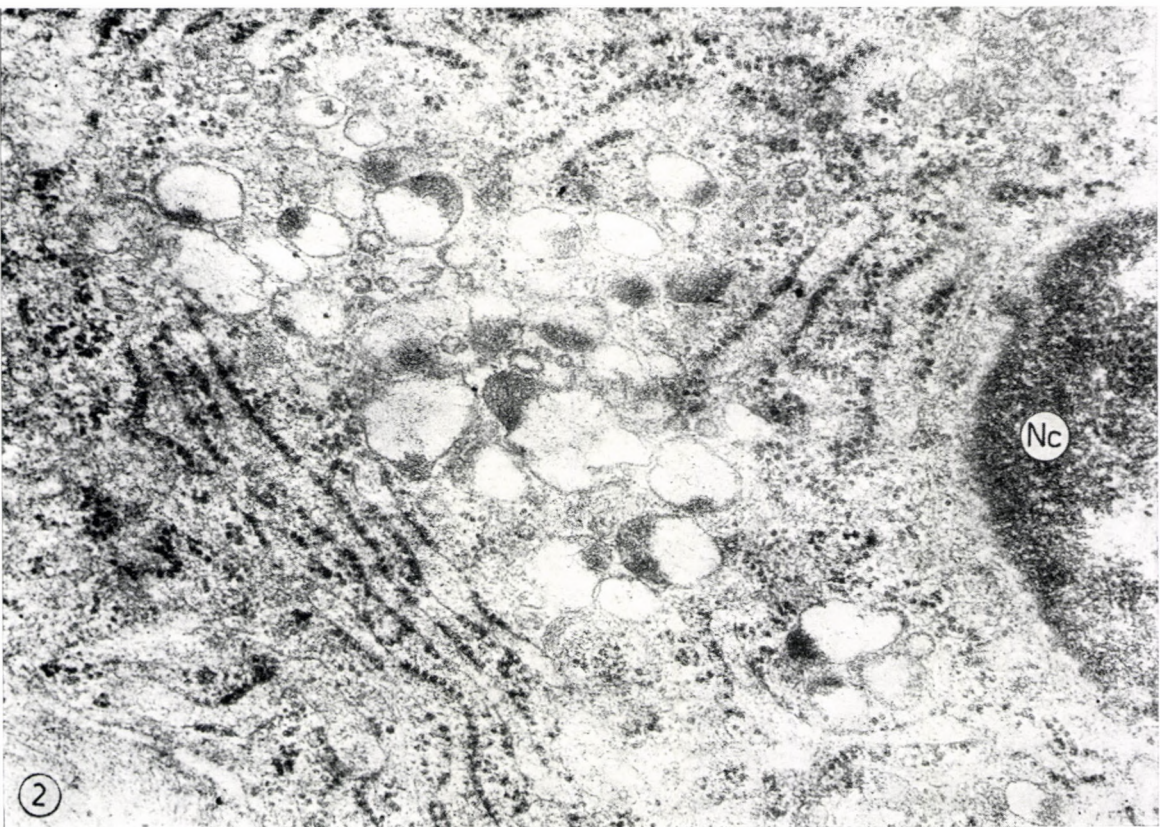


Fig. 2. Aortic arch SMC from colchicine-treated rabbit. Numerous secretory granules. The rough endoplasmic reticulum cisternae keep their long and flattened pattern of organization. Nucleus (Nc). $\times 20,000$

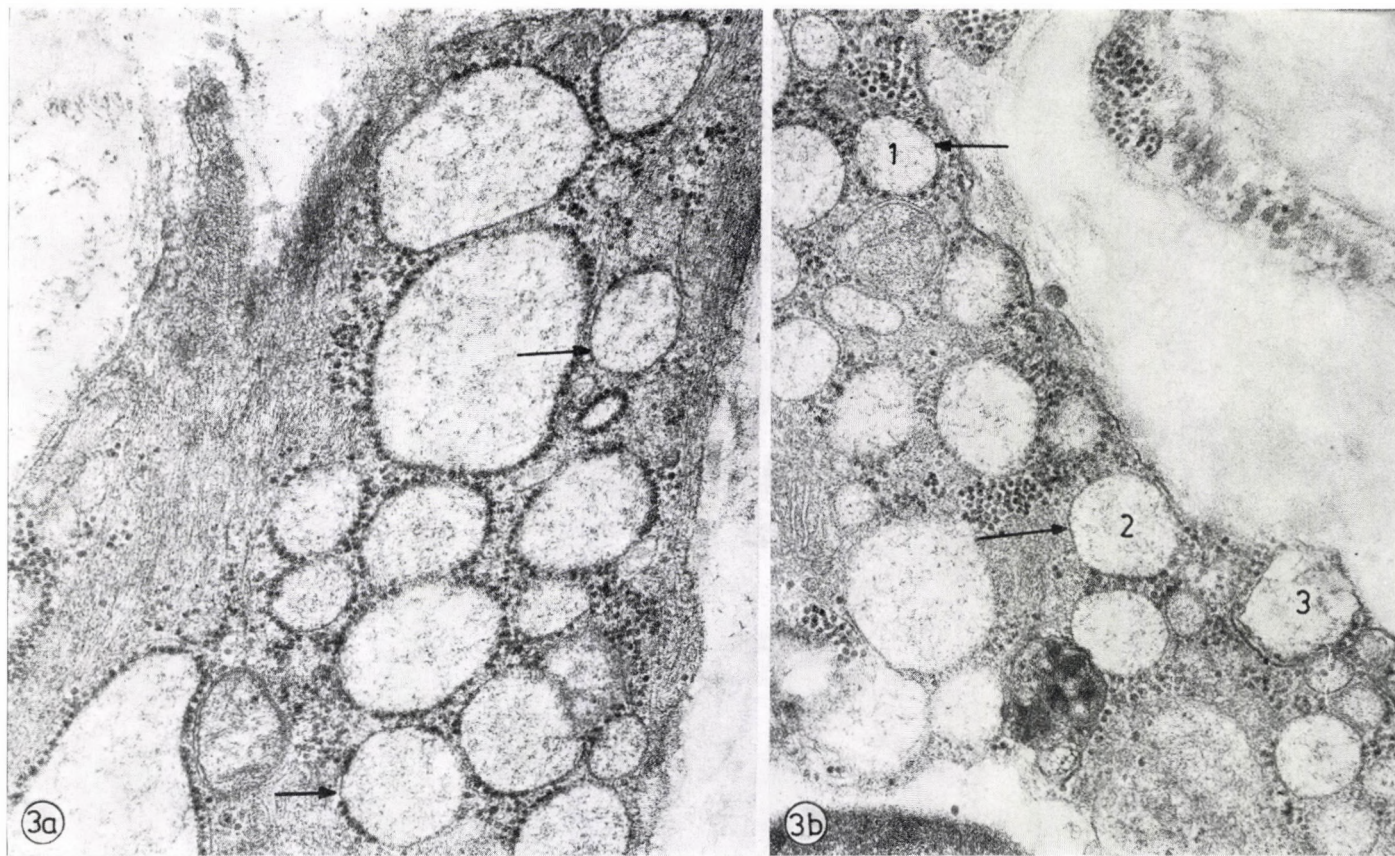


Fig. 3. Aortic arch SMC from colchicine-treated rabbit. Numerous round-shaped and separate vacuoles of rough endoplasmic reticulum. They contain no secretory granules. In Fig. 3/b, two vacuoles (1 and 2) are closely approached the sarcolemma, and another (3) seems to be discharged from the cell. Parts of the vacuolar surfaces are devoid of ribosomes (arrows) $\times 20,000$

Results

The SMC from control animals showed well-developed rough endoplasmic reticulum (RER), Golgi complex, and abundant Mt (Fig. 1/a). The myofilament system of these cells was less developed and occupied small areas beneath the sarcolemma. The cisternae of the RER were long and flat, and ribosomes were regularly attached onto their surface. The Golgi complex consisted of stacks of flattened cisternae, numerous small coated and smooth-surfaced vesicles, and possessed a few SGr. Numerous Mt were localized between these two secretory organelles, *i.e.* RER and Golgi complex. The perinuclear space displayed its usual appearance.

Colchicine treatment resulted in an almost total loss of Mt, an increased number of SGr and an evident alteration in RER. The SMC from the three arterial vessels studied showed the same response to colchicine treatment. In contrast, the SMC from each individual vessel wall was affected differently by colchicine; two distinct populations of SMC were found.

Colchicine increased the number of SGr in one group of SMC. An accumulation of SGr without any alteration in RER was the prominent feature of these cells. These SGr seemed somewhat modified in their appearance; they were enlarged, had altered in shape and a "capping" of their matrix occurred (Fig. 2). The accumulated SGr was observed chiefly in perinuclear Golgi regions. An increased presence of Golgi-related vacuoles was also found (Fig. 1/b).

Colchicine caused a vacuolar dilatation of the cisternae of RER in another group of SMC. In these cells a striking dilatation of RER cisternae occurred which lead to formation of numerous roundish, independently situated vacuoles of various sizes (Fig. 3). Some vacuoles were close to the plasma membrane; a few were encountered outside the cell. Most of the RER dilated cisternae kept their ribosomes attached whereas some displayed surface regions devoid of ribosomes. The matrix of the cisternae consisted of a network of filamentous material.

An outpocketing of the outer nuclear membrane resulting in vacuole-like dilatation of the perinuclear space was frequently observed. These SMC contained no SGr.

Discussion

Although in recent years considerable progress has been made towards the understanding of the connective tissue matrix producing function of SMC, detailed morphological knowledge of the secretory process in arterial SMC is still lacking. In particular, nothing is available in the literature concerning the possible role of Mt in their secretory ability, while an extensive body of

evidence has implicated them in intracellular transport and release of the secretory products of different types of secretory cells [6, 7, 16, 18].

Colchicine has been shown to affect the Mt and to prevent tubulin assembly by its tubulin-binding property [3, 4, 28]. That may be the most likely reason for the loss of Mt in SMC, observed after colchicine treatment.

It seems puzzling that two groups of SMC should respond differently to the antimicrotubular effect of colchicine. In the first group, the number of SGr increased while in the other, the presence of numerous dilated cisternae of the RER was the prominent finding. The appearance of RER was unchanged in the former, whereas no SGr were found in the latter. One may assume a heterogeneity within the SMC studied in respect to the behaviour of their secretory processes in the absence of Mt. As for the increased number of SGr after colchicine treatment we believe that the present results give a meaning to the relationship between SGr and Mt described previously [5]. In addition, these results support the suggestion that RER-Golgi complex-SGr-Mt secretory pathway operates in arterial SMC [5]. Thus, the Mt might participate in the secretory process in SMC in a manner similar to that in glandular and other mesenchymal cells. Taking into account the other functions of the colchicine-binding protein [2, 14, 29] it seems, however, difficult to evaluate precisely which step(s) of the secretory process in SMC is (are) more influenced by colchicine.

The apparent characteristic of the second group of SMC after colchicine treatment is the presence of numerous vacuolarly dilated RER cisternae and their "movement" towards the sarcolemma, where most likely both membranes fuse and a subsequent discharge takes place.

The precise sequence of events resulting in dilatation of the cisternae of RER is difficult to imagine. Whether such a dilatation is due to the lack of Mt [8] or to some colchicine-binding properties of the cisternal membrane itself, remains unclear.

Nevertheless, the behaviour of the RER in response to colchicine, suggests the existence of a direct RER secretory pathway in the arterial SMC. To our knowledge, a report presuming such a pathway in aorta SMC is that of KARRER [12]. Thus, like fibroblasts [21; CHALDAKOV and KÁDÁR in preparation], the arterial SMC are probably capable by bypassing the Golgi complex and discharging secretory products into the cell exterior directly *via* the dilated RER cisternae. It is another question how effective [20, 25] such secretory pathway may be. Since all steps of the proposed direct secretory pathway operate in the absence of Mt, it is tempting to postulate that it is Mt-independent, in contrast to the pathway through the Golgi-complex, which requires an intact Mt system. Which of these can be chosen by a smooth muscle cell probably depends on the cellular status of the Mt apparatus. In this respect, the dynamic equilibrium of assembly and disassembly of Mt [1, 4] might

be taken into account. Since the cyclic nucleotides are believed to control both, cell Mt status [15] and cell secretion [17, 19], these substances might be considered as eventual candidates triggering one or the other secretory pathway in arterial SMC.

Acknowledgement

The authors are indebted to Dr. Anna KÁDÁR for valuable discussions and help in preparing the manuscript, to Dr. Z. R. ANGELOV for discussions, Dr. P. GENEV for co-operation, and to Miss Lillia PASTARMADGIEVA and Mrs Stela VLADIMIROVA for technical assistance.

REFERENCES

1. BEHNKE, O.: (1967) Incomplete microtubules in mammalian blood platelets during microtubule polymerization. *J. Cell Biol.* **34**, 697–701. — 2. BHATTACHARYYA, B., WOLFF, J.: (1975) Membrane-bound tubulin in brain and thyroid tissue. *J. biol. Chem.* **250**, 7639–7646. — 3. BORISY, G. G., TAYLOR, E. W.: (1967a) The mechanism of action of colchicine. Binding of colchicine ^3H to cellular protein. *J. Cell Biol.* **34**, 525–533. — 4. BORISY, G. G., TAYLOR, E. W.: (1967b) The mechanism of action of colchicine. Colchicine binding to sea urchin eggs and the mitotic apparatus. *J. Cell Biol.* **34**, 534–548. — 5. CHALDAKOV, G. N., NIKOLOV, S., VANKOV, V.: (1976) Fine structure of the secretory process in arterial smooth-muscle cells. I. Secretion granules. Submitted for publication. — 6. EHRLICH, H. P., BORNSTEIN, P.: (1972) Microtubules in transcellular movement of procollagen. *Nature new Biol.* **238**, 257–260. — 7. EHRLICH, H. P., BORNSTEIN, P., ROSS, R.: (1974) Effects of anti-microtubular agents on the secretion of collagen. A biochemical and morphological study. *J. Cell Biol.* **62**, 390–405. — 8. FELDMAN, G., MAURICE, M., SAPIN, C., BENHAMON, J. P.: (1975) Inhibition by colchicine of fibrinogen translocation in hepatocytes. *J. Cell Biol.* **67**, 237–243. — 9. KÁDÁR, A., VERESS, B., JELLINEK, H.: (1969) Ultrastructural elements in experimental intimal thickening. II. Study of the development of elastic elements in intimal proliferation. *Exp. molec. Path.* **11**, 212–223. — 10. KÁDÁR, A., GARDNER, D. L., BUSH, V.: (1971) The relation between the fine structure of smooth muscle cells and elastogenesis in chick-embryo aorta. *J. Path.* **104**, 253–260. — 11. KÁDÁR, A., GARDNER, D. L., BUSH, V.: (1972) Glycosaminoglycans in developing chick-embryo aorta revealed by ruthenium red: an electron microscope study. *J. Path.* **108**, 275–280. — 12. KARRER, H. E.: (1960) Electron microscope study of developing chick-embryo aorta. *J. Ultrastruct. Res.* **4**, 420–454. — 13. NARAYANAN, A. S., SANDBERG, L. R., ROSS, R., LAYMAN, D. L.: (1976) The smooth-muscle cells. III. Elastin synthesis in arterial smooth-muscle cell culture. *J. Cell Biol.* **68**, 411–419. — 14. OLIVER, J. M., UKENA, T. E., BERLIN, R. D.: (1974) Effects of phagocytosis and colchicine on the distribution of lectin-binding sites on cell surface. *Proc. nat. Acad. Sci. (Wash.)* **71**, 394–398. — 15. OLIVER, J. M., KRAWIEC, J. A., BERLIN, R. D.: (1976) Carbamylcholine prevents giant granule formation in cultured fibroblasts from beige (Chediak-Higashi) mice. *J. Cell Biol.* **69**, 205–210. — 16. OLSEN, B. R., PROCKOP, D. J.: (1974) Ferritin-conjugated antibodies used for labeling of organelles involved in the cellular synthesis and transport of procollagen. *Proc. nat. Acad. Sci. (Wash.)* **71**, 2033–2037. — 17. PETTERS, H. D., KARZEL, K., PADBERG, D., SCHÖNHÖFER, P. S., DINNENDAHL, V.: (1974) Influence of PG-E₁ on cAMP levels and glycosaminoglycan secretion of fibroblasts cultured in vitro. *Pol. J. Pharmacol. Pharm.* **26**, 41–49. — 18. POISNER, A. M., COOK, P.: (1975) Microtubules and the adrenal medulla. *Ann. N. Y. Acad. Sci.* **253**, 653–669. — 19. RASMUSSEN, H.: (1970) Cell communication, calcium ion, and cyclic adenosine monophosphate. *Science* **170**, 404–412. — 20. ROSS, R., BENDITT, E. P.: (1964) Wound healing and collagen formation. IV. Distortion of ribosomal patterns of fibroblasts in scurvy. *J. Cell Biol.* **22**, 365–389. — 21. ROSS, R., BENDITT, E. P.: (1965) Wound healing and collagen formation. V. Quantitative electron microscope radioautographic observations of prolin H³ utilization by fibroblasts. *J. Cell Biol.* **27**, 83–106. — 22. ROSS, R., KLEBANOFF, S. J.: (1971) The smooth-muscle cells. I. In vivo synthesis of connective tissue proteins. *J. Cell Biol.* **50**, 159–171. — 23. ROSS, R.: (1971) The smooth-muscle cells. II. Growth of smooth-muscle in culture and formation of elastic fibers. *J. Cell Biol.* **50**, 172–186. — 24. ROSS, R.: (1975) Connective tissue cells, cell proliferation

and synthesis of extracellular matrix — a review. *Phil. Trans. roy. Soc. (Lond.) B.* **271**, 247—269. — 25. SCHAFER, I. A., SULLIVAN, J. C., SILVERMAN, L.: (1966) Evidence for ascorbic acid deficiency in cultured human fibroblasts. *J. Cell Biol.* **31**, 98 A. — 26. WIGHT, N. T., ROSS, R.: (1975a) Proteoglycans in primate arteries. I. Ultrastructural localization and distribution in the intima. *J. Cell Biol.* **67**, 660—674. — 27. WIGHT, N. T., ROSS, R.: (1975b) Proteoglycans in primate arteries. II. Synthesis and secretion of glycosaminoglycans by arterial smooth-muscle cells in culture. *J. Cell Biol.* **67**, 675—686. — 28. WILSON, L., BAMBURG, J. R., MIZEL, S. B., GRISHAM, L. M., GRESWELL, K. M.: (1974) Interaction of drug microtubule proteins. *Fed. Proc.* **33**, 158—166. — 29. YAHARA, I., EDELMAN, G. M.: (1975) Modulation of lymphocyte receptor mobility by concanavalin A and colchicine. *Ann. N. Y. Acad. Sci.* **253**, 455—469.

MORPHOLOGISCHE ASPEKTE DER SEKRETIONSPROZESSE IN DEN GLATTEN MUSKELZELLEN

(Die Rolle der Mikrotubuli)

G. N. CHALDAKOV, S. NIKOLOV und V. VANCOV

Die Ergebnisse der vorläufigen Untersuchungen klärten die Rolle des mikrotubulären Systems in den Sekretionsprozessen, die in der Aorta und in den glatten Muskelzellen des A.-pulmonalis-Stammes von Kaninchen vor sich gehen.

Die bisherigen elektronenmikroskopischen Beobachtungen basieren auf der In-vivo-Wirkung des Kolchizins. Die Akkumulation der Sekretionsgranula und die Erweiterung der Zysternen vakuolären Typs in den endoplasmatischen Retikula mit grober Oberfläche machen es möglich, die glatten Muskelzellen zwei Gruppen zuzuordnen. Die Autoren sind der Meinung, daß sich in diesen Zellen zwei Sekretionsbahnen (pathways) finden. Die das mikrotubuläre System enthaltenden Zellen spielen hier eine entscheidende Rolle im Zusammenhang mit der einen oder anderen Sekretionsbahn.

МОРФОЛОГИЧЕСКИЕ АСПЕКТЫ СЕКРЕТОРНЫХ ПРОЦЕССОВ В КЛЕТКАХ ГЛАДКИХ МЫШЦ

(Роль микротрубочек)

Г. Н. ХАЛДАКОВ, Ш. НИКОЛОВ и В. ВАНЦОВ

Результаты предварительных исследований выяснили роль микротубулярной системы в секреторных процессах, происходящих в аорте и в клетках гладких мышц ствола легочной артерии у кроликов.

Проводившиеся до сих пор электронномикроскопические исследования основываются на действии колхицина in vivo. Аккумуляция секреторных зернышек и расширение цистерн вакуолярного типа в эндоплазматических сеточках с грубой поверхностью предоставляют возможность для обособления клеток гладких мышц на две группы. По мнению авторов в этих клетках существуют два секреторных пути (pathways). Клетки, содержащие микротубулярную систему, играют при этом решающую роль в связи с одним или другим секреторным путем.

G. N. CHALDAKOV	}	Department of Anatomy and Histology, Medical Faculty, Varna, Bulgaria
S. NIKOLOV		
V. VANCOV		

First Institute of Anatomy, Histology and Embryology, Semmelweis University Medical School, Budapest and *Laboratory of Clinical Science, National Institute of Mental Health, Bethesda, USA

ASCENDING PROJECTIONS TO THE HYPOTHALAMUS AND LIMBIC NUCLEI FROM THE DORSOLATERAL PONTINE TEGMENTUM: A BIOCHEMICAL AND ELECTRON MICROSCOPIC STUDY

L. ZÁBORSZKY, M. J. BROWNSTEIN* and M. PALKOVITS

(Received July 2, 1977)

Axons arising from the dorsolateral pontine tegmentum of the rat were traced in various hypothalamic and limbic nuclei by the electron microscopic degeneration method (0.5–8 day survival times) and by measuring regional norepinephrine (NE) concentrations after 12 days of survival using a radioenzymatic method. Significant reductions (41–85%) in NE contents were observed in the supraoptic, arcuate, basal and lateral amygdaloid nuclei and in the hippocampus 12 days after the bilateral electrolytic lesions of the locus coeruleus. No changes in NE concentrations were observed in the ventromedial, septal, central amygdaloid nuclei, in the median eminence and olfactory tubercle. Parabrachial lesions resulted in a decrease of NE content only in the olfactory tubercle. By means of electron microscopy terminal degeneration was found in the hypothalamic paraventricular, dorsomedial nuclei, in the median eminence, in the bed nucleus of the stria terminalis, in the central, lateral and basal amygdaloid nuclei, in the hippocampus and in the anterior ventral thalamic nucleus.

Introduction

In the rat 15 pathways could be identified ascending from the brain stem [50]. A part of these innervates the cell groups of the hypothalamus and limbic system. From the dorsolateral pontine tegmentum three separate, long ascending systems arise: the noradrenergic projections of the locus coeruleus [14, 15]; the tertiary gustatory projections from the pontine parabrachial nuclei [31] and the ventral tegmental acetylcholinesterase-containing pathway originating from the dorsolateral tegmental nuclei [36]. The projections to the hypothalamic and limbic regions of the noradrenergic cell bodies of the locus coeruleus have been demonstrated by fluorescence histochemical [2, 10, 25, 32, 47], autoradiographic [28, 38, 15], electrophysiological [30, 31], biochemical [3, 4, 20, 22, 39, 48, 14] and horseradish peroxidase methods [24]. The projections of a third order gustatory relay in the dorsolateral pons (parabrachial region) have been studied by autoradiography and antidromic activation [31].

The axons from the locus coeruleus and the parabrachial nuclei have partially overlapping paths and termination areas. Considering the vicinity of the two cell groups and the possibility of diffusion of labeled amino acids in an autoradiographic study, a careful reinvestigation of these two systems seemed to be necessary. The pitfalls of autoradiography, in case of such closely located areas, were thought to be avoided by measuring NE concentrations in various hypothalamic and limbic regions following the separate lesions of the locus coeruleus and parabrachial nuclei. The biochemical results were correlated with the distribution of degenerated terminals as revealed by electron microscopy. With regard to the fact that the sensitivity of the present combined approach seemed to be superior to the methods of previous experiments, the scope of this work was extended to areas not investigated so far for NE fibers.

Material and methods

Male Sprague-Dawley rats weighing 160–180 g were anesthetized with ether. In animals fixed in a Horsley–Clarke stereotaxic apparatus (nose angled 5° downward from the horizontal) two types of lesions were made: 1. bilateral lesion of the locus coeruleus (co-ordinates: 1.8 and 1.4 mm posterior to the interauricular line; 1.1 mm lateral and 6 mm beneath the brain surface); 2. parabrachial lesion (P = 1.3 mm, L = 2.2 mm, V = 6 mm). Electrolytic lesions were made by passing 2 mA current for 10 sec through a small monopolar Nichrome electrode insulated with Teflon, except for a 0.2 mm part at the tip. For electron microscopy large lesions were used including both the locus coeruleus and the parabrachial region (Fig. 1A). For the biochemical measurements finer lesions were performed restricted in one group of the animals to the locus coeruleus and its close vicinity, and to the parabrachial region only in the other group (Figs 1B, C).

For electron microscopic degeneration studies animals were sacrificed 0.5, 1, 2, 4 and 8 days postoperatively by the intraaortic perfusion of Karnovsky's paraformaldehyde–glutaraldehyde fixative. Brains were cut frontally into 0.5–1.0 mm slices. Under stereomicroscope, pellets of tissue from the required brain regions were punched out [33]. Small tissue blocks were immersed into 1% osmic acid for 1 h, dehydrated through an ethanol series and embedded in Durcupan (Fluka). Ultrathin sections were cut with a Reichert ultramicrotome, stained with uranyl acetate and lead citrate and examined under a Tesla BS 413 electron microscope at 8000× primary magnification.

NE concentrations were assayed 12 days after bilateral locus coeruleus and parabrachial lesions using a sensitive radioenzymatic method [12]. Results were expressed as mg NE/mg protein. The NE levels in each brain region were compared with those in samples from sham-operated animals which served as controls. In both experimental and control groups 6 animals were studied.

Results

Electron microscopy. The early signs of degeneration of the putative NE axons are rather inconspicuous and thus might be easily confused with fixation artifacts (ZÁBORSZKY, LÉRÁNT and PÁLKOVITS, in preparation). Therefore, the accumulation of phagosomes (Fig. 4B) and/or multilocular degenerated complexes (Fig. 5B) were considered as necessary to evaluate degeneration.

In the *hypothalamus* between 2–8 postoperative days degeneration was seen in the paraventricular (Fig. 2) and dorsomedial (Fig. 3) nuclei. In the

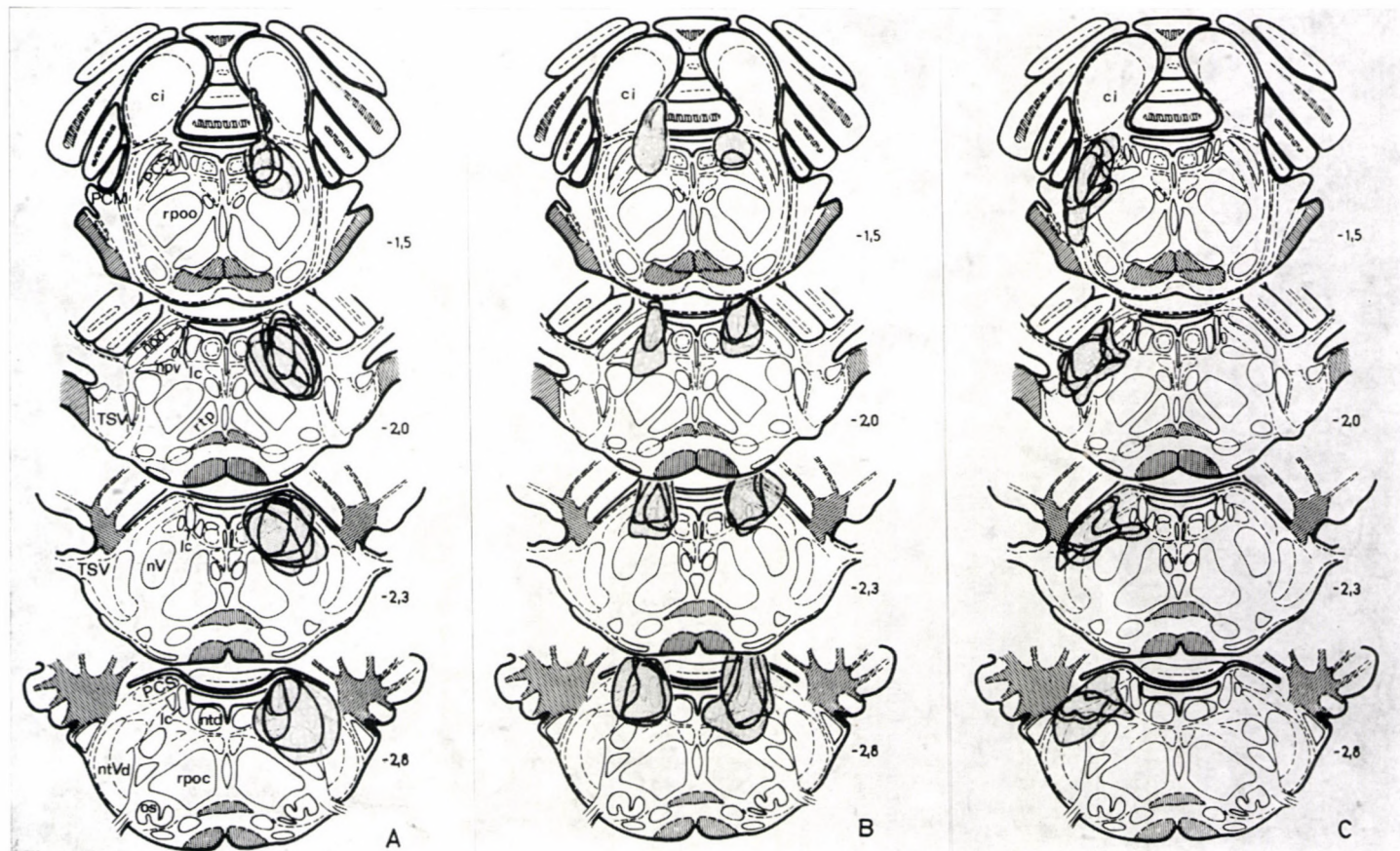


Fig. 1. Schematic illustration of the superimposed outlines of lesions plotted on frontal brain stem sections redrawn from the atlas of Palkovits and Jacobowitz [34]. Numbers indicate the distance in mm from the interauricular line. Abbreviations: ci — colliculus inferior, rpo — nucleus reticularis pontis oralis, lc — locus coeruleus, npd — nucleus parabrachialis dorsalis, npv — nucleus parabrachialis ventralis, rtp — nucleus reticularis tegmenti pontis, nV — nucleus originis nervi trigemini, ntd — nucleus tegmenti dorsalis Gudden, ntvd — nucleus tractus spinalis nervi trigemini, pars dorsomedialis, os — oliva superior, PCM — pedunculus cerebellaris medius, PCS — pedunculus cerebellaris superior, TSV — tractus spinalis nervi trigemini

periventricular and arcuate nuclei many lysosomes and pleomorphic vesicles were found one day after surgery (Figs 3B, D). These might be considered as early degeneration signs but we have no data in these regions at later survival periods. In the median eminence degeneration was found in the zona externa and interna mainly 4 days postoperatively (Fig. 3C).

Within the *limbic system* the bed nucleus of the stria terminalis (Figs 4A, B, C) and the lateral amygdaloid nucleus (Fig. 5A) showed the most pronounced degeneration between 2—4 days, whereas in the central and basolateral amygdaloid nuclei this peak was observed between 4—8 and 8 postoperative days, respectively (Figs 5B, D).

Biochemistry. There were significant changes in NE concentrations in several brain regions after bilateral locus coeruleus lesions (Table I and Fig. 6). NE was strikingly reduced in the supraoptic and arcuate nuclei. In the amygdala a significant reduction in NE was found only in the basal and lateral nuclei. No changes occurred in the ventromedial, septal and central amygdaloid nuclei, in the median eminence and in the olfactory tubercle.

After parabrachial lesions (Fig. 6) no change of NE content was observed in the regions studied except for a 34% decrease in the olfactory tubercle.

Table I

Norepinephrine concentrations of hypothalamic and limbic nuclei after bilateral locus coeruleus lesions

	Controls	Lesioned
	(ng/mg protein)	
<i>Hypothalamus</i>		
supraoptic nucleus	24.76±3.55 (6)*	10.76±1.28 ⁺⁺ (4)
ventromedial nucleus	20.50±1.32 (6)	17.76±2.28 (6)
arcuate nucleus	42.67±5.04 (6)	20.58±1.35 ⁺⁺ (4)
median eminence	19.91±6.22 (6)	15.63±2.28 (6)
<i>Limbic system</i>		
olfactory tubercle	3.48±0.19 (6)	3.69±0.54 (6)
dorsal septal nucleus	5.29±0.99 (6)	3.62±0.75 (4)
lateral septal nucleus	9.49±0.71 (6)	8.32±0.97 (6)
medial septal nucleus	6.73±0.70 (6)	6.41±0.97 (6)
medial amygdaloid nucleus	9.37±1.10 (6)	9.00±1.39 (6)
basal amygdaloid nucleus	11.26±1.57 (6)	6.74±0.83 ⁺ (4)
central amygdaloid nucleus	15.12±1.30 (6)	13.93±1.99 (6)
lateral amygdaloid nucleus	12.00±1.37 (6)	4.94±1.52 ⁺⁺ (4)

mean ± S.E.M.

+ = $p < 0.05$

++ = $p < 0.001$

* = Number of animals in brackets

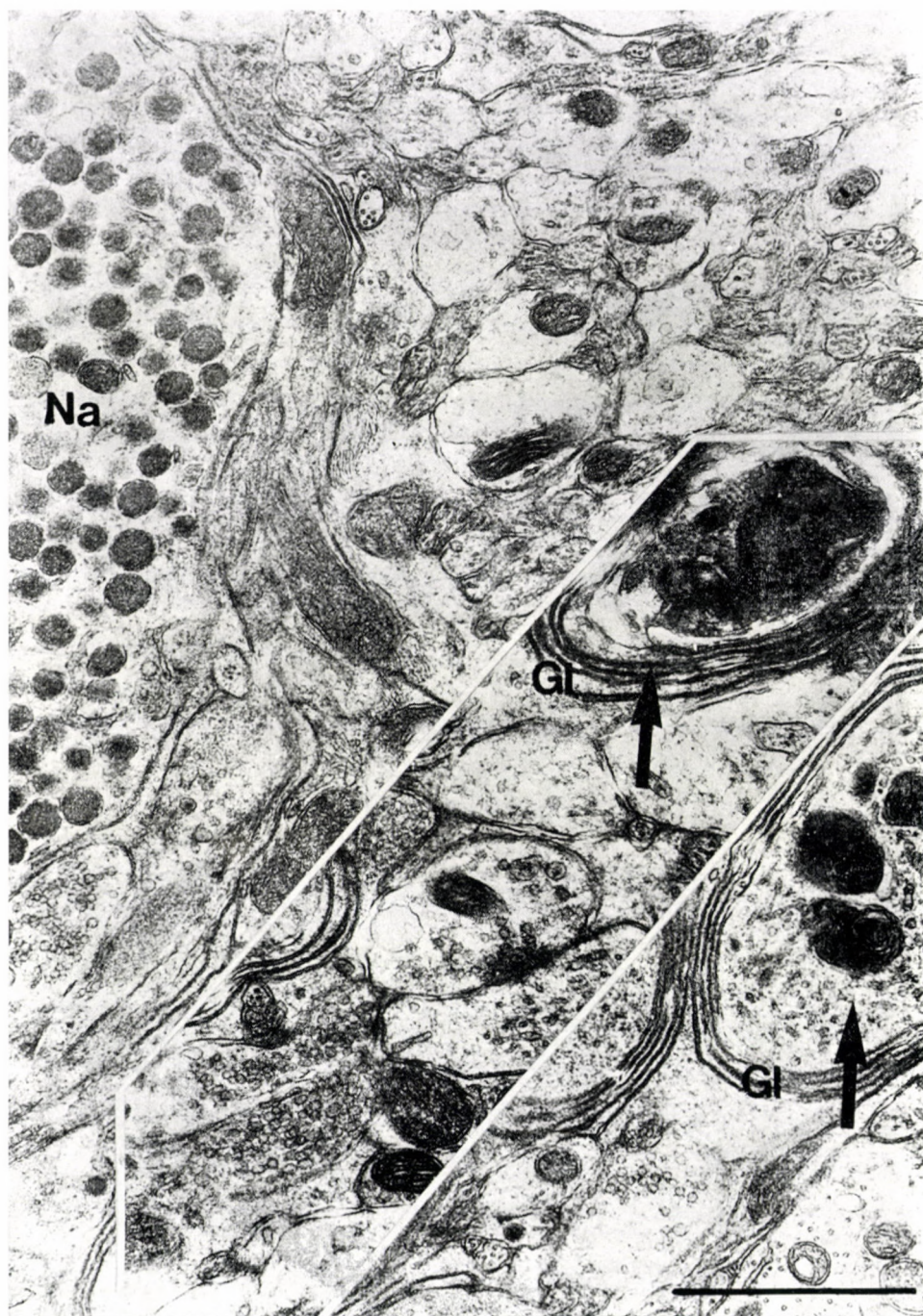


Fig. 2. Electron micrographs showing the ensheathment by glial processes (Gl) of degenerated axons in the paraventricular nucleus; 12 h survival. NA = neurosecretory axon. Bar scale = $1 \mu\text{m}$

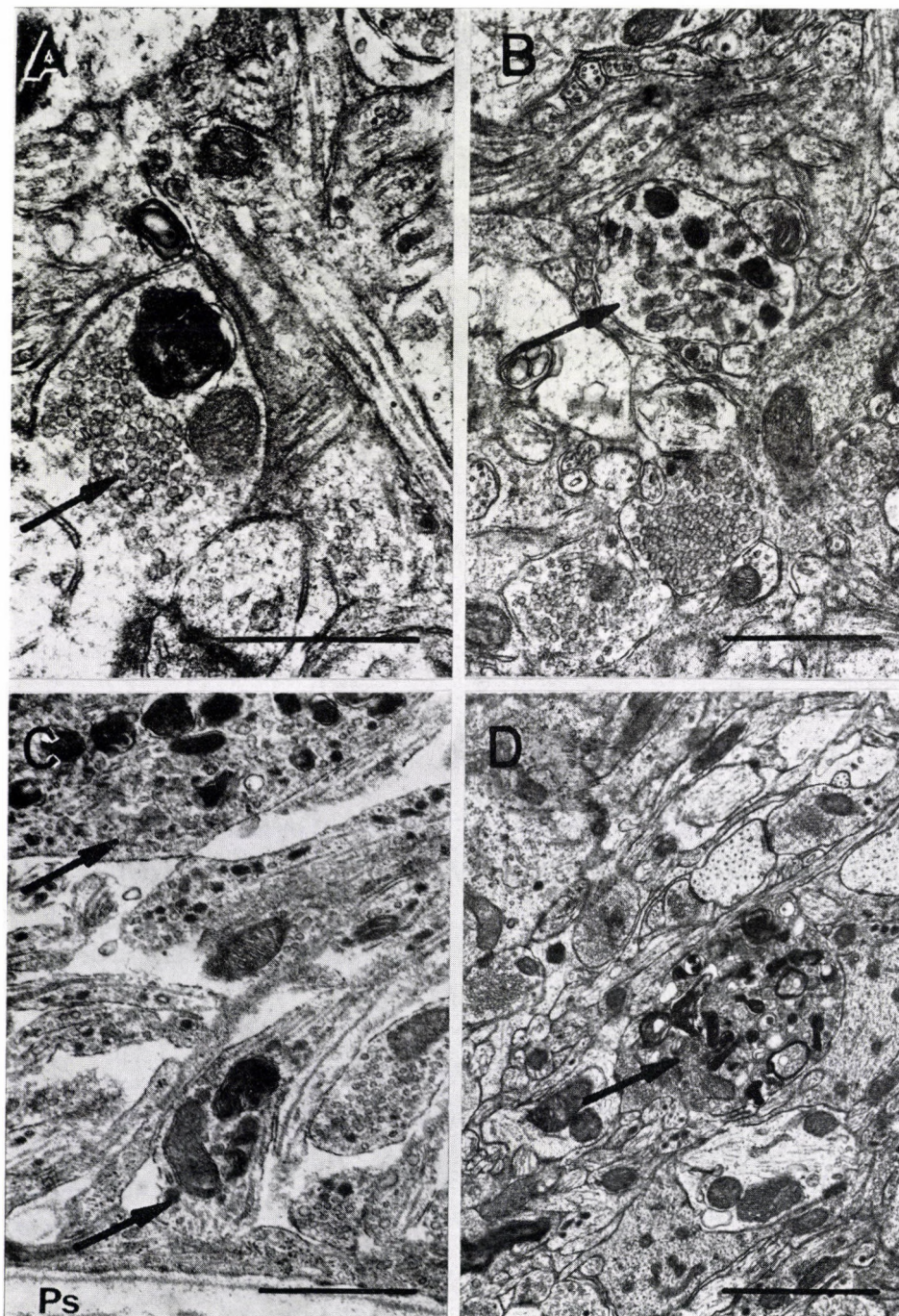


Fig. 3. Structures in various stages of degeneration in the hypothalamus. A = 4 days survival. A dense body in the dorsomedial nucleus. B = 1 day survival. Lysosomes and pleomorphic vesicles in the periventricular nucleus. C = 4 days survival. Lysosomes and dense bodies in the median eminence. D = 1 day survival. Lysosomes and a dense body in the arcuate nucleus. Bar scale = 1 μ m

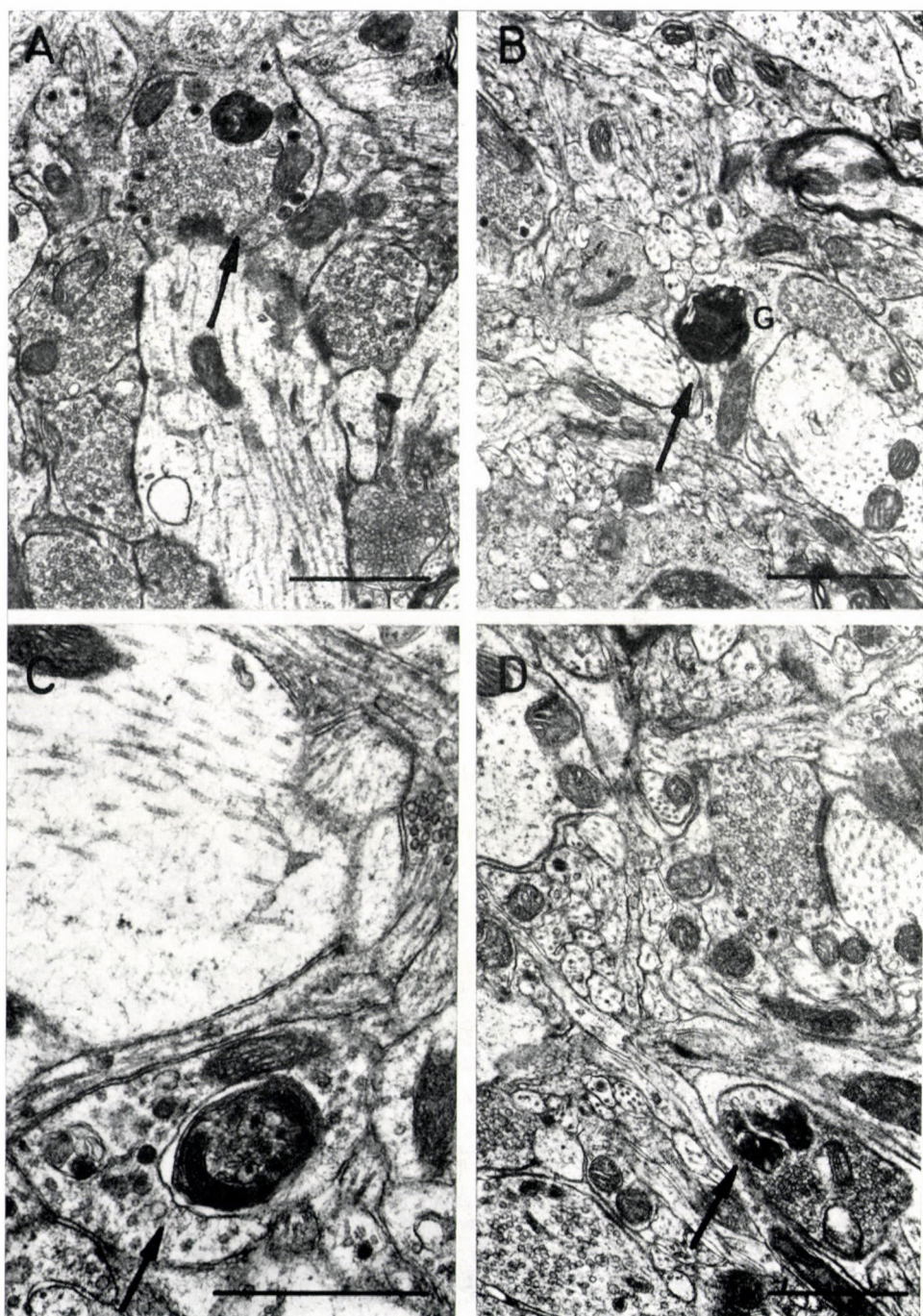


Fig. 4. Electron micrographs taken from different parts of the limbic system. (A, B, C: bed nucleus of the stria terminalis; D: hippocampus) A = dense body, 2 days. B = dark degenerating bouton (phagosome) engulfed by a glial (G) process, 2 days. C = dense body with recognizable dense core vesicle, 4 days. D = dense bodies in an axon terminal, 2 days. Bar scale = $1\text{ }\mu\text{m}$

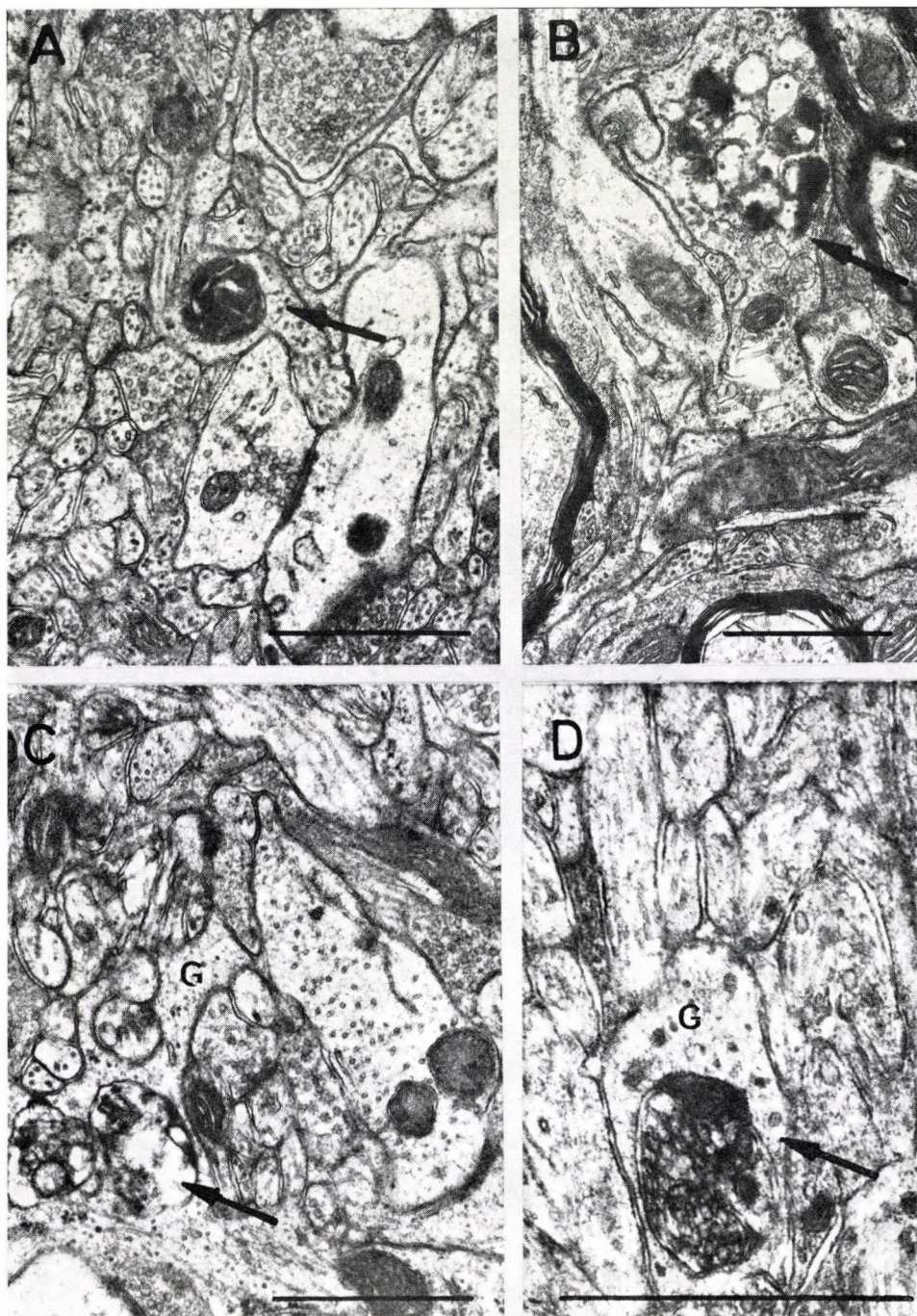


Fig. 5. Terminal degenerations in different limbic nuclei. A = degenerating bouton engulfed by a glial cell in the lateral amygdaloid nucleus, 8 days. B = multilocular degenerating structure in the anterior ventral thalamic nucleus, 8 days. C = multilocular degenerating structure within the glial cytoplasm in the basolateral amygdaloid nucleus, 8 days. D = dense body within a glial cell in the central amygdaloid nucleus, 4 days. Bar scale = 1 μ m

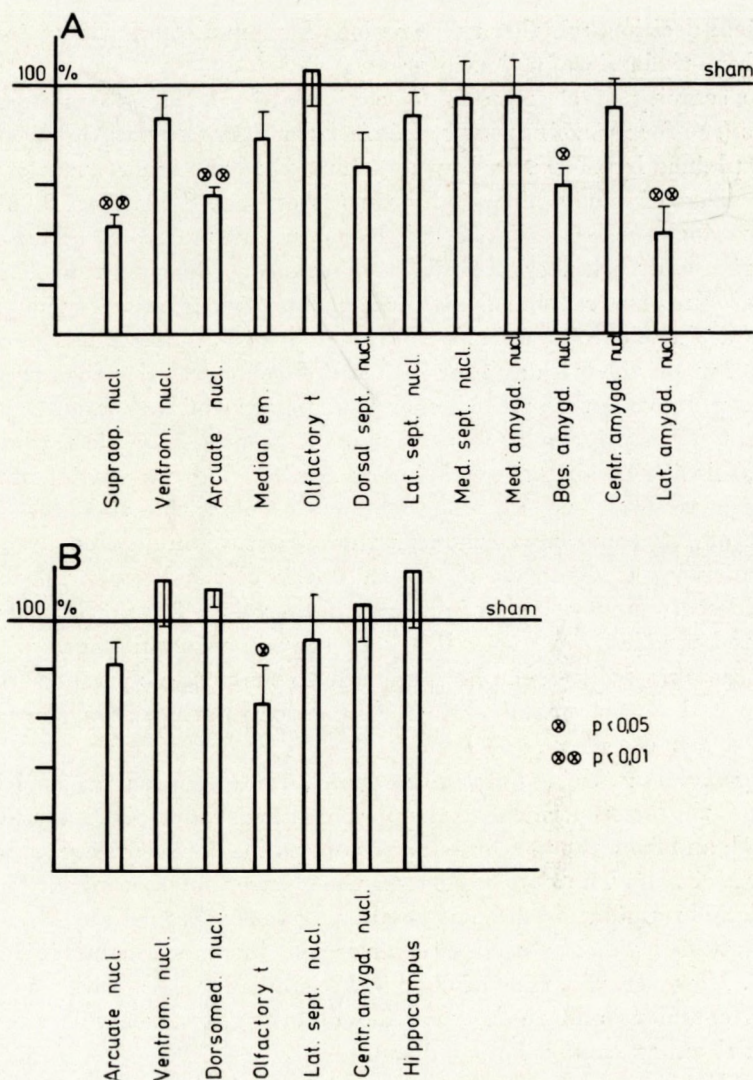


Fig. 6. Changes in the norepinephrine levels of individual brain regions after locus coeruleus (A) and parabrachial lesions (B). Data are expressed in percentage of the sham-operated animals

Discussion

A comprehensive analysis of ascending locus coeruleus [14, 15] and parabrachial [31] projections has recently been performed using light microscopic autoradiography. A major drawback of this technique is the impossibility to distinguish with certainty between a pathway and a terminal area and the most likely error in the autoradiographic material to mistake fiber of passage for terminals. Therefore, an adequate electron microscopic analysis is necessary

for the final decision, whether these regions have monosynaptic projections to discrete hypothalamic and limbic areas.

The scarcity of electron microscopic data relevant to monoaminergic pathways (see for ref. ZÁBORSZKY, LÉRÁNT and PALKOVITS, in preparation) can be explained by their very low contribution to the innervation of an area. The percentage of monoaminergic boutons is estimated between 0.02–2% in different regions of the CNS [1, 18, 21]. Hence it is difficult to recognize subtotal degeneration and to distinguish it from spontaneous degeneration. The choice of the optimum survival time is also crucial. The degeneration of the aminergic terminals are asynchronous. Its earliest signs can be observed 12 hours after the lesion but on the 8th day there are still degenerated elements present. An additional problem is that the degeneration pattern of monoaminergic terminals do not differ principally from that of non-monoaminergic terminals (ZÁBORSZKY, LÉRÁNT and PALKOVITS, in preparation). The coagulation of the locus coeruleus destroys also the non-monoaminergic cells within this area. The measurement of NE content was thought therefore to complement usefully any electron microscopic observations as to the nature of the degenerated terminals. This enables a one-way evaluation only: if there is a fall in NE content the degenerated terminals are very likely to contain this substance whereas in negative cases no decision can be made due to the possible presence on monoaminergic and non-monoaminergic terminals originating from sources other than the locus coeruleus.

Hypothalamus. Using light microscopic autoradiography axons have been traced from the locus coeruleus to the paraventricular, dorsomedial and arcuate nuclei [15], and from the parabrachial regions to the paraventricular and dorsomedial nuclei [31]. The only report on the electron microscopically verifiable hypothalamic termination of locus coeruleus axons was made by BLOOM et al. [6] who studied the hypothalamus after the intraventricular injections of 6-OHDA. However, this type of chemical lesion is not necessarily confined to the locus coeruleus and the destruction of other noradrenergic sites and/or preterminal axons cannot be ruled out.

According to our recent electron microscopic investigations the locus coeruleus region projects to the paraventricular and dorsomedial nuclei and to the median eminence. In addition, degenerated axons found in the supraoptic nucleus after lesions directed to the central grey matter but also affecting the dorsal NE bundle were likely to be derived from the locus coeruleus [49].

In earlier studies a marked decrease of NE content was found in the paraventricular nucleus after both locus coeruleus [17] and dorsal bundle [39] lesions. Present biochemical measurements showed additional noradrenergic innervation of the supraoptic and arcuate nuclei.

Although terminal degeneration was detected in the dorsomedial nucleus, the level of NE did not change after either locus coeruleus or parabrachial

lesions. Perhaps the non-aminergic neurons of the pontine taste area [31] or those of the dorsal nucleus of GUDDEN [29] project to the dorsomedial nucleus; the diffusion of labeled amino acids to the immediate vicinity of the injection site [15] may be responsible for the labeling of non-aminergic areas. The possibility that a small fraction of locus coeruleus cells are non-aminergic has also to be taken into consideration. DAHLSTRÖM and FUXE [8] have described all locus coeruleus neurons to contain catecholamines. However, the recent quantitative study of SWANSON [44] questions this statement. Finally, the lack of change of NE content in the dorsomedial nucleus in spite of the degenerated terminals present can be explained by a negligible contribution of the locus coeruleus to the monoaminergic innervation of this nucleus.

A similar discrepancy between the electron microscopic image and biochemical measurements was observed in the median eminence. Recent studies [35, 37] have shown that the median eminence receives axons also from the A2 and A8 catecholaminergic cell groups. Upon selective destruction neither of these pathways can be expected to produce measurable changes in the NE content of the median eminence, the more so since a compensatory increase of NE production occurs in the remainder.

Limbic system. The hippocampus is richly innervated by noradrenergic fibers [5, 45, 47]. After locus coeruleus lesions these fibers disappear [47] and the NE content in the hippocampus falls [17]. Degenerated terminals were also observed in this region. On the basis of these findings it can be assumed that the locus coeruleus has a monosynaptic connection with the hippocampus and that NE may act as a transmitter at these synapses [42]. This might well apply for the anterior ventral thalamic nucleus which by its connections can be regarded as a part of the limbic system.

According to light microscopic autoradiography, both the locus coeruleus [15] and the parabrachial nuclei [31] project to the central amygdaloid nucleus and to the bed nucleus of the stria terminalis. In the amygdala terminal degenerations were found under the electron microscope in the basal, lateral and central nuclei. A significant reduction (41–59%) in NE concentrations was found in the basal and lateral nuclei which may point to the role of NE at these terminals. No change in the NE level was found in the central nucleus. Here the degenerated terminals can be considered either as non-aminergic ones or as belonging to a pathway providing this nucleus only with a small fraction of its NE content.

In the bed nucleus of the stria terminalis contrasting to the positive ultrastructural findings no change in NE content could be pointed out. The histofluorescence studies of OLSON and FUXE [32], UNGERSTEDT [47] and the combined biochemical and electron microscopic studies of PALKOVITS et al. [37] have shown that this nucleus receives most of its noradrenergic terminals from the A1, A2, A5 and A7–A8 catecholaminergic cell groups. Of

course it cannot be excluded that a small proportion of NE in the bed nucleus of the stria terminalis is contained by the locus coeruleus axons.

The present findings argue for the existence of massive projections from the dorsolateral pontine tegmentum to the hypothalamus and limbic system and lend support to the view that these projections might have partially overlapping termination areas. Studies were focussed on nuclei of high NE content some of which were found to receive their main aminergic input from the dorsolateral pons. The contribution of this area to the aminergic innervation of other hypothalamic and limbic nuclei must also be kept in evidence.

REFERENCES

1. AJIKA, K., HÖKFELT, T.: (1973) Ultrastructural identification of catecholamine neurones in the hypothalamic periventricular-arcuate nucleus-median eminence complex with special reference to quantitative aspects. *Brain Res.* **57**, 97–117. — 2. ANDÉN, N.—E., DAHLSTRÖM, A., FUXE, K., LARSSON, K., OLSON, L., UNGERSTEDT, U.: (1966) Ascending monoamine neurons to the telencephalon and diencephalon. *Acta physiol. scand.* **67**, 313–326. — 3. ANLEZARK, G., CROW, T., GREENWAY, A.: (1973) Impaired learning and decreased cortical norepinephrine after bilateral locus coeruleus lesions. *Science* **181**, 682–684. — 4. ARBUTHNOTT, G., CHRISTIE, J., CROW, T., ECCLESTON, D., WALTER, D.: (1973) The effect of unilateral and bilateral lesions in the locus coeruleus on the levels of 3-methoxy-4-hydroxyphenylglycyl in neocortex. *Experientia (Basel)* **29**, 52–53. — 5. BLACKSTADT, T., FUXE, K., HÖKFELT, T.: (1967) Noradrenaline nerve terminals in the hippocampal region of the rat and guinea pig. *Z. Zellforsch.* **78**, 463–473. — 6. BLOOM, F.—E., ALGERI, S., GROPEL, A., REVUELTA, A., COSTA, E.: (1969) Lesions of central norepinephrine terminals with 6-hydroxydopamine: biochemistry and fine structure. *Science* **166**, 1284–1286. — 7. BROWNSTEIN, M., SAAVEVEDRA, J. M., PALKOVITS, M.: (1974) Norepinephrine and dopamine in the limbic system of the rat. *Brain Res.* **79**, 431–436. — 8. DAHLSTRÖM, A., FUXE, K.: (1964) Evidence for the existence of monoamine-containing neurons in the central nervous system. I. Demonstration of monoamine in the cell bodies of brain stem neurons. *Acta physiol. scand.* **62**, Suppl. 232, 1–55. — 9. DESCARRIES, L., LAPIERRE, Y.: (1973) Noradrenergic axon terminals in the cerebral cortex of rat. I. Radioautographic visualization after topical application of DL ³H norepinephrine. *Brain Res.* **51**, 141–160. — 10. FUXE, K.: (1965) Evidence for the existence of monoamine neurons in the central nervous system. IV. Distribution of monoamine nerve terminals in the central nervous system. *Acta physiol. scand.* **64**, Suppl. 247, 39–85. — 11. FUXE, K., HAMBURGER, B., HÖKFELT, T.: (1968) Distribution of noradrenaline nerve terminals in cortical areas of the rat. *Brain Res.* **8**, 125–131. — 12. HENRY, D. P., STARMAN, B. J., JOHNSON, D. G., WILLIAMS, R. H.: (1975) A sensitive radioenzymatic assay for norepinephrine in tissue and plasma. *Life Sci.* **16**, 375–384. — 13. JACOBOWITZ, D. M.: Effects of 6-hydroxydopa. In: *Frontiers in Catecholamine Research*. Eds: Usdin, E., Snyder, S., pp. 729–739, Pergamon Press, Oxford 1973. — 14. JONES, B. E., HALARIS, A. E., McILHANY, M., MOORE, R. Y.: (1977) Ascending projections of the locus coeruleus in the rat. I. Axonal transport in central noradrenaline neurons. *Brain Res.* **127**, 1–21. — 15. JONES, B. E., MOORE, R. Y.: (1977) Ascending projections of the locus coeruleus in the rat. II. Autoradiographic study. *Brain Res.* **127**, 23–53. — 16. KIZER, J. S., MUTH, E., JACOBOWITZ, D. M.: (1976) The effect of bilateral lesions of the ventral noradrenergic bundle on endocrine-induced changes of tyrosine hydroxylase in the rat median eminence. *Endocrinology* **98**, 886–898. — 17. KOBAYASHI, R. M., PALKOVITS, M., KOPIN, I. J., JACOBOWITZ, D. M.: (1975) Biochemical mapping of noradrenergic nerves arising from the rat locus coeruleus. *Brain Res.* **77**, 269–279. — 18. KODA, L. Y., BLOOM, F. E.: (1977) A light and electron microscopic study of noradrenergic terminals in the rat dentate gyrus. *Brain Res.* **120**, 327–335. — 19. KOOB, G. F., BALCOM, G. J., MEYERHOFF, J. L.: (1967) Increase in intracranial self-stimulation in the posterior hypothalamus following unilateral lesions in the locus coeruleus. *Brain Res.* **101**, 554–560. — 20. KORF, J., AGHAJANIAN, G., ROTH, R.: (1973) Stimulation and destruction of the locus coeruleus: opposite effects on 3-methoxy-4-hydroxy-phenylglycol sulfate levels in the rat cerebral cortex. *Europ. J. Pharma-*

- col. **21**, 305–310. — 21. LAPIERRE, Y., BEAUDET, N., DEMIANCZUK, L., DESCARRIES, L.: (1973) Noradrenergic axon terminals in the cerebral cortex of rat. II. Quantitative data revealed by light and electron microscope radioautography of the frontal cortex. *Brain Res.* **63**, 175–182. — 22. LIDBRINK, P.: Noradrenaline nerve terminals in the rat cerebral cortex following lesion of the dorsal noradrenaline pathway: a study on the time course of their disappearance. In: *Dynamics of Degeneration and Growth in Neurons*. Eds: Fuxe, K., Olson, L., Zotterman, Y. Wenner Gren Center Int. Symp. Ser. Vol. 22, pp. 141–149. Pergamon Press, Oxford–New York–Toronto–Sydney 1974. — 23. LINDVALL, O., BJÖRKLUND, A.: (1974) The organization of the ascending catecholamine neuron system in the rat brain as revealed by the glyoxylic acid fluorescence method. *Acta physiol. scand. Suppl.* **412**, 1–48. — 24. LLAMAS, A., REINOSO-SUÁREZ, F., MARTINEZ-MORENO, E.: (1975) Projections to the gyrus prorus from the brain stem tegmentum (locus coeruleus, raphe nuclei) in the cat, demonstrated by retrograde transport of horseradish peroxidase. *Brain Res.* **89**, 331–336. — 25. LOIZOU, L.: (1969) Projections of the locus coeruleus in the albino rat. *Brain Res.* **15**, 563–564. — 26. LOWRY, O., ROSEBROUGH, N., FARR, A., RANDALL, R.: (1951) Protein measurement with the Folin phenol reagent. *J. biol. Chem.* **193**, 265–275. — 27. MAEDA, T., PIN, C., SALVERT, D., LIGIER, M., JOUVET, M.: (1973) Les neurones contenant des catécholamines du tegmentum pontique et leurs voies de projection chez le chat. *Brain Res.* **57**, 119–152. — 28. McBRIDE, R. L., SUTIN, I.: (1976) Projections of the locus coeruleus and adjacent pontine tegmentum in the cat. *J. comp. Neurol.* **165**, 265–284. — 29. MOREST, D. K.: (1961) Connexions of the dorsal tegmental nucleus in the rat and rabbit. *J. Anat. (Lond.)* **95**, 229–246. — 30. NAKAMURA, S., IWAMA, K.: (1975) Antidromic activation of the rat locus coeruleus neurons from hippocampus, cerebral and cerebellar cortices. *Brain Res.* **99**, 372–376 (1975). — 31. NORGREN, R.: (1976) Taste pathways to hypothalamus and amygdala. *J. comp. Neurol.* **166**, 17–30. — 32. OLSON, L., FUXE, K.: (1972) Further mapping out of central noradrenaline neuron system: Projections of the 'subcoeruleus' area. *Brain Res.* **43**, 289–295 (1972). — 33. PALKOVITS, M.: (1973) Isolated removal of hypothalamic or other brain nuclei of the rat. *Brain Res.* **59**, 449–450. — 34. PALKOVITS, M., JACOBOWITZ, D. M.: (1974) Topographic atlas of catecholamine and acetylcholinesterase-containing neurons in the rat brain. II. Hindbrain (mesencephalon, rhombencephalon). *J. comp. Neurol.* **157**, 29–42. — 35. PALKOVITS, M., LÉRÁNT, Cs., ZÁBORSZKY, L., BROWNSTEIN, M. J. (1977) Electron microscopic evidence of direct neuronal connections from the lower brain stem to the median eminence. *Brain Res.* **136**, 339–344. — 36. PALKOVITS, M., RICHARDSON, J. S., JACOBOWITZ, D. M.: A histochemical study of ventral tegmental acetylcholinesterase-containing pathway following destructive lesions. *Brain Res.* **81**, 183–188. — 37. PALKOVITS, M., ZÁBORSZKY, L., FEKETE, M., SZABÓ, D., HERMAN, J. P., FEMINGER, A., KANYICSKA, B.: (In press) Biochemical and morphological changes in the hypothalamic and limbic nuclei following electrolytic lesions of mesencephalic-pontine catecholaminergic cell groups (A5, A7 and A8) in rat. *Brain Res.* — 38. PICKEL, V. M., SEGAL, M., BLOOF, F. E.: (1974) A radioautographic study of the efferent pathways of the nucleus locus coeruleus. *J. comp. Neurol.* **155**, 15–42. — 39. ROIZEN, M. F., KOBAYASHI, R. M., MUTH, E. A., JACOBOWITZ, D. M.: (1976) Biochemical mapping of noradrenergic projections of axons in the dorsal noradrenergic bundle. *Brain Res.* **104**, 384–389. — 40. ROSS, R., REISS, D. J.: (1974) Effect of lesions of locus coeruleus on regional distribution of dopamine- β -hydroxylase activity in rat brain. *Brain Res.* **73**, 161–166. — 41. SACHS, Ch., JOHNSON, G., FUXE, K.: (1973) Mapping of central noradrenaline pathways with 6-hydroxy-DOPA. *Brain Res.* **63**, 249–261. — 42. SEGAL, M., BLOOM, F. E.: (1974) The action of norepinephrine in the rat hippocampus. II. Activation of the input pathway. *Brain Res.* **72**, 99–114. — 43. SHIMIZU, N., OHNISHI, S., TOHYAMA, M., MAEDA, T.: (1974) Demonstration by degeneration silver method of the ascending projection from the locus coeruleus. *Exp. Brain Res.* **21**, 181–192. — 44. SWANSON, L. W.: (1976) The locus coeruleus: a cytoarchitectonic, Golgi and immunohistochemical study in the albino rat. *Brain Res.* **110**, 39–56. — 45. SWANSON, L. W., HARTMAN, B.: (1975) The central adrenergic system. An immunofluorescence study of the location of cell bodies and their efferent connections in the rat utilizing dopamine- β -hydroxylase as a marker. *J. comp. Neurol.* **163**, 467–506. — 46. TOHYAMA, M., MAEDA, T., SHIMIZU, N.: (1974) Detailed noradrenaline pathways of locus coeruleus neuron to the cerebral cortex with use of 6-hydroxy-dopa. *Brain Res.* **79**, 139–144. — 47. UNGERSTEDT, U.: (1971) Stereotaxic mapping of the monoamine pathways in the rat brain. *Acta physiol. scand. Suppl.* **367**, 1–48. — 48. WORTH, W. S., COLLINS, J., KETT, D., AUSTIN, J. H.: (1976) Serial changes in norepinephrine and dopamine in rat brain after locus coeruleus lesion. *Brain Res.* **106**, 198–203. — 49. ZÁBORSZKY, L., LÉRÁNT, Cs., MAKARA, G. B., PALKOVITS, M.: (1975) Quantitative studies on the supra-optic nucleus in the rat. II. Afferent fiber connections. *Exp. Brain Res.* **22**, 525–540. — 50. ZÁBORSZKY, L., PALKOVITS, M.: (In press) Ascending brain stem pathways to the hypothalamus and limbic regions: a light and electron microscopic study in the rat. *Acta Morph. Acad. Sci Hung.*

AUFSTEIGENDE BAHNEN ZU DEM HYPOTHALAMUS UND ZU DEN LIMBISCHEN KERNEN VON DER DORSOLATERALEN PONSREGION: BIOCHEMISCHE UND ELEKTRONENMIKROSKOPISCHE UNTERSUCHUNGEN

L. ZÁBORSZKY, M. J. BROWNSTEIN und M. PALKOVITS

Nach der elektrolytischen Läsion des Locus coeruleus und der parabrachialen Kerne untersuchten wir mit dem Elektronenmikroskop in den verschiedenen Kernen des Hypothalamus und des limbischen Systems die Endigungen der von obigen Gebieten aufsteigenden Axone nach 5–8-tägiger Überlebenszeit. 12 Tage nach ähnlichen Läsionen wurden in verschiedenen cerebralen Regionen mit Enzym-Isotopentechnik die Norepinephrin (NE) Konzentration gemessen.

Eine signifikante Verminderung der NE-Konzentration wurde nach der Läsion des Locus coeruleus im Nucleus supraopticus, Nucleus arcuatus, in den lateralen und basalen Amygdala-Kernen, bzw. im Hippocampus beobachtet. Unverändert blieb die NE Konzentration im Nucleus ventromedialis, Nucleus amygdaloideus centralis, in den septalen Kernen, in der Eminentia mediana und im Tuberculum olfactorium.

Nach parabrachialer Läsion verminderte sich die NE Konzentration nur im Tuberculum olfactorium.

Mit dem Elektronenmikroskop fanden wir terminale Degeneration im Nucleus hypothalamicus dorso-medialis, paraventricularis, in der Eminentia mediana, im Nucleus interstitialis striae terminalis, in den zentralen, lateralen, basalen Amygdala-Kernen, im Hippocampus und im ventralen Nucleus anterior thalami.

ПРОЕКЦИЯ ДОРЗОЛАТЕРАЛЬНОЙ ЧАСТИ МОЗГА К ЛИМБИЧЕСКИМ И ГИПОТАЛАМИЧЕСКИМ ЯДРАМ: БИОХИМИЧЕСКОЕ И ЭЛЕКТРОННОМИКРОСКОПИЧЕСКОЕ ИССЛЕДОВАНИЕ

Л. ЗАБОРСКИ, М. Е. БРОНШТЕЙН и М. ПАЛКОВИЧ

Авторы провели электронномикроскопический анализ аксональных окончаний в различных ядрах гипоталамуса и лимбической системы, после электролитического повреждения локуса цорилеуса и парабрахияльных ядер (животные забивались через 0,5–8 дней после электролитического повреждения вышеуказанных ядер). Проведено, также, измерение концентрации норэпинефрина (НЭ), методом, предложенным ХЕНРИ и др. [12] в различных конкретных частях мозга через 12 дней после повреждения вышеуказанных ядер.

Выявлено, что после повреждения локуса цорилеуса достоверно уменьшается концентрация НЭ в латеральных и базальных ядрах амигдалы, гипоталамуса, в нуклеус супраоптикуса и нуклеус аркуатуса. Не меняется концентрация НЭ в центральном ядре амигдалы, септальных ядрах, в нуклеус вентромедialis, эминенция медиана и туберкулум олфакториум. После повреждения парабрахияльных ядер, достоверное уменьшение концентрации НЭ можно было выявить только в туберкулум олфакториум.

Электронномикроскопический анализ показал дегенерацию аксональных окончаний в дорсомедиальном и паравентрикулярном ядрах гипоталамуса, в эминенция медиана, в центральном, латеральном и базальном ядрах амигдалы, гипоталамуса, в переднем ядре таламуса, в интерстициальном ядре стрии терминалис.

Dr. László ZÁBORSZKY	} Semmelweis Orvostudományi Egyetem I. sz. Anatómiai Intézet, H-1450 Budapest, Tüzoltó u. 58., Hungary
Dr. Miklós PALKOVITS	
M. J. BROWNSTEIN	} Laboratory of Clinical Science, National Institute of Mental Health, Bethesda, USA

National Institute for Nervous and Mental Diseases, Budapest, and Balassa János Hospital, Szekszárd, Hungary

XERORADIOGRAPHIC DEMONSTRATION OF SOFT TISSUES OF THE EXTREMITIES

R. PÁLVÖLCGYI and Z. PÉNTEK

(Received May 3, 1977)

The authors gave a useful sketch of the essence of xeroradiography. Their method has proved to be optimal in demonstrating the soft tissues of the extremities *in vivo*. The paper provides us with a better cognition of the morphology and pathomorphology of soft tissues of the extremities.

The X-ray permeability of soft tissues is remarkably greater than that of the bones, that is why their shadow cannot be analysed. With the use of special finegrain films and soft X-rays, pictures can be taken on which the musculature, the fascia, the subcutis with its vessels, and the cutis can clearly be recognized. These pictures proved to be appropriate for the demonstration of various structural alterations of the soft tissues.

A new xeroradiographic method has been elaborated to take pictures of the soft tissues of extremities, providing a wide range of information.

Material and methods

The theoretical background and practical application of xeroradiography is discussed in several papers [1, 2, 7].

In this method of radiological diagnosis the image is not produced by photographic but an electrical process.

In principle, instead of an X-ray film, an aluminium plate with electrically charged selenium layer is exposed in the usual manner. Soft X-rays of 35 kV have to be used and filtration must be reduced to a minimum. The rays pass through the soft tissues of the extremity. Then they strike the positively charged selenium layer producing on it positive and negative charges in proportion to the intensity and the wave length discharging thereby the selenium. A negatively charged bluish powder cloud is forced into the developing chamber, producing a vertical field component with distinct outlines. The powder is then transferred on paper by an electrostatic process and fixed by heat.

The xeroradiographic image gives a weak overall contrast but a sharp local one due to the characteristic intensity of the borders (Figs 1–8).

Xeroradiography has proved most suitable for the *in vivo* demonstration of the soft tissues of the extremities. Its clinical application and advantages have been discussed previously [2–6]. The method is thought to add to our knowledge of the morphology and pathology of the soft tissues of extremities — mainly of the muscles — and will be useful in teaching anatomy.

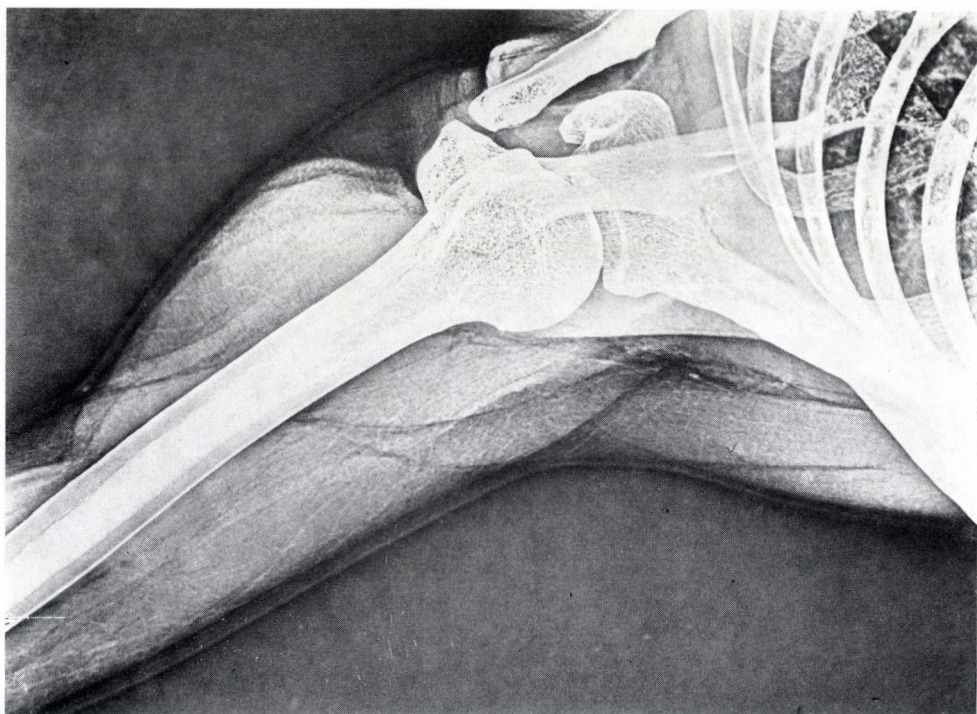


Fig. 1. Shoulder musculature. The intermuscular fat tissue is darker, the single muscles can clearly be recognized by this line-like shadow

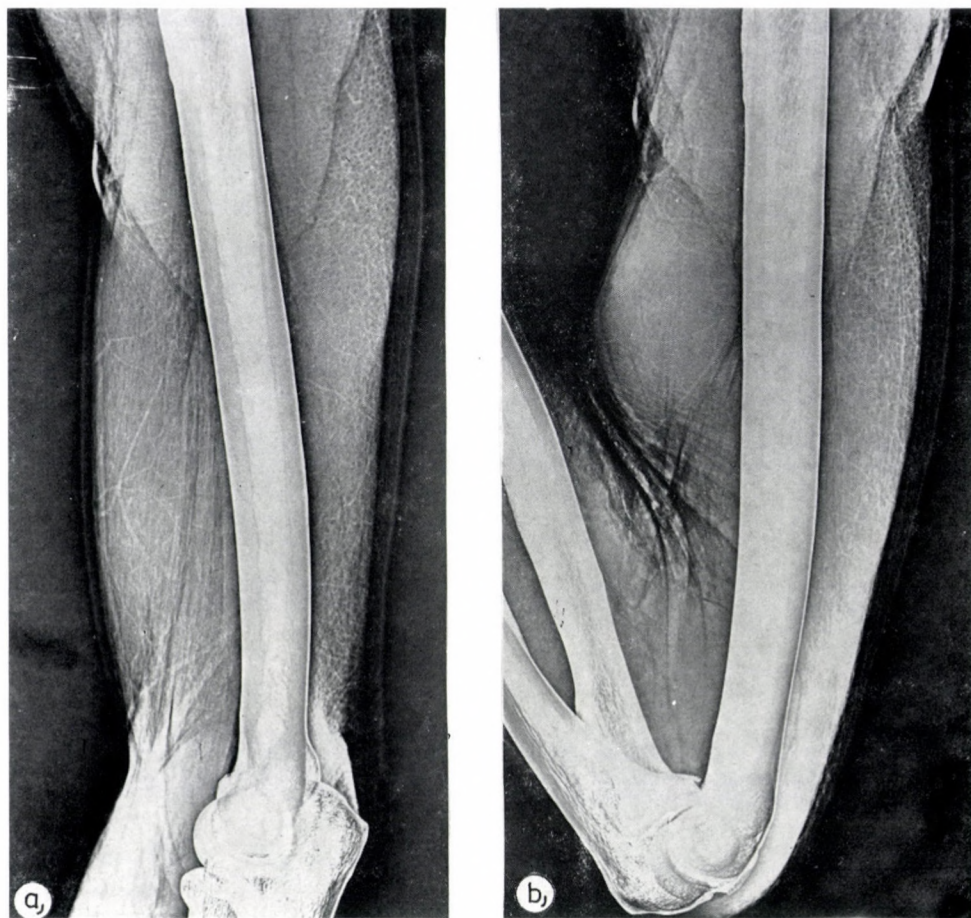


Fig. 2. Arm musculature at rest (a) and actively flexed (b)

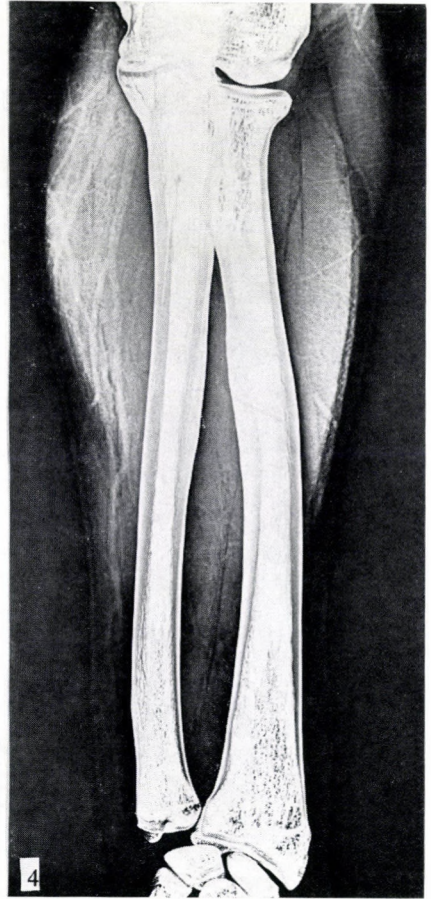
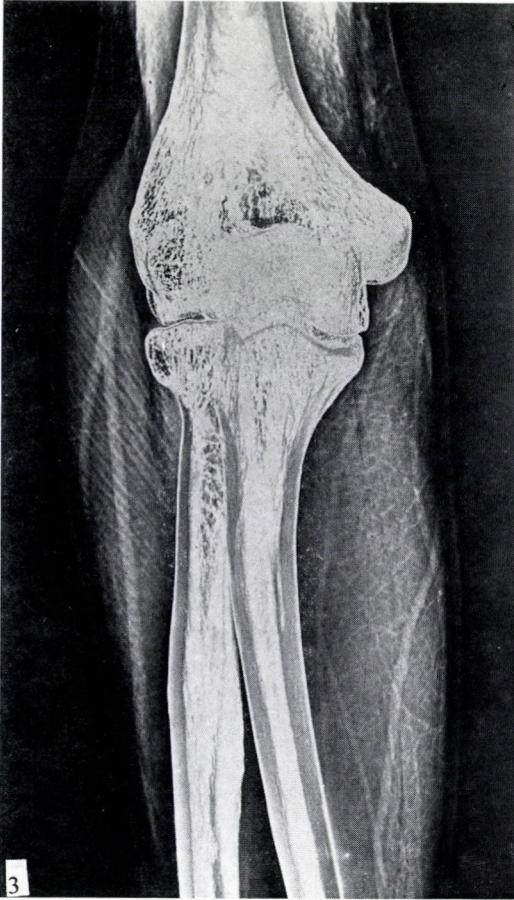


Fig. 3. Soft tissues surrounding the elbow joint. The stripiness of the brachioradial muscle deserves attention

Fig. 4. The muscles of the forearm in balling the hand

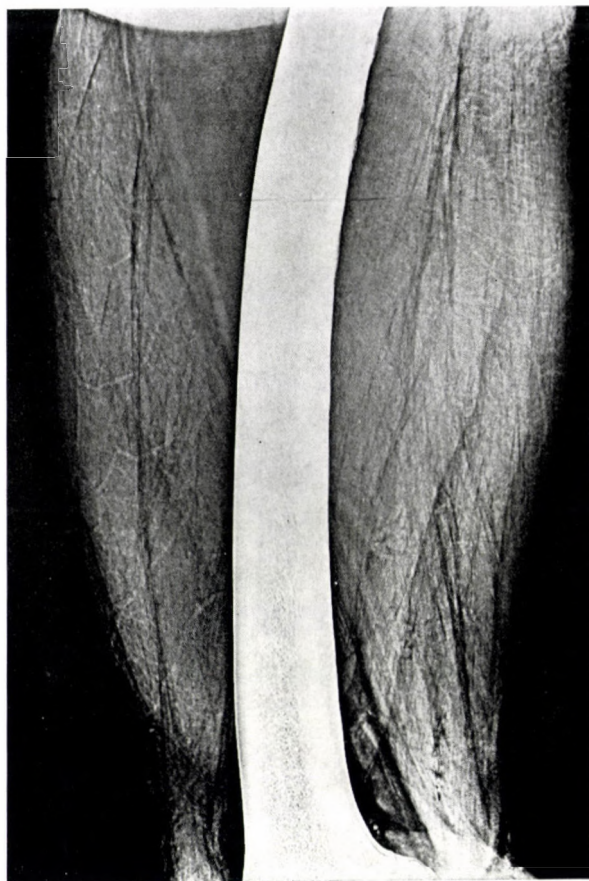


Fig. 5. Lateral picture of the thigh-muscles

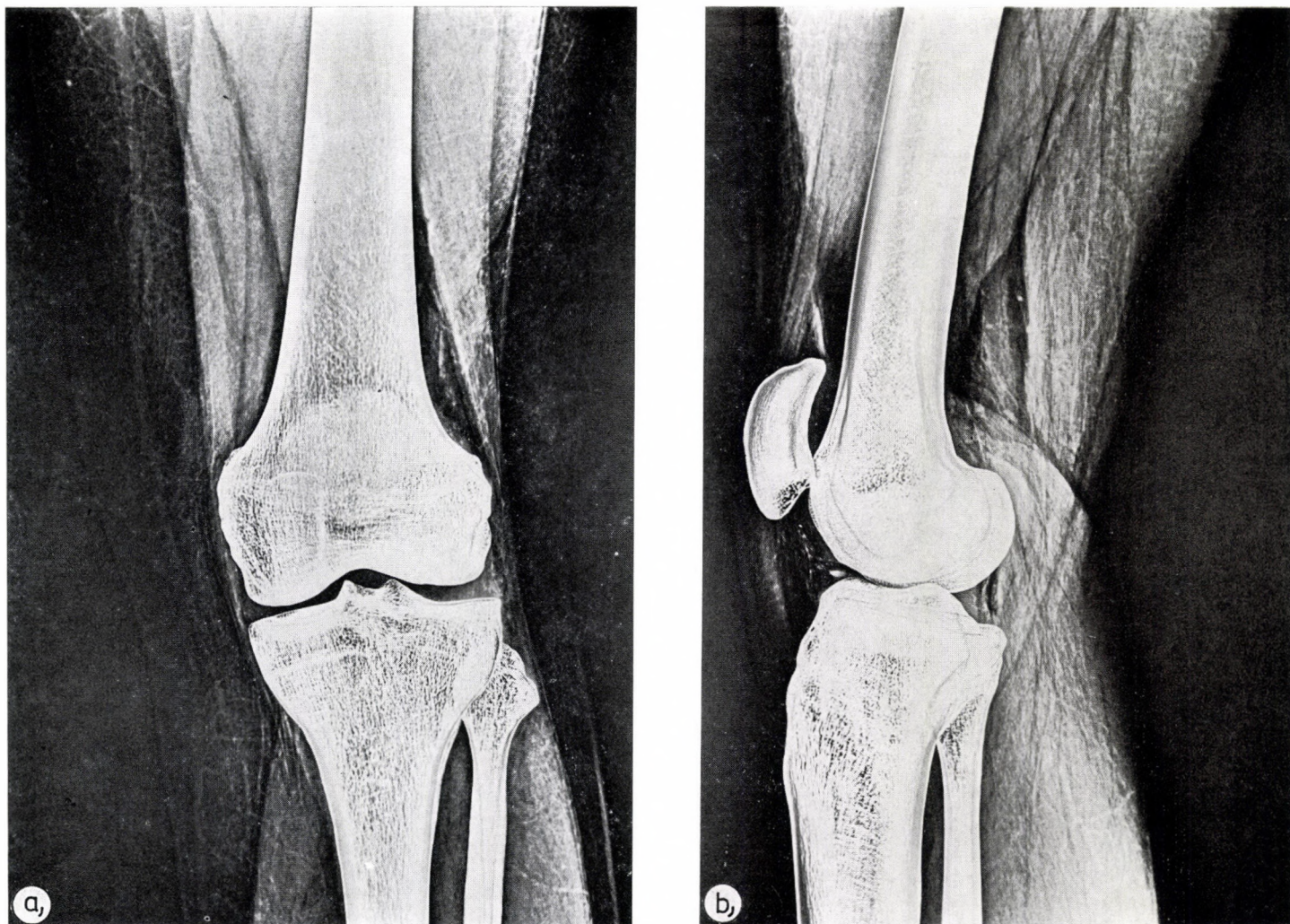


Fig. 6. Knee-joint with the surrounding soft tissues from front (a) and side (b)

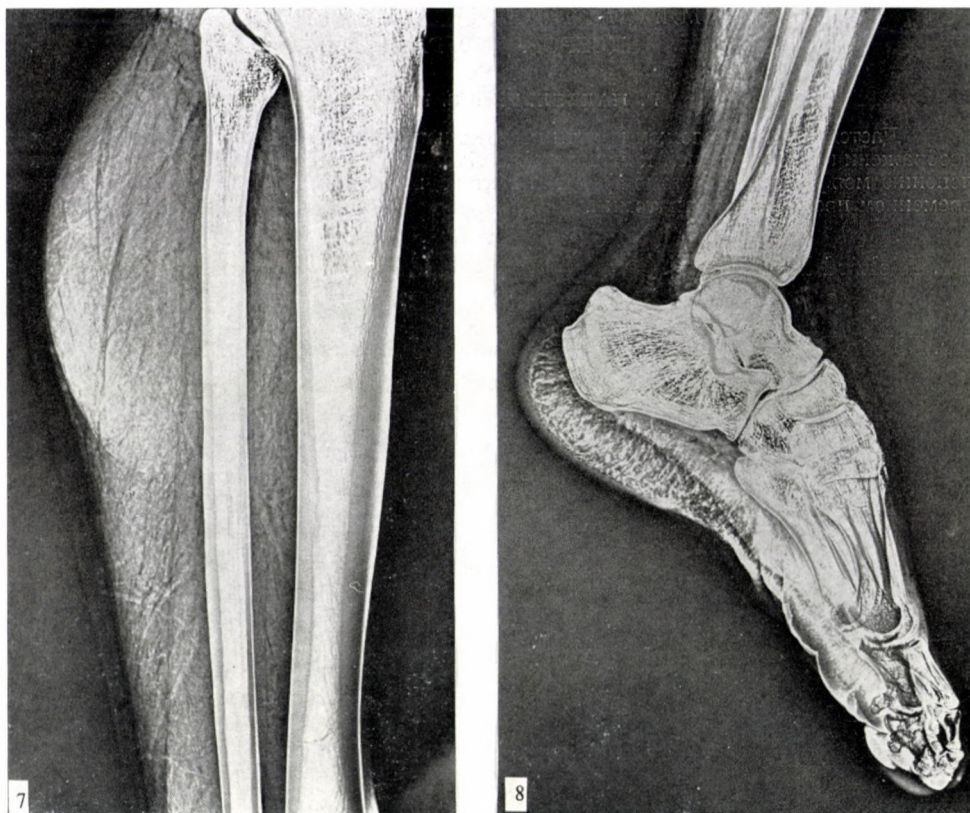


Fig. 7. Lateral picture of the leg
Fig. 8. Soft tissues of the foot, from the side

REFERENCES

1. BOAG, J. W.: (1973) Xeroradiography. Phys. in Med. Biol. **18**, 3–37. — 2. GRAVELLE, J. H., HALLETT, P.: (1975) Xeromammography — the process and image characteristics. Med. Biol. Illust. **25**, 93–96. — 3. PÁLVÖLGYI, R.: (1975) A lágyrésztechnikáról, Radiológiai Közlemények **2**, 136–163. — 4. PÁLVÖLGYI, R.: (1976) Röntgendiagnostik der Extremitätenweichteile. Röntgen **24**, 3–11. — 5. PÁLVÖLGYI, R., PÉNTEK, Z.: Weichteilveränderungen bei Pseudopseudohypoparathyreoidismus. Fortschr. Röntgenstr. in Press. — 6. PÁLVÖLGYI, R., PÉNTEK, Z.: Xeroradiographie in der Diagnostik von Extremitätenweichteilen. Fortschr. Röntgenstr. in Press. — 7. WOLFE, J. N.: (1973) Xeroradiography: Image content and comparison with film roentgenograms. Amer. J. Roentgenol. **117**, 690–695.

UNTERSUCHUNG DER WEICHTEILE VON EXTREMITÄTEN MITTELS XERORADIOGRAPHIE

R. PÁLVÖLGYI und Z. PÉNTEK

Das Wesen der Xeroradiographie wird kurz umrissen, das sich zur In-vivo-Darstellung der Weichteile von Extremitäten als optimal geeignet erwiesen hat. Sie hilft die Morphologie und Pathomorphologie der Weichteile besser aufzuklären und dürfte auch beim zeitgemäßen Anatomieverricht nützlich sein.

ИЗУЧЕНИЕ МЯГКИХ ТКАНЕЙ КОНЕЧНОСТЕЙ МЕТОДОМ
КСЕРОРАДИОГРАФИИ

Р. ПАЛВЕЛЬДИ и З. ПЕНТЕК

Дается краткое изложение сути ксерорадиографии, оказавшейся оптимальной для изображения мягких тканей конечностей *n vivo*. Метод способствует более точному выяснению морфологии и патоморфологии мягких частей и может быть полезным при современном преподавании анатомии.

Dr. Richárd PÁLVÖLGYI: Országos Ideg- és Elmegyógyintézet
H-1281 Budapest, Hungary

Dr. Zoltán PÉNTÉK: Szekszárdi Balassa János Kórház
H-7100 Szekszárd, Hungary

Second Department of Anatomy, Semmelweis University Medical School,
Budapest, Hungary

DESCENDING COURSE OF PRIMARY AFFERENT COLLATERALS IN THE CAT'S SPINAL CORD*

(Short Communication)

MÁRIA KAUSZ and M. RÉTHELYI

(Received December 2, 1977)

After injecting horseradish-peroxidase into the lower thoracic, lumbar and sacral spinal cord segments of cats, labelled perikarya were found in several spinal ganglia localized cranially to the site of injection. The segmental distance between the injection site and the rostralmost localized ganglion with labelled cells varied depending on the medio-lateral localization of the injection. The longest distance (10 segments) was achieved by medial injections. Primary sensory neurones with long descending collaterals belong to large ganglion cells.

Collaterals of primary afferent fibres are issued mainly to the segment of entry, but also to higher as well as lower spinal segments. Ascending collaterals were followed through 8 to 13 segments in cats and monkeys, whereas descending collaterals were assumed to take a shorter intersegmental course [1, 3, 10]. Electrophysiological evidence of long descending primary afferent collaterals (5 to 6 segments) was shown recently in the lumbar region of the cat [13].

The present paper aims at giving some indication about the maximum length of intersegmental course of descending collaterals, and about the size of perikarya in the spinal ganglia giving rise to long descending collaterals to lower thoracic, lumbar and sacral segments. Retrograde axoplasmic transport of horseradish-peroxidase (HRP) [4, 5, 6, 7] was used to study the distribution of primary afferent collaterals in the spinal cord.

In 9 cats single or multiple injections of 0.8–2.0 μ l of 30% HRP (Sigma Type VI and Boehringer) were made unilaterally into the spinal grey matter of lower thoracic, lumbar and sacral segments, from Th₁₁ to S₃ (see Table I). In all but one animal the needle of the Hamilton syringe (701-N) was inserted through the dorsal funiculus. In the remaining one (TM-26) it was introduced obliquely through the dorsal portion of the lateral funiculus. Unfortunately, even in this case the most ventral portion of the dorsal funiculus was moderately injured. After 48 hours survival time the animals were anesthetized and perfused with saline followed by a phosphate buffered solution of 0.5% paraformaldehyde and 2.5% glutaraldehyde, pH = 7.2. The spinal cord and the spinal ganglia were removed and stored in the fixative for 4 hours, then in

* Presented at the Congress of Hungarian Anatomists, Histologists and Embryologists, Budapest, April 6–8, 1977.

Table I

Localization of HRP injection and the distribution of labelled perikarya in spinal ganglia cranial to the injection

Animal	Injected segment	Cranial most ggl. with labelled perikarya	Segmental distance of descending collaterals
TM-2	L ₆₋₇	Th ₉	10
TM-24	L ₅	Th ₉	9
TM-16	L ₅	Th ₁₀	8
TM-13	L ₅	Th ₁₁	7
TM-26	L ₄	Th ₁₁	6
TM-8	Th ₁₁₋₁₂	Th ₆	5
TM-5	L ₁₋₂	Th ₉	4
TM-22	S ₃	L ₆	4
TM-11	L ₆	L ₃	3

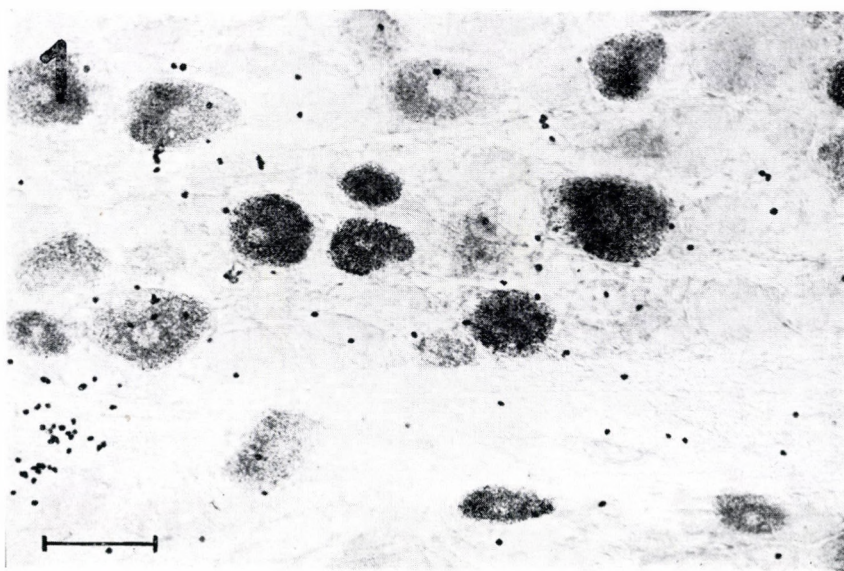
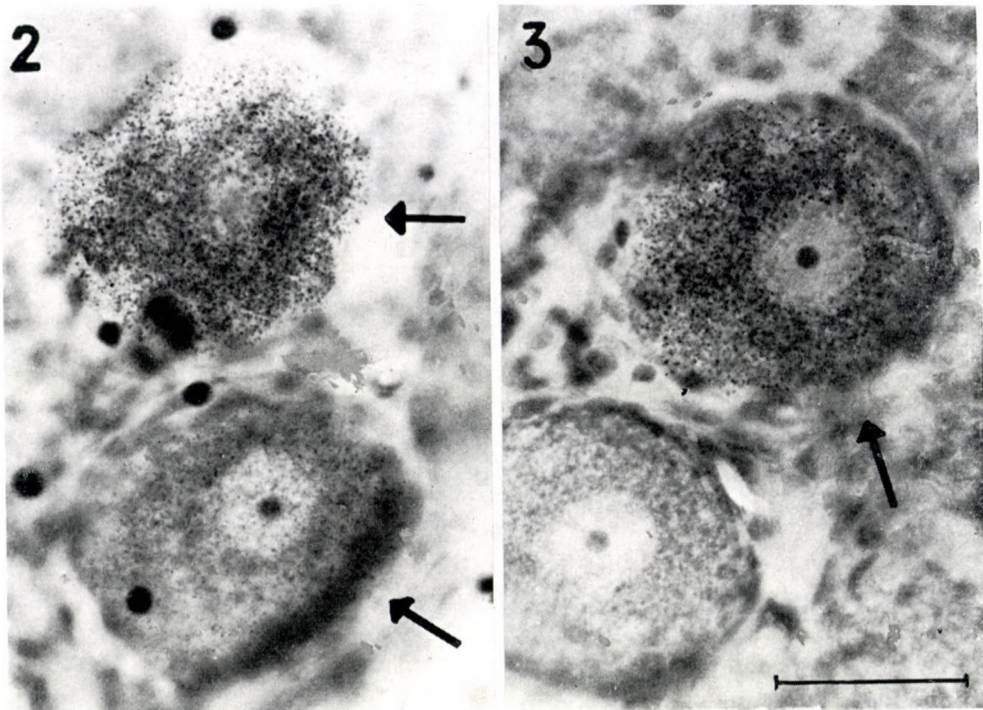


Fig. 1. Labelled neurones of various sizes in ganglion L₅ from animal TM-24. The density of the reaction product in the cells varies from high to low. Scattered black dots are red blood cells. Scale: 100 μ m



Figs 2 and 3. Large labelled neurones (arrows) in ganglion Th₁₁ of the same animals as in Fig. 1. They occur singly or occasionally in small groups. The size of HRP granules in the cytoplasm of the labelled neurones varies from fine (Fig. 2, bottom neurones) to medium (the other two neurones in both pictures) resulting in low to moderate density of the reaction product. Black dots on Fig. 2, are red blood cells. Scale: 50 μ m

buffered 5% sucrose solution for 1 or several days at 4°C temperature. Forty μ m thick frozen sections were cut from the injected segment of the spinal cord (transverse sections), and from the ganglia at both sides (longitudinal sections). The sections were incubated for HRP reaction product in diaminobenzidine (Sigma) and hydrogen peroxide, as described by NAUTA et al. [8], and counter-stained with cresyl violet.

The injection site was reconstructed from the localization of the needle track. The tip of the needle was usually confined to the intermediate grey matter; occasionally it reached the ventral horn and the ventral funiculus as well. In agreement with recent findings in the rat [9], numerous labelled cells were found in the ganglia corresponding and adjacent to the injected spinal cord segments in all animals. In these specimens both small and large neurones were filled with the reaction product (Fig. 1). The number of labelled cells diminished sharply in the cranial direction, but scattered labelled neurones could still be seen in several ganglia. The latter were mostly large nerve cells (Figs 2–3).

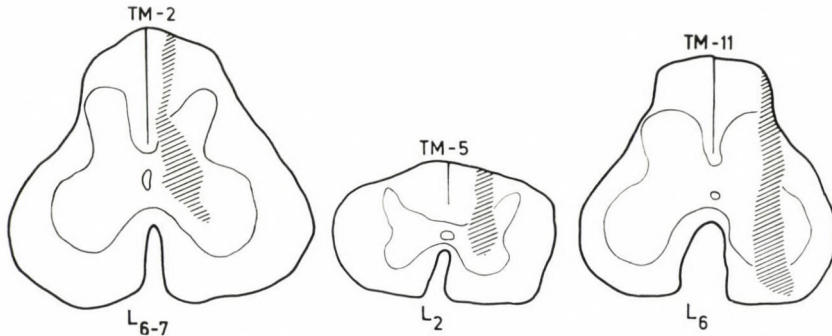


Fig. 4. Drawings of spinal cord cross sections of animals TM-2, TM-5, and TM-11. The hatched area corresponds to the needle track in each drawing. Compare the mediolateral localization of the needle track with the distribution of labelled spinal ganglion cells (see Table I)

The segmental distance between the injected segment and the most cranial ganglion in which labelled perikarya were found depended on mediolateral localization of the injection. Injections confined to the medial part of the spinal cord cross section resulted in the longest segmental distance (Fig. 4 and Table I). This finding confirms the known principles that descending primary afferent collaterals are shifted medially along their course in the dorsal funiculus [1, 12] and that they terminate mainly in the medial portion of the laminae V, VI, and VII [2]. Both injured fibres in the dorsal funiculus and axon terminals in the grey matter did probably contribute to the labelling of the perikarya. Labelled ganglion cells in the contralateral ganglia indicating a crossing of primary afferent collaterals were rarely observed. The long intersegmental course (up to 10 segments) of the descending collaterals of primary afferent fibre was unexpected and suggested an extensive convergence of primary afferent fibres to the lumbar spinal cord segments. Mainly the intraspinal arborization of the large neurones was distributed over many segments. This observation confirmed the results of recent electrophysiological studies [13] which showed that the long descending primary afferent collaterals are of thick myelinated nature (conduction velocity up to 40 m/sec). We have no direct evidence for the functional characteristics of these nerve fibres, but the findings of SELZER and SPENCER [11] concerning the long course of visceral afferents up and down the spinal cord might suggest that at least some of the neurones revealed in the present study have visceral connections at the periphery.

Acknowledgements

The authors are indebted to Mrs. Zs. TEGZES and Mr. Zs. BÁRTFAI for expert technical assistance. The HRP used in this study was generously provided by Dr. E. R. PERL.

REFERENCES

1. Bok, Th.: 1928, Das Rückenmark. In: Handbuch der mikroskopischen Anatomie des Menschen, Bd. 4, Teil 1, Nervensystem, ed. W. Möllendorff. Springer, Berlin pp. 478—578. — 2. CARPENTER, M. B., STEIN, B. M., and SHRIVER, J. E.: (1968) Central projections of spinal dorsal roots in the monkey. II. Lower thoracic, lumbosacral and coccygeal dorsal roots. Amer. J. Anat. **123**, 75—118. — 3. IMAI, Y., and KUSAMA, T.: (1969) Distribution of the dorsal root fibers in the cat. An experimental study with the Nauta method. Brain Res. **13**, 339—359. — 4. KRISTENSSON, K., and OLSSON, Y.: (1971) Retrograde axonal transport of protein. Brain Res. **29**, 363—365. — 5. KRISTENSSON, K., and OLSSON, Y.: (1974) Retrograde transport of horseradish peroxidase in transected axons. 1. Time relationships between transport and induction of chromatolysis. Brain Res. **79**, 101—109. — 6. KUYPERS, H. G. J. M., and MAISKY, V. A.: (1975) Retrograde axonal transport of horseradish peroxidase from spinal cord to brain stem cell groups in the cat, Neurosci. Letters **1**, 9—14. — 7. La VAIL, J. H., and La VAIL, M. M.: (1972) Retrograde axonal transport in the central nervous system, Science **176**, 1416—1417. — 8. NAUTA, H. J. V., PRINZ, M. B., and LASEK, R. J.: (1974) Afferents to the rat caudoputamen studied with horseradish peroxidase. An evaluation of a retrograde neuroanatomical research method. Brain Res. **67**, 219—238. — 9. NEUHUBER, W., NIEDERLE, B., and ZENKER, W.: (1977) Somatopetal transport of horseradish peroxidase (HRP) in the peripheral and central branches of dorsal root ganglion cells. Cell Tiss. Res. **183**, 395—402. — 10. SCHIMERT, J.: (1939) Das Verhalten des Hinterwurzelkollateralen im Rückenmark, Z. Anat. Entwickl.-Gesch. **109**, 665—687. — 11. SELZER, M., and SPENCER, A. W.: (1969) Convergence of visceral and cutaneous afferent pathways in the lumbar spinal cord. Brain Res. **14**, 311—348. — 12. SPRAGUE, J. M.: (1958) The distribution of the dorsal root fibres on motor cells in the lumbosacral spinal cord of the cat and the pathways. Proc. Roy. Soc. B. **149**, 534—556. — 13. WALL, P. D., and WERMAN, R.: (1976) The physiology and anatomy of long ranging afferent fibres within the spinal cord, J. Physiol. (Lond.) **255**, 321—334.

DAS VERHALTEN DER ABSTEIGENDEN KOLLATERALEN DER PRIMÄREN SENSIBLEN NEURONEN IM RÜCKENMARK DER KATZE

MARIA KAUSZ und M. RÉTHELYI

In die unteren thorakalen, lumbalen und sakralen Segmente des Rückenmarks von Katzen wurde Horseradish-Peroxidase eingespritzt. Nach der Injektion fanden sich in mehreren, kranialwärts der Injektionsstelle gelegenen Spinalganglien markierte Neurozyten. Die in Segmenten gemessene Entfernung von der Injektionsstelle bis zu dem am weitesten kranial gelegenen, markierten Neurozyten enthaltenden Ganglion war anscheinend von der Lokalisation der Einstichstelle abhängig. Die größte Entfernung (10 Segmente) wurde bei medialem Einstich ermittelt. Die primären sensiblen Neuronen mit langen absteigenden Kollateralen gehören zu den über große Neurozyten verfügenden Ganglionzellen.

НИСХОДЯЩИЕ КОЛЛЯТЕРАЛИ ПЕРВИЧНЫХ ЧУВСТВУЮЩИХ НЕВРОНОВ СПИННОГО МОЗГА КОШКИ

МАРИЯ КАУС и М. РЕТХЕЙИ

Авторы вводили horseradish-пероксидазу в нижние грудные, поясничные и крестцовые сегменты спинного мозга кошки. После инъекции препарата в нескольких спинальных ганглиях, располагающихся в краниальном направлении от места укола, наблюдались меченные нервные клетки. Определяемое в сегментах расстояние от места инъекции до наиболее краниально расположенного ганглия, содержащего меченные нервные клетки, повидимому зависит от места укола. Наибольшее расстояние (10 сегментов) было определено после инъекций, введенных медиально. Первичные чувствительные нейроны с длинными нисходящими коллятералами, относятся к ганглиозным клеткам, обладающим крупными нейронами.

Dr. Mária KAUSZ Dr. Miklós RÉTHELYI	}	Semmelweis Orvostudományi Egyetem II. sz. Anatómiai Intézet H-1094 Budapest, Tűzoltó u. 58.
--	---	---

RECENSIONES

E. HOLTZMAN: *Lysosomes: A Survey*. Cell Biology Monographs Vol. 3. Springer Verlag, New York, 1976. XI. 298 pages 56 figures.
Price: DM 130,—

The lysosome concept and discovery is a result of biochemical research, however, its full potential was realized only through modern morphological investigations. The morphological and biochemical experiments together, brought about the present knowledge of the cell physiological and pathological significance of the lysosomes. The book provides the reader with a well designed picture of the above topics.

Individual chapters deal with the concept of the lysosomes, their enzymes, the questions of the hetero and autophagy, the types of lysosomes and their functions, the known lysosome theories and their role in various pathological processes.

Regarding the origins of the lysosomes, the author attempts to bridge the differences of views in the De Duve and Novikoff schools of thought. Testing the pathological functions of the lysosomes is among pathology's most comprehensive research subjects.

Their role in storage and infectious disorders as well as in various inflammatory maladies is surveyed. According to the author, in background of the pathological processes, damages of the lysosomal membrane and their reduced functions (or lack of it) could be observed.

The subject on the role of the lysosomes in securing the cell's turnover is also adequately covered. A separate chapter discusses those lysosomes which are found in alkaloid cells and the role and functions of lysosomes in the endocrine secretions and germinal cells.

The illustrations greatly assist the reader in better understanding of the lysosomes, making the book concise and easy to read. The bibliography contains almost every significant data pertaining to the subject.

The timeliness of the lysosome topic makes this book a most useful tool for biologists, medical researchers as well as practicing clinicians.

P. SÓTONYI

JOHANN AMBROSIOUS BARTH. *Nova Acta Leopoldina NF Nr. 217/Bd. 41. Pathologie Heute* Halle, 1975. Pages 560, Figs 300 Tab. 54.
Price: DM 109,—

The publication contains the lectures delivered at the Halle scientific conference, held in honour of the 60th anniversary of Professor Günter Bruns, on February 3rd, 1974.

The well designed volume, besides surveying the development of pathology, sums up the research, the methods and the goals of today's pathologists.

Introducing the cases is a lecture heard on the changes of anatomical investigation of the central nervous system and the effect of these changes on various aspects of pathology itself. Other lectures cover a rather wide scale of topics, among them the localization frequency of head injuries, pathological analysis of experimental traumatological material, including reports on various tests done by electron microscopical, histochemical, polarization filter, fluorescence microscopy and other up to date methods.

A special asset of the book is that the lectures are well connected with one another, thus giving the reader a unified picture and in the same time informing him of the newest results available within a subject.

The well placed and numerous figures convincingly present the facts mentioned in the text.

Pathologie Heute is a book that can equally be useful for clinicians and pathologists.

J. LUKÁCS

R. ERIC LOMBARD: *Comparative Morphology of the Inner Ear in Salamanders (Caudata: Amphibia)*. Contributions to Vertebrate Evolution, Vol. 2. Eds: Hecht, M. K., Szalay, F. S. S. Karger, Basel 1977. 140 pages, 63 Figs, 1 Tab.
Price: DM 75,—

This monograph is based on the study of larval and adult specimens of 55 species belonging to 35 Salamander genus.

It gives a detailed review of the structure of their inner ear. Since few data is known concerning the gross and microscopic anatomy of the organs of hearing and equilibrium of ten caudate Amphibia, and their majority is outdated, the work fills a gap in the literature.

The study is based chiefly on gross and histological findings. It supplies a detailed and exact description on the inner ear, the spatial situation of the labyrinth as well as of the histological structure of its single parts. The electron microscopic data, which form a minor part of the work, concern the ultrastructure of the sensory papillae.

Following a general anatomical description of the inner ear, the characteristics of the different species are discussed. A separate chapter deals with the causes and significance of the structural diversity observed in the systematic groups.

The book is a well-edited, valuable summary containing a rich figure material. It is recommended to all who are engaged in the comparative anatomy of the organ of hearing and balance.

J. KOVÁCS

H. TEDESCHI: *Mitochondria: Structure, Biogenesis and Transducing Functions*. Springer Verlag, Vienna, New York, 1976. Vol. 4 X., 164 pages, 18 figures.
Price: DM 89,—

One of the central questions of cytological research is the biochemistry and structural organization of the multi-enzyme systems of mitochondria. The timeliness of the book is obvious in this respect.

The well-articulated volume emphasises the basic fact: the simultaneous examinations of structure and function is possible and necessary today. The function is realized through the molecular membrane.

Individual chapters deal with the energy production within the mitochondrion, the morphological structure, the workings of the inner and outer membranes, the cation—anion permeability, the metabolic carriers, the electron transport and the ATP-ase connected to it. The author also gives a detailed explanation of the theories regarding "high-energy" state (chemical, chemical-osmotic, amount of protein).

An especially well-edited part of the book concerns protein synthesis, where the author provides us with a rather comprehensive discussion on the problems of mitochondrial DNA and RNA synthesis.

The figures are complementing the text well, and the bibliography used by the author covers almost all available literature on the subject.

The book, in our opinion, will be widely read and used by biochemists, morphologists, or any other professionals working on mitochondria research.

P. SÓTONYI

INDEX

Pathologia

<i>Bély, M.—Kempelen, I.</i> : Early Diagnosis of Cancer by Gastric Biopsy	73
<i>Betléri, I.—Bély, M.</i> : Dangers of Positive Pressure Respiration Breathing with Special Reference to the So-called "Surfactant Factor"	91
<i>Fodor, I.</i> : Histogenesis of Beryllium-Induced Bone Tumours	99
<i>Keller, Mária—Tanka, D.</i> : Effect of Ultrasonic Treatment on the Organs of Experimental Animals. III. Enzyme-Histochemical Examination of the Prolonged Effect	107
<i>Neumark, T.</i> : Cell-to-Cell Contacts Between Lymphoreticular Cells in Rheumatoid Synovial Membrane	121
<i>Tanka, D.—Keller Mária</i> : Electron Transporting Enzymes of Rheumatoid Connective Tissue	137

Morphologica Normalis et Experimentalis

<i>Csonka Éva—Bernolák, B.—Koch, A. S.—Jellinek, H.</i> : Influence of Membrane Active Substances on Cell Surface Morphology of Cultured Aortic Endothelial Cells	147
<i>Sidhu, K. S.—Guraya, S. S.</i> : Comparative Dimensional Characteristics of Spermatozoa in Muridae	161
<i>Chaldakov, G. N.—Nikolov, S.—Vancov, V.</i> : Fine Morphological Aspects of the Secretory Process in Arterial Smooth Muscle Cells. II. Role of Microtubules	167
<i>Záborszky, L.—Brownstein, M. J.—Palkovits, M.</i> : Ascending Projections to the Hypothalamus and Limbic Nuclei from the Dorsolateral Pontine Tegmentum: A Biochemical and Electron Microscopic Study	175
<i>Pálvölgyi, R.—Péntek, Z.</i> : Xeroradiographic Demonstration of Soft Tissues of the Extremities	189
<i>Kausz Mária—Réthelyi, M.</i> : Descending Course of Primary Afferent Collaterals in the Cat's Spinal Cord (Short Communication)	197
Recensiones	203

Printed in Hungary

A kiadásért felel az Akadémiai Kiadó igazgatója

Műszaki szerkesztő: Zacsik Annamária

A kézirat nyomdába érkezett: 1977. XI. 23. — Terjedelem: 11,90 (A/5) ív, 66 ábra

78.5211 Akadémiai Nyomda, Budapest — Felelős vezető: Bernát György

ERRATUM

Acta Morphologica Tomus XXIV Fasciculus 3

pp. 285

An Animal is presenile when its irregular cycle, and pregnancy occurs infrequently.

pp. 287

Only the fifth mouse (36 month old) had an irregular pattern during the 9 additional cycles, consisting of a 2-day oestrous period, than a 20-day dioestrous period, 2 normal cycles and than again a 2-day oestrous period.

pp. 292

Sz. Ottó

The Acta Morphologica publish papers on experimental medical subjects in English.
The Acta Morphologica appear in parts of varying size, making up volumes.
Manuscripts should be addressed to:

Acta Morphologica, 1091 Budapest, Üllői út 93.

Correspondence with the editors and publishers should be sent to the same address.
Subscription: \$ 36.00 per volume.

Orders may be placed with "Kultura" Foreign Trading Company (1389 Budapest 62, P.O.B. 149. Account No. 218-10990) or its representatives abroad.

Les Acta Morphologica paraissent en anglais et publient des travaux du domaine des sciences médicales expérimentales.

Les Acta Morphologica sont publiés sous forme de fascicules qui seront réunis en volumes.

On est prié d'envoyer les manuscrits destinés à la rédaction à l'adresse suivante:

Acta Morphologica, 1091 Budapest, Üllői út 93.

Toute correspondance doit être envoyée à cette même adresse.

Le prix de l'abonnement: \$ 36.00 par volume.

On peut s'abonner à l'Entreprise du Commerce Extérieur «Kultura» (1389 Budapest 62, P.O.B. 149. Compte-courant No. 218-10990) ou chez représentants à l'étranger.

«Acta Morphologica» публикуют трактаты из области экспериментальных медицинских наук на английском языке.

«Acta Morpholog» выходят отдельными выпусками разного объема. Несколько выпусков составляют один том.

Предназначенные для публикации авторские рукописи следует направлять по адресу:

Acta Morphologica, 1091 Budapest, Üllői út 93.

По этому же адресу направлять всякую корреспонденцию для редакции и администрации. Подписная цена — \$ 36.00 за том.

Заказы принимает предприятие по внешней торговле «Kultura» (1389 Budapest 62, P.O.B. 149. Текущий счет № 218-10990) или его заграничные представительства и уполномоченные.

Reviews of the Hungarian Academy of Sciences are obtainable
at the following addresses:

AUSTRALIA

C.B.D. LIBRARY AND SUBSCRIPTION SERVICE,
Box 4886, G.P.O., Sydney N.S.W. 2001
COSMOS BOOKSHOP, 145 Ackland Street, St.
Kilda (Melbourne), Victoria 3182

AUSTRIA

GLOBUS, Höchstädtplatz 3, 1200 Wien XX

BELGIUM

OFFICE INTERNATIONAL DE LIBRAIRIE, 30
Avenue Marnix, 1050 Bruxelles
LIBRAIRIE DU MONDE ENTIER, 162 Rue du
Midi, 1000 Bruxelles

BULGARIA

HEMUS, Bulvar Ruszki 6, Sofia

CANADA

PANNONIA BOOKS, P.O. Box 1017, Postal Sta-
tion "B", Toronto, Ontario M5T 2T8

CHINA

CNPICOR, Periodical Department, P.O. Box 50,
Peking

CZECHOSLOVAKIA

MAD'ARSKÁ KULTURA, Národní třída 22,
115 66 Praha

PNS DOVOZ TISKU, Vinohradská 46, Praha 2

PNS DOVOZ TLAČE, Bratislava 2

DENMARK

EJNAR MUNKSGAARD, Norregade 6, 1165
Copenhagen

FINLAND

AKATEEMINEN KIRJAKAUPPA, P.O. Box 128,
SF-00101 Helsinki 10

FRANCE

EUROPERIODIQUES S.A., 31 Avenue de Ver-
sailles, 78170 La Celle St. Cloud

LIBRAIRIE LAVOISIER, 11 rue Lavoisier, 75008
Paris

OFFICE INTERNATIONAL DE DOCUMENTA-
TION ET LIBRAIRIE, 48 rue Gay-Lussac, 75240
Paris Cedex 05

GERMAN DEMOCRATIC REPUBLIC

HAUS DER UNGARISCHEN KULTUR, Karl-
Liebknecht-Straße 9, DDR-102 Berlin

DEUTSCHE POST ZEITUNGSVERTRIEBSAMT,
Straße der Pariser Kommune 3-4, DDR-104 Berlin

GERMAN FEDERAL REPUBLIC

KUNST UND WISSEN ERICH BIEBER, Postfach
46, 7000 Stuttgart 1

GREAT BRITAIN

BLACKWELL'S PERIODICALS DIVISION, Hythe
Bridge Street, Oxford OX1 2ET

BUMPUS, HALDANE AND MAXWELL LTD.,
Cowper Works, Olney, Bucks MK46 4BN

COLLET'S HOLDINGS LTD., Denington Estate,
Wellingborough, Northants NN8 2QT

W.M. DAWSON AND SONS LTD., Cannon House,
Folkestone, Kent CT19 5EE

H. K. LEWIS AND CO., 136 Gower Street, London
WC1E 6BS

GREECE

KOSTARAKIS BROTHERS, International Book-
sellers, 2 Hippokratous Street, Athens-143

HOLLAND

MEULENHOF-BRUNA B.V., Beulingstraat 2,
Amsterdam

MARTINUS NIJHOFF B.V., Lange Voorhou-
9-11, Den Haag

SWETS SUBSCRIPTION SERVICE, 347b Heere-
weg, Lisse

INDIA

ALLIED PUBLISHING PRIVATE LTD., 13/14
Asaf Ali Road, New Delhi 110001

150 B-6 Mount Road, Madras 600002

INTERNATIONAL BOOK HOUSE PVT. LTD.,
Madame Cama Road, Bombay 400039

THE STATE TRADING CORPORATION OF
INDIA LTS., Books Import Division, Chandralok,
36 Janpath, New Delhi 110001

ITALY

EUGENIO CARLUCCI, P.O. Box 252, 70100 Bari
INTERSCIENTIA, Via Mazzé 28, 10149 Torino

LIBRERIA COMMISSIONARIA SANSONI, Via
Lamarmora 45, 50121 Firenze

SANTO VANASIA, Via M. Macchi 58, 20124
Milano

D. E. A., Via Lima 28, 00198 Roma

JAPAN

KINOKUNIYA BOOK-STORE CO. LTD., 17-7
Shinjuku-ku 3 chome, Shinjuku-ku, Tokyo 160-91

MARUZEN COMPANY LTD., Book Department,
P.O. Box 5050 Tokyo International, Tokyo 100-31

NAUKA LTD. IMPORT DEPARTMENT, 2-30-19
Minami Ikebukuro, Toshima-ku, Tokyo 171

KOREA

CHULPANMUL, Phenjan

NORWAY

TANUM-CAMMERMEYER, Karl Johansgatan
41-43, 1000 Oslo

POLAND

WĘGIERSKI INSTYTUT KULTURY, Marszał-
kowska 80, Warszawa

CKP I W ul. Towarowa 28 00-958 Warszawa

ROMANIA

D. E. P., București

ROMLIBRI, Str. Biserica Amzei 7, București

SOVIET UNION

SOJUZPETCHATJ — IMPORT, Moscow

and the post offices in each town

MEZHDUNARODNAYA KNIGA, Moscow G-200

SPAIN

DIAZ DE SANTOS, Lagasca 95, Madrid 6

SWEDEN

ALMQVIST AND WIKSELL, Gamla Brogatan 26,
101 20 Stockholm

GUMPERTS UNIVERSITETSBOKHANDEL AB,
Box 346, 401 25 Göteborg 1

SWITZERLAND

KARGER LIBRI AG, Petersgraben 31, 4011 Basel

USA

EBSCO SUBSCRIPTION SERVICES, P.O. Box
1943, Birmingham, Alabama 35201

F. W. FAXON COMPANY, INC., 15 Southwest
Park, Westwood, Mass. 02090

THE MOORE-COTTRELL SUBSCRIPTION

AGENCIES, North Cohocton, N. Y. 14868

READ-MORE PUBLICATIONS, INC., 140 Cedar
Street, New York, N. Y. 10006

STECHELT-MACMILLAN, INC., 7250 Westfield
Avenue, Pennsauken N. J. 08110

VIETNAM

XUNHASABA, 32, Hai Ba Trung, Hanoi

YUGOSLAVIA

JUGOSLAVENSKA KNJIGA, Terazije 27, Beograd
FORUM Vojvode Mišića 1, 21000 Novi Sad

Acta

Morphologica

Academiae
Scientiarum
Hungaricae

ADIUUVANTIBUS

I. TÖRŐ, J. BALÓ, E. BEREI, P. ENDES,
B. HALÁSZ, H. JELINEK, I. KROMPECHER,
K. LAPIS, GY. RAPPAY, GY. ROMHÁNYI, P. RÖHLICH,
J. SUGÁR, J. SZENTÁGOTAI, I. TARISKA

REDIGIT

E. SOMOGYI

TOMUS XXV * FASCICULUS 4



1977

Akadémiai Kiadó Budapest

ACTA MORPH. HUNG.

ACTA MORPHOLOGICA

A MAGYAR TUDOMÁNYOS AKADÉMIA ORVOSTUDOMÁNYI KÖZLEMÉNYEI

SZERKESZTŐSÉG ÉS KIADÓHIVATAL: 1054 BUDAPEST, ALKOTMÁNY U. 21.

Az Acta Morphologica angol nyelven közöl értekezéseket a kísérletes orvostudomány tárgyköréből.

Az Acta Morphologica változó terjedelmű füzetekben jelenik meg. Több füzet alkot egy kötetet.

A közlésre szánt kéziratok a következő címre küldendők:

Acta Morphologica, 1091 Budapest, Üllői út 93.

Ugyanerre a címre küldendő minden szerkesztőségi és kiadóhivatali levelezés.

Megrendelhető a belföld számára az Akadémiai Kiadónál (1368 Budapest Pf. 24. Bankszámla: 215-11488), a külföld számára pedig a „Kultura” Külkereskedelmi Vállalatnál (1389 Budapest 62, P.O.B. 149 Bankszámla: 218-10990) vagy annak külföldi képviselőinél.

Die Acta Morphologica veröffentlichen Abhandlungen aus dem Bereich der experimental-medizinischen Wissenschaften in englischer Sprache.

Die Acta Morphologica erscheinen in Heften wechselnden Umfanges. Mehrere Hefte bilden einen Band.

Die zur Veröffentlichung bestimmten Manuskripte sind an folgende Adresse zu senden:

Acta Morphologica, 1091 Budapest, Üllői út 93.

An die gleiche Anschrift ist jede für die Schriftleitung und den Verlag bestimmte Korrespondenz zu richten. Abonnementspreis pro Band: \$ 36.00.

Bestellbar bei »Kultura« Außenhandelsunternehmen (1389 Budapest 62, P.O.B. 149. Bankkonto Nr. 218-10990) oder seinen Auslandsvertretungen.

First Department of Ophthalmology, Semmelweis University
Medical School, Budapest

MYOFIBRE ABNORMALITIES OF ORBICULAR MUSCLE IN MALPOSITION OF THE EYELID

J. FEHÉR

(Received March 11, 1977)

Fifty-five cases of senile entropion and ectropion have been studied electron microscopically. In both senile entropion and ectropion significant ultrastructural abnormalities were found in the orbicular muscle fibres, such as a disruption of fibres, Z line streaming, rod formation, Z line duplication and cytoplasmic body formation. These alterations have been described only in neuromuscular disorders and systemic diseases affecting the skeletal muscles. Our observations have confirmed that these abnormalities are not specific signs of any given disease, they rather represent the ultrastructural background of impaired muscle function independently of the aetiology of the disease.

There are two main theories to explain the pathomechanism of senile entropion and ectropion, the spastic and the atonic theory. These malpositions of the lower eyelid are therefore often called spastic entropion or ectropion as well as atonic entropion or ectropion. Both ascribe essential importance to orbicular muscle function, although few morphological and function observations have been carried out to reveal the pathologic background of abnormal muscle activity [10, 37–39], and we are far from knowing the exact ultrastructural features of the orbicular muscle affected by senile involution, which could explain the clinical picture.

This paper has been devoted to the study of the myofibrillar abnormalities.

Materials and methods

Fifty-five patients with senile entropion and ectropion were studied electron microscopically. Forty-two had senile entropion and twelve, senile ectropion. Thirty-seven cases were unilateral and seventeen cases were bilateral, and one patient had senile entropion of the left lower eyelid and senile ectropion of the right lower eyelid. Their mean age was 72.5 years. All these patients were operated upon and small pieces of the orbicular muscle were dissected at the surgical intervention. The muscle specimens were fixed in 2% osmium tetroxide pH 7.2, buffered with veronal-acetate, embedded in Araldite, sectioned with Reichert Ultramicrotome and contrasted by Reynolds' technique with uranyl acetate and lead citrate for examination in the JEM 7A electron microscope.

Observations

Dissolution of filaments

Disruption of the normal banding pattern and loss of myofilaments were the most common ultrastructural changes in the orbicular muscle. In some sites there were only small focal changes, whereas at other places the damage extended over many sarcomeres and even many fibres (Fig. 1). Most areas of myofibre damage were filled with glycogen particles, remnants of sarcoplasmic reticulum, T tubules as well as mitochondria, most of which showed abnormalities.

Z line streaming

A focal widening of the Z line, or sometimes widening of the whole Z line in one or more sarcomeres were common in both apparently normal and abnormal orbicular muscles. The lesions sometimes involved one or more sarcomeres in one fibre or in several neighbouring fibres (Fig. 2). Under higher power the Z line streaming displayed a longitudinal fibrillar structure, which continued into the I band next to the abnormal Z line. No transversal periodicity was seen in these extended Z lines (Fig. 3). The sarcomeres around Z line streaming had either a normal or an abnormal banding pattern.

Rod formation

This alteration was characterized by paracrystalline accumulation of Z line material. The myofibrillar structure was more or less irregular and the normal banding pattern disrupted. The intermyofibrillar spaces had widened, and in those spaces, tubules of sarcoplasmic reticulum, glycogen particles, mitochondria and a few T tubules could be seen (Fig. 4). Under high magnification, the enlarged Z lines showed a typical paracrystalline structure (Fig. 5). They consisted of a lattice-like arrangement of squares measuring about 100 Å on each side. The enlarged Z line was three to five times wider than the normal but we have never observed such paracrystalline bodies, which would have extended over several sarcomeres. On both sides of the rods, fine filaments penetrated into the substance of the accumulated Z line material.

Double Z band

A duplication of the Z line occurred in one of the cases, a man 65 year of age who had a senile ectropion and no symptoms of systemic neuromuscular or metabolic disease. The Z line duplication appeared in several neighbouring fibres (Fig. 6). On both sides of each pair of Z lines, fine fibrils could be seen.

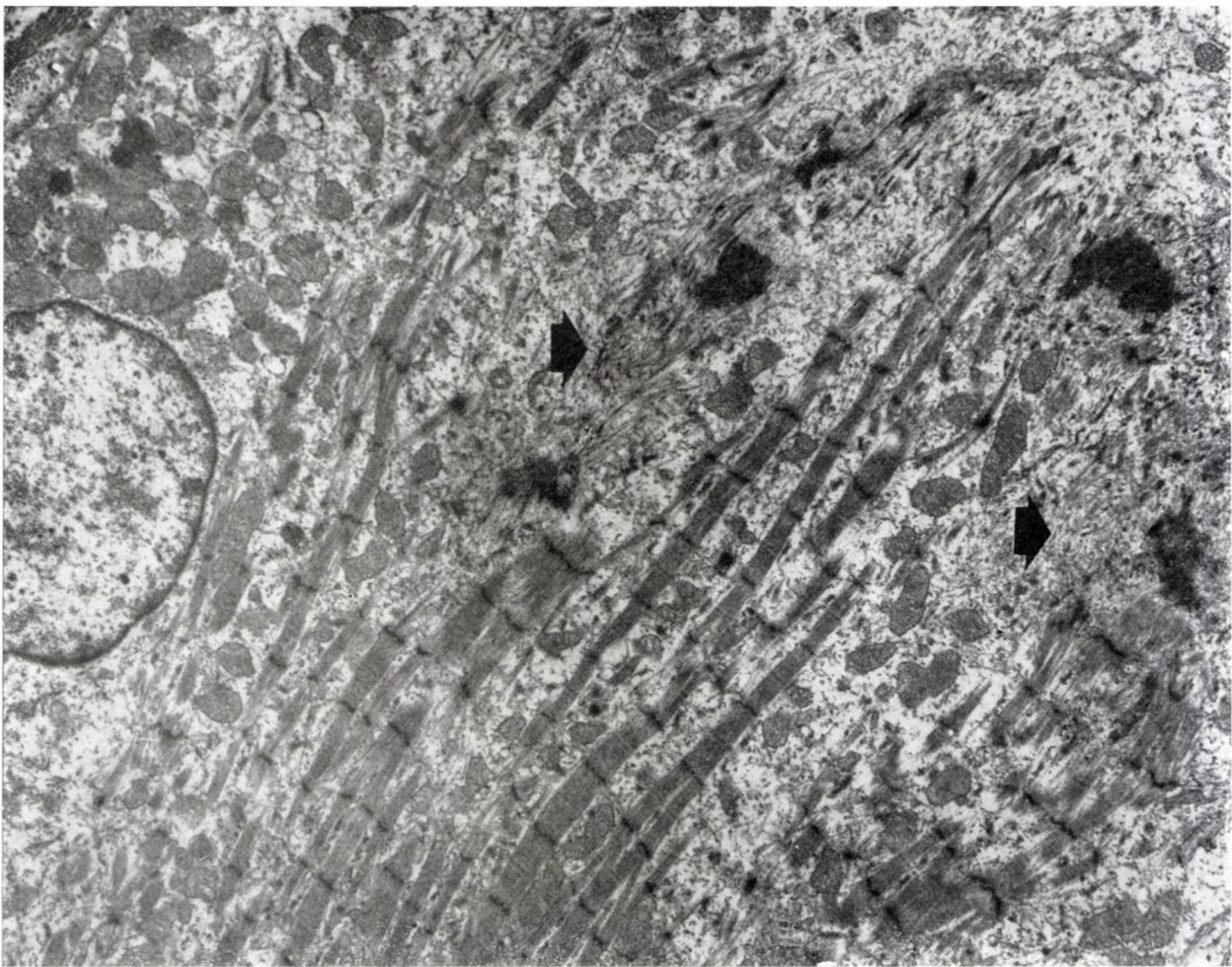


Fig. 1. Focal disruption of myofibres (arrow). The normal banding pattern has disappeared, large masses of Z line material and irregular fibrillar network are seen. N. I. 69 years. Senile entropin. $\times 11,400$



Fig. 2. Z line streaming in apparently normal muscle. The normal banding pattern is well preserved. The sarcoplasmic reticulum and mitochondria seem to be intact. T.A. 87 years. Senile entropion. $\times 22,000$



Fig. 3. Excessive Z line streaming. The normal banding pattern is highly disturbed, most of the Z line are widened. Between the irregular fibres mitochondria, glycogen particles and tubules of sarcoplasmic reticulum can be seen. S.M. 68 years. Senile entropion. $\times 19,200$

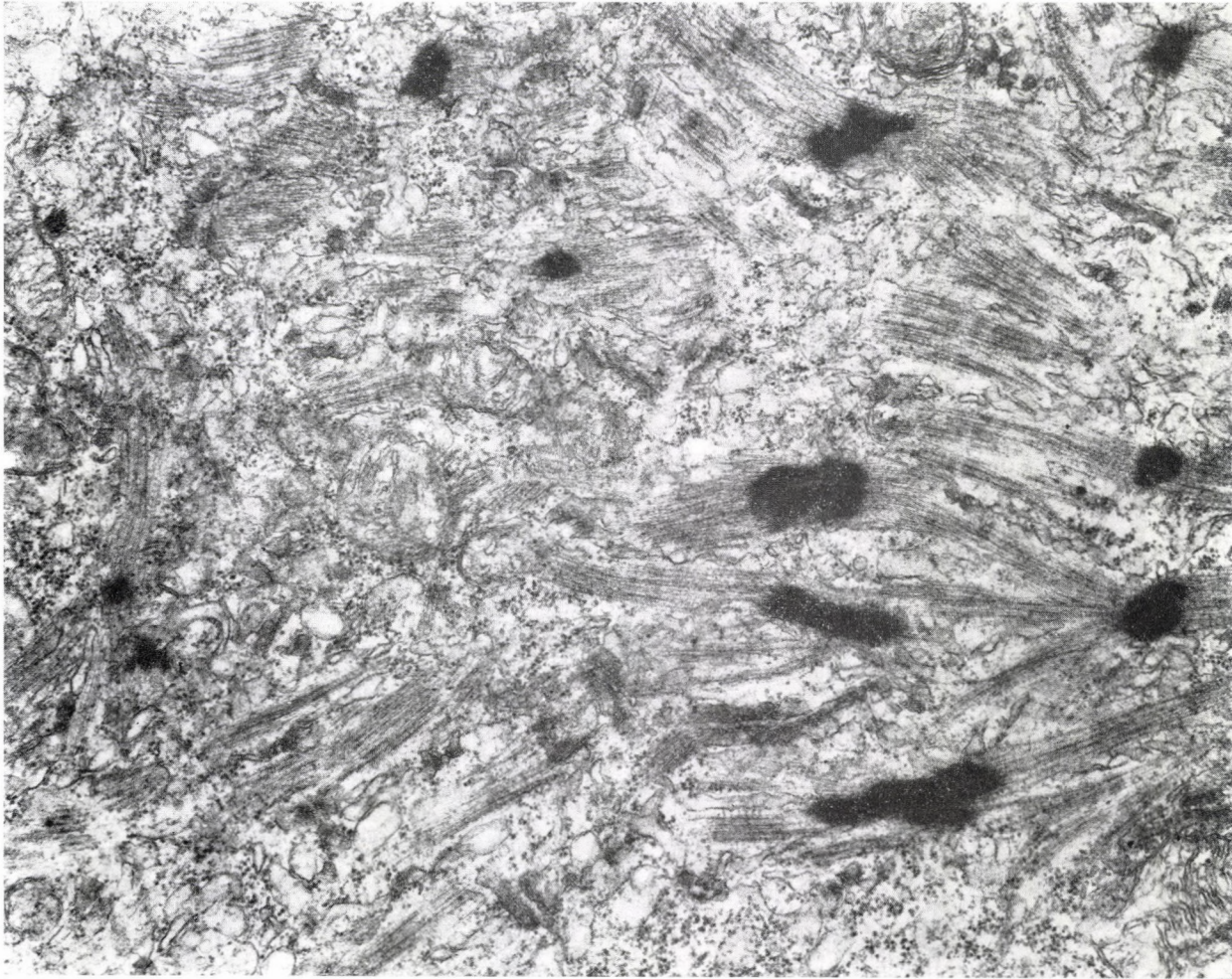


Fig. 4. Rod formation corresponding to a paracrystalline accumulation of Z line material. S.G. 76 years. Senile entropion. $\times 28,000$

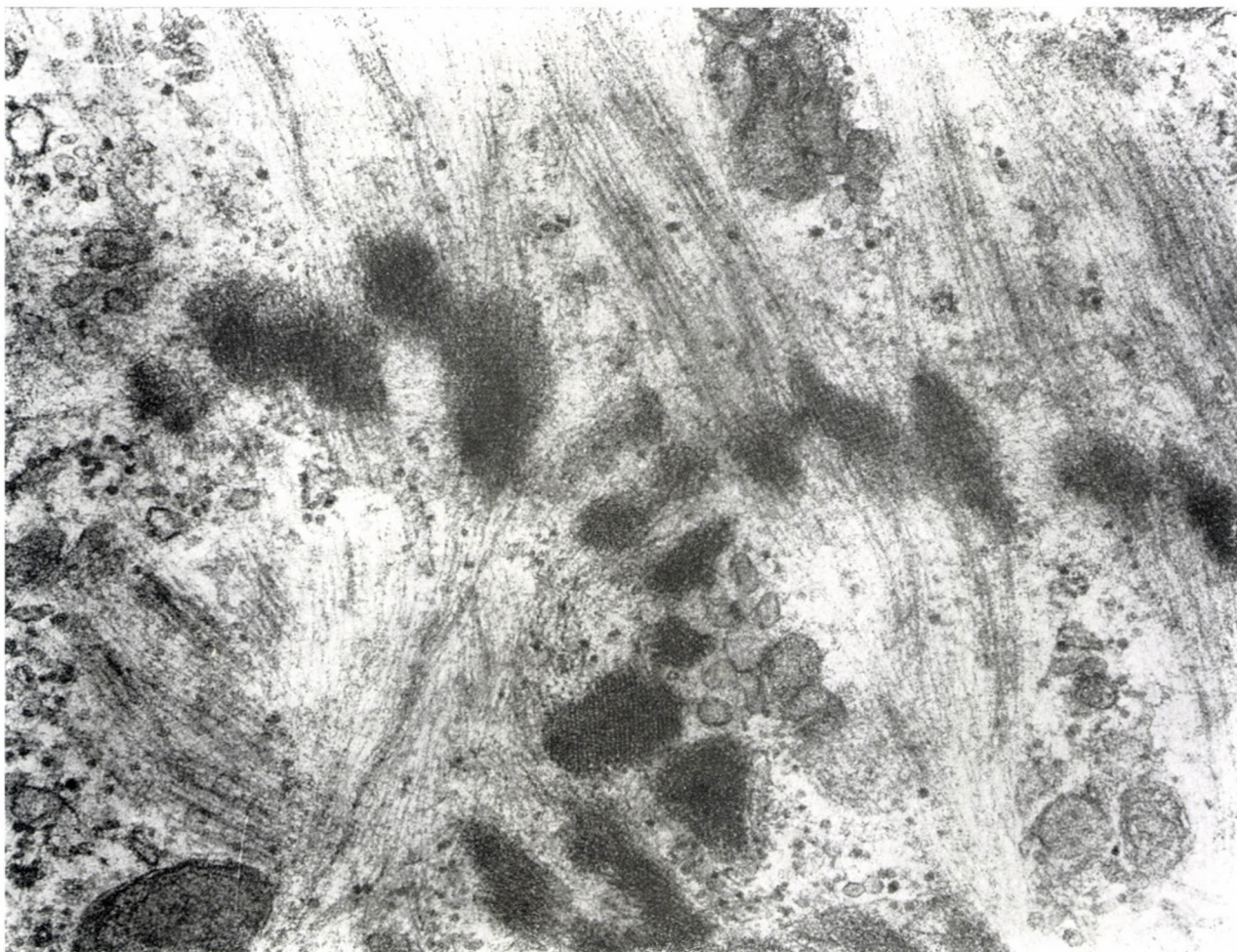


Fig. 5. The rods under high magnification show a typical paracrystalline structure. The thin filaments are in connection with the rods. E.J. 73 years. Senile entropion. $\times 99,000$

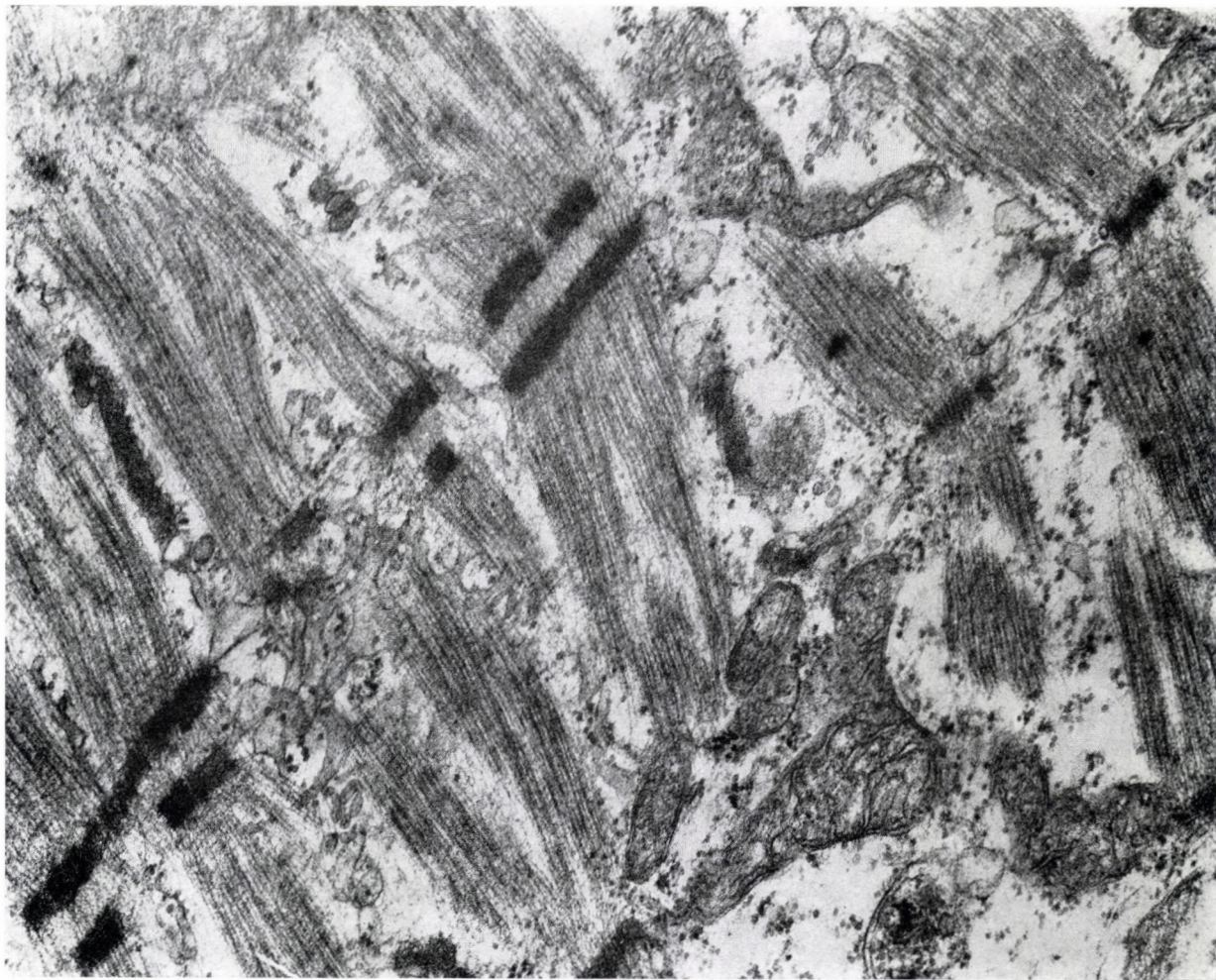


Fig. 6. Duplication of the Z lines in some neighbouring fibres. Between the slightly irregular fibres, well-developed tubules of sarcoplasmic reticulum, mitochondria and glycogen particles. V.F. 65 years. Senile ectropion. $\times 66,000$

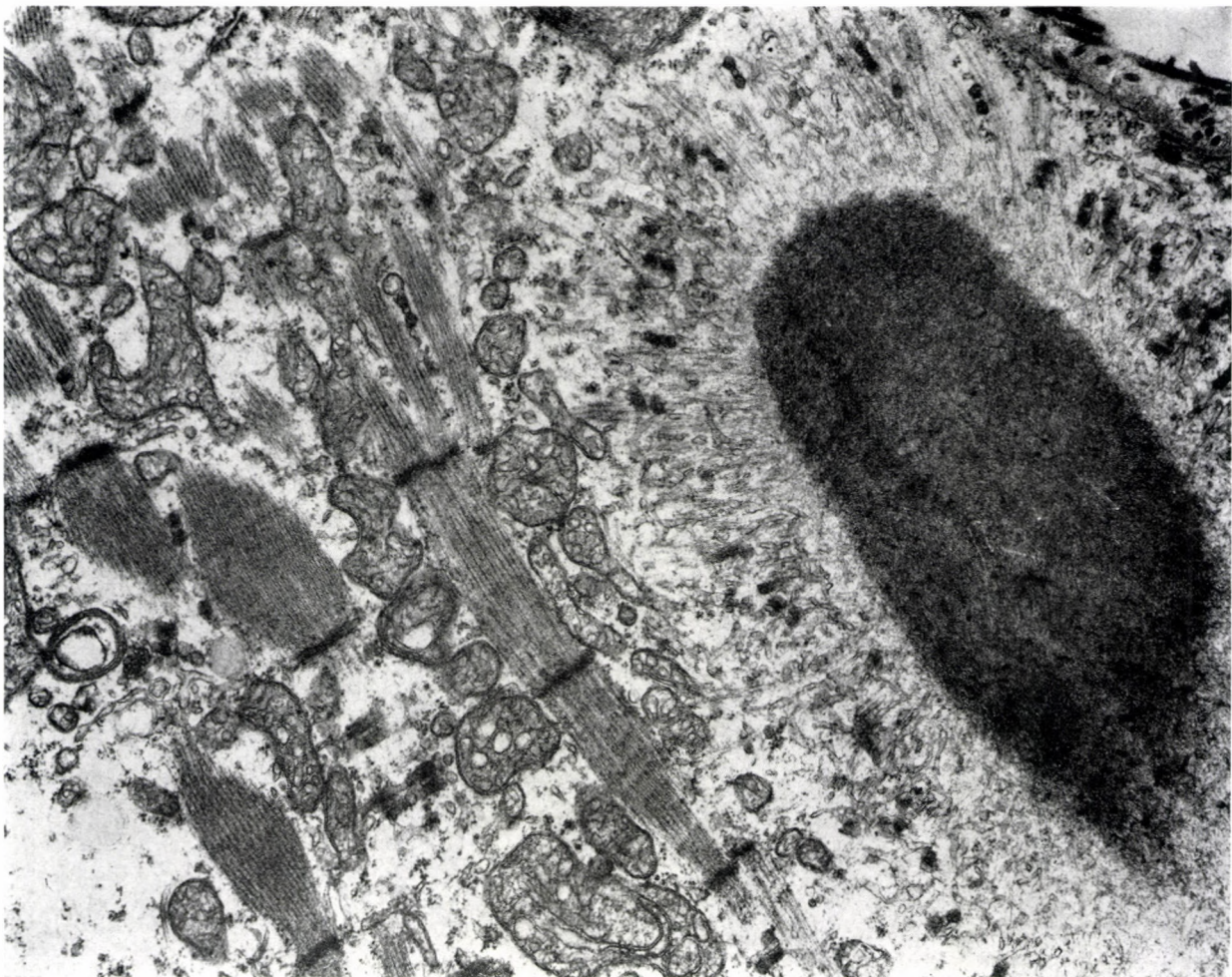


Fig. 7. Cytoplasmic body formation in the sarcoplasm. The electron-dense oval area is surrounded by a halo of fine filaments, tubules of sarcoplasmic reticulum and T tubules. B.F. 82 years. Senile entropion. $\times 22,000$

Between these fibrils glycogen particles, mitochondria and tubes of sarco-plasmic reticulum were observed. This duplication of the Z line was certainly no artefact.

Cytoplasmic bodies

This curious structure varied widely in size and shape, but had a characteristic appearance. It consisted of a round or oval, amorphous, osmiphilic central area surrounded by a halo of lighter, less dense amorphous material (Fig. 7). Fine filaments from the adjacent muscle fibres passed through this outer zone and entered into the electron-dense central region. Between the fine filaments a few T tubules, glycogen particles and a rich network of sarco-plasmic reticulum appeared.

Discussion

There is a general agreement that a disruption of the filament arrangement is not specific for any given disease. The alteration has been described in numerous unrelated diseases, such as muscular dystrophies [18, 26, 42, 45], periodic paralysis [24, 47], steroid myopathy [37], neurogenic atrophies [1, 50], glycogen storage diseases [5, 12, 27, 41].

Recently RADNÓT [37, 38], RADNÓT and FOLLMAN [39] described marked destruction and diminution of the orbicular muscle in cases of senile entropion, ectropion and eyelid tumours. The alterations were considered to represent senile changes. Our observations confirmed their findings and showed some more ultrastructural abnormalities of the orbicular muscle, such as Z line streaming, rod formation, Z line duplication and cytoplasmic body formation. These abnormalities have not been described in the orbicular muscle of apparently healthy patients.

Z line streaming may occur in normal muscles, but it is more common in muscle diseases such as muscular dystrophies [16, 34], denervation atrophies [44], collagen vascular diseases [32, 43, 49], hypothyroid myopathy [19] and central core disease [4, 11, 21].

Z line streaming has often been found in senile entropion and ectropion and sometimes enormous masses of filamentous Z line material could be observed.

A number of authors have considered these rods to be a unique pathological change found in congenital myopathy [9, 25, 48]. The specificity of rod formation seems to be doubtful since typical rods were observed in late onset myopathy of adults [13], collagen vascular disease [16, 43], central core disease [2], muscular dystrophies [16], after tenotomy [51], in the heart muscle of the cat [17] as well as in extraocular muscles [8, 33, 40].

According to the earlier opinion, the electrodense rods originated from the Z line and consisted of Z line material [14, 21, 22, 29, 30, 36]. This view was based on the finding of focal enlargements of the Z line, and on the ultrastructural similarities between the Z line and rods with regard to their electron density and lattice-like pattern. The biochemical composition of the rods is unknown [54]. Several authors suggested that the rods are the result of an excessive production and accumulation of tropomyosin [36]. This hypothesis was based on the apparent continuation of the rods into the Z lines, which earlier were believed to be tropomyosin, as well as on the ultrastructural similarities between the rods and tropomyosin crystals. Subsequent antibody localization studies [35], Z line reconstruction experiments [53] and X-ray diffraction studies [7] have considerably undermined the evidence concerning the presence of tropomyosin in the Z line. There is growing evidence suggesting that the tropomyosin localized in the thin filaments and the protein which the Z lines consist is mostly alpha actin [20]. On the other hand, remarkable myosin abnormalities have recently been described in muscle biopsies from a patient with characteristic clinical and pathological phenomena of rod myopathy. These abnormalities were accompanied by decreased ATP-ase activity of the myofibres and the sarcoplasmic reticulum [52]. In our cases of senile entropion and ectropion the rods had undoubtedly originated from the Z lines. In some places the Z lines had thickened and formed lattice-like structures, and their continuity with the filaments was always obvious. Although the size of the rods varied widely, the paracrystalline structure was typical and constant.

Duplication of the Z line is a very rare change. Only two cases of this abnormality have been reported, one in regenerating muscle [23] and one in a case of thyrotropin deficiency [15]. One case with this abnormality showed widened pairs of Z lines with paracrystalline structure.

The origin, the chemical composition and significance of cytoplasmic bodies are not known, but they appear to contain Z line material as well as myofilaments [29, 34]. These abnormalities are accompanied with other Z line alterations such as Z line streaming or rod formation. Cytoplasmic bodies were found in muscle dystrophies [30, 46], periodic paralysis [28, 31], and collagen vascular diseases [49, 55]. Two of our cases showed typical cytoplasmic body formation accompanied by other abnormalities such as Z line streaming and rod formation.

REFERENCES

1. ADACHI, M., TORII, J., SHER, J., RATNOFF, E., ARONSON, S. M., LAPOVSKY, A.: (1971) Ultrastructural and histochemical features of skeletal muscle in the Wohlfahrt-Kugelberg-Welander syndrome. *J. neurol. Sci.*, **13**, 13-20. — 2. AFIFI, A. K., SMITH, J. W., ZELLWEGER, H.: (1965) Congenital nonprogressive myopathy. Central core and nemaline myopathy in one family. *Neurology (Minneapolis)*, **15**, 371-381. — 3. AFIFI, A. K., BERGMAN, R. A., HARVEY,

- J. C. (1968): Steroid myopathy: clinical, histologic and cytologic observations. *Johns Hopkins med. J.*, **123**, 158—166. — 4. ARMSTRONG, R. M., KOENIGSBERGER, R., MELLINGER, J., LOVEFACE, R. E.: (1971) Central core disease with congenital hip dislocation: study of two families. *Neurology (Minneap.)*, **21**, 369—380. — 5. BRUNBERG, J. A., McCORMICK, W. F., SCHOCHET, S. S. Jr.: (1971) Type III glycogenosis. An adult with diffuse weakness and muscle wasting. *Arch. Neurol.*, **25**, 171—178. — 6. CAPE, C. A., JOHNSON, W. W., PITNER, S. E.: (1970) Nemaline structures in polymyositis. *Neurology (Minneap.)*, **20**, 494—502. — 7. CASPAR, D. L. D., COHEN, C., LONGLEY, W.: (1969) Tropomyosincrystal structure, polymorphism and molecular interactions. *J. molec. Biol.*, **41**, 87—95. — 8. CHENG-MINODA, K.: (1970) Aging changes in human extraocular muscles. *J. clin. Electron Micr.*, **2**, 590—601. — 9. CONEN, P. E., MURPHY, R. G., DONOHUE, W. L.: (1963) Light and electron microscopic studies of 'myo-granules' in a child with hypotonia and muscle weakness. *Canad. med. Ass. J.*, **89**, 983—987. — 10. DALGLEISH, R., SMITH, J. L. S.: (1966) Mechanism and histology of senile entropion. *Brit. J. Ophthalm.*, **50**, 79—91. — 11. DUBOWITZ, V., ROY, S.: (1970) Central core disease of muscle: clinical, histochemical and electronmicroscopic studies of an affected mother and child. *Brain*, **93**, 133—140. — 12. ENGEL, A. G.: (1970) Acid maltase deficiency in adults: Studies in four cases of a syndrome which may mimic muscular dystrophy or other myopathies. *Brain*, **93**, 599—616. — 13. ENGEL, W. K., RESNICK, J. S.: (1966) Late-onset rod myopathy: a newly recognised, acquired and progressive disease. *Neurology (Minneap.)*, **16**, 308—309. — 14. ENGEL, A. G., GOMEZ, M. R.: (1967) Nemaline (Z disc) myopathy: observations on the origin, structure and solubility properties of the nemaline structures. *J. Neuropath. exp. Neurol.*, **26**, 601—609. — 15. ENGEL, A. G., MACDONALD, R. D.: (1970) Ultrastructural reactions in muscle disease and their light-microscopic correlates. In: *Muscle Diseases*. Eds. Walton, J. N., Canal, N. and Scarlato, G., p. 71. I.C.S. No. 199. Excerpta Medica, Amsterdam. — 16. FARDEAU, M.: (1970) Ultrastructural lesions in progressive muscular dystrophies. A critical study of their specificity. In: *Muscle Diseases*. Eds. Walton, J. N., Canal, N. and Scarlato, G., p. 98. I.C.S. No. 199. Excerpta Medica, Amsterdam. — 17. FAWCETT, D. M.: (1968) The sporadic occurrence in cardiac muscle of anomalous Z-bands exhibiting a periodic structure suggestive of tropomyosin. *J. Cell Biol.*, **36**, 266—270. — 18. FISHER, E. R., COHN, R. E., DANOWSKY, T. S.: (1966) Ultrastructural observation of skeletal muscle in myopathy and neuropathy with special reference to muscular dystrophy. *Lab. Invest.*, **15**, 778—790. — 19. GODET-GUILLIAIN, J., FARDEAU, M.: (1970) Hypothyroid myopathy. Histological and ultrastructural study of an atrophic form. In: *Muscle Diseases*. Eds. Walton, J. N., Canal, N. and Scarlato, G. P. 512, I.C.S. No. 199, Excerpta Medica, Amsterdam. — 20. GOLL, D. E., MOMMAERTS, W. F. H. M., REEDY, M. K., SERAYDARIN, K.: (1969) Studies on alfa actin-like proteins liberated during trypsin digestion of alfa actin and of myofibril. *Biochim. biophys. Acta (Amst.)*, **175**, 174—194. — 21. GONATAS, N. K.: (1966) The fine structure of the rod-like bodies in nemaline myopathy and their relation to the Z-discs. *J. Neuropath. exp. Neurol.*, **25**, 409—417. — 22. GONATAS, N. K., SHY, G. M., GODFREY, E. H.: (1966) Nemaline myopathy. The origin of nemaline structures. *New Engl. J. Med.*, **274**, 535—539. — 23. GRABOW, J. D., CHOU, S. M.: (1969) Thyrotropin hormone deficiency with a peripheral neuropathy. *Arch. Neurol.*, **19**, 284—291. — 24. HOWES, E. L., PRICE, H. M., PEARSON, C. M., BLUMBERG, J. M.: (1966) Hypokalemic periodic paralysis, electronmicroscopic changes in the sarcoplasm. (Minneap.), **16**, 242—249. — 25. JENIS, E. H., LINDQUIST, R. R., LISTER, R. C.: (1969) New congenital myopathy with crystalline intranuclear inclusions. *Arch. Neurol.*, **20**, 281—292. — 26. KLINKERFUSS, G. H.: (1967) An electronmicroscopic study of myotonic dystrophy. *Arch. Neurol.*, **16**, 181—190. — 27. KOEPPEN, A. H., BISHOP, M. B., KONDAURIS, S.: (1976) Polymyositis in Kaposi's syndrome. *J. neurol. Sci.*, **27**, 123—126. — 28. MACDONALD, R. D., REWCASTLE, N. B., HUMPHREY, J. G.: (1968) The myopathy of hyperkalemic periodic paralysis. *Arch. Neurol.*, **19**, 274—282. — 29. MACDONALD, R. D., ENGEL, A. G.: (1969) The cytoplasmic body: another structural anomaly of the Z disc. *Acta neuropath. (Berl.)*, **14**, 99—104. — 30. MACDONALD, R. D., ENGEL, A. G.: (1970) Experimental chloroquine myopathy. *J. Neuropath. exp. Neurol.*, **24**, 479—499. — 31. MACDONALD, R. D., REWCASTLE, N. B., HUMPHREY, J. C.: (1969) Myopathy of hypokalemic periodic paralysis. *Arch. Neurol.*, **20**, 565. — 32. MASTAGLIA, F. L., WALTON, J. N.: (1971) An ultrastructural study of skeletal muscle in polymyositis. *J. neurol. Sci.*, **12**, 473—481. — 33. MUKUNO, K.: (1969) Electron microscopic studies on human extraocular muscles under pathologic conditions. I. Rod formation in normal and diseased muscles (polymyositis and ocular myasthenia). *Jap. J. Ophthalm.*, **13**, 35—40. — 34. NAKASHIMA, N., TAMURA, Z., OKAMOTO, S., GOTO, H.: (1970) Inclusion bodies in human neuromuscular disorders. *Arch. Neurol.*, **22**, 270—280. — 35. PEPE, F. A.: (1966) Some aspects of the structural organisation of the myofibril as revealed by antibody-staining methods. *J. Cell Biol.*, **28**, 505—525. — 36. PRICE, H. M., GORDON, G. B., PEARSON, C. M., MUNSAT, T. L., BLUMBERG, J. M.: (1965) New evidence for excessive accumulation of

Z-ban material in nemaline myopathy. *Proc. nat. Acad. Sci. (Wash.)*, **54**, 1398–1406. — 37. RADNÓT, M.: (1973) Degenerative Veränderungen in der Feinstruktur des M. orbicularis oculi. *Klin. Mbl. Augenheilk.*, **162**, 493–498. — 38. RADNÓT, M.: (1974) A m. orbicularis oculi ultrastrukturája hibás szemhéjállás eseteiben. *Szemészet* **111**, 81–88. — 39. RADNÓT, M., FOLLMAN, P.: (1974) Ultrastructural changes in senile atrophy of the orbicularis oculi muscle. *Amer. J. Ophthalm.*, **78**, 689–699. — 40. RADNÓT, M., VARGA, M.: (1974) Az egyenes szemizmok ultrastrukturája. *Szemészet* **111**, 241–249. — 41. SALTER, R. H., ADAMSON, D. G., PEARCE, G. W.: (1967) McArdle's syndrome (myophosphorylase deficiency). A study of a family. *Quart. J. Med.*, **36**, 565–570. — 42. SANTA, T.: (1969) Fine structure of the human skeletal muscle in myopathy. *Arch. Neurol.*, **20**, 488–496. — 43. SATO, T., WALKER, D. L., PETERS, H. A., REESE, H. H., CHOU, S. M.: (1971) Chronic polymyositis and myxovirus-like inclusions. Electron microscopic and viral studies. *Arch. Neurol.*, **24**, 409–418. — 44. SCHOTLAND, D. L.: (1969) An electron microscopic study of target fibers, target-like fibers and related abnormalities in human muscle. *J. Neuropath. exp. Neurol.*, **28**, 214–225. — 45. SCHOTLAND, D. L.: (1970) An electron microscopic investigation of myotonic dystrophy. *J. Neuropath. exp. Neurol.*, **29**, 241–257. — 46. SCHRODER, J. M., ADAMS, R. D.: (1968) The ultrastructural morphology of the muscle fiber in myotonic dystrophy. *Acta neuropath. (Berl.)*, **10**, 218–225. — 47. SCHUTTA, H. S., ARMITAGE, J. L.: (1969) Thyrotoxic hypokalemic periodic paralysis. *J. Neuropath. exp. Neurol.*, **28**, 321–330. — 48. SHAFIQ, S. A., DUBOWITZ, V., PETERSON, H. de C., MILHORAT, A. T.: (1967) Nemaline myopathy: report of a fatal case, with histochemical and electron microscopic studies. *Brain*, **90**, 817–828. — 49. SHAFIQ, S. A., MILHORAT, A. T., GORYCKI, M. A.: (1967) An electronmicroscope study of muscle degeneration and vascular changes in polymyositis. *J. Path. Bact.*, **94**, 139–145. — 50. SHAFIQ, S. A., MILHORAT, A. T., GORYCKI, M. A.: (1967) Fine structure of human muscle in neurogenic atrophy. *Neurology (Minneap.)*, **17**, 934–942. — 51. SHAFIQ, S. A., GORYCKI, M. A., ASIEDU, S. A., MILHORAT, A. T.: (1969) Tenotomy; effect on the fine structure of the soleus of the rat. *Arch. Neurol.*, **20**, 625–633. — 52. SRETER, F. A., ASTRÖM, K. E., ROMANUL, F. C. A., YOUNG, R. R., JONES, H. R.: (1976) Characteristics of myosin in nemaline myopathy. *J. neurol. Sci.*, **27**, 98–116. — 53. STROMER, M. H., HARTSHORNE, D. J., MUELLER, H., RICE, R. V.: (1969) The effect of various protein fractions on Z and M line reconstruction. *J. Cell Biol.*, **40**, 167–168. — 54. SUGITA, H., MASAKI, T., EBASHI, S., PEARSON, C. M.: (1971) Protein composition of rods in nemaline myopathy. I.C.S. No. 237. *Excerpta Medica, Amsterdam (Abstract)*. — 55. YUNIS, E. J., SAMAHA, F. J.: (1971) Inclusion body myositis. *Lab. Invest.*, **25**, 240–250.

VERÄNDERUNGEN DER MUSKELFASERN BEI FALSCHER AUGENLIDSTELLUNG

J. FEHÉR

Der Musculus orbicularis oculi wurde bei 55 Patienten, die wegen Entropium oder Ectropium senile operiert wurden, elektronenoptisch untersucht. Sowohl beim senilen Entropium als auch beim senilen Ectropium wurden charakteristische ultrastrukturelle Veränderungen festgestellt, wie Auflösung der Muskelfasern, Verbreiterung der Z-Linie, Stäbchenbildung, Z-Linienverdopplung und Bildung von Zytoplasmakörperchen. Diese Veränderungen wurden früher nur im Zusammenhang mit verschiedenen neuromuskulären Erkrankungen und anderen, auf die Skelettmuskulatur übergreifenden Systemerkrankungen beschrieben. Die Ergebnisse bestätigen die Ansichten, nach denen die erwähnten ultrastrukturellen Veränderungen nicht als eine für bestimmte Krankheiten spezifische Veränderung anzusehen sind, vielmehr die ultrastrukturellen Grundlagen der geschädigten Muskeltätigkeit darstellen, unabhängig von der Ätiologie der Krankheit.

ИЗМЕНЕНИЯ МЫШЕЧНЫХ ВОЛОКОН ПРИ НЕПРАВИЛЬНОМ ПОЛОЖЕНИИ ВЕК

Й. ФЕХЕР

В электронном микроскопе была исследована круговая мышца глаза у 55 больных, оперированных по поводу старческого выворота или заворота век. При обоих патологических процессах в мышечных волокнах были обнаружены характерные изменения, в том

числе растворение мышечного волокна, расширение линии Z, образование полочек, удвоение линии Z и образование цитоплазматических телец. Раньше эти изменения были описаны только в связи с различными нейромускулярными заболеваниями и прочими системными заболеваниями, распространяющимися на скелетную мышцу. Результаты исследований подкрепляют взгляды, согласно которым упомянутые ультраструктурные изменения не являются специфическими для определенного заболевания, а представляют собой ультраструктурные основы нарушенной мышечной функции, независимо от этиологии заболевания.

Dr. János FEHÉR: Semmelweis Orvostudományi Egyetem I. sz. Szemklinika
H-1083 Budapest, Tömő u. 25—29, Hungary

Second Institute of Anatomy, Histology and Embryology,
Semmelweis University, Medical School, Budapest

INFLUENCE OF THE INTESTINAL EPITHELIUM TO THE PLASMA CELL DIFFERENTIATION INJECTED INTO THE THYMUS

I. TÖRŐ

(Received April 26, 1977)

Physiological saline solution of enzyme-isolated small intestinal epithelium of rat embryos was injected into the thymus of adult rats, thus increasing the number of epithelial cells in the parenchyma. The effect on the cellular composition of the thymus parenchyma was studied with special regard to plasma cells. Considering the functional importance of epithelial elements in the lymphoepithelial organs, the intervention rendered the thymus similar to the lymphoid organs of the intestinal tract. Plasma cells failed to appear in the thymus, but their number in the lymph nodes surrounding the thymus was considerably increased. It is supposed that under normal circumstances the thymus contains an inhibitory factor, which would make it possible to induce plasma cell transformation, but would inhibit maturation during the presence of the cells in the thymus.

Studies on the cellular composition of the thymus reveal certain contradictions as under normal circumstances they failed to demonstrate plasma cells. This is in agreement with the finding that no antibodies are produced in the thymus and on this basis point to a functional difference between thymus and lymph nodes. The difference is farther supported by the differences in structure, since the thymus, though by its composition a lymphoid organ is still of epithelial origin differing from lymph nodes by its lobulation, the expressed variability of its cellular elements and chiefly by its entodermal basement reticulum. These structural differences by themselves explain that the function of the thymus is characteristically different from that of other lymphoid organs and it is this structural difference which might explain the absence of plasma cells. This seems to allow the assumption that the presence of epithelial cell is connected with the absence of plasma cells. Thus, since the plasma cells are endproducts of the maturation process of lymphocytes, it may be supposed that something necessary for lymphocyte maturation is missing or something inhibiting the maturation process is present, in the thymus. Whichever of these factors may be responsible for the absence of plasma cells, the factor would be possibly controlled by the characteristic basement reticulum. The question arose, what would happen if the number of the basement reticulum cells would increase or that the normal ration of lymphoid and epithelial cells would be shifted in favour of the epithelial cells.

The epithelial cells of the thymus are entodermal in origin and all the thymo-lymphatic organs are connected with the entodermal epithelium cells,

thus in the tonsils, Peyer's plaques or in the bursae of the birds. The intestinal epithelium, similar to the epithelial elements of the thymus, are in close structural and functional connection with the lymphoid cellular elements. Therefore, intestinal epithelial cells of the rat embryo were injected into the thymus, thus increasing there the number of epithelial elements. Then their effect on the cellular composition of the thymus has been studied, chiefly in respect of plasma cell maturation. This observation seemed to promise results all the more, since, except the thymus, all lymphoepithelial organs contain a considerable number of plasma cells.

Materials and methods

From the intestines of rat embryos removed between the 16th and 20th days of pregnancy, intestinal epithelial cell suspensions were prepared, following digestion of the intestine in 1% trypsin solution at 38°C for 90 minutes, then after repeated shaking and washing in physiological saline, the epithelial elements were separated by layer centrifugation for 2×10 minutes. The layer above the sediment contained the majority of intestinal epithelial cells, partly adhering to each other, partly isolated. The layer was pipetted and suspended in physiological saline. The suspension thus obtained was injected into the jugular fossa of rats of 100 to 200 g body weight, at identical depth into the thymus. Identical depths were ensured by a narrow metal collar welded at 5 mm from the point of the injection canule. The thymus of the rats thus treated was removed at different time intervals, after glutaraldehyde and osmium fixation and embedding into Durcupan, semithin as well as ultra thin sections were prepared and examined by the electron microscope.

In some cases the thymus adhered to the pleura or displayed a tumour-like enlargement (Fig. 1); the latter was conspicuous by a considerable protrusion of the thorax. In these

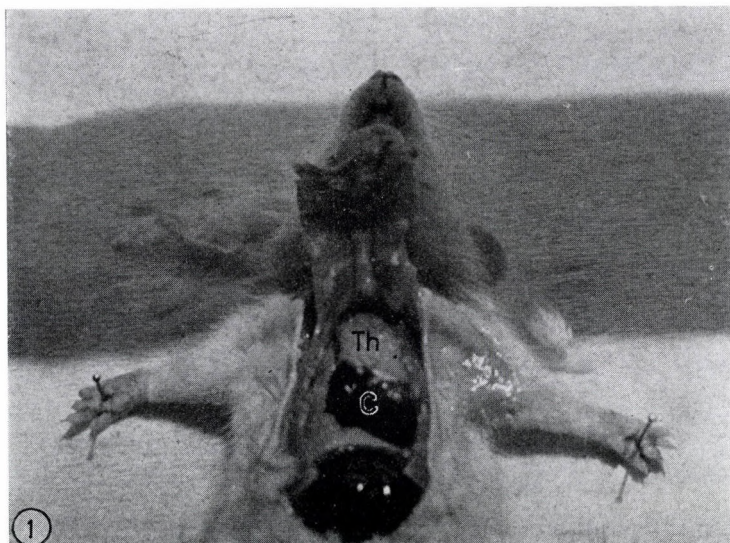


Fig. 1. Open thorax of white rat of 120 g, 20 days before an autopsy, suspension of the small intestinal epithelium of a 19 days rat embryo was injected into the thymus. The picture demonstrates a considerable increase in the size of the thymus, with nodules on its surface.

Th = Thymus, C = heart

cases the enlargement was induced by cavities containing a mucous milky fluid in the interior of the thymus. The neighbouring lymph nodes often showed enlargement or discoloration and the otherwise smooth thymus surface was uneven and nodular.

Examinations

The intestinal epithelial cells injected into the thymus parenchyma continued to lie in a satisfactory state (Fig. 2), and several goblet cells containing granules (Fig. 3) could be found among them. The mucus containing cavities were the products of secretory intestinal epithelium. Some intestinal epithelial cells displayed microvilli on their surface towards the mucus-filled cavities (Fig. 4). The intestinal epithelial cells were mostly found in groups, forming smaller or larger cavities. In the luminal part of the epithelial cells the number of mitochondria of roughly equal size was increased (Fig. 5). In their environment, the cellular substance of the parenchyma was loosened, wide intercellular gaps, containing electron-dense material (Fig. 6) were observed. This material was probably secreted of the epithelial cells. In the intercellular spaces some intercellular bridges were observed, allowing the union of cytoplasm and by this way the exchange of cellular components (Fig. 7). In the wide intercellular gaps the cells could move freely and form variable shapes with processes. Among the lymphoid elements, apart from small thymocytes, numerous lymphoblasts and mitotic forms were observed (Fig. 8), showing both possibilities of transformation, i.e. blast formation and macrophage transformation. Their nuclei displayed blebs and cytoplasmic tunnels. The transitory cells had a rich structure; they contained lysosomes, dense bodies and numerous vacuoles. The epithelial cells of the basement reticulum were arranged in groups, with interdigitating complicated cytoplasmic processes, intertwined with those of the macrophages. Endocytosis of the macrophages demonstrated intact thymocytes and cells in various stages of digestion, thus indicating their destruction. The emperipolesis of the epithelial cells was somewhat increased, pointing to and increased activity of the thymus. The cells termed by us specific epithelial cells could clearly be observed, in contrast with some data in literature, we consider them to represent transformed epithelial cells. With their complicated light, gyrificated cytoplasmic lobules they surrounded closely a great number of thymocytes: structurally the picture indicates a close functional cooperation of the two types of cell. Despite the complex cellular picture, no plasma cells could be observed.

Since the phenomenon has been explained by assuming a blood-thymus barrier that would inhibit antigens to enter into the parenchyma, it was interesting to observe the conspicuous capillary walls (Figs 9–10) and the passage of lymphoid cells across them. The behaviour of endothelial cells was also conspicuous as these demonstrated considerable thickenings, a marked structure of the cytoplasm processes penetrating deep into the lumen and connected with pinocytosis indicated by vacuoles in the cytoplasm. The wide pericapillary spaces contained a granular substance (Fig. 10) and were covered by distended epithelial cells. This looked like a real barrier, all the more since frequently the epithelial cells formed several layers surrounding the vessel.

At other sites collagenous fibre bundles too participated in forming the barrier, seeming to isolate the blood stream from the parenchyma. In spite of this, a penetration of lymphoid cells into the vascular wall was quite frequent. Originally, the lymphoid cells is lying beside the vascular wall and although it cannot be decided whether the cell then moves into or out of the lumen, the structural picture seems to support the former possibility.

The paratracheal lymph nodes near the thymus have also been studied (Figs 11, 12); they contained a large number of plasma cells. There were regions, where almost all the cells mature or maturing plasma cells.



Fig. 2. A suspension of small intestinal epithelium of a 18 days rat embryo was injected into the thymus of a white rat of 60 g. The animal was killed 17 days later. The epithelial cells are in a good condition, cuticle, microvilli are absent. Wide intercellular spaces in the epithelium. IE = Intestinal epithelium; M = $\times 3900$

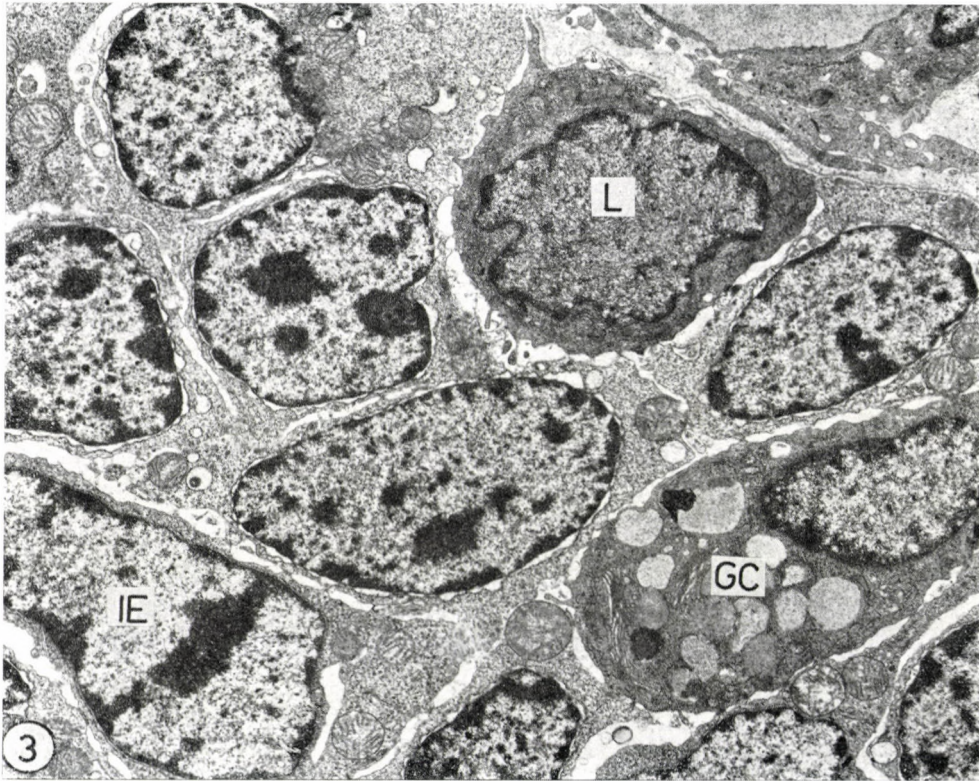


Fig. 3. White rat of Fig. 2. GC = Goblet cell; L = lymphocyte; IE = intestinal epithelium; M = $\times 3900$

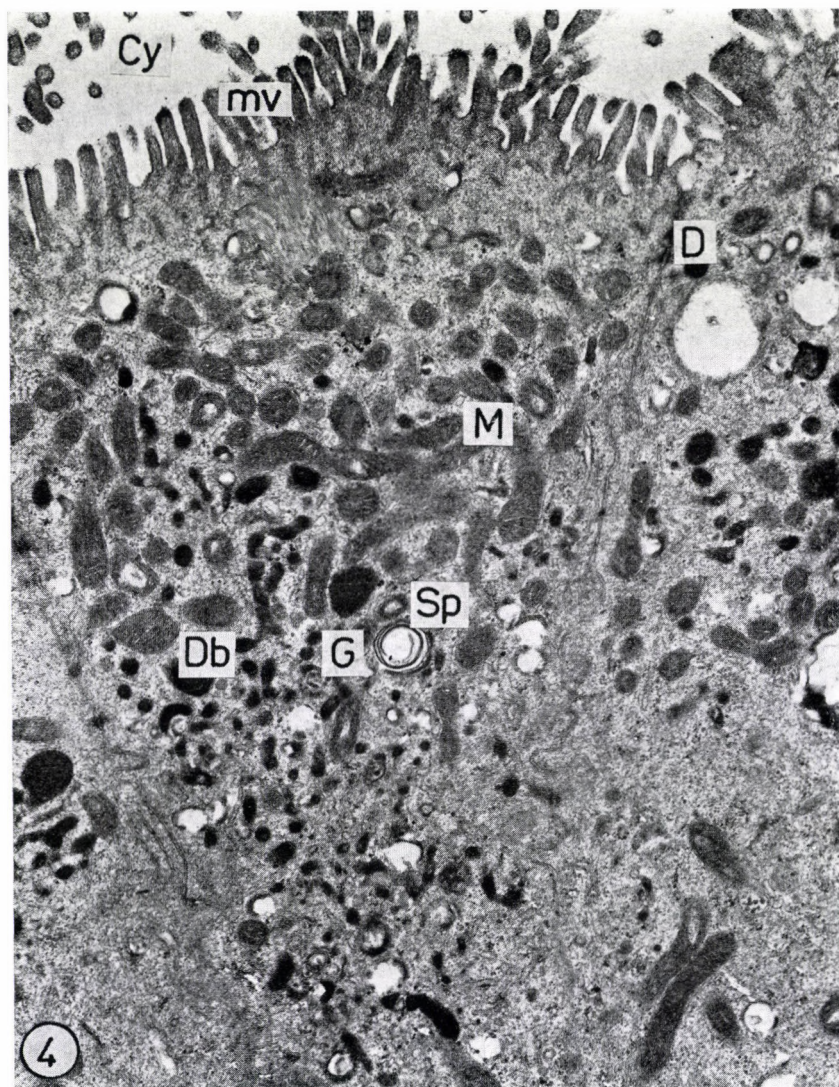


Fig. 4. Small intestinal epithelial cells of a 18 days rat embryo were injected into the thymus of an adult rat. mv: Microvilli; Cy = cyst lumen; M = mitochondrion; D = desmosome; Sp = specific vacuole; Db = dense body; G = granules; M = $\times 2400$

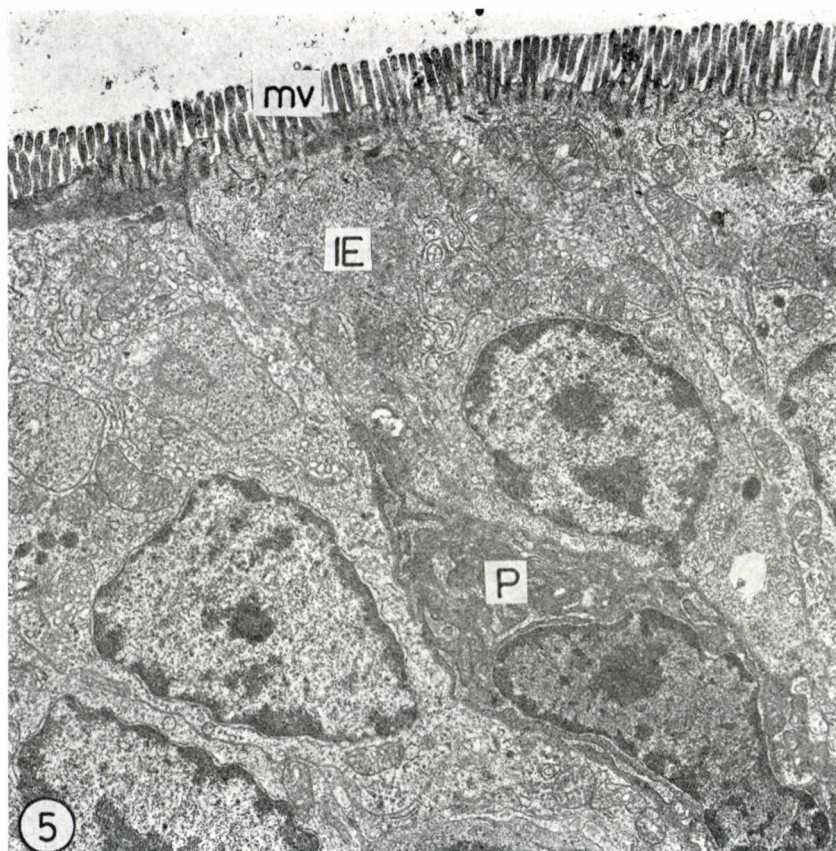


Fig. 5. Small intestinal epithelial cells of a 18 days rat embryo were injected into the thymus of a white rat of 55 g. 19 days later the cyst in the thymus is lined with epithelial cells possessing microvilli. mv = Microvilli; IE = intestinal epithelium; P = plasma cell; M = $\times 4300$

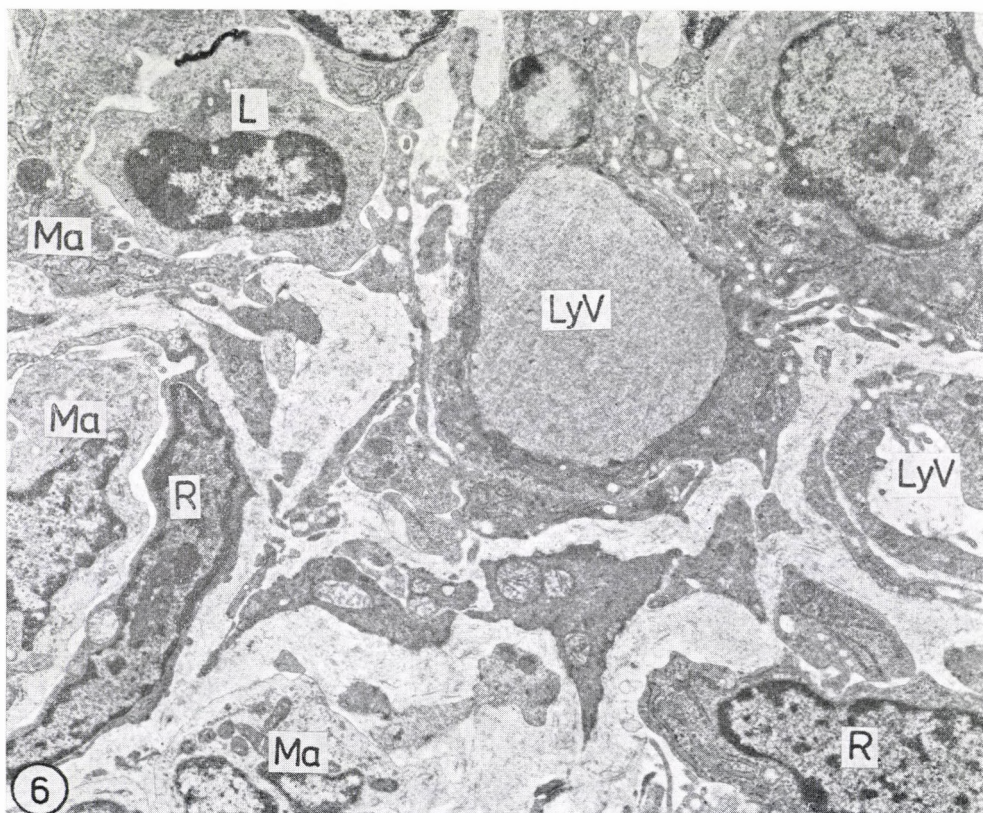


Fig. 6. Loosened parenchyma of thymus of adult rat, with the injected small intestinal epithelial cells of a rat embryo. Widened intercellular spaces containing electron-dense substance. LyV = lymph vessel; Ma = macrophage; L = lymphoid cell; R = reticulum cell; M = 13,700

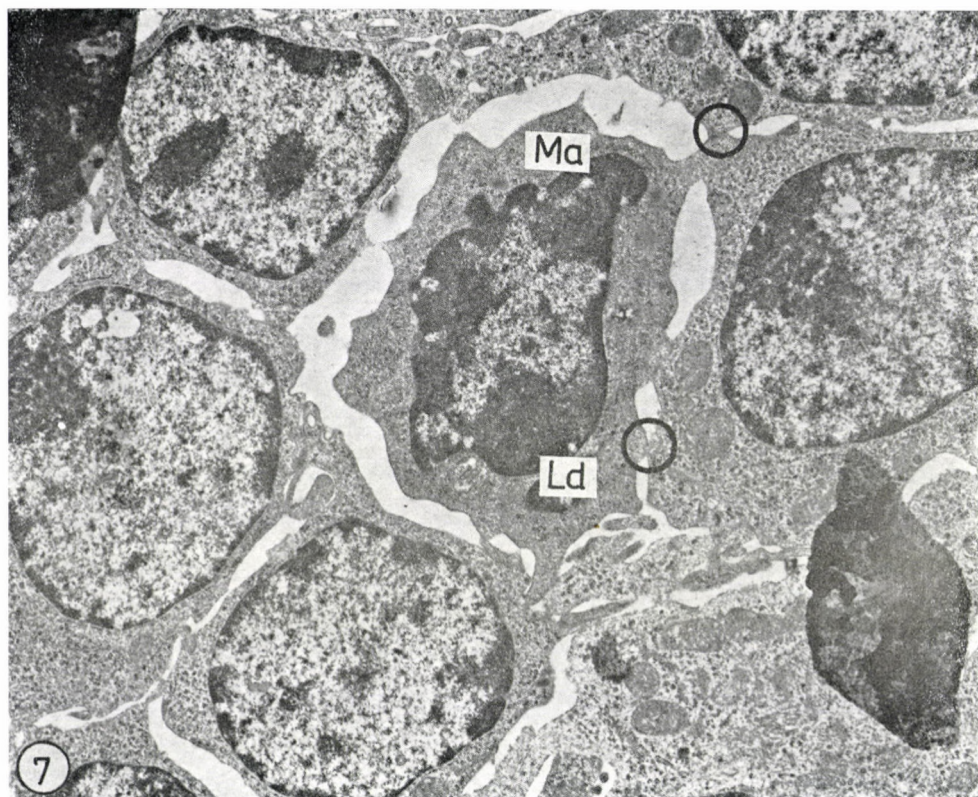


Fig. 7. Thymus of a white rat of 160 g body weight, 15 days after injection of a suspension of small intestinal epithelium of rat embryo. The thymus is increased on size and contains a cyst filled with mucous substance. Intracellular cytoplasmic bridges between lymphoblasts and macrophages. Ma = Macrophage; Ld = lymphocytic debris; ○ = plasma bridge; M = $\times 14,000$

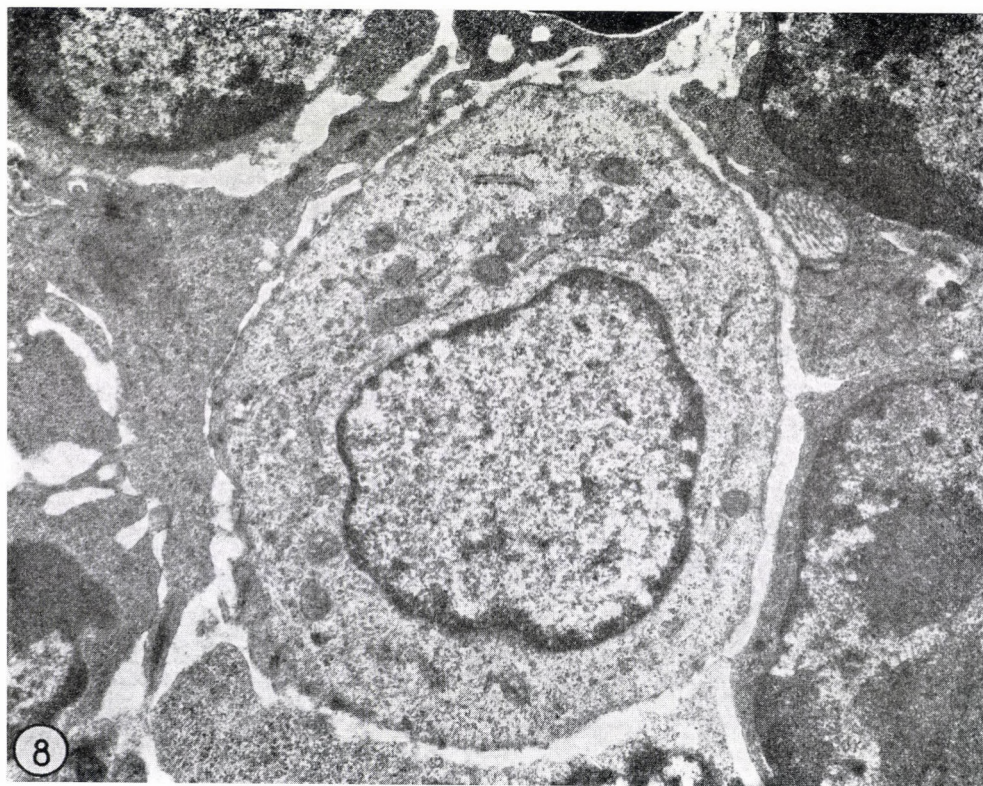
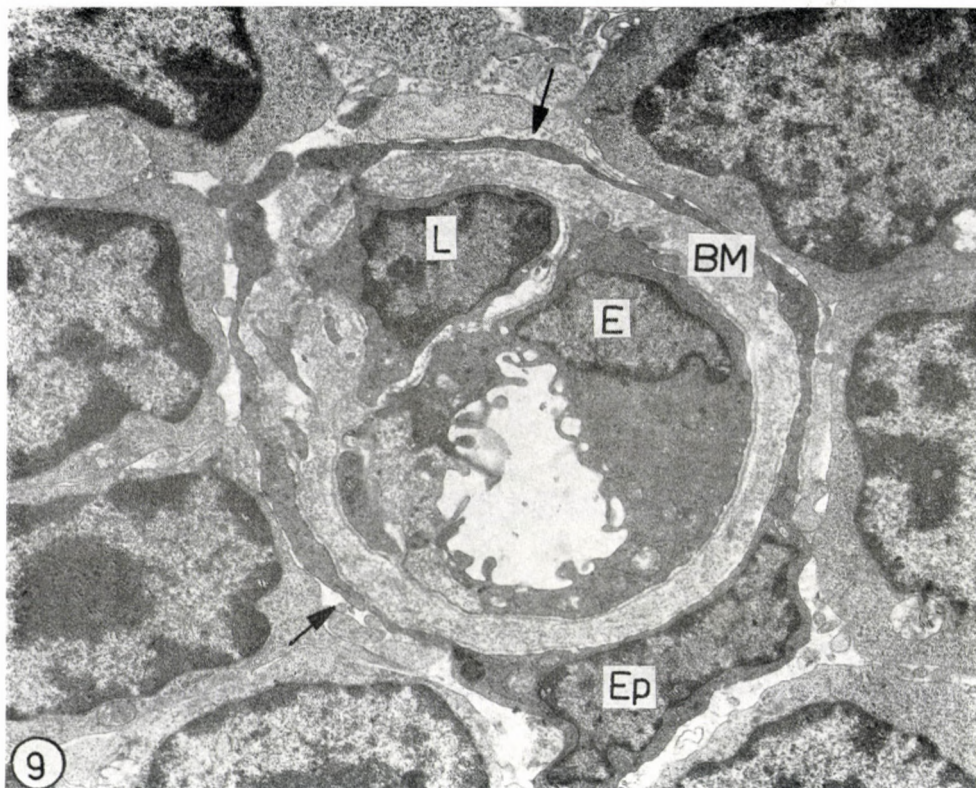


Fig. 8. Small intestinal epithelium of 19 days rat embryo, injected into thymus of rat of 180 g weight. Transformation cell in the thymus



Figs 9–10. Thymus of adult rat injected with a suspension of small intestinal epithelium of 18 days rat embryo, 4 days later lymphoid cell penetration across the wall of a capillary. E = Endothelium; Ep = epithelial barrier; Lu = lumen; L = lymphocyte; BM = basal membrane

Figure 9: $M = \times 13,700$; Figure 10: $M = \times 15,800$

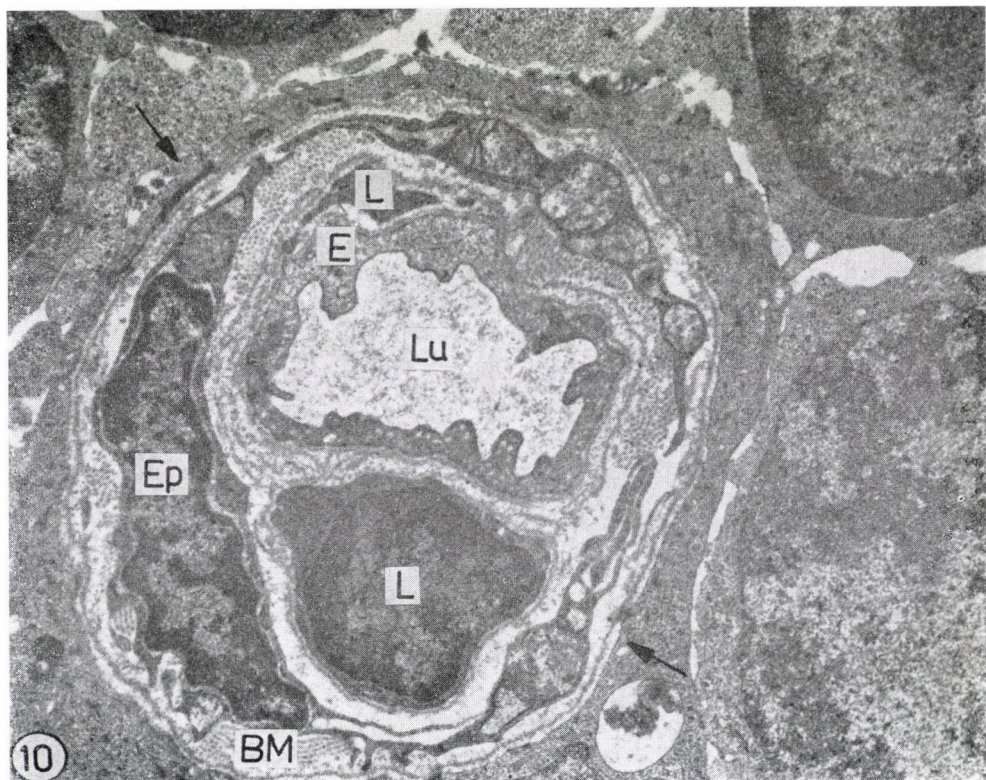


Fig. 10

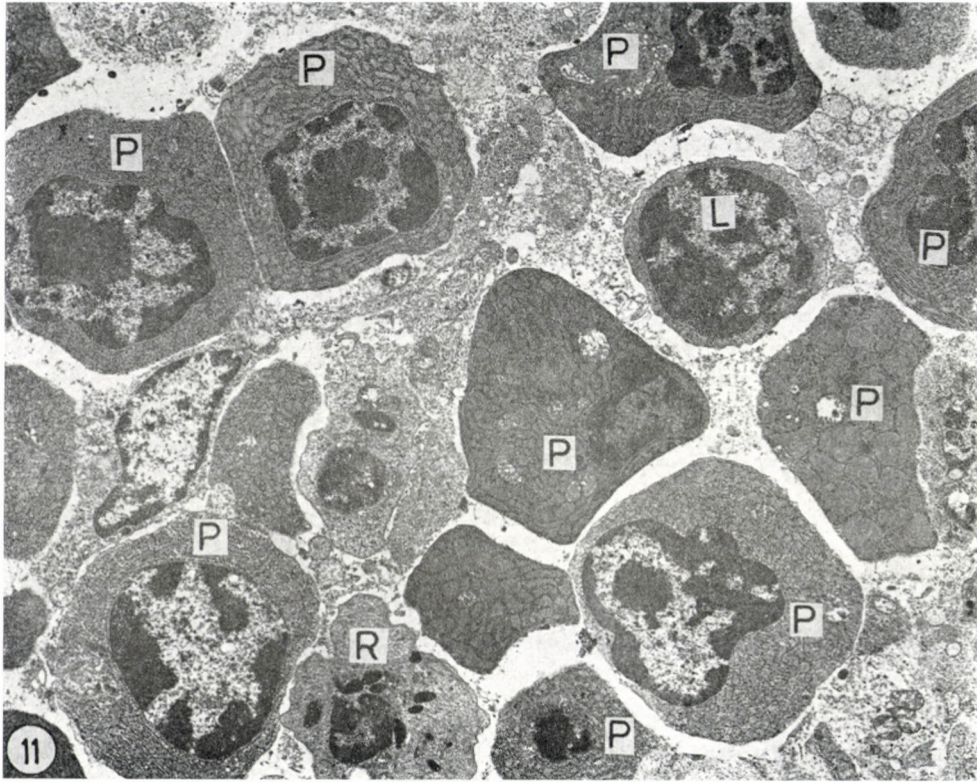


Fig. 11. Parathymic lymph node of a rat of 120 g, 6 weeks after injection into the thymus of embryonic small intestinal epithelium. The lymph node is filled with plasma cells. P = Plasma cell; L = lymphocyte; M = $\times 4200$

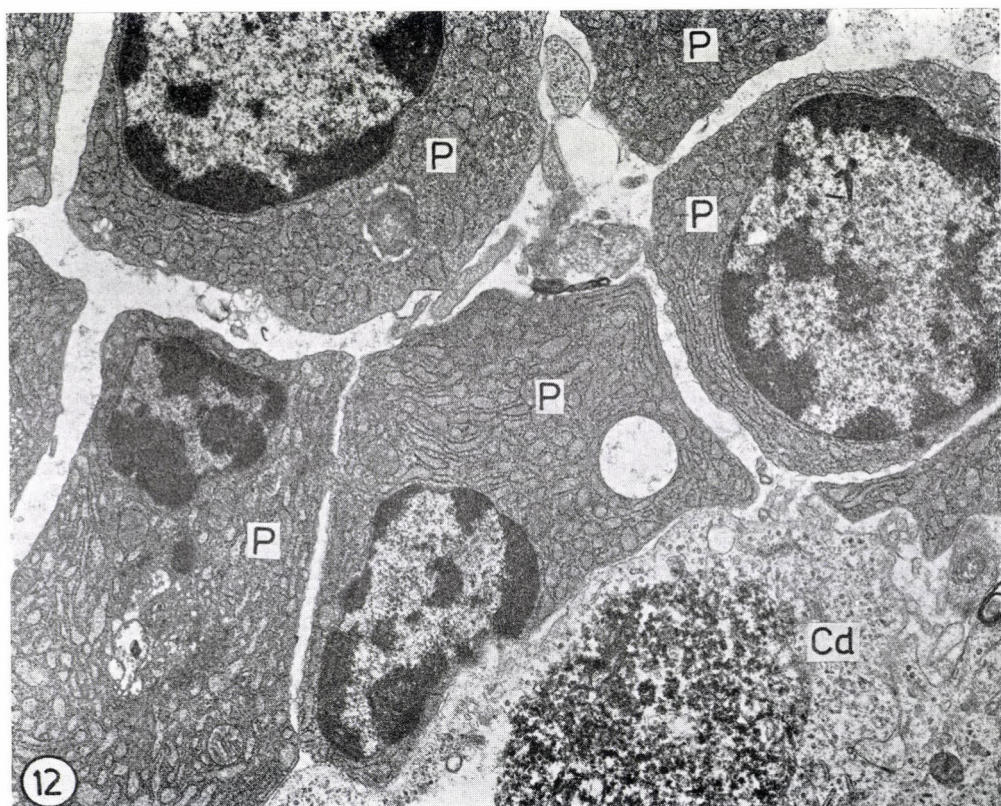


Fig. 12. Perithymic lymph node of a rat of 120 g, filled with plasma cells. 30 days after injection into the thymus of embryonic intestinal epithelium. L = Lymphocyte; P = plasma cell; Cd = cell degeneration; M = $\times 13,700$

Discussion

All lymphoepithelial organs originate from the entoderm. The epithelium of entodermal origin has a characteristic affinity to lymphoid cells, from which the antibody-producing plasma cells differentiate. This is explained by the fact that the intestinal epithelium is in constant and close contact with the intestinal contents containing antigens and toxic elements. Thus, these organs contain a large number of plasma cells and so do the intestinal lymphoreticular organs and the milk-spots [5]. In the rabbit appendix, plasma cells appear much earlier than at other sites [32]. In the oral mucosa e.g. in the subepithelial connective tissue of the human gingiva, plasma cell aggregates occur regularly [25].

Everywhere, where there are numerous plasma cells, there are many lymphocytes. This is due to the fact that the plasma cells are transformed small lymphocytes. Under the effect of antigens and mitogens this transformation occurs both *in vitro* and *in vivo*. MÖNNINGHOF et al. examined the light and electron microscopic changes of the thymus in young rats and followed the plasma cell transformation after intravenous application of anti-lymphocyte serum. In the epithelium of the palatine tonsil numerous immature, but sometimes even mature plasma cells were found [33]. The study of the axolotl intestine offers a good opportunity to examine the connection between intestinal entoderm and plasma cells [39]; both in the connective tissue and the intestinal epithelium a high number of plasma cells were found. No such active penetration of plasma cells into the crypt could be observed, which was similar as the penetration of lymphocytes. Numerous lymphocytes were seen in the stage of plasma cell differentiation. The cytoplasm of the small lymphocytes increases, the nucleus is shifted towards the capillary, the nuclear chromatin reaches its characteristic marginal and central position, meanwhile the relation of plasma cells to epithelial cells is getting more close. WARREN even observed cytoplasmic bridges between the two cell types. According to FICHTELIUS, the lymphoid cells produce immunoglobulin on contact with the intestinal epithelium. OWEN demonstrated in the Peyer plaques of the axolotl intestine a so-called microfold cell (M cell) which contained chiefly plasma cells in the network of its processes. According to this author in the reticulum formed by the M cells the antigens of the intestinal lumen reach the lymphoid cells by way of the M cells. The M cells may connect IgA to the secretion and release the immunoglobulin complex into the lumen. Characteristic cells with a function similar as that of M cells may be found in the other lymphoepithelial organs too, e.g. the specific cells of the thymus [24/a], the covering cells of the tonsils or the epithelial cells covering the bursa. The importance of the contact with the intestinal lumen is clearly demonstrated by bursa grafts implanted into the peritoneum of the chick embryo: the bursa will lose its lymphoid character on the day of hatching [3]. Also the appendix of the rabbit is ligated

after birth, it will lose its lymphoid character; this will, however, return on restoring the communication with the intestinal lumen. The microenvironment for the differentiation of plasma cells is created by the epithelium. Since the thymus in the course of evolution has lost its contact with the intestinal lumen, its difference from the other lymphoepithelial organs may easily be understood despite the structural similarity. Is the absence of mature plasma cells [1, 11, 16, 26, 29, 38] explained by the absence of precursor cells, which at the periphery are responsible for the differentiation of plasma cells? The plasma cells are responsible for antibody production [28], and each mature plasma cell produces only one kind of immunoglobulin. In experiments carried out with labelled antibodies, the antibodies are selectively bound to the plasma cells, which array on their surface the immunoglobulin. When labelled basophilic lymphoid cells stimulated with antigen are injected into lymph nodes, their cells will be transformed into plasma cells [6]. In the lymph nodes, there are many plasma cells and many transitory forms between lymphocytes and plasma cells [2, 24]. If the lymphocytes of immunized mice are transferred into irradiated mice incapable of producing antibodies, they regain their antibody-producing capacity. Immunofluorescence studies demonstrated that lymphocytes injected under the skin were transformed into plasma cells without mitotic activity [4]. Thus, the lymphocytes are plasma cell precursors [7, 9, 41]. Electron microscopic autoradiography revealed that on antigenic stimulation some lymphoid cells will take up thymidine; the cells contain many RNP granules and small Golgi apparatus and will be transformed into plasma cells [6]. On the basis of immunofluorescent and autoradiographic examinations antibody production is attributed to the plasma cells [13]. The plasmoblast, being a younger cell form, has a large nucleus with a markedly pyroninophilic cytoplasm, where increased RNA synthesis occurs. In the plasmoblast or immunoblast, many free ribosomes are found, with little rough endoplasmic reticulum, which then increases in amount in the course of maturation. The Golgi apparatus is less developed. It has been stated that antibody production starts in the ergastoplasm of the perinuclear space, pointing also to the role of the nucleus. In the mature plasma cells, in the cisterns of the endoplasmic reticulum, large nodules may be observed. The plasma cells contain less receptors than the other cells, since many receptors are lost during differentiation, but they are the most active in antibody synthesis as well as in secretion of antibodies into the circulation. In New Zealand Black (NZB) mice, plasma cell proliferation is regulated by the thymus [12]. According to MILLER, there exists a thymus-dependent lymphocyte population responsible for plasma cell production, able to produce also immunoglobulin and antibodies. The B lymphocytes are transformed into plasma cells, which secrete 2000 identical antibody molecules every second. This cell has a short life span; it is destroyed in a few days [40].

In cells isolated from lymph nodes of immunized rabbits and labelled with tritiated leucine, the site of protein formation was observed by WEISS by means of autoradiography. He intended to find the site of antibody formation during the 30 minutes between formation and secretion in the plasma cell. It was found that during the latent period of secretion, the antibody travels into the Golgi complex and from there to site of synthesis, the ergastoplasm [10, 21].

Thus, among the lymph-epithelial organs the thymus alone has no contact with the intestinal lumen and contains no plasma cells. According to METCALF the thymus exerts its influence upon the immune response by speeding up by antigenic stimulation the proliferation of plasma cell precursors. When spleen and thymus pieces are transplanted into mice, within one month a well-developed mosaic tissue is formed from the mixed graft. The growth of spleen and thymus beside each other was satisfactory, but even in this case plasma cells failed to appear in the thymus tissue, whereas they were present in the spleen. The thymus differs from the other tissues also by epithelial basement reticulum. Thus, it seemed interesting to investigate the causal relation of the two different factors and it seemed indicated to shift the tissular equilibrium of the thymus towards the epithelial elements, in order to observe the effect on the other factor responsible for the difference. No plasma cells appeared in the thymus but an abnormally high number of chiefly mature plasma cells was found in those lymph nodes, through which the lymph circulates on its way from the thymus. Thus, it seemed justified to suppose that the stimulation of plasma cell formation had occurred in the thymus, but since the tissue environment in the latter inhibited plasma cell differentiation, this had to occur outside the thymus, in the lymph nodes. Thus, the occurrence in the thymus of a factor has to be supposed, which would potentiate plasma cell formation, but simultaneously an inhibitory factor too, might be present, perhaps identical to the former, which inhibits the process of plasma cell differentiation; this factor might be bound to the entodermal epithelial elements. As long as the thymus is active, the inhibitory factor will exert its influence. For plasma cell differentiation in the thymus, thymic function and production of the inhibitory factor must cease. The easiest way to achieve this by removing the thymus. WAKSMAN et al. found increased numbers of plasma cells subsequent to thymectomy. Following X-ray irradiation, which decreases thymic function, the number of plasma cells in the thymus will be increased, just as under the effect of cortisone which too decreases the function of the thymus. Freund adjuvant will induce the accumulation of plasma cells in the thymus [15, 31]; in this case the thymus displays degenerative phenomena: tubuli, cysts appear, just as in massive involution. Similarly, the number of plasma cells increases with age, parallel to the physiological involutions of the thymus. In the thymus of a two years old boy suffer-

ing from myasthenia gravis many plasma cells were found [34]. NAHMAS supposed the dissociation of the origin of lymphocytes and plasma cells, since in an athymic female infant in the presence of normal serum globulin no lymphocytes were found, neither in the lymph nodes nor in the spleen or the intestines, but plasma cells were present. JANKOVIC et al. observed that following calf serum antigen injection the number of small lymphocytes decreased, that of pyroninophilic cells increased in the thymus. This too indicated that the cells of the thymus have a capacity to differentiate locally into plasma cells under the effect of direct antigen. In athymic NZB mice or other thymectomized mouse strains an intense proliferation of plasma cells was seen [12]. When three weeks old rats were thymectomized, 16 days later lymphocytopenia, leukopenia and plasmocytosis appeared. After 31–32 days the plasma cell concentration in peripheral blood might reach 10 per cent. This seems to indicate that plasmoblasts are formed at a different site, but also to the inhibition of formation in the thymus under normal conditions. MILLER et al. reported on an increase in the number of myeloid elements following thymectomy, indicating thus the suppression of myeloid element formation or the inhibition of their maturation by the thymus. AZAR found in rats no change in the plasma cell count after thymectomy. SVET observed in thymectomized mice hyperplastic paratracheal lymph nodes with plasma cells. MARSHALL and WHITE injected antigen into the thymus and observed the appearance of plasma cells. Similar observations were made in C3H mice after prolonged administration of Salmonella antigen or bovine serum albumin. According to METCALF, STUTMAN and LIBGALLE, when the host was stimulated with antigen, follicles and plasma cells were formed in the thymic graft, MILLER found no decrease in plasma cell count after neonatal thymectomy.

REFERENCES

1. AZAR, H. A.: (1963) Role of adult thymus in immunity and lymphopoiesis. *Arch. Path.*, **76**, 653–658. — 2. BLAZSEK, J., GYÉVAI, A., BALÁZS, A.: (1972) Electron microscopic study of spontaneous transformation of lymphocytes and monocytes in tissue culture. *Symp. biol. hung.* 14, on Ultrastructural Features of Cells and Tissues in Culture. Ed. Hung. Academy of Sciences. — 3. BOCKMAN, D. E., COOPER, D.: (1973) Pynocytosis by epithelium associated with lymphoid follicles in the bursa of Fabricius, appendix, and Peyer's patches. An electron microscopic study. *Amer. J. Anat.*, **136**, 455–478. — 4. BRAUNSTEINER, H., FELKNER, K., PAKESCH, F.: (1953) Demonstration of a cytoplasmic structure in plasma cells. *Blood*, **8**, 916. — 5. CARR, J.: (1967) The fine structure of the cells of the mouse peritoneum. *Z. Zellforsch.*, **80**, 534–555. — 6. CARR, J.: (1970) The fine structure of the mammalian lymphoreticular system. *Int. Rev. Cytol.*, **27**, 283–348. — 7. CATOVSKY, D., HOLT, P. J. L., GALTON, D. A. G.: (1972) Binucleated blastcells in lymphocyte cultures from myelomatosis. *Immunology*, **22**, 1103–1109. — 8. CLARK, S. L.: (1963) The thymus in mice of strain 129/Y studied with the electronmicroscope. *Amer. J. Anat.*, **112**, 1–33. — 9. CLARK, S. L.: (1963) Isolated environment of lymphoid tissues of the intestine. *Fed. Proc.*, **22**, 1339–1348. — 10. CLARK, S. L.: (1966) The synthesis and storage of protein by isolated lymphoid cells examined by autoradiography with the electron microscope. *Amer. J. Anat.*, **119**, 375–404. — 11. DIOMEDE-FRESA, V., FUMAROLA, D., PANTALEO, R.: (1964) Thymectomy and experimental plasmacytosis from DDT. *Med. exp. (Basel)*, **11**, 217–223. — 12. EAST, J., DeSousa, MARIA A. B.: (1965) The Thymus Autoimmunity and Malignancy in New Zealand Black Mice. *Proc. Conf.*

- Murine Leukemia, Philadelphia, Pa. Ed.: Harper and Row, N. Y. — 13. FAGRAENS, A.: (1948) Antibody production in relation to the development of plasma cells. *Acta med. scand.*, **130**, (Suppl. 204) 3. — 14. FICHTELIUS, K. E.: (1968) The gut epithelium, a first level lymphoid organ? *Exp. Cell Res.*, **104**, 49–87. — 15. ISAKOVIC, K., JANKOVIC, B. D.: (1967) Germinal Centers and Plasma Cells in the Thymus of the Chicken. In: *Proc. Symp. on Germinal Centers in Immune Response*. Bern 1966. Springer Verlag, Berlin–Heidelberg–New York, 379–382. — 16. JOFFEY, J. M., COORTICE, F. C.: (1956) *Lymphatics, Lymph and Lymphoid Tissue*, 2nd ed. Harvard Univ. Press, Cambridge, Mass. — 17. MARSHALL, A. H. E., WHITE, R. G.: (1961) The immunological reactivity of the thymus. *Brit. J. exp. Path.*, **42**, 379–385. — 18. METCALF, D.: (1958) The Thymic Lymphocytosis Stimulating Factor. *Ann. N. Y. Acad. Sci.*, **73**, 113–119. — 19. MILLER, J. F. A. D.: (1963) Origins of immunological competence. *Brit. med. Bull.*, **19**, 214. — 20. MILLER, J. F. A. P., DUKOR, P.: (1964) Die Biologie des Thymus. S. Karger Verlag, Basel and New York. — 21. MILLER, J. F. A. P., BLOCK, M., ROWLANDS, D. T., JR., P. KIND: (1965) Effect of Thymectomy in Hemopoietic Organs of the Opposum Embryo. *Proc. Soc. exp. Biol. (N. Y.)*, **118**, 916–921. — 22. MÖNNINGHOFF, W., THEMANN, H., WIRTH, W., WEIKERT, C., TAKEBAYASHI, S.: (1972) Die Feinstruktur des lymphatischen Gewebes der Ratte nach Behandlung mit antithymocytenserum. *Beitr. path. Anat.*, **145**, 51–67. — 23. NAHMIA, A. J., GRIFFITH, D., SALSBERY, C., YOSHIDA, K.: (1967) Thymic Aplasia With Lymphopenia, Plasma Cells and Normal Immunglobulins. *N. Amer. med. Ass.*, **201**, 729–734. — 24. NOSSAL, G. J. V.: (1959) Antibody production by single cells. III. The histology of antibody production. *Brit. J. exp. Path.*, **40**, 301–311. — 24/a. OLÁH, J., DUNAI, Cs., RÖCHLICH, P., TÖRÖ, I.: (1968) A special type of cells in the medulla of the rat thymus. *Acta biol. Acad. sci. hung.*, **19**, 97–113. — 25. OSOGOE, EL. B. M., SHIOTA, I.: (1958) Plasma Cells and Lymphocytes in the Healthy Human Gingiva. *Okajimas Folia anat. jap.*, **31**, (5–6) 401–405. — 26. OTANI, T.: (1957) Hematological studies of the lymph nodes and the thymus. *Hiroshima J. med. Sci.*, **6**, No. 1. 55–64. — 27. OWEN, R. L., JONES, A. L.: (1974) Epithelial cells specialization within human Peyer's patches. An ultrastructural study of intestinal lymphoid follicles. *Gastroenterology*, **66**, 189–203. — 28. SCHWENKE, H.: (1970) Die Lymphozytenkultur und ihre Anwendungsmöglichkeiten. *Z. inn. Med.*, **256** — 29. SHIER, K. J.: (1963) The morphology of the epithelial thymus observation on lymphocyte depleted and fetal thymus. *Lab. Invest.*, **12**, 316–326. — 30. STUTMAN, O.: (1975) The post-thymic precursor cell. *Biological Activity of Thymic Hormones*. Kooyher Scientific Publications, Rotterdam, 87–97. — 31. SVET-MOLDAVSKY, G. J., RAFFLON, L. J.: (1963) Thymus-lymphatic nodes interrelations following injection of Freund's adjuvant. *Nature (London)*, **197**, 52–53. — 32. THORBECKE, G. J., COHEN, M. W.: (1964) Immunological Competence and Responsiveness of the Thymus. In: *The Thymus*. Ed.: Defendi and D. Metcalf. The Wistar Institute, Philadelphia. — 33. TÖRÖ, I., OLÁH, I.: (1972) Elektronenmikroskopische Struktur und Antigenrezeption in der Gaumenmandel des Kaninchens. *Anat. Anz.*, **130**, 109–119. — 34. VAN DER VELDA, H.: (1969) The Fine Structure of the thymus in Congenital Myasthenia Gravis. *Abst. Fourth Meeting of the Northern and Southern California Societies for Electron Microscopy*. San Francisco. J. Ultrastruct. Res. — 35. VAN DER VELDE, H., OOSTERHUIS, H. J. G. H.: (1963) Muscle and thymus antibodies in myasthenia gravis. *Vox Sang.*, **8**, 196–204. — 36. VAN HAELST, U.: (1967) Light and electron microscopic study of the normal and pathological thymus of the rat. *Z. Zellforsch.*, **77**, 534–553. — 37. WAKSMAN, B. H., ARNASON, B. G., JANKOVIC, B. D.: (1962) Role of the Thymus in Immune Reactions in Rats. III. Changes in the lymphoid organs of thymectomized rats. *J. exp. Med.*, **116**, 187–206. — 38. WARNER, N. L.: (1967) The Immunological Role of the Avian Thymus and Bursa of Fabricius. *Fol. biol. (Praha)*, **13**, 1–17. — 39. WARREN, A.: (1975) Origin and Life History of Plasma Cells in the Intestinal Mucosa of the Axolotl, *Amblystoma Mexicanum*. *Proc. 10th int. Congr. Anatomy*, Tokyo, P. 380. — 40. WEISS, L.: (1972) *The Cells and Tissues of the Immune System, Structure, Function, Interaction*. Prentice Hall, Englewood Cliffs. — 41. WOODS, PH. A.: (1964) Local Labelin of thymocytes in the guinea-pig with tritiated thymidine. *Anat. Rec.*, **148**, 352.

DIE WIRKUNG DES EMBRYONALEN DARMEPITHEL AUF DIE DIFFERENZIERUNG DER PLASMAZELLEN

I. TÖRÖ

Die mit Enzym isolierte und aus physiologischer Kochsalzlösung hergestellte Suspension von Rattenembryonen wurde in den Thymus erwachsener Ratten injiziert und dadurch die Anzahl der Epithelzellen im Thymusparenchym erhöht. Die Wirkung dieses Eingriffs auf

die Veränderungen in der Zellzusammensetzung des Thymusparenchyms wurde — unter besonderer Berücksichtigung der Plasmazellen — elektronenoptisch untersucht. Im Hinblick auf die funktionelle Bedeutung der Epithelzellen in den lympho-epithelialen Organen wurden diese durch den Eingriff den lymphoiden Organen des Darmkanals ähnlich gemacht, wobei es sich herausstellte, daß die Plasmazellen im Thymus zwar nicht in Erscheinung traten, ihre Zahl jedoch in den Lymphdrüsen der Thymusumgebung erheblich zunahm. Es wird angenommen, daß unter normalen Verhältnissen im Thymus ein Hemmfaktor zugegen ist, der die Induktion der plasmazytären Transformation potentiell zuläßt, doch die Zellreifung solange hintanhält, bis die Zelle im Thymus verbleibt.

ДЕЙСТВИЕ ЭМБРИОНАЛЬНОГО КИШЕЧНОГО ЭПИТЕЛИЯ, ВВЕДЕННОГО
В ЗОБНУЮ ЖЕЛЕЗУ, НА ДИФФЕРЕНЦИАЦИЮ ПЛАЗМОЦИТОВ

И. ТЁРЁ

Взвесь зародиша крысы, изолированная энзимом и изготовленная из физиологического раствора поваренной соли, была введена в зобную железу взрослой крысы, вследствие чего в паренхиме зобной железы повысилось число эпителиальных клеток. При помощи электронной микроскопии было проведено исследование действия указанного вмешательства на изменения состава клеток в паренхиме зобной железы, с особым вниманием на плазмоциты. Принимая во внимание их функциональное значение в лимфо-эпителиальных органах эпителиальные элементы при помощи вышеизложенного вмешательства были сделаны подобными лимфоидным органам кишечного канала. Таким образом было установлено, что плазматические клетки не появляются в зобной железе, в то время как их число в значительной мере повышается в лимфатических узлах около зобной железы. Полагается, что в норме в зобной железе присутствует тормозящий фактор, потенциально возволяющий индукцию плазмоклеточной трансформации, но препятствующий созреванию клеток до тех пор, пока они остаются в зобной железе.

Dr. Imre TÖRÖ: Semmelweis Orvostudományi Egyetem
II. sz. Anatómiai, Szövet és Fejlődéstani Intézet
H-1094 Budapest, Tüzoltó u. 58., Hungary

First Institute of Pathology and First Institute of Biochemistry,
Semmelweis University Medical School, Budapest

CYTOPLASMIC AGGREGATES IN D-GALACTOSAMINE INDUCED LIVER INJURY

Anna TOMPA, K. LAPIS, Zsuzsa SCHAFF, K. MÉSZÁROS, J. MANDL,
T. GARZÓ and F. ANTONI

(Received August 15, 1977)

D-galactosamine treatment leads to the formation of PAS-positive granules or aggregates in the cytoplasm of mouse liver cells. Ultrastructural observations show that the granules consist of particles surrounded by membranes of rough endoplasmic reticulum. Cytochemical results reveal that part of the particles is pronase-sensitive and amylase resistant, staining positively by the Thiéry silver proteinate method. The other part is stained positively by EDTA preferential staining. According to the cyto- and histochemical results the granules consist of ribosomes and abnormal basic glycogen. The aggregates are removed from the cytoplasm mostly by lysosomal degradation.

Discovery of the specific hepatotoxic effect of D-galactosamine (DGA) [5] has been followed by a number of morphological and biochemical studies (for reviews see DECKER and KEPPLER [2, 3, 7]). Several morphological features resembling those of human viral hepatitis (inflammation and focal necroses, Councilman bodies, balloon cells, etc.) have drawn attention to this experimental liver disease which can be elicited in a variety of animal species. The ultimate mechanism of cellular necrosis is not known. The primary biochemical lesion is considered to be a depletion of the uridine triphosphate (UTP) pool [3] which entails the drastic inhibition of RNA synthesis [19]. Biochemical alterations include the decrease of protein synthesis [8, 15, 19, 22] which cannot, however, be interpreted as a mere consequence of impaired RNA synthesis in the early stage. Some direct damage to the protein synthesizing machinery has been suggested by electron microscopic observations [9, 14, 22] demonstrating a degranulation of the rough endoplasmic reticulum and the formation of cytoplasmic electrondense aggregates. The purpose of present study was to elucidate the structure, composition and fate of the cytoplasmic aggregates.

Materials and methods

Treatment of animals (see Table I).

Male Swiss mice weighing 20 to 25 g were used. Starvation for 48 hours was applied to deplete liver glycogen. Galactosamine treatment was performed by a single intraperitoneal (i.p.) injection of 1 g/kg body weight of D-galactosamine HCl (DGA) (Fluka AG, Buchs, Switzerland), if not otherwise stated. D-glucose was injected i.p. in a single dose of 5 g/kg body weight. The controls received i.p. physiological saline. Each experimental group contained at least five mice. The animals were sacrificed by decapitations.

Light microscopy. Liver samples excised from the middle large lobe were fixed in 4% neutral buffered formalin and in Dubosque-Brasil-Bouin fixative. Paraffin sections were stained with haematoxylin and eosin and PAS, with or without amylase treatment. Neutral lipids were demonstrated in frozen sections by oil-red staining.

Electron microscopy. Samples were fixed in 2% OsO_4 for 2 hours, or in 2.5% glutaraldehyde for 3 hours at 4°C. The fixatives were dissolved in cacodylate buffer pH 7.2. Samples were dehydrated in increasing concentrations of ethanol, and propylenoxide, and embedded in Durcupan (Fluka ACM). Ultrathin sections cut with an LKB ultratome III were stained with uranyl acetate and lead citrate and examined with a JEM 100B electron microscope.

Cytochemical methods. Polysaccharides were stained for electron microscopy with thio-carbohydrazide-silver proteinate according to THIÉRY [24]. Ribonucleoproteins were demonstrated in glutaraldehyde fixed ultrathin sections stained by the method of BERNHARD [1] applying EDTA.

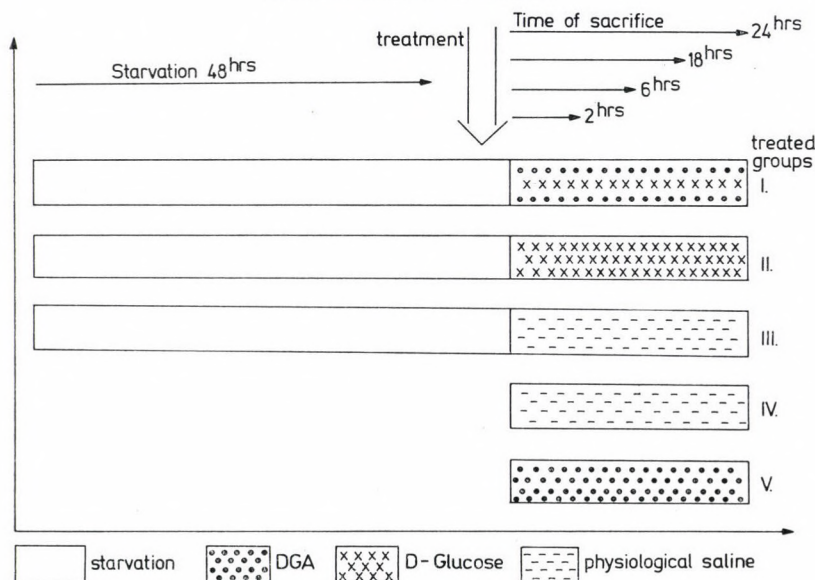
Amylase and pronase treatments were performed according to MONNERON and BERNHARD [17]. Sample sections were digested in a 0.1% solution of alpha-amylase (65.7 U per mg, Worthington Biochem. Corp.) or in a 0.5% solution of pronase (Grade B, Calbiochem.) at pH 7.4 at 37°C for 20 minutes. Samples treated with periodic acid only served as controls. Acid phosphatase activity was demonstrated by the method of NOVIKOFF et al. [18]. Glucose-6-phosphatase activity was demonstrated according to the method of WACHSTEIN and MEISEL [26] as modified by TICE and BARNETT [25].

Cell fractionation. Rough (heavy) endoplasmic membranes were isolated as described [16] with some modifications. Postmitochondrial supernatants of liver homogenates were prepared as before. The postmitochondrial supernatant of a single liver was layered gently over a discontinuous sucrose gradient in 12 ml cellulose nitrate tubes (from bottom to top, 2.5 ml L2-65B ultracentrifuge for 120 minutes). The resulting pellet was washed with 3.2% sucrose dissolved in cacodylate buffer pH 7.4, in order to remove excess sucrose and centrifuged at 900 g for one minute. The sediment was fixed in OsO_4 for 30 minutes and processed for electron microscopy as described above.

Polysaccharide analysis. Glycogen was isolated from the perchloric acid supernatant of liver homogenates. The amount of glucose was determined by the cysteine-sulphuric acid reaction [4]. Hydrolysis of the polysaccharides was performed with 4 N HCl at 100°C for 12 hours. Glucosamine was demonstrated by automated amino acid analyzer. Protein was estimated according to LOWRY et al. [12] using serum albumin as standard.

Table I

SCHEME OF THE TREATMENT



Results

1. Controls

In the livers of normally fed mice treated with physiological saline no particular alterations were seen (Fig. 1/A). PAS staining demonstrated large amounts of glycogen of normal localization. Starvation for 48 hours depleted the hepatic glycogen and oil-red staining demonstrated a finely dispersed fatty infiltration. The injection of D-glucose (5 g per kg body weight) led to the re-appearance of glycogen which was easily digested by amylase.

2. Galactosamine induced alterations

Light microscopy. Mice starved for 48 hours received a single injection of DGA (1 g/kg body weight) and were sacrificed after various intervals. Two hours after the injection a basophilic granulation appeared on the sinusoidal surface of the liver cells (Fig. 1/B). The granules were resistant against alpha-amylase digestion (Fig. 1/C). In the period from 6 to 18 hours after the administration of galactosamine, light microscopic signs of liver damage developed: unicellular necroses surrounded by round cell infiltration (Table III). In the liver of normally fed mice treated with galactosamine, the light microscopic alterations were similar to those of the starved animals, but the amount of basophilic granulation was considerably larger.

Electron microscopy. At 6 hours following the treatment of starved mice with galactosamine, electron microscopic examination of the liver revealed the dilatation of the endoplasmic reticulum and the formation of vesicles. Between the cisternae several aggregates were seen, consisting of electrondense particles of 10 to 20 nm. The structure of the mitochondria was unchanged apart from a slight swelling. The appearance of lipid droplets, lysosomes and microbodies accompanied the changes. Later excessive formation and segregation of electrondense aggregates became the dominant alteration. The change of the nucleolus deserved attention: the electrondense spots around it reminded one of the "spotted nucleolus" (Fig. 1/D).

3. Formation and fate of the cytoplasmic aggregates induced by galactosamine (see Table II)

PAS staining. The basophilic granulation appearing in the haematoxylin-eosin stained liver sections of fasted and galactosamine treated mice gave an intense reaction on PAS staining (Fig. 1/B) and resisted amylase digestion for 20 minutes (Fig. 1/C), although prolonged treatment with alpha-amylase diminished somewhat the amount of PAS positive granulation. The site of the

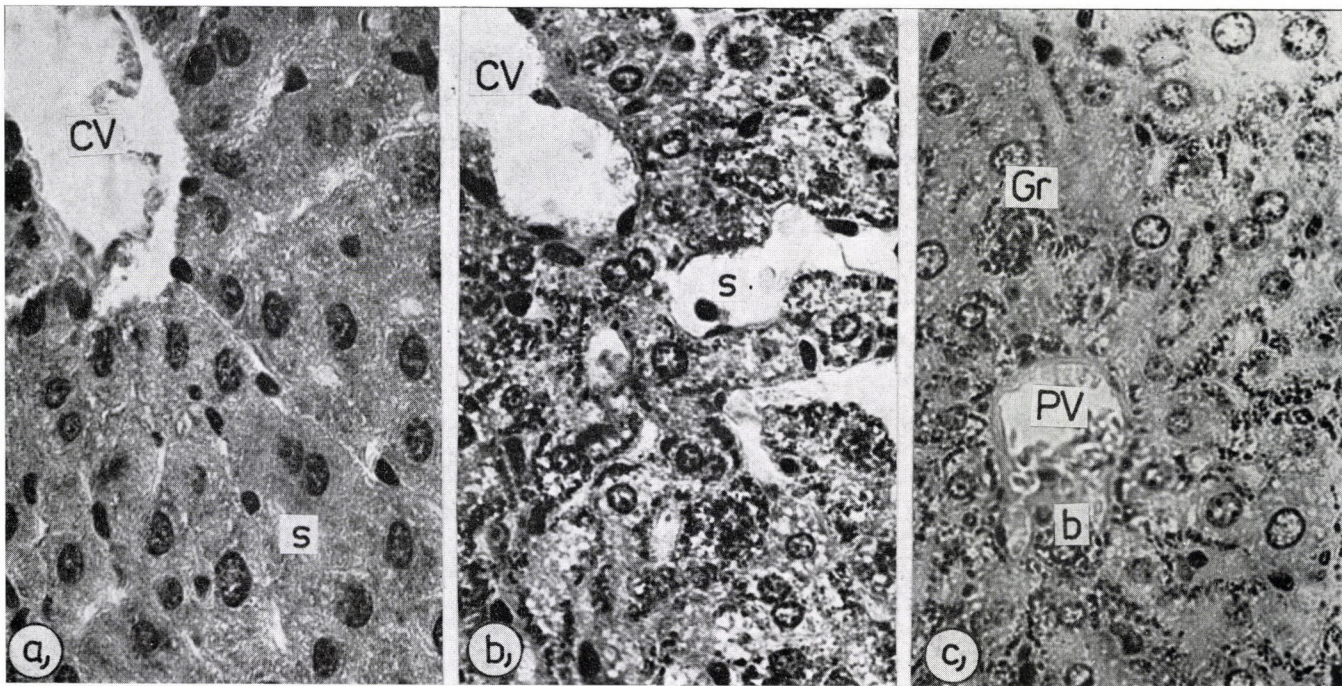


Fig. 1a. Control mouse liver: finely dispersed PAS positivity throughout the cytoplasm. PAS reaction. $\times 400$; cv = central vein; s = sinusoid

Fig. 1b. 2 hours after galactosamine (DGA) treatment. PAS positive granulation on the sinusoidal surface of liver cells PAS reaction. $\times 400$; cv = central vein; s = sinusoid

Fig. 1c. DGA treated liver from the animal shown in Fig. 1b. 30 min after alpha-amylase digestion. The PAS positive granulation is unchanged. Amylase-digested PAS reaction. $\times 400$; Pv = portal vein; Gr = Granulation; b = bile canal

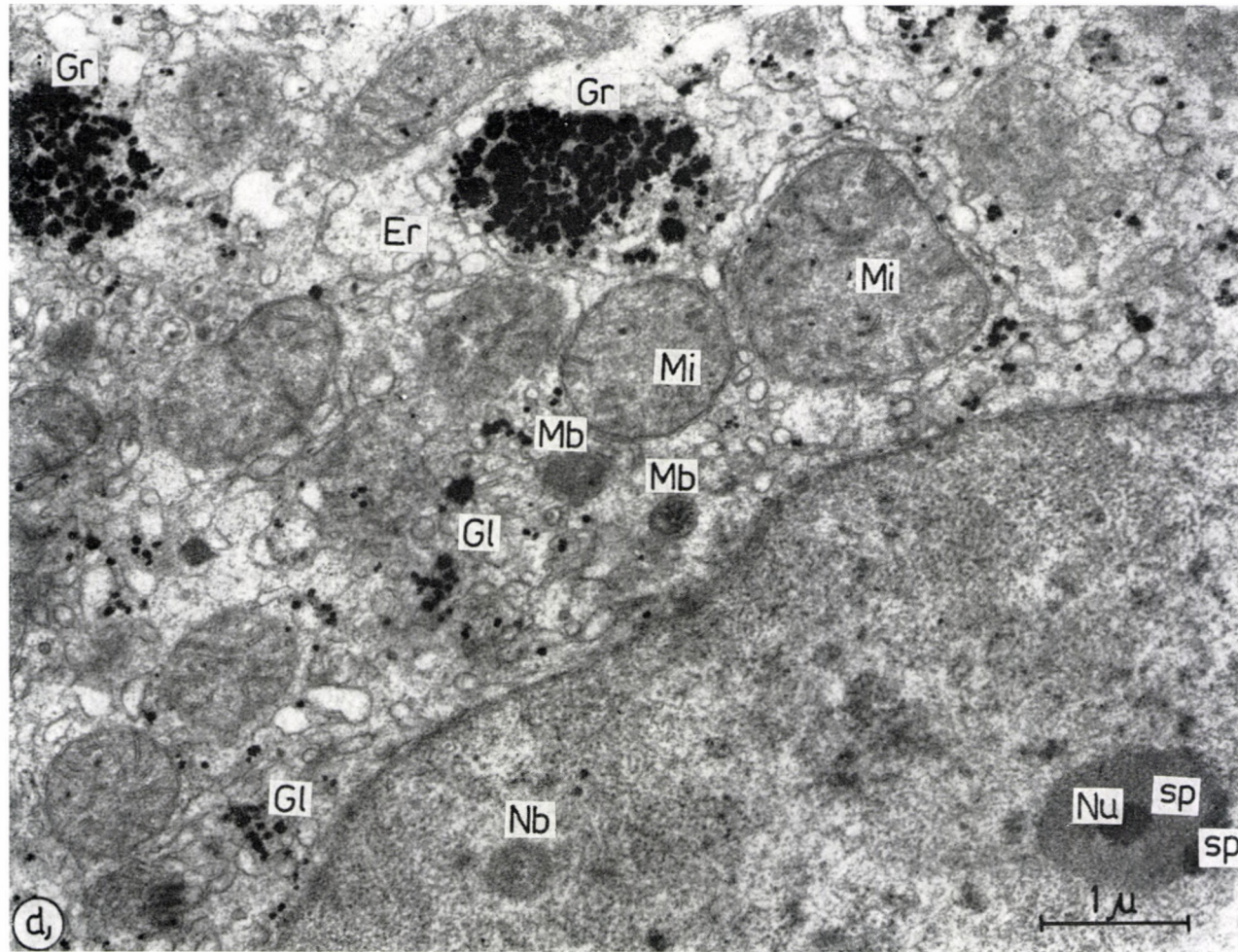


Fig. 1d. Electronmicrograph of liver cell 6 hr after DGA treatment. Note electron-dense spots (sp) in the nucleoli. Endoplasmic reticulum (Er) exhibits vesicular transformation. Granular aggregates (Gr) stained by the Thiéry-method. OsO_4 fixation — Thiéry staining. $\times 21,440$; Nu = nucleolus; Gl = glycogen; Mi = mitochondria; Mb = microbody; Nb = nuclear body

Table II*Cytochemical nature of the DGA induced granules*

	DGA treat- ment	DGA D-glucose treatment	Starvation and DGA treatment
Amylase digestion	—	—+	—
Pronase digestion	+	+	+
EDTA positivity	+	+	++
Thiéry positivity	+	++	+
Glucose-6-P-ase activity in the bile canal	+	++	+
Acid-P-ase activity in the granules	++	+	++

granulation corresponded to the midzonal localization of normal glycogen in the liver lobule. Six hours after the injection of galactosamine, marked PAS staining was observed in each of the livers examined. Thereafter, the PAS positive granulation was found to diminish: 18 hours after the injection it was restricted to a few cells, whereas in the 24th hour, glycogen of normal morphology was seen only (Table III). A large amount of PAS positive material was observed in the livers of normally fed mice treated with galactosamine, or

Table III*Results*

Time	DGA	DGA + D-glucose	D-glucose	Control	48 ^h starva- tion DGA	36 ^h starva- tion control
1—6 ^{hrs} granules	++	+++	—	—	+	—
6—18 ^{hrs} unicellular necroses	++	—	—	—	+++	—
18—36 ^{hrs} round cell infiltration	+++	++	—	—	+++	—
36—96 ^{hrs} regeneration	+++	—	—	—	++	—

+ mild
++ moderate degree of the given alteration
+++ severe

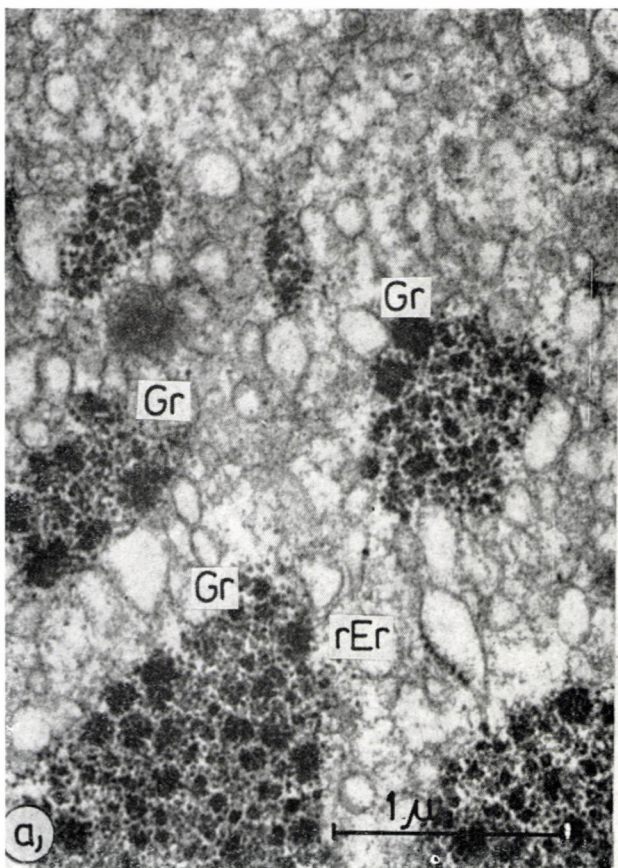


Fig. 2a. DGA treatment, 2 hr after injection. Degranulation of rough endoplasmic reticulum (rEr). OsO_4 fixation: $\times 32,000$; Gr = aggregates

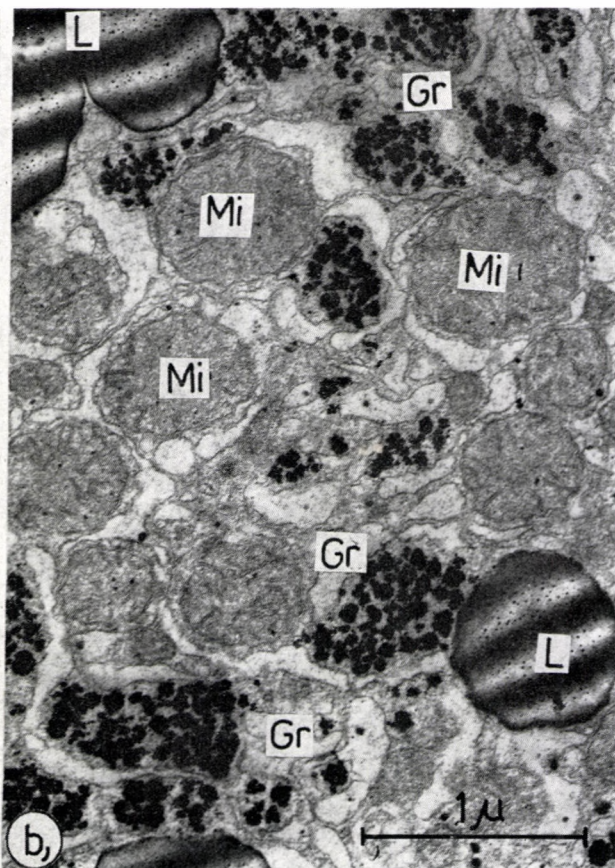


Fig. 2b. DGA treatment, 6 hr after injection. Polysaccharide substance in the aggregates (Gr). OsO_4 fixation, Thiéry staining. $\times 29,600$; L = lipid; Mi = mitochondria

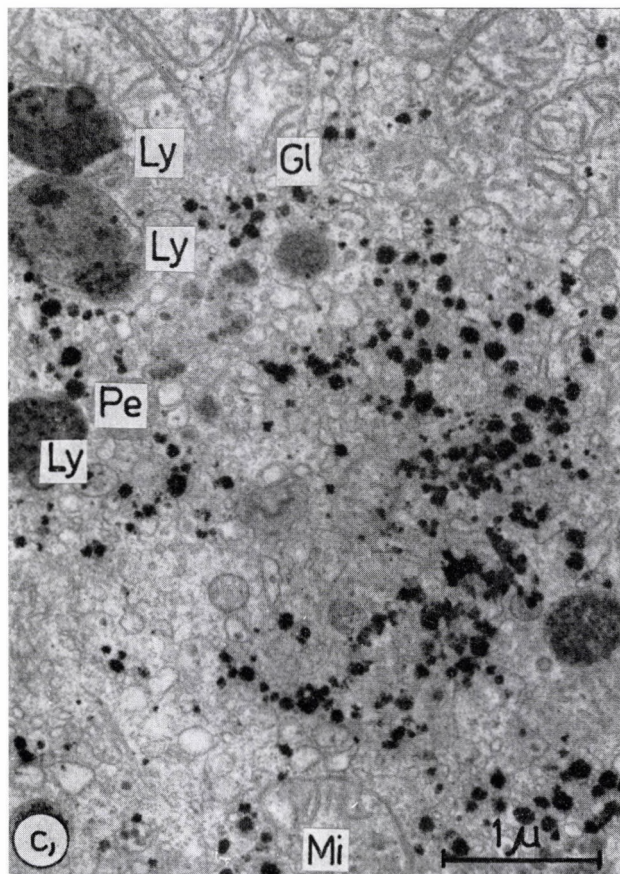


Fig. 2c. DGA treatment, 18 hr after injection. At the optimal point of time for inducing hepatitis-like alterations. A number of lysosomes contains Thiéry-positive material. OsO₄ fixation. $\times 21,440$; Ly = lysosomes; Gl = glycogen; Pe = peroxisome; Mi = mitochondria

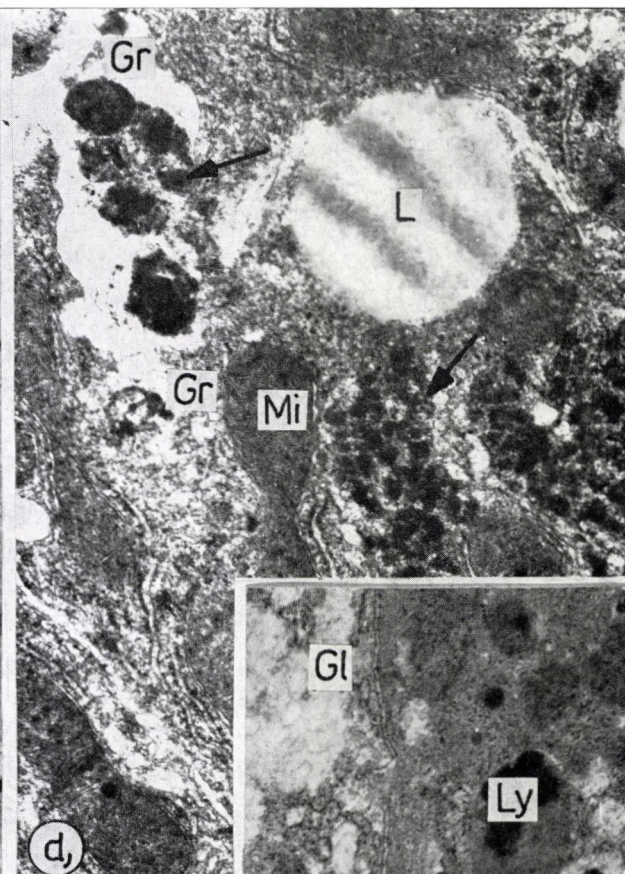


Fig. 2d. DGA treatment, 24 hr after injection. Acid-Ph-ase positivity in the aggregates: arrow; Glutaraldehyde fixation. $\times 21,440$; Gr = aggregates; Mi = mitochondria; Li = lipid droplets *Insert*: In the control liver cell the glycogen areas are negative after acid-Ph-ase reaction. Glutaraldehyde fixation. $\times 13,000$; Gl = glycogen; Ly = lysosome

of starved mice after treatment with galactosamine and glucose. In the latter case, the amount of PAS positive material could be reduced but not completely abolished by treatment with amylase.

Electron microscopy. Aggregates of electrondense particles (Fig. 1/d) appeared in increasing amounts 2 to 6 hours after galactosamine treatment of fasted mice.

Two hours after the treatment (Fig. 2/a) aggregation of electrondense particles was seen between the cisternae of rough endoplasmic reticulum (Fig. 2/a). Six hours after treatment an increase in the amount of dense granulation was observed (Fig. 2/b). 18 hours after treatment, the aggregates were partly surrounded by membranes of rEr; at this stage the lysosomes contained densely stained material on Thiéry's glycoprotein-specific staining (Fig. 2/c).

Considering the difficulties of distinction between cytoplasmic electrondense granules, i.e. glycogen particles and polyribosomes, polysaccharides were demonstrated by the method of THIÉRY [24]. The aggregates formed six hours after galactosamine treatment of starved animals showed intense staining by this method (Fig. 3/a). The amount of polysaccharide was much larger when glucose too was injected. The reaction was similar in intensity as the staining of glycogen, but the localization and distribution of the grains was different from that of the normally stored polysaccharide. Diastase treatment of the specimens caused a slight decrease in the amount of this unusual polysaccharide (Fig. 3/c), in accordance with the behaviour of the PAS positive material. Pronase treatment caused the granules to disappear (Fig. 3/d).

Ribonucleoprotein was detected by Bernhard's method [1] demonstrating the ribosomes (polysomes) as well as the nucleolar ribonucleoprotein. At variance with the regular arrays of ribosomes along the rough endoplasmic reticulum in the starved controls, ribonucleoprotein particles were trapped in the cytoplasmic aggregates induced by galactosamine (Fig. 3/b).

Acid phosphatase activity was detected in several of the large electrondense aggregates in the liver of galactosamine treated animals (Fig. 2/d). This was in agreement with the finding that the cytoplasmic aggregates were present in the lysosomes 18–24 hours after treatment. No acid phosphatase reaction was seen around the glycogen in the controls (Fig. 2/d) (insert).

Glucose-6-phosphatase activity was shown to be localized around the aggregates as well as on the bile canalicular surface of liver cells in the galactosamine treated animals (Fig. 4/b). In the controls, the reaction appeared normally within the cisternae of the endoplasmic reticulum (Fig. 4/a).

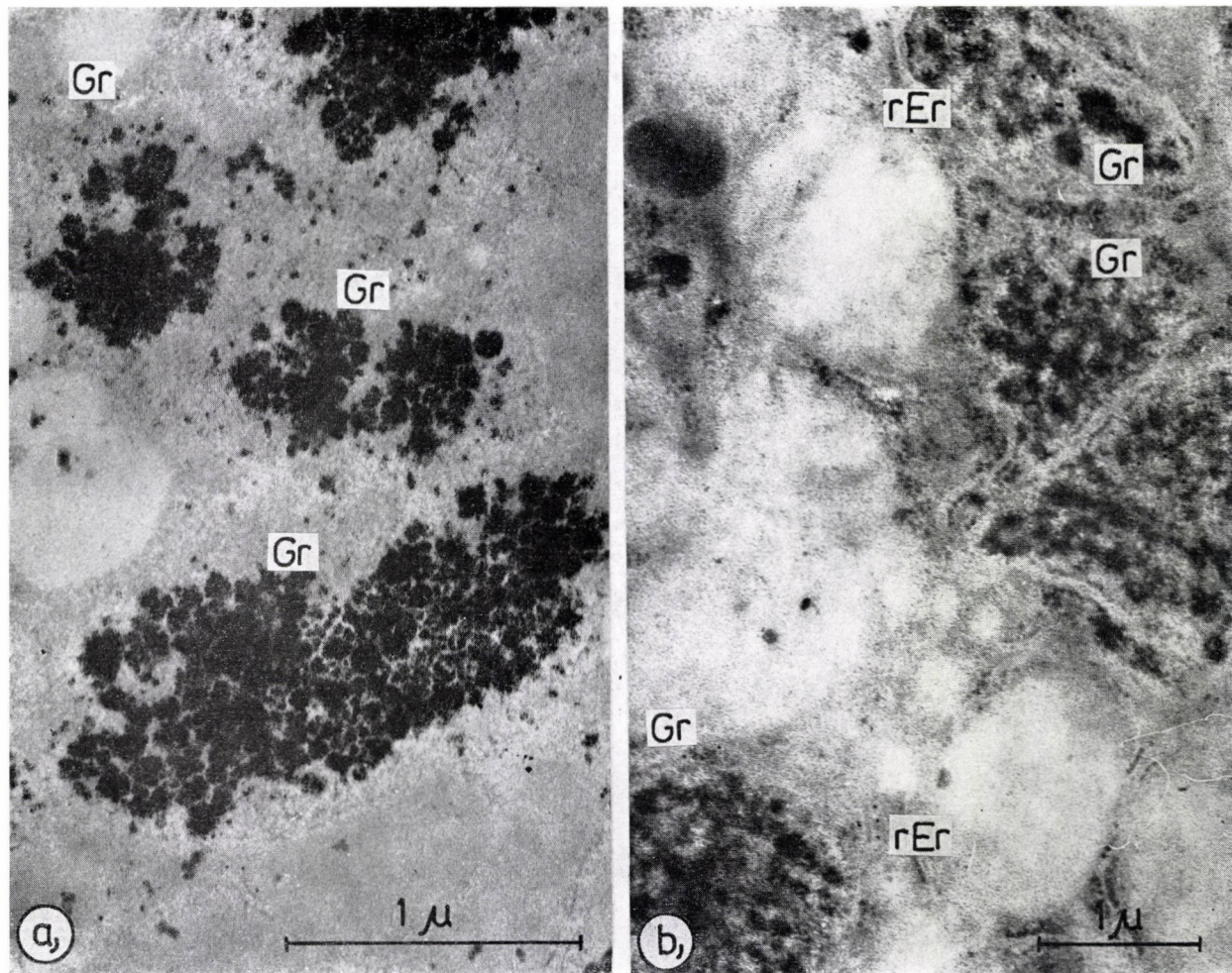
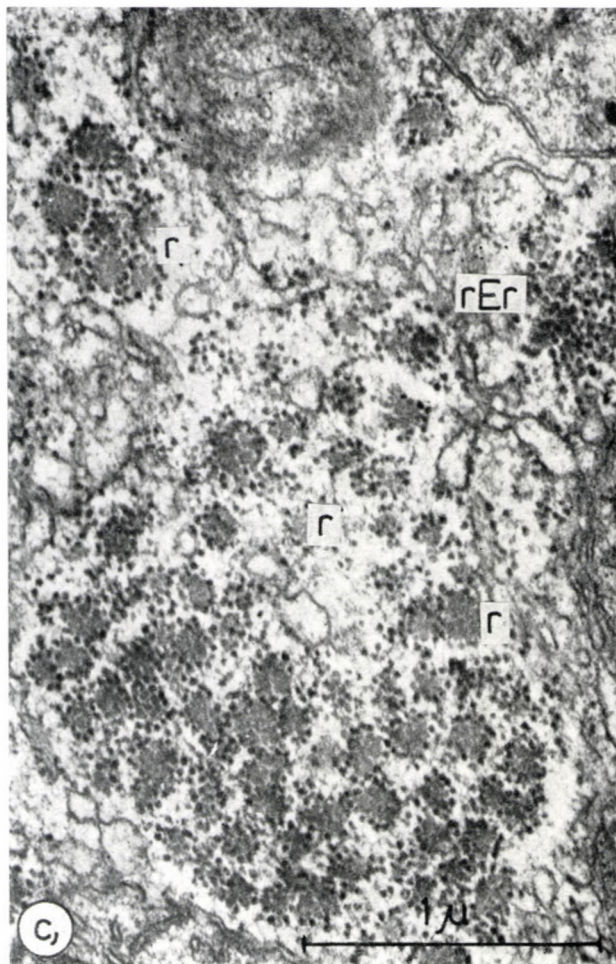
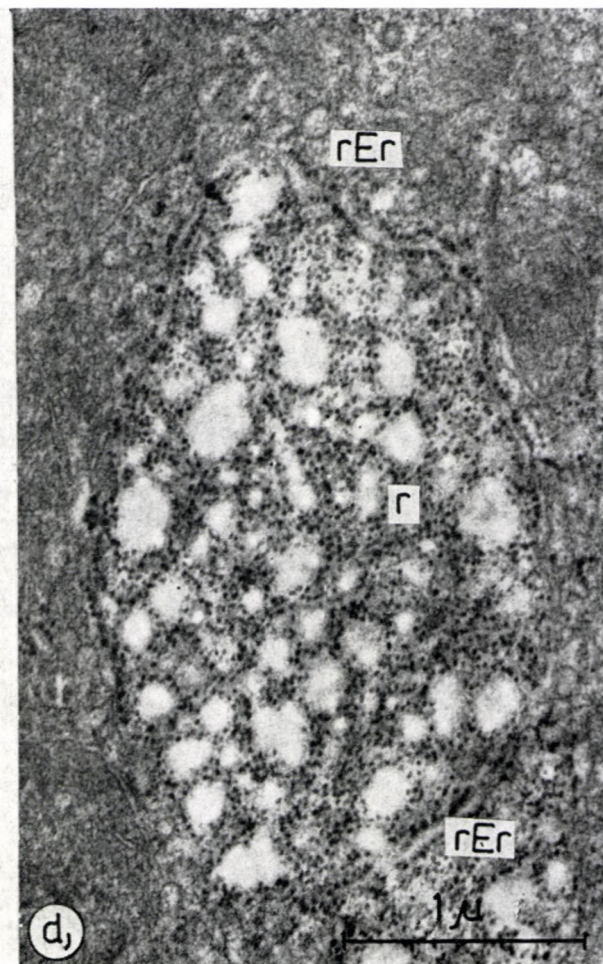


Fig. 3a. to d. DGA treatment 6 hr after injection. a. Thiéry staining: the positive reaction shows the presence of the polysaccharide component. OsO₄ fixation. $\times 21,440$; Gr = aggregates.

b. Bernhard staining: the EDTA positive material was found also in the aggregates, proving RNP containing structure. Glutaraldehyde fixation. $\times 21,440$; rEr = rough endoplasmic reticulum; Gr = aggregates.



c. Alpha-amylase treatment: the aggregates were resistant to 30 minutes digestion. OsO_4 fixation. $\times 39,960$; rEr = rough endoplasmic reticulum; r = ribosome.



d. Pronase treatment: 30 minutes after digestion, the polysaccharide components of the aggregates disappeared. OsO_4 fixation. $\times 32,000$; r Er = rough endoplasmic reticulum; r = ribosomes

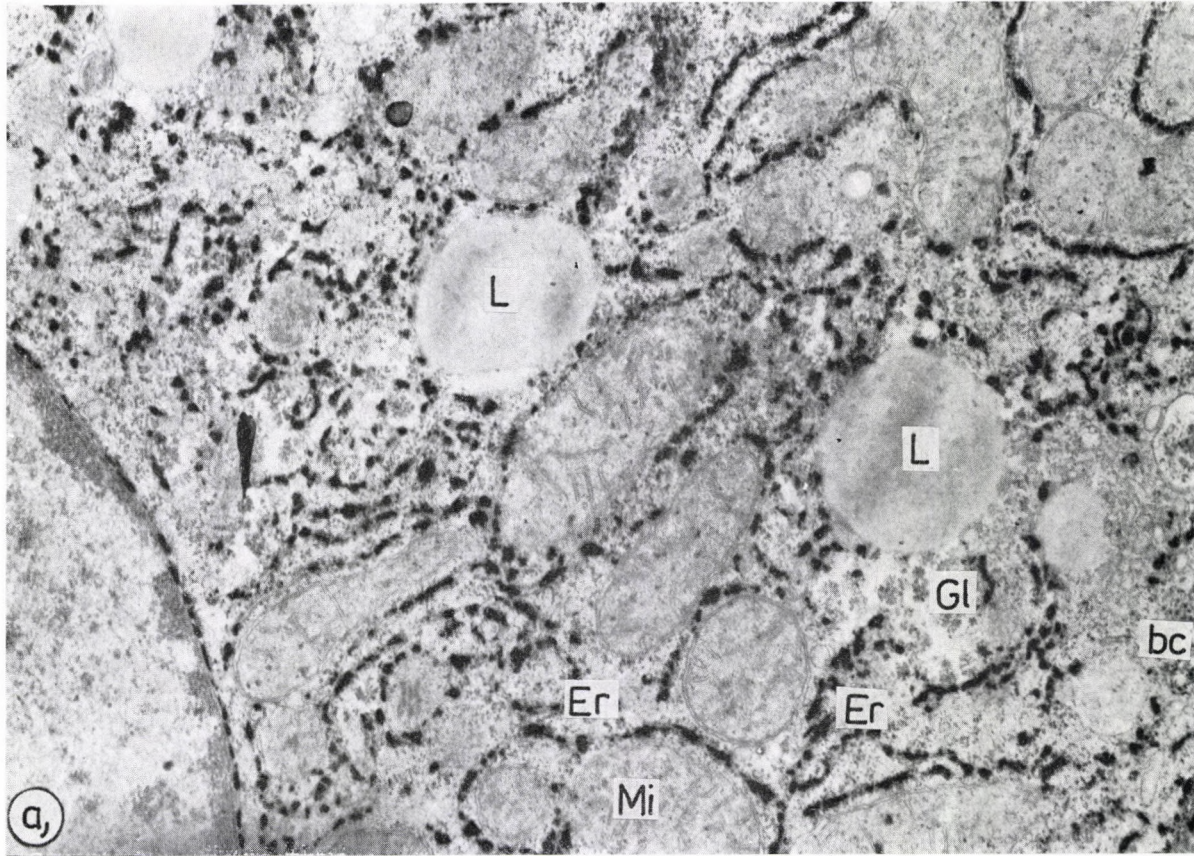


Fig. 4a. Control liver: in the endoplasmic reticulum (Er) cisterns the reaction is well-preserved, but the bile canalicular membranes show point-like positivity. Glutaraldehyde fixation, Glucose-6-Ph-ase reaction. $\times 21,440$; bc = bile canal; L = lipid droplets; Mi = mitochondria; Gl = glycogen

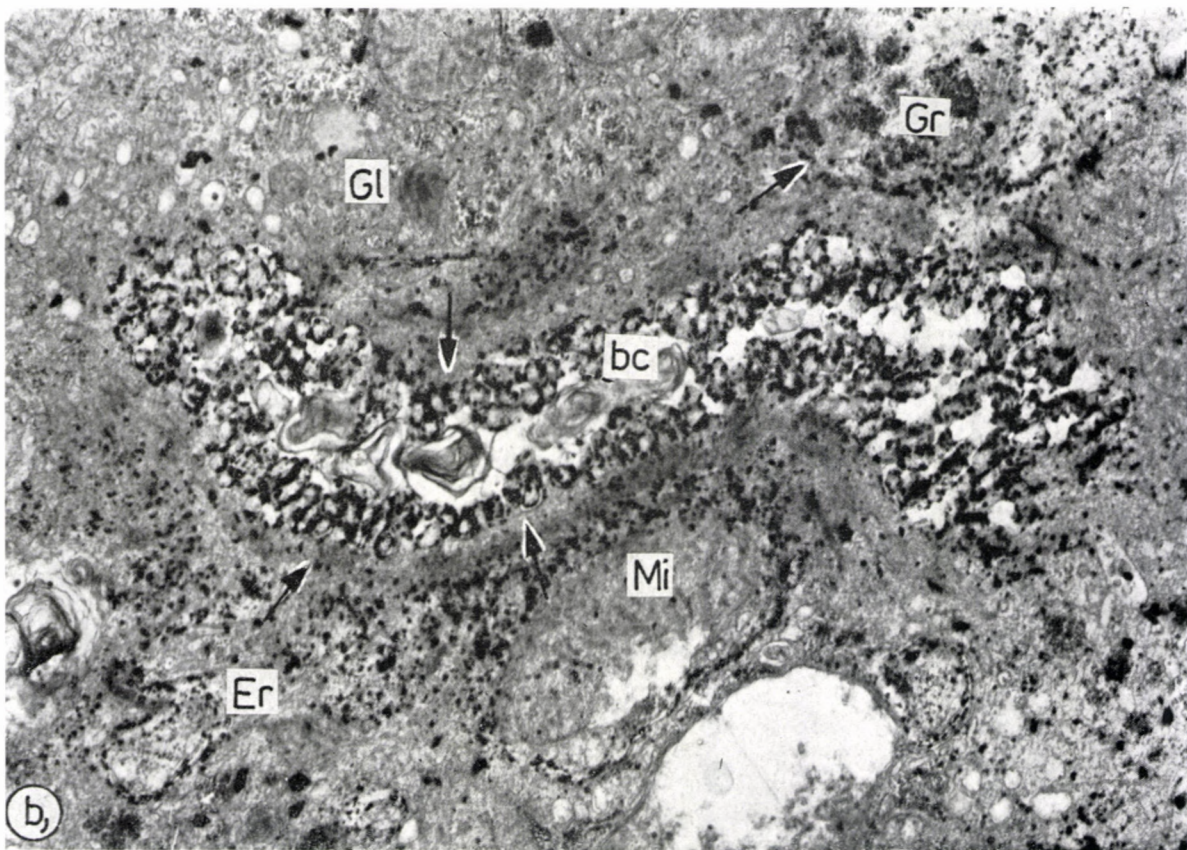


Fig. 4b. DGA treatment: 36 hr after injection, glucose-6-Ph-ase reaction in the bile canicular (bc) membranes and around the aggregates (Gr): arrow. Glutaraldehyde fixation, glucose-6-Ph-ase reaction. $\times 21,440$; Er = endoplasmic reticulum; Gl = glycogen; Mi = mitochondria

4. Isolation and electron microscopic examination of the cell fraction corresponding to the cytoplasmic aggregates.

Previous work on the fractionation of microsomal membranes [16] has shown a characteristic increase in the density of the rough endoplasmic reticulum membranes isolated from galactosamine treated mice. For electron microscopic examination of this cell fraction, the earlier method had to be modified in order to obtain both the altered and the normal rough membranes at the bottom of the ultracentrifuge tubes as pellets, separated from the smooth membranes by a layer of 1.3 M sucrose. Mice starved for 48 hours were injected intraperitoneally with DGA—HCl 250 mg per kg body weight, and D-glucose, 5 g per kg. Previously, this treatment has been shown to produce large amounts of cytoplasmic aggregates, but no hepatic necrosis. The controls received glucose only. After 120 minutes the livers were processed as described in Methods. The smooth membranes were recovered at the interfaces of the sucrose layers: similar amounts were found in the controls and the experimental samples.

The pellet containing the rough (heavy) membranes was examined by electron microscopy. The pellets obtained from the controls showed more or less uniform vesicles derived from the rough endoplasmic reticulum (Fig. 5/a). The fraction gained from galactosamine treated mice by the same procedure contained amorphous electrondense material containing irregular fragments and degranulated vesicles of the rough endoplasmic membranes (Fig. 5/b). The involvement in the formation of cytoplasmic aggregates of endoplasmic membranes carrying the ribosomes was clearly demonstrated by these experiments.

5. Chemical composition of the atypical polysaccharide.

The incorporation of D-glucosamine into hepatic glycogen following D-galactosamine administration has been described and elucidated by MALEY et al. [13]. For analytical purposes, the polysaccharides were isolated from mice receiving similar treatments as in the cell fractionation experiment, in order to ensure the high yield of the material. Both the normal and the atypical glycogen, isolated from the perchloric acid supernatant of liver homogenates, contained 97 to 99% glucose and 0.3 to 0.5% protein. No hexosamine was found in the hepatic glycogen of the glucose treated mice. In the acid hydrolysate of the hepatic polysaccharide of mice treated with galactosamine and glucose, 1.3% glucosamine was demonstrated. The purified polysaccharide was not resistant to digestion with amylase.

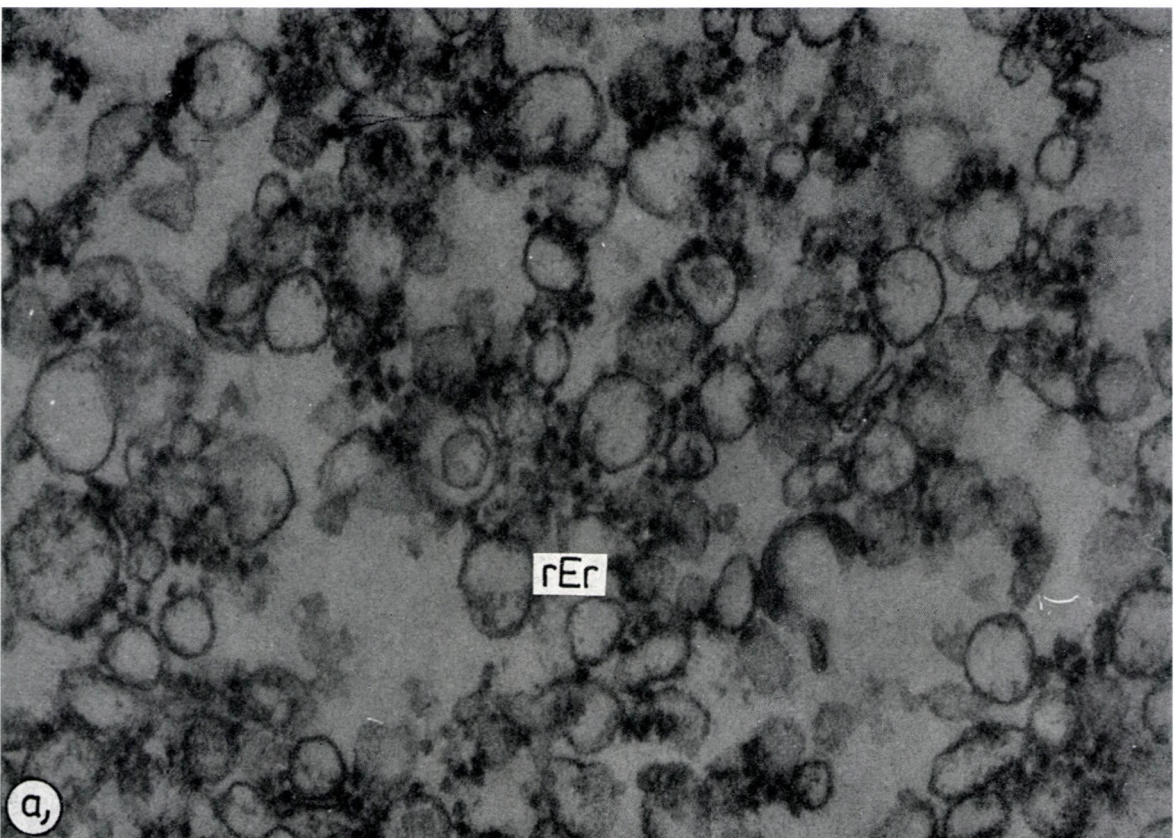


Fig. 5a. Control mouse liver: ultrastructure of heavy microsomal fraction. Normal pellet. OsO_4 fixation. $\times 60,000$;
rEr = rough endoplasmic reticulum membranes

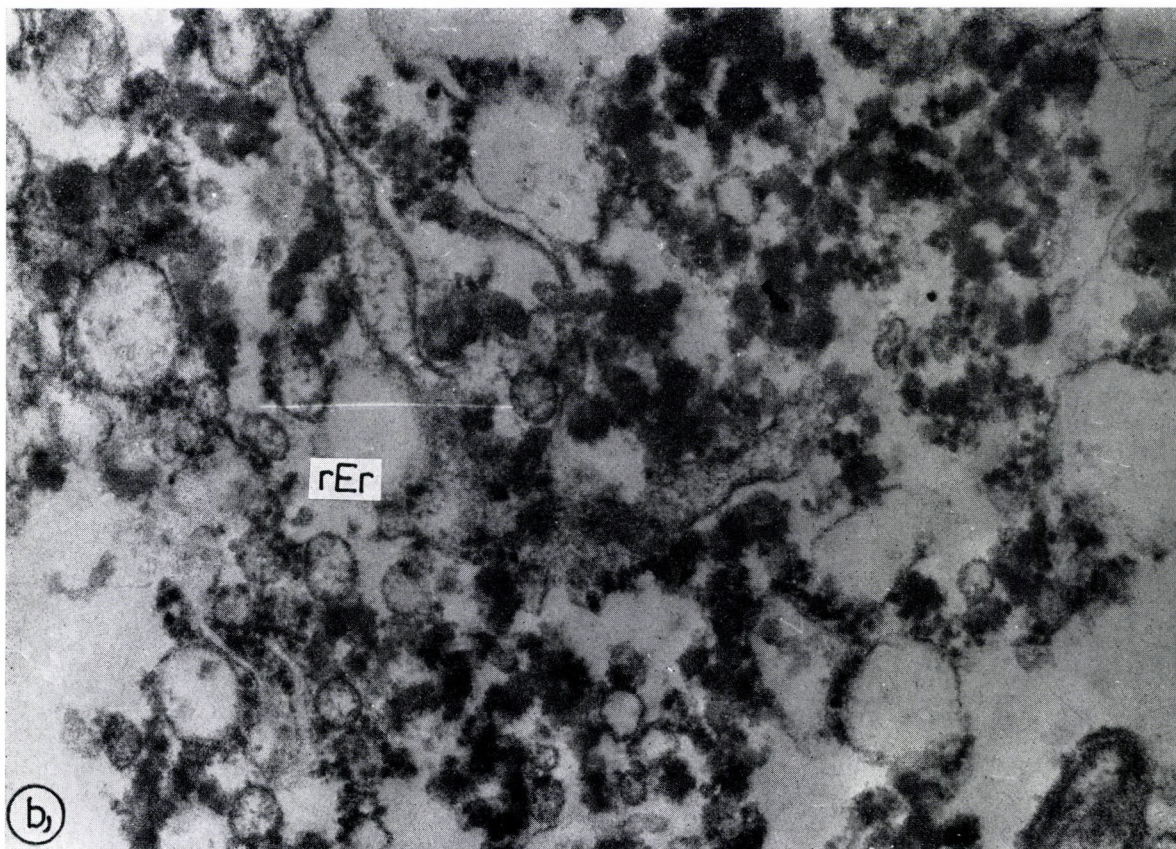


Fig. 5b. DGA treatment: ultrastructure of heavy microsomal fraction after 3 hr DGA treatment. Uncommon sedimented pellet. The membranes were attached to electrondense substance. OsO_4 fixation. $\times 60,000$; rEr = rough endoplasmic reticulum

Discussion

Cytoplasmic aggregates have been observed in galactosamine hepatitis of the rat by SCHARNBECK et al. [21], LAPIS and SCHAFF [9], who interpreted this material as abnormal glycogen. This opinion was opposed by SHINOZUKA et al. [23] mainly because of the unusual morphology and atypical localization of the granulation, and its resistance to digestion with diastase. The latter authors detected irregular stacks of ribosomes in the aggregates and speculated on the formation of complexes of ribosomes with some unknown carbohydrate due to the disturbance of glycoprotein synthesis. LAPIS and SCHAFF [9] suggested that the atypical polysaccharide might be formed on the route demonstrated by MALEY et al. [13]. Uridine failed to prevent the formation of aggregates [23].

According to LESCH et al. [10] the aggregates or atypical dense bodies (ADB) can be classified into three types; the early, the intermediate and the late type and they are never enclosed by a limiting membrane. The ADB has two constituents; RNase-sensitive and RNase and diastase resistant PAS-positive components. The latter represents some abnormal metabolite of glycogen [10]. We had come to the same conclusion. Part of the particles found in ADB are stain positively on Bernhard's preferential staining for RNA containing structures, and part of the granules take Thiéry's polysaccharide-specific stain but they are diastase-resistant. The pronase digested the glycoprotein component but did not attack the RNA-containing particles similar to the ribosomes.

Most authors share the opinion that the inhibition of protein synthesis in galactosamine hepatitis is difficult to explain solely on the basis of UTP deficiency, defined as a primary biochemical lesion by DECKER and KEPPLER [3]. Unlike the decrease of RNA synthesis, the inhibition of protein synthesis was not completely reverted by administration of uridine [23].

The study of the formation and composition of cytoplasmic aggregates in galactosamine hepatitis has led us to suggest an explanation for the inhibition of protein synthesis in the early stage of galactosamine induced liver injury in mice. The morphological and biochemical findings presented indicate that the cytoplasmic aggregates consist of atypical basic glycogen and ribosomes detached from the rough endoplasmic reticulum. The formation of aggregates is preceded by the incorporation into glycogen of non-N-acetylated glucosamine. The resulting basic polysaccharide is presumably attached to the rough endoplasmic reticulum which is the framework supporting the polyribosomes, particles of strongly acid character. The interaction may result in the detachment of ribosomes from the membranes, or it may cause a fragmentation of the rough endoplasmic membrane system. Such a severe damage to the supramolecular structure of the protein synthesizing apparatus most probably impairs its function, too.

The formation of the aggregates could be a factor in the inhibition of protein synthesis which is certainly not counteracted by uridine. The significance of this factor is determined by the amount and basicity of the polysaccharide. The amount of glycogen is decreasing in galactosamine treated, normally fed rats [11], but this should be interpreted in terms of a turnover with a negative balance, permitting the incorporation of glucosamine into glycogen. The abundance of the aggregates in the mouse liver indicates that the phenomenon is of great importance in this species. Elimination of the aggregates is due to lysosomal degradation of the complexes. In galactosamine hepatitis, autophagic vacuoles containing glycogen were observed by SCHARNBECK et al. [21], LAPIS and SCHAFF [9] and by RUMPELT et al. [20].

From the point of view of cell death, the aggregates seem to be of secondary importance because low doses of galactosamine combined with glucose maximally stimulate the formation of aggregates, while no significant hepatocellular necrosis is induced. Nevertheless, in the sequence of events leading to hepatic damage, the formation of cytoplasmic aggregates and the resulting decrease of protein synthesis is certainly one of the factors to be considered.

REFERENCES

1. BERNHARD, W.: (1969) A new staining procedure for microscopical cytology. *J. Ultrastruct. Res.* **27**, 250. — 2. DECKER, K., KEPPLER, D.: (1973) The regulation of pyrimidine nucleotide level and its role in experimental hepatitis. In: Weber, G. (Ed.), *Advances in enzyme regulation*, Vol. 11, p. 205–229. Pergamon Press, Oxford. — 3. DECKER, K., KEPPLER, D.: (1974) Galactosamine hepatitis: Key role of the nucleotide deficiency period in the pathogenesis of cell injury and cell death. *Rev. Physiol.* **71**, 78. — 4. DISCHE, Z.: (1955) New color reactions for determination of sugars in polysaccharides. In: Glick, D. (Ed.), *Methods of biochemical analysis*, Vol. 11, p. 327. Interscience Publishers, New York. — 5. KEPPLER, D., LESCH, R., REUTTER, W., DECKER, K.: (1968) Experimental hepatitis induced by D-galactosamine. *Exp. molec. Path.* **9**, 279. — 6. KEPPLER, D., DECKER, K.: (1969) Studies on the mechanism of galactosamine hepatitis: Accumulation of galactosamine-1-phosphate and its inhibition of UDP-glucose pyrophosphorylase. *Europ. Biochem.* **10**, 219. — 7. KEPPLER, D., PAUSCH, J., DECKER, K.: (1974) Selective uridine-triphosphate deficiency induced by D-galactosamine in liver and reversed by pyrimidine nucleotide precursors. Effect on ribonucleic acid synthesis. *J. biol. Chem.* **249**, 211. — 8. KOFF, R. S., GORDON, G., SABESIN, S. M.: (1971) D-galactosamine hepatitis. I. Hepatocellular injury and fatty liver following a single dose. *Proc. Soc. exp. Biol. (N. Y.)* **137**, 696. — 9. LAPIS, K., SCHAFF, Zs.: (1973) Ultrastructural studies on D-galactosamine-HCl induced liver injury in mice. *Morph. Igazs. Orv. Szle* **13**, 276. — 10. LESCH, R., MEINHARDT, K., HÄBERLE, B., ENZAN, H.: (1976) The appearance and degradation of specific hepatocellular cytoplasmic inclusion bodies in rat liver due to D-galactosamine. *Virchows Arch. path. Anat. B. Cell Path.* **21**, 313. — 11. LESCH, R., REUTTER, W., KEPPLER, D., DECKER, K.: (1970) Liver restitution after acute galactosamine hepatitis: Autoradiographic and biochemical studies in rats. *Exp. molec. Path.* **12**, 58. — 12. LOWRY, O. H., ROSEBROUGH, N. J., FARR, A. L., RANDALL, R. J.: (1951) Protein measurement with the Folin phenol reagent. *J. biol. Chem.* **193**, 264. — 13. MALEY, F., TARENTINO, A. L., MCGARRAHAN, J. F., DELGIACCO, R.: (1968) The metabolism of D-galactosamine and N-acetyl-D-galactosamine in rat liver. *Biochem. J.* **107**, 637. — 14. MEDLINE, A., SCHAFFNER, F., POPPER, H.: (1970) Ultrastructural features in galactosamine-induced hepatitis. *Exp. molec. Path.* **12**, 201. — 15. MÉSZÁROS, K., ANTONI, F., HRABÁK, A., SZIKLA, R., GARZÓ, T., TOMPA, A., LAPIS, K.: (1973) Prevention of the hepatotoxic effects of D-galactosamine by D-galactose. *FEBS Letters* **35**, 1. — 16. MÉSZÁROS, K., ANTONI, F., MANDL, J., HRABÁK, A., GARZÓ, T.: (1974) Effects of D-galactosamine on nucleotide metabolism and on microsomal membranes in mouse liver. *FEBS Letters* **44**, 141. — 17. MONNERON, A., BERNHARD, W.: (1966) Action

des certaines enzymes sur des tissus inclus en Epon. *J. Micr. (Paris)* **5**, 697. — 18. NOVIKOFF, A. B., OGAWA, K., MASUTANI, K., SHINONAGA, K.: (1962) Electron histochemical demonstration of acid phosphatase in the normal rat jejunum. *J. Histochem. Cytochem.* **10**, 228. — 19. REUTTER, W., KEPPLER, D., LESCH, R., DECKER, K.: (1969) Zum Glycoproteidstoffwechsel bei der Galactosamin-induzierten Hepatitis. *Verh. dtsch. Ges. inn. Med.* **75**, 363. — 20. RUMPELT, H. J., ALBRING, M., THOENES, W.: (1974) Prevention of D-galactosamine-induced hepatocellular autophagocytosis by cytohexamine. *Virchows Arch. path. Anal. B. Cell Path.* **16**, 195. — 21. SCHARNBECK, H., SCHAFFNER, F., KEPPLER, D., DECKER, K.: (1972) Ultrastructural studies on the effect of choline orotate on galactosamine-induced hepatic injury in rats. *Exp. molec. Path.* **16**, 33. — 22. SHINOZUKA, H., FARBER, J. L., KONISHI, Y., ANUKARAHANONTA, T.: (1973a) D-galactosamine and acute liver cell injury. *Fed. Proc.* **32**, 1516. — 23. SHINOZUKA, H., MARTIN, J. T., FARBER, J. L.: (1973b) The induction of fibrillar nucleoli in rat liver cells by D-galactosamine and their subsequent re-formation into normal nucleoli. *J. Ultrastruct. Res.* **44**, 279. — 24. THIÉRY, J. P.: (1967) Mise en évidence des polysaccharides sur coupes fines en microscopie électronique. *J. Micr. (Paris)* **6**, 85A. — 25. TICE, L. W., BARNETT, R. J.: (1962) The fine structural localisation of glucose-6-phosphatase in rat liver. *J. Histochem. Cytochem.* **10**, 754. — 26. WACHSTEIN, M., MEISEL, E.: (1956) On the histochemical demonstration of glucose-6-phosphatase. *J. Histochem. Cytochem.* **4**, 592.

KENNZEICHNUNG DER BEI D-GALACTOSAMIN-BEDINGTER LEBERSCHÄDIGUNG BEOBACHTETEN ZYTOPLASMA-AGGREGATE

ANNA TOMPA, K. LAPIS, ZSUZSA SCHAFF, K. MÉSZÁROS, J. MANDL, T. GARZÓ und F. ANTONI

Unter D-Galactosaminwirkung entstehen im Zytoplasma der Mäuse-Leberzellen PAS-positive Granula oder Aggregate. In den Untersuchungen ihrer Ultrastruktur wurde aufgezeigt, daß die Granula von der Membran des endoplasmatischen Retikulums mit grober Oberfläche umgeben sind.

Die Ergebnisse der zytochemischen Untersuchungen deuten darauf hin, daß ein Teil dieser Aggregate Pronase-empfindlich und Amylase-resistent ist und sich mit dem Thiéryschen Silberproteinatverfahren positiv anfärbt. Der andere Teil färbt sich mit der EDTA-Präferenzfärbung positiv an. Gemäß zytochemischen und biochemischen Untersuchungsergebnissen bestehen die Granula aus Ribosomen und aus abnormalem basischem Glykogen. Die Aggregate verschwinden aus dem Zytoplasma zumeist infolge lysosomaler Degradation.

ХАРАКТЕРИСТИКА АГРЕГАТОВ, НАБЛЮДАЕМЫХ ПРИ ПОВРЕЖДЕНИИ ПЕЧЕНИ, ВЫЗВАННОМ Д-ГАЛАКТОЗАМИНОМ

АННА ТОМПА, К. ЛАПИШ, ЖУЖА ШАФФ, К. МЕСАРОШ, Й. МАНДЛ, Т. ГАРЗО и Ф. АНТОНИ

Под действием Д-галактозамина в цитоплазме печеночных клеток мыши образуются ПАСК-положительные гранулы или агрегаты. Исследования ультраструктуры показывают, что зернышки окружены мембраной эндоплазматической сеточки с грубой поверхностью.

Результаты цитохимических исследований показали, что часть гранул чувствительна к проназу, устойчива против амилазы и при окрашивании методом протенината серебра по Тиери положительно окрашивается. Другая часть агрегатов положительно окрашивается при предпочтительном окрашивании ЭДТА. На основе цитохимических и биохимических исследований эти гранулы состоят из рибосом и из ненормального щелочного гликогена.

Dr. Anna TOMPA
Dr. Károly LAPIS
Dr. Zsuzsa SCHAFF

Semmelweis Orvostudományi Egyetem
I. sz. Kórbonctani Intézet
H-1085 Budapest, Üllői út 26, Hungary

Dr. Károly MÉSZÁROS
Dr. József MANDL
Dr. Tamás GARZÓ
Dr. Ferenc ANTONI

Semmelweis Orvostudományi Egyetem
I. sz. Kémiai-Biokémiai Intézet
H-1088 Budapest, Puskin u. 9, Hungary

First Institute of Anatomy, Histology and Embriology,
Semmelweis University Medical School, Budapest, Hungary

BLOOD SUPPLY OF THE RAT HYPOTHALAMUS. V. THE MEDIAL HYPOTHALAMUS (NUCLEUS VENTROMEDIALIS, NUCLEUS DORSOMEDIALIS, NUCLEUS PERIFORNICALIS)

G. AMBACH and M. PALKOVITS

(Received October 12, 1977)

Using the India ink double-perfusion technique, the blood vessels of the rat's medial hypothalamus were reconstructed from serial sections. The area studied comprised the ventromedial, dorsomedial and perifornical nuclei. The arterial supply of this territory comes from the middle hypothalamic and the anterior, middle and posterior tuberal arteries. The drainage is strictly undirectional: ventralward by the anterior, middle and posterior ventromedial, the posteromedial and posterolateral hypothalamic veins, all ending in the basal vein.

The arteries of the ventromedial and dorsomedial nuclei are distinct from those of the arcuate nucleus and median eminence, and their drainage is not connected with the portal vessels. The nuclei studied, even at the levels of their subdivisions, possess own arteries whose territories of supply can well be distinguished with a minimum of overlap. The topography of these arteries is described in detail.

The medial hypothalamus has no vascular connections with other regions of the diencephalon including the thalamus.

Introduction

Earlier studies with double injections of India ink [2, 3, 4, 5] have shown that the hypothalamic nuclear groups have fairly independent blood supplies. Those located in the central part of the medial hypothalamus (arcuate, ventromedial and dorsomedial nuclei) were distinct from the anterior [4, 5] and pre-mammillary cell groups as far as their blood supply was concerned (AMBACH and PALKOVITS in preparation). Even within the medial hypothalamus, the median eminence and the arcuate nucleus have an own vascular system which has few or no connections with the dorsally situated ventromedial and dorsomedial nuclei [5].

The ventromedial and dorsomedial nuclei have an important role in neuroendocrine control and, as indicated by their volume and cell number, their contribution to the mass of the hypothalamus is substantial. The fact that, this territory often serves as the target of experimental surgery, has prompted us to investigate its blood supply in detail. Studies were focused on the following problems. 1) Do the ventromedial (NVM), dorsomedial (NDM)

and perifornical (NPF) nuclei possess independent blood supplies? 2) Is there any vascular relationship between this area and the median eminence and hypophysis? 3) Have the subdivisions of the above nuclei own arteries and veins? 4) What is the pattern of venous drainage in these nuclei? 5) Do they have any vascular connection with the thalamus?

Materials and methods

The blood vessels of 40 albino rats were filled with India ink. After fixation the brains were processed as described below. Ink perfusions were made with two colours as described earlier [2]. Through the common carotid artery, blue ink (Rotring) was injected into the arteries of the head, then red ink of higher viscosity was pumped in, pressing the blue one into the veins. Due to its high viscosity the red ink did not pass through the capillaries thus the arterial side of the circulation became filled with red and the venous one with blue ink. When only one of the two were filled up, a 5–6% black ink-gelatin solution was administered. Brains were removed from the skull and fixed for 8–10 days in 10% formaldehyde. Serial sections of 100–400 μ thickness were cut mainly in the frontal, in some cases in the sagittal plane. Sections were cleared for stereo-microscopic study. This allowed a complete reconstruction of the vessels. Their localization was made using the coordinates of the cytoarchitectonic atlas of the hypothalamus [PALKOVITS in preparation]. The blood supply of the medial hypothalamic nuclei (NVM, NDM, NPF) was investigated systematically.

Results

The term “medial hypothalamus” usually refers to the rostro-caudal middle part of the hypothalamus. This corresponds to what is termed the pars tuberalis in another terminology. In front of it is the anterior hypothalamus (pars optica), from behind it is bordered by the premammillary region. It consists of a medial and lateral part. The latter is situated lateral to the vertical plane through the fornix and comprises the medial forebrain bundle with its enclosed cell groups.

Within the medial hypothalamus the basally located arcuate nucleus and median eminence are distinguished as the medial-basal hypothalamus from the ventromedial, dorsomedial and perifornical nuclei situated dorso-laterally.

From the cytoarchitectonic aspect the ventromedial and dorsomedial nuclei can be subdivided (PALKOVITS, in preparation). Six subdivisions can be distinguished in the ventromedial and three in the dorsomedial nucleus. The anterior cell group of the NVM is the most prominent (NVMA). Rostrally there is a medial (NVMma) central (NVMc) and lateral (NVMla) subdivision whereas caudally only medial (NVMmp) and lateral (NVMlp) subdivisions can be found. The dorsomedial nucleus contains in the dorso-ventral direction the dorsal (NDMd), central (NDMc) and ventral (NDMv) subdivisions. The perifornical nucleus, homogeneous in cell density, is situated above the fornix (Figs 5D, 5E).

Arterial input to the medial hypothalamus

The medial hypothalamus is supplied by the tuberal arteries. These arise from the internal carotid artery or from the hypophyseal and posterior cerebral arteries. They enter the hypothalamus from the base of the brain 1000—1200 μ laterally from the midline. Tuberal branches are given off also by the hypophyseal arteries but their contribution to the blood supply of the NVM is negligible. The more important tuberal branches are as follows (Figs 1A—D, 2).

Middle hypothalamic artery issuing from the internal carotid at a distance of 3500 μ behind the bregma. It forms an arch running an antero-medial course, and at a length of approx. 1.5 mm it enters the diencephalon between the internal carotid and anterior hypophyseal arteries. At the point of entry a thin branch directed antero-laterally emerges from the trunk contributing to the blood supply of the pretuberal part of the supraoptic nucleus (NSO) [2]. The trunk runs on the side of the NVM to the top of this nucleus where it divides into terminal branches. Occasionally, this artery comes from the initial part of the anterior hypothalamic artery (Figs 1A, 2).

The *anterior tuberal artery* emerges from the initial part of the anterior hypothalamic, in some cases from the internal carotid arteries. It passes upwards 2500—2600 μ behind the bregma between the anterior ventromedial and subfornical nuclei and divides into terminal branches near the NVMc (Figs 1B, 2).

A branch of the internal carotid is the *middle tuberal artery*. It enters the hypothalamus 3500 μ from the bregma behind the entry of the middle hypophyseal artery. It runs on the outer side of the postero-lateral part of the ventromedial nucleus to reach the dorsomedial nucleus. Just before its entry into the brain this artery gives off 3—4 branches which penetrate the brain at the bifurcation of the internal carotid and posterior cerebral arteries. The branches supply the MFB (Figs 1C, 2, 4B).

The *posterior tuberal artery* is in most cases an independent branch of the posterior cerebral artery but sometimes it originates from the internal carotid as a trunk common with the posterior hypophyseal artery. From its origin (4200 μ behind the bregma) it runs medialwards and then shortly divides into several branches. The side ones (*rr. posterolaterales*) contribute to the supply of the MFB, whereas those directed medialwards (*rr. posteromediales*) run to the premammillary region. The trunk proper lies initially on the base of the brain then enters it at a postbregmal distance of 3500 μ and either through or below the fornix it runs to the NDM. Along its course it lies medial to the parallel veins. It divides within or just before the NDM (Figs 1D, 2, 4C.)

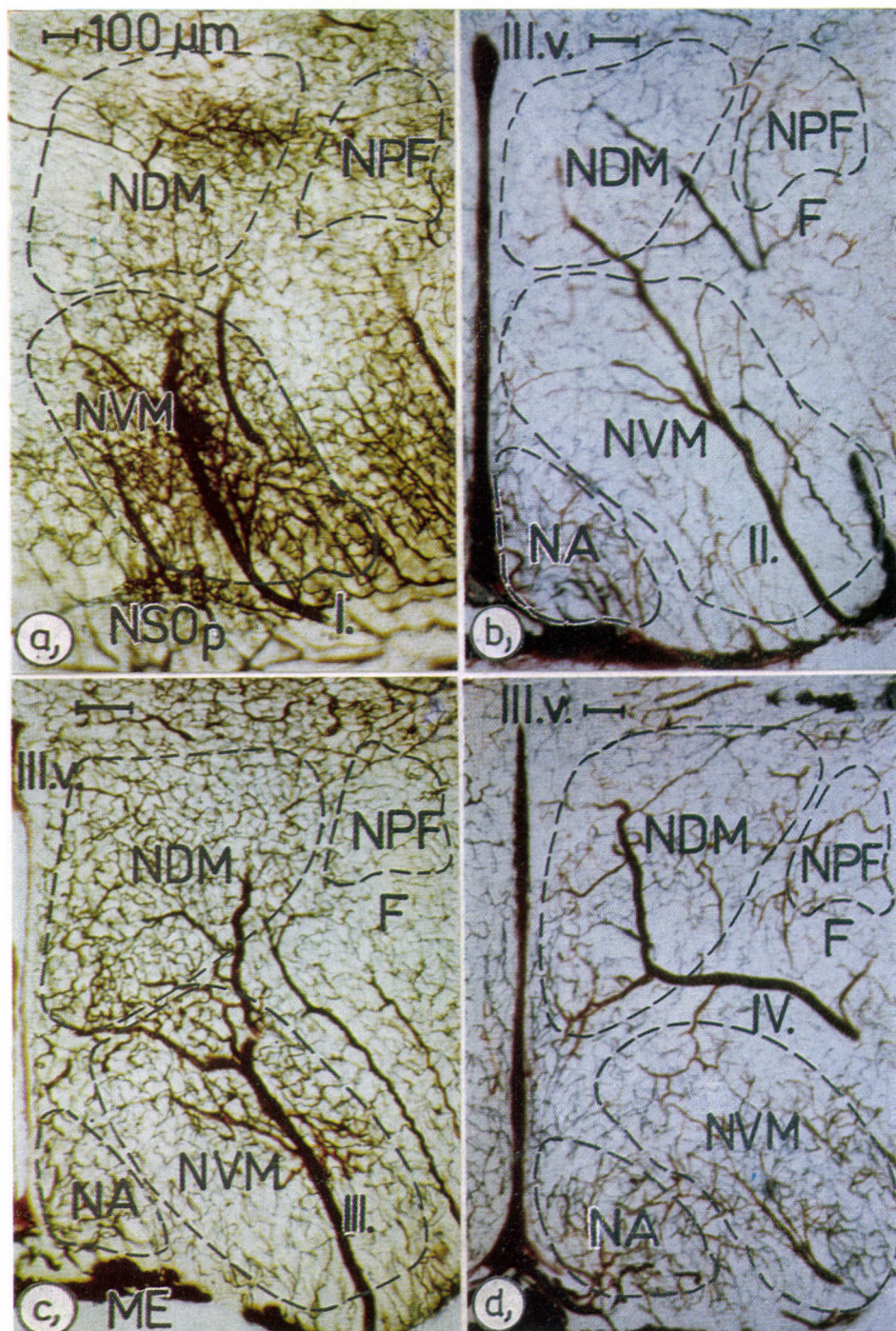


Fig. 1. Arteries of the middle part of the hypothalamus. *a* = middle hypothalamic artery, 400 μ section in the sagittal plane; *b* = anterior tubular artery; *c* = middle tubular artery; *d* = posterior tubular artery in a 300 μ frontal section. *Abbr.*: see Table I and list of Abbreviations

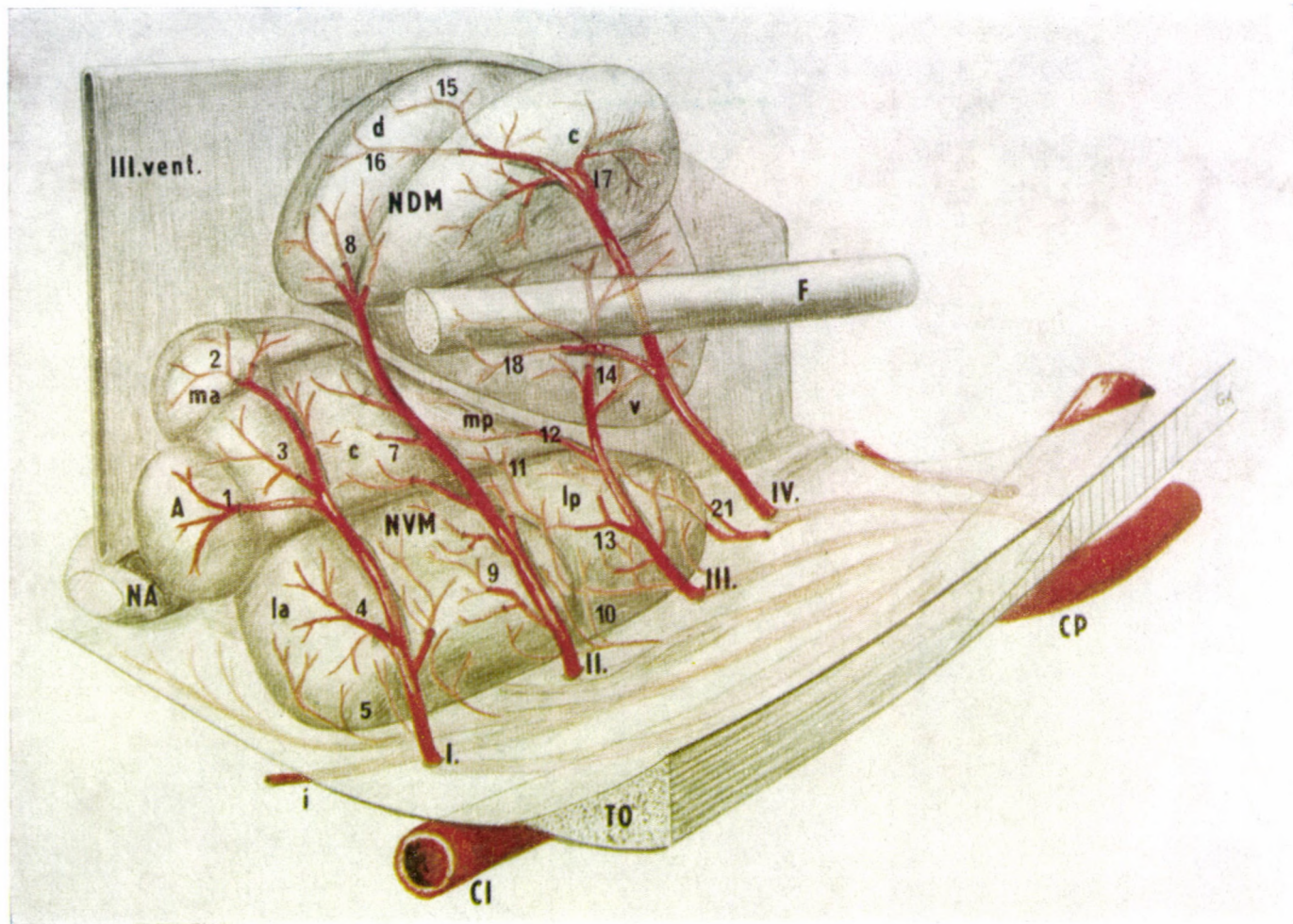


Fig. 2. Arterial supply of the dorsomedial and ventromedial nuclei. *Abbr.*: see Table I and list of Abbreviations

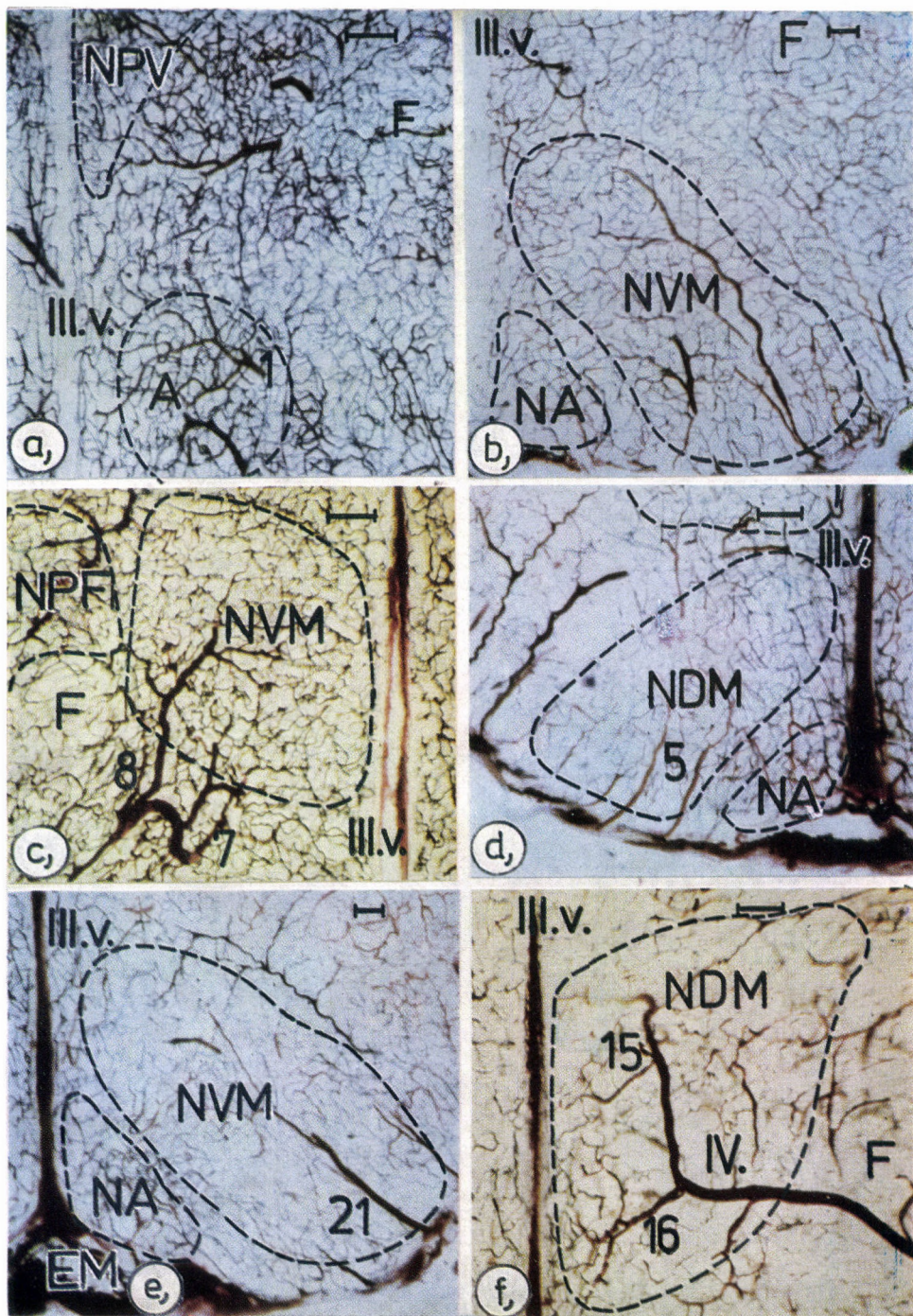


Fig. 3. Arteries of the ventromedial nucleus. *a* = 300 μ frontal section behind the paraventricular nucleus; *b* = oblique frontal section at the level of the middle hypothalamic artery; *c* = terminal branches of the anterior tuberal artery; *d* = small terminal branches of the ventromedial nucleus of the anterior hypophyseal artery; *e* = arteries of the pars lateralis posterior of the ventromedial nucleus; *f* = terminal ramifications of the main artery of the dorsomedial nucleus. *Abbr.*: see Table I and list of Abbreviations

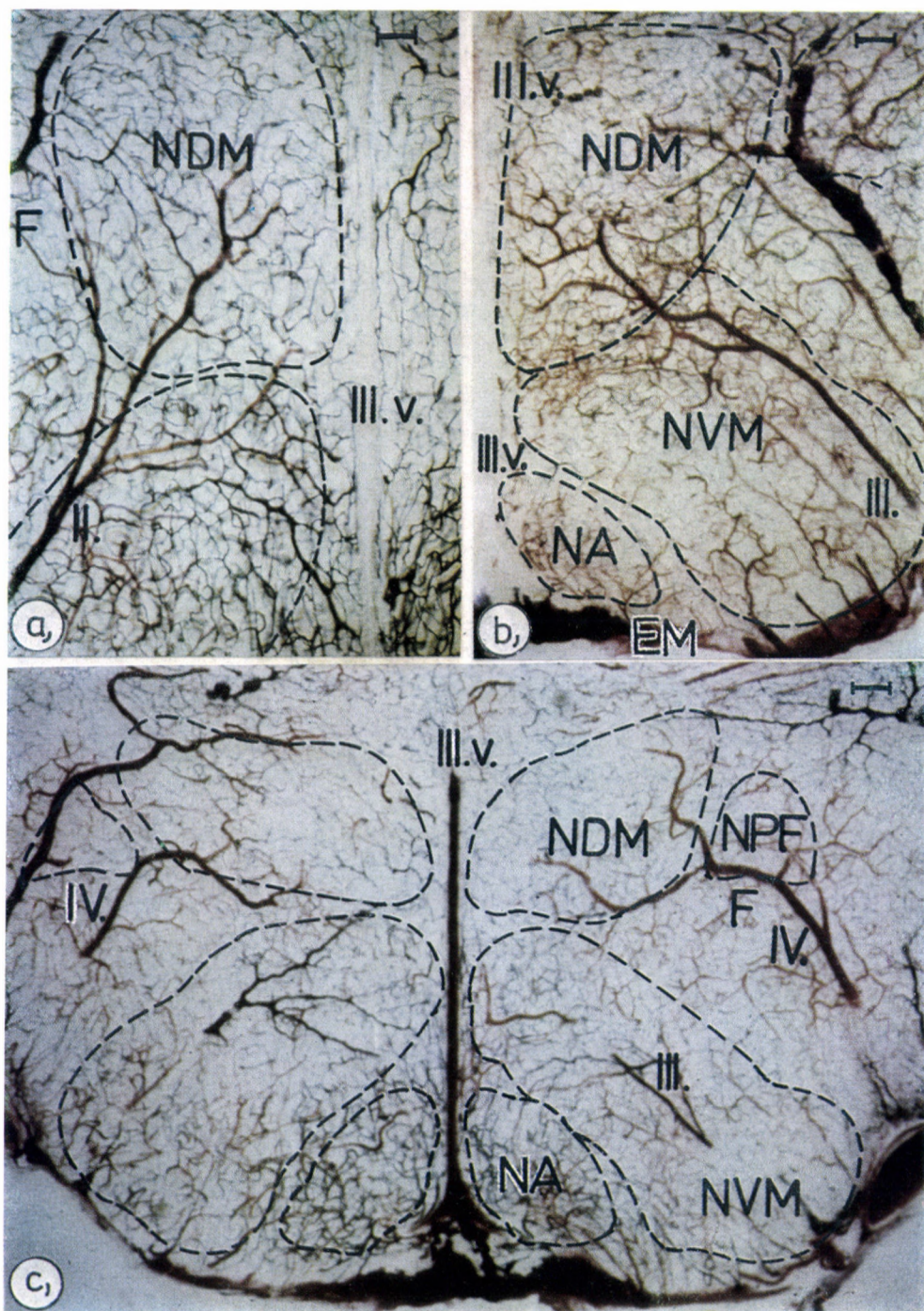


Fig. 4. Arteries of the dorsomedial nucleus. *a* = terminal branch of the anterior tuberal artery; *b* = branches of the middle tuberal artery; *c* = ramifications of the posterior tuberal artery. Abbr.: see Table I and list of Abbreviations

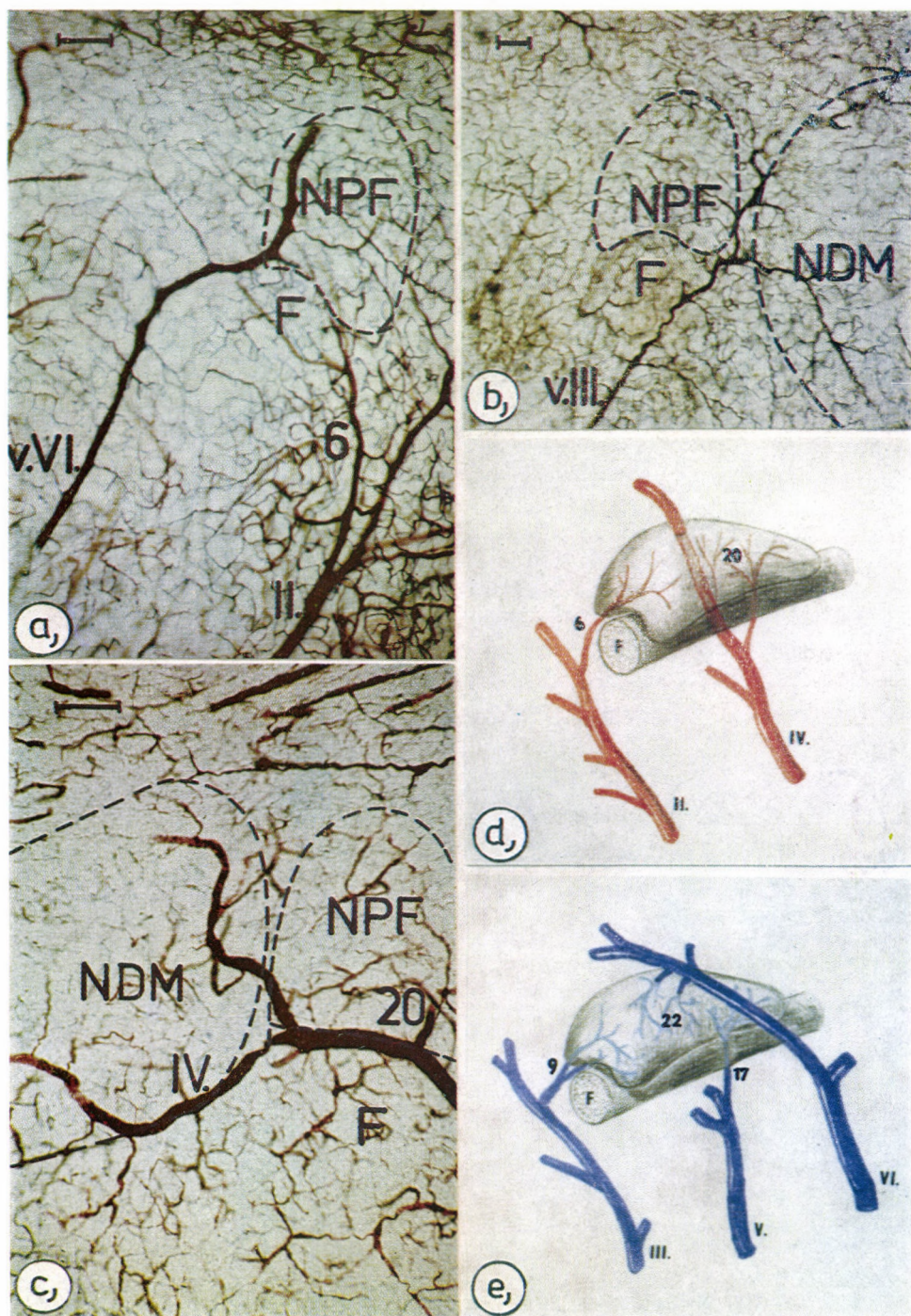


Fig. 5. Arteries and veins of the perifornical nucleus. a, b and c = 400 μ frontal sections; d = arteries of the perifornical nucleus; e = veins of the perifornical nucleus. Abbr.: see Tables I and II and list of Abbreviations

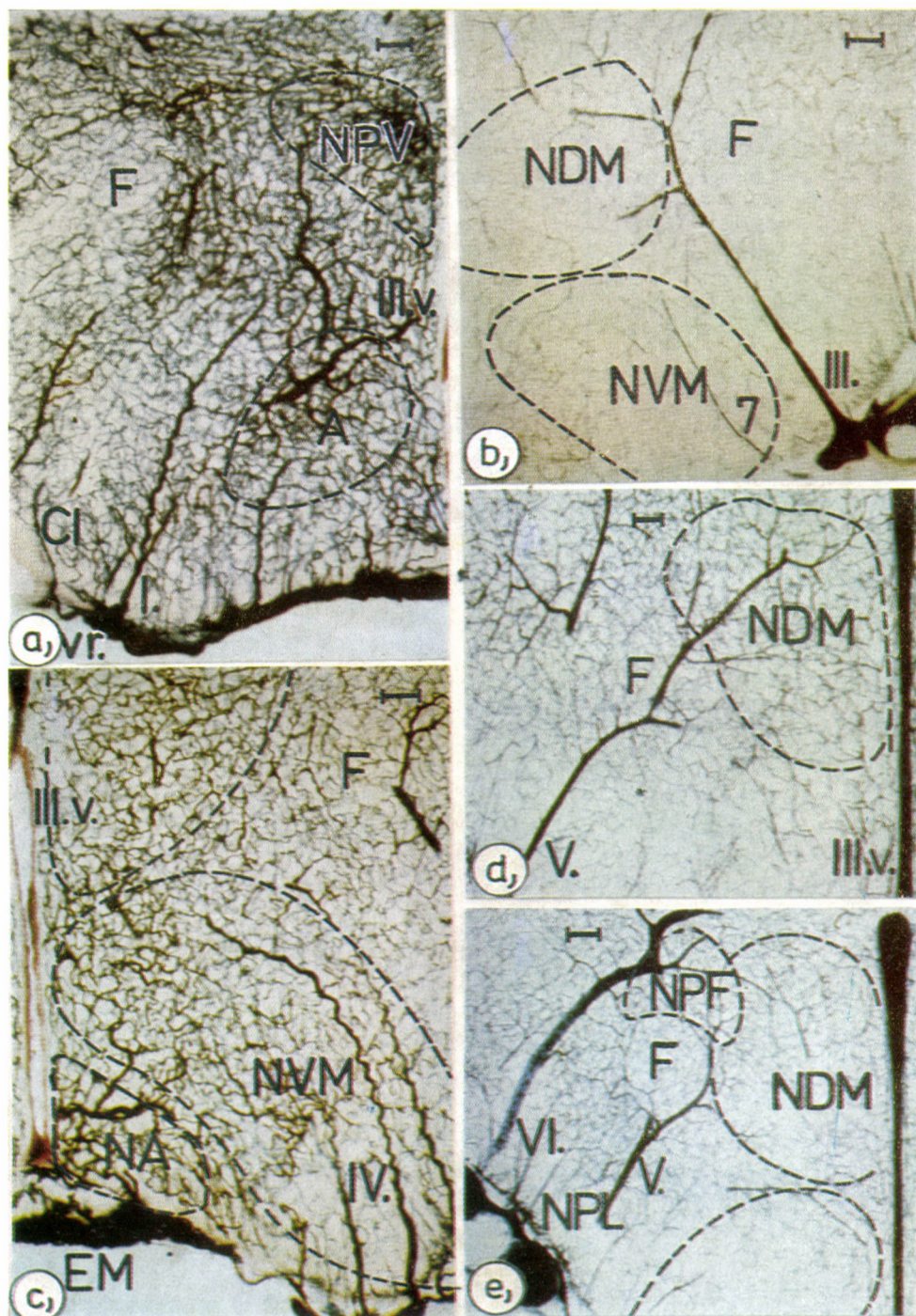


Fig. 6. a—e = veins of the middle part of the hypothalamus. 300 μ frontal sections. Abbr.: see Table II and list of Abbreviations

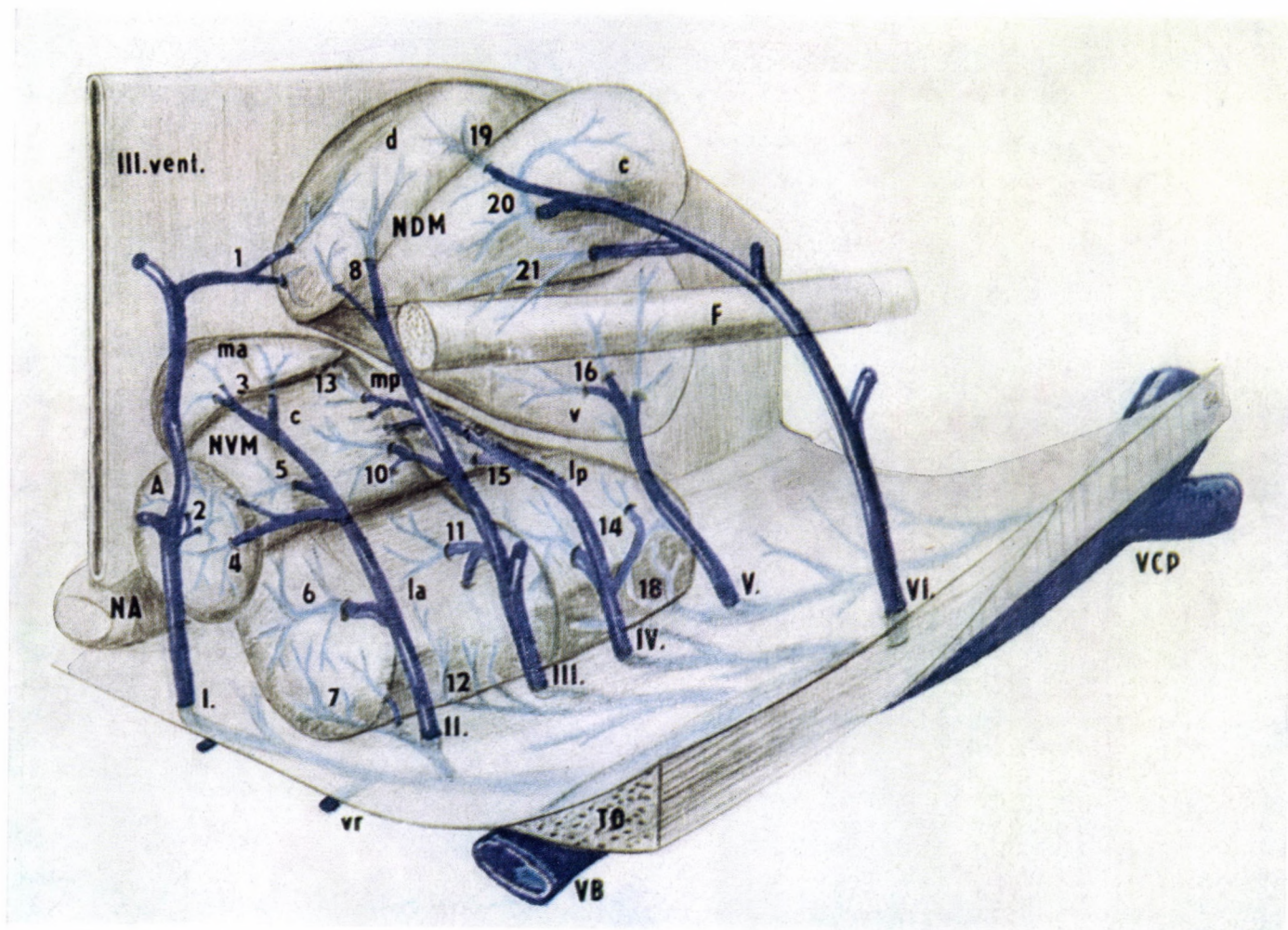


Fig. 7. Veins of the dorsomedial and ventromedial nuclei. *Abbr.*: see Table II and list of Abbreviations

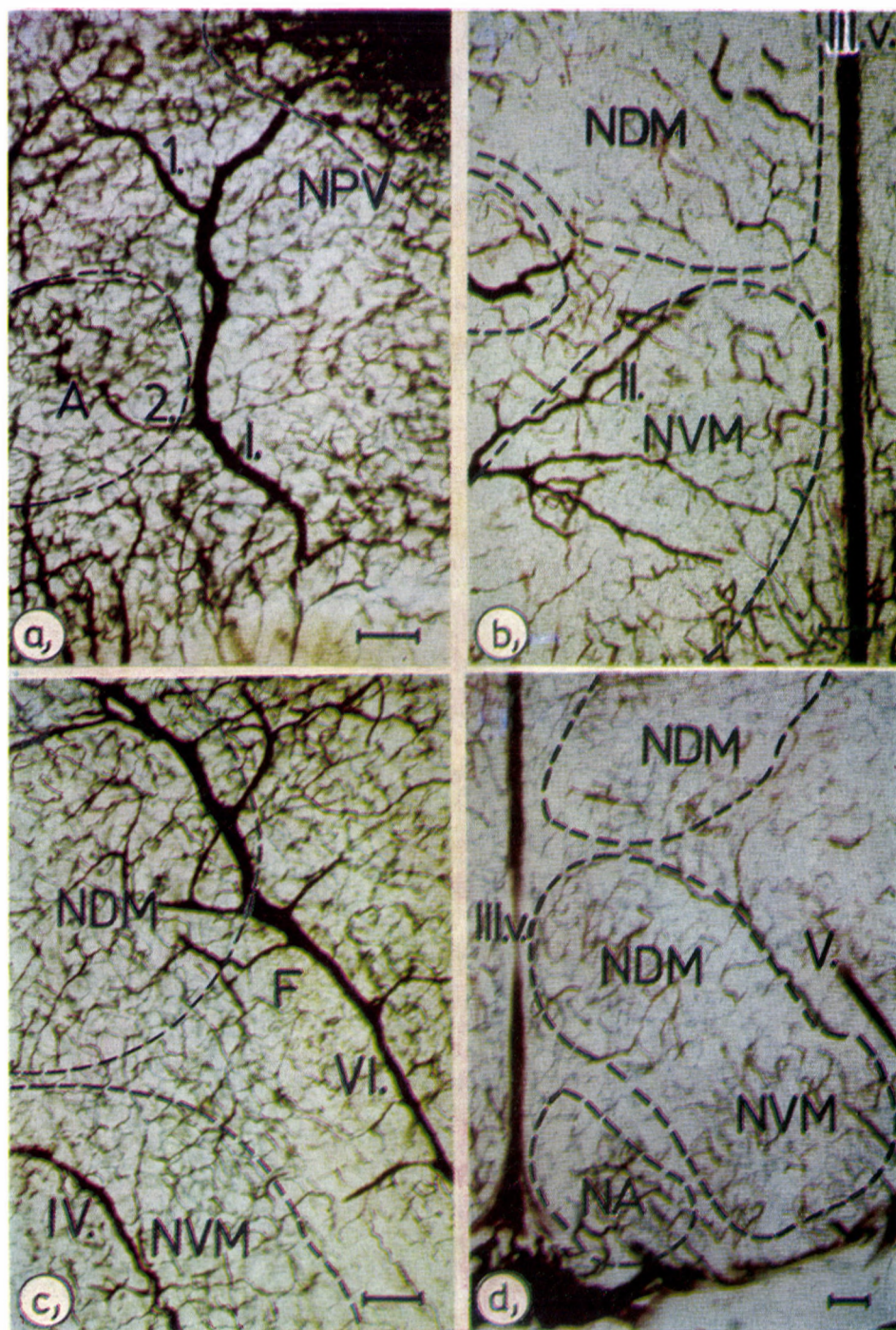


Fig. 8. *a* = the posterior hypothalamic vein and its tributaries. 400 μ sagittal section; *b*, *c* and *d* = veins of the dorsomedial and ventromedial nuclei in a 300 μ frontal section.
Abbr.: see Table II and list of Abbreviations

Arteries of the ventromedial nucleus (Table I)

The artery of the *anterior ventromedial nucleus* (NVMA) (1800—2100 μ) is a branch (*r. anterior*) of the middle hypothalamic artery. It penetrates the NVMA from behind and bifurcates in the core of the nucleus (Figs 2, 3A). In a few cases, this nucleus receives small arteries also from below *via* the tuberal branches of the anterior hypothalamic artery.

The *pars medialis anterior of the ventromedial nucleus* (NVMma) is supplied by the middle hypothalamic artery. It enters the nucleus from lateral and divides into three branches (*rr. superiores*). In one-third of the animals studied, one of these branches constituted the posterior artery to the NVMA (Figs 2, 3B).

The *pars centralis of the ventromedial nucleus* (NVMc) has two arteries. The narrow frontal zone (between 2100—2400 μ) gets two laterally entering branches (*rr. centrales anteriores*) from the middle hypothalamic artery. The major, caudal, portion of the nucleus is supplied by the anterior tuberal artery which divides either in the outer third of the NVMc or beside the nucleus. Among its branches the 2—3 (*rr. centrales posteriores*) are the most pronounced, running and dividing further from lateral towards the ventricle (Figs 2, 3C).

The *pars medialis posterior of the ventromedial nucleus* (NVMmp) receives blood in its upper two-third through a branch of the middle tuberal artery (*r. medialis posterior*) entering the nucleus from lateral. The lower third is reached from below by one or two branches of the same artery arising on the base of the brain (Fig. 2).

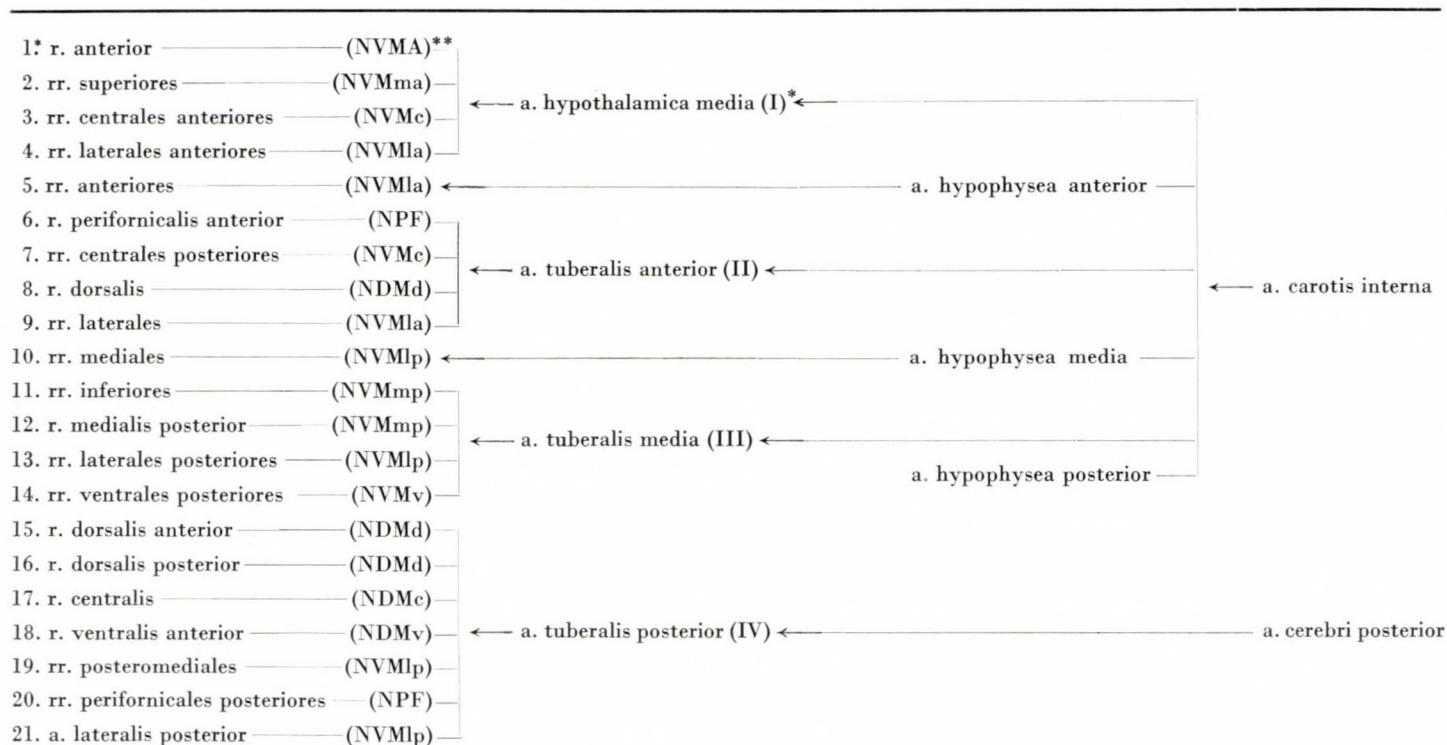
Similarly as the posterior part the blood supply of the *pars lateralis anterior of the ventromedial nucleus* (NVMla) is multilateral with overlapping fields (Figs 2, 3B). 1) The middle hypothalamic artery provides the *rr. laterales anteriores* (2100—2400 μ). 2) The short branches of the anterior tuberal artery (*rr. laterales*) cover the area between 2400—2600 μ . 3) From below the small branches of the anterior hypophyseal artery (*rr. anteriores*) enter the nucleus at 800—1000 μ from the midline before the infundibular branches.

The anterior part of the *pars lateralis posterior of the ventromedial nucleus* (NVMlp) receives its arterial supply from lateral through the branches of the middle tuberal artery (*rr. laterales posteriores*) running upwards from the base from the posterior tuberal artery, then bifurcating and reaching the nucleus at its ventromedial side (Fig. 3F). Finally, to supply the premammillary region, small branches called the *rr. posterolaterales* enter from below and cover also the posterior medial part of the NVMlp.

Arteries of the dorsomedial nucleus (Table I)

Each subdivision of the NDM receives a separate branch mainly from the posterior tuberal artery. There is, however, a considerable overlap between the terminal supply territories.

Table I

Arteries of the ventromedial, dorsomedial and perifornical nuclei

* The roman and Arabic numerals stand for identification of the branches in the Figure

** Subdivisions supplied by the branches. *Abbr.* see in text

The *pars dorsalis of the dorsomedial nucleus* (NDMd) gets a branch (*r. dorsalis*) of the anterior tuberal artery running an upward course on the side of the NVMc between the medial forebrain bundle and the NVMla. Its divisions occur in the frontal part (2400—2700 μ) of the nucleus (Figs 1B, 2). To the NDMd, the posterior tuberal artery gives usually two branches, in the back two-thirds of the nucleus the ramifications of the *r. dorsalis posterior*, in front those of the *r. dorsalis anterior* are found (Figs 2, 3F).

The *pars centralis of the dorsomedial nucleus* (NDMc) comprises the main terminal territory of the posterior tuberal artery. Mostly a strong branch, the *r. centralis*, reaches the pars centralis from its side and supplies it after a regular bifurcation (Figs 2, 4C). In the rostral area of the pars centralis a few terminal branches of the *r. dorsalis* of the anterior tuberal artery are found.

The *pars ventralis of the dorsomedial nucleus* (NDMv) receives in its rostral part a branch (*r. ventralis anterior*) of the posterior tuberal artery (Figs 2, 4C). The rest of the nucleus is supplied by those 2—3 branches (*rr. ventrales posteriores*) of the middle tuberal artery that pass backward above the NVMmp.

Arteries of the perifornical nucleus (NPF)

The *r. perifornicalis anterior* is coming from antero-medial to the NPF, given off by the anterior tuberal artery (Figs 5A, 5D). A more important source of arterial supply to this nucleus is the posterior tuberal artery which passes through the nucleus over the fornix. Usually, two branches (*rr. perifornicales posteriores*) run to the NPF (Figs 5C, 5D).

Veins

The blood of the tuberal nuclei is collected by the veins of the basis such as the retrochiasmatic, the anterior, middle and posterior tuberal veins (Table II). The veins on the base of the brain pass lateralwards and drain the blood into the basal vein [1]. The main veins of the medial hypothalamus are as follows.

The *posteromedial hypothalamic vein* is formed lateral to the caudal edge of the paraventricular nucleus by the posterolateral paraventricular branches and the anterior vein of the anterior nucleus of the NDM. It passes towards the base between the anterior hypothalamic nucleus and NVM receiving branches from both nuclei. On the base it drains the blood into the retrochiasmatic vein (Figs 6A, 7, 8A) 700—800 μ from the midline and approximately 1600 μ behind the bregma.

The *middle hypothalamic vein* runs downward on the lateral side of the

anterior part of the NVM. It reaches the base at 2200–2300 μ where it ends either in the retrochiasmatic vein or in a basal branch of the latter, the anterior tuberal vein (Figs 6B, 7).

The *anterior ventromedial vein* emerges at the border of the NVMma and NVMmp and passes downward on the lateral side of the NVMc. This is an important vein whose uppermost branch arises in the NDMd, then runs between the fornix and NVM collecting veins from the periventricular and ventromedial nuclei and from the medial forebrain bundle. At 2500 μ behind the bregma it reaches the base of the brain and ends in one of the middle tuberal veins (Figs 6C, 7).

The *middle ventromedial vein* is thinner than the former one and runs medialward behind it along the NVMmp to the base (Figs 6D, 7). There it ends in one of the middle tuberal veins 2700–2800 μ behind the bregma. At a post-bregmal distance of 3000–3500 μ a long vein, the *posterior ventromedial* connects the NDMv with the posterior tuberal vein running at its beginning near the posterior edge of the NVMmp then on the side of the NVMIp (Figs 6E, 7).

The *posterolateral hypothalamic vein* is the outermost vein of the tuberal nuclei and the main venous drainage of the NDM. After turning from behind around the fornix, it pursues a course towards the base of the brain and at 3000 μ it drains the blood into the basal vein (Figs 6E, 7). It receives branches from above the fornix and some negligible ones from the ventral thalamus and contributes to the drainage of the NPF. The lateral subfornical branches issue from the lateral hypothalamus.

Veins of the ventromedial nucleus (Table II)

The venous drainage of the NVMA is bidirectional. From its core a thin branch, *r. anterior minor*, is directed towards the posteromedial hypothalamic vein that passes in front of the nucleus. From the posterior part of the nucleus a thicker branch, *r. posterior major*, is formed running backwards and lateralwards into the middle hypothalamic vein (Figs 7, 8A).

Those 3–4 branches (*rr. mediales anteriores*) collecting in the NVMma are the only veins of this area. They run towards the lateral edge of the nucleus where they unite to form the middle hypothalamic vein (Figs 7, 8B).

From the NVMc blood is drained in three directions. From the anterior part the *r. centralis anterior* collects several small branches and passes lateralwards at the side of the nucleus into the middle hypothalamic vein. From the lower two-thirds of the pars centralis, usually 2–3 branches (*rr. centrales mediae*) and lateralwards in the anterior ventromedial vein. From the upper dorsal part of the NVMc the *rr. centrales posteriores* come usually together in a com-

mon trunk that ends in the middle ventromedial vein. Rarely the back branches turn to dorsolateral and drain the blood into the posterior ventromedial vein (Fig. 7).

From the NVMmp 3—4 branches, *rr. mediales posteriores* emerge. The front ones are thicker and run into the middle ventromedial, the back ones into the posterior ventromedial veins.

A bidirectional drainage can be observed from the NVMLa and NVMLp. Thin branches run to the base, ending in the tuberal veins. The lateral branches fuse with the successive veins (Fig. 7). From the anterior part of the NVMLa 2—3 thin branches (*rr. inferiores anteriores*) run into the anterior tuberal vein whereas the lower ones are collected by a thicker, laterally directed branch (*r. lateralis anterior*) ending in the middle hypothalamic vein. The posterior part of the NVMLa gives rise to the inferior branches (*rr. inferiores mediae*) draining the blood into the middle tuberal veins. The lateral branches (*rr. laterales*) unite with the anterior ventromedial vein. The small *rr. inferiores posteriores* that run from the NVMLp to the base of the brain are the branches of the posterior tuberal vein (Fig. 7). The *rr. laterales posteriores* emerging from the front two-thirds of the nucleus unite with the middle ventromedial vein passing near this nucleus.

Veins of the dorsomedial nucleus (Table II)

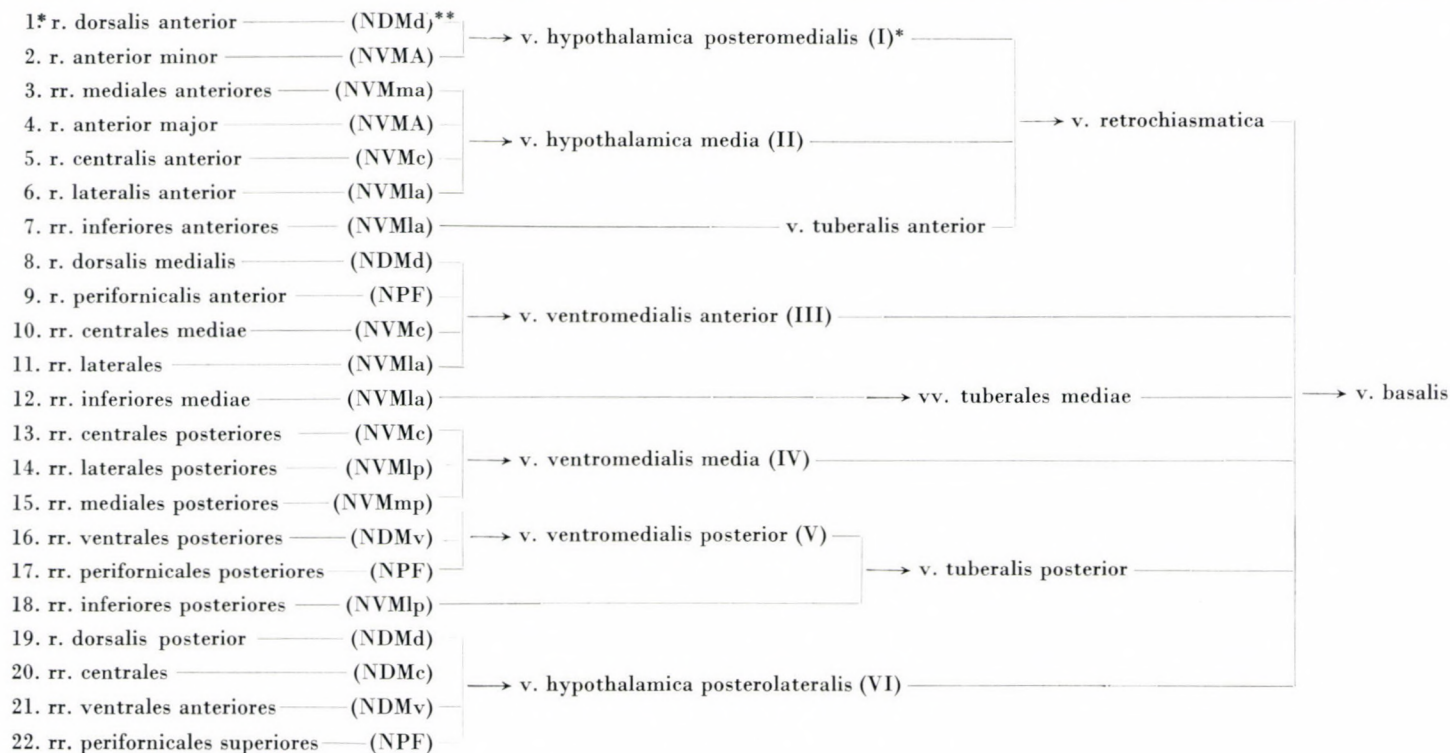
The NDMd is drained by three veins (Fig. 7). 1) From the anterior part the *r. dorsalis anterior* passes antero-laterally ending in the posteromedial hypothalamic vein. 2) The middle third is drained by 2—3 branches uniting in the *r. dorsalis medialis* to form the initial part of the anterior ventromedial vein. 3) At the posterior end of the dorsal part emerges the slender *r. dorsalis posterior* which runs lateralwards into the posterolateral hypothalamic vein.

From the NDMc usually two branches come (*rr. centrales*) that unite with the *r. dorsalis posterior* near the nucleus. The NDMv gives rise to several branches. The *rr. ventrales anteriores* come from the front and drain their blood into the posterolateral hypothalamic vein. The thicker hind branches, *rr. ventrales posteriores* run a downward course to reach the posterior ventromedial vein (Figs 6B, 7, 8C—D).

Veins of the perifornical nucleus (Table II)

From the anterior part of the NPF emerges the *r. perifornicalis anterior* running medial to the fornix into the anterior ventromedial vein (Figs 5B, 5E). The major part of this nucleus is drained by the *rr. perifornicales superiores*, the branches of the posterolateral hypothalamic vein (Fig. 5A). From the core of the nucleus they pass ventrolaterally, ending in the vein near the nucleus.

Table II

Veins of the ventromedial, dorsomedial and perifornical nuclei

* The roman and Arabic numerals stand for identification of the branches in the Figure

** Subdivisions supplied by the branches. *Abbr.* see in text

The small branches, *rr. perifornicales posteriores* drain the posterior part of the NPF into the posterior ventromedial vein (Fig. 5E).

Discussion

Data concerning the blood supply of the medial hypothalamus are not comprehensive. The vessels entering from the base of the brain have been described in the rat [1, 6, 7, 10, 12, 13], rabbit [8, 9, 11] and cat [1, 7, 10] but their further tracing and the elucidation of their contribution to the blood supply of the nuclei has not been accomplished.

As far as volume and cell number are concerned, the ventromedial and dorsomedial nuclei are encountered as large hypothalamic nuclei. Their physiological role has been investigated extensively. A knowledge of their blood supply might be relevant to the function and experimental surgery of this area. From the present studies the following conclusions have been drawn.

(i) As it has been observed earlier [5], the vessels supplying the medial basal hypothalamus (arcuate and ventromedial nuclei) have a terminal territory different from that of the dorsal nuclei with practically no vascular link between them. The veins of the ventromedial and dorsomedial nuclei do not drain the blood into the portal vessels of the median eminence.

(ii) The ventromedial, dorsomedial and perifornical nuclei have an independent arterial supply. In most cases, the subdivisions of these nuclei have their own arteries with a minimum of overlap between their supply territories of.

(iii) The medial and central parts of the ventromedial nucleus are poorly vascularized, whereas the lateral subdivisions are more abundantly supplied by receiving arteries from the basis.

(iv) The ventromedial nucleus receives small branches also from the hypophyseal arteries. These issue lateral from the median eminence before the infundibular branches.

(v) All the three subdivisions of the dorsomedial nucleus have their own arteries.

(vi) With regard to its blood supply, the perifornical nucleus appears to belong to the medial hypothalamus by receiving its main arteries from the posterior tuberal artery.

(vii) Although the ventromedial and dorsomedial nuclei can be distinguished by their blood supply patterns, their arterial trunks, the anterior and middle tuberal arteries, are common.

(viii) The medial hypothalamus has no significant vascular link with the structures located dorsally (thalamus), and its drainage is directed downward. All the veins are collected on the basis by the tuberal veins formed from their tributaries lateral to the median eminence.

Abbreviations

a	—	artery
CI	—	a. carotis interna
CP	—	a. cerebri posterior
EM	—	eminentia mediana
F	—	fornix
i	—	a. infrachiasmatica
NA	—	nucleus arcuatus
NDM	—	nucleus dorsomedialis
NDMc	—	nucleus dorsomedialis, pars centralis
NDMd	—	nucleus dorsomedialis, pars dorsalis
NDMv	—	nucleus dorsomedialis, pars ventralis
NPF	—	nucleus perifornicalis
NPV	—	nucleus paraventricularis
NSF	—	nucleus subfornicalis
NSOp	—	nucleus supraopticus, pars posterior
NVM	—	nucleus ventromedialis
NVMA	—	nucleus ventromedialis, pars anterior
NVMC	—	nucleus ventromedialis, pars centralis
NVMla	—	nucleus ventromedialis, pars lateralis anterior
NVMlp	—	nucleus ventromedialis, pars lateralis posterior
NVMma	—	nucleus ventromedialis, pars medialis anterior
NVMmp	—	nucleus ventromedialis, pars medialis posterior
TO	—	tractus opticus
V	—	vein
vB	—	v. basalis
vCP	—	v. cerebri posterior
vr	—	v. retrochiasmatica
III.V	—	ventriculus tertius

REFERENCES

1. AKMAYEV, I. G.: (1971) Morphological aspects of the hypothalamic-hypophyseal system. III. Vascularity of the hypothalamus, with special reference to its quantitative aspects. *Z. Zellforsch.* **116**, 195—204. — 2. AMBACH, G., PALKOVITS, M.: (1974) Blood supply of the rat hypothalamus I. Nucleus supraopticus. *Acta morph. Acad. Sci. hung.* **22**, 291—310. — 3. AMBACH, G., PALKOVITS, M.: (1974) Blood supply of the rat hypothalamus II. Nucleus paraventricularis. *Acta morph. Acad. Sci. hung.* **22**, 311—320. — 4. AMBACH, G., PALKOVITS, M.: (1975) Blood supply of the rat hypothalamus III. Anterior region of the hypothalamus (Nucleus suprachiasmaticus, nucleus hypothalamicus anterior, nucleus periventricularis). *Acta morph. Acad. Sci. hung.* **23**, 21—49. — 5. AMBACH, G., PALKOVITS, M., and SZENTÁGOTAI, J.: Blood supply of the rat hypothalamus. IV. Area retrochiasmatica. (1976) median eminence, arcuate nucleus. *Acta morph. Acad. Sci. hung.* **24**, 93—119. — 6. CRAIGIE, E. H.: (1940) Measurements of vascularity in some hypothalamic nuclei of the albino rat. *Res. Publ. Ass. nerv. ment. Dis.* **20**, 310—319. — 7. DANIEL, P. M., PRICHARD, M. L.: (1975) Studies of the hypothalamus and the pituitary gland, with special reference to the effects of transection of the pituitary stalk. *Acta Endocr. (Kbh.)* **80**, Suppl. 201. — 8. HASEGAWA, K.: (1954) On the vascular supply of the hypophysis and of the hypothalamus of rabbits. I. The arterial supply. *Fukuoka Acta med.* **45**, 430—437. — 9. HASEGAWA, K.: (1954) On the vascular supply of the hypophysis and of the hypothalamus of rabbits. II. On the systemic and the portal veins. *Fukuoka Acta med.* **45**, 504—511. — 10. LIERSE, W.: (1963) Über die Beeinflussung der Hirnangioarchitektur durch die Morphogenese. *Acta anat. (Basel)* **53**, 1—54. — 11. PROLO, D. J., STILWELL, D. L.: (1962) Arterial supply of the diencephalon and some associated areas of the rabbit brain. *J. comp. Neurol.* **119**, 229—254. — 12. SCREMIN, O. U.: (1970) The vascular anatomy of the rat's hypothalamus in stereotaxic coordinates. *J. comp. Neurol.* **139**, 31—52. — 13. SPENGLER, J., HUBER, P.: (1959) Topographische Beziehungen zwischen neurosekretorischen Ganglienzellen und arteriellen Gefäßen in Ratten-Hypothalamus. *Pflügers Arch. ges. Physiol.* **269**, 31—37.

**DIE BLUTVERSORGUNG DES HYPOTHALAMUS BEI RATTEN. V.
DER MEDIANE HYPOTHALAMUS (NUCLEUS VENTROMEDIALIS,
NUCLEUS DORSOMEDIALIS, NUCLEUS PERIFORNICALIS)**

G. AMBACH und M. PALKOVITS

Die Gefäßtopographie in dem aus Serienschritten rekonstruierten mittleren Hypothalamusgebiet von Ratten wurde mit doppelter Tuscheauffüllung untersucht. Das untersuchte Gebiet umfaßt den Nucleus ventromedialis, den N. dorsomedialis und den N. perifornicalis. Es wird durch die A. hypothalamica media, die A. tuberalis anterior, media und posterior mit Blut versorgt. Eine venöse Ableitung geht nur in ventraler Richtung vor sich: die Vv. ventromedialis, anterior, media und posterior, ferner die V. hypothalamica posteromedialis und posterolateralis münden in die V. basalis.

Die den N. ventromedialis und den N. dorsomedialis versorgenden Arterien sind von den N. arcuatus und die Eminentia mediana versorgenden Arterien scharf abgegrenzt und ihr venöses Blut steht mit den portalen Gefäßen in keinem Zusammenhang. Die untersuchten Nuclei und sogar ihre Subdivisionen verfügen über selbständige Arterien, deren Versorgungsbereiche mit gewisser Überlappung sich voneinander gut absondern lassen. Die Topographie dieser Arterien wird eingehend besprochen.

Der mediale Hypothalamus hat mit den anderen Gebieten des Dienzephalons, auch den unmittelbar dorsal von ihm gelegenen Thalamus einbegriffen, keine vaskuläre Verbindung.

**КРОВΟΣНАБЖЕНИЕ ГИДРОТАЛЯМУСА У КРЫСЫ. V. СРЕДНЯЯ ГРУППА ЯДЕР
ГИПОТАЛЯМУСА (NUCLEUS VENTROMEDIALIS, NUCLEUS DORSOMEDIALIS,
NUCLEUS PERIFORNICALIS)**

Г. АМБАХ и М. ПАЛКОВИЧ

Методом двойного заполнения тушью авторы изучали у крысы топографию кровеносных сосудов средней группы ядер гипоталамуса, реконструированного из серийных срезов. Исследованная область содержит Nucleus ventromedialis, N. dorsomedialis и N. perifornicalis. Кровоснабжение этой области обеспечивается A. hypothalamica media, A. tuberalis anterior, media и posterior. Венозное отведение осуществляется только в вентральном направлении: Vv. ventromedialis, anterior, media и posterior, а также V. hypothalamica posteromedialis и posterolateralis втекают в V. basalis.

Артерии, снабжающие Nucleus ventromedialis и dorsomedialis резко обособляются от артерий, обеспечивающих кровоснабжение Nucleus arcuatus и Eminentia mediana и их венозная кровь не имеет связи с воротными сосудами. Исследованные ядра и даже их субдивизии имеют свои собственные артерии, области снабжения которых с некоторым перекрытием хорошо отграничиваемы друг от друга. Дается подробное описание топографии этих артерий.

Средняя группа ядер гипоталамуса не имеет васкулярной связи с другими областями промежуточного мозга, включая также таламус, располагающийся непосредственно дорсально от медиального гипоталамуса.

György AMBACH: H-6239 Császártöltés, Keceli út 5, Hungary

Miklós PALKOVITS: Semmelweis Orvostudományi Egyetem
I. sz. Anatómiai Intézet
H-1054 Budapest, Tűzoltó u. 58, Hungary

Institute of Forensic Medicine, and Institute of Vascular Surgery,
Semmelweis University Medical School, Budapest, Hungary

INTERMITTENT HYPOXIC LOADING: A MODEL SYSTEM TO STUDY THE EARLY STAGES OF MYOCARDIAL LESIONS

(Short communication)

E. SOMOGYI, P. SÓTONYI, A. NEMES and S. JUHÁSZ-NAGY

(Received March 3, 1978)

Authors applied the model system of intermittent hypoxic loading to study the development of early myocardial alterations. It was found that a primary role is played by the deficiency of high-energy phosphate synthesis and by the disturbance of energetic and transport processes. The change of Ca^{2+} -control, activation of anaerobic glycolysis and intracellular acidosis were found to be instrumental in decreasing contractility, impairing membranes and finally in a diffuse destruction of myofilaments

Recent efforts to clarify the molecular basis of early hypoxic changes of the myocardium provided data that question current views and inspire the formulation of new ones [1–5, 8–17, 19, 20, 22]. The study of early or initial myocardial alterations constitute an essential problem in the research of myocardial hypoxia. With the model systems available serious difficulties emerge when this question has to be investigated. It can be, of course, argued that the different agents damaging heart muscle cells and causing thereby hypoxia may have different targets. Evidence is, however accumulating for a uniform action of the irreversibly progressive hypoxia, irrespective of its cause [18–20]. The necessity of an experimental model is underlined by the fact that it could yield informations for the clinician concerning the mechanism of myocardial insufficiency. Adequate models may serve also for the testing of methods of protection [2, 4, 5, 11].

Interruption of the coronary circulation even for a single cardiac cycle brings about a well-measurable post-occlusion reactive hyperaemia [6, 7, 19–20]. Several authors concur in the opinion that this reactive hyperaemia is the most reliable phenomenon currently available to quantitate adaptation capacity of the coronary system (Fig. 1). Inducing reactive hyperaemia the adaptation capacity of a vessel is stretched to the extreme as the adaptation reaction is driven by its strongest stimulus: the lack of oxygen. The reactive

Abbreviations

I = I-band
Z = Z-band
M = Mitochondria

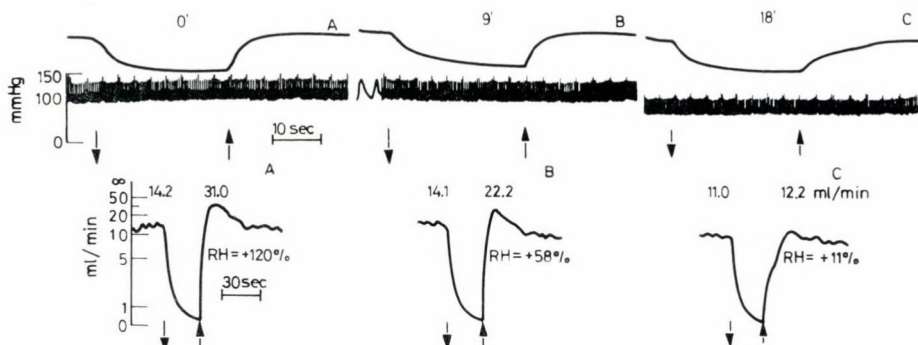


Fig. 1. Decrease of reactive hyperaemia in intermittent hypoxia tolerance test. RH: reactive hyperaemia excess. A: control state B: 9 minutes, C: 18 minutes tolerance test

hyperaemic vasodilatation is easy to reproduce. It ceases relatively soon and if carried out with caution the experimental territory can fully recover. All these justify to consider reactive hyperaemia as the best means for testing the general reactivity of coronaries.

The adaptation disturbance of the coronaries can be induced by interferences exhausting the capacity for adaptation. One of these is the selective exhaustion of the myocardium by prolonged or periodic hypoxia. Similar factors may be instrumental after circulatory arrest for heart operations in causing adaptation disturbances in young patients with intact coronary circulation.

In our experience intermittent hypoxic loading results in myocardial alterations characteristic for angina pectoris. From this aspect angina pectoris can be regarded as an exhaustion of adaptation capacity of the coronaries against hypoxia.

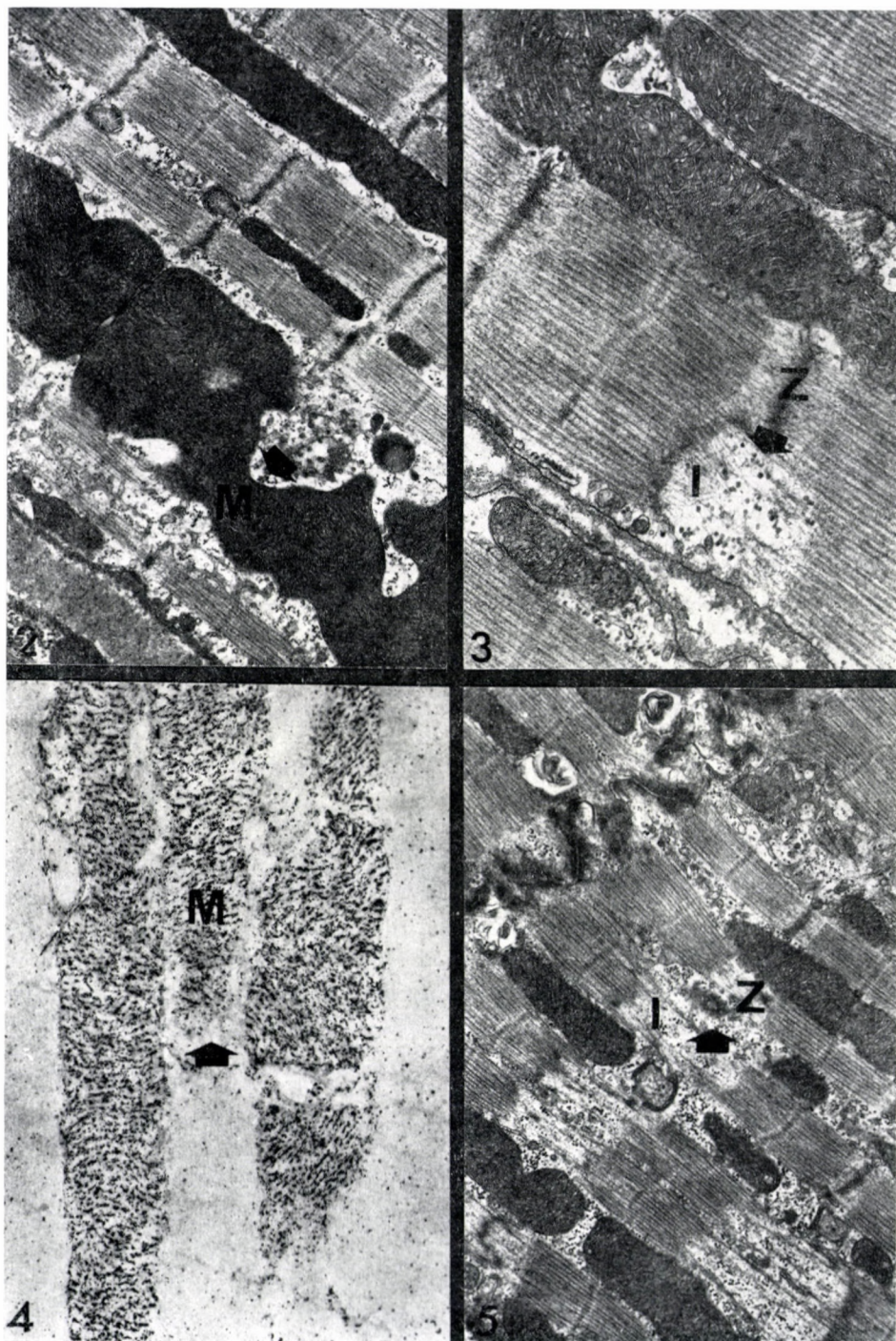
The blood supply of the heart cannot be characterized with one single parameter of coronary circulation. The possible reserves of adaptation-capacity are unknown. The "biological value" of blood supply of the myocardium is not determined by the actual volume of streaming but rather by the inherent sensitivity of the vascular system to oxygen deprivation. Parallel to the decrease of reactive hyperaemic responses various forms of structural and functional alterations develop (Figs 2–5). Methods to study the postadaptation state of coronaries can be applied according to their sensitivity.

Fig. 2. After 9 minutes intermittent hypoxia some mitochondria showed an end-to-end fusion. 17,000 ×

Fig. 3. The arrow points to focal destruction of I-band. 23,000 ×

Fig. 4. The cytochemical reaction showed a marked increase of calcium. 17,000 ×

Fig. 5. After 18 minutes of intermittent hypoxia, there were places of focal destruction of I-band, loss of actin filaments and irregular Z-bands. 17,000 ×



The leading factor responsible for the state after intermittent hypoxia is the disturbance of energy metabolism (ATP, CP). According to our observations, in the initial stage the change in ATP levels is not significant unlike to that in CP levels that decrease rapidly.

The change of ATP level elicits the disturbance of Ca^{2+} regulation. The sacs of the sarcoplasmic reticulum are dilatated. With electron microscopic cytochemistry a substantial increase of Ca^{2+} activated ATPase activity can be demonstrated.

It seems that the increase of intracellular calcium causes initially an ATP breakdown through an extreme activation of ATPase. Mitochondria accumulate high amounts of divalent cations. This process is energy dependent untill the electron microscopically verified destruction of mitochondrial membranes. Then it continues as a passive ion uptake. It is assumed that mitochondria act as buffers to control intracellular Ca^{2+} levels. Structural damage to mitochondria results in a further degradation of the process of phosphorylation. The increase of intracellular Ca^{2+} could be demonstrated by the electron microscopic visualization of Ca^{2+} and by the measuring of Ca^{45} uptake with liquid isotope techniques. Coinciding with the increase of intracellular Ca^{2+} characteristic alterations occur in the Z-membranes and actin filaments. The disturbance of enzyme system binding and transferring Ca^{2+} to the sarcoplasmic reticulum may also be responsible for the changes of filaments. Glycogen content decreases at a later stage as a manifestation of the enhancement of anaerobic glycolysis and a result of a shift of intracellular pH to acidic. This shift blocks the Ca^{2+} binding sites of troponine-C. This can also bring about filament alterations. According to our observations intracellular acidosis is a sign of irreversible changes leading to diffuse myocardial damage.

The reproducibility of the hypoxic model enables protective compounds to be tested. A prerequisite to counteract the effects of hypoxia is to restore energy metabolism, increase membrane stability and improve Ca^{2+} control. The increase of high-energy phosphates can be achieved by the protection and stimulation of intracellular energy production. Using our model several protective agents were tested. A typical drug of this type, Solcoseryl® (Solco., Basel) for example, proved to increase tolerance against hypoxia. The degree of osmotic swelling of mitochondria diminished, glycogen levels remained unchanged. This latter indicated that the onset of anaerobic glycolysis and concomitant intracellular acidosis was delayed. A protective effect was encountered also on energy production and conservation by a slower decrease of high-energy phosphate stores. The increase of membrane stability is of basic importance: their irreversible damage means the death of the cell. Alas, effective membrane protection cannot be performed until after the mechanism leading to membrane destruction is understood. Besides electron microscopy, polarized light microscopy seems to be a suitable means to investigate this problem.

Topo-optical reactions reveal early changes in the geometry of membrane lipoproteins. The quantitative expression of these changes may provide valuable informations about early membrane impairments. The molecular background of the mechanism of alterations in membrane function requires elucidation by future research.

REFERENCES

1. DHALLA, N. S., TOMLINSON, C. W., LEE, S. L., VARLEY, K. G., BOROWSKY, I. P., BARWINSKY, J.: (1975) Role of mitochondrial calcium transport in failing heart. In: *Basic Function of Cations in Myocardial Activity*. Edited by: Fleckenstein, A., Dhall, N. S. Urban and Schwarzenberg. Vol. 5, 177. — 2. FERRANS, J. V.: (1975) Morphological methods for evaluation of mitochondrial protection. *Ann. Thorac. Surg.* **20**, 11. — 3. FLECKENSTEIN, A.: (1975) Metabolische Faktoren bei der Entstehung von Myokardnekrosen und Mikroinfarkten. *Triangel*. **14**, 27. — 4. FLECKENSTEIN, A., DÖRING, H. J., JANKE, J., BYON, Y. K.: (1975) Basic actions of ions and drugs on myocardial high-energy phosphate metabolism and contractility. In: *Handbuch der experimentellen Pharmacologie*. Edited by: BORN, G. V. R., EICHLER, O., FARAH, A., HERKEN, H., WELCH, A. D. Springer Verlag. Vol. XVI/3, 345. — 5. JENNINGS, R. B., GANOTE, C. E.: (1974) Structural changes in the myocardium during acute ischemia. *Circulat. Res. Suppl.* **35**, 156. — 6. JUHÁSZ-NAGY, S., SZENTIVÁNYI, M.: (1973) Effect of alpha-adrenergic coronary constriction on myocardial tissue blood flow. *Arch. int. Pharmacodyn.* **206**, 19. — 7. JUHÁSZ-NAGY, S., SZODORAY, P.: (1972) Effect of transitory myocardial ischemia on coronary adaptability and on heart production of the left ventricle. *Acta. Physiol. Acad. sci. Hung.* **42**, 275. — 8. KATZ, A. M.: (1970) The contractile proteins of the heart. *Physiol. Rev.* **50**, 63. — 9. KATZ, A. M., TADA, M., REPKE, D., IORIO, J. A., KIRCHENBERG, M. A.: (1974) Adenylate cyclase: Its probable localization in sarcoplasmic reticulum as well as sarcolemma of the canine heart. *J. Mol. Cell. Cardiol.* **4**, 673. — 10. KATZ, A. M.: (1975) Congestive heart failure. Role of the altered myocardial cellular control. *New England J. Med.* **293**, 1184. — 11. NAYLER, W. G., GRAU, A., SLADE, A.: (1976) Eine Shutzwirkung von Verapamil auf den hypoxischen Herzmuskel. *Cardiovasc. Res.* **10**, 650. — 12. NAYLER, W. G., SEABRA-GOMES, R.: (1975) Excitation-contraction coupling in cardiac muscle. *Progress in Cardiovasc. Res.* **13**, 75. — 13. OLSON, R. E., DHALLA, N. S., SUN, C. N.: (1972) Changes in energy stores in the hypoxic heart. In: *Metabolism of the Hypoxic and Ischemic Heart*. Edited by: MORET, P., FEJFAR, Z. Karger: Basel. 114. — 14. REUTER, H.: (1974) Exchange of calcium ions in the mammalian myocardium: mechanisms and physiological significance. *Circ. Res.* **34**, 599. — 15. POOL, P. E., COVELL, J. W., CHIDSEY, C. A., BRAUNWALD, E.: (1966) Myocardial high energy stores in acutely induced hypoxic heart failing. *Circ. Res.* **19**, 221. — 16. SHEN, A. C., JENNINGS, R. B.: (1972) Kinetics of calcium accumulation in acute myocardial ischemic injury. *Am. J. Path.* **67**, 441. — 17. SIMPSON, F., RAYNS, D. G., LEDINGHAM, J. M.: (1974) Fine structure of mammalian myocardial cells. In: *Advances in Cardiology. The Myocardium*. Edited by: Reader, R. Karger: Basel. **12**, 15. — 18. SOMOGYI, E., BALOGH, I., SÓTONYI, P.: (1976) Alterations of the Z-band in cardiac and skeletal muscles. *Acta Morph. Acad. sci. Hung.* **24**, 35. — 19. SOMOGYI, E., SÓTONYI, P., LUKÁCS, J., NEMES, A.: (1976) Changes in energy stores and cytochromeoxidase activity in the intermittent hypoxia. *Proc. XVth Conf. Electron Micr. (Prague)* Vol. A. 319. — 20. SÓTONYI, P., SOMOGYI, E., NEMES, A., JUHÁSZ-NAGY, S.: (1976) Ultrastructure and cytochemistry of cardiac intramitochondrial glycogen. *Acta Morph. Acad. sci. Hung.* **24**, 379. — 21. TRUMP, B. F., MERGNER, W. J., KAHNG, M. W., SALADINO, A.: (1976) Studies on the subcellular pathophysiology of ischemia. *Circulat.* **53**, 17. — 22. YATES, J. C., DHALLA, N. S.: (1975) Structural and functional changes associated with failure and recovery of hearts after perfusion with Ca^{++} free medium. *J. Molec. Cell. Cardiol.* **7**, 91.

INTERMITTIERENDE HYPOXISCHE BELASTUNG ALS UNTERSUCHUNGS MODEL DER FRÜHZEITIGEN HERZMUSKEL VERÄNDERUNGEN

E. SOMOGYI., P. SÓTONYI., A. NEMES und S. JUHÁSZ-NAGY

Verfasser konnten feststellen das die intermittierende hypoxische Belastung ein geeignetes Untersuchungs model ist der frühzeitigen Herzmuskel veränderungen. Es wurde festgestellt das Energietransport Verwirrung und Verminderung der Macroerg-phosphat verbindung eine primäre Rolle spielen. Die Schädigung der Ca^{++} Regulation, Änderung des Gewebes pH und Aktivaton des Anaeroben glycolise führt zu Minderung der Kontractions Kraft, Membranen Schädigungen und später zu disseminierten und diffusen Filamenten Destruction.

ПЕРЕМЕЖАЮЩАЯСЯ ГИПОКСИЧЕСКАЯ НАГРУЗКА — МОДЕЛЬ ИССЛЕДОВАНИЯ РАННИХ ИЗМЕНЕНИЙ СЕРДЕЧНОЙ ТКАНИ

Э. ШОМОДЬИ, П. ШОТОНЬИ, А. НЕМЕШ и Ш. ЮХАС-НАДЬ

Модель нагрузки перемежающейся гипоксии подходящей к исследованию формирования ранних изменений сердечной ткани. Авторы констатировали что дефицит формирующей из макроэрг-фосфатных соединений и энергетический транспорт имеют первичную роль. Изменение регуляции- Ca^{++} , активация анаэробного гликолиза, кислое смещение pH ткани вызывают понижение сокращения, разрушение мембран, потом рассеянный или диффузный некроз ниточек.

Dr. Endre SOMOGYI

Dr. Péter SÓTONYI

} Semmelweis Orvostudományi Egyetem,
Igazságügyi Orvostani Intézet,
H-1450 Budapest, Pf. 9/41, Hungary

Dr. Attila NEMES

Dr. Sándor JUHÁSZ-NAGY

} Semmelweis Orvostudományi Egyetem
Érsebészeti Klinika
H-1122 Budapest, Városmajor u. 68., Hungary

Regional Blood Transfusion Centre and County Hospital, Pécs, Hungary

DETECTION OF HEPATITIS B SURFACE ANTIGEN IN ISOLATED HEPATOCYTES

Mária PAÁL, G. BAJTAI, Mária AMBRUS, Györgyi HORVÁTH,
Márta KOVÁCS and K. BARNA

(Received February 10, 1977)

HB_sAg was detected by indirect immunofluorescent method in liver biopsy specimens of 60 symptom-free HB_sAg positive volunteers. An effort was made to separate from the material intact cells suitable for studying HB_sAg localization in the liver cells.

Introduction

The immunofluorescent technique is indispensable for the detection of cell antigens but use of the method is somewhat limited by some technical difficulties. One of the main problems is to obtain satisfactory preparations of the small biopsy material and often there are no sections sufficient for microscopic examinations. To avoid this problem, we isolated intact cell populations from human liver biopsy specimens and performed the immunofluorescent demonstration of hepatitis B surface antigen (HB_sAg) on the single cells. This allowed to demonstrate the occurrence and frequency of HB_sAg in the liver cells of seropositive, symptom-free volunteers, who were chronic carriers of HB_sAg.

Materials and methods

Sixty HB_sAg seropositive volunteer blood donors were subjected to percutaneous liver biopsy. The material obtained was prepared as follows.

1. The specimen was cut into small pieces with fine scissors.
2. The pieces were gently homogenized by slow shaking in 2 ml modified, Ca⁺⁺ free Hanks' solution pH 7.4 containing 0.5 mM EDTA for Ca⁺⁺ extraction [2, 5].
3. The isolated cell suspension was washed in 1 ml modified Hanks' solution twice, then centrifuged at low speed (50–70 g) for 5 min.
4. One drop of the cell suspension was placed on a slide and kept in a moist chamber for 30 min. During the incubation period the cells settled and adhered to the slide, bringing about a monolayer. The procedure was carried out at +4°C.
5. The cell preparation then was fixed by drying in air at room temperature for 10 min.

The indirect immunofluorescent method of COYNE et al. [1] and RAY and DESMAL [3] was used to detect HB_sAg intracellularly. The applied antisera were rabbit anti-HB_sAg (Behringwerke), and goat anti-rabbit 7-S globulin conjugated with fluorescein isothiocyanate (FITC) (Progr. Lab. Inc., Baltimore, USA). With the control normal rabbit serum no immunofluorescence was obtained, neither with anti-HB_sAg immune serum absorbed with serum containing HB_sAg. FITC anti-rabbit 7-S globulin was applied directly.

Results and conclusions

The single cell separation technique from liver biopsy specimens seems to be a suitable laboratory tool for the detection of HB_sAg (Fig. 1). To distinguish positive and negative tissue samples, it is easier to investigate single cells than to work with cryostat sections.

The percentage of antigen positive cells was easily determined by the method (Table I) because it results in an isolated cell population. Furthermore a detailed morphological analysis could be made of single cells, revealing

Table I

*Percentage distribution of HB_sAg containing cells
in 32 out of 60 cases giving
a positive immunohistochemical reaction with IIF*

Percentage of HB _s Ag positive cells	No. of cases
1—20	20
20—40	5
40—	7
Total	32

clearly the diffuse cytoplasmic, perimembraneous, or perinuclear localization of fluorescence (Figs 1/a, 1/b, 2 and 3), much better than it was seen in frozen sections. The cell isolation method is recommended for immunofluorescent studies, especially if the tissue specimen is very small. This is mostly the case when examining symptom-free HB_sAg carriers, and a liver biopsy is made for the sake of early diagnosis.

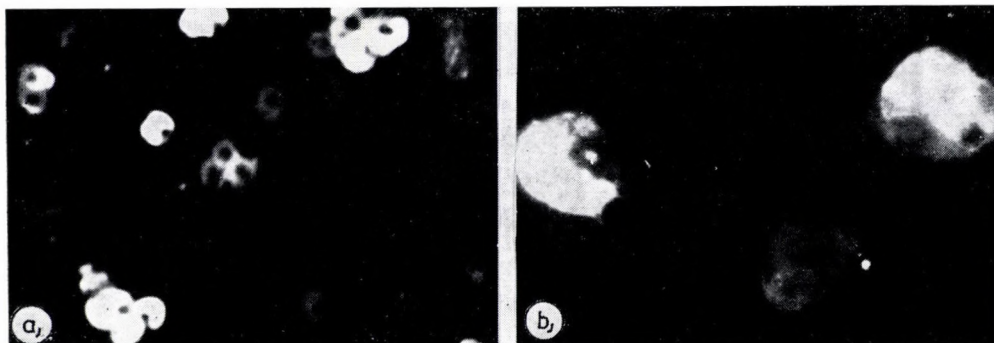


Fig. 1. Cytoplasmic localization of HB_sAg in hepatocytes (IIF) 1a ($\times 160$), 1b ($\times 600$)



Fig. 2. Peripheral fluorescence in the cell membrane (IIF) ($\times 600$)



Fig. 3. Perinuclear fluorescence in hepatocytes (IIF) ($\times 640$)

REFERENCES

1. COYNE (ZAVATONE), V. E., MILLMAN, I., CERDA, J., GERSTLY, B. J. S., LONDON, T., SUTNICK, A., BLUMBERG, B. S.: (1970) The localisation of Australia antigen by immunofluorescence. *J. exp. Med.* **131**, 307. — 2. JACOB, S. T., BHARGAVA, P. M.: (1962) New method for the preparation of liver cell suspensions. *Exp. Cell Res.* **27**, 453. — 3. RAY, M. B., DESMET, V. J.: (1975) Immunofluorescent detection of hepatitis B antigen in paraffin-embedded liver tissue. *J. immunol. Methods* **6**, 283. — 4. SAMPLINER, R.: (1977) Chronic active hepatitis in hepatitis B surface antigen (HB_sAg) carriers. *J. Amer. med. Ass.* **237**, 50. — 5. SEGLEN, P. O.: (1972) Preparation of rat liver cells. I. Effect of Ca⁺⁺ on enzymatic dispersion of isolated, perfused liver. *Exp. Cell Res.* **74**, 450.

NACHWEIS DES HEPATITIS B OBERFLÄCHENANTIGENS IN ISOLIERTEN LEBERZELLEN

M. PAÁL, G. BAJTAI, M. AMBRUS, GY. HORVÁTH, M. KOVÁCS und K. BARNA

Im Leberbiopsiematerial von 60 symptomfreien Blutspendern wurde das Vorkommen des Hepatitis B Oberflächenantigens (HB_sAg) mit indirekten Immunfluoreszenzverfahren untersucht. Aus den mittels Nadelbiopsie entnommenen Proben wurden intakte Zellen isoliert. Die auf diese Weise gewonnenen Zellen wurden zur Untersuchung der Intrazellulären Lokalisation und der Häufigkeit des HB_sAg mit Erfolg angewandt.

ВЫЯВЛЕНИЕ ПОВЕРХНОСТНОГО АНТИГЕНА ГЕПАТИТА В ИЗОЛИРОВАННЫХ ПЕЧЕНОЧНЫХ КЛЕТКАХ

М. ПААЛ, Г. БАЙТАИ, М. АМБРУШ, Д. ХОРВАТ, М. КОВАЧ и К. БАРНА

Авторы изучали методом иммунофлюоресценции в материале биопсии печени 60 бессимптомных доноров встречаемость поверхностного антигена гепатита В (HB_sAg). Из образцов, полученных при помощи биопсии, изолировали неповрежденные клетки. Полученные таким образом отдельные клетки успешно применялись для исследования внутриклеточной локализации и частоты встречаемости поверхностного антигена гепатита В.

Dr. Mária PAÁL

Dr. Gábor BAJTAI

Dr. Mária AMBRUS

} Megyei Vértanszfúziós Állomás, Pécs
H-7621 Pécs, Dischka Gy. u. 7, Hungary

Dr. Gyöngyi HORVÁTH

Dr. Márta KOVÁCS

Dr. Kornél BARNA

} Baranya Megyei Tanács Kórháza, Pécs
Fertőző Osztály
H-7623 Pécs, Rákóczi u. 2, Hungary

Péterfy Hospital, Budapest, Hungary

POST MORTEM DETECTION OF EARLY MYOCARDIAL INFARCTION BY DETERMINATION OF THE TISSUE K^+/Na^+ RATIO

Alice DECASTELLO, Éva REMENÁR, Jeannette TÓTH,
Borbála POZDERKA and I. BARTÓK

(Received May 20, 1977)

The K^+/Na^+ ratio was determined in myocardial specimens obtained post mortem from a total of 90 patients. The ratio was 1.0 or higher in 25 cases in which there was firm evidence against myocardial infarction, and 0.7, or less in 30 cases with grossly visible signs of myocardial necrosis. The remaining 35 cases were suspect of myocardial infarction on the grounds of either clinical observation or sudden death, without gross change. Out of these the K^+/Na^+ ratio was above 0.7, histological evidence of myocardial infarction was absent, but other changes accounting for death were present in 17 cases. In another 16 cases a K^+/Na^+ ratio of 0.7 or less was the sole indication of myocardial infarction, and any other change likely to be responsible for death was absent. In two further cases a false negative result was obtained for the K^+/Na^+ ratio, owing in all probability to some technical error. The findings suggest that determination of the myocardial K^+/Na^+ ratio is a great aid in detecting early myocardial infarction. The technique is not affected by post mortem autolysis, and is simple enough for routine use.

Traditional approaches to post mortem diagnosis do not always furnish evidence of the cause of sudden death. Myocardial infarction (MI) may cause sudden death even in young age [9] without giving rise to gross or conventionally detectable microscopic lesions in patients surviving for less than 12 hours [10, 11, 15, 18, 22, 23, 25]. If no obstruction of the coronary arteries is present, the suspicion of MI can be founded only on indirect signs, such as an arteriosclerotic stenosis of coronary artery, or the presence of an infarction scar [9], and clinical data. A further difficulty is that MI may occur without producing characteristic clinical signs [9, 14]. In view of this, all techniques allowing a reliable diagnosis of early MI are welcome by the pathologists. The requirements of such techniques are that, in addition to simplicity and accuracy, they should reflect also short-term ischaemia, and should not be affected by autolysis.

Disappearance of glycogen from the heart muscle, identified in animal experiments as one of the earliest signs of MI [1, 6, 11, 22], is not conclusive at autopsy owing to the considerable reduction of myocardial glycogen by autolysis [11, 22]. The reliability of the initially promising acid fuchsin staining [13, 15, 19] and of the haematoxylin — basic fuchsin — picric acid method [4, 8, 14] seem to be doubtful in the light of more recent findings [7, 11, 17, 25]. The microscopic [11, 21] and gross histochemical techniques [2, 12, 16] based

on the decreased dehydrogenase activity are greatly influenced by post mortem autolysis [2, 10, 22]. TORACK [20] has attempted to utilize the peroxidase activity of erythrocytic haemoglobin for the demonstration of myocardial circulatory disturbances but little experience has been obtained with this technique.

A simple biochemical method measuring the sodium potassium ratio in heart muscle, was elaborated by ZUGIBE et al. [23] for the detection of early MI. Since ischaemia soon gives rise to cell membrane injury, the cellular electrolyte transport mechanism becomes disturbed resulting in an influx of sodium ions into the cell and a loss of potassium ions by the cell. Consequently, the myocardial Na^+ -concentration increases, while the K^+ -concentration tends to decrease, since collateral circulation, usually functioning in the ischaemic area [5], can drain the K^+ lost from the cells. It follows that the K^+/Na^+ ratio decreases considerably in the infarcted heart muscle [10, 23–25]. Evidence has accumulated [10, 17, 23–25] that the determination of the K^+/Na^+ ratio meets all requirements of a post mortem diagnostic test of early MI.

In several necropsied cases the suspicion of MI arose on the grounds of the clinical history or sudden death, but no evidence could be obtained by routine histologic techniques. This has prompted us to introduce a new technique for the detection of MI in cases where the usual staining procedures fail. The macroscopic dehydrogenase technique would have also failed, most necropsies being carried out about 24 hr after death. Efforts were subsequently centred on measuring being the K^+/Na^+ ratio. These studies are reported in the present paper.

Materials and methods

Heart muscle specimens were obtained from a total of 90 patients, in most cases 24 to 30 hr after death. The cases were divided into three groups.

Group 1. 25 myocardial samples, without gross or microscopic indication of MI, and without clinical suspicion of MI while the patients were alive (negative controls).

Group 2. 30 myocardial samples with both gross and microscopic evidence of MI. The interval between onset of symptoms and death varied from 18 to 48 hr (positive control).

Group 3. 35 myocardial samples from cases suspected of early MI, but exhibiting neither coronary obstruction nor gross myocardial changes. The clinical and laboratory findings (pain in the chest, abnormal ECG, increased serum transaminase, shock, severe circulatory failure) had been indicative of MI in part of these cases. The onset of symptoms was followed by death within 1.5 to 10 hr. The rest of the patients had been treated for various disorders before sudden death, of which no satisfactory explanation could be found at necropsy.

The K^+ and Na^+ contents were determined in the necrotic myocardial area (group 2) or, there was no gross change (groups 1 and 3), in the anterior and posterior wall of the left ventricle, 5 and 8 cm away from the ostia of the anterior descending coronary artery and circumflex artery, respectively. Each specimen weighed about 1.5 g. A specimen was secured from the adjacent myocardial region for histological examination. In 16 cases belonging to group 2, additional specimens were removed from remote, normal-appearing areas of the myocardium.

The specimens were trimmed of pericardium, fat tissue and endocardium, wrapped into aluminium foil, and stored at -20°C until examination 1–7 days later [23]. According

to earlier studies [10, 23, 24], storage under such conditions does not affect the result. Before use the samples were minced, weighed, and deionized distilled water was added to give a weight to volume ratio of 1 : 20. The mixture was homogenized for 10 minutes. The homogenate was centrifuged for 10 minutes at 3000 r.p.m. The Na^+ and K^+ contents were determined in the 1 : 10 diluted supernatant by flame photometry, using Na^+ and K^+ reference standards for comparison. Initially larger myocardial specimens were taken from the controls (groups 1 and 2), and each was homogenized half by half in a ground glass homogenizer and Waring blender. Homogenation and centrifugation were carried out at 0°C or at room temperature. Since identical results were yielded by both procedures and at both temperatures, in later work the Waring blender was employed and homogenation and centrifugation were uniformly done at room temperature.

The specimens secured for histological examination were fixed in 10% neutral formalin. Paraffin sections were stained with H. and E., PATH, and PAS, with and without previous diastase digestion.

Results

Results are summarized in Table I.

Table I

K⁺/Na⁺ ratios determined in 90 myocardial specimens

Groups	No. of cases	K ⁺ /Na ⁺		
		range	mean	standard deviation
Group 1 (negative controls)	25	1 — 2.2	1.58**	± 0.33
Group 2 (positive controls)	30	0.1 — 0.7	0.42**	± 0.17
Group 3 (suspicion of early MI)				
a)	19*	0.8 — 2.2	1.41	± 0.38
b)	16	0.2 — 0.7	0.5	± 0.13

* In 2 cases histological evidence of minor necrosis (false negative result) was obtained.

** The difference established by the unpaired *t*-test was highly significant (*p* < 0.01).

Group I (negative controls). The age of the patients ranged from 22 to 91 years. The cause of death was pulmonary embolism in nine cases, congestive heart failure in eight cases, renal failure after chronic pyelonephritis in two cases and after acute tubular necrosis in one case, liver cirrhosis with parenchymal and vascular decompensation in one case, acute diffuse peritonitis in one case, and pneumonia in three cases. Hyperpotassaemia, with serum K^+ values of 5.8, 6.8 and 6.9 mEq/l, respectively, was found in three cases. Several small, dispersed fibrotic foci were visible in five cases, and post-infarction scars in two cases. Hypertrophy of the left ventricle was found in 12 cases.

The K^+/Na^+ ratio varied between 1.0 and 2.2, irrespective of the serum K^+ level.

Scattered focal fibrotic changes were demonstrated histologically in about half of the cases. On staining with PATH, focal rarification and an indistinct cross striation were observed in several cases. Glycogen could be detected by PAS reaction in a minor part of muscle cells.

Group 2 (positive controls). The patients of this group were 38 to 89 years old. In three cases MI was followed by rupture of the left ventricle. Occlusion of a coronary artery by a fresh thrombus occurred in 15 cases, and scars indicating earlier MI were found in five samples.

The K^+/Na^+ ratio was 0.7, 0.6 and 0.5 or less in two, six and 22 specimens of necrotic myocardial tissue, respectively.

Sections stained with H and E showed the characteristic picture of myocardial infarction. The cross striation was not recognizable on staining with PATH; the cells contained only contraction bundles and coarse granules. A small amount of glycogen was detectable by PAS-reaction in some myocardial cells.

Among the specimens appearing preserved on gross examination, 14 had a K^+/Na^+ ratio higher than 1.0, but two only 0.6 and 0.4, respectively, without any histological sign of MI.

Group 3: suspicion of early MI. The patients were 52–89 years old.

a) In 17 cases the K^+/Na^+ ratio ranged from 1.0 to 2.2 in both samples, but in two other cases it was within these limits in one sample and had a value of 0.8 and 0.9, respectively, in the other. Post-infarction scar was grossly visible in one case, and dispersed focal scars occurred in three cases. Histological evidence of MI was absent in 17 cases including those two in which the tissue K^+/Na^+ ratio was 0.8 and 0.9. The cause of death was severe congestive heart failure after a valvular defect or hypertrophy and dilatation of both ventricles in 10 cases, pneumonia in two cases, endstage carcinoma with multiple metastases in three cases, and advanced liver cirrhosis in two cases.

Unlike the above cases on staining with H, and E, and PTAH two further myocardial specimens showed, despite high values for the K^+/Na^+ ratio, fresh necrosis of minor groups of muscle cells adjacent to extensive fibrous scars. Factors other than myocardial necrosis had also a role in the death of these two patients. One had had systemic lupus erythematosus, and emboli were found in several secondary branches of the pulmonary artery. The other patient had uterine carcinoma with metastases, and a myocardial post-infarction scar. The ECG had suggested MI in both cases.

b) The K^+/Na^+ ratio ranged from 0.2 to 0.7 in 16 cases, of which four showed this value in both specimens, and 12 in one specimen only, while the other specimens showed values of 0.8–0.9 in three cases and of 1.0 or more in the rest. No other change which could be held responsible for death was

found. Post-infarction scar was grossly visible in four specimens and dispersed minute scars in three. The microscopic appearance of the myocardium did not differ from the negative controls in any of the 16 cases.

Discussion

In the present material MI could be excluded with certainty in 25 cases. Although focal rarefication or indistinctness of cross striation was demonstrable by PTAH staining in several such cases, it differed considerably from the alterations found in MI, and represents in all probability a post-mortem artifact. The K^+/Na^+ ratio was 0.1 or higher in each case, irrespective of the presence of left ventricular hypertrophy, congestive heart failure, or hyperpotassaemia. The high K^+/Na^+ ratio was not affected by digitalis intoxication and external heart massage in the cases seen by McVIE [10]. The K^+/Na^+ ratio never exceeded 0.7 in 30 cases with gross evidence of MI. A similar alteration of myocardial K^+ and Na^+ contents was reported in experimental MI [3, 17, 23, 24]. It seems therefore improbable that the K^+/Na^+ ratio should be low in non-necrotic myocardial tissue, or high where necrosis had occurred.

Most of our cases were necropsied 24—30 hr after death. The K^+/Na^+ ratio was always high in the negative controls and always low in the positive controls, indicating that autolysis did not affect the diagnostic value of the K^+/Na^+ ratio in 30 hr. McVIE [10] and ZUGIBE et al. [23—24] observed no change of the K^+/Na^+ ratio in specimens of normal and necrotic myocardial tissue after storage at room temperature for 5 and 10 days, respectively. Post-mortem shifts certainly occur in electrolyte distribution between cells and intercellular fluid, but this is of no avail since the ion ratio depends on the total electrolyte content [24].

In view of the foregoing considerations, K^+/Na^+ ratios of 1.0 or higher have been considered normal in this study, while those of 0.7 or less have been taken as evidence of MI. Values of 0.8 and 0.9, found in a few group 3 patients, were regarded as questionable.

Sixteen myocardial specimens without indication of necrosis showed K^+/Na^+ ratios of 0.7 or less. None of these specimens differed from the negative controls in microscopic appearance. It follows that the low K^+/Na^+ ratio was the sole indication of MI in all 16 cases, and in none was found any other change which could have been incriminated as the cause of death. In the cases seen by us, the shortest interval between onset of symptoms and death was 1.5 hours, but the MI-associated decrease of the K^+/Na^+ ratio could be detected within a shorter time [23, 24]. A low K^+/Na^+ ratio signifying early MI was also found in two histologically normal specimens obtained from myocardial regions distant to the grossly visible necrosis.

A clinical suspicion of MI had arisen in 19 additional cases, but in these the K^+/Na^+ ratio was 1.0 or higher. Necrosis was absent in 17 cases and in these, death could be explained by causes other than MI. In the remaining two cases, fresh myocardial necrosis was found. Since autolysis had no influence on the ionic composition and, on the other hand, a necrotic heart muscle did not ever give a negative result, the sole explanation of the false negative findings is a technical error. The accuracy of K^+/Na^+ determination depends on two preconditions. One is accurate sampling, which is a blind manipulation without topographic localization of infarction; for this reason the site of sampling should always be in the area supplied by the anterior descending and circumflex coronary arteries. The other prerequisite is a careful removal of all extraneous tissues [10, 23, 24]. In the above two cases with false negative results the first requirement had been met because the samples were taken from an area adjacent to histologically detectable necrosis, but the site of sampling must have been outside the necrotic involvement. The necrotic area was evidently quite small, because it was not grossly visible. Considerable fibrotic alterations were present in the surroundings of the necrosis in both cases, and thus a substantial amount of connective tissue may have been excised along with specimen, which may in fact have influenced the ionic composition. A further explanation for the error is that the myocardium had not been satisfactorily trimmed of extraneous tissues.

The aim of the present studies was not so much to compare the value of different techniques as to employ a routinely applicable procedure for the demonstration of early MI, not effected by post-mortem autolysis. The technique based on determination of the myocardial K^+/Na^+ ratio was found to meet these requirements. The ratio was high in all negative controls and low in all those used as positive controls; in 16 of the 90 cases studied, the low K^+/Na^+ ratio was the sole indication of MI. We believe that the two false negative results do not diminish the merits of the technique. Since no mention was made of such errors in earlier reports [10, 23, 24], false results can in all probability be prevented by greater experience and caution.

REFERENCES

1. BAJUSZ, E., JASMIN, G.: (1964) Histochemical studies on the myocardium following experimental interference with coronary circulation in the rat. I. Occlusion of coronary artery. *Acta histochem. (Jena)* **18**, 222. — 2. BRODY, G. L., BELDING, W. A., BELDING, R. M., FELDMAN, S. A.: (1967) The identification of myocardial infarcts. *Arch. Path.* **84**, 313. — 3. CROUT, J. R., JENNINGS, R. B.: (1957) An improved histochemical method for the demonstration of potassium. *J. Histochem. Cytochem.* **5**, 170. — 4. FEKETE, J. F.: (1974) Staining techniques. *Arch. Path.* **98**, 67. — 5. JENNINGS, R. B., WARTMAN, W. B.: (1957) Production of an area of homogeneous myocardial infarction in the dog. *Arch. Path.* **63**, 580. — 6. KLIONSKY, B.: (1960) Myocardial ischemia and early infarction: a histochemical study. *Amer. J. Path.* **36**, 575. — 7. LICHTIG, C., BROOKS, H., CHASSAGNE, G., GLAGOV, S., WISSLER, R. W.: (1975) Basic fuchsin picric-acid method to detect acute myocardial ischemia. An experimental study in swine. *Arch. Path.* **99**, 158. — 8. LIE, J. T., HOLLEY, K. E., KAMPA, W. R., TITUS, J. L.: (1971) New histochemical method for morphologic diagnosis of early

stages of myocardial ischemia. Mayo Clin. Proc. **46**, 319. — 9. LUCKE, J. L., HELPERN, M.: (1968) Sudden unexpected death from natural causes in young adults. Arch. Path. **85**, 10. — 10. McVIE, J. G.: (1970) Postmortem detection of inapparent myocardial infarction. J. clin. Path. **23**, 203. — 11. MORALES, A. R., FINE, G.: (1966) Early human myocardial infarction. A histochemical study. Arch. Path. **82**, 9. — 12. NACHLAS, M. M., SHNITKA, T. K.: (1963) Microscopic identification of early myocardial infarction by alteration in dehydrogenase activity. Amer. J. Path. **42**, 379. — 13. NIELSEN, K., RENAUD, S., LEMIRE, Y., SELYE, H.: (1958) "Fuchsinophilic degeneration" of myocardial fibers. Meeting of the Canadian Federation of Biological Societies, Kingston, Ont. (cit. by Poley et al.) — 14. OLSEN, E. G. J.: (1974) The Pathology of the Heart. Chapter 5, p. 47. G. Thieme, Stuttgart. — 15. POLEY, R. W., FOBES, C. D., HALL, M. J.: (1964) Fuchsinophilia in early myocardial infarction using acid fuchsin staining. Arch. Path. **77**, 325. — 16. RAMKISSOON, R. A.: (1966) Macroscopic identification of early myocardial infarction by dehydrogenase alterations. J. clin. Path. **19**, 479. — 17. ROSE, A. G., OPIE, L. H., BRICKNELL, O. L.: (1976) Early experimental myocardial infarction. Evaluation of histologic criteria and comparison with biochemical and electrocardiographic measurements. Arch. Path. **100**, 516. — 18. SAPHIR, O.: (1958) A Text on Systemic Pathology. Vol. 1, p. 87. Grune and Stratton, New York 1958. — 19. SELYE, H.: The Chemical Prevention of Cardiac Necroses. The Ronald Press, New York 1958, p. 43, footnote. (cit.: Poley et al.) (1958) — 20. TORACK, R. M.: (1974) Peroxidase activity in autopsy material. Evaluation of microcirculation. Arch. Path. **98**, 233. — 21. WACHSTEIN, M., MEISEL, E.: (1955) Succinic dehydrogenase activity in myocardial infarction and in induced myocardial necrosis. Amer. J. Path. **31**, 353. — 22. ŽUGIBE, F. T.: (1970) Diagnostic Histochemistry. C. V. Mosby Co., Saint Louis 1970, p. 156. — 23. ŽUGIBE, F. T., BELL, P., CONLEY, T., STANDISH, M. L.: (1966) Determination of myocardial alterations at autopsy in the absence of gross and microscopic changes. Arch. Path. **81**, 409. — 24. ŽUGIBE, F. T., CONLEY, T. L., BELL, P., JR., STANDISH, M.: (1972) Enzyme decay curves in normal and infarcted myocardium. Arch. Path. **93**, 308. — 25. ŽUGIBE, F. T., JR., ŽUGIBE, F. T.: (1973) Fuchsinophilia, fuchsinorrhagia staining techniques. Arch. Path. **96**, 243.

NACHWEIS DES FRÜHEN MYOKARDINFARKTS BEI DER AUTOPSIE AUFGRUND DES K/Na-QUOTIENTEN

ALICE DECASTELLO, ÉVA REMENÁR, JEANNETTE TÓTH, BORBÁLA POZDERKA und I. BARTÓK

Im Myokard von 90 Verstorbenen wurde der K/Na-Quotient bestimmt. In 25 Fällen, in denen ein frischer Infarkt mit Sicherheit ausgeschlossen werden konnte, betrug der Ionenquotient 1,0 oder mehr und in 30 Herzmuskeln, in denen makroskopisch ein Myokardinfarkt wahrgenommen wurde, betrug der Quotient 0,7 oder weniger. In weiteren 35 Fällen, in denen aufgrund der klinischen Symptome oder des plötzlichen Todes der Verdacht auf Herzinfarkt aufkam, war mit freiem Auge weder ein Verschluß der Koronararterie, noch Myokardnekrose zu sehen. In 17 dieser Fälle betrug der Ionenquotient mehr als 0,7, eine Nekrose ließ sich auch histologisch nicht nachweisen, und der Tod konnte auf andere Ursachen zurückgeführt werden. In anderen 16 Fällen war ein Ionenquotient von 0,7 oder weniger das einzige Zeichen der Herzmuskelnekrose, und andere Todesursachen kamen nicht in Frage. In weiteren 2 Fällen war der K/Na-Quotient aufgrund des histologischen Befundes falsch-negativ, allem Anschein nach infolge eines technischen Fehlers. Aufgrund dieser Ergebnisse bietet die Bestimmung des K/Na-Quotienten in der Diagnose des frühen Herzinfarkts eine bedeutende Hilfe. Ein Vorteil des Verfahrens ist, daß die post-mortale Autolyse die Resultate unbeeinflusst läßt und daß es routinemäßig durchgeführt werden kann.

ВЫЯВЛЕНИЕ РАННЕГО ИНФАРКТА СЕРДЦА НА ВСКРЫТИИ МЕТОДОМ ОПРЕДЕЛЕНИЯ КОЭФФИЦИЕНТА

АЛИС ДЕКАСТЕЛЛО, ЕВА РЕМЕНАР, ЖАНЕТТ ТОТ, БОРБАЛА ПОЗДЕРКА и И. БАРТОК

В сердечной мышце 90 умерших авторы определили коэффициент K/Na. В 25 случаях, в которых можно было бесспорно исключить свежий инфаркт, ионный коэффициент оказался 1,0 или больше, а в 30 случаях, в которых невооруженным глазом наблюдался инфаркт миокарда, коэффициент K/Na был 0,7 или меньше. В дальнейших 35 случаях на основе клинических симптомов или внезапной смерти возникло подозрение и

инфаркт сердца, невооруженным глазом не было видно ни закупорки коронарной артерии, ни некроза сердечной мышцы. В 17 этих случаев коэффициент K/Na был больше 0,7, при гистологическом исследовании не удалось выявить некроза, и смерть больных можно было привести в связь с другими причинами. В других 16 случаях единственным признаком некроза сердечной мышцы был ионный коэффициент в 0,7 или меньше, а другой причины смерти не было. В дальнейших 2 случаях коэффициент на основе гистологического исследования оказался ошибочно-отрицательным, по всей вероятности из-за технической ошибки. На основе исследований авторов определение коэффициента K/Na оказывает значительную помощь при распознавании раннего инфаркта миокарда. Преимуществом описанного метода является, что посмертный автолиз не влияет на результаты и что его можно поводить в качестве рутинного метода исследования.

Dr. Alice DECASTELLO
Dr. Éva REMENÁR
Dr. Jeannette TÓTH
Dr. Borbála POZDERKA
Dr. István BARTÓK

} Péterfy Sándor u. Kórház
H-1441 Budapest, Pf. 76, Hungary

RECENSIONES

JANSSEN W.: *Forensische Histologie. Arbeitsmethoden der medizinischen und naturwissenschaftlichen Kriminalistik. Forensic Histology. Method in Medical and Scientific Criminology.* Vol. 10. Verlag Max Schmidt-Römhild, Lübeck, 1977. 400 pages with 125 figures and 10 tables. Price: DM 180.—

This book is given a particular actuality by the fact that it abridges a gap in the literature of forensic medicine. Textbooks available are concerned with a narrower field of histopathology and they consider it primarily from the pathologist's angle. A comprehensive histopathology treating the subject with the special situation and demands of forensic pathology in mind was painfully missing. The intention of the author is most appreciated because his book is an important contribution to the literature of forensic medicine and will certainly be wellcome by those who are engaged with this field.

The construction of the book is clear offering an easy orientation. Earlier and recent data are considered in a harmonic summary of views. Each chapter is concluded by a comprehensive list of references. For the reader's great help are the high-quality illustrations, colour and black-and-white as well. The author attempts at dealing with the forensic pathology in a detailed and objective manner and this aim is fully reached. The literature with its controversial issues is reviewed critically similarly to author's own results. This critical attitude is an assurance for the reader that the pending questions of forensic medicine are approached in a most unprejudiced and realistic way.

The methodical section gives a detailed description of procedures and contains also relevant critical remarks. In the chapter dealing with *post-mortem* changes the methods for determination of the time of death are surveyed. Their potentialities are discussed with special reference to the *post-mortem* period when they can be used most efficiently to obtain realistic values. The chapter dealing with the differentiation of *in vivo* and *post-mortem* damages is particularly rich comprising almost all possible approaches to this problem (histochemistry, fluorescent-, polarized light-, and electron-microscopy). The clear construction of this chapter calls the attention to the types of histopathological diagnoses that can be made. The chapter considering the conditions of hypoxia is also comprehensive. The section on the subject of sudden death besides its detailed discussions reveals a wide scale of diagnostic problems and lists almost all the forms of sudden death which are met with in the forensic medicine. A separate chapter is devoted to the cases of hanging and suffocation completed with relevant biochemical results. Useful informations can be gained from the chapters on the damaging effects of heat and electric current. To show the histopathological changes following these injuries, the most recent scanning electron microscopic data are cited. Similarly excellent chapters are those considering the shot wounds and poisonings. Special attention is paid to the forensic histopathology of atypical shot wounds. Of great value is the histopathological differentiation of almost all types of poisonings. The summarizing tables after each chapter show briefly but efficiently the most important points of the histopathological investigation for each case.

This book is also excellent from the didactical point of view without being verbose. Informations are well-grouped covering practically every field of forensic histopathology. Documentation is of high quality. The book is therefore thought to be most useful for forensic physicians, pathologists and also for those who are concerned with interdisciplinary studies.

E. SOMOGYI

SCHUMACHER, G. H.—GEYER, G.: *Neurowissenschaft im Licht morphologischer Forschungen. Ergebnisse der experimentellen Medizin* vol. 25. VEB Verlag Volk und Gesundheit, Berlin, 1977. 238 pages + illustrations.
Price: M 34,—

The Societies of the Anatomists, Histochemists and Electron Microscopists of the German Democratic Republic hold their first joint Congress in 1974 at Binz. One of the main topics of this meeting was nervous system and sensory organs. The 25. volume of the results of experimental medicine contains the two reviews and the 32 short communications related to the mentioned topic and presented at the Congress. The first review type paper (by Prof. W. Kirsche) is devoted to the functional morphology of the neuronal organization. It is an excellent survey discussing cellular (focusing on synaptology, i.e. synaptic formations, plasticity of synapses, etc.), supracellular (dealing mainly with neural networks, particularly¹ of the cerebral cortex) and macromorphological levels. More than 400 publications are listed in the references. In the second comprehensive and outstanding paper Prof. J. Szentágothai presents his very exciting concept on the neural organization of various central nervous system structures. Largely based on own findings on the spinal cord, lateral geniculate body and cerebellar cortex, he proposes that the specific neuronal network of various regions is built of regular structural units overlapping in several cases. The assumption of the repetition of such units appears to help to explain the occurrence of systematic specificity of neuronal connections of the various CNS structures. The short communications deal with a great variety of different neuromorphological questions (such as normal morphology including neural connections of certain regions, ontogenesis of some structures, morphological changes in certain areas after various interventions, etc.) having studied them at gross anatomical, light microscopical or electron microscopical level. Illustrations are of good quality, but are separated from the text (attached to the end of the volume). The pages of the figures are not numbered. Therefore, it is not so easy to find the propiate figure referred to in the text. The volume may be recommended to all those interested in the field of neuroscience.

B. HALÁSZ

UNGVÁRY, GY.: *Functional Morphology of the Hepatic Vascular System*. Akadémiai Kiadó, Budapest, 1977

This book summarizes more than a decade's systematic research of the author on the hepatic circulation under normal and pathological conditions. The unitarian concept of the entity of structure and function and a multilateral approach to the understanding of circulation-control characterizes the whole work.

The reviewer cannot undertake the task of highlighting some new results or to enlarge on some interesting details. A general consideration of the scope, methods and — being a morphological work — the quality of illustrations is given instead.

Investigations were carried out on livers of humans (adult and fetal) and of several other species. The methods are selected to tackle the problem from various aspects. The potentialities of injection-corrosion techniques (ink, PVC), portography, stereomicroscopy, histochemistry, fluorescence microscopy, transmission electronmicroscopy, etc., are well exploited. Some questions are studied in different species: partial hepatectomy in rats, ligature of the hepatic artery in cats, ligature of the common bile duct in guinea pigs and rats. Circulatory changes following acute hepatic injuries are considered in CCl₄-intoxicated rat and yellow cirrhotic human livers.

The list of references also comprises recent (1975) data indicating the relatively short time elapsing between the finalization of the manuscript and the publishing of the book. Nowadays, this has to be appreciated.

The illustrations are abundant and of high-quality. Legends are clear and grasp the very essence of the figure. Out of 127 pictures 102 are in black-and-white, 25 in colour. Similarly to the methods illustrations also reflect the multilateral approach of the author.

The book is thought useful primarily for anatomists and histologists but contains valuable informations also for workers of other theoretical or diagnostic fields such as pathophysiology, experimental and human pathology and pharmacology. In practical medicine this work can be of use in abdominal surgery. This latter field is currently showing an increasing interest towards the liver. The number of partial hepatectomies carried out for therapeutical reasons increases constantly.

G. KENDREY

SCHUMACHER, G. H.: *Embryonale Entwicklung des Menschen* (Thesaurus Reihe). *Human Embryonic Development* (Thesaurus Series) VEB Verlag Volk und Gesundheit, Berlin, 1977. (Third revised and completed edition) 206 pages (19 × 12 cm), 96 illustrations (G. Ritschel and R. Schiller)
Price: M 5.75

This is a well constructed, didactically illustrated introductory book of the professor in anatomy of the Wilhelm Pieck University of Rostock. Unfortunately, it suffers from the main drawback of many similar books by missing the adequate proportions of the fields surveyed. For example, extremely rare developmental malformations are detailedly considered whereas the development of the immune-system is treated rather laconically. Moreover very little is found in this book of the haemopoiesis and its onset in the bone marrow. There is no mention of some important disturbances such as the discrepancies in the growth-parameters in early embryonic age. Nor is the list of references enough comprehensive.

Because of its low price and page number and for its didactical illustrations this book can be recommended to students or to post-graduate beginners in the field. Finally, it has to be noted that it comprises all the advantages what a third, revised and completed edition of any book can offer.

E. KELEMEN

SCHUMACHER, G. H.—SCHMIDT, H.: *Anatomie und Biochemie der Zähne. Anatomy and biochemistry of teeth.* Verlag Volk und Gesundheit, Berlin, 1976. 589 pages with 349 figures and 301 tables
Price: M 125.70

The second revised edition of the book of professor G. H. Schumacher, director of the Anatomy Department of Wilhelm Pieck University in Rostock, and H. Schmidt, director of the Department of Physiology and Chemistry of Martin Luther University in Wittenberg, has been reedited since the first edition was sold out shortly after its appearance in 1971.

The authors' functional and modern attitude is well mirrored by the book's title and classification, for chapters and dental development, anatomy and morphology are supplemented by just the right amount of biochemical and histochemical knowledge. The work consists of six main parts.

1. The introductory chapter deals with dental anatomy, structural aspects of teeth, their setting in the jaws, their pattern and function are discussed together with such important items as the unity of the maxillo-mandibular apparatus and their tasks.

2. The chapter on phylogenesis and comparative anatomy of the teeth discusses their origin, the comparative anatomy of the hard dental tissue, the teeth's topography and fixing as well as their formations.

3. The chapter on development consists of four parts, a) a historical review; b) genesis and histogenesis (tooth and dental lamina, dentin, papilla, enamel, the structure and ultrastructure of the tissues and evolution of the paradontium). There is an excellent table showing the chronology of development and growth of human teeth; c) eruption and shedding of teeth, sexual and population differences and chronological data; d) anomalies including hyperdontia and hyperodontia.

4. The histology and molecular structure of the dental tissue is the longest chapter in the book, describing the light microscopical and ultramicroscopical structure of dental enamel, dentin, cement and pulp. Especially valuable are the excellent electron microscopic pictures. Studies of tooth structure, histochemical and biochemical methods and their results, estimation of organic and inorganic components, their topography and, where it is known, their significance are discussed.

5. The chapter on the morphology of teeth and of human dentition contains much practical information equally useful for the dentist and the anatomist and could prove to be important in forensic medicine for the identification of corpses. A comprehensive picture is given of the general and special questions of permanent teeth, the differences in primary teeth, masticatory function, the structure of the dental arch, occlusion, eugnathia dysgnathia and abrasion.

6. The chapter entitled "parodontium" is devoted mainly to morphology; the gums, the desmodontium, cementum and the anatomical structure of the alveolar bones. It also touches upon the functions of the parodontium, the parodontal cleft and the physiological movement of teeth.

The book under review is based on substantial experience, thorough information and knowledge, as indicated by the list of nearly fifteen hundred pertaining references. The black and white figures are of good quality, the tables illustrate well the text.

The appendix by W. Richter explains the Greek and Latin terminology. It is supplemented by a short dictionary and a grammatical table.

The book is an excellent and modern work, offering valuable and detailed information for students, clinicians, dentists, oral surgeons, chemists, morphologists and specialists of forensic medicine.

I. KENYERES

INDEX

Morphologica Normalis et Experimentalis

<i>Fehér, J.</i> : Myofibre Abnormalities of Orbicular Muscle in Malposition of the Eyelid	205
<i>Törő, I.</i> : Influence of the Intestinal Epithelium to the Plasma cell Differentiation Injected Into the Thymus	219
<i>Tompa, Anna—Lapis, K.—Schaff, Zsuzsa—Mészáros, K.—Mandl, J.—Garzó, T.—Antoni, F.</i> : Cytoplasmic Aggregates in D-Galactosamine Induced Liver Injury	239
<i>Ambach, G.—Palkovits, M.</i> : Blood Supply of the Rat Hypothalamus. V. The Medial Hypothalamus (Nucleus Ventromedialis, Nucleus Dorsomedialis, Nucleus Perifornicalis)	259
<i>Somogyi, E.—Sótonyi, P.—Nemes, A.—Juhász-Nagy, S.</i> : Intermittent Hypoxic Loading: A Model System to Study the Early Stages of Myocardial Lesions. (Short communication)	279

Pathologia

<i>Paál, Mária—Bajtai, G.—Ambrus, Mária—Horváth, Györgyi—Kovács, Márta—Barna, K.</i> : Detection of Hepatitis B Surface Antigen in Isolated Hepatocytes	285
<i>Decastello, Alice—Remenár, Éva—Tóth, Jeanette—Pozderka, Borbála—Bartók, I.</i> : Post Mortem Detection of Early Myocardial Infarction by Determination of the Tissue K^+/N^+ Ratio	289
Recensiones	297

Printed in Hungary

A kiadásért felel az Akadémiai Kiadó igazgatója.

Műszaki szerkesztő: Zacsik Annamária

A kézirat nyomdába érkezett: 1978. I. 23. — Terjedelem: 8,75 (A/5) ív, 35 ábra (8 színes)

78.5427 Akadémiai Nyomda, Budapest — Felelős vezető: Bernát György

The Acta Morphologica publish papers on experimental medical subjects in English. The Acta Morphologica appear in parts of varying size, making up volumes. Manuscripts should be addressed to:

Acta Morphologica, 1091 Budapest, Üllői út 93.

Correspondence with the editors and publishers should be sent to the same address. Subscription: \$ 36.00 per volume.

Orders may be placed with "Kultura" Foreign Trading Company (1389 Budapest 62, P.O.B. 149. Account No. 218-10990) or its representatives abroad.

Les Acta Morphologica paraissent en anglais et publient des travaux du domaine des sciences médicales expérimentales.

Les Acta Morphologica sont publiés sous forme de fascicules qui seront réunis en volumes.

On est prié d'envoyer les manuscrits destinés à la rédaction à l'adresse suivante:

Acta Morphologica, 1091 Budapest, Üllői út 93.

Toute correspondance doit être envoyée à cette même adresse.

Le prix de l'abonnement: \$ 36.00 par volume.

On peut s'abonner à l'Entreprise du Commerce Extérieur «Kultura» (1389 Budapest 62, P.O.B. 149. Compte-courant No. 218-10990) ou chez représentants à l'étranger.

«Acta Morphologica» публикуют трактаты из области экспериментальных медицинских наук на английском языке.

«Acta Morphologica» выходят отдельными выпусками разного объема. Несколько выпусков составляют один том.

Предназначенные для публикации авторские рукописи следует направлять по адресу:

Acta Morphologica, 1091 Budapest, Üllői út 93.

По этому же адресу направлять всякую корреспонденцию для редакции и администрации. Подписная цена — \$ 36.00 за том.

Заказы принимает предприятие по внешней торговле «Kultura» (1389 Budapest 62, P.O.B. 149. Текущий счет № 218-10990) или его заграничные представительства и уполномоченные.

Reviews of the Hungarian Academy of Sciences are obtainable
at the following addresses:

AUSTRALIA

C.B.D. LIBRARY AND SUBSCRIPTION SERVICE,
Box 4886, G.P.O., Sydney N.S.W. 2001
COSMOS BOOKSHOP, 145 Ackland Street, St.
Kilda (Melbourne), Victoria 3182

AUSTRIA

GLOBUS, Höchstädtplatz 3, 1200 Wien XX

BELGIUM

OFFICE INTERNATIONAL DE LIBRAIRIE, 30
Avenue Marnix, 1050 Bruxelles
LIBRAIRIE DU MONDE ENTIER, 162 Rue du
Midi, 1000 Bruxelles

BULGARIA

HEMUS, Bulvar Ruszki 6, Sofia

CANADA

PANNONIA BOOKS, P.O. Box 1017, Postal Sta-
tion "B", Toronto, Ontario M5T 2T8

CHINA

CNPICOR, Periodical Department, P.O. Box 50,
Peking

CZECHOSLOVAKIA

MAD'ARSKÁ KULTURA, Národní třída 22,
115 66 Praha

PNS DOVOZ TISKU, Vinohradská 46, Praha 2

PNS DOVOZ TLACE, Bratislava 2

DENMARK

EJNAR MUNKSGAARD, Norregade 6, 1165
Copenhagen

FINLAND

AKATEMINEN KIRJAKAUPPA, P.O. Box 128,
SF-00101 Helsinki 10

FRANCE

EUOPERIODIQUES S. A., 31 Avenue de Ver-
sailles, 78170 La Celle St. Cloud

LIBRAIRIE LAVOISIER, 11 rue Lavoisier, 75008
Paris

OFFICE INTERNATIONAL DE DOCUMENTA-
TION ET LIBRAIRIE, 48 rue Gay-Lussac, 75240
Paris Cedex 05

GERMAN DEMOCRATIC REPUBLIC

HAUS DER UNGARISCHEN KULTUR, Karl-
Liebknecht-Straße 9, DDR-102 Berlin

DEUTSCHE POST ZEITUNGSVERTRIEBSAMT,
Straße der Pariser Kommune 3-4, DDR-104 Berlin

GERMAN FEDERAL REPUBLIC

KUNST UND WISSEN ERICH BIEBER, Postfach
46, 7000 Stuttgart 1

GREAT BRITAIN

BLACKWELL'S PERIODICALS DIVISION, Hythe
Bridge Street, Oxford OX1 2ET

BUMPUS, HALDANE AND MAXWELL LTD.,
Cowper Works, Olney, Bucks MK46 4BN

COLLET'S HOLDINGS LTD., Denington Estate,
Wellingborough, Northants NN8 2QT

W.M. DAWSON AND SONS LTD., Cannon House,
Folkestone, Kent CT19 5EE

H. K. LEWIS AND CO., 136 Gower Street, London
WC1E 6BS

GREECE

KOSTARAKIS BROTHERS, International Book-
sellers, 2 Hippokratous Street, Athens-143

HOLLAND

MEULENHOF-BrUNA B.V., Beulingstraat 2,
Amsterdam

MARTINUS NIJHOFF B.V., Lange Voorhou-
9-11, Den Haag

SWETS SUBSCRIPTION SERVICE, 347b Heere-
weg, Lisse

INDIA

ALLIED PUBLISHING PRIVATE LTD., 13/14
Asaf Ali Road, New Delhi 110001

150 B-6 Mount Road, Madras 600002

INTERNATIONAL BOOK HOUSE PVT. LTD.,
Madame Cama Road, Bombay 400039

THE STATE TRADING CORPORATION OF
INDIA LTS., Books Import Division, Chandralok,
36 Janpath, New Delhi 110001

ITALY

EUGENIO CARLUCCI, P.O. Box 252, 70100 Bari

INTERSCIENTIA, Via Mazzè 28, 10149 Torino

LIBRERIA COMMISSIONARIA SANSONI, Via

Lamarmora 45, 50121 Firenze

SANTO VANASIA, Via M. Macchi 58, 20124

Milano

D. E. A., Via Lima 28, 00198 Roma

JAPAN

KINOKUNIYA BOOK-STORE CO. LTD., 17-7
Shinjuku-ku 3 chome, Shinjuku-ku, Tokyo 160-91

MARUZEN COMPANY LTD., Book Department,
P.O. Box 5050 Tokyo International, Tokyo 100-31

NAUKA LTD. IMPORT DEPARTMENT, 2-30-19
Minami Ikebukuro, Toshima-ku, Tokyo 171

KOREA

CHULPANMUL, Phenjan

NORWAY

TANUM-CAMMERMEYER, Karl Johansgatan
41-43, 1000 Oslo

POLAND

WĘGIERSKI INSTYTUT KULTURY, Marszał-
kowska 80, Warszawa

CKP I W ul. Towarowa 28 00-958 Warszawa

ROMANIA

D. E. P., București

ROMLIBRI, Str. Biserica Amzei 7, București

SOVIET UNION

SOJUZPETCHATJ — IMPORT, Moscow
and the post offices in each town

MEZHDUNARODNAYA KNIGA, Moscow G-200

SPAIN

DIAZ DE SANTOS, Lagasca 95, Madrid 6

SWEDEN

ALMQVIST AND WIKSELL, Gamla Brogatan 26,
101 20 Stockholm

GUMPERTS UNIVERSITETSBOKHANDEL AB,
Box 346, 401 25 Göteborg 1

SWITZERLAND

KARGER LIBRI AG, Petersgraben 31, 4011 Basel

USA

EBSCO SUBSCRIPTION SERVICES, P.O. Box
1943, Birmingham, Alabama 35201

F. W. FAXON COMPANY, INC., 15 Southwest
Park, Westwood, Mass. 02090

THE MOORE-COTTRELL SUBSCRIPTION

AGENCIES, North Cohocton, N. Y. 14868

READ-MORE PUBLICATIONS, INC., 140 Cedar
Street, New York, N. Y. 10006

STECHERT-MACMILLAN, INC., 7250 Westfield
Avenue, Pennsauken N. J. 08110

VIETNAM

XUNHASABA, 32, Hai Ba Trung, Hanoi

YUGOSLAVIA

JUGOSLAVENSKA KNJIGA, Terazije 27, Beograd
FORUM Vojvode Mišića 1, 21000 Novi Sad